Horsing around with *Anoplocephala perfoliata*:

A Polyomic Investigation of the Host–Parasite Interface

By

Boontarikaan Wititkornkul

A thesis submitted at the Department of Life Sciences,

Aberystwyth University, for the degree of Doctor of Philosophy

September 2023

DECLARATION/STATEMENTS

Word Count of thesis: DECLARATION	66,377
This work has not previously been accepted in substance for any degree and is not concurrently submitted in candidature for any degree.	
Candidate name	Boontarikaan Wititkornkul
Signature:	BOONTARIKAAN
Date	14/09/2023

STATEMENT 1

This thesis is the result of my own investigations, except where otherwise stated. Where ***correction services** have been used, the extent and nature of the correction is clearly marked in a footnote(s).

Other sources are acknowledged by footnotes giving explicit references. A bibliography is appended.

Signature:	BOONTARIKAAN
Date	14/09/2023

[*this refers to the extent to which the text has been corrected by others]

STATEMENT 2

I hereby give consent for my thesis, if accepted, to be available for photocopying and for inter–library loan, and for the title and summary to be made available to outside organisations.

Signature:	BOONTARIKAAN
Date	14/09/2023

NB: *Candidates on whose behalf a bar on access (hard copy) has been approved by the University should use the following version of Statement 2:*

I hereby give consent for my thesis, if accepted, to be available for photocopying and for inter–library loans after expiry of a bar on access approved by Aberystwyth University.

Signature:	BOONTARIKAAN
Date	14/09/2023

ACKNOWLEDGEMENTS

First and foremost, I would like to extend my heartfelt appreciation to the Faculty of Veterinary Science at Rajamangala University of Technology Srivijaya for generously sponsoring my PhD studies, enabling me to carry out this thesis at Aberystwyth University, United Kingdom.

I am deeply grateful to my exceptional supervisors, Ruth Wonfor and Russell Morphew, for their unwavering support, encouragement, and guidance throughout my PhD research. I cannot thank both of you enough for accompanying me on this journey.

I would like to express my gratitude to the following individuals who have contributed to the success of this research:

- Martin Swain and Matthew Hegarty for their invaluable work in transcriptome analysis.
- The staff at Lluest Equine Centre, including Hannah Appleton, Jennifer Lawrence, and Caryl Thomas, for their support and assistance in the yard, as well as the wonderful horses that participated in my experiments.
- Technicians Julie Hirst, Susan Girdwood, Hilary Worgan, Mike Holland, Natalie Meades, Helen McAnulty–Jones, Robert Darby, Rory Geoghegan, Alan Cookson, and Helen Phillips, as well as research staff and fellow PhD students John Tomes, Sarah Davey, Benjamin Hulme, and Josephine Forde–Thomas, for their technical support in areas such as worm collection, sample analyses, bioinformatics, statistics, TEM, and more, throughout my journey.
- The VetHub1 team, including Amanda Gibson, Chelsea Davis, Oktawia Polak, Juan Carlos Cabulao, and Shane Collett, for their kind support in the cell culture laboratory work.
- Dylan Phillips for his expertise in confocal microscopy.
- Our lab group, including Debbie Nash, Nicholas Shorten, Joanna Giles, and Nathan Allen, as well as my parasitology lab mates Holly Marie Northcote and Jacob Leonard, and past BSc and MSc students, for the cherished time we spent together in the lab.
- My dear friends who have provided constant cheer and moral support, including Lai Shu Zhan, Thanyarat, Rawikan, Dilaka, Phuthita, and the Thai ladies in Aberystwyth, for their kind help and support that have made my time in the UK truly wonderful.

Last but certainly not least, I must mention my family, especially my parents and sister, whose unwavering belief in me has kept my spirits high and motivation strong throughout the entire PhD process.

Words cannot fully express my gratitude to each and every one of you.

PUBLICATION LISTS

Wititkornkul, B., Hulme, B.J., Tomes, J.J., Allen, N.R., Davis, C.N., Davey, S.D., Cookson, A.R., Phillips, H.C., Hegarty, M.J., Swain, M.T. and Brophy, P.M., 2021. Evidence of immune modulators in the secretome of the equine tapeworm *Anoplocephala perfoliata*. Pathogens, 10(7), p.912. Available at: https://doi.org/10.3390/pathogens10070912.

Stuart, R.B., Zwaanswijk, S., MacKintosh, N.D., **Witikornkul, B.,** Brophy, P.M. and Morphew, R.M., 2021. The soluble glutathione transferase superfamily: role of Mu class in triclabendazole sulphoxide challenge in *Fasciola hepatica*. Parasitology Research, 120, pp.979-991. Available at: https://doi.org/10.1007/s00436-021-07055-5.

Northcote, H., **Wititkornkul, B**., Cutress, D. J., Allen, N. R., Brophy, P. M., Wonfor, R. E. & Morphew, R. M. (*In Prep*.) 'Dominance of Mu class glutathione transferases within the equine tapeworm *Anoplocephala perfoliata'*. Target Journal: Journal of Proteome Research.

PRESENTATIONS

Title: Polyomics of the neglected equine tapeworm *Anoplocephala perfoliata*. The 65th American Association of Veterinary Parasitologists (AAVP) Annual Meeting. Virtual Meeting. Date: 20th–23rd June 2020.

Title: Control of equine tapeworms through praziquantel: The hidden impact on the equine microbiome. British Society for Parasitology (BSP) Spring Meeting 2022, University of York, United Kingdom. Date: 20th–23rd June 2020.

AWARDS

Title: Polyomics of the neglected equine tapeworm *Anoplocephala perfoliata*. The 65th American Association of Veterinary Parasitologists (AAVP) Annual Meeting. Virtual Meeting. Date: 20th–23rd June 2020. AAVP–Student Poster Presentation Awards: an honourable mention award.

CONTENTS

LIST OF FIGURES

LIST OF TABLES

LIST OF ABBREVIATIONS

Abbreviation	Definition
°C	degrees Celsius
0–3hRP	0–3 hour released preparation
1D SDS–PAGE	One Dimensional Sodium Dodecyl Sulfate–Polyacrylamide Gel Electrophoresis
1DE	1–Dimensional Electrophoresis
3D–SIM	3–dimensional structured illumination microscopy.
A. perfoliata or AP	*Anoplocephala perfoliata*
Abs	Apoptotic bodies/apoptotic blebs
ACN	Acetonitrile
ALIX	ALG–2–interacting protein X
AMBIC	Ammonium bicarbonate
AMPs	Antimicrobial peptides
ANOVA	Analysis of variance
APS	Ammonium persulfate
Arg–1	Arginase 1
BI	Bayesian inference
Bis	Bisacrylamide
BLAST	Basic Local Alignment Search Tool
BLASTp	Protein–protein Basic Local Alignment Search Tool
bp	Base pairs
BW	Body Weight
$Ca(C_2H_3O_2)_2$	Calcium acetate
CAESITEC	Caecum simulation technique
CBSS	Sterile Chernin's balanced salt solution
CD	Cluster of differentiation
cDNA	Complementary deoxyribonucleic acid
CHAPS	3–[(3–cholamidopropyl)dimethylammonio]–1–propanesulfonate
CME	Clathrin–mediated endocytosis
ConA	Concanavalin–A
CstN	Cystatin, papain–like cysteine protease inhibitors
CTCF	Corrected total cell fluorescence
CTD	C–terminal domain
DAPI	4',6–diamidino–2–phenylindole
DC	Differential centrifugation
ddH2O	Double–distilled water
dH2O	Distilled water
disc–UC	Density gradient Centrifugation
DMEM	Dulbecco's Modified Eagle's Medium
DMSO	Dimethyl sulfoxide
DNA	Deoxyribonucleic acid
ds cDNA	Double–stranded Complementary deoxyribonucleic acid
DTT	Dithiothreitol
dUC	Differential Ultracentrifugation
DUSP1	Dual Specificity Phosphatase 1
EDTA	Ethylenediaminetetraacetic acid
EEs	Early endosomes
ELISAs	Enzyme–linked immunosorbent assays
EMCCD	Electron Multiplying Charge–Coupled Device
EQUITEC	Modified RUSITEC for horses
ESI MS/MS	Electrospray mass spectrometry
ESPs	Excretory–Secretory Products
e–value	Expectation–value

Abbreviation	Definition
EVs	Extracellular vesicles
ExPASy	Expert Protein Analysis System
FABPs	Fatty–acid binding proteins
FACS	Fluorescence–activated cell sorting
FEC	Faecal egg count
FFFF	Flow Field–Flow Fractionation
Fg	femtogram, an SI unit of mass equal to 10−15 grams
FOXP3	forkhead box P3
FT–IR	Fourier–transform infrared spectroscopy
GAPDH	glyceraldehyde–3–phosphate dehydrogenase
GC	Gas chromatography
GIT	Gastrointestinal Tract
GO	Gene ontology
GOEA	Gene Ontology terms enrichment analysis
GRP	Glucose–regulated protein
GSTO	Omega–class Glutathione S transferase protein
GSTs	Glutathione S transferase protein
HDMs	Helminth defence molecules
HEPES	N–(2–Hydroxyethyl)piperazine–N'–(2–ethanesulfonic acid)
HF	Hydatid Fluid
HFD	Hydrostatic Filtration Dialysis
HSPs	Heat shock proteins
HUVECs	Human umbilical vein endothelial cells
IAA	Iodoacetic acid
IEF	Isoelectric Focusing
IFN–γ	Interferon gamma
IgG	Immunoglobulin G
IL	Interleukin
IL1RL1	Interleukin 1 Receptor Like 1
ILCs	Innate lymphoid cells
ILVs	Intraluminal vesicles
iNOS	Inducible nitric oxide synthase
IRF5	Interferon Regulatory Factor 5
IRF–5	Interferon regulatory factor 5
L	Larva
LC MS/MS	Liquid Chromatography–Tandem–Mass–Spectrometry
LEs	Late endosomes
LMW	Low Molecular Weight
LPS	Lipopolysaccharides
LRR1	Leucine–rich repeat 1
LVC	Left ventral colon
M	Molar
MALDI–TOF/TOF–MS/MS	Matrix–Assisted Laser Desorption/Ionization Time–of–Flight Mass Spectrometry
MCMC	Multi–chain Markov chain Monte Carlo
mBMDMs	Murine bone marrow–derived macrophages
MDR:TAP	ATP binding cassette subfamily B
MEGA	Molecular Evolutionary Genetics Analysis
$MgSO_4$	Magnesium sulphate
MHC	Major histocompatibility complex
miRNA	Small non–coding RNAs
mL	Millilitre
ML	Maximum likelihood
mm	millimetre
mM	Millimolar

Abbreviation	Definition
moDCs	Human monocyte–derived dendritic cells
MODE–K cells	Mouse small intestinal epithelial cells
mRNA	Messenger RNA
MTT	3–(4,5–dimethylthiazol–2–yl)–2,5–diphenyl–2H–tetrazolium bromide
MVB	Multivesicular body
MVs	Shedding microvesicles (SMVs) or ectosomes
MW	Molecular Weight
MyD88	Myeloid differentiation primary response 88
NanoESI–QqTOF–MS	Nano electrospray hybrid quadrupole–time of flight mass spectrometry
Nano–LC–MS/MS	Nanoscale capillary Liquid chromatography–tandem–mass spectrometry
NBL	New born larvae
NCBI	National Center for Biotechnology Information
NF–κB	Nuclear factor kappa–beta
NGS	Next generation sequencing
nm	Nanometre
NO	Nitric oxide
NTA	Nanoparticle tracking analysis
NTD	N–terminal domain
OTUs	Operational taxonomic units
PBMCs	Sheep peripheral blood mononuclear cells
PBS	Phosphate–buffered saline
PCA	Principal component analysis
PCR	Polymerase chain reaction
PEG	Polyethylene Glycol
PFA	Paraformaldehyde
PM	Plasma membrane
PZQ	Praziquantel
RDC	Right dorsal colon
RefSeq	Reference Sequence
RELMα	Resistin–like molecule alpha
RIN	Ribonucleic acid Integrity Number
RPMI	Roswell Park Memorial Institute
RNA	Ribonucleic acid
RNase	Ribonuclease
RNA–seq	Ribonucleic acid–sequencing
rRNA	Ribosomal Ribonucleic acid
RT–PCR	Quantitative polymerase chain reaction
RUSITEC	Rumen simulation technique
RVC	Right ventral colon
SC	Small colon
SCFAs	Short–chain fatty acids
SDCBP	Syndecan Binding Protein
SEC	Size exclusion chromatography
sELISA	Sandwich enzyme–linked immunosorbent assay
Shotgun–LC–MS/MS	shotgun liquid chromatography tandem–mass spectrometry
sMB–R	Secreted midbody remnant
Sp1	Primary Sporocyst
TAE	Tris Acetate Ethylenediaminetetraacetic acid
TBE	Tris Borate Ethylenediaminetetraacetic acid
tBLASTn	Search translated nucleotide databases using a protein query
TCA	Trichloroacetic Acid
TEM	Transmission electron microscopy
TEMED	Tetramethylethylenediamine
TGF–β	Transforming growth factor beta

Abbreviation	Definition
Th	T helper cells
Th1	T helper 1–type immune response
Th2	T helper 2–type immune response
TLR	Toll–like receptor
TNF–α	Tumour necrosis factor
TOF–MS	Time–of–flight mass spectrometry
Tregs	Regulatory T cells
TRFLP	Terminal restriction fragment length polymorphism
Tris–HCl	Tris(hydroxymethyl)aminomethane hydrochloride
TRPS	Tunable Resistive Pulse Sensing
TSP	Tetraspanin
UF	Ultrafiltration
UV	Ultraviolet
V	Voltage
VFAs	Volatile fatty acids
VOC	The volatile organic compound
WDFY3	WD repeat and FYVE domain–containing protein 3
βME	Beta–mercaptoethanol
µg	Microgram
µL	Microlitre

ABSTRACT

The equine tapeworm, *Anoplocephala perfoliata,* is the principal tapeworm species commonly infecting horses worldwide. Clusters of *A. perfoliata* are found primarily attached to the caecal wall, close to the ileocaecal valve. A light infection is often asymptomatic, whereas a severe infection from large clusters of *A. perfoliata* is likely to cause significant damage and dysfunction at the site of attachment and has been linked to colic. Given a status as a neglected helminth, many aspects of the fundamental biology, such as understanding of *A. perfoliata* infection and its interaction with the digestive physiology and health of its host, have yet to be thoroughly researched.

In the current thesis, I have generated molecular tools using a polyomic approach, transcriptomics and proteomics, supported with bioinformatics to explore *A. perfoliata*. In doing so, this work has successfully generated the first *de novo* assembled transcriptome for adult *A. perfoliata* providing an in–depth insight into the parasites fundamental biology. Transcriptomic analysis revealed various key sequences likely expressed as proteins potentially involved in host–parasite interactions including glutathione transferases (both Sigma and Omega classes), Heat shock protein 90 alpha and alpha–Enolase.

During infection, helminths secrete excretory–secretory products (ESPs), designated as the secretome, into the host environment. Of note are the extracellular vesicles (EVs) which are secreted as part of this secretome and are likely involved in cell–cell communication and host–parasite interactions. Given this, I first confirmed that EVs are secreted within *A. perfoliata* secretome during *in vitro* maintenance; these EVs were purified using size exclusion chromatography (SEC). Furthermore, I present the first analysis into the *A. perfoliata* secretome using GeLC (for whole EVs and EV depleted ESPs>10 kDa) and Gel free (for EV surface shaves) proteomic approaches supported by the newly developed *A. perfoliata* transcriptome. EV proteomic profiles resolved contained known EV biomarkers (i.e. annexins and tetraspanins) alongside putative immune modulators highlighting EVs secreted into the host environment as likely capable of interacting directly or indirectly with the host.

I further investigated *A. perfoliata* EV interaction with mammalian host cells, including EV uptake (confocal and flow cytometry analyses), cell viability (trypan blue, MTT assays and

flow cytometry) and cytokine secretion (Milliplex) after THP–1 cells were exposed to EVs. This study demonstrated that *A. perfoliata* EVs are taken up by mammalian cells and have immune modulatory activities and functions, primarily stimulating a Th1–driven immune response.

The current thesis also includes a praziquantel (PZQ)–equine hindgut microbiome interaction study, examining the effect of PZQ on the equine gut microbiome in *in vitro* hindgut microbial fermentation model over 72 hours. Results demonstrated PZQ at any dosage seems unlikely to have widespread changes on the overall equine hindgut microbiome. However, PZQ at a higher than recommended dose may alter the fermentation pathways in the equine hindgut, which could impact on the nutritional function of the caecum.

All discoveries from the current research have uncovered many aspects of *A. perfoliata* fundamental biology including the dataset of *A. perfoliata* transcriptome and proteomics of the secretome, key secretory proteins and potential immune modulators. In conjunction with the establishment of an interaction between EVs and mammalian immune cells, this thesis provides a basis for the further study into the host–parasite interaction. Furthermore, my investigation into the interaction between PZQ and the equine hindgut microbiome gives further insight into the impact of parasite treatment methods on the host hindgut microbiome and nutritional functioning. The comprehensive data generated from my research serve as a foundation for future studies, mainly aiming to advance my understanding of this infection. Furthermore, this knowledge holds the potential to drive the creation of efficacious strategies for further diagnosis, treatment, and prevention of *A. perfoliata* infections.

CHAPTER 1:

INTRODUCTION

1.1 EQUINE TAPEWORMS

1.1.1 Basic biology

The equine tapeworms are classified in the order Cyclophyllidea, the family Anoplocephalidae and genus *Anoplocephala.* Horses and donkeys are commonly infected with three species of tapeworm, including *Anoplocephala perfoliata* (Goeze, 1782) (Lee & Tatchell, 1964), *Anoplocephala magna* (Abildgaard, 1789) and *Anoplocephaloides mamillana* (formerly *Paranoplocephala mamillana)* (Mehlis, 1831). Among these three equine tapeworm species, *A. perfoliata* is the most prevalent that infect horses worldwide followed by *A. magna*, and less commonly, *A. mammilana* (Gasser *et al.*, 2005; Nielsen, 2016). The morphological characteristics and location in the gastrointestinal tract (GIT) of the host differs between species (Figure 1.1A–B and Table 1.1) (Gasser *et al.*, 2005; Walden *et al.*, 2014; Nielsen, 2016).

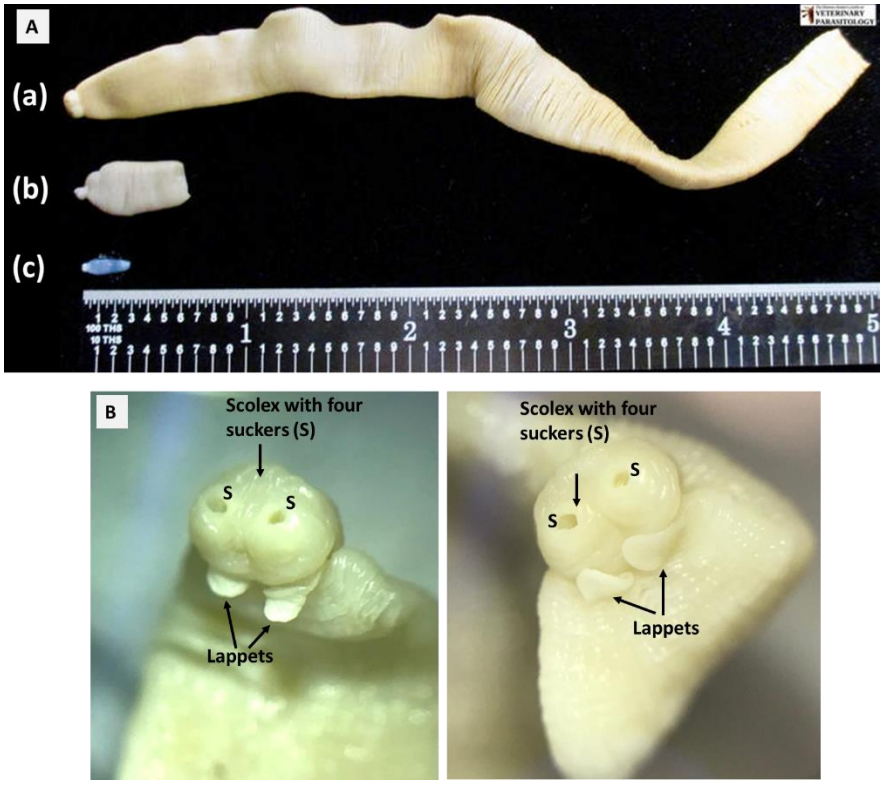

Figure 1.1 Adult equine tapeworm (A) Three adult equine tapeworm species: (a) *Anoplocephala magna*, (b) *Anoplocephala perfoliata* and (c) *Anoplocephala mamillana* (B) Scolex of adult *Anoplocephala perfoliata*, demonstrating four forward–pointing suckers (S), with a backward–pointing lappet behind each (showing 2 of 4 lappets) (The Monster Hunter's Guide to Veterinary Parasitology, 2018) (Photographer: Holly Northcote, 2022 used with permission).

Table 1.1 Comparison of the morphological characteristics of three adult *Anoplocephala* species (Adapted from Gasser et al., 2005; Walden et al., 2014; Nielsen, 2016).

Species	*A. perfoliata*	*A. magna*	*A. mamillana*
Host	Horses and donkeys	Horses and donkeys	Horses
Location	ileum & adjacent large intestine, adjacent to the ileo–caecal valve	Posterior small intestine; Jejunum & occasionally in the stomach	Anterior small intestine; mainly jejunum & ileum & occasionally in the stomach
Length of gravid adult specimens	2.5–40 mm, up to 80 mm	up to 80 cm	6–50 mm
Width of the body	9–15 mm	25 mm	4–6 mm
Scolex, muscular suckers	4 no rostellum or hooks, round suckers	4 4 to 6 mm wide no rostellum or hooks	4 slit–like, point dorsally & ventrally
Lappets	4 ear–shaped lappets, 0.5 to 1.0 mm, posterior to muscular suckers	No	No
Mature eggs	~65–80 µm in diameter	~50–60 µm in diameter	~37 x 51 µm

1.1.2 Life cycle

The life cycle of *A. perfoliata* (Figure 1.2) is indirect with horses as the definitive hosts and free–living oribatid mites as the intermediate hosts (Pashkirova, 1941; Denegri, 1993). There are numerous species of oribatid mites, around 20 species are considered potential vectors of anoplocephalid infections in animals (Denegri, 1993; Michael McAloon, 2004; Shimano, 2004; Tomczuk *et al.*, 2015). In infected horses, common species of oribatid mites have been reported, including *Achipteria* spp., *Carabodes* spp., *Ceratozetes bulanovae, Eremaeus oblongus, Galumna dimofica*, *G. nervosus, G. obvius, Hermanniella granulata*, *Liacaruss* spp., *Liebstadia similis*, *Parachipteria punctata, Platynothrus peltifer, Scheloribates laevigatus*, *S. latipes, Scheloribates* spp., *Trichoribates incisellus, Urubambates schachtachtinskoi*, *Zygoribatula microporosa* (Denegri, 1993). Pastures with higher humidity and moderate temperatures are known to harbour a greater number of mites in anoplocephalid infections (GergóCS *et al.*, 2011).

In the GIT of infected horses, cysticercoids develop into adult *A. perfoliata* and attach on the intestinal mucosa of the small intestine, colon and caecum, particularly at the ileocaecal region and the caecal wall (Slocombe, 1979; Lyons *et al.*, 1987; Fogarty *et al.*, 1994; Williamson *et al.*, 1997). The strobila of immature *A. perfoliata* are lance–shaped–like (Figure 1.3–A). Once

proglottids (gravid segments; Figure 1.3–B) of adult *A. perfoliata* are mature, a large number of tapeworm eggs are released and passed out in faeces where oribatid mites within the pasture are infected by the ingestion of faecal tapeworm eggs. Cysticercoids continue to develop into larvae in the body cavity of oribatid mites. Finally, ingestion of infected mites by horses during grazing begins the new life cycle of *A. perfoliata* (Gasser *et al.*, 2005; Nielsen, 2016). During the pre–patent period, the tapeworm larvae undergo various stages of development to the development of adult tapeworms within the host's digestive system, which takes approximately 6–14 weeks (Bain & Kelly, 1977; Bucknell et al., 1995). Once they mature into adult tapeworms, they attach themselves to the intestinal wall and start releasing eggs, which can be detected in the host's faeces (Bain & Kelly, 1977; Bucknell et al., 1995).

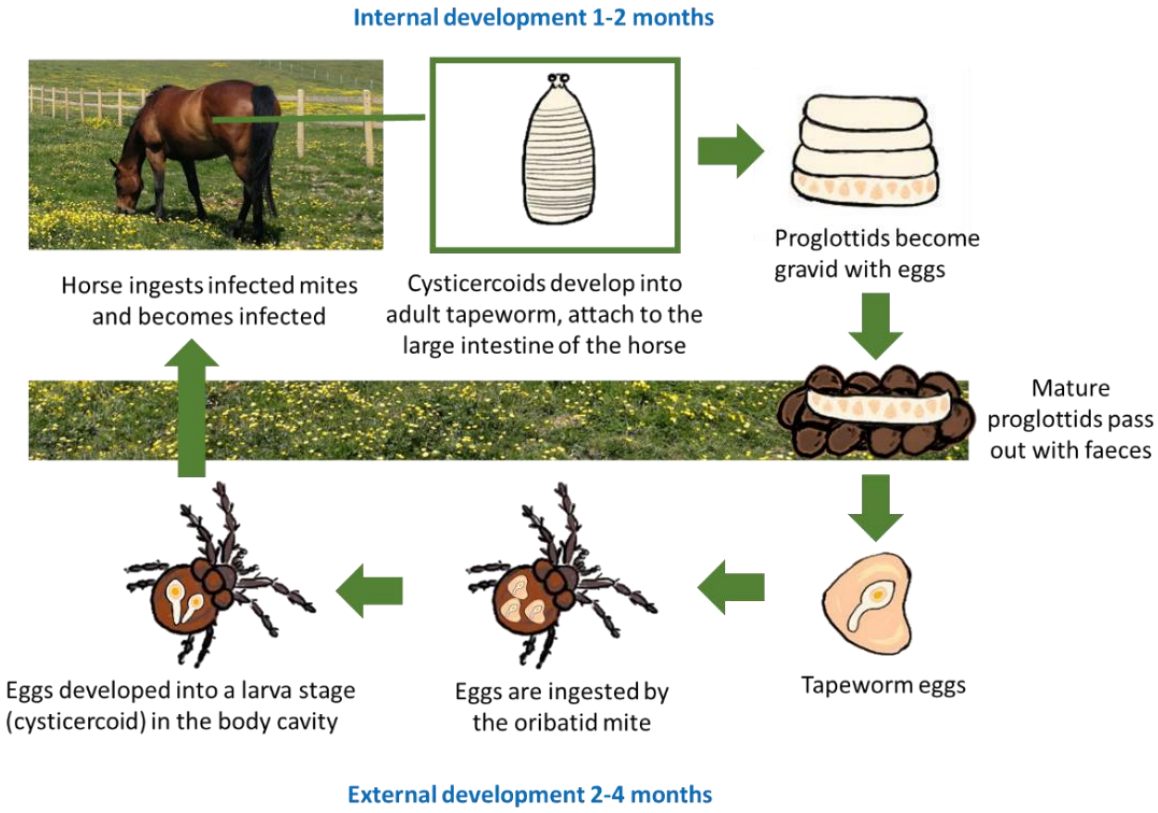

Figure 1.2 The life cycle of an equine tapeworm begins when mature proglottids (containing tapeworm eggs) of adult tapeworm pass out in faeces. These eggs are ingested by the oribatid mite (an intermediate host) and developed into a larva stage (cysticercoid) in the body cavity. Horse ingests infected mites and becomes infected. Cysticercoids develop and attach to the large intestine of the horse, particularly at the ileocaecal junction. Once proglottids of mature tapeworms becomes gravid with eggs, they are released with the host faeces (Photographer: Boontarikaan Wititkornkul, 2019).

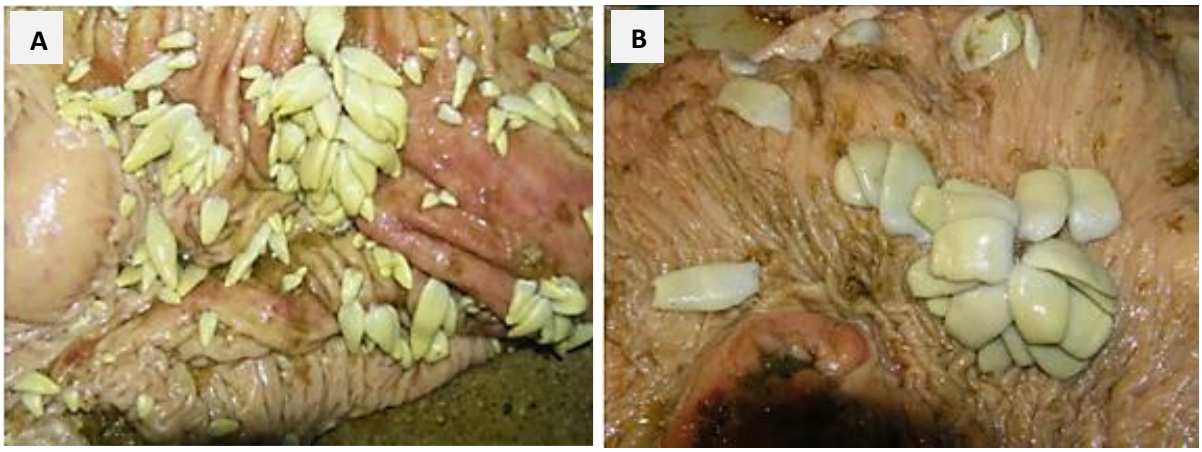

Figure 1.3 The period of invasion of *A. perfoliata* (A) Lance–shaped–like strobila of immature *A. perfoliata* during the prepatent period of invasion (B) Tapeworms with gravid segments during the patent period (Tomczuk et al., 2014).

1.1.3 Prevalence of infection

The prevalence and distribution of *A. perfoliata* infection can be influenced by various factors (Denegri, 1993; Rehbein *et al.*, 2013; Tomczuk *et al.*, 2017). Particularly, the presence of oribatid mites in the environment as these mites are involved in pedogenesis as intermediate hosts in the lifecycle (Denegri, 1993; Shimano, 2004; Tomczuk *et al.*, 2015). The geographical distribution and climate also play a crucial role in the transmission of diseases. In European countries, different zones can have different invasion dynamics of *A. perfoliata* infection in horses in different seasons (Rehbein *et al.*, 2013; Tomczuk *et al.*, 2015). Countries in Eastern, Western or Southern Europe, such as Germany (Rehbein *et al.*, 2013) and Spain (Meana *et al.*, 2005), have a high prevalence of infection during autumn and winter rather than in spring and summer (Meana *et al.*, 1998, 2005; Rehbein *et al.*, 2013). Meanwhile, prevalence in European countries with a maritime climate, such as the Netherlands and Denmark, remains more consistent throughout the year (Meana *et al.*, 1998). This discrepancy is primarily influenced by the climate conditions, characterised by early and prolonged winters, which directly impact the seasonality of *A. perfoliata* infections due to the presence of prepatent and patent periods of the invasion stages within a particular year (Tomczuk *et al.*, 2015). Additionally, Meana *et al.* (2005) concluded that *A. perfoliata* show an infection pattern of having only one generation per year with a marked dependence on humidity, which is in contrasts to *A. magna*, whose infection is detected throughout the year with higher prevalence during autumn.

The prevalence of *A. perfoliata* infection in equids can be determined by faecal examination, serological assays and necropsy, the most reliable technique being necropsy (Gasser *et al.*, 2005). From 2010 onwards, the reported prevalence of *A. perfoliata* has varied between 2.0–75.7% in horses (Tavassoli *et al.*, 2010; Hinney *et al.*, 2011; Zerihun *et al.*, 2011; Rehbein *et al.*, 2013; Pittaway *et al.*, 2014; Tomczuk *et al.*, 2015, 2017; Lyons *et al.*, 2018; Hreinsdóttir *et al.*, 2019; Gehlen *et al.*, 2020; Jürgenschellert *et al.*, 2020; Sallé *et al.*, 2020; Mathewos *et al.*, 2021; Roba and Hiko, 2022) and 0.4–34% in donkeys (Getachew *et al.*, 2010, 2012; Zerihun *et al.*, 2011; Matthews and Burden, 2013; Fesseha *et al.*, 2022; Roba and Hiko, 2022) around the world, with different diagnostic techniques and distribution in a range of different countries and geographic regions.

1.1.4 Pathology changes

Tapeworms attach throughout the hindgut, and primarily at the small intestine, colon and caecum (Slocombe, 1979). The proportion of *A. perfoliata* between 2 common attachment sites was greater at the caecal wall (81.1–91%) than at the ileocaecal region (17–53%) (Fogarty *et al.*, 1994; Williamson *et al.*, 1997). However, large clusters of *A. perfoliata* are found mostly at the ileocaecal valve (Williamson *et al.*, 1997) (Figure 1.4 and 1.5). The severity of histological and pathological changes at the attachment site is proportional to the number of worms (Figure 1.6) (Fogarty *et al.*, 1994). A particular number of *A. perfoliata* at the attachment site can cause various pathological changes of the GIT mucosa and submucosa including irritation, thickening, hyperaemia, oedema, necrotic ulceration, diphtheresis and eosinophil infiltration (Figure 1.6) (Barclay *et al.*, 1982; Pearson *et al.*, 1993; Fogarty *et al.*, 1994; Williamson *et al.*, 1997; Pavone *et al.*, 2011; Hreinsdóttir *et al.*, 2019; Lawson *et al.*, 2019). Ulceration tends to be found in light infections with less than 20 tapeworms on both attachment sites of the caecal wall and the ileocaecal region (Figure 1.4 and 1.5). Furthermore, mucosal thickening and ulceration with diphtheresis can be found in horses infected with more than 21 tapeworms (Figure 1.4 and 1.5) (Pearson *et al.*, 1993; Fogarty *et al.*, 1994). The severity of symptoms is increased in burdens of over 100 tapeworms at the ileocecal junction (Pearson *et al.*, 1993), whereby attachment of *A. perfoliata* can cause circular muscle layer hypertrophy and damage to the enteric nervous system of the GIT (Pavone *et al.*, 2011).

Figure 1.4 Large clusters of adult *Anoplocephala perfoliata* attach to the caecal mucosal membrane adjacent to the ileocecal valve (arrow) (Photographer: Boontarikaan Wititkornkul, 2019).

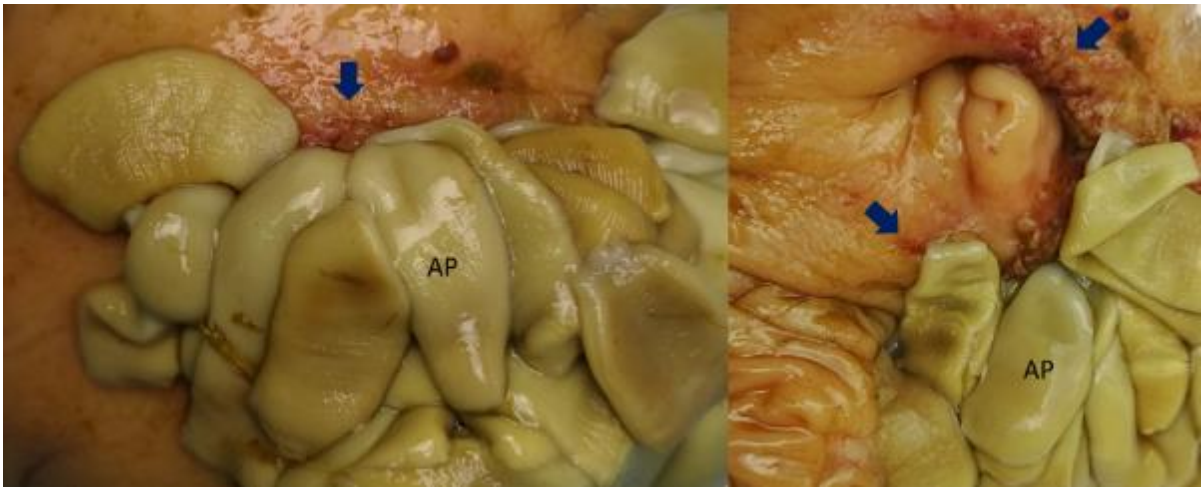

Figure 1.5 Adult *Anoplocephala perfoliata* (AP) in a naturally infected horse, attached to the caecal mucosal membrane resulting in pathological changes at the attachment site such as hyperaemia and ulceration (arrow) (Photographer: Boontarikaan Wititkornkul, 2019).

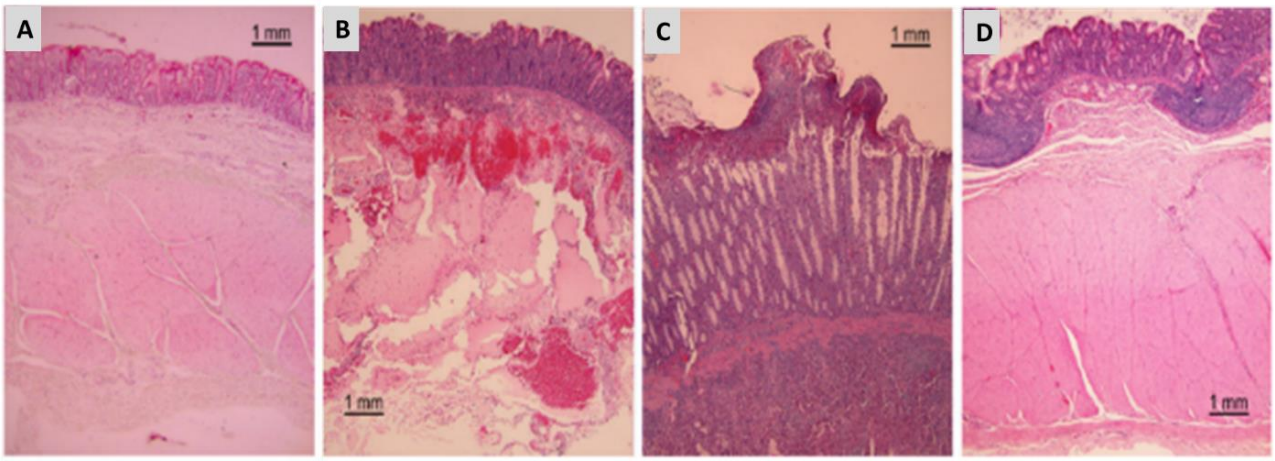

Figure 1.6 A representative of a histological section of a caecall wall of a horse close to the site of *A. perfoliata* attachment and without *A. perfoliata* infection, at x40 magnification, (A) non *A. perfoliata*–infected horse showing the entire thickness of the caecal mucosa. (B) an early infection showing an inflamed area of caecal wall with some hyperplasia of the epithelium, eosinophils and lymphocyte infiltrations in the lamina propria and submucosa. (C) the late summer phase of the infection (only the mucosa and submucosa fit within the frame) showing the marked hyperplasia of all tissue layers of the caecal mucosa, with increased goblet cells and necrosis of the superficial epithelial layers, extensive eosinophils and lymphoid cells infiltration of the submucosa. (D) a late–stage infection showing less severe hyperplasia of the mucous membrane, with eosinophils, leucocytes and lymphoid follicle infiltration in the submucosa, markedly hyperplastic muscular layer (Lawson *et al.*, 2019).

1.1.5 Clinical signs

Clinical tapeworm infections range from acute to chronic symptoms such as anorexia, weight loss, dull hair coats, malnutrition, abdominal pain or discomfort from GIT disturbance, anaemia and decreased performance (Gasser *et al.*, 2005; Nielsen, 2016), although infection can be harmless in small infection burdens. An acute tapeworm infection may also be asymptomatic (Gasser *et al.*, 2005; Nielsen, 2016). Chronic tapeworm infection is associated with severe GIT health problems (Gasser *et al.*, 2005), and can cause various types of colic such as, spasmodic colic and ileal impaction colic, particularly at the ileocecal region (Proudman and Edwards, 1993; Proudman *et al.*, 1998; Proudman and Trees, 1999; Boswinkel and Sloet van Oldruitenborgh-Oosterbaan, 2007; Back *et al.*, 2013), ileocaecal or caeco–caecal intussusception (Barclay *et al.*, 1982; Beroza *et al.*, 1986; Cosgrove *et al.*, 1986; Edwards, 1986; Owen *et al.*, 1989; Mezerova *et al.*, 2007), caecal perforation and peritonitis (Barclay *et al.*, 1982; Beroza, 1983; Beroza *et al.*, 1986; Mezerova *et al.*, 2007), caecal rupture (Ryu *et al.*, 2001) and intestinal obstruction by large clustering of tapeworms (Slocombe, 1979; Beroza,

1983; Carmel, 1988). In spite of the importance of understanding the impact of tapeworms on the host for effective horse health management, few studies have quantified their effect on the host, highlighting a crucial research gap (Lawson *et al.*, 2019; Slater *et al.*, 2021).

1.1.6 Diagnosis

Adult equine tapeworms can be found in the GIT during a post–mortem examination, despite an absence of clinical signs in the live animal (Proudman and Trees, 1999). The conventional routine diagnostic technique is faecal egg counting for the detection of characteristic D–shaped tapeworm eggs (Figure 1.7) via coprological methods (sensitivity 7.4–61%), including the simple flotation of *A. perfoliata* eggs and McMaster using a counting chamber (sensitivity 16.7%) and sedimentation methods (sensitivity 8.3%) (Proudman and Edwards, 1992; Nilsson *et al.*, 1995; Meana *et al.*, 1998; Williamson *et al.*, 1998; Bohórquez *et al.*, 2014; Tomczuk *et al.*, 2014; Hreinsdóttir *et al.*, 2019). However, both techniques differ in their principles and procedures.

Relying on a single timed faecal examination may not consistently provide an effective and sufficient diagnostic result, especially when dealing with light tapeworm infections where the number of tapeworms is less than 100 (Boswinkel and Sloet van Oldruitenborgh-Oosterbaan, 2007; Nielsen, 2016). This is because tapeworm eggs are released intermittently during the patent period, making their detection in a single examination challenging (Meana et al., 1998; Gasser *et al*., 2005; Nielsen, 2016). Moreover, the simple flotation method may not be adequate for detecting tapeworm eggs as they may not float properly (Hreinsdóttir *et al.*, 2019). Thus, to enhance the accuracy of diagnosis up to a sensitivity ranging from 61% to 97.3% and specificity of 98%, a combination and modification of coprological techniques, such as centrifugation, flotation, and sedimentation, have been applied (Proudman and Edwards, 1992; Meana *et al.*, 1998; Traversa *et al.*, 2008; Rehbein *et al.*, 2011; Back *et al.*, 2013; Norris *et al.*, 2018). Additionally, commercially available products like the Mini–FLOTAC® technique have been utilised to improve diagnostic capabilities (Boelow *et al.*, 2022).

Figure 1.7 Eggs of *Anoplocephala perfoliata* with the characteristic pyriform apparatus (oncosphere) containing the hexacanth embryo. A) The typical crest is seen when focusing on the external features of the egg, B) the D–shaped tapeworm eggs found during faecal examination (Nielsen, 2016).

Alternatively, immunological and molecular diagnostic tools have also been developed to enhance the accuracy and reliability of tapeworm diagnosis, e.g. various immunological techniques such as enzyme–linked immunosorbent assays (ELISAs)–based on faecal or serum samples (Höglund *et al.*, 1995; Proudman and Trees, 1996; Proudman and Holdstock, 2000; Kjaer *et al.*, 2007; Abbott *et al.*, 2008; Traversa *et al.*, 2008; Bohórquez *et al.*, 2012; Back *et al.*, 2013; Pittaway *et al.*, 2014; Gehlen *et al.*, 2020; Jürgenschellert *et al.*, 2020). For example, the potential and non–invasive diagnostic ELISA–based techniques such as coproantigen ELISAs (with a sensitivity of 74% and specificity of 92%) (Kania and Reinemeyer, 2005; Skotarek *et al.*, 2010), and a commercially available saliva–based diagnostic test called EquiSal® Tapeworm test (with a sensitivity of 83% and specificity of 85%) (Lightbody *et al.*, 2016, 2018; Jürgenschellert *et al.*, 2020). Furthermore, molecular diagnostic tools such as Polymerase Chain Reaction (PCR)–based assays are commonly used in research and farm–level settings to detect and amplify specific DNA sequences (Bracken *et al.*, 2012; Baltrušis *et al.*, 2019; Baltrušis and Höglund, 2023; Jawad and Alfatlawi, 2023). It is particularly useful in studying *A. perfoliata* infection, as PCR–based assays can provide detailed information about the presence and abundance of the *A. perfoliata* in samples such as faeces or serum (Drogemuller et al., 2004; Bohórquez et al., 2015; Gehlen et al., 2020). This method allows for accurate identification and characterisation of *A. perfoliata*, contributing to a better understanding of the parasite and facilitating effective control strategies (Drogemuller *et al.*, 2004; Bohórquez *et al.*, 2015; Gehlen *et al.*, 2020).

1.1.7 Treatment and control

Anthelmintics available for *A. perfoliata* treatment and control are primarily limited to praziquantel (PZQ) and pyrantel, mainly as a pamoate salt. PZQ is the anthelmintic of choice for *A. perfoliata* treatment, with various PZQ oral formulations in paste, gel, suspension and tablet forms as a single administration (Lyons *et al.*, 1995; Roelfstra *et al.*, 2006; Slocombe, 2006; Slocombe *et al.*, 2007; Getachew *et al.*, 2013). Moreover, PZQ at a dosage between 1.0 and 2.5 mg/kg BW has been shown to reduce *A. perfoliata* faecal egg counts in naturally infected horses, with an efficacy of 90 to 100% (Grubbs *et al.*, 2003; Holm-Martin *et al.*, 2005; Slocombe, 2006; Rehbein *et al.*, 2007; Slocombe *et al.*, 2007; Getachew *et al.*, 2013; Lyons *et al.*, 2017). Pyrantel pamoate is also recommended for treatment of *A. perfoliata* at double the dosage of the therapeutic dose for nematodes at 13.2 mg/kg BW (Slocombe, 1979; Craig *et al.*, 2003) which provides 97.8%–99 reduction of the tapeworms and with no adverse effects under field use conditions (Slocombe, 1979; Craig *et al.*, 2003; Marchiondo *et al.*, 2006; Jürgenschellert *et al.*, 2020).

To date, anthelmintic resistance is a growing concern in equine parasite management. However, no resistance to either PZQ (Rehbein *et al.*, 2007; Elsener and Villeneuve, 2011; Lyons *et al.*, 2017) or pyrantel pamoate in equine tapeworm has been reported (Lyons et al., 2017). However, this is most likely associated with unremarkable clinical signs in infected horses (Proudman and Trees, 1999). Hence, it is crucial to follow the recommended dosing guidelines and consult a veterinarian when administering PZQ to horses to ensure both effective treatment and the reduction of the risk of drug resistance. Recently, Nielsen, (2023) reported the failure of PZQ (23.5%) and pyrantel pamoate (50.9%) to eliminate anoplocephalid eggs in tapeworm–positive yearlings and mares, as evidenced by mean Faecal Egg Count Reductions (FECRs) test from Thoroughbred horses in Central Kentucky. The potential decrease in effectiveness of both anthelmintics raises concerns regarding the development of anthelmintic resistance, emphasising the necessity for alternative treatment options and enhanced methods for assessing treatment efficacy (Nielsen, 2023).

1.1.8 Praziquantel: Battling *Anoplocephala perfoliata* Infections

PZQ, a broad–spectrum anthelmintic, belongs to the class of pyrazine–isoquinoline derivatives, widely recognised as a potent anti–trematodes and cestodes agent (Andrews *et al.*, 1983; Andrews, 1985; Redman *et al.*, 1996; Chai, 2013). PZQ is readily absorbed from the GIT in experimental animals and humans, with an absorption rate of approximately 75–100%. PZQ is distributed throughout the body, then disrupt the outer layer of tapeworm integument through a calcium influx mechanism (Greenberg, 2005; Alsaqabi, 2014; Thomas and Timson, 2018; S.-K. Park *et al.*, 2021; Nogueira *et al.*, 2022). This results in muscle spasms and paralysis of the worms, leading to natural detachment from the intestinal wall and eventual elimination in the faeces (Greenberg, 2005; Alsaqabi, 2014; Thomas and Timson, 2018; S.-K. Park *et al.*, 2021; Nogueira *et al.*, 2022). PZQ is metabolised in the liver, and excreted primarily through the bile into the faeces, where an unchanged PZQ is excreted in the urine, with a relatively short elimination half–life (1–1.5 hours), and more than 80% is completed after 24 hours (Steiner *et al.*, 1976).

At the recommended dosage, in field conditions, most studies have consistently reported no adverse reactions, including clinical or neurological signs, associated with PZQ treatment (Grubbs *et al.*, 2003; Marley *et al.*, 2004; Holm-Martin *et al.*, 2005; Slocombe *et al.*, 2007; Getachew *et al.*, 2013). However, growing awareness of PZQ's efficacy and resistance is driving the demand for improved *A. perfoliata* infection management strategies. Consequently, ongoing research on long–term effects of PZQ on horse health is essential to comprehensively investigate. Particularly noteworthy is the fact that *A. perfoliata* shares its habitat with the host gut microbiome (Slater *et al.*, 2021). Moreover, our understanding of the interplay between *A. perfoliata*, PZQ, and the horse's gut microbiome remains relatively understudied (Slater *et al.*, 2021). Thus, exploring this interaction can provide insights into how PZQ influences the composition and function of the gut microbiota, ultimately leading to more refined treatment strategies and minimised unintended consequences.

1.2 HELMINTH SECRETOMES

1.2.1 Introduction to Excretory–Secretory Products (ESPs)

Excretory–secretory products (ESPs), or the secretome, are secreted by live parasitic helminths during infection from different excretory or secretory organs such as the digestive tract, reproductive organs, the cuticular/ tegmental surface, or through specialised structures (Rhoads, 1981; Maizels *et al.*, 1982; Lightowlers and Rickard, 1988). For example, *Schistosoma mansoni* cercariae secrete ESPs from the acetabular and head glands to facilitate entry into the host via direct skin penetration (Curwen *et al.*, 2006; Paveley *et al.*, 2009; Wilson, 2012). Various studies of ESPs in nematodes (Wang *et al.*, 2017; Wangchuk *et al.*, 2019; Grzelak *et al.*, 2020), trematodes (Liu *et al.*, 2009; Robinson *et al.*, 2009; Morphew *et al.*, 2011; Marcilla *et al.*, 2012; Sotillo *et al.*, 2019) and cestodes (Victor *et al.*, 2012; Wang *et al.*, 2015; Bień *et al.*, 2016; Vendelova *et al.*, 2016; Pan *et al.*, 2017; Hautala *et al.*, 2022), have demonstrated that helminth ESPs derived from *in vitro* culture contain a variety of molecules with various functions, such as nucleic acids, soluble proteins, glycoproteins, carbohydrates and lipids and metabolites.

Given their size, helminths cannot prevent host immune attack while living in the host habitat. Thus, strategies to modulate these immune responses are required. Therefore, many ESPs assist helminths in development, penetration of host defensive barriers, reduction of oxidative stress, and avoidance of the host immune system (Gillis-Germitsch *et al.*, 2021). Additionally, they are well–known to have significant immunomodulatory effects on the host immune system, allowing parasitic helminths to survive for extended periods in their host environment (Harnett, 2014; Kobpornchai *et al.*, 2020).

1.2.2 Preparation and characterisation of ESPs

The common method employed for collecting helminths ESPs is *in vitro* culture of live helminths in tissue culture medium (Table 1.2), supplemented with essential nutrients as a source of energy, antimicrobial and antifungal drugs and buffering agents to represent the host intestinal environment (Li *et al.*, 2020). The procedure for *in vitro* culture differs depending on the helminth species, stage of life–cycle and viability in culture system. For example, the majority of proteins in *S. mansoni* cercaria ESPs are released within the first three hours after transformation, termed 0–3 hour released preparation (0–3hRP),

representing the first parasite–derived molecules encountered by innate immune cells in the skin (Jenkins *et al.*, 2005).

Helminths have complex life cycles and this, along with differences in sex, result in a greater range and unique ESP components at certain life stages which are excreted/secreted to the host. Furthermore, these different ESP components will also elicit a variety of immunological responses from the host (Stirewalt, 1963; Lightowlers and Rickard, 1988; Wang *et al.*, 2013; Maruszewska-Cheruiyot *et al.*, 2021; Kenney *et al.*, 2022). Characterisation of key secretory proteins in ESPs is therefore important to gain an in–depth understanding of the complex mechanisms occurring at the host–parasite interface. Proteomics approaches based on mass spectrometry (MS) have become widely used to identify the protein components of ESPs, and undertake structural analyse of endogenous protein complexes (Han *et al.*, 2008; Rogawski and Sharon, 2022). In helminths, various mass spectrometry techniques have been employed for ESP analysis as shown in Table 1.2. Furthermore, genomics, transcriptomics, immunoproteomics, and bioinformatics combined with the proteomics approach have been employed for the functional characterisation of molecules in ESPs, which enhancing an improved ESPs profiling (Robinson *et al.*, 2009; Pan *et al.*, 2014; Wang *et al.*, 2017; Grzelak *et al.*, 2020; Gillis-Germitsch *et al.*, 2021; Chen *et al.*, 2022).

Table 1.2 Example of representative helminths Excretory–Secretory Products (ESPs) which have been characterised using a proteomics approach based on mass spectrometry.

Phylum	Species	Stage	Culture medium & conditions	MS/MS techniques	References
Nematode	*Angiostrongylus cantonensis*	L3, Young adult	RPMI, 24–96h, 37°C, 5% CO_2	LC–MS/MS	Chen *et al.* (2019)
	Angiostrongylus vasorum	Adult: M/F	RPMI, 24h, 37°C, 5% CO_2	LC–MS/MS	Gillis-Germitsch *et al.* (2021)
	Heligmosomoides polygyrus bakeri	L4: M/F	RPMI, 600 larvae/mL, 72h, 37°C	LC–MS/MS	Maruszewska-Cheruiyot *et al.* (2021)
	Haemonchus contortus	L3, L4, Adult: M/F	RPMI, 30,000 L3, 100 L4, 30 Af, 2 Am worms/10 mL, 12h, 37°C, 10% v/v CO_2	High throughput LC–MS/MS	Wang *et al.* (2019)
	Nippostrongylus brasiliensis	Adult	PBS, 100 worms/well/10 mL, 72h, 37°C, 5% CO_2	GC–MS & LC–MS/MS	Wangchuk *et al.* (2019)
	Toxocara canis	L3	RPMI, $1X10^7$ larvae, 30 days (collected weekly), 37°C, 5% CO_2	LC–MS/MS	Sperotto *et al.* (2017)
	Trichinella spiralis	Muscle L1	RPMI, 5000 worms/mL, 18h, 37°C, 5% CO_2	LC–MS/MS	Grzelak *et al.* (2020); Kobpornchai *et al.* (2020)
	Trichinella pseudospiralis	Adult, NBL	RPMI, 5000 worms/mL, 20h, 37°C, 5% CO_2	MALDI–TOF/TOF–MS/MS	Wang *et al.* (2017)
	Trichuris muris	Adult	PBS, 100 worms/well/10 mL, 72h, 37°C, 5% CO_2	GC–MS & LC–MS/MS	Wangchuk *et al.* (2019)
Trematode	*Calicophoron daubneyi*	Adult	DMEM, 1 fluke/mL, 39°C, 6h	LC–Q–TOF–MS/MS	Huson *et al.* (2018)
	Clonorchis sinensis	Adult	Locke's medium, 48h, 37°C, 5% CO_2	Shotgun LC–MS/MS	Ma *et al.* (2021)
	Echinostoma caproni	Adult	RPMI, 10 worms/mL, 12h, 37°C	TOF–MS/MS	Cortés *et al.* (2016)
	Echinostoma caproni	Adult	PBS, 10 worms/mL, 12h, 37°C	Shotgun LC–MS/MS	Sotillo *et al.* (2010)
	Echinostoma caproni	Sp1	CBSS, 425,000 Sp1, 24h, 26°C	Nano–LC–MS/MS	Guillou *et al.* (2007)
	Fascioloides magna	Adult	RPMI, 15 worms, 6h, 37°C	LC–MS/MS	Cantacessi *et al.* (2012)
	Fasciola hepatica	Adult	RPMI, 1 fluke/2 mL, 24h, 37°C	MALDI–TOF/TOF–MS/MS	Jefferies *et al.* (2001)
	Fasciola hepatica	Immature (21–D)	RPMI 1640, 32 flukes/ group, 24h, 37°C	ESI MS/MS	Cwiklinski *et al.* (2021)
	Fasciola hepatica	Sp1	CBSS, 388,000 Sp1, 24h, 26°C	Nano–LC–MS/MS	Gourbal *et al.* (2008)
	Fasciola gigantica	Adult	RPMI, 12h, 37°C	Shotgun LC–MS/MS	Huang *et al.* (2019)
	Schistosoma haematobium	Adult, Egg	Serum–free Basch medium, 50 fluke pairs/4 mL (7 days), 50,000 eggs/5 mL (72h), 37°C, 5% CO_2	LC–MS/MS	Sotillo *et al.* (2019)
	Schistosoma japonicum	Adult: M/F	PBS, 800 mixed sex/mL, 10 min, room temperature	Nano–LC–MS/MS	Liu *et al.* (2009)
	Schistosoma mansoni	Adult: M/F	DMEM, 24h interval (7 days), 37°C, 5% CO_2	NanoESI–QqTOF–MS	Kenney *et al.* (2022)
	Schistosoma mansoni	Sp1	CBSS, 120,700 Sp1, 24h, 26°C	Nano–LC–MS/MS	Guillou *et al.* (2007)
Cestode	*Echinococcus granulosus*	Protoscoleces	PBS, 13–48h, 37°C, 5% CO_2	LC–MS/MS	Virginio *et al.* (2012)
	Echinococcus granulosus	Adult	RPMI, 500 worms/mL, 24h, 37°C	MALDI–TOF/TOF–MS/MS	Wang *et al.* (2015)
	Taenia solium	Metacestodes	RPMI, 50 cysts/20 mL, 6h then 18h, 37°C, 5% CO_2	Nano–LC–MS/MS	Victor *et al.* (2012)
	Hymenolepis diminuta	Adult	Eagle's media, 5 tapeworms/Petri dish, 5h & 18h, 37°C	LC–MS/MS	Bień *et al.* (2016)
	Mesocestoides corti	Tetrathyridia	DMEM, 100 tetrathyridia/mL, 14 days (collected every 24h), 37°C, 5% CO_2	NanoLC–MS/MS	Vendelova *et al.* (2016)

Abbreviations: New born larvae (NBL), Larva (L), Primary Sporocysts (Sp1), Male (M), Female (F), Liquid chromatography–tandem–mass spectrometry (LC–MS/MS), shotgun liquid chromatography tandem–mass spectrometry (Shotgun LC–MS/MS), Time–of–flight mass spectrometry (TOF–MS), nanoscale capillary LC–MS/MS (Nano–LC–MS/MS), Electrospray mass spectrometry (ESI MS/MS), Nano electrospray hybrid quadrupole–time of flight mass spectrometry (NanoESI–QqTOF–MS), Matrix–Assisted Laser Desorption/Ionization Time–of–Flight Mass Spectrometry (MALDI–TOF/TOF–MS/MS), Gas chromatography (GC).

1.2.3 Key proteins in ESPs and interaction with the host

ESPs derived from representative helminths (Table 1.2) include key proteins, such as glutathione transferases (GSTs), fatty–acid binding proteins (FABPs), heat shock proteins (HSPs), helminth defence molecules (HDMs), cathepsin proteases, thioredoxin peroxidase, enolase, actin, 14–3–3 proteins, dynein light chain and myoferlin. There is convincing evidence that whole ESPs, as well as individual secretory molecules in ESPs of helminths, have potential immunomodulatory capabilities that trigger T helper 2 (Th2)–type immune response in host immune cells such as macrophages, dendritic cells, T lymphocytes, eosinophils, basophils, mast cell and others (Donnelly *et al.*, 2005; Hewitson *et al.*, 2009; Dowling *et al.*, 2010; White and Artavanis-Tsakonas, 2012; Nono *et al.*, 2012, 2020; Harnett, 2014; Vendelova *et al.*, 2016; Pan *et al.*, 2017; Lawson *et al.*, 2019; Ryan *et al.*, 2020). The pro–inflammatory response of the host is diminished by suppressing Th1/Th17 responses and stimulating the response of the regulatory T cells (Tregs) and B10 cells (Harnett, 2014; Johnston *et al.*, 2017; Nono *et al.*, 2020). Furthermore, an induction of anti–inflammatory cytokines, such as interleukin 10 (IL–10) and transforming growth factor beta (TGF–β) allow parasites to survive longer in their hosts (Harnett, 2014; Johnston *et al.*, 2017; Nono *et al.*, 2020). Moreover, there are likely interactions with the microbial community due to the helminth ESPs containing a repertoire of antimicrobial peptides (AMPs) and antimicrobial proteins (Reynolds *et al.*, 2014; Midha *et al.*, 2018; Eline P. Hansen *et al.*, 2019; Rooney *et al.*, 2022).

Comprehensive research has been performed on the interactions of whole ESPs derived from helminths and selected antigenic proteins identified in helminth ESP with the host immune response (Sperotto *et al.*, 2017; Han *et al.*, 2019; Kobpornchai *et al.*, 2020). For example, in nematodes, whole ESPs derived from *Trichinella spiralis* suppresses mRNA expression of toll–like receptor 2 (TLR2)/ TLR4 and inhibit the Myeloid differentiation primary response 88 (MyD88) and Nuclear factor kappa–beta (NF–κB) subunit p65, in Lipopolysaccharides (LPS)–stimulated RAW264.7 macrophages (Han et al., 2019). Furthermore, studies have demonstrated that TsCstN, a novel papain–like cysteine protease inhibitor derived from muscle–stage larvae (L1) of *T. spiralis*, acted as a type 2 cystatin (Kobpornchai *et al.*, 2020). Additionally, TsCstN effectively modulated host immune responses by inhibiting inflammation in murine bone marrow–derived macrophages (mBMDMs) that are treated with LPS (Kobpornchai *et al.*, 2020). The presence of mucins

(Tcan_15190), the main *Toxocara canis* ESP component in L3s aids helminths survive in host tissue by resisting attacks from the host immune system (Sperotto *et al.*, 2017). Upon binding of mucin to specific glycoproteins found in the helminths cuticle such as glycans, C–type lectin, N–acetylglucosamine and others, they form glycaemic chains on host cells, subsequently preventing leukocyte infiltration into invaded tissues (Maizels and Page, 1990; Maizels, 2013; Prasanphanich *et al.*, 2013; Sperotto *et al.*, 2017; Shanawany *et al.*, 2019).

In trematodes, the characterisation of ESP derived from the adult stage of *Echinostoma caproni*, *Schistosoma* spp., *Fasciola* spp. and *Clonorchis sinensis,* reveals that the most abundant molecules are involved in detoxification, stress response (GST and protein disulfide isomerase, heat shock proteins and the 14–3–3 proteins) and the glucose metabolism in the glycolytic pathway (enolase, aldolase, phosphoglycerate kinase, triose phosphate isomerase, and glyceraldehyde–3–phosphate dehydrogenase (GAPDH), suggesting that these secretory molecules support the long term survival in the host (Liu *et al.*, 2009; Sotillo *et al.*, 2010; Ryan *et al.*, 2020). Interestingly, FABPs are found as a major component of *S. japonicum* ESPs, while, HSP70s, HSP90, and HSP97 are the most abundant protein families, with these proteins playing a crucial role in host immunomodulation (Liu *et al.*, 2009). In *C. sinensis* ESPs, proteins involved in body movement and energy metabolism including dynein light chain–1, dynein light chain–2 and myoferlin were identified in all infection periods and a highly expressed at different life stages (Ma *et al.*, 2021). In addition, these proteins are postulated to act as an energy reservoir, supporting *C. sinensis* in the establishment of chronic infection (Ma *et al.*, 2021). GSTs (FhGSTs), one of the major secretory protein (Mu–class GST as a major isoform) identified in *F. hepatica* ESPs account for up to 4% of the total protein and are involved in detoxification, functioning as antioxidants (Dowling *et al.*, 2010; LaCourse *et al.*, 2012; Aguayo *et al.*, 2019; Ryan *et al.*, 2020). A recent investigation of a novel *F. hepatica* omega–class GST 2 (FhGSTO2) demonstrated an ability to regulate the physiological functions of RAW264.7 murine macrophages and their cytokine expression, thus suggesting that FhGSTO2 may play an immunomodulatory role via the immune–evasion mechanism, and anti–inflammatory roles during infection (Wang *et al.*, 2022).

In cestodes, the most identified ESPs derived proteins from *Hymenolepis diminuta* are similar to those found in other helminths, with predominant functions associated metabolism and catalytic activity, such as in host immune evasion mechanisms and immunomodulatory

processes, in response to detoxification/oxidative stress (peroxidasin, HSPs, receptor type tyrosine protein phosphatase, glutamate dehydrogenase) or metabolic processes (pyruvate kinase, deoxyhypusine hydroxylase, glyceraldehyde 3 phosphate dehydrogenase) (Bień *et al.*, 2016). Apart from the interactions with the host, whole ESPs of *Echinococcus granulosus* `producing B cells (B17) and Th17 cells in *in vitro* B cell culture from CD19+ B and naïve CD4+ T cells (Pan *et al.*, 2017). Likewise, in *Echinococcus multilocularis* metacestodes, ESPs stimulates host T–cells to secrete higher levels of immunosuppressive cytokine IL–10 and contributes to the expansion of TGF–β –driven Foxp3+ Treg cells implying that the expansion of this cell type after ESP stimulation aids parasite establishment and proliferation (Nono *et al.*, 2012, 2020).

Although, various helminth ESP evidence has demonstrated the modulation of the host immune system, limited research has been undertaken to investigate whether *A. perfoliata* secrete ESP during *in vitro* culture that is similar to other closely related species and whether this can regulate the host immune response. Lawson *et al.* (2019) demonstrated that *A. perfoliata* ESPs are able to inhibit growth and induce cell death in the Jurkat cells (Human T-cell line). Moreover, after *in vitro* treatment of equine lymphocytes activated by Concanavalin-A (ConA) with *A. perfoliata* ESPs, there is a signification reduction in transcription of the cytokines IL–1, IL–2, IL–5, IL–17 and Interferon gamma (IFN–γ), indicating downregulation of T–cell responses to *A. perfoliata* during infection (Lawson *et al.*, 2019). However, the characterisation of essential secretory molecules in *A. perfoliata* ESP, as well as the exploration of the underlying mechanisms and pathways involved in host–parasite interactions, remains unexplored. Therefore, further studies are needed to enhance my comprehension of *A. perfoliata* infection and develop effective control strategies.

1.2.4 Introduction to Extracellular vesicles (EVs)

Extracellular vesicles (EVs) comprise a diverse array of small, lipid–bilayer membrane–bound vesicles released by various cell types into the extracellular space and interact with cell recipients (Valadi *et al.*, 2007; Marcilla *et al.*, 2012; Buck *et al.*, 2014; Cwiklinski *et al.*, 2015; Ancarola *et al.*, 2017; Samoil *et al.*, 2018; de la Torre-Escudero *et al.*, 2019). EVs were first discovered by Chargaff and West (1946) in platelet–free sera as procoagulant platelet–derived particles within the unnecessary secretions of metabolic pathways. Since then, EVs have been extensively studied. They were initially developed to isolate exosomes using differential centrifugation (DC) and were reported as intraluminal vesicles (ILVs) originating

from multivesicular endosomes within sheep reticulocyte tissue culture medium, and associated with plasma membrane activities (Johnstone *et al.*, 1987).

EVs have been secreted and isolated from multiple cell types (Table 1.3) through various biological fluid samples in *vivo* or from *in vitro* cell–culture supernatants (Table 1.2 and 1.3) (Keller *et al.*, 2011). EVs are not exclusively secreted by mammalian cells; microorganisms, such as bacteria (commonly referred to as bacterial extracellular vesicles or BEVs) (Jung *et al.*, 2021; Le *et al.*, 2023; Sartorio *et al.*, 2023), and parasites also contribute to the secretion of EVs as part of ESPs (Section 1.2.2; Table 1.2). Additionally, my thesis is exclusively focused on the investigation of EVs derived from *A. perfoliata*. Given an ability of EVs to circulate in bodily fluids under various physiological or pathological conditions, with distinct functions involved in most biological processes, there has been a substantial surge in interest as diagnostic biomarkers, therapeutic agents, and vaccine candidates across diseases, including cancer (Lane *et al.*, 2018; Hoshino *et al.*, 2020; Xia Wang *et al.*, 2022), respiratory diseases (Jiang *et al.*, 2020; Cappellano *et al.*, 2021; Jung *et al.*, 2021) and parasitic diseases (Cheng *et al.*, 2020; Mossallam *et al.*, 2021; Opadokun and Rohrbach, 2021). EVs are also being explored for therapeutic potential to deliver specific cargo molecules or serve as vehicles for drug delivery (Walker *et al.*, 2019; Buschmann *et al.*, 2021).

Table 1.3 An example of a cell type that secretes extracellular vesicles (EVs) and biological fluid samples obtained from these cells.

Categories	Example
Cell type	cancer cells (Xu *et al.*, 2018; Zhang *et al.*, 2021; Kalluri and McAndrews, 2023) stem cells (Keshtkar *et al.*, 2018; Hur *et al.*, 2020; Kou *et al.*, 2022) neurons and glial cells (Prada *et al.*, 2018; Datta Chaudhuri *et al.*, 2020) endothelial cells (Ravera *et al.*, 2020; Gao *et al.*, 2022; Elsner *et al.*, 2023) red blood cells (RBCs) (Straat *et al.*, 2015; Nguyen *et al.*, 2016, 2022; Yang *et al.*, 2022) platelets (Cappellano *e*(Lopez *et al.*, 2019; Suades *et al.*, 2022; Zhang *et al.*, 2022)*t al.*, 2021) epithelial cells (Mills *et al.*, 2019; Huang *et al.*, 2020; Devulder *et al.*, 2021) adipocytes (Crewe *et al.*, 2021; Blandin *et al.*, 2023)
Biological fluid samples	Blood (Palviainen *et al.*, 2020; Alberro *et al.*, 2021) milk (Hansen *et al.*, 2022) saliva (Nawaz *et al.*, 2020) urine (Zhang *et al.*, 2021) amniotic fluid (Gebara *et al.*, 2022) uterine flush (Almiñana *et al.*, 2021) bronchoalveolar lavage fluid (Höglund *et al.*, 2022)

1.2.5 Extracellular vesicle biogenesis and morphology

EVs are comprised of mixed populations that vary in size, properties, and secretion pathway, and are differentiated based on their cellular origin and mode of biogenesis; namely exosomes, microvesicles (MVs) (also referred to shedding microvesicles (SMVs) or ectosomes) and apoptotic bodies (also referred to apoptotic blebs (ABs)) (Figure 1.8, Table 1.4) (Mathivanan *et al.*, 2010; Raposo and Stoorvogel, 2013; Doyle and Wang, 2019).

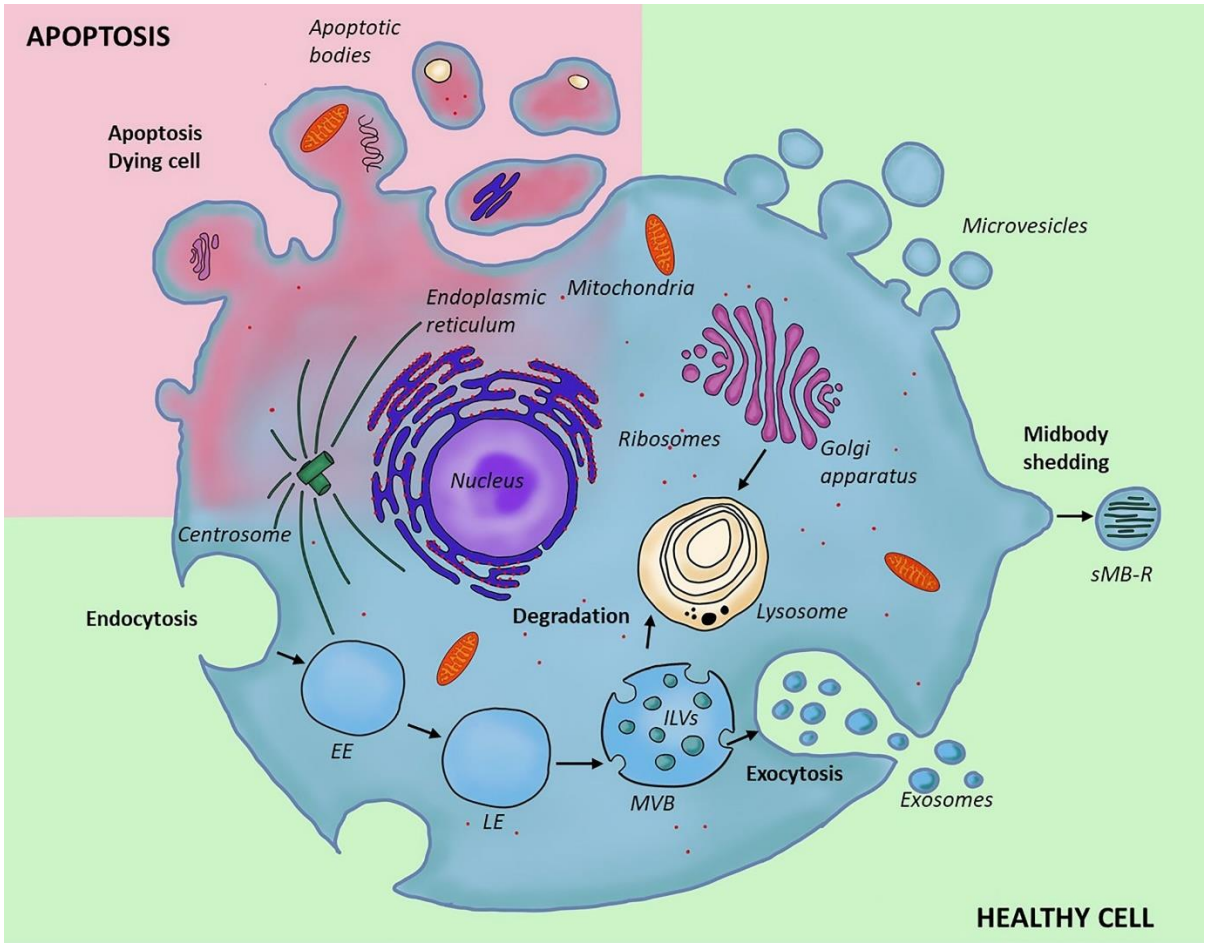

Figure 1.8 The overview of the biogenesis of exosomes, microvesicles and apoptotic bodies. Two types of EVs; microvesicles (a healthy cell) and apoptotic bodies (programmed cell death) and also secreted midbody remnant (sMB–R) are formed through outward invagination of the plasma membrane. Within the endocytic system, a multivesicular body (MVB) containing multiple intraluminal vesicles (ILVs) are formed by inward budding of early endosome (EE) to late endosome (LE). The content of MBV is either digested after fusion with lysosome (Hovhannisyan *et al.*, 2021).

Exosomes are the smallest EV sub–population, and are generated through endocytosis of the plasma membrane to form early endosomes (EEs), then transition to late endosomes (LEs). An inward budding of LEs once they are mature accumulate in intraluminal vesicles (ILVs) results in the formation of a multivesicular body (MVB), containing multiple ILVs. At this point, through the secretory pathway; MVBs fuse with the plasma membrane (PM) via exocytosis, subsequently, ILVs within MVBs are released from the cell into the extracellular space as exosomes. Alternatively, through the degradative pathway, MVBs fuse with the lysosome, where ILVs are degraded. The morphology of exosomes is a cup–shaped like vesicle when characterised using Transmission electron microscopy (TEM), with size ranging from 30–100 nm and up to 150 nm. Microvesicles are generated by an outward budding or exocytosis of the plasma membrane and subsequent release directly from the plasma membrane. The morphology of microvesicles is in various shapes and the size is larger than exosomes, approximately 100 nm up to 1000 nm in diameter. Apoptotic bodies, are generated by blebbing of plasma membrane in dying cells undergoing the later stages of apoptosis in the context of programmed cell death. Apoptotic bodies display a diverse range of shapes, and their diameter can vary from 50 nm to 5000 nm (Figure 1.8 and Table 1.4) (Mathivanan *et al.*, 2010; Raposo and Stoorvogel, 2013; Doyle and Wang, 2019; Hovhannisyan *et al.*, 2021).

Table 1.4 Characterisation of extracellular vesicles include exosomes, microvesicles and apoptotic bodies. Adapted from (Mathivanan *et al.*, 2010; Doyle and Wang, 2019; Sivanantham and Jin, 2022).

Characterisation	Exosomes	Microvesicless	Apoptotic bodies
Size (diameter in nm)	30–100 up to150	100–1000	50–500 up to 5000
Flotation density (rate zonal centrifugation)	1.10–1.21 g/mL	Not known	1.16–1.28 g/mL
Morphology	Cup–shaped/ Spherical	Various shapes	Heterogeneous
Lipid composition	Low phosphatidylserine exposure, cholesterol, ceramide, contains lipid rafts, sphingomyelin	High phosphatidylserine exposure, cholesterol	High
Protein markers	ALG–2–interacting protein X, Tumour susceptibility gene 101, Heat shock cognate 70, Heat shock protein 90–beta, Tetraspanins (CD63, CD81, CD9)	Selectins, integrins, CD40, metalloproteinases	Histones
Surface markers	Tetraspanins (CD9, CD63, CD81 and CD82)	Selectins, integrin, CD40, CD31+, CD235a+, CD42b–, CD45, CD61+, CD62E+, CD144+	Apoptotic cell markers
Cargos and other markers	Podocalyxin–like protein 1, Heat shock protein 70, Heat shock protein 90	Cytoskeletal proteins, Heat shock proteins, Proteins containing post–translational modifications (glycosylation & phosphorylation)	Intact chromatin, Glycosylated proteins, Caspase 3, Heat shock protein 60, 78–kDa glucose–regulated protein (GRP78)
Site of origin	Multivesicular bodies	Plasma membrane	–
Mode of extracellular release	Constitutive and regulated	Regulated	Regulated
Mechanism of discharge	Exocytosis of multivesicular bodies	Budding from plasma membrane	Cell shrinkage & death
Release or response	Cellular stress or activation signals	Cell injury, Proinflammatory stimulants, Hypoxia, Oxidative stress or Shear stress	Apoptosis
Composition	Proteins, miRNA, mRNA	Proteins, miRNA, mRNA	Proteins, DNA, miRNA, mRNA

1.2.6 EV isolation and characterisation methods

In this thesis, my focus is on the isolation and characterisation methods of EVs derived from helminths. EVs are commonly isolated from the supernatants after *in vitro* culture of helminth derived ESP (Section 1.2.2). There are various techniques utilised for isolation of EVs, particularly for exosomes. However, the yield and purity of EVs vary depending upon the technique (Table 1.5) due to the complexity of different sources of biological fluids EVs are derived from, the type of EV of interest, and level of homogeneity required (Zhang *et al.*, 2018; Davis *et al.*, 2019; Doyle and Wang, 2019; Freitas *et al.*, 2019). Currently, there is no single gold standard for EV isolation, differential centrifugation (DC) has been considered as a primary method for EVs isolation; as it is the first developed and still widely applied for exosome isolation (Théry *et al.*, 2006; Zhang *et al.*, 2018; Doyle and Wang, 2019; Stam *et al.*, 2021). DC involves a series of centrifugation steps at varying speeds and durations for the separation of particles or molecules, making it a time–intensive process. While, a size based technique, size exclusion chromatography (SEC), has recently gained attention and is being used for EV isolation in helminths such as in *Ascaris suum* (Hansen *et al.*, 2019; Borup *et al.*, 2022)*, F. hepatica* (Davis *et al.*, 2019, 2020; Sánchez-López *et al.*, 2020), *C. daubneyi* (Huson *et al.*, 2018; Allen *et al.*, 2021) and *Teladorsagia circumcincta* (Rooney *et al.*, 2022). SEC is less time consuming and simpler method than DC/Ultracentrifugation (UC), especially when using a commercial kit. Furthermore, EV integrity is not altered during SEC isolation (Konoshenko *et al.*, 2018; Zhang *et al.*, 2018; Monguió-Tortajada *et al.*, 2019; Guan *et al.*, 2020).

For example, In *Ascaris suum*, three EV isolation methods were employed, including SEC, Differential Ultracentrifugation (dUC), and the combination of SEC and dUC, to separate *Ascaris suum* EVs (Borup *et al.*, 2022). These methods exhibited a similar EV yield and performance in reducing LPS–induced levels of Tumor Necrosis Factor (TNF–α) (Borup *et al.*, 2022). However, the combination method showed slightly higher EV purity compared to either method alone (Borup *et al.*, 2022). Therefore, the combined method is recommended for EV isolation to achieve better EV purity (Stam *et al.*, 2021). In *F. hepatica* SEC and DC methods were used to isolate differential EV sub-populations (Davis et al., 2019). The EV purity to protein yield ratio from SEC is higher than DC as indicated by decreasing in soluble free cathepsin L proteases, less free ES proteins and tegumental based protein components in SEC purified EVs. The higher purity of EV isolated by SEC, it is the potential EV purification

method, particularly for protein functional downstream analysis in helminths studies (Davis *et al.*, 2019).

Isolated EVs can be characterised (e.g. particle shape, size, particle size distribution and concentration) using a physical analysis, such as Brownian motion of small particles, visualisation using Nanoparticle Tracking Analysis (NTA), a single–particle measurement technique using Tunable Resistive Pulse Sensing (TRPS), visualisation of the characteristic feature of exosomes using Transmission electron microscopy (TEM). Other chemical, biochemical and composition analyses such as Flow Cytometry, Western Blotting and MS/MS (Table 1.5) (Zhang *et al.*, 2018; Doyle and Wang, 2019).

Table 1.5 Isolation and characterisation methods of extracellular vesicles (Zhang *et al.*, 2018; Doyle and Wang, 2019).

Procedure	**Methods**	
Isolation	**Ultracentrifugation techniques**	• Differential ultracentrifugation (dUC) • Density gradient Centrifugation (disc–UC)
	Size Based Techniques	• Ultrafiltration (UF) • Exosome isolation kit • Sequential filtration • Size Exclusion Chromatography (SEC) • Flow Field–Flow Fractionation (FFFF) • Hydrostatic Filtration Dialysis (HFD)
	Immunoaffinity Capture–Based Techniques	• Enzyme–Linked Immunosorbent Assay (ELISA) • Magneto–Immunoprecipitation
	Exosome Precipitation–based Techniques	• Polyethylene Glycol (PEG) precipitation • Lectin induced agglutination
	Microfluidic based isolation techniques	• Acoustic nanofilter • Immuno–based microfluidic isolation
Characterisation: Physical analysis	**Nanoparticle Tracking Analysis (NTA),** minimum 10 nm **Transmission electron microscopy (TEM),** minimum < 1 nm **Scanning electron microscopy (SEM)** **Dynamic Light Scattering (DLS)** **Tunable Resistive Pulse Sensing (TRPS),** minimum <100 nm, depend on pore size	
Characterisation: Chemical, Biochemical & Compositional analyses	**Immunodetection:** • Flow Cytometry (minimum 100 nm) • Western Blotting • Integrated Immuno–Isolation and Protein Analysis of Exosomes	
	Thermophoretic Profiling	
	Mass Spectrometry (MS)–Based Proteomic Analysis • Global Proteomic Approaches • Targeted Proteomic Approaches	

1.2.7 Key proteins in helminths extracellular vesicles

The identification and functional characterisation of molecules in EVs demonstrate that each EVs sub–population contains unique bioactive molecules, including lipids, proteins, metabolites, genomic DNA, RNAs, and non–coding RNAs, termed "EVs markers" (Mathivanan *et al.*, 2010) (Table 1.4). EVs in helminths are also considered as key components for cellular crosstalk and host–parasite interactions (Valadi *et al.*, 2007; Marcilla *et al.*, 2012; Cwiklinski *et al.*, 2015; Ancarola *et al.*, 2017; de la Torre-Escudero *et al.*, 2019). Some examples of protein and surface markers associated with different types of EVs are as follows (Figure 1.9 and 1.10): ALG–2–interacting protein X (ALIX), Tumour susceptibility gene 101 (TSG101), Heat shock cognate 70 (HSC70), Heat shock protein 90–beta (HSP90β), Tetraspanins (CD63, CD81, CD9). For microvesicles, the markers include Selectins, integrins, CD40, and metalloproteinases. Histone is a marker specifically associated with apoptotic bodies, as indicated in Table 1.4 (Théry *et al.*, 2001; Mathivanan *et al.*, 2010; Baietti *et al.*, 2012; Doyle and Wang, 2019; Sivanantham and Jin, 2022). Tetraspanin, membrane proteins involved in EV function which CD63, CD9 and CD81 are well–known exosome protein markers and found to be highly abundant on the EV surface of *H. polygyrus* (Buck *et al.*, 2014) and *Schistosoma* spp. (Samoil *et al.*, 2018; Mekonnen *et al.*, 2020). For example, EVs (exosomes and microvesicles) derived from the metacestode stages of cestodes, *Taenia crassiceps*, *Mesocestoides corti* and *E. multilocularis*, contain miRNA and protein cargo such as heat shock proteins, annexin, enolase, phosphoglycerate kinase, actin, tubulin and elongation factors (Ancarola *et al.*, 2017) which are typically found in other platyhelminths such as *F. hepatica* (Marcilla *et al.*, 2012; Davis *et al.*, 2019). EVs derived from the larval stage of *E. granulosus* contain exosomal protein markers (ALIX, TSG101, Syndecan Binding Protein (SDCBP), 14–3–3 proteins and Tetraspanins), vesicle–related transport proteins that are homologous to the mammalian proteins in the immune response (Bp29, basigin, and maspardin), and parasite antigens involved in parasite–host relationship (antigen 5, P29 and endophilin–1) (Nicolao *et al.*, 2019).

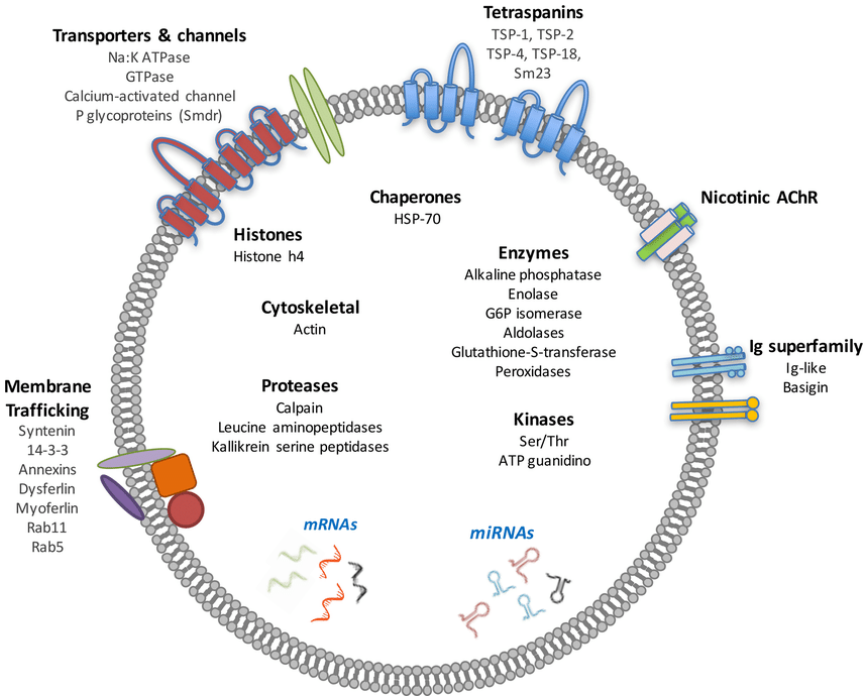

Figure 1.9 Schematic representation of a platyhelminth EV showing selected proteins of interest. This specific example demonstrates proteins identified from larval and adult Schistosoma mansoni derived EVs (Kifle et al., 2017).

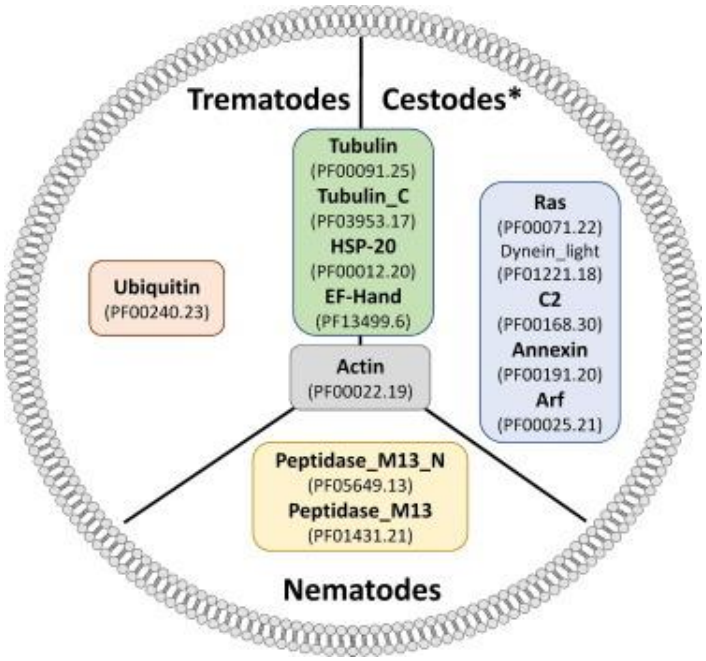

Figure 1.10 Schematic representation of the most abundant protein families and domains (Pfam) detected in helminth EVs across phyla analysed from each lineage of trematodes, nematodes and cestodes. For clarity in cestode (*), only the top ten protein families and domains based on occurrence are shown (Sotillo et al., 2020).

1.2.8 EV internalisation and interaction with the host

EVs released by donor cells deliver their cargo and can be internalised by recipient cells via various mechanisms, including clathrin–mediated endocytosis (CME), caveolin–mediated endocytosis, lipid rafts–mediated endocytosis, phagocytosis, micropinocytosis, and plasma or endosomal membrane fusion (Figure 1.11) (Mulcahy *et al.*, 2014). The transportation of EV cargo molecules results in cell to cell intercommunication. Furthermore, the interaction of EV molecules causes downregulation of type 1 (classical) and type 2 (alternative) immune–response–associated molecules (IL–6 and Tumor Necrosis Factor (TNF), Ym1 and Resistin–Like Molecule Alpha (RELMα), and inhibition of the expression of the IL–33 receptor subunit ST2 of the host to facilitate parasite survival during infection (Mulcahy *et al.*, 2014; Coakley *et al.*, 2017).

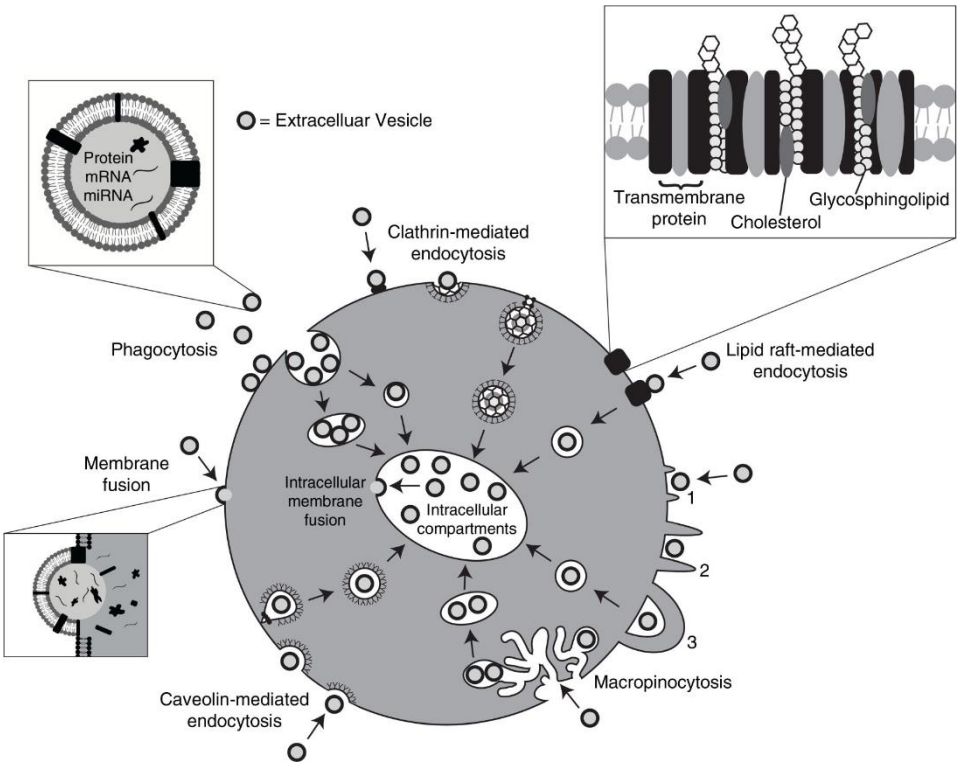

Figure 1.11 Pathways shown to participate in EV uptake by target cells and EVs transport signals between cells (Mulcahy et al., 2014).

Currently, it has been demonstrated that the internalisation of helminth–derived EVs into host cells leads to the activation of various functions within the host cell mediated by EV cargoes. For example, following *in vitro* co–culture of *H. polygrus* exosomes with mouse small intestinal epithelial cells (MODE–K cells) for 1 h, the exosomes are internalised by over 60% of MODE–K cells. Furthermore, *H. polygrus* exosomes suppress an innate Type 2 response *in vivo* which leads to the significant decrease of eosinophils in bronchoalveolar lavage; suppresses the expression of type 2 cytokines (IL–5 and IL–13) by innate lymphoid cells (ILCs); and downregulates gene expression of DUSP1 (Dual Specificity Phosphatase 1) and IL1RL1 (Interleukin 1 Receptor Like 1) (Buck *et al.*, 2014).

In trematodes, both *S. mansoni* derived EVs and miRNA extracted from EVs are 50% internalised by primary Th cells (purified from spleen and lymph nodes of mice and stimulated with anti–CD3 and anti–CD28 antibodies) after an *in vitro* co–culture for 10 minutes (Meningher *et al.*, 2020). An internalisation of *S. mansoni* EVs (exosome–like vesicles (ELVs) and microvesicles (MVs)) by human umbilical vein endothelial cells (HUVECs) induces differential gene expression in HUVECs (Kifle *et al.*, 2020). In a study conducted by de la Torre-Escudero *et al.* (2019), it was demonstrated that RAW246.7 macrophages actively internalised the surface–derived *F. hepatica* EVs. The researchers provided further confirmation of this active internalisation process by demonstrating that treatment with cytochalasin D, a blocker of actin polymerization and endocytosis pathways, as well as glycosidase treatment, inhibited the internalisation of these EV surface (de la Torre-Escudero *et al.*, 2019). Furthermore, EV surface proteins (DM9–containing protein, CD63 receptor, and myoferlin) enhance cellular internalisation of *F. hepatica* derived EV surface, highlighting EV biogenesis and trafficking pathways as well as potential fusogenic properties (de la Torre-Escudero *et al.*, 2019).

In cestodes, EVs derived from *E. granulosus* also demonstrate uptake by murine peripheral blood mononuclear cells after co–culture (Yang *et al.*, 2021). Following uptake, immunomodulatory functions of the EVs are demonstrated through upregulation of T lymphocyte functions via inhibition of the proliferation of murine lymphocytes, CD4+ T cells, and CD8+ T cells in a dose–dependent manner (Zhou *et al.*, 2019). *E. granulosus* exosome–like vesicles are also internalised by murine dendritic cells, and demonstrate an increase in CD86 and decrease in the MHCII molecule expression, which induces the murine dendritic cells maturation, implying that *E. granulosus* EVs induce immunoregulation in the host by

interfering with the antigen presentation pathway of murine dendritic cells (Nicolao *et al.*, 2019). The internalisation of *E. granulosus*–derived EVs from the 110 K hydatid fluid by sheep peripheral blood mononuclear cells (PBMCs) serves as evidence of their role in immune responses during *E. granulosus* infection (Yang *et al.*, 2021). This internalisation leads to the induction of IL–10, TNF–α, an upregulation of Interferon Regulatory Factor 5 (IRF5), and a downregulation of IL–1β, IL–17, and CD14 (Yang *et al.*, 2021). To this end, the information on EV uptake in representative platyhelminths provided above are essential for gaining a thorough understanding of the role of EVs in parasite survival strategies. Therefore, it is hypothesised that *A. perfoliata* can secreted EVs with a potential to modulate the host immune responses.

1.3 EQUINE DIGESTIVE PHYSIOLOGY

1.3.1 Equine hindgut digestion

Horses are non–ruminant herbivorous animals and therefore rely on plant species, especially grasses, as the main source for energy and nutrients to the host, formulating a high–fibre diet (Janis, 1976). To support the high–fibre diet, the GIT of the horse is divided into two main parts, the foregut, the stomach and small intestine, responsible for the initial mechanical and enzymatic digestion, and the hindgut, i.e. large intestine, caecum and colon, responsible for the fermentation of the highly fibrous plant matter (Figure 1.12). Within hindgut fermenters, a symbiotic relationship is established between the host and numerous microorganisms in the hindgut ecosystem to enhance degradation, fermentation and utilisation of structural or insoluble carbohydrates in plant cell walls, such as hemicellulose and cellulose, which cannot be digested by the host alone (Janis, 1976; Julliand and Grimm, 2016). Microbes in the equine hindgut include bacteria, fungi, protozoa, bacteriophages, and archaea and are located mostly in the caecum and colon (Janis, 1976; Mackie and Wilkins, 1988; Dicks *et al.*, 2014; Julliand and Grimm, 2016). The populations in the large colon and caecum are accountable for the majority of fermentation activities, with fibrolytic bacteria implicated in the digestion and absorption of nutrients for energy production (Mackie and Wilkins, 1988; Dicks *et al.*, 2014). Therefore, to support a high–fibre diet for energy production, the horse utilises hindgut fermentation, which employs enzymes produced by the

gut microbiota (Janis, 1976). The equine gut microbiota is also involved in various significant roles in enhancing vitamins B and K, nutrients, as well as providing energy (Costa and Weese, 2012; Dicks *et al.*, 2014; Venable *et al.*, 2016). Volatile fatty acids (VFAs) are short–chain fatty acids (SCFAs) including acetate, butyrate, and propionate, and the predominant metabolite products generated by the gut microbiota in the hindgut through the anaerobic fermentation of dietary fibres that are used by the horse as an energy source (Bergman, 1990; Costa and Weese, 2012). Moreover, the microbiota helps to maintain the GIT health status, toxin neutralisation and promotion of the host immune system (Maslowski and Mackay, 2011; Hooper *et al.*, 2012; Sommer and Bäckhed, 2013; Belkaid and Hand, 2014; Venable *et al.*, 2016). However, further studies and more understanding of the equine hindgut microbiome are required to better understand its structure and function (Costa and Weese, 2012; Dicks *et al.*, 2014; Julliand and Grimm, 2016; Venable *et al.*, 2016).

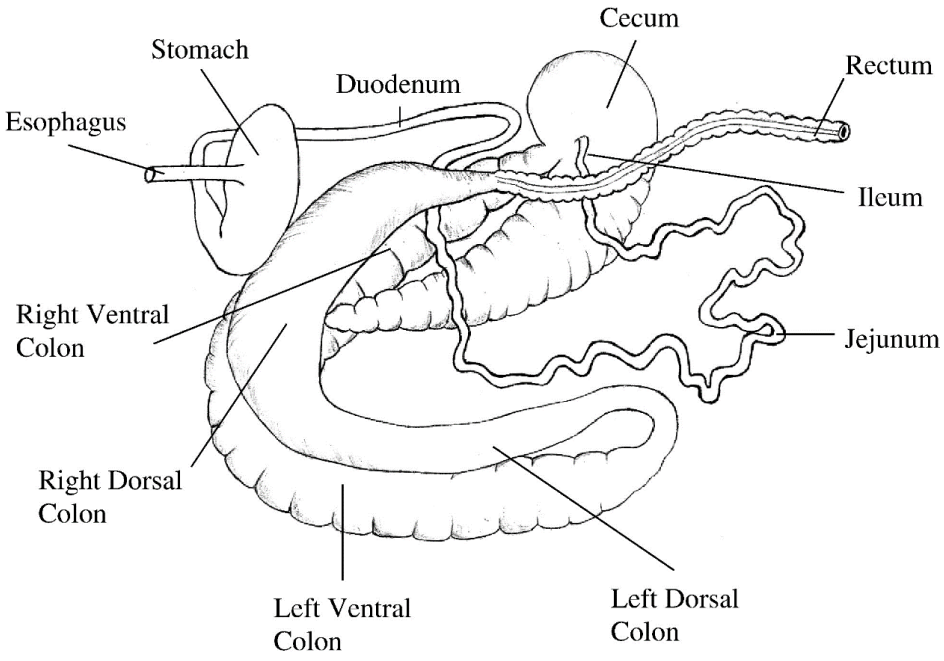

Figure 1.12 Gastrointestinal tract of the adult horse (Van Weyenberg et al., 2006).

1.3.2 Investigation of equine gut microbiota

In early gut microbiome studies, bacterial communities in the equine hindgut as well as faecal samples were primarily investigated using standard microbiological techniques, such as *in vitro* culturing (Mackie and Wilkins, 1988; de Fombelle *et al.*, 2003; Respondek *et al.*, 2008). Due to the complexity of the microbiome in the GIT and a predominance of anaerobes (Hao and Lee, 2004), culture techniques likely lead to an under–estimation or over–estimation of the microbiota (Vendelova *et al.*, 2016). Consequently, various non–culture–dependent, molecular based techniques are now the most commonly used methods to understand the microbiome. These include techniques such as polymerase chain reaction (PCR) (Hastie *et al.*, 2008a; Górniak *et al.*, 2021), amplicon next generation sequencing (NGS) analysis of bacterial 16S ribosomal RNA (16S rRNA) gene (Whitfield-Cargile *et al.*, 2021; Morrison *et al.*, 2018; Mshelia *et al.*, 2018; Whitfield-Cargile *et al.*, 2018; Kunz *et al.*, 2019; Lindenberg *et al.*, 2019; Arnold *et al.*, 2020; Paßlack *et al.*, 2020; Collinet *et al.*, 2021; T. Park, Cheong, *et al.*, 2021; Liepman *et al.*, 2022), bacterial 16S ribosomal RNA (16S rRNA) terminal restriction fragment length polymorphism (TRFLP) (Willing *et al.*, 2009; Dougal *et al.*, 2012; Blackmore *et al.*, 2013; Schoster *et al.*, 2013; Crotch-Harvey *et al.*, 2018; Morrison *et al.*, 2018) and metagenomics/metabolomics approaches (Papaiakovou *et al.*, 2022). Recently, bioinformatics platforms and the combination of culture and non–culture techniques have been applied widely for more reliable and accurate microbiome identification (Dicks *et al.*, 2014; Venable *et al.*, 2016).

Faecal samples have been widely used as an alternative to caecal or colonic fluid to represent the microbial population within the GIT of horses, due to the ethical and practical concerns for sampling in live horses (Lowman *et al.*, 1999). It has been noted that bacterial communities found in faeces are not exactly representative of bacterial communities within caecum (Dougal *et al.*, 2012), where the majority of bacterial fermentation occurs. Dougal et al. (2012) and Costa et al. (2015) revealed that the microbiome from faecal samples were similar to the gut microbiomes from the right ventral colon. In contrast, Fliegerova et al. (2016) revealed that the microbiome from faecal samples were similar to the gut microbiomes from the left ventral colon, and that the number of total bacteria were highest in the right ventral colon . Therefore, it is considered that different regions of GIT may harbour different bacterial communities.

1.3.3 Gut microbiota communities

In healthy horses, the most abundant bacterial phylum found throughout the GIT is Firmicutes (47–74%), followed by Bacteroidetes (14–34.5%) as the second most abundant phylum. Other phyla which contribute less than 10% of the core microbiome include Spirochaete (6.3%), Verrucomicrobia (4.1%), Proteobacteria (0.95–10%), and Fibrobacteres (2–6.4%) (Costa *et al.*, 2012; Shepherd *et al.*, 2012; Steelman *et al.*, 2012; Blackmore *et al.*, 2013; Dougal *et al.*, 2014; Fernandes *et al.*, 2014; Costa *et al.*, 2015; Zhao *et al.*, 2016; Mach *et al.*, 2017; Salem *et al.*, 2018). The predominance of the Firmicutes phyla is commonly found in animals that utilise the hindgut, cecum and large colon, as the main site of fermentation. Therefore, their presence is probably associated with the anatomical physiology and feeding habits of these animals (Costa et al., 2012).

Furthermore, investigations into the faecal microbiomes between two breeds, Mongolian and Thoroughbred horses have been conducted using both 16S rRNA gene (Zhao *et al.*, 2016) and metagenomic sequencing (Gilroy *et al.*, 2021). These studies revealed that the bacterial community compositions were similar in both breeds (Zhao *et al.*, 2016; Gilroy *et al.*, 2021). The dominant phyla were Firmicutes, comprising 56% and 53% in Mongolian and Thoroughbred horses, respectively, followed by Bacteroidetes at 33% and 32%, respectively. Additionally, Spirochaete, Verrucomicrobia, Proteobacteria, and Fibrobacteres phyla each accounted for less than 10% (Zhao *et al.*, 2016). However, noteworthy differences were observed in the abundance of specific bacterial genera between the two breeds. *Treponema* was more prevalent in Mongolian horses, while *Oscillibacter* was found in higher abundance in Thoroughbred horses (Zhao *et al.*, 2016). Interestingly, the donkey (*Equus asinus*), which is a herbivorous hindgut fermenter in the same genus as the horse (*Equus caballus*), has a similar faecal microbiota to the healthy horse (Liu *et al.*, 2014). Despite the limited information available about gut homeostasis in other equid species, the knowledge gained from studying horses can still provide valuable insights into digestive physiology and health. By leveraging the understanding of horses' digestive processes, researchers can potentially apply that knowledge to benefit other equid species. This cross–species approach holds the potential to enhance my comprehension of digestive physiology and promote better digestive health across different equid species.

The diversity and species richness of the microbiome in each particular region of the equine GIT increases towards the distal gut compartments, due to the fermentation activities, with the highest diversity and species richness at the right ventral colon and declining through faeces (Table 1.6) (Dougal et al., 2012, 2013; Costa et al., 2015; Ericsson et al., 2016). Consequently, the large intestine harbours a greater diversity and species richness of the microbiome compared with the small intestine, yet within each particular region of the large intestine there is a slight variation in the microbiome (Dougal et al., 2013).

Table 1.6 The core bacterial communities of the large intestine of the horse (Dougal *et al.*, 2013).

Location	Most abundant (Family)	Predominant of core bacterial community
All regions of the large intestine		Firmicutes (46%) and Bacteroidetes (43%) phyla
Proximal large intestine (Caecum, RVC and LVC)	*Lachnospiraceae*	Order *Bacteroidales*, the family *Lachnospiraceae* (Firmicutes phyla) following by *Prevotellaceae* (Bacteroidetes phyla), *Erysipelotrichaceae*, *Ruminococcaceae* (Firmicutes phyla), *Fibrobacteraceae* (Fibrobacteres phyla)
Distal large intestine (RDC, SC and faeces)	*Prevotellaceae*	*Prevotellaceae*, *Fibrobacteraceae*, *Lachnospiraceae*, unclassified family only classified to phyla level as *Bacteroidetes* and *Clostridiaceae* 1 (Firmicutes phyla)
Left dorsal colon		*Lachnospiraceae*, *Clostridiaceae* 1, unclassified family order *Bacteroidales* and *Erysipelotrichaceae*

Abbreviations: RVC: right ventral colon; LVC: left ventral colon; RDC: right dorsal colon; SC: small colon and faeces.

1.3.4 Microbiome alterations

Importantly, the horse has a very small, less diverse core gut microbiome (key microbes) and low abundance of species richness in the large intestine (Blackmore *et al.*, 2013; Dougal *et al.*, 2013) compared to that of the rumen of adult ruminants, that is characterised by a remarkably diverse gut microbiome (Weimer, 1998, 2015; Petri et al., 2013; Malmuthuge & Guan, 2016). Consequently, ruminants possess a stable rumen microbiome due to minimal susceptibility to changes caused by factors like dietary modifications (Weimer, 1998, 2015; Petri et al., 2013; Malmuthuge & Guan, 2016). Conversely, horses are highly susceptible to GIT disturbances from opportunistic species that take over as predominant species (Dougal et al., 2013). The proportion of Firmicutes to Bacteroidetes (F/B), is known as a relevant marker of gut dysbiosis (Costa *et al.*, 2012; Park, Cheong, *et al.*, 2021; Park, Yoon, *et al.*, 2021). The ideal proportion of F/B in healthy adult horses has been reported in a ratio at 68:14 and 30:40, respectively (Costa *et al.*, 2012). Whereas the proportion of F/B of horses

with diarrhoea and colic were in a ratio at 4:1 (Costa *et al.*, 2012; Park, Cheong, *et al.*, 2021; Park, Yoon, *et al.*, 2021).

There are numerous factors that can influence the overall gut microbiome in horses, either at the level of the horse itself or environmental factors (Table 1.7) (Theelen *et al.*, 2021). The alteration of the equine hindgut microbiota homeostasis can cause consequential effects on equine digestive physiology and health status, and is associated with various serious metabolic disorders and diseases including diarrhoea, colitis, colic and laminitis (Garber *et al.*, 2020; T. Park, Cheong, *et al.*, 2021; Liepman *et al.*, 2022).

Table 1.7 Key selected factors altering the equine gut microbiota.

Factors	Factors	Sample	Method	Effect on microbiota	Authors
Diets, Supplements	Meal size and frequency	Caecal	16S rRNA gene sequence analyses	• One large meal having different microbial community both abundance and composition of the ceacal microbiota than fed three smaller meals throughout the day • Treatment affected *Prevotella, YRC22, Lactobacillus, Streptococcus, Coprococcus,* and *Phascolarctobacterium*	Venable *et al.* (2017)
	Cellobiose (prebiotics)	Faecal	16S rRNA gene sequence analyses VFAs analyses	A dose–dependent • Increase of the relative abundance of Firmicutes, *Coriobacteriales* and *Clostridium* indicates a bacterial fermentation of cellobiose in the equine intestine • Decrease of the relative abundance of *Bacteroidetes*	Paßlack *et al.* (2020)
Management & others: Stress	Exercise & Physical training (Intense Exercise in Thoroughbred Racehorses)	Faecal	DNA isolation and real–time–PCR analysis	• Significant increase on both Firmicutes and Bacteroidetes phyla after exercise • no significant changes on facultative aerobes; *Lactobacillaceae* family (Firmicutes phylum)	Górniak *et al.* (2021)
	Transportation	Faecal	Prokaryotic community profiling by 16S metagenomic analysis	• 48 hours after transport, increased Bacteroidetes, decreased Firmicutes phyla	Szemplinski *et al.* (2020)
Antimicrobial drugs	Procaine penicillin Ceftiofur sodium Trimethoprim sulfadiazine	Faecal	16S rRNA gene sequence analyses	• Significant reduction in bacterial species richness and diversity. • Greatest effects on population structure, specifically targeting members of the Verrucomicrobia phylum	Marcio C Costa *et al.* (2015)
	Metronidazole	Faecal, Caecal	16S rRNA gene sequence analyses and metabolomics analyses	• Reduced of OTU, Shannon and Chao 1 metrics in cecal samples on day 14 post treatment. Lowest alpha diversity in fecal samples on day 3 post treatment • No effects in beta diversity in cecal samples. • Significant effects on alpha and beta diversity in faecal samples on day 3 and day 14 post treatment	Arnold *et al.* (2020)
	Ceftiofur, enrofloxacin and oxytetracyclines	Faecal	16S rRNA gene sequence analyses	• Significant reduces richness but diversity of microbiota • Genus–level OTU richness for ceftiofur greater on day 0	Liepman *et al.* (2022)
Anti–inflammatory drugs	Phenylbutazone	Faecal, Blood	16S rRNA gene sequence analyses	• Increases bacterial numbers 16S rDNA in circulation by 3.02–fold & induces specific changes in the microbiota including a loss of *Pseudobutyriovibrio* of family *Lachnospiraceae.* • Minimal changes in beta diversity	Whitfield-Cargile *et al.* (2021)
	Phenylbutazone/Firocoxib & combination	Faecal	16S rRNA gene sequence analyses	• Phenylbutazone and firocoxib decrease microbial diversity profiles significantly on day 10 post treatment • Temporary alterations of the faecal microbiota and inferred metagenome	Whitfield-Cargile *et al.* (2018)

Abbreviations: 16S ribosomal RNA (16S rRNA), OTUs: operational taxonomic units (OTUs), The volatile organic compound (VOC), GCMS: Gas Chromatography Mass Spectrometry, FEC: Faecal egg count, FT–IR: Fourier–transform infrared spectroscopy, T–RFLP: Restriction Fragment Length Polymorphism.

Table 1.7–Continued2 Key selected factors altering the equine gut microbiota.

Factors	Factors	Sample	Method	Effect on microbiota	Authors
Gastrointestinal parasites	Acute larval cyathostominosis	Faecal, Blood	Clinicopathological, faecal egg count analyses and 16s rRNA gene sequencing	• Bacterial overgrowth in the mucosa of the large intestine • Faecal microbiota reflected the large intestinal microbiota, not represent changes directly • Decreased alpha–diversity of the faecal microbiota and greater relative abundance of the genus *Streptococcus*, class Bacilli, order *Lactobacillales* and family *Streptococcaceae*, and *Prevotelleceae* in clinically affected horses • Increase obligate fibrolytic bacteria in the clinically normal group: the phylum Fibrobacteres, the order *Fibrobacterales*, class Fibrobacteria, genus *Fibrobacter* and the family *Ruminococcaceae*, genus *Ruminococcaceae*	Walshe *et al.* (2021)
	Anoplocephala perfoliata	colonic contents	16s rRNA gene sequencing (V4 region) VOC metabolome by GCMS	• Bacterial diversity (alpha and beta) was similar between tapeworm infected and non–infected controls • Down–regulation of OTUs belonging to the symbiotic families of *Ruminococcaceae* and *Lachnospiraceae*	Slater *et al.* (2021)

	Grazing ponies with an extreme phenotypic resistance or susceptibility toward natural strongyle infection	Faecal, Blood	V3V4 16S rRNA gene sequencing
			Illumina MiSeq
			Functional Metagenomic Predictions for the 16S rRNA marker gene sequences by the phylogenetic investigation
				• The overall alpha and beta diversity did not differ significantly between resistance (R) and susceptibility (S) group following the infection
				• Transitioning period/mild parasite exposure (day 0–43)
				  ○ no significant alterations in the overall gut microbial community structure, the phylum or family levels nor at the genera level
				  ○ higher anaerobic fungal concentrations, lower protozoan concentrations in S relative to R
				  ○ bacterial concentrations & pH remain similar between groups of ponies within each time point.
				• Natural strongyle infection (day 92–132)
				  ○ increase in observed species richness and Chao1 indexes relative to the other time points
				  ○ minor differences in microbiota composition between 2 groups
				  ○ differed gut microbiota structure compared to the other time points
				  ○ a reduction of bacteria such as *Ruminococcus*, *Clostridium* XIVa and members of the *Lachnospiraceae* family, which may have promoted a disruption of mucosal homeostasis.
				• Day 92: changes in relative abundance of certain genera concomitantly arose with strongyle egg excretion
				• higher anaerobic fungi and protozoa concentrations in the S group, did not alter bacterial concentrations & fecal pH in both groups
					Clark *et al.* (2018)

Abbreviations: 16S ribosomal RNA (16S rRNA), OTUs: operational taxonomic units (OTUs), The volatile organic compound (VOC), GCMS: Gas Chromatography Mass Spectrometry, FEC: Faecal egg count, FT–IR: Fourier–transform infrared spectroscopy, T–RFLP: Restriction Fragment Length Polymorphism.

Table 1.7–Continued3 Key selected factors altering the equine gut microbiota.

Factors	Factors	Sample	Method	Effect on microbiota	Authors

Gastrointestinal parasites	Cyathostomin	Faecal	High–throughput sequencing of bacterial 16S rRNA	• Cyathostomin infection in horses was associated with global shifts in faecal microbial composition and diversity when
				  ○ FEC of ≥100 (Chigh) versus FEC of ≤10 eggs per gram (Clow)
				  ○ FEC of ≥200 eggs per gram (C200) versus FEC of 0 (C0)
				• No significant differences in OTU alpha diversity (Shannon Index) between Chigh and Clow, or between samples collected at D0, D2 and D14 post–treatment.
				• A trend towards increased alpha diversity in Chigh versus Clow at all time–points, C200 compared with C0 at D0
				• No significant differences in beta diversity between groups.
				• There were differences in abundance of individual taxa at the phylum, class, order, family, genus and species level between Chigh and Clow samples, as well as between samples collected at D0, and D2 and D14 p.t.
				• A trend towards increased populations of Methanomicrobia (class), *Dehalobacterium* (genus) and unclassified *Dehalobacterium* and *Ruminococcus* (species) in C0 compared with C200, with the addition of methanogens of the Family *Methanocorpusculacaea*, Order *Endomicrobiales*, *Rickettsiales*, Family *Bacteroidaceae*, genus BF311 and species RFN20
				• The taxa GMD14H09 of the Phylum Proteobacteria were increased in samples from C200 compared with C0
					Peachey *et al.* (2018)

Anthelmintics	Moxidectin (*in vivo*)	Faecal	16S rRNA gene sequence analyses, fermentation kinetics and metabolic profiling	• Between 16– 160 h, small effect on the taxonomic community profile of faecal microbiota • Decrease of *Cyanobacteria*, Increase in Deferribacters (*Mucispirilllum)*, Spirochaetes (*Treponema*) in 16 hours • Increase of Deferribacter in 40– 160 hours, Increase in Spirochaetes 160 hours • Significant reduction of hay degration half way and total gas pool half way fermentation changes • Moxidectin alters carbohydrate metabolism	Daniels *et al.* (2020)
	Moxidectin & Praziquantel (*in vitro*)	Faecal	FEC analyses, 16S rRNA gene sequence analyses	• Decrease in alpha diversity, No effect on beta diversity • No changes in overall population structure or taxanomic microbiota composition	Kunz *et al.* (2019)
	Ivermectin (*in vivo*)	Faecal	FEC analyses, 16S rRNA gene sequence analyses and NMR spectroscopy	• Significant increase in microbial eveness and Shannon index. • Increase in abundance of *Clostridiales* and *Prevotellaceae* and reduced *Lactobacillaceae* and *Mogibacteriaceae* in high parasitic burden animals. • Reduced of α– and β–Proteobacteria in low parasite burden animals	Peachey *et al.* (2019)

Abbreviations: OTUs: operational taxonomic units (OTUs), The volatile organic compound (VOC), GCMS: Gas Chromatography Mass Spectrometry, FEC: Faecal egg count, FT–IR: Fourier–transform infrared spectroscopy, T–RFLP: Restriction Fragment Length Polymorphism.

Table 1.7–Continued4 Key selected factors altering the equine gut microbiota.

Factors	Factors	Sample	Method	Effect on microbiota	Authors
Anthelmintics	Fenbendazole (10 mg/kg orally for five successive days), Moxidectin (0.4 mg/kg orally) (*in vivo*)	Faeca, blood	16S rRNA gene sequence analyses	• Decrease in beta diversity in both groups at Day 7 post–treatment compared with both Day 0 & Day 14 • Decreases in both alpha & beta diversity at Day 7, reversed by Day 14 & accompanied by increases in inflammatory biomarkers • There were no significant differences in alpha diversity between moxidectin or fenbendazole sub– groups at any point. • In Group 1, alpha diversity was significantly decreased for both sub–groups on Day 7 compared with both pre–treatment and DAY 14 as assessed using the Simpson and Shannon index.	Walshe *et al.* (2019)
	Ivermectin 0.2 mg/kg (*in vivo*)	Faecal	16S rRNA sequencing (V3–V4 region)	• No significance of clustering according to time point pre– and post– anthelmintic treatment (D0 versus D14). • Anthelmintic treatment in Chigh (FEC of ≥100 eggs per gram) was associated with a significant reduction of the bacterial Phylum TM7 at D14 post–ivermectin administration, as well as a transient expansion of *the taxa Adlercreutzia* and R445B at D2 and D14 post–treatment, respectively. • In Clow, treatment was also associated with an increase in R445B (family, genus, species) at D14 • Differences in bacterial alpha diversity (Shannon diversity) between groups	Peachey *et al.* (2018)
	Panacur paste (fenbendazole 7.5 mg/ kg) (*in vivo*)	Faecal	FT–IR analysis T–RFLP analysis	• based on FT–IR data, no obvious difference in metabolite patterns could be detected.	Crotch-Harvey *et al.* (2018)
	Pyrantel pamoate paste/ Pyrantel pellet (*in vivo*)	Faecal	16S rRNA gene sequences (V2–V3 region)	• Mares in the paste group showed greater change in diversity immediately follow treatment • Mares in the pellet group showed a gradual change in microbial diversity during exposure to the anthelmintic	Rowe (2017)
	Fenbendazole, over the course of five days Ivermectin on the fifth and final day (*in vivo*)		Illumina MiSeq Genomic DNA Extraction 16S v4 rRNA PCR Amplification Illumina 16S rRNA	• In the 'pre–treatment' samples, Bacteriodetes predominated (42.6%) followed by Firmicutes (27.1%) and Verrucomicrobia (12.7 %). • Firmicutes was the most prevalent phylum among the 'post–treatment' samples accounting for 34.6 % of sequences, followed by Bacteriodetes (31.5%) and Verrucomicrobia (21.7%)	Sirois (2013)

Abbreviations: OTUs: operational taxonomic units (OTUs), The volatile organic compound (VOC), GCMS: Gas Chromatography Mass Spectrometry, FEC: Faecal egg count, FT–IR: Fourier–transform infrared spectroscopy, T–RFLP: Restriction Fragment Length Polymorphism.

1.4 EQUINE HELMINTH HOST INTERACTIONS

To date, there are an increasing of evidences in horses (Table 1.7) that parasitic infections (Clark *et al.*, 2018; Peachey *et al.*, 2018, 2019; Walshe *et al.*, 2019, 2021; Slater *et al.*, 2021) and anthelmintic administration (Rowe, 2017; Peachey *et al.*, 2018; Kunz *et al.*, 2019; Walshe *et al.*, 2019) can have an impact on the microbial community, and as such could affect the health and nutritional functionality of the horse.

1.4.1 Helminth infections and host interactions

GIT parasite–gut microbiome interactions have been studied and discussed widely in laboratory animals (Reynolds et al., 2014; Fricke et al., 2015; Holm et al., 2015; Houlden et al., 2015; McKenney et al., 2015; Cattadori et al., 2016; Parfrey et al., 2017; Su et al., 2017), livestock (Li *et al.*, 2011, 2012, 2016; S. Wu *et al.*, 2012; Zhu *et al.*, 2016; Ramírez *et al.*, 2021; Paz *et al.*, 2022) and companion animals (Šlapeta *et al.*, 2015; Duarte *et al.*, 2016; Clark *et al.*, 2018; Peachey *et al.*, 2018, 2019; Walshe *et al.*, 2019, 2021; Berg *et al.*, 2020; Slater *et al.*, 2021). These studies contribute to an enhanced comprehension of gastrointestinal parasite biology and the intricate interactions involved, including insights into improved control strategies and the prevention of anthelmintic resistance. According to Daniels *et al.*, (2020), parasites in the host alter the microbiota composition, rather than anthelminthics. However, such changes mostly do not alter the total composition and the diversity of the gut microbiome, but rather a few specific groups of gut microbial populations (Peachey et al., 2017). Nevertheless, the varying types of GI parasite infections is a likely explanation for the variability in results between studies, most likely because of the differences in experimental settings. As an example, nematode infections typically result in an increased abundance of *Bacteroidetes* (Rausch *et al.*, 2013). Theoretically, inflammation within the GIT and systemic diseases are associated with a reduction in alpha–diversity, specifically the species richness within the gut bacterial population (Manichanh et al., 2006; Sepehri et al., 2007; Abrahamsson et al., 2012 & 2014; Costa et al., 2012; Schoster et al., 2017). However, these parasites may counterintuitively inhibit inflammatory responses of the host, promoting gut homeostasis and consequently leading to an increase in alpha–diversity within the gut

microbial population. This phenomenon could support the prolonged survival of gastrointestinal parasites within the host (Walk *et al.*, 2010; Glendinning *et al.*, 2014).

In strongyle infected Welsh ponies, faecal microbial community structure, namely species richness and α–diversity in both susceptible (S) and resistant (R) to strongyle infection was not considerably altered during a mild infection period (at 43 day of grazing) (Clark *et al.*, 2018). The dominant phyla of faecal microbiota were Firmicutes and Bacteroidetes phyla followed by Fibrobacteres and Spirochaetes phyla (Clark *et al.*, 2018). In addition, species richness and abundance of faecal microbiota were increased in natural strongyle infection period (at grazing day 92 and 132) (Clark *et al.*, 2018). Due to changes in immunological pathways and energy homeostasis, carbohydrate–degrading bacteria including *Pseudomonas* and *Campylobacter* were increased in S ponies at grazing day 92. Meanwhile, butyrate–producing bacteria including *Ruminococcus*, *Clostridium* XIVa and unclassified *Lachnospiraceae* family that inhibit the inflammatory effect in the gut, were decreased in S ponies but abandoned in R ponies. Thus, S ponies are possibly prone to the disruption of mucosal homeostasis. However, the decrease in *Clostridium* XIVa could enhance the immune system in S ponies against the overgrowth of *Pseudomonas* and *Campylobacter* (Clark *et al.*, 2018). Remarkably, the protozoan concentrations also increased at grazing day 92 in S ponies and was likely associated with the host carbohydrate metabolism providing for against Strongyle infection (Dougal *et al.*, 2012). In line with Strongyle infection may enhance the appropriate environment in the large intestine of horses for commensal protozoa (Clark *et al.*, 2018).

In Cyathostomin infected horses, different dominant phyla have been observed. Peachey *et al.* (2018 & 2019) demonstrated that Bacteroidetes (42.3%) and Firmicutes (42.1%) were the dominant phyla in all samples, followed by Verrucomicrobia, Spirochaetes. Whereas Walshe *et al.* (2019) reported that the dominant phyla were Firmicutes, Bacteroidetes and Proteobacteria followed by Spirochaetes and Fibrobacteres. Notably, in Cyathostomin infected horses, the core faecal microbiota was not significantly altered (although there was a trend towards changes in faecal microbial composition and increased alpha diversity in high infection) (Peachey et al., 2018), yet changes to the faecal microbiome were found in the minor phyla, specific in some genus, class or species (Peachey et al., 2018; Walshe et al., 2019). Horses with a high faecal Cyathostomin egg count found a decrease of

Class Methanomicrobia, Genus *Dehalobacterium,* unclassified *Dehalobacterium spp. and Ruminococcus spp.* populations. As such, Cyathostomin infections may inhibit the growth of methanogens and induce changes in host–mucosal immunity (Peachey et al., 2017).

To date, there is limited evidence of the effect of *A. perfoliata* on the equine hindgut microbiome (Slater *et al.*, 2021). Furthermore, as the caecum is an essential region for hindgut fermentation, it is unclear how the presence of *A. perfoliata* will affect the digestive physiology of the horse. In *A. perfoliata* infected horses (Slater *et al.*, 2021), the presence *of A. perfoliata* reduced the abundance of some fibrolytic bacteria belonging to the family *Ruminococcaceae* UCG–004, which is similar to susceptible ponies infected with strongyles (Clark *et al.*, 2018). Consequently, a reduction in *Ruminococcus*, suggests a reduction in butanoic acid, which can lead to an increase of the inflammation (Clark *et al.*, 2018), yet this requires further investigation. Additionally, the genus *Selenomonas* 3 is more abundant in *A. perfoliata* infected animals, which is also suggested to be associated with inflammation and involved in the fermentation pathway of starch and sugars in the hindgut (Slater et al., 2021). As a result, this may be attributable to the diet or to an adaption of the host or gut microbiota to compete for nutrients with the parasite (Slater et al., 2021). *A. perfoliata* cohabit with the gut microbiota in the hindgut of the horse. Thus it is hypothesised that the gut microbiome within the hindgut including structure, species richness and functions can be altered by *A. perfoliata* infection, as with other equine gastrointestinal parasites (Clark *et al.*, 2018; Peachey *et al.*, 2018, 2019; Walshe *et al.*, 2019, 2021).

1.4.2 Anthelmintic administration

Anthelmintic treatment in horses is as a risk factor for colic (Kunz *et al.*, 2019), colitis and other inflammatory diseases (Costa *et al.*, 2012). Essentially, the alteration of the gut microbiome and faecal microbiota following anthelmintic administration for cyathostomin infections is associated with a change of immune suppressive activity, gut dysbiosis and inflammation (Costa et al., 2012; Schoster et al., 2017) e.g. a significant reduction of phylum TM7 on day 14 following ivermectin treatment (Peachey et al., 2018), a significant proliferation of Proteobacteria, decrease in Bacteroidetes as well as a considerably decreased alpha diversity and richness on day 7 following moxidectin and fenbendazole treatment (Walshe *et al.*, 2019).

On assessment of the use of the macrocyclic lactones, Moxidectin alone, Walshe *et al.* (2019) demonstrated a decrease in both alpha diversity and beta diversity of the faecal microbiota at Day 7 post–treatment, although this was reversed by Day 14. Whereas Daniels *et al.* (2020) reported that Ivermectin had a minor effect on both the community structure and the function of the gut microbiome in horses with low strongyle burdens (FEC of ≤ 50 eggs per gram) via reduced *in vitro* fibre fermentation, lower pH, altered metabolic profiles particularly at 16 hours post moxidectin treatment, indicating altered carbohydrate metabolism. However, there was no change in alpha diversity following Moxidectin treatment (Daniels *et al.*, 2020). On assessment of the use of the Ivermectin, Peachey *et al.* (2018) observed no change on core microbiota, however, a specific population, such as in horses with FEC of ≥ 100 eggs per gram (C–High), was associated with a significant reduction of the bacterial Phylum TM7 at 14 days and transient expansion of *Adlercreutzia* spp. at 2 days post–ivermectin administration. Peachey *et al.* (2019) also observed that faecal metabolites did not change in C–high horses, but in faecal samples from C–low horses (FEC of ≤ 10 eggs per gram) found increased glucose, uracil, inosine and trehalose 14 days post–treatment, indicating a reduction in the absorption of microbial metabolism products. Hu *et al.* (2021) demonstrated that overall function did not change after Ivermectin treatment for 7 days, some populations were altered such as increased the genera of *Clostridium* and *Eubacterium* and decreased *Bacteroides* and *Prevotella* which related to immunity and digestion.

I*n vivo* studies of Fenbendazole of Sirois, (2013) demonstrated a change of predominant phylum from Bacteriodetes in pre–treatment group to Firmicutes in post–treatment group. Goachet *et al.*, (2004) demonstrated changes in anaerobe bacteria, *lactobacillus* and cellulolytic bacteria, however, pH post–administration 24–48 hours were not altered. Whereas Crotch-Harvey *et al.*, (2018) did not observe any alteration on the microbial community composition and metabolites 14 days following Fenbendazole. Walshe *et al.*, (2019) found that administering Fenbendazole once daily orally for five consecutive days resulted in a significant decrease in beta diversity and richness on Day 7, followed by a significant increase in alpha diversity on Day 14 relative to Day 7 post–treatment. Study of Pyrantel from Boisseau *et al.* (2022) revealed a microbial community shifted towards another interacting and unstable state after six weeks of pyrantel treatment, however, in conjunction with cyathostomin infection. Rowe (2017) demonstrated changes in the faecal microbial

diversity following Parental pamoate for 14 days, a single dose of Pyrantel paste had greater and immediately changes in the microbial profiles following treatment, whereas horses given the Pyrantel tartrate pellet once daily had a gradual change in the microbial profiles compared to pre–treatment.

Anthelminthics will also lead to bacterial overgrowth which results in the disruption of the mucosal barrier, which could be a significant contributing factor to further deterioration in gut health and metabolic processes (Kunz *et al.*, 2019; Walshe *et al.*, 2020).

1.5 THESIS AIMS

- To improve fundamental biology of a neglected parasite, *A. perfoliata* particularly at the molecular level via transcriptomics and bioinformatics approach (Chapter 2)
- To facilitate an in–depth understanding of the potential molecular mechanisms that *A. perfoliata* utilises to interact with the host via proteomics of the adult *A. perfoliata* secretome and potential immune modulatory proteins (Chapter 3).
- To determine how *A. perfoliata EVs* demonstrate immunomodulatory functions and thus influence the mammalian immune response (Chapter 4)
- To incorporate praziquantel–equine hindgut microbiome interactions for further understanding of host–parasite (*A. perfoliata)* interaction which useful on parasite management and control (Chapter 5).

CHAPTER 2:

DE NOVO TRANSCRIPTOME CONSTRUCTION REVEALS POTENTIAL IMMUNE MODULATORS FROM ADULT *ANOPLOCEPHALA PERFOLIATA*

2.1 INTRODUCTION

At present, *A. perfoliata,* a neglected equine tapeworm is being considered widely in host–parasite interactions; however, evidence of how *A. perfoliata* interacts with the digestive physiology and health of its host horse is still limited (Lawson *et al.*, 2019; Slater *et al.*, 2021). A deeper understanding of molecular biology in *A. perfoliata* is necessary to assist further exploration of host–parasite interactions. To date, molecular analysis of *A. perfoliata* has thus far focussed on mitochondrial (mt) genome sequence data as a molecular marker of the ecological and phylogenetic relationship among the 4 families of the order *Cyclophyllidea* (Guo, 2015), and supporting morphological analyses within the Anoplocephalidae family (Guo, 2016). Nevertheless, there is no whole reference genome or supporting transcriptome profiles for further biological discovery in *A. perfoliata*, which precludes further in–depth functional genomics and proteomics profiling of *A. perfoliata* to better understand host–parasite interactions.

Current effective "omic" based technologies have been extensively used to generate in–depth molecular database resources, often transcriptomics and proteomics combined, aimed at developing sustainable control strategies for several important helminths (Cantacessi *et al.*, 2012; Choudhary *et al.*, 2015; Liu *et al.*, 2016; X.-X. Zhang *et al.*, 2017; Huson *et al.*, 2018; Cwiklinski *et al.*, 2021). Transcriptomic analysis is a powerful tool that provides insights into various aspects of gene expression and related biological processes. It allows us to understand the expression levels of messenger RNAs (mRNAs) within a cell or tissue. By exploring the transcriptome, we can gather information about gene structure, the regulation of gene expression, potential functional roles of genes, dynamics of the genome, and even the mechanisms underlying diseases caused by pathogens. High–throughput RNA sequencing (RNA–Seq) is a widely used transcriptomic technology and allows the entire transcriptome of parasitic organisms to be explored with high levels of reproducibility with relatively low cost (Wang *et al.*, 2009; Nagalakshmi *et al.*, 2010; Li *et al.*, 2014; Kukurba and Montgomery, 2015). Particularly, RNA–Seq enables transcriptomic profiling in non–model organisms or in cases where a reference genome is unavailable (Chang *et al.*, 2015; Hölzer and Marz, 2019).

The first transcriptome of parasitic flatworms (Platyhelminthes) was generated for *Fasciola hepatica* (Young *et al.*, 2010). Since then, this methodology has been further expanded to various species and life–stages in helminths (Table 2.1). Transcriptomics has been primarily dedicated to investigating various aspects such as the gene expression profiles in different tissues related to development and interactions between parasites and hosts (Huang *et al.*, 2013). Additionally, it has been employed to unravel the molecular basis of anthelmintic resistance and identify susceptible strains, aiding in the development of effective strategies for parasite control (Miranda-Miranda *et al.*, 2021). Consequently, transcriptomics offers valuable insights into the underlying molecular biology of individual parasites, shedding light on the mechanisms by which neglected parasites establish infections in hosts and adapt for long–term survival in their host environments.

Table 2.1 Transcriptomic study in trematode and cestode species from different life–stages.

Classes	**Species**
Trematodes	*Fasciola hepatica* (Cwiklinski *et al.*, 2021)
	Fasciola gigantica (Young *et al.*, 2011; X.-X. Zhang *et al.*, 2017)
	Fascioloides magna (Cantacessi *et al.*, 2012),
	Opisthorchis viverrini (Young *et al.*, 2010)
	Clonorchis sinensis (Young 2010; Yoo *et al.*, 2011)
	Paramphistomum cervi (Choudhary *et al.*, 2015)
	Eurytrema pancreaticum (Liu *et al.*, 2016)
	Calicophoron daubneyi (Huson *et al.*, 2018)
	Schistosoma mansoni (Wangwiwatsin *et al.*, 2020)
	Schistosoma japonicum (Liu *et al.*, 2020; Cheng *et al.*, 2022)
Cestodes	*Echinococcus multilocularis* (Liu *et al.*, 2017)
	Echinococcus granulosus (Pan *et al.*, 2014; Liu *et al.*, 2017; Bai *et al.*, 2020; Debarba *et al.*, 2020; Fan *et al.*, 2020; Mohammadi *et al.*, 2021)
	Hymenolepis microstoma (Preza *et al.*, 2021)
	*Taenia crassiceps (*García-Montoya *et al., 2016)*
	*Taenia pisiformis (*Yang *et al., 2012;* Chen *et al., 2018;* Zhang*, 2019)*
	Taenia multiceps (Wu *et al.*, 2012; Li *et al.*, 2021)

2.1.1 Helminth immune modulation of the host environment

Helminths have the ability to survive in the host through a variety of mechanisms. Most notably through molecules secreted into the host environment during infection, (as a part of the Excretory–Secretory Products (ESPs) (Harnett, 2014; Kobpornchai *et al.*, 2020; Gillis-Germitsch *et al.*, 2021). Various potent immune modulators have been identified in helminths, however, in this chapter we focus on Glutathione transferases (GSTs), Heat shock proteins 90 (HSP90s) and Alpha–Enolase (α–Enolase). These three immune modulators are just examples for an initial studying in *A. perfoliata* and further candidates could be investigated. GSTs are primarily known for their detoxification functions (Brophy and Barrett, 1990; Barrett, 1997, 2009; Line *et al.*, 2019), an area of expertise within my lab group Alpha–Enolase, on the other hand, functions as a metabolic enzyme in glycolysis and plays a role in the degradation of the host's extracellular matrix (Pancholi, 2001; Jolodar *et al.*, 2003; Díaz-Ramos *et al.*, 2012; Figueiredo *et al.*, 2015). Both GSTs and α–Enolase are well–established immune modulators and are increasingly recognised for their potential as immune modulators in Platyhelminths (Liebau *et al.*, 2000; Alexandra *et al.*, 2003; Burmeister *et al.*, 2008; Dowling *et al.*, 2010; LaCourse *et al.*, 2012; Kim *et al.*, 2016, 2017; Wang *et al.*, 2022). In contrast, while HSP90s are well–known for their roles in cellular homeostasis (Johnson, 2012; Roy *et al.*, 2012; Gillan and Devaney, 2014; Hoter *et al.*, 2018; Zininga *et al.*, 2018; Biebl and Buchner, 2019; Backe *et al.*, 2020), they have received relatively limited exploration as novel immune modulators in Platyhelminths. Consequently, these three immune modulators have captured my interest and motivated me to conduct extensive research in *A. perfoliata.*

In helminths, a crucial role of the GST superfamily (GSTs, EC 2.5.1.18) is in the detoxification system (Brophy and Barrett, 1990; Barrett, 1997, 2009; Line *et al.*, 2019). The cytosolic GST classes identified in helminths are Mu, Pi and Sigma, with some also demonstrating Alpha and Omega classes (Rossum *et al.*, 2001; Chemale *et al.*, 2006; Burmeister *et al.*, 2008; Nguyen *et al.*, 2010; Iriarte *et al.*, 2012; LaCourse *et al.*, 2012; Morphew *et al.*, 2012; Bae *et al.*, 2016; Kim *et al.*, 2016, 2017; Ferguson and Bridge, 2019; Miles *et al.*, 2022). However, several GST classes, including Sigma and Omega, have also been identified to have a role in immune modulation. Based on Sigma class GSTs known prostaglandin D synthase activity, they have been indicated to have the potential to modulate

the host immune response (Alexandra *et al.*, 2003; Dowling *et al.*, 2010; LaCourse *et al.*, 2012). Omega class GSTs, play a major role in the response to oxidative stress (Liebau *et al.*, 2000; Burmeister *et al.*, 2008; Kim *et al.*, 2017) and the protection of the reproductive system during maturation in *C. sinensis* (Kim *et al.*, 2016). Interestingly, a novel *F. hepatica* Omega class GST (GSTO2) has recently been discovered in modulating murine macrophages which repressed the cell viability, and induced apoptosis of RAW264.7 macrophages, as well as inhibiting pro–inflammatory cytokine and enhancing anti–inflammatory cytokine expression (Wang *et al.*, 2022). Of note, there is no evidence at present which indicates that Mu class GSTs have an immune modulatory potential.

HSP90s play essential roles in the stress response as well as molecular chaperone proteins for major cellular homeostasis (Johnson, 2012; Roy *et al.*, 2012; Gillan and Devaney, 2014; Hoter *et al.*, 2018; Zininga *et al.*, 2018; Biebl and Buchner, 2019; Backe *et al.*, 2020). HSP90 has also been thought to be involved in host immune system modulation via platyhelminth secretomes (Liu *et al.*, 2009; Xu *et al.*, 2020). However, less evidence of HSP90s is available for platyhelminths than other protein superfamilies including GSTs. Moreover, information on the role of HSP90s as an immune modulator in helminth infections is sparse. Xu *et al.* (2020) demonstrated that *S. japonicum* HSP90 (Sjp90α) is found in soluble egg antigens and egg secretory proteins, located in the Reynolds' layer within mature eggs, on the tegument of adult, suggesting its involvement in triggering the host immune response. Furthermore, recombinant Sjp90α demonstrated the ability to stimulate dendritic cells expression and elicit a T helper 17 (Th17) response (Xu *et al.*, 2020).

Enolase (EC 4.2.1.11) is a key glycolytic enzyme (Fukano and Kimura, 2014). α–Enolase (α, Eno1) is expressed in most tissue and has multi–functional roles, including the plasminogen activation system, plasminogen receptor, plasmin role in apoptosis, plasmin and intracellular signalling (Pancholi, 2001; Díaz-Ramos *et al.*, 2012). α–Enolase possesses immunomodulatory properties in binding with the host plasminogen or fibrinogen and activating plasmin–mediated proteolysis, resulting in the degradation of the extracellular matrix of the host as well as preventing clot formation around the parasites which eventually facilitate helminth penetration into the host tissue (Jolodar *et al.*, 2003; Marcilla *et al.*, 2007; Ramajo-Hernández *et al.*, 2007; Wang *et al.*, 2011; Figueiredo *et al.*, 2015; Maizels *et al.*, 2018; Jiang *et al.*, 2019).

The comprehensive analysis, which includes the construction and exploration of the adult *A. perfoliata* transcriptome, has the potential to provide a detailed understanding of the unique biological characteristics of *A. perfoliata*. Furthermore, the transcripts obtained from *A. perfoliata* can aid in the identification of significant RNA sequences that are likely expressed as candidates for known immune modulators. Due to how little is known about immune modulators in *A. perfoliata*, this study would provide an initial key knowledge associated with host–parasite interactions, as well as the support for further proteomic analysis of the *A. perfoliata* secretome.

2.1.2 AIMS AND OBJECTIVES

To address the lack of fundamental biological knowledge of *A. perfoliata*, I aimed to generate a transcriptome of adult *A. perfoliata*. To utilise this transcriptome to better understand host–parasite interactions, I aimed to identify *A. perfoliata* transcripts encoding genes that are known to have immune modulatory roles in other platyhelminth species. To achieve these aims, RNA was extracted from whole adult *A. perfoliata* isolated from natural infections within the equine caecum. RNA was sequenced via Illumina sequencing and *de novo* assembly used to generate a transcriptome. Bioinformatic approaches were then used to identify transcripts of known immune modulators and further investigate isoforms.

It was hypothesised that there will be expression of known immune modulatory proteins identified in other platyhelminth species within the adult *A. perfoliata* transcriptome; Key immune modulatory RNA sequences of interest will include GST (Sigma and Omega classes), Heat shock protein 90 (alpha and beta isoforms) and alpha–Enolase within the adult *A. perfoliata* transcriptome.

2.2 MATERIALS AND METHODS

2.2.1 Collection of adult *Anoplocephala perfoliata*

Six individual biological replicates of live adult *A. perfoliata* were collected from the ileocecal valve of six naturally infected horses immediately post–slaughter from a commercial abattoir (Swindon, UK). All horses used in this study were killed for purposes unrelated to this research. Following removal of the caecum from the horse, the organ was opened at the ileocaecal valve and live adult *A. perfoliata* specimens were collected. The worms were identified as *A. perfoliata* based on their unique morphology (4 ear–shaped lappets posterior to muscular suckers) and location within the host (ileum & adjacent large intestine, adjacent to the ileo–caecal valve) (Gasser *et al.*, 2005; Walden *et al.*, 2014; Nielsen, 2016). Specimens were thoroughly washed thrice in pre–warmed sterile phosphate–buffered saline (PBS; pH 7.4; Thermo Scientific, Loughborough, UK) at 39 °C to remove contamination including caecal fluid, bacteria and host materials. Each live adult *A. perfoliata* was subsequently transferred into a 2 mL microcentrifuge tube, immediately snap–frozen in liquid nitrogen for 1 minute and stored on dry ice for transportation to the laboratory, where they were stored at -80°C until further analysis.

2.2.2 Total RNA extraction and purification

Total RNA was extracted and purified from adult *A. perfoliata* (n = 6) using the Direct–zol™ RNA MiniPrep Plus Kit (Zymo Research, Cambridge, UK) with the Tough–to–Lyse Samples (cells and tissue) procedure, according to the manufacturer's protocol. *A. perfoliata* were removed from -80 °C and ≤50 mg of the adult worm containing the anterior end (scolex) was removed and chopped into small pieces before transferring into a 2 mL microcentrifuge tube containing 600 µL of RNA Isolation Reagent, TRI Reagent® (Zymo Research, Cambridge, UK). Tissue samples were subsequently disrupted via bead beating by adding a pre–frozen (-80 °C) 5 mm stainless–steel bead in each tube (Qiagen, Manchester, UK) and placing in a TissueLyser LT (Qiagen, Manchester, UK) for 2 minutes at 50 oscillations per second. Where complete tissue disruption was not achieved, the bead beating process was repeated. To separate any remaining debris, samples were centrifuged at 14,000 *x g* for 30 seconds at 4°C and the supernatant transferred into a RNase–free tube for subsequent RNA purification. The

protocol provided by the manufacturer was followed from this point. Following purification, RNA was stored at −80 °C for subsequent analysis.

2.2.3 RNA Quantity and Quality Assessment

RNA concentration of each purified RNA sample was determined using a NanoDrop1000 spectrophotometer (Thermo Scientific, Loughborough, UK). The overall quality and integrity of the purified RNA were initially determined by agarose gel electrophoresis to inspect the presence of the 28S and 18S rRNA bands. A 1% w/v agarose gel was prepared containing 0.5 g of agarose (Thermo Scientific, Loughborough, UK) and 5 µL of SafeView Nucleic Acid Staining Solution (NBS Biologicals, Cambridgeshire, UK) in 50 mL of 0.5x TBE gel electrophoresis buffer (0.89 mM Tris–base, 0.89 mM Boric acid, 20 mM EDTA, pH 8.0). The same preparation of 0.5x TBE buffer was also used as a TBE gel electrophoresis buffer to fill the electrophoresis apparatus (Thermo Scientific, Loughborough, UK). For each sample, 4 µL of purified RNA was mixed with 2 µL of 6x Sample Loading Buffer (PCR Biosystems, London, UK) and loaded onto the 1% w/v agarose gel alongside 3 µL of a PCRBIO Ladder IV (PCR Biosystems, London, UK), ranging from 100 bp to 1500 bp. Samples were run on the gel at a constant voltage of 120 V using a Biorad PowerPac 300 Electrophoresis Power Supply (BioRad, Hemel Hempstead, UK) for approximately 30–45 minutes or until the gel–loading buffer stain reached approximately ¾ of the way down to the end of the gel. The gel was visualised using a Molecular Imager® Gel Doc™ XR+ System (BioRad, Hemel Hempstead, UK). If RNA integrity was demonstrated by clear 28S and 18S rRNA bands, samples were then subjected to assessment via a Bioanalyzer (Agilent 2100 Technologies, CA, USA) to generate a RIN value, following the manufacturer's instructions (Agilent RNA 6000 Pico Kit).

2.2.4 RNA–Seq library construction and next generation sequencing

Purified RNA from 6 biological replicates of individual adult *A. perfoliata* underwent next generation sequencing at the Translation Genomics facility, Institute of Biological, Environmental & Rural Sciences (IBERS), Aberystwyth University. Briefly, RNA purity was assessed using Qubit® RNA HS Assay Kits with the Qubit® Fluorometer (Invitrogen, Thermo Scientific, Loughborough, UK). cDNA libraries were then constructed by reverse transcribing 500 ng of total RNA from each sample using the TruSeq RNA Library Preparation Kit v2

according to the Low Sample (LS) Workflow (Illumina, Cambridge, UK) with all reagents supplied by Illumina (Cambridge, UK). RNA adapter indexes were added and ligated on both ends of cDNA to allow multiple indexing of samples pooled together. To this end, cDNA libraries synthesis was accomplished then cDNA fragments with adapters were amplified through PCR amplification (Illumina, Cambridge, UK).

Following amplification, cDNA quality was determined on a 1.2% w/v agarose gel containing 1.2 g of agarose (Melford Laboratories, Suffolk, UK) in 100 mL of 1x TAE gel electrophoresis buffer (40 mM Tris, 20 mM Acetate, 1 mM EDTA, pH 8.0) mixed with GelRed® Nucleic Acid Gel Stain (5 µL per 100 mL; Biotium, Cambridge Bioscience, Cambridge, UK). The same preparation of 1x TAE buffer was used as a TAE gel running buffer. HyperLadder™ 100 bp (Bioline Meridian Life Science, London) was run on the gels with the samples at a voltage of 300 V (Apelex PS 304 MiniPac II Electrophoresis Power Supply; Apelex, Lisses, France) for approximately 30 minutes or until the dye migrated down ¾ of the gel. Gels were imaged using a GelDoc Red system (Alpha InnoTech Ltd).

Amplified cDNA libraries were quantified using an Ultrospec EPOCH (BioTek, China), at an absorbance measurement of 280 nm to normalise a pooling volume of each sample library prior to sequencing. Following cDNA library concentration, the 6 individual sample cDNA libraries were pooled at equal concentrations to construct the final library. The final concentration of pooled cDNA libraries was quantified using Qubit™ dsDNA BR Assay Kits with the Qubit® 2.0 Fluorometer (Invitrogen, Life Technologies, Paisley, UK), according to the manufacturer's protocol. Cluster generation and sequencing were performed according to the MiSeq Workflow using MiSeq Reagent Kit v3 (Illumina, Cambridge, UK). Briefly, cDNA libraries were adjusted in equimolar concentration to 10 nM concentration with 10 nM Tris HCl (Melford Laboratories, Suffolk, UK) and 0.05 % v/v Tween–20 solution (Sigma–Aldrich, Merck Life Sciences, Dorset, UK), followed by diluting to 2 nM with buffer EB (Qiagen, Manchester, UK). cDNA libraries were denatured to a single stranded DNA using 0.1 M NaOH (Sigma–Aldrich, Merck Life Sciences, Dorset, UK) and diluted again to a final loading concentration at 6 pM in hybridisation buffer (Illumina, Cambridge, UK). The library mixes were loaded onto the reagent cartridge followed by loading the MiSeq flow cell and reagent cartridge for clustering and paired–end sequencing on a Illumina Miseq™, according to standard protocols (Illumina, Cambridge, UK). Base pairs (bp) per read were generated in 2x75

bp format. A total of 36 sequencing output files (two for each sample from 3 runs) were then saved for subsequent bioinformatics analysis.

2.2.5 *De novo* transcriptome assembly and bioinformatics analysis

The sequencing bioinformatics pipeline was performed through the Galaxy web platform hosted by IBERS, Aberystwyth University (version 17.01; https://galaxy.ibers.aber.ac.uk/; (Goecks *et al.*, 2010; Afgan *et al.*, 2018; Jalili *et al.*, 2020).

2.2.5.1 Quality control assessment

Prior to assembly, all raw FASTQ sequencing data files were assessed via FastQC (Galaxy tool version 0.69; Babraham Bioinformatics; Andrews, 2010; Andrews *et al.*, 2015). All reads with a phred quality scores <20 were discarded (although no reads were found below this cut–off). Based on the FastQC assessment, the reads were trimmed via Trimmomatic (Galaxy Version 0.36.0; Bolger *et al.*, 2014). Illuminaclip was initially used to remove Truseq Illumina adapter contamination followed by Slidingwindow to remove from the 3' end (4–*base* wide sliding window, cutting once the average quality per base dropped below 20) and Minlen to remove any reads below 36 bp long. Trimmed reads were again assessed through FastQC to ensure that the read quality of the new RNA-Seq datasets had phred scores of ≥30 across more than 70% of the bases.

2.2.5.2 *De novo* transcriptome sequencing analysis pipeline

The trimmed reads after the quality filtering were subjected to *de novo* assembly and each of the 6 *A. perfoliata* sequencing samples were assembled individually in Trinity (v2.11.0; https://github.com/trinityrnaseq/trinityrnaseq/wiki; Grabherr *et al.*, 2011; Haas *et al.*, 2013), using default parameters. To determine a common set of transcripts between all 6 biological replicates, all 6 assemblies were clustered together with Cluster Database at High Identity with Tolerance (cd–hit) software (version 4.8.1; http://weizhongli-lab.org/cd-hit/ref.php; Li *et al.*, 2001& 2002; Li and Godzik, 2006; Huang *et al.*, 2010; Fu *et al.*, 2012). All coding regions within transcript sequences were identified using the assembled contigs as input through Transdecoder software (part of the Trinity package, version Trinity–v2.11.0; http://transdecoder.sf.net; Haas *et al.*, 2013). The parameter setting used to detect the open reading frames (ORFs) in the transcript sequences, and to produce a list of protein sequences

according to identify ORFs were at least 100 amino acid long and the ORFs retention of 3000. This process led to version 1.0 of the *A. perfoliata* transcriptome.

To identify the possible host (horse) contamination in the parasite transcriptome, the set of protein sequences derived from the clustered transcripts was compared to the protein and CDS files from the *Equus caballus* genome from Ensemble (version 3.0 https://www.ensembl.org), and *Hymenolepis microstoma* as the closest relative genome sequenced cestode (PRJEB124 available at https://parasite.wormbase.org/; Tsai *et al.*, 2013). In each case BLASTp or BLASTx was used with default options, with a minimum e–value of 0.1. Transcripts which were more similar (i.e. lower e–values) to the host (horse) rather than to a related flatworm (*H. microstoma*) were deemed to be likely host contaminants and were subsequently removed from the transcriptome. Each transcript sequence was initially labelled as a "Horse", "Worm" and "N/A" (not assigned as horse or worm) according to the bit–scores for each BLAST. Subsequently, the same transcript that contained more than 1 opening reading frames were grouped together. The groups of "Worm and Worm", "Horse and Worm", "Worm and N/A", "Horse and N/A" and "N/A and N/A" were kept as likely worm transcripts. Whereas the group of "Horse and Horse" were removed as a host contaminant. This process led to the compiled *A. perfoliata* transcriptome version 2.0 (74607 records), which was used for further bioinformatics analysis.

2.2.5.3 Functional annotation and Gene Ontology (GO) terms analysis

The resulting *A. perfoliata* assembly was functionally annotated to predict the functional description (DE) and GO functional classification of the unitranscripts, describing the Biological Processes (BP), Molecular Functions (MF), and Cellular Components (CC). The GO terms dataset were summarised and visualised using OmicsBox (BioBam Bioinformatics, 2019; Götz *et al.*, 2008). The expression level of transcripts using RNA–seq data was quantified by Salmon (https://combine-lab.github.io/salmon/; Patro *et al.*, 2017) and the expression value was expressed in units of Transcripts Per Million mapped reads (TPM). Subsequently, the top 50 most expressed genes identified by TPM value were then searched against the Omicsbox annotation output to obtain the summary descriptive data. Transcripts that were not in the annotated output were subsequently translated into protein sequences using ExPASy Translate tools (https://web.expasy.org/translate/; Gasteiger *et al.*, 2003), followed by

manual BLASTp against the NCBI (nr) protein database using a protein query (BLASTp; https://blast.ncbi.nlm.nih.gov/Blast.cgi; Altschul *et al.*, 1997) and a cutoff set at $1.0E^{-03}$ to obtain the protein description.

2.2.6 Bioinformatic analysis of potential immune modulators

The transcriptome was initially analysed for the presence of characterised immune modulators, previously identified in helminths (*Schistosoma mansoni*, *Fasciola hepatica*, *Onchocerca volvulus, Clonorchis sinensis*, *Opisthorchis viverrini*, *Trichinella spiralis*, *Hymenolepis microstoma*, *Ancylostoma caninum*, *Ancylostoma ceylanicum*, *Toxocara canis, Nippostrongylus brasiliensis*, *Necator americanus*, *Brugia malayi*, *Heligmosomoides polygyrus* and *Acanthocheilonema viteae*) by performing tBLASTn searched against the *A. perfoliata* transcriptome (Section 2.2.5.2) through BioEdit Sequence Alignment Editor (Version 7.2.6.1; Hall, 1999). The number of expected hits of similar quality (e–value) cutoff was set at $1.0E^{-15}$ using 76 immunomodulator bait peptide sequences retrieved from Genbank and NCBI Reference Sequence (http://www.ncbi.nlm.nih.gov/) (see immunomodulators listed in Appendix 2.1). Subsequently, the top 5 hits from each bait sequence were searched and translated with ExPASy Translate tools (https://web.expasy.org/translate/; Gasteiger *et al.*, 2003) to identify the best opening reading frames (ORFs). The peptide sequence of the bait proteins were submitted to Pfam database (version 34.0; http://pfam.xfam.org/; Mistry *et al.*, 2021) to confirm protein domain conservation.

Key potential immune modulatory transcripts for Glutathione transferase (GSTs) Superfamily, Cytoplasmic Heat Shock Protein 90 (HSP90) and Alpha–Enolase (α–Enolase) were further investigated within the *A. perfoliata* transcriptome, version 2.0. Protein sequences from all three potential immune modulators (GSTs, HSP90s and α–Enolase) were put through the same bioinformatics pipeline, multiple sequence alignment and phylogenetic analysis. Briefly, the *A. perfoliata* transcript was uploaded to a local nucleotide database using a Basic Local Alignment Search Tool (BLAST) in BioEdit Sequence Alignment Editor (Version 7.2.6.1; Hall, 1999). Subsequently, protein sequences of recognised GST superfamily (Alpha, Delta, Epsilon, Kappa, Mu, Nu, Omega, Pi, Sigma, Theta and Zeta GST classes), HSP90 family (Alpha and Beta isoforms) and α–Enolase from 15, 22 and 14 different species, respectively (mammalian, nematode, trematodes, cestodes and insects) were retrieved from Genbank and

NCBI Reference Sequence (http://www.ncbi.nlm.nih.gov/) (see recognised GSTs, HSP90 and α–Enolase proteins sequences in Appendix 2.2). Recognised sequences were blasted (tBLASTn; Altschul *et al.*, 1997) against the *A. perfoliata* transcript version 2.0 through BioEdit Sequence Alignment Editor (Version 7.2.6.1; Hall, 1999). The number of expected hits of similar quality (e–value) was set at $1.0E^{-15}$, $1.0E^{-20}$ and $1.0E^{-15}$ for GSTs, HSP90s and α–Enolase, respectively.

The tBLASTn output which was homologous with the top hits (highest e–value) of recognised GSTs, HSP90s and α–Enolase protein sequences, was taken as the representative *A. perfoliata* nucleotide sequences and translated into protein sequences using ExPASy Translate tools (https://web.expasy.org/translate/; Gasteiger *et al.*, 2003) to identify the best open reading frames. To ensure that the selected protein sequences represented potential candidates, each protein sequence underwent an additional search against the NCBI (nr) protein database using a protein query (BLASTp; https://blast.ncbi.nlm.nih.gov/Blast.cgi; Altschul *et al.*, 1997). Subsequently, all representative protein sequences were classified into protein super–families, domain prediction and functional site analysis through InterProScan (version 77.0; http://www.ebi.ac.uk/interpro/; Jones *et al.*, 2014; Blum *et al.*, 2021). The resulting InterPro domains classified as GSTs, HSP90s and α–Enolase with N–terminal domain (NTD) and C–terminal domain (CTD) were retained as a unique confirmed protein sequence. Non–GSTs, HSP90s and α–Enolase protein sequences, very short protein sequences (less than 50 amino acids) and fragmented split sequences were manually selected and then excluded. All unique classified sequences, or one representative if isoforms were present, were taken as a final representative *A. perfoliata* GSTs, HSP90s and α–Enolase protein sequences for subsequent sequence alignment and phylogenetic analysis.

2.2.7 Sequence alignment and phylogenetic analysis of potential immune modulators

The resulting representative *A. perfoliata* sequences (GSTs, HSP90s and α–Enolase) and their recognised protein sequences were ClustalW aligned using BioEdit Sequence Alignment Editor (Version 7.2.6.1; Hall, 1999). To initially determine the overall evolutionary relationship between each *A. perfoliata* GST class and recognised GST protein sequences, all final representative sequences of *A. perfoliata* GST were put through phylogenetic trees analysis with their recognised protein sequences. All unrooted phylogenetic trees were constructed and visualised in MEGA X (version 10.1.7; Hall, 2013; Kumar *et al.*, 2018).

Reliability of the phylogenetic tree was estimated with 1000 bootstrap replicates, using a Maximum Likelihood (ML) method. For the ML method the parameters were set with a likelihood of amino acid data determined based upon 5 discrete gamma rate categories. An initial tree for the heuristic search was obtained automatically by applying ML Heuristic method with Nearest–Neighbor–Interchange (NNI) and number of threads at 3. Additional phylogenetic trees for individual GST classes of Sigma and Omega, unrooted phylogenetic trees for HSP90s and α–Enolase were also constructed, as described above.

The secondary structures (included beta sheets and alpha helixes) for the resulting representative Sigma and Omega GST classes (identified during phylogenetic analysis), HSP90s and α–Enolase were predicted using the Predict Secondary Structure Protein Analysis Workbench (PSIPRED 4.0; http://bioinf.cs.ucl.ac.uk/psipred/; Jones, 1999; Buchan and Jones, 2019). Following that, protein domain identification and architecture were analysed using Simple Modular Architecture Research (SMART) tools (http://smart.embl.de; Letunic and Bork, 2018; Letunic *et al.*, 2021) to obtain novel *A. perfoliata* Sigma and Omega classes GSTs, HSP90α and α–Enolase sequences.

2.3 RESULTS

2.3.1 Sequencing of the *A. perfoliata* transcriptome

RNA integrity of all samples (n=6) was demonstrated on 1% w/v agarose gel by clear 28S and 18S rRNA bands (Appendix 2.3). The mean ± SD RNA integrity numbers (RIN values) was 2.35 ± 0.07 and ranging from 2.2 and 2.4. Miseq Illumina sequencing was completed on cDNA, resulting in a total of 36 raw reads obtained from 3 technical replicates. The mean ± SD reads per sample was approximately 3.0 ± 0.6 million reads per sample. This provided a dataset of *A. perfoliata* RNA–sequencing containing 109,267,236 paired–end reads for subsequent bioinformatics analysis (Table 2.2).

Table 2.2 The summary statistics of the raw Illumina sequencing and the *de novo* transcriptome assembly of the adult *A. perfoliata* from naturally infected horses (n=6).

Illumina RNA sequencing	**Raw reads**	**Trimmed reads**
Total reads (bp)	109,267,236	104,519,050
Mean ± SD reads per sample (bp)	3,035,201 ± 633,399	2,903,307 ± 608,363
Sequence length (bp)	35–76	36–76
GC percentage (%)	46	46
***De novo* Trinity assembly**	**Assembled transcript V1.0**	**Assembled transcript V2.0**
Total assembled length (bp)	60,821,233	56,913,324
Number of contigs	76,917	74,607
Number of contigs (without Isoforms)	26,985	26,653
Mean ± SD contig lengths per sample (bp)	791 ±797	763 ± 762
Max. contig lengths (bp)	11,266	11,266
Min. contig lengths (bp)	201	201
Contigs N50	1,214	N/A
TransDecoder	**Protein Dataset V1.0**	**Protein Dataset V2.0**
Number of protein sequences	36,694	34,341

2.3.2 *De novo* assembly of the *A. perfoliata* transcriptome

Raw reads were trimmed following quality control analysis, leaving a mean ± SD of 2.9 ± 0.6 million reads per sample and final read lengths between 36 and 76 bp (Table 2.2). For each biological replicate, the trimmed reads underwent *de novo* assembly and a total of 199,943 transcripts sequences were obtained across all samples. Following removal of homologous sequences (redundant sequences) of the merged assembled transcripts, the resulting clustered non–redundant (nr) database had 76,917 contigs including isoforms. To this end,

the *A. perfoliata* transcriptome was named as *A. perfoliata* transcript version 1.0 containing the total assembled contigs length of 60,821,233 bp (Table 2.2). The total assembled 76,917 contigs were used as nucleotide sequences for converting to protein sequences, providing 36,694 protein sequences in *A. perfoliata* transcriptome version 1.0.

A total of 2,353 sequences were determined to be host (*E. caballus*) when the protein candidates were blasted against the *E. caballus* genome and related flatworm genome (*Hymenolepis microstoma*). These sequences were removed from the dataset, leaving all sequences that were deemed to be 'worm' (27,603 sequences) or 'N/A' (6,738 sequences). Therefore, following the removal of homologous sequences and host contamination, a total of 74,607 decontaminated transcript sequences (contained 34,341 protein sequences) remained to comprise the compiled *A. perfoliata* transcript version 2.0 for downstream bioinformatics analysis, with the total assembled contigs length of 56,913,324 bp (Table 2.2). The complete *A. perfoliata* transcriptome version 2.0 is available for interrogation at https://sequenceserver.ibers.aber.ac.uk. The Transcriptome Shotgun Assembly project has been deposited at DDBJ/EMBL/GenBank, under the accession GJFT00000000.

2.3.3 Transcriptome functional annotation, Gene Ontology terms analysis

Omicsbox functional annotation revealed that 3,244 (9.4%) protein sequences could not be annotated, while 19,445 (56.6%) sequences were successfully fully annotated and the remaining sequences were annotated with BLAST hits only. Of the annotated sequences, the top 3 species hits were to the tapeworm species, *H. diminuta*, *E. granulosus* and *H. microstoma* (Figure 2.1). Annotated sequences were associated with 59,828 high–quality GO terms, with a mean ± SD GO level of 6.277 ± 2.441 (Figure 2.2). The majority of GO terms were classified according to the three main GO categories; Biological process (BP; 20,030 GO terms, 33.5%) followed by Molecular function (MF; 23,775 GO terms, 39.7%) and Cellular component (CC; 16,023 GO terms, 26.8%). The most frequent GO terms identified by GO level 3 were related to organic substance metabolic process, cellular metabolic process and primary metabolic process under BP category; organic cyclic compound binding, heterocyclic compound binding and ion binding under MF category; membrane, intrinsic component of membrane and intracellular anatomical structure among CC category (Figure 2.3).

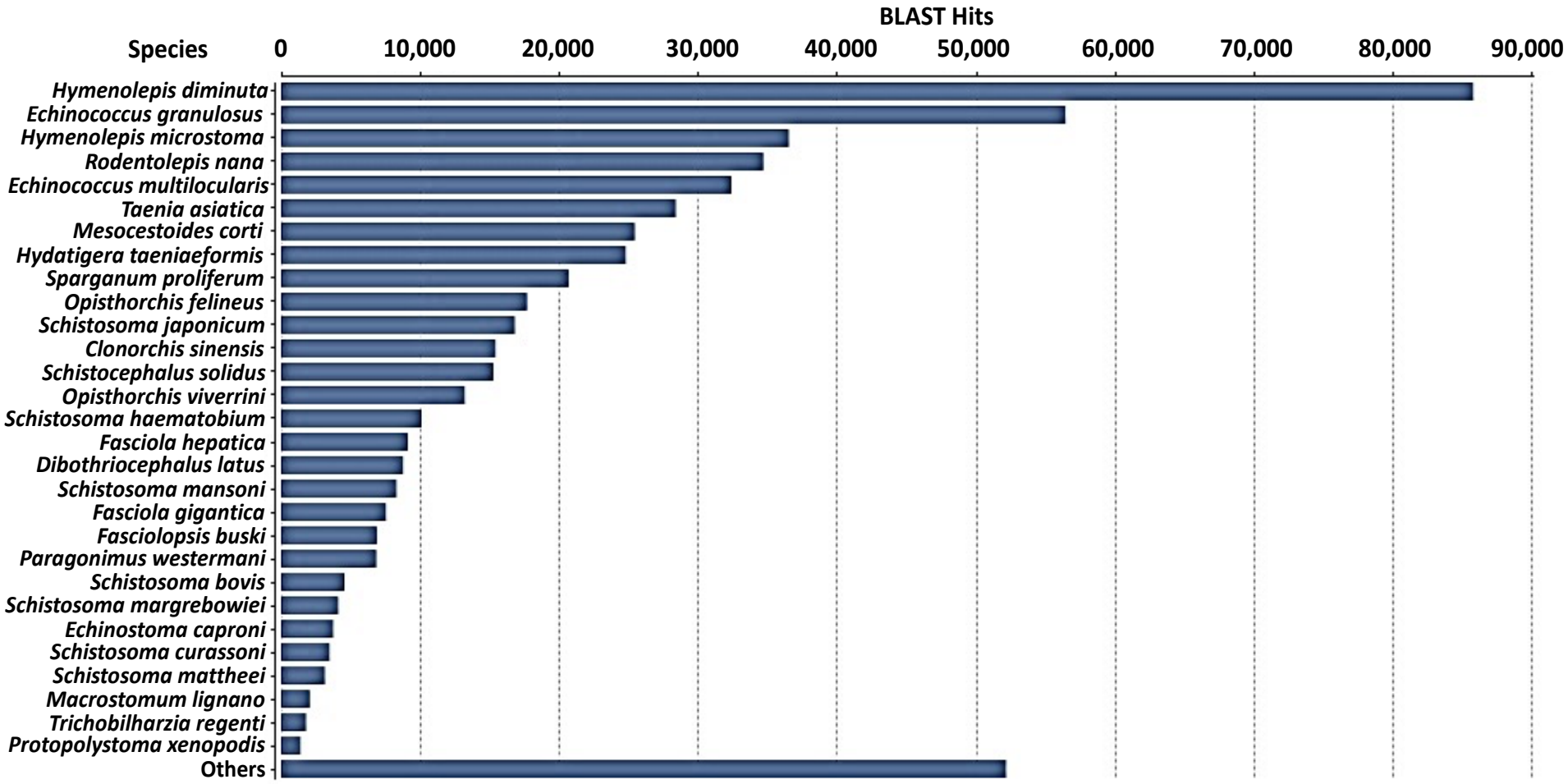

Figure 2.1 Species distribution of the BLAST hits found for proteins predicted from annotated sequences within the *A. perfoliata* transcriptome with OmicsBox functional annotation.

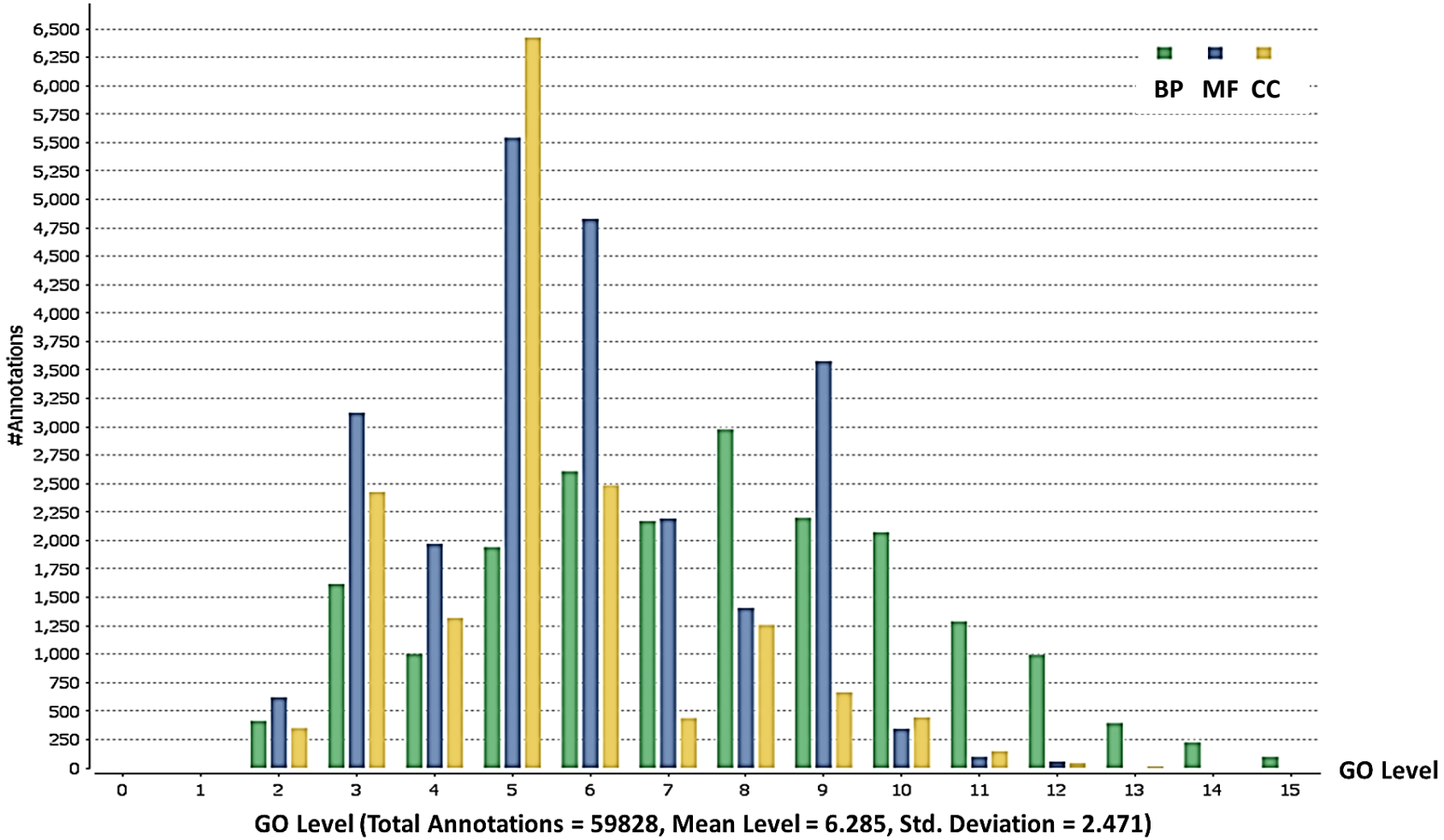

Figure 2.2 The distribution of annotated sequences within the *A. perfoliata* transcriptome per GO level using OmicsBox functional annotation, according to the Biological process (BP), Molecular function (MF) and Cellular component (CC). The GO level distribution graph showed a total of 59828 annotations with a mean level of 6.285 and standard deviation 2.471.

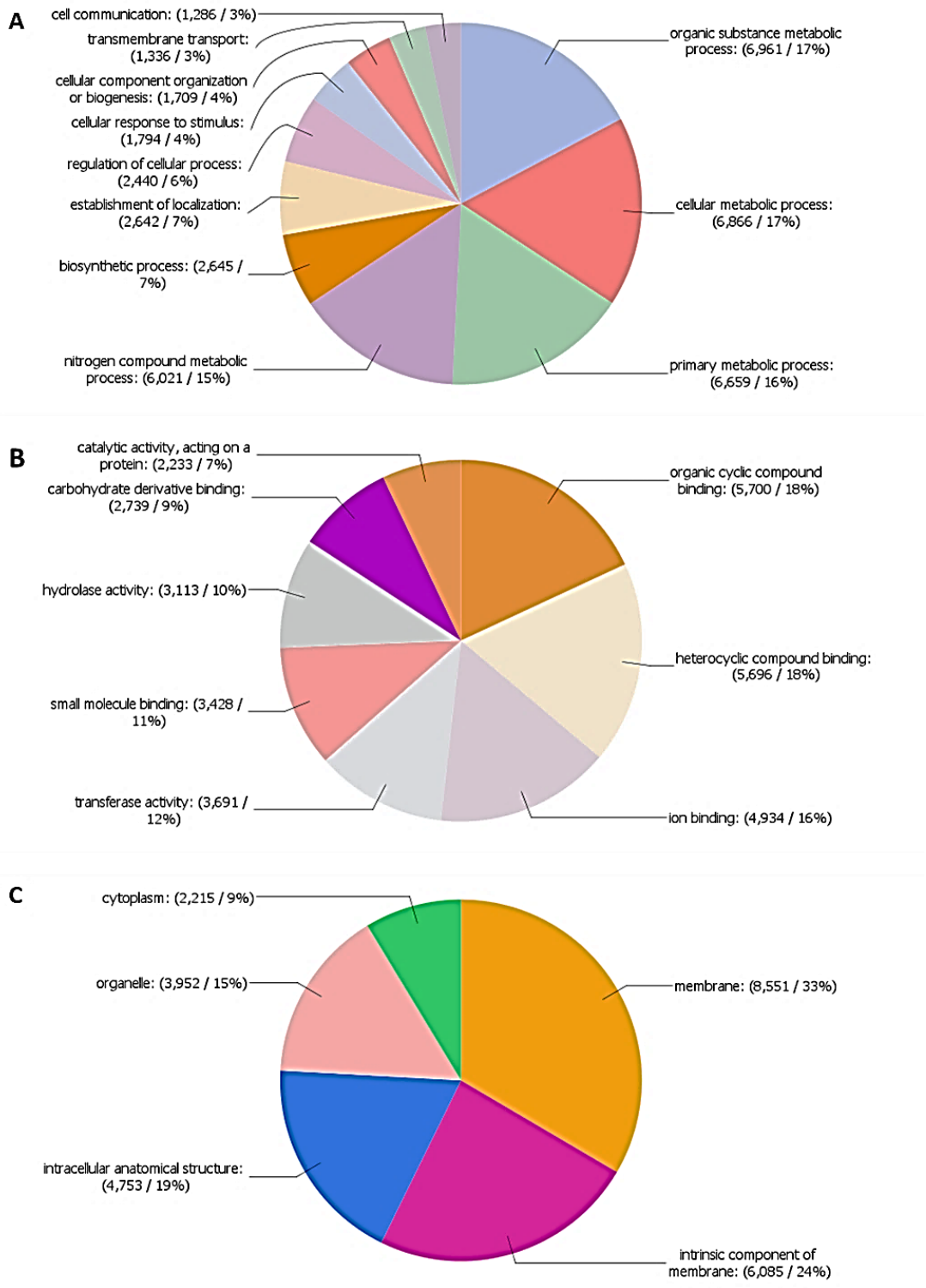

Figure 2.3 Summary of the distribution of GO terms in the *A. perfoliata* transcriptome at level 3 representing the relative abundance of GO terms in each of the three main categories: (A) Biological process (BP), Molecular function (MF) and Cellular component (CC).

2.3.4 Transcripts expression analysis of *A. perfoliata* transcriptome

The mean ± SD TPM was 12.4 ± 222. The top 50 TPM across the 6 biological replicates of *A. perfoliata*, are summarised in Table 2.3, with the transcript description from the functional annotation through Omicsbox. Known genes of interest in other platyhelminths were noted amongst the top 50 abundance transcripts such as, protein superfamilies including Dynein light chain (IPR037177) superfamily, EF–hand domain pair (IPR011992), Armadillo–like helical (IPR011989), Armadillo–type fold (IPR016024) and Profilin superfamily (IPR036140). Of note, 33 (66%) of the top 50 most abundant transcripts in *A. perfoliata* were classified as uncharacterised transcripts.

Table 2.3 The top 50 most abundant transcripts in *A. perfoliata* (across all 6 biological replicates) calculated from Salmon and expressed as a TPM value. The description of each transcript is demonstrated from Omicsbox functional annotation.

Rank	Gene ID	Length	Mean Effective Length	Mean Number Reads	Mean TPM	Description
1	DN10805_c3_g6_i1_11702	1036	858	407936	46601	Uncharacterised
2	DN10805_c3_g2_i9_11698	1754	1591	264055	16600	Uncharacterised
3	DN6887_c0_g1_i1_76818	384	212	34703	16001	Uncharacterised
4	DN8498_c0_g2_i2_20529	333	162	17101	10383	Uncharacterised
5	DN14755_c0_g1_i1_41815	314	148	10387	6916	Uncharacterised
6	DN8064_c0_g1_i1_68336	477	315	13860	4289	Uncharacterised
7	DN8427_c0_g1_i1_72770	410	234	10236	4283	Uncharacterised
8	DN7932_c0_g1_i1_6806	401	225	9709	4239	Uncharacterised
9	DN12386_c1_g1_i9_39644	4006	3843	158692	4199	Transcript antisense to ribosomal rna protein
10	DN10805_c3_g2_i7_11692	3260	3097	133004	4199	Uncharacterised
11	DN3788_c0_g1_i1_50567	426	265	10398	3869	Uncharacterised
12	DN8606_c1_g1_i3_340	314	146	5533	3826	Uncharacterised
13	DN12640_c1_g1_i8_71952	9547	9384	316400	3293	Uncharacterised
14	DN10987_c0_g1_i3_65072	874	711	23587	3277	Expressed conserved protein
15	DN5384_c0_g1_i1_75533	414	241	8058	3248	Uncharacterised
16	DN8805_c0_g1_i1_60212	444	283	8962	3129	Uncharacterised
17	DN12068_c0_g3_i1_63804	1028	851	25275	2996	Expressed conserved protein
18	DN13746_c0_g1_i1_26674	358	199	5871	2919	Uncharacterised
19	DN10069_c0_g1_i3_2055	985	809	21491	2662	Expressed conserved protein
20	DN11085_c1_g1_i5_42186	381	221	5786	2641	Uncharacterised
21	DN9799_c0_g1_i1_46050	508	346	9173	2617	Dynein light chain 1, cytoplasmic
22	DN118_c0_g1_i1_52814	595	420	10683	2540	Tegumental protein
23	DN10418_c3_g5_i1_34715	483	311	8002	2501	Immunogenic protein
24	DN6144_c0_g1_i1_49576	641	469	11504	2425	Dynein light chain type 1 2
25	DN3712_c0_g1_i1_698	602	440	10689	2400	Dynein light chain 1, putative
26	DN10763_c1_g5_i1_22341	281	128	3136	2298	Uncharacterised
27	DN7817_c0_g1_i1_51569	1013	850	19568	2191	Expressed conserved protein
28	DN9590_c0_g2_i1_51137	480	318	6844	2115	Uncharacterised

Table 2.3–continued. The top 50 most abundant transcripts in *A. perfoliata* (across all 6 biological replicates) calculated from Salmon and expressed as a TPM value. The description of each transcript is demonstrated from Omicsbox functional annotation.

Rank	Gene ID	Length	Mean Effective Length	Mean Number Reads	Mean TPM	Description
29	DN10367_c0_g1_i3_29401	1522	1347	28911	2057	Expressed conserved protein
30	DN3791_c0_g1_i1_14014	632	470	9552	2007	Uncharacterised
31	DN4055_c0_g1_i1_61482	518	346	7092	1989	Dynein light chain type 1 2
32	DN6146_c0_g1_i2_38481	514	352	6601	1906	Uncharacterised
33	DN15763_c0_g1_i1_57495	831	668	12973	1887	Tegumental protein
34	DN10204_c0_g1_i2_51272	516	354	6655	1828	Uncharacterised
35	DN12126_c0_g1_i9_41589	2283	2120	38789	1826	Uncharacterised
36	DN502_c0_g1_i1_32021	462	284	5326	1809	Uncharacterised
37	DN10922_c1_g1_i5_14239	1292	1129	19933	1778	Deoxyhypusine hydroxylase
38	DN5442_c0_g1_i1_26423	439	261	4666	1728	Uncharacterised
39	DN5954_c0_g1_i2_54752	370	201	3606	1703	Uncharacterised
40	DN9433_c0_g1_i5_18544	424	251	4344	1674	8 kDa glycoprotein
41	DN12201_c0_g3_i1_43360	334	176	3135	1672	Uncharacterised
42	DN11009_c0_g1_i1_3069	711	535	9247	1669	Uncharacterised
43	DN11588_c0_g1_i4_75797	406	245	4072	1669	Uncharacterised
44	DN10667_c1_g1_i2_72481	469	296	5181	1666	Uncharacterised
45	DN5960_c0_g1_i2_30732	274	122	1928	1571	Uncharacterised
46	DN7341_c0_g1_i1_31615	484	322	4974	1532	Dynein light chain 1, cytoplasmic
47	DN1202_c0_g1_i1_62670	642	470	7386	1532	Profilin allergen
48	DN10641_c0_g1_i1_57690	585	423	6391	1528	Uncharacterised
49	DN15681_c0_g1_i1_62555	578	416	6427	1513	Uncharacterised
50	DN9547_c0_g1_i1_1108	381	221	3260	1477	Uncharacterised

2.3.5 Bioinformatics of potential immune modulators

Initial *A. perfoliata* transcriptome analysis by tBLASTn and Pfam demonstrated significant hits for 46 of the 76 bait immune modulators, leading to a total of 566 contigs (462 unique contigs) which were identified as potential immune modulator homologs (cutoff 1 x 10^{-15}) (Table 2.4, Appendix 2.1). After the Pfam domain searches from the top 5 hits for each of the 46 bait proteins (152 contigs with 122 unique contigs), confirmed a total of 96 unique contigs as potential immune modulators with over 70% domain conservation and 26 unique contigs hits with less than 70% domain conservation.

Table 2.4 Immune modulator bait sequences from transcriptome and proteome analysis and contig ID hits from the *A. perfoliata* transcriptome analysis. The top 5 translated hits from each bait sequence were confirmed using PFAM. The hits with >70% functional domain conservation are shaded in green or <70% functional domain conservation are shaded in yellow (see full information in Appendix 2.1).

No.	Name of bait sequence	Total Hits	Hits Contig ID	Description
1	*Schistosoma mansoni* Calpain 1 (Smp_214180)	14	DN4288_c0_g1_i1_31793	Calpain
			DN8134_c0_g1_i2_2225	Calpain
			DN9786_c0_g1_i2_72693	Calpain A
			DN9786_c0_g1_i1_72692	Calpain A
			DN8870_c0_g2_i5_9689	Calpain A
2	*Schistosoma mansoni* Calpain 2 (Smp_137410)	19	DN9786_c0_g1_i2_72693	Calpain A
			DN9786_c0_g1_i1_72692	Calpain A
			DN11727_c0_g1_i2_61275	Family C2 unassigned peptidase (C02 family)
			DN8870_c0_g2_i5_9689	Calpain A
			DN11280_c0_g3_i1_60806	Calpain A
3	*Schistosoma mansoni* TSP2 (Smp_335630)	37	DN12118_c0_g3_i5_41623	Leukocyte surface antigen CD53
			DN10515_c0_g1_i10_29170	Leukocyte surface antigen CD53
			DN11070_c1_g1_i4_16427	Leukocyte surface antigen CD53
			DN12587_c0_g3_i1_73053	Leukocyte surface antigen CD53
			DN10391_c0_g1_i10_3751	Leukocyte surface antigen CD53
4	*Schistosoma mansoni* Sm23 transmembrane protein (Smp_017430)	47	DN11950_c0_g1_i3_46360	Uncharacterised
			DN11950_c0_g1_i2_46359	Uncharacterised
			DN5933_c0_g1_i1_30778	Uncharacterised
			DN9904_c0_g1_i4_4304	Uncharacterised
			DN10515_c0_g1_i7_29168	Leukocyte surface antigen CD53
5	*Schistosoma mansoni* Cathepsin B (Smp_085180)	2	DN9013_c0_g2_i3_9574	Cathepsin b
			DN6585_c0_g1_i2_52284	Cathepsin b
6	*Schistosoma mansoni* Cathepsin D (Smp_013040)	1	DN1780_c0_g1_i1_17249	Cathepsin d (lysosomal aspartyl protease)
7	*Fasciola hepatica* Cathepsin L Peptidase	27	DN10215_c0_g1_i10_1389	Cysteine protease
			DN10215_c0_g1_i8_1388	Cysteine protease
			DN12594_c0_g1_i4_73468	Cathepsin L cysteine protease
			DN11706_c0_g1_i7_61136	Cathepsin L cysteine protease
			DN12173_c0_g1_i11_41498	Cathepsin L cysteine protease
8	*Fasciola hepatica* Cathepsin 2L Peptidase	27	DN10215_c0_g1_i10_1389	Cysteine protease
			DN11706_c0_g1_i7_61136	Cathepsin L cysteine protease
			DN12594_c0_g1_i4_73468	Cathepsin L cysteine protease
			DN10215_c0_g1_i8_1388	Cysteine protease
			DN12173_c0_g1_i11_41498	Cathepsin L cysteine protease
9	*Schistosoma mansoni* Leucine aminopeptidase 1 (Smp_030000)	3	DN8903_c0_g1_i1_52178	Putative aminopeptidase W07G4.4
			DN11744_c0_g1_i1_48021	Putative aminopeptidase W07G4.4
			DN11744_c0_g1_i2_48022	Leucyl aminopeptidase
10	*Schistosoma mansoni* Leucine aminopeptidase 2 (Smp_083870)	3	DN8903_c0_g1_i1_52178	Putative aminopeptidase W07G4.4
			DN11744_c0_g1_i1_48021	Putative aminopeptidase W07G4.4
			DN11744_c0_g1_i2_48022	Leucyl aminopeptidase
11	*Schistosoma mansoni* Arginase (Smp_059980)	6	DN10464_c0_g1_i2_59297	Agmatinase mitochondrial–like
			DN11086_c0_g1_i4_42134	Agmatinase mitochondrial–like
			DN11086_c0_g1_i2_42133	Agmatinase mitochondrial–like
			DN11086_c0_g1_i6_42135	Agmatinase mitochondrial–like
			DN9955_c0_g1_i1_17555	Agmatinase mitochondrial–like
12	*Schistosoma mansoni* BMP (Smp_343950)	1	DN15780_c0_g1_i1_57523	Bone morphogenetic protein 2

Table 2.4–continued 2. Immune modulator bait sequences from transcriptome and proteome analysis and contig ID hits from the *A. perfoliata* transcriptome analysis. The top 5 translated hits from each bait sequence were confirmed using PFAM. The hits with >70% functional domain conservation are shaded in green or <70% functional domain conservation are shaded in yellow (see full information in Appendix 2.1).

No.	Name of bait sequence	Total Hits	Hits Contig ID	Description
13	*Schistosoma mansoni* Acetylcholinesterase (Smp_154600)	7	DN10838_c0_g1_i1_62967	Acetylcholinesterase
			DN11171_c0_g1_i1_62356	BC026374 protein (S09 family)
			DN11307_c0_g1_i1_39219	Acetylcholinesterase
			DN5821_c0_g1_i2_36524	Neuroligin–4, Y–linked
			DN6095_c0_g2_i1_68248	Neuroligin–4, Y–linked
14	*Nippostrongylus brasiliensis* Acetylcholinesterase	6	DN10838_c0_g1_i1_62967	Acetylcholinesterase
			DN11171_c0_g1_i1_62356	BC026374 protein (S09 family)
			DN5821_c0_g1_i2_36524	Neuroligin–4, Y–linked
			DN5090_c0_g2_i1_63985	Uncharacterised
			DN6095_c0_g2_i1_68248	Neuroligin–4, Y–linked
15	*Schistosoma mansoni* Phosphatidylserine decarboxylase proenzyme 1 (Smp_021830)	4	DN6014_c0_g1_i2_68245	Phosphatidylserine decarboxylase proenzyme
			DN6014_c0_g1_i1_68244	Phosphatidylserine decarboxylase proenzyme
			DN979_c0_g1_i1_39046	phosphatidylserine decarboxylase proenzyme
			DN13199_c0_g1_i1_36812	phosphatidylserine decarboxylase proenzyme
16	*Schistosoma mansoni* Phosphatidylserine synthase 1 (Smp_127890)	1	DN6150_c0_g1_i2_49591	phosphatidylserine synthase 1
17	*Schistosoma mansoni* Phosphatidylserine synthase 2 (Smp_125780)	1	DN6150_c0_g1_i2_49591	phosphatidylserine synthase 1
18	*Schistosoma mansoni* Serpin (Serine protease inhibitor) (Smp_090080)	4	DN12464_c0_g1_i3_71373	Unnamed protein product
			DN10645_c0_g1_i6_57768	Serine protease inhibitor
			DN5832_c0_g1_i1_36564	Serpin B8
			DN11133_c0_g2_i3_24057	Serine protease inhibitor
19	*Schistosoma mansoni* Superoxide dismutases (SODs) (Smp_176200)	1	DN7926_c0_g1_i1_57618	Superoxide dismutase [Cu–Zn]
20	*Schistosoma mansoni* Glutathione–S–transferase 28 kD (GST 28) (Smp_306860)	2	DN3993_c0_g1_i1_58938	Glutathione S–transferase class–mu 28 kda isozyme
			DN10944_c0_g1_i2_40229	ADP ribosylation factor 2
21	*Schistosoma mansoni* Glutathione–S–transferase 26 kD (GST 26) (Smp_163610)	227	DN10359_c1_g2_i1_29384	Glutathione S–transferase
			DN10325_c1_g7_i1_3824	Glutathione S–transferase
			DN11650_c5_g1_i4_54174	Glutathione S–transferase
			DN12274_c0_g2_i15_43535	Glutathione S–transferase
			DN12275_c2_g2_i1_68703	Glutathione S–transferase
22	*Schistosoma mansoni* thioredoxin glutathione reductase (TGR) (Smp_048430)	4	DN10093_c0_g1_i4_2011	Thioredoxin glutathione reductase
			DN6580_c0_g2_i1_15786	Thioredoxin glutathione reductase
			DN10491_c0_g1_i3_59313	Dihydrolipoamide dehydrogenase
			DN10491_c0_g1_i2_59312	Dihydrolipoamide dehydrogenase
23	*Fasciola hepatica* TPx (Thioredoxin peroxidase)	2	DN3303_c0_g1_i1_3647	Peroxiredoxin 1
			DN10337_c2_g3_i2_29708	Uncharacterised
24	*Schistosoma mansoni* Peroxiredoxin (Smp_322080)	2	DN3303_c0_g1_i1_3647	Peroxiredoxin 1
			DN10337_c2_g3_i2_29708	Uncharacterised
25	*Fasciola hepatica* Peroxiredoxin (A0A2H1CGV5/D915_05992)	2	DN3303_c0_g1_i1_3647	Peroxiredoxin 1
			DN10337_c2_g3_i2_29708	Uncharacterised
26	*Fasciola hepatica* Peroxiredoxin (A0A2H1C7L1/D915_10207)	2	DN3303_c0_g1_i1_3647	Peroxiredoxin 1
			DN10337_c2_g3_i2_29708	Uncharacterised

Table 2.4–continued 3. Immune modulator bait sequences from transcriptome and proteome analysis and contig ID hits from the *A. perfoliata* transcriptome analysis. The top 5 translated hits from each bait sequence were confirmed using PFAM. The hits with >70% functional domain conservation are shaded in green or <70% functional domain conservation are shaded in yellow (see full information in Appendix 2.1).

No.	Name of bait sequence	Total Hits	Hits Contig ID	Description
27	*Schistosoma mansoni* Thioredoxin (Smp_054470)	18	DN11064_c0_g2_i2_53099	Uncharacterised
			DN12253_c1_g2_i7_68485	Uncharacterised
			DN12253_c1_g2_i1_68480	Uncharacterised
			DN16298_c0_g1_i1_39003	Uncharacterised
			DN10913_c1_g1_i4_14323	Uncharacterised
28	*Schistosoma mansoni* VAL6 (Smp_124050)	3	DN5797_c0_g1_i1_52760	Golgi–associated plant pathogenesis–related protein
			DN4751_c0_g1_i2_8068	Uncharacterised
			DN10072_c0_g1_i1_40924	Venom allergen (val) protein
29	*Ancylostoma caninum*, Ancylostoma secreted protein	8	DN11836_c0_g2_i1_69709	Peptidase inhibitor
			DN11047_c0_g2_i1_67118	Venom allergen (val) protein
			DN11047_c0_g1_i4_67120	Venom allergen
			DN11047_c0_g1_i3_67119	Venom allergen
			DN4099_c0_g1_i2_36713	Uncharacterised
30	*Necator americanus*, Ancylostoma secreted protein	9	DN9093_c0_g1_i2_60117	Uncharacterised
			DN11047_c0_g1_i4_67120	Venom allergen
			DN11047_c0_g1_i3_67119	Venom allergen
			DN4099_c0_g1_i2_36713	Uncharacterised
			DN4099_c0_g1_i1_36712	Uncharacterised
31	*Schistosoma mansoni* Sm14 (Fatty acid binding protein) (Smp_095360)	3	DN10318_c0_g1_i1_67570	Fatty acid–binding protein FABP2
			DN1125_c0_g1_i1_57386	Fatty acid–binding protein
			DN9249_c0_g1_i2_7433	Fatty acid–binding protein FABP2
32	*Fasciola hepatica* Fatty acid–binding protein type 3	2	DN10318_c0_g1_i1_67570	Fatty acid–binding protein FABP2
			DN9249_c0_g1_i2_7433	Fatty acid–binding protein FABP2
33	*Brugia malayi* Asparagine tRNA Synthetase (AsnRS)	7	DN12226_c0_g1_i2_68698	Asparaginyl tRNA synthetase cytoplasmic
			DN9945_c0_g1_i1_4316	Asparaginyl tRNA synthetase cytoplasmic
			DN10561_c0_g1_i7_29119	Asparaginyl tRNA synthetase cytoplasmic
			DN11509_c1_g1_i9_62133	Asparaginyl tRNA synthetase cytoplasmic
			DN10561_c0_g1_i5_29118	Asparaginyl tRNA synthetase cytoplasmic
34	*Necator americanus* Metalloproteinase	2	DN9257_c0_g1_i1_57880	Family M13 unassigned peptidase (M13 family)
			DN9191_c0_g1_i2_6454	Endothelin–converting enzyme
35	*Schistosoma mansoni* SmInAct	1	DN12824_c0_g1_i1_54884	Inhibin beta B chain
36	*Schistosoma mansoni* SmATPDase1 (Smp_042020)	1	DN8415_c0_g1_i1_7791	Ectonucleoside triphosphate diphosphohydrolase
37	*Schistosoma mansoni* Ectonucleotide pyrophosphatase (SmNPP–5) (Smp_153390)	5	DN1832_c0_g1_i1_13035	Ectonucleotide pyrophosphatase:phosphodiesterase
			DN8881_c0_g1_i1_47537	Ectonucleotide pyrophosphatase:phosphodiesterase
			DN14098_c0_g1_i1_63192	Ectonucleotide pyrophosphatase:phosphodiesterase
			DN5273_c0_g1_i1_59766	Ectonucleotide pyrophosphatase:phosphodiesterase
			DN3258_c0_g1_i1_44766	Uncharacterised
38	*Onchocerca volvulus* Alpha–enolase	5	DN14469_c0_g1_i1_24672	Enolase
			DN7852_c0_g1_i1_40713	Enolase
			DN9213_c0_g1_i1_45970	Enolase
			DN13262_c0_g1_i1_2554	Enolase B
			DN14116_c0_g1_i1_34224	Enolase
39	*Brugia malayi* BmK1	2	DN10317_c0_g1_i12_53432	Astacin protein
			DN10317_c0_g1_i9_53429	Astacin protein

Table 2.4–continued 4. Immune modulator bait sequences from transcriptome and proteome analysis and contig ID hits from the *A. perfoliata* transcriptome analysis. The top 5 translated hits from each bait sequence were confirmed using PFAM. The hits with >70% functional domain conservation are shaded in green or <70% functional domain conservation are shaded in yellow (see full information in Appendix 2.1).

No.	Name of bait sequence	Total Hits	Hits Contig ID	Description
40	*Schistosoma mansoni* Serine Protease–2 (SmSP–2)	26	DN11035_c1_g3_i1_42129	Mastin precursor
			DN11087_c0_g1_i2_53046	Mastin precursor
			DN11087_c0_g1_i1_53045	Mastin precursor
			DN12112_c0_g1_i3_66557	Subfamily S1A unassigned peptidase (S01 family)
			DN10312_c2_g3_i6_3805	Mastin precursor
41	*Fasciola hepatica* Heat shock protein 90 alpha (Fhep THD20903.1)	9	DN11960_c0_g1_i1_46290	Molecular chaperone HtpG
			DN9350_c0_g1_i2_37241	Putative endoplasmin
			DN11414_c0_g1_i1_45013	Endoplasmin
			DN11437_c0_g1_i3_56596	Heat shock protein 90
			DN11205_c0_g2_i1_23358	Heat shock protein 90
42	*Hymenolepis microstoma* Sigma Class Glutathione Transferase like (Hmic CDS25704)	1	DN5806_c0_g1_i1_22697	AChain A, Glutathione S–transferase 28 Kda
43	*Hymenolepis microstoma* Sigma Class Glutathione Transferase like (Hmic CDS28394)	3	DN3993_c0_g1_i1_58938	Glutathione S–transferase class–mu 28 kda isozyme
			DN10944_c0_g1_i2_40229	ADP ribosylation factor 2
			DN8069_c0_g1_i1_4835	Uncharacterised
44	*Clonorchis sinensis* Omega Class Glutathione Transferase 1 (Csin ANK78262)	6	DN9643_c1_g1_i1_33799	Stringent starvation protein A
			DN9643_c2_g1_i3_33801	Stringent starvation protein A
			DN8371_c0_g1_i1_36357	Stringent starvation protein A
			DN9506_c0_g1_i2_1042	Stringent starvation protein A
			DN11078_c1_g1_i6_53065	Stringent starvation protein A
45	*Schistosoma mansoni* Omega Class Glutathione Transferase (Sman Q86LC0)	1	DN11479_c1_g2_i1_45003	Stringent starvation protein A
46	*Schistosoma mansoni* Omega Class Glutathione Transferase (Sman AAO49385)	2	DN11078_c1_g1_i6_53065	Stringent starvation protein A
			DN11524_c0_g1_i1_75686	Stringent starvation protein A
47	*Schistosoma mansoni* Sm16 (SPO–1 and SmSLP) (Smp_341790)	No hits	No hits	No hits
48	*Schistosoma mansoni* Alpha–1/IPSE (Smp_334590)	No hits	No hits	No hits
49	*Schistosoma mansoni* Omega–1 (Smp_334170, Smp_333930, Smp_334240)	No hits	No hits	No hits
50	*Toxocara canis* TES–32	No hits	No hits	No hits
51	*Toxocara canis* TES–70	No hits	No hits	No hits
52	*Schistosoma mansoni* Cystatin B (cysteine protease inhibitor) (Smp_006390)	No hits	No hits	No hits
53	*Schistosoma mansoni* SmKL–1 (Serine–protease inhibitor) (Smp_307450)	No hits	No hits	No hits
54	*Schistosoma mansoni* Sm29 Tegumental Protein (Smp_072190)	No hits	No hits	No hits
55	*Heligmosomoides polygyrus* Alarmin Release Inhibitor (HpARI)	No hits	No hits	No hits

Table 2.4–continued 5. Immune modulator bait sequences from transcriptome and proteome analysis and contig ID hits from the *A. perfoliata* transcriptome analysis. The top 5 translated hits from each bait sequence were confirmed using PFAM. The hits with >70% functional domain conservation are shaded in green or <70% functional domain conservation are shaded in yellow (see full information in Appendix 2.1).

No.	Name of bait sequence	Total Hits	Hits Contig ID	Description
56	*Opisthorchis viverrini* (Ov–GRN–1)	No hits	No hits	No hits
57	*Fasciola hepatica* helminth defense molecule-1 (FhHDM–1 Fragment)	No hits	No hits	No hits
58	*Brugia malayi* Macrophage Migration Inhibitory Factor (MIF)	No hits	No hits	No hits
59	*Trichinella spiralis* Macrophage Migration Inhibitory Factor (MIF)	No hits	No hits	No hits
60	*Ancylostoma caninum* Neutrophil Inhibitory Factor (AcNIF)	No hits	No hits	No hits
61	*Brugia malayi* TGF–ß homolog–2 (TGH–2)	No hits	No hits	No hits
62	*Helig62mosomoides polygyrus* TGF–ß m63imic (TGM)	No hits	No hits	No hits
63	*Acanthocheilonema viteae* ES–62	No hits	No hits	No hits
64	*Fasciola hepatica* Fatty acid binding protein Fh15	No hits	No hits	No hits
65	*Fasciola hepatica* Mucin–like polypeptide Fhmuc	No hits	No hits	No hits
66	*Brugia malayi* Abundant larval transcript–2 protein (alt–2)	No hits	No hits	No hits
67	*Ancylostoma caninum* AcK1 (Inhibitor of potassium channel) (ANCCAN_23812)	No hits	No hits	No hits
68	*Necator americanus* Anti–inflammatory protein–1 (W2TPY4)	No hits	No hits	No hits
69	*Necator americanus* Anti–inflammatory protein–2 (W2SWZ9)	No hits	No hits	No hits
70	*Acanthocheilonema viteae* Cystatin	No hits	No hits	No hits
71	*Brugia malayi* Cystatin (CPI2_BRUMA)	No hits	No hits	No hits
72	*Onchocerca volvulus* Cystatin (CYTX_ONCVO)	No hits	No hits	No hits
73	*Clonorchis sinensis* Cystatin	No hits	No hits	No hits
74	*Schistosoma japonicum* Cystatin	No hits	No hits	No hits
75	*Schistosoma mansoni* SmKI–1 Kunitz–type serine protease inhibitor (Smp_307450)	No hits	No hits	No hits
76	*Ancylostoma ceylanicum* Tissue Inhibitor of Metalloprotease Ace–MTP–2	No hits	No hits	No hits

2.3.5.1 Characterisation of novel *A. perfoliata* Glutathione Transferases (GSTs)

The initial identification of *A. perfoliata* GST sequences within the *A. perfoliata* transcriptome by tBLASTn demonstrated a total of 330 *A. perfoliata* GST sequences, which were homologous to recognised GST superfamily sequences from mammals, insects and helminths (cutoff 1 x 10^{-15}). InterProScan of all 330 sequences followed by manual BLASTp against NCBI (nr) database predicted a total of 309 sequences as GST superfamily membership (IPR040079), thus 21 sequences were removed as non–GST sequences given they were lacking GST domains of importance. Of the 309 predicted sequences, 110 sequences were further predicted as Glutathione Transferase family (IPR040079) and 59 sequences as Glutathione transferase, Mu class membership (IPR003081), with the class of the remaining 140 GST sequences undetermined but also containing GST domain and homologous superfamily.

Of the total 309 confirmed GST sequences, 214 sequences were removed prior to phylogenetic tree construction (non–representatives chosen sequences where isoforms were presented (180), very short sequences (19) and alternative splice variant, missing exon or fragmented split sequences (15)). A phylogenetic analysis of the remaining 95 *A. perfoliata* potential GST representative sequences and 58 recognised GST sequences (mammal, helminths and insects) demonstrated that there were no *A. perfoliata* GST sequences belonging to Alpha, Delta, Epsilon, Kappa, Pi, Theta or Zeta classes based on the current transcriptome assembly (Figure 2.4). Among the group of GST classes, the largest cluster of 83 *A. perfoliata* GST sequences were clustered in the Mu class GST group, while 3 and 9 *A. perfoliata* GST sequences were clustered in Sigma and Omega GST class groups, respectively (Figure 2.4).

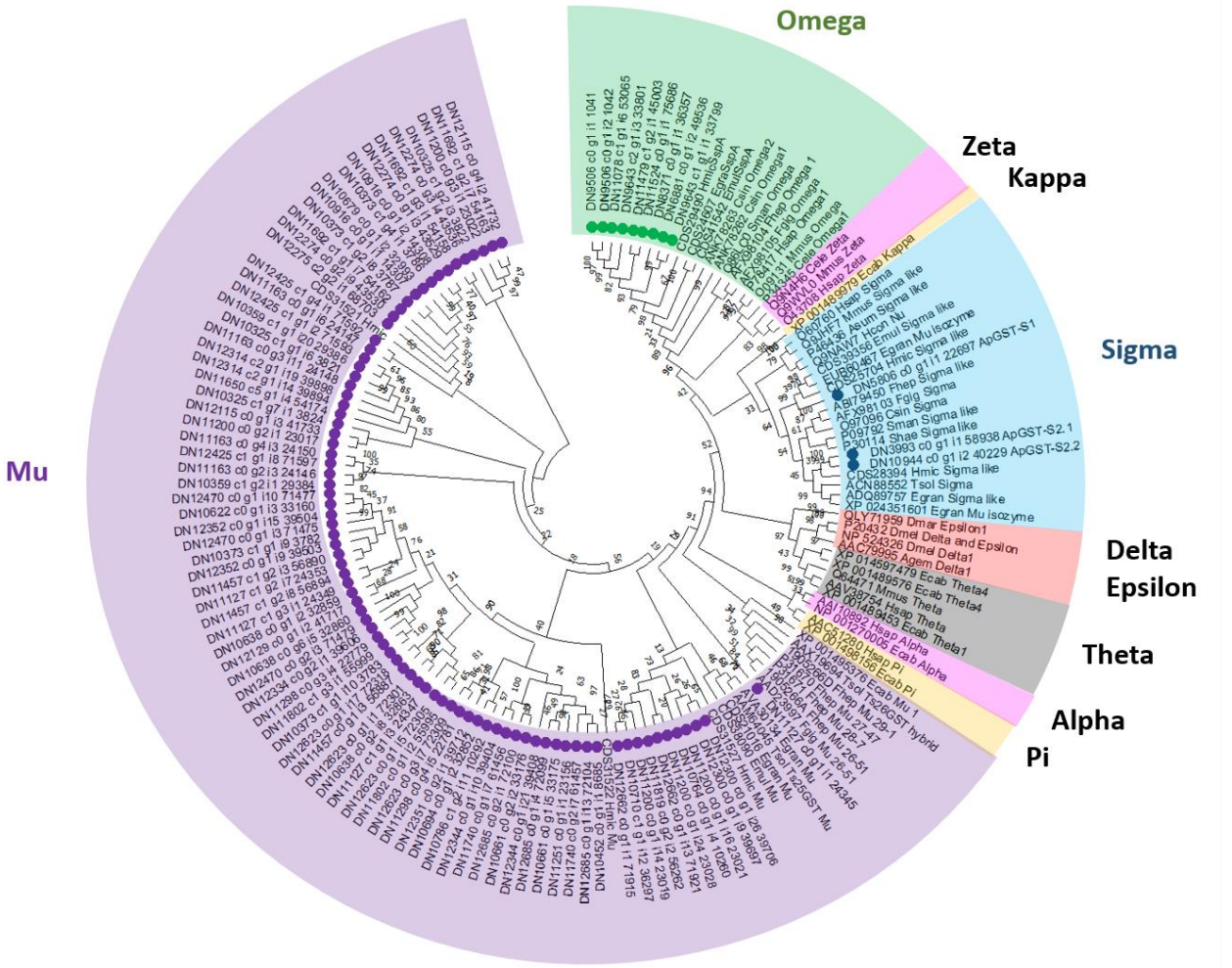

Figure 2.4 Maximum likelihood (ML) tree with JTT matrix–based model inferred from *Anoplocephala perfoliata* (AP) Glutathione Transferase (GSTs) amino acid sequences. The bootstrap consensus tree inferred from 1000 replicates. Initial tree(s) for the heuristic search were obtained automatically by applying Neighbor–Joining and BioNJ algorithms to a matrix of pairwise distances estimated using a JTT model, and then selecting the topology with superior log likelihood value. A discrete Gamma distribution was used to model evolutionary rate differences among sites (5 categories (+G, parameter = 2.2434)). This analysis involved 153 amino acid sequences. There was a total of 384 positions in the final dataset. Evolutionary analyses were conducted in MEGA X. The coloured dots in purple, green and blue demonstrate Mu, Omega and Sigma class GST sequences from *A. perfoliata*, respectively. **Abbreviations:** Agem: *Anopheles gambiae*, Asum: *Ascaris suum*, Cele: *Caenorhabditis elegans*, Csin: *Clonorchis sinensis,* Dmar: *Dermacentor marginatus*, Dmel: *Drosophila melanogaster*, Egra: *Echinococcus granulosus*, Emul: *Echinococcus multilocularis,* Ecab: *Equus caballus*, Fgig: *Fasciola gigantica,* Fhep: *Fasciola hepatica,* Hcon: *Haemonchus contortus,* Hsap: *Homo sapiens*, Hmic: *Hymenolepis microstoma*, Mmus: *Mus musculus*, Shae: *Schistosoma haematobium*, Sman: *Schistosoma mansoni*, Tsol: *Taenia solium*.

Despite Mu class GST sequences being the most commonly identified GSTs within *A. perfoliata* transcripts, there is no evidence supporting the role in immune modulation. Therefore, we only further investigated Sigma and Omega class GSTs, according to evidence indicating potential immune modulatory properties in helminths (Alexandra *et al.*, 2003; Dowling *et al.*, 2010; LaCourse *et al.*, 2012; Wang *et al.*, 2022). Of the GST sequences, 4 and 9 sequences were identified as potential Sigma and Omega class GST proteins, respectively, based on homology searching alone.

One of the 4 putative Sigma class GSTs was only a partial sequence and thus was removed from future analysis leaving 3 potential Sigma class GSTs from *A. perfoliata*. Manual BLASTp against the NCBI (nr) database supported these three putative Sigma class GST sequences as potential *A. perfoliata* Sigma class GST sequences. These 3 sequences represented two distinct enzymes; namely ApGST–S1 (DN5806_c0_g1_i1_22697, 218 amino acids) and ApGST–S2 (212 amino acids) [2.1 (DN3993_c0_g1_i1_58938) and 2.2 (DN10944_c0_g1_i2_40229)], where ApGST–2.1 and 2.2 shared 100% amino–acid sequence identity hence these two clustering with 99% bootstrap support (Figure 2.4).

The nine sequences designated as potential Omega class GSTs clustered strongly with Omega class GSTs from other platyhelminths with a high bootstrap support (96%) (Figure 2.4). These nine *A. perfoliata* sequences likely represented eight distinct enzymes based on homology (ApGST–O1 [1.1 (DN9506_c0_g1_i1_1041, 203 amino acids) and 1.2 (DN9506_c0_g1_i2_1042, 211 amino acids)], ApGST–O2 (DN11078_c1_g1_i6_53065, 182 amino acids), ApGST–O3 (DN9643_c2_g1_i3_33801, 236 amino acids), ApGST–O4 (DN11479_c1_g2_i1_45003, 236 amino acids), ApGST–O5 (DN11524_c0_g1_i1_75686, 161 amino acids), ApGST–O6 (DN8371_c0_g1_i1_36357, 236 amino acids), ApGST–O7 (DN9643_c1_g1_i1_33799, 244 amino acids) and ApGST–O8 (DN6881_c0_g1_i2_49536, 124 amino acids)), where ApGST–O1.1 and 1.2 shared 87.6% amino–acid sequence identity).

2.3.5.2 Characterisation of novel *A. perfoliata* Sigma class GSTs

A total of 2 novel *A. perfoliata* Sigma class GST (GSTS) sequences; ApGST–S1 and ApGST–S2 [2.1 and 2.2] were multiple sequence aligned separately with 16 recognised Sigma class GST sequences from mammals and helminths (Figure 2.5). The secondary characteristic structure of multiple aligned *A. perfoliata* Sigma GST homolog sequences were predicted, and overlayed on the multiple sequence alignment, with 3 β–strands and 9 α–helices, demonstrating the consistency of the secondary characteristic structure between ApGST–S1, ApGST–S2.1 and ApGST–S2.2 and the recognised Sigma class GST sequences (Figure 2.5). The Sigma class GST homologs were investigated based on the GSH–binding sites in the N–terminal domain (the catalytic tyrosine residue at the end of the first β–strand (Tyr^{8}), Phe^{9}, Arg^{14}, Trp^{39}, Lys^{43}, Pro^{52}, and Ser^{64})) and the substrate binding sites in the C–terminal domain (Yamamoto *et al.*, 2007; Nguyen *et al.*, 2010; Iriarte *et al.*, 2012; Xie *et al.*, 2015; Bae *et al.*, 2016; Zhang *et al.*, 2020). It is demonstrated that ApGST–S2.1 and 2.2 contained the highly conserved catalytic tyrosine residue (Tyr^{8}) at the end of the first β–strand and also demonstrated a high homology to other GSH–binding sites (Figure 2.5). However, the catalytic Tyrosine residues (Y) of ApGST–S1 likely shifted the alignment to the left (highlight in green colour), which is similar to *H. microstoma* Sigma like GST (HmicGST–S2, accession number CDS25704) (Figure 2.5).

A phylogenetic tree generated from the 3 *A. perfoliata* and 16 recognised Sigma class GST sequences demonstrated that ApGST–S1, ApGST–S2.1 and ApGST–S2.2 were clustered in a cestode clade, which further suggested that all three should be included in the Sigma class of the GST superfamily (Figure 2.6). ApGST–S1 clustered closest to *H. microstoma* Sigma like GST (accession number CDS25704) with a moderately bootstrap supported (52%), and also strongly clustered in the Sigma group of *E. multilocularis* Sigma like GST (accession number CDS39356) and *E. granulosus* isozyme (accession number EUB60467) with a high bootstrap value (100%). Whereas ApGST–S2.1 and 2.2 were clustered with all recognised Sigma class GST sequences from mammals and helminths (Figure 2.6).

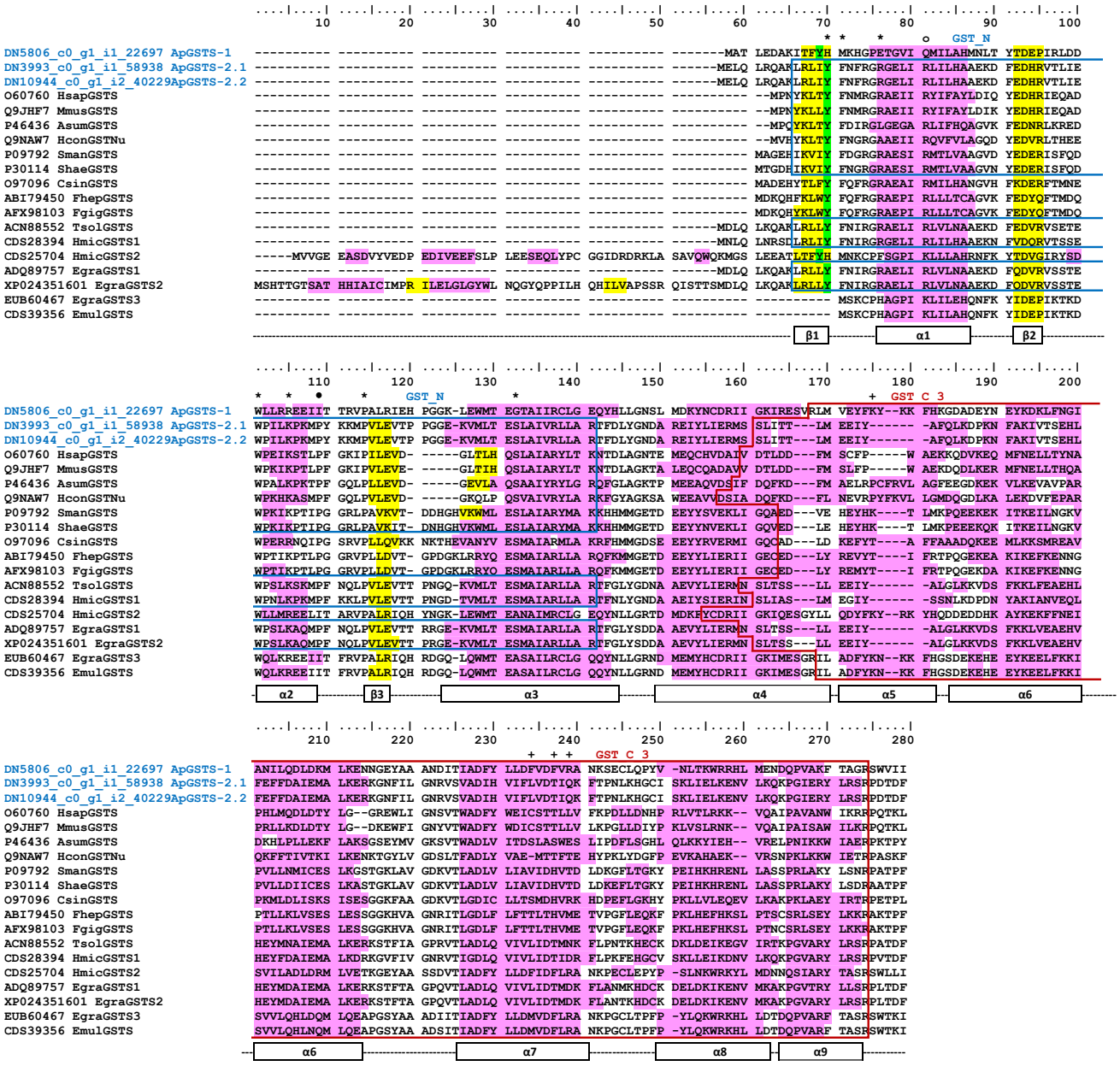

Figure 2.5 Multiple sequence alignment of the two novel Sigma class GSTs (GSTS) identified in *Anoplocephala perfoliata* (AperGST–S1 and S2). Secondary protein structure prediction using the PSIPRED Protein Analysis Workbench is presented below the alignment and is comprised of 3 β–strands, shaded in yellow, and 9 α–helices, shaded in pink. The catalytic Tyrosine residues (Y), the GSH–binding sites (Tyr[8], Phe[9], Arg[14], Trp[39], Lys[43], Pro[52], and Ser[64] and the substrate binding sites (as denoted by Yamamoto *et al.* (2007), Nguyen *et al.* (2010), Iriarte *et al.* (2012), Xie *et al.* (2015), Kim *et al.* (2016), Zhang *et al.* (2020) are shaded in green, indicated by asterisks (*) and indicated by a cross (+), respectively. The predicted N– and C–terminal GST domain profiles are indicated by blue– and red–boxes, respectively. **Abbreviations:** Hsap: *Homo sapiens*, Mmus: *Mus musculus*, Asum: *Ascaris suum*, Hcon: *Haemonchus contortus,* Sman: *Schistosoma mansoni,* Shae: *Schistosoma haematobium*, Csin: *Clonorchis sinensis,* Fhep: *Fasciola hepatica,* Fgig: *Fasciola gigantica*, Tsol: *Taenia solium*, Hmic: *Hymenolepis microstoma*, Egra: *Echinococcus granulosus*, Emul: *Echinococcus multilocularis.*

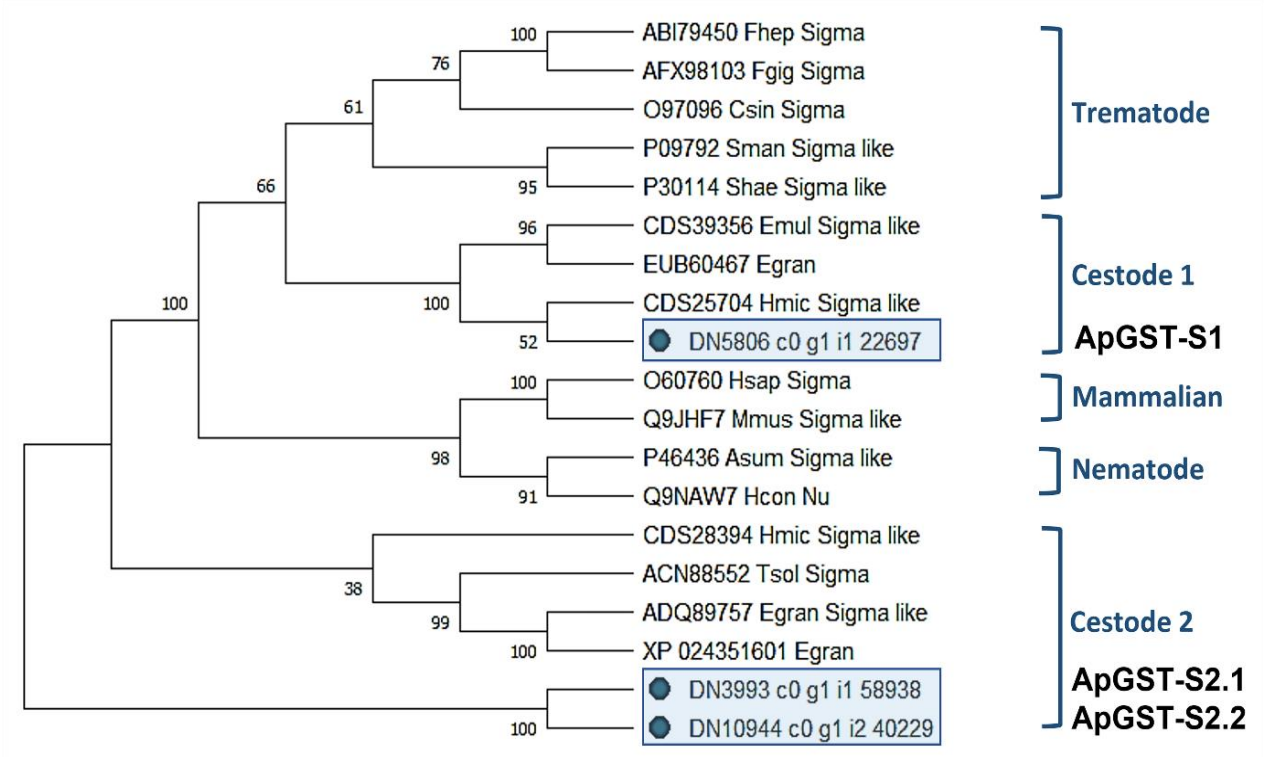

Figure 2.6 Maximum likelihood (ML) tree with JTT matrix–based model inferred from *Anoplocephala perfoliata* (AP) Sigma class GST (GSTS) amino acid sequences. The bootstrap consensus tree inferred from 1000 replicates. Initial tree(s) for the heuristic search were obtained automatically by applying Neighbor–Joining and BioNJ algorithms to a matrix of pairwise distances estimated using a JTT model, and then selecting the topology with superior log likelihood value. A discrete Gamma distribution was used to model evolutionary rate differences among sites (5 categories (+G, parameter = 4.2179)). This analysis involved 19 amino acid sequences. There was a total of 279 positions in the final dataset. Evolutionary analyses were conducted in MEGA X. **Abbreviations:** Fhep: *Fasciola hepatica,* Fgig: *Fasciola gigantica*, Csin: *Clonorchis sinensis,* Sman: *Schistosoma mansoni,* Shae: *Schistosoma haematobium*, Emul: *Echinococcus multilocularis*, Egran: *Echinococcus granulosus*, Hmic: *Hymenolepis microstoma,* Hsap: *Homo sapiens,* Mmus: *Mus musculus*, Asum: *Ascaris suum*, Hcon: *Haemonchus contortus,* Tsol: *Taenia solium*.

2.3.5.3 Characterisation of novel *A. perfoliata* Omega class GSTs

A total of 8 novel *A. perfoliata* Omega class GST (GSTO) sequences; ApGST–O1 [1.1 and 1.2] to ApGST–O8 clustered in Omega class GST branch within the whole GST phylogenetic tree were multiple sequence aligned with 11 recognised Omega class GST sequences from mammals and helminths (Figure 2.7). The secondary characteristic structure of multiple aligned *A. perfoliata* Omega GST homolog sequences predicted 3 β–strands and 5 α–helices, demonstrating the consistency of the secondary characteristic structure between ApGST–O1.1 to ApGST–O8 and 11 recognised Omega class GST sequences (Figure 2.7). Following the investigation of Omega class GST sequences based on the GSH–binding sites in the N–terminal domain, all eight novel *A. perfoliata* Omega class GST sequences had a high homology to other GSH–binding sites (Burmeister *et al.*, 2008; Kim *et al.*, 2016), conserved catalytic cysteine residue characteristic of Omega class GSTs, particularly at positions 32 (Cys^{32}) (Morphew *et al.*, 2012; Meng *et al.*, 2014; Kim *et al.*, 2016). However, all lacked the proline–rich residues in the Omega class characteristic N–terminal extension (PXXP motif) (Morphew *et al.*, 2012). Of note, the amino acid length of ApGST–O8 was truncated (DN6881_c0_g1_i2_49536; 124 amino acids), and therefore, it was excluded for further phylogenetic tree analysis.

A phylogenetic tree was generated from the 7 novel *A. perfoliata* Omega class GST sequences (ApGST–O1.1 to ApGST–O7) and 11 recognised Omega class GST sequences. It is demonstrated that all seven *A. perfoliata* Omega class GST sequences were clustered with the homologous Stringent starvation protein A (SspA) sequence from cestode clade. Additionally, they were well characterised to *H. microstoma* (accession number CDS29490) with a high bootstrap supported (78%) and, *E. granulosus* (accession number CDS24607) and *E. multilocularis* (accession number CDS41542) with a strongly bootstrap supported (96%) (Figure 2.8).

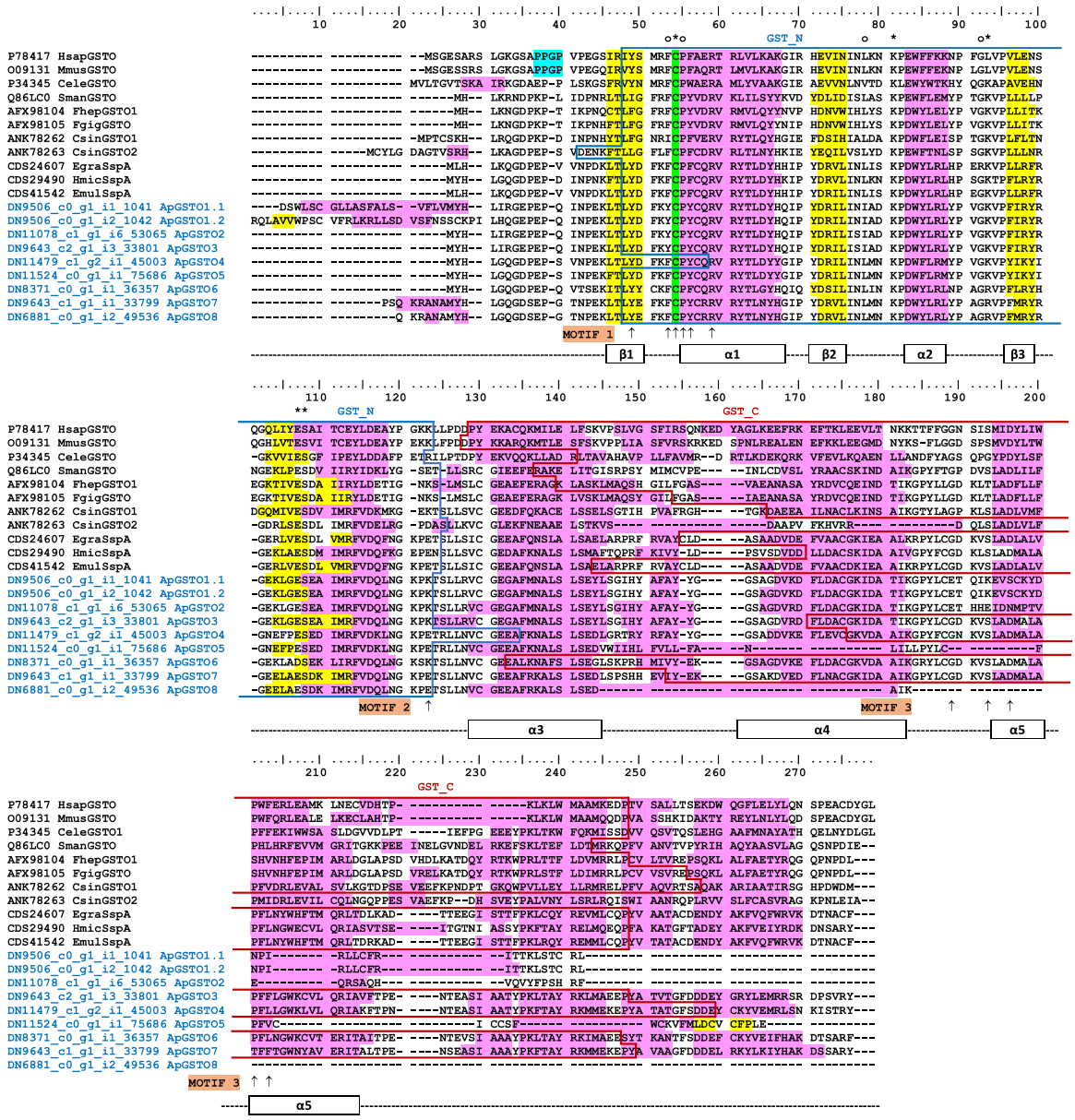

Figure 2.7 Multiple sequence alignment of the 8 novel Omega class GSTs (GSTO) identified in *Anoplocephala perfoliata* (ApGST–O1.1 to ApGST–O8). Secondary protein structure prediction using the PSIPRED Protein Analysis Workbench is presented below the alignment and is comprised of 3 β–strands, shaded in yellow, and 5 α–helices, shaded in pink. The proline–rich residues in the Omega class characteristic N–terminal extension as denoted by Morphew *et al.* (2012) are shaded in blue. The catalytic cysteine residues characteristic of Omega class GSTs as denoted by Morphew *et al.* (2012), Meng *et al.* (2014) and Kim *et al.* (2016) are shaded in green. Amino acids residues directly in contact to glutathione are indicated by asterisks (*) (Burmeister *et al.*, 2008; Kim *et al.*, 2016). Glutathione–binding residues are indicated by closed circles (o) (Kim *et al.*, 2016). The Omega class GST signature motifs as denoted by (Chemale *et al.*, 2006) are marked by arrows (↑). The predicted N– and C–terminal GST domain profiles are indicated by blue–and red–boxes, respectively. **Abbreviations:** Hsap: *Homo sapiens,* Mmus: *Mus musculus,* Cele: *Caenorhabditis elegans,* Sman: *Schistosoma mansoni,* Fhep: *Fasciola hepatica*, Fgig: *Fasciola gigantica,* Csin: *Clonorchis sinensis,* Egran: *Echinococcus granulosus*, Hmic: *Hymenolepis microstoma,* Emul: *Echinococcus multilocularis*.

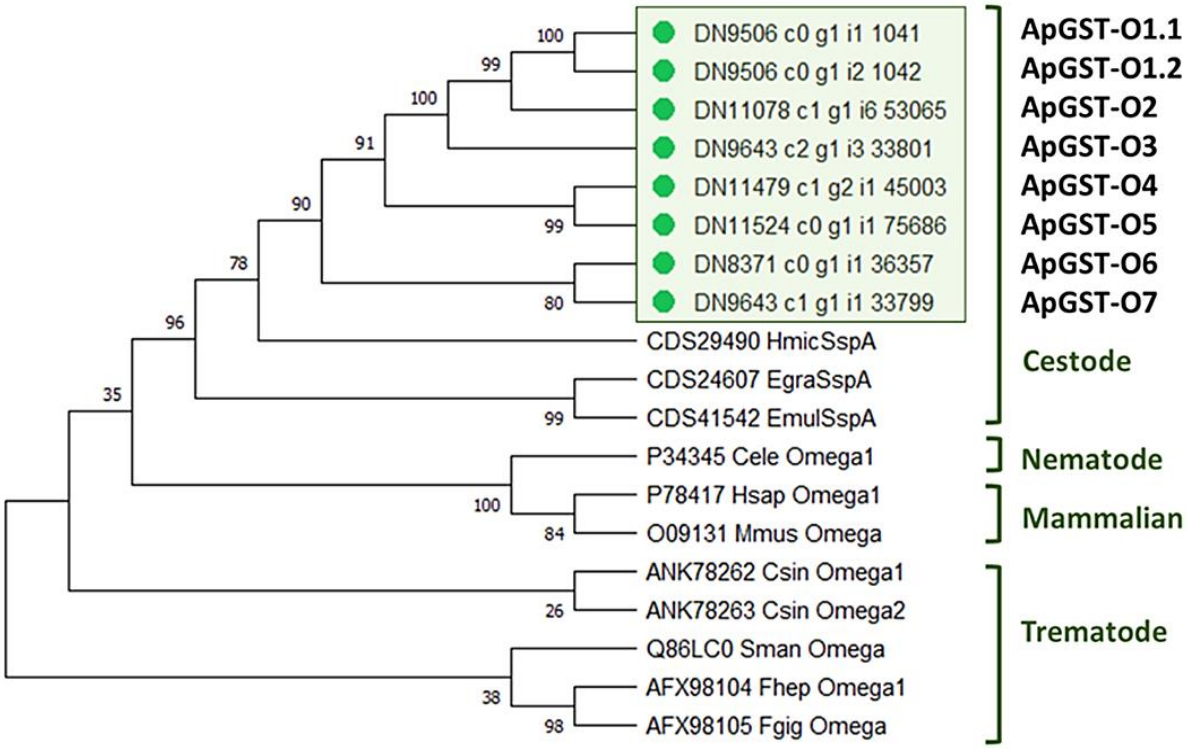

Figure 2.8 Maximum likelihood (ML) tree with JTT matrix–based model inferred from *Anoplocephala perfoliata* (AP) Omega class GST (GSTO) amino acid sequences. The bootstrap consensus tree inferred from 1000 replicates. Initial tree(s) for the heuristic search were obtained automatically by applying Neighbor–Joining and BioNJ algorithms to a matrix of pairwise distances estimated using a JTT model, and then selecting the topology with superior log likelihood value. A discrete Gamma distribution was used to model evolutionary rate differences among sites (5 categories (+G, parameter = 1.9774). This analysis involved 19 amino acid sequences. There was a total of 279 positions in the final dataset. Evolutionary analyses were conducted in MEGA X. **Abbreviations:** Hmic: *Hymenolepis microstoma*, Egra: *Echinococcus granulosus*, Emul: *Echinococcus multilocularis*, Cele: *Caenorhabditis elegans*, Hsap: *Homo sapiens*, Mmus: *Mus musculus*, Csin: *Clonorchis sinensis*, Sman: *Schistosoma mansoni*, Fhep: *Fasciola hepatica*, Fgig: *Fasciola gigantica.*

2.3.5.4 Characterisation of novel *A. perfoliata* Heat shock protein 90 (HSP90)

A total of 9 *A. perfoliata* sequences were identified by tBLASTn as potential HSP90 protein sequences either as alpha or beta isoforms. These sequences were homologous to protein sequences of recognised HSP90 family, following searches including alpha and beta isoforms from mammals and helminths (cutoff 1 x 10^{-20}). Due to the amino acid length of DN5627_c0_g2_i1_9552 sequence being short (196 amino acids), this sequence was excluded from further analysis, leaving 8 *A. perfoliata* sequences (mean sequence length ± SD of 643 ± 180 amino acids).

The InterProScan followed by manual BLASTp against NCBI (nr) database confirmed 8 *A. perfoliata* sequences as part of the HSP90 protein family (IPR001404) representing 5 likely distinct *A. perfoliata* HSP90s; ApHSP90–1 [1.1 (DN10172_c0_g2_i2_35191, 673 amino acids) and 1.2 (DN11738_c0_g1_i3_48033, 356 amino acids)], ApHSP90–2 [2.1 (DN11205_c0_g2_i1_23358, 688 amino acids) and 2.2 (DN11437_c0_g1_i3_56596, 677 amino acids)], ApHSP90–3 (DN10943_c0_g2_i1_50836, 654 amino acids), ApHSP90–4 (DN11960_c0_g1_i1_46290, 743 amino acids), ApHSP90–5 [5.1 (DN9350_c0_g1_i2_37241, 777 amino acids) and 5.2 (DN11414_c0_g1_i1_45013, 575 amino acids)]. All potential HSPs top scored to matches from HSP90α representatives; thus, ApHSP90–1–5 are likely putative HSP90 alphas.

The secondary characteristic structure of multiple aligned putative HSP90 alpha (HSP90α) *A. perfoliata* homologous sequences was predicted, with 17 β–strands and 25 α–helices, demonstrating the consistency of the secondary characteristic structure between all 8 novel *A. perfoliata* and recognised HSP90α sequences (Figure 2.9). Among the 8 novel isoforms of *A. perfoliata* HSP90α sequences, the most unique motif; the MEEVD peptide sequence in the C–terminal end of cytoplasmic HSP90 isoforms was found in ApHSP90–4. Whereas ApHSP90–5.1 and ApHSP90–5.2 contained KEEL peptide sequence which were 75% identical to KDEL peptide sequence of unique endoplasmic reticulum isoforms (human GRP94) (Skantar and Carta, 2004). The cytosolic HSP90α was investigated based on a signature sequence LIP and EDD peptide sequences at residues 80–82 and 701–703, respectively (Chen *et al.*, 2006). However, all *A. perfoliata* sequences lacked this signature, as did the additional included cestode sequences. Of note, none of 8 novel *A. perfoliata* HSP90 sequences had any beta isoform specific; LKID peptides at residues 71–74 (Chen *et al.*, 2006).

The analysis of the evolutionary relationships between the 8 *A. perfoliata* HSP90 and 27 recognised HSP90 protein member sequences demonstrated that, as expected, there were no *A. perfoliata* HSP90 sequence clustered within HSP90 beta (HSP90β) clades (Figure 2.10). All 8 potential *A. perfoliata* HSP90 sequences; ApHSP90–1 [1.1 and 1.2], 2 [2.1 and 2.2], 3, 4 and 5 [5.1 and 5.2] were clustered in a branch of HSP90α into a cestode and trematode specific clade (Figure 2.10). The phylogenetic analysis suggested five *A. perfoliata* HSP90s of which ApHSP90–1 [1.1 and 1.2], 2 [2.1 and 2.2] and 3 were clustered into a cestode specific clade of 3 recognised HSP90s. Whereby, ApHSP90–1 [1.1 and 1.2], 2 [2.1 and 2.2] were well characterised to *H. microstoma* (accession number CDS28179.1) with a high bootstrap value of 100% and 82% to *E. granulosus* (accession number CDS25067.1) and *E. multilocularis* (accession number CDS39694.1). ApHSP90–3 was characterised with a moderately bootstrap supported (69%) to *H. microstoma* (accession number CDS28179.1), however, well–supported to *E. granulosus* (accession number CDS25067.1) and *E. multilocularis* (accession number CDS39694.1) with a high bootstrap value (82%). Whereas ApHSP90–4 was strongly clustered in a HSP90α cestode specific clade containing *E. granulosus* (accession number XP_024345770.1 and CDI70178.1) with a high bootstrap value (97%). However, ApHSP90–5.1 and 5.2 were clustered into both cestode and trematode specific clade as well as HSP90s and HSP90α (Figure 2.10).

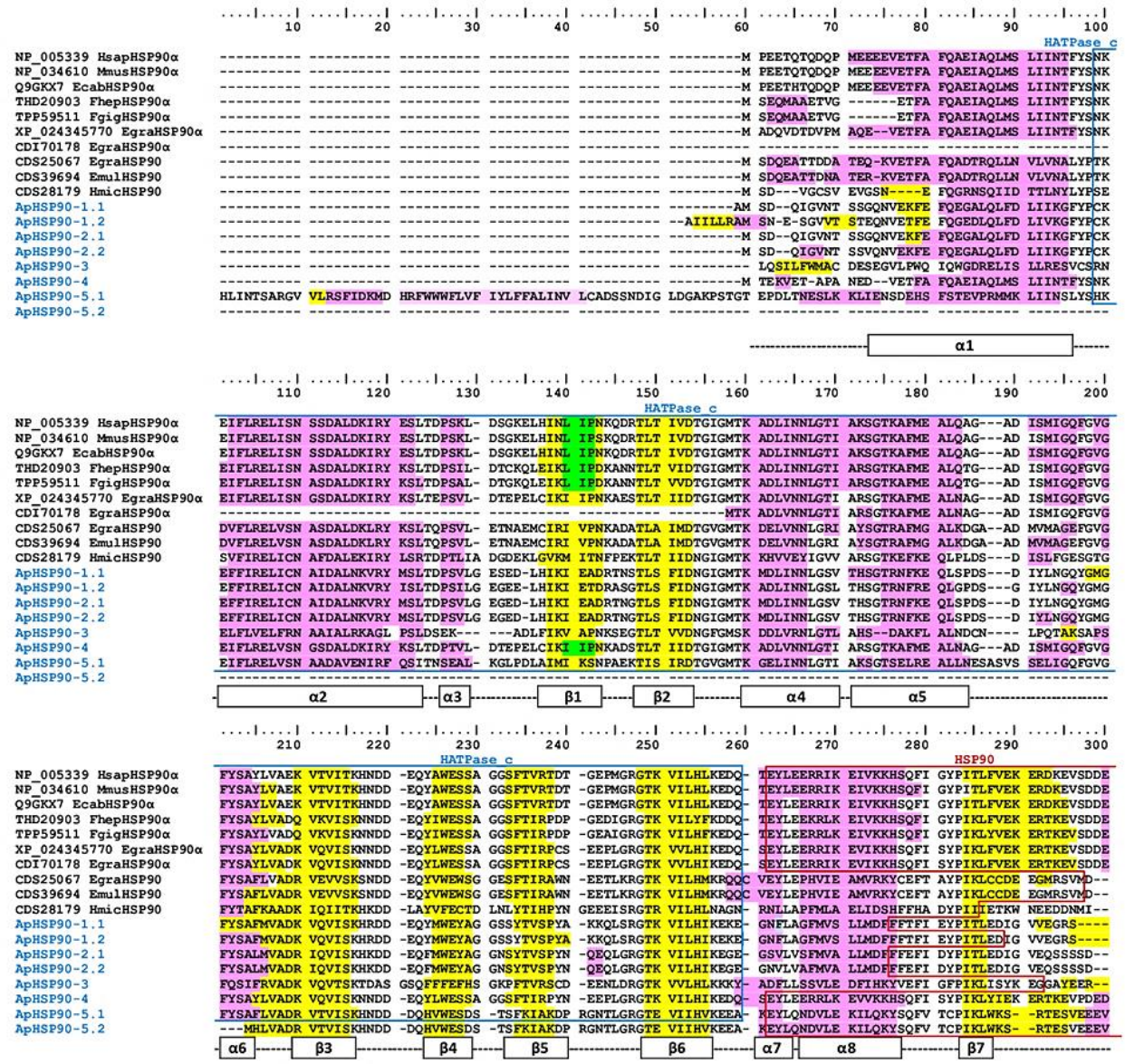

Figure 2.9 Multiple sequence alignment of the 5 novel *Anoplocephala perfoliata* (AP) Heat Shock Protein 90 alpha (HSP90α) sequences (including isoforms of each) with recognised HSP90α BLAST hits sequences. The secondary protein structure prediction the HSP90α characteristic structure using the PSIPRED Protein Analysis Workbench (presented below the alignment). Each β–strand or α–helix is numbered and shaded in yellow and pink, respectively. The domain analysis of C–terminal and N–terminal domain of HSP90α using SMART tools is boxed in blue and red, respectively. Unique cytosolic HSP90, MEEVD peptide sequences are in green type and the unique cytosolic HSP90α, LIP and EDD peptide sequences are shaded in green (Skantar and Carta, 2004; Chen *et al.*, 2006). **Abbreviations:** Hsap: *Homo sapiens*, Mmus: *Mus musculus*, Ecab: *Equus caballus*, Fhep: *Fasciola hepatica*, Fgig: *Fasciola gigantica*, Egra: *Echinococcus granulosus*, Emul: *Echinococcus multilocularis,* Hmic: *Hymenolepis microstoma*.

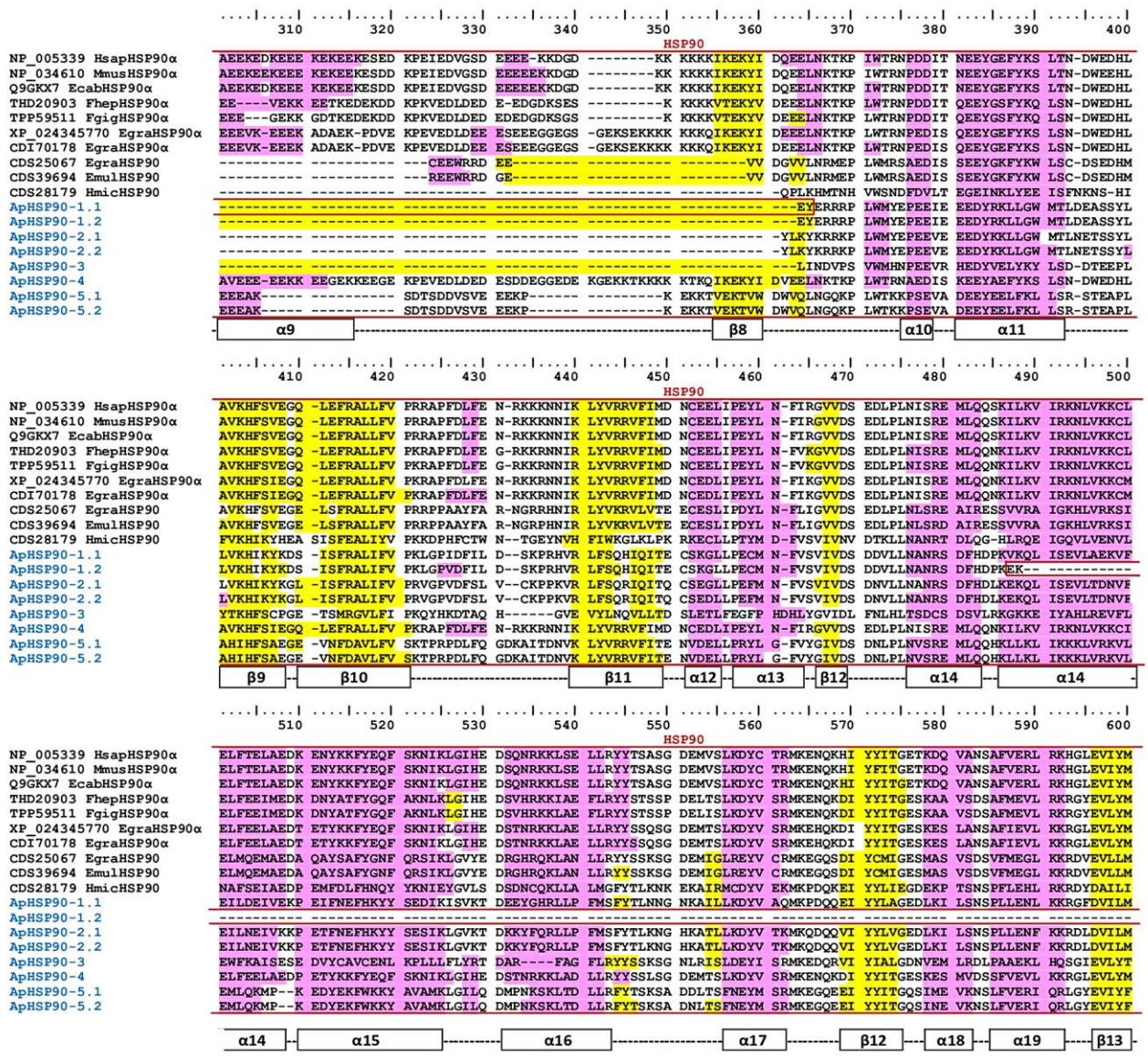

Figure 2.9–Continued 2. Multiple sequence alignment of the 5 novel *Anoplocephala perfoliata* (AP) Heat Shock Protein 90 alpha (HSP90α) sequences (including isoforms of each) with recognised HSP90α BLAST hits sequences. The secondary protein structure prediction the HSP90α characteristic structure using the PSIPRED Protein Analysis Workbench (presented below the alignment). Each β–strand or α–helix is numbered and shaded in yellow and pink, respectively. The domain analysis of C–terminal and N–terminal domain of HSP90α using SMART tools is boxed in blue and red, respectively. Unique cytosolic HSP90, MEEVD peptide sequences are in green type and the unique cytosolic HSP90α, LIP and EDD peptide sequences are shaded in green (Skantar and Carta, 2004; Chen *et al.*, 2006). **Abbreviations:** Hsap: *Homo sapiens*, Mmus: *Mus musculus*, Ecab: *Equus caballus*, Fhep: *Fasciola hepatica*, Fgig: *Fasciola gigantica*, Egra: *Echinococcus granulosus*, Emul: *Echinococcus multilocularis,* Hmic: *Hymenolepis microstoma*.

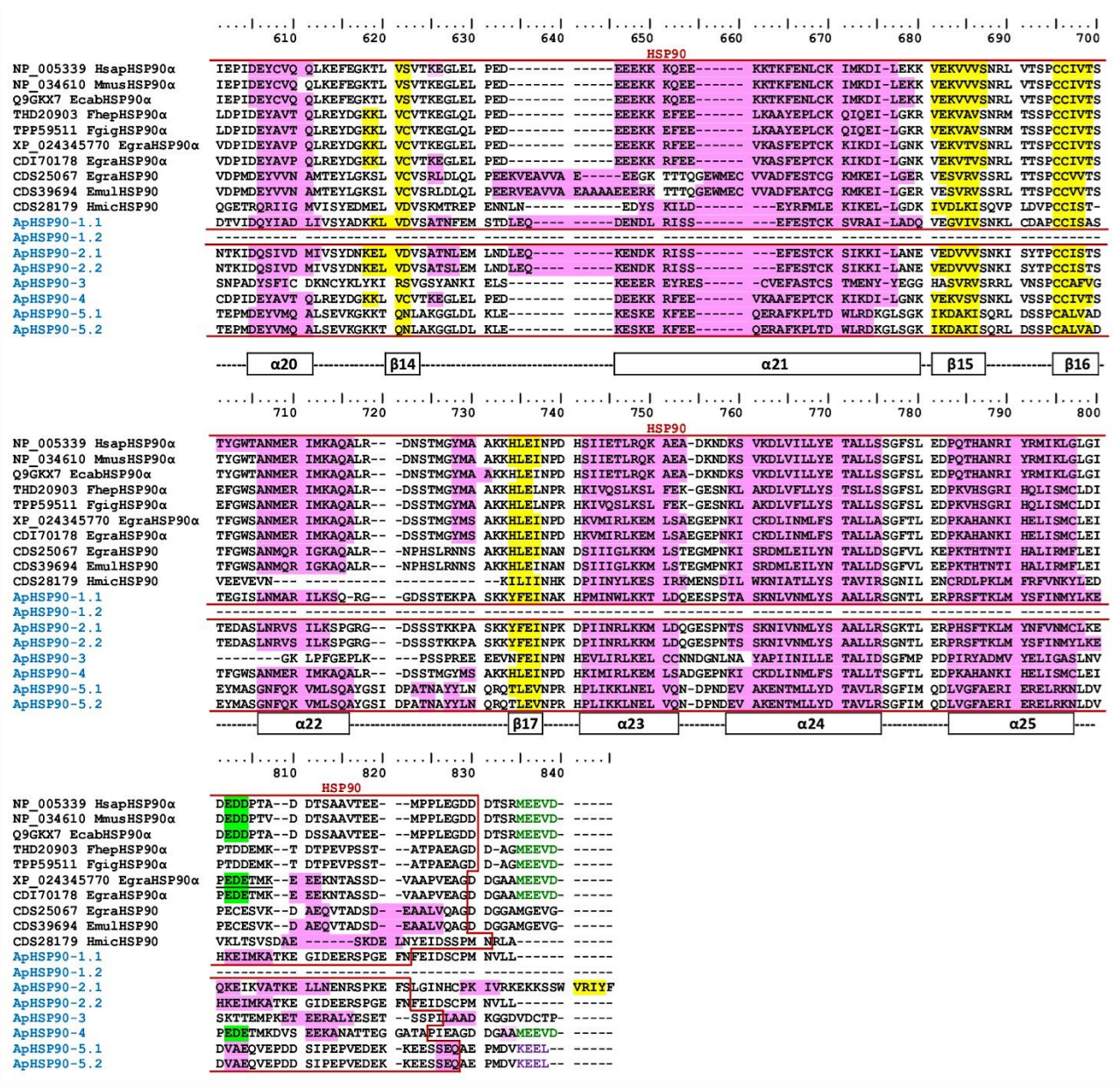

Figure 2.9–Continued 3. Multiple sequence alignment of the 5 novel *Anoplocephala perfoliata* (AP) Heat Shock Protein 90 alpha (HSP90α) sequences (including isoforms of each) with recognised HSP90α BLAST hits sequences. The secondary protein structure prediction the HSP90α characteristic structure using the PSIPRED Protein Analysis Workbench (presented below the alignment). Each β–strand or α–helix is numbered and shaded in yellow and pink, respectively. The domain analysis of C–terminal and N–terminal domain of HSP90α using SMART tools is boxed in blue and red, respectively. Unique cytosolic HSP90, MEEVD peptide sequences are in green type and the unique cytosolic HSP90α, LIP and EDD peptide sequences are shaded in green (Skantar and Carta, 2004; Chen *et al.*, 2006). **Abbreviations:** Hsap: *Homo sapiens*, Mmus: *Mus musculus*, Ecab: *Equus caballus*, Fhep: *Fasciola hepatica*, Fgig: *Fasciola gigantica*, Egra: *Echinococcus granulosus*, Emul: *Echinococcus multilocularis,* Hmic: *Hymenolepis microstoma.*

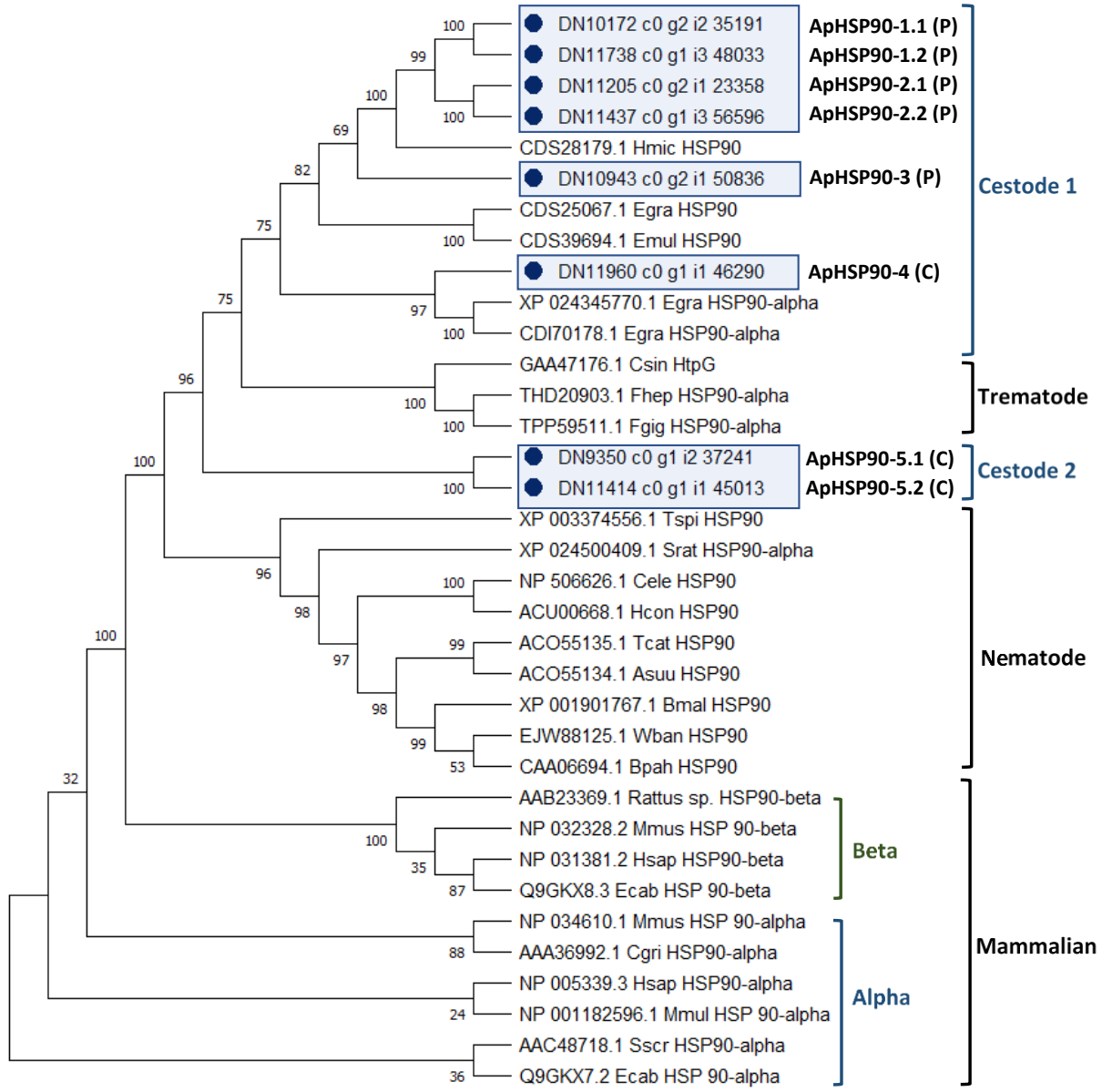

Figure 2.10 The phylogenetic tree of *Anoplocephala perfoliata* (AP) Heat Shock Protein 90 (HSP90) inferred by using Maximum likelihood (ML) method and JTT matrix–based model. The bootstrap consensus tree inferred from 1000 replicates. The tree with the highest log likelihood (–16485.50) is shown. Initial tree(s) for the heuristic search were obtained automatically by applying Neighbor–Joining and BioNJ algorithms to a matrix of pairwise distances estimated using a JTT model, and then selecting the topology with superior log likelihood value. A discrete Gamma distribution was used to model evolutionary rate differences among sites (5 categories (+G, parameter = 1.4964)). This analysis involved 35 amino acid sequences. There was a total of 885 positions in the final dataset. Evolutionary analyses were conducted in MEGA X. The predicted and constant–alpha are noted in (P) and (C), respectively. **Abbreviations:** Hmic: *Hymenolepis microstoma*, Egra: *Echinococcus granulosus*, Emul: *Echinococcus multilocularis*, Csin: *Clonorchis sinensis*, Fhep: *Fasciola hepatica*, Fgig: *Fasciola gigantica,* Tspi: *Trichinella spiralis*, Srat: *Strongyloides ratti*, Cele: *Caenorhabditis elegans*, Hcon: *Haemonchus contortus*, Tcat: *Toxocara cati*, Asuu: *Ascaris suum*, Bmal: *Brugia malayi*, Wban: *Wuchereria bancrofti*, Bpah: *Brugia pahangi*, Mmus: *Mus musculus*, Hsap: *Homo sapiens*, Ecab: *Equus caballus*, Cgri: *Cricetulus griseus*, Mmul: *Macaca mulatta,* Sscr: *Sus scrofa*.

2.3.5.5 Characterisation of novel *A. perfoliata* Alpha–Enolase

A total of 5 *A. perfoliata* sequences were identified by tBLASTn as potential alpha–Enolase (α–Enolase) protein sequences, homologous to protein sequences of recognised α–Enolase from mammals and helminths (cutoff 1 x 10^{-15}). Subsequently, InterProScan followed by manual BLASTp against the NCBI (nr) database confirmed that all 5 of these sequences were potential α–Enolase *A. perfoliata* sequences (Enolase superfamily IPR000941) (mean sequence length ± SD of 443 ± 12). There were three *A. perfoliata* α–Enolase enzymes; Apα–Enolase–1 (DN14469_c0_g1_i1_24672, 433 amino acids), Apα–Enolase–2 (DN7852_c0_g1_i1_40713, 456 amino acids) and Apα–Enolase–3 (DN9213_c0_g1_i1_45970, 438 amino acids) that retained all catalytic residues and, therefore are likely to be catalytically functional. The remaining two sequences (not shown in the analysis; DN14116_c0_g1_i1_34224 (88 amino acids) and DN13262_c0_g1_i1_2554 (48 amino acids)) represented likely incomplete fragments and were therefore excluded from further characterisation.

All three α–Enolase *A. perfoliata* sequences; Apα–Enolase–1, 2 and 3 showed comparable numbers of β–strands and α–helices when compared to α–Enolase of human, nematodes, trematodes and cestodes (10 β–strands and 15 α–helices) demonstrating the consistency of the secondary characteristic structure between the three novel α–Enolase from *A. perfoliata* and recognised α–Enolase sequences (Figure 2.11). Apα–Enolase–1, 2 and 3 showed 87.7%, 69.6% and 64.8% identity to α–enolases of cestodes; *E. multilocularis* (accession number CDS37852), 87.2%, 69.6% and 64.8% to *E. granulosus* (accession number ACY30465), 84.7%, 65.8% and 61.4% to *H. microstoma* (accession number CDS30005), 64.1%, 59.1% and 77.8% to *H. microstoma* (accession number CDS26422), and 75.1%, 65% and 62.5% to human (accession number CAA59331). All three α–Enolase *A. perfoliata* sequences and recognised α–Enolase sequences had conserved amino acid residues imperative for proper catalytic function (His^{158}, Glu^{167}, Glu^{210}, Lys^{343}, Lys^{394}, respective positions in human α–Enolase) (Pancholi, 2001). Moreover, these three α–Enolase *A. perfoliata* sequences contained an enolase fingerprint motif (SHRSGETED; Babbitt *et al.*, 1996: Apα–Enolase–1, 2 and 3 ASVPSGASAGIH (100% identity), domain for a hydrophobic putative signal peptide (AAVPSGASTGIY; Jolodar *et al.* 2003: Apα–Enolase–1 and 2 AAVPSGASTGI**H** (91.7% identity) and 3 A**S**VPSGAS**A**GI**H** (75% identity)) and putative plasminogen–binding motif in surface displayed α–enolase (GKVXIAMDCAASEFYKEGKYDLDF; Bergmann *et al.* 2003 and Bernal *et al.*, 2004: Apα–

Enolase–1 GKV**K**I**G**MDCAASEFYKEGKYDLDF (90.9% identity) and 2 **DRIR**IA**T**D**V**AASEFY**RD**G**L**YDLDF (68.2% identity) and 3 GK**IL**I**GI**D**V**AASEFY**ENG**KY**N**L**G**F (63.6% identity)).

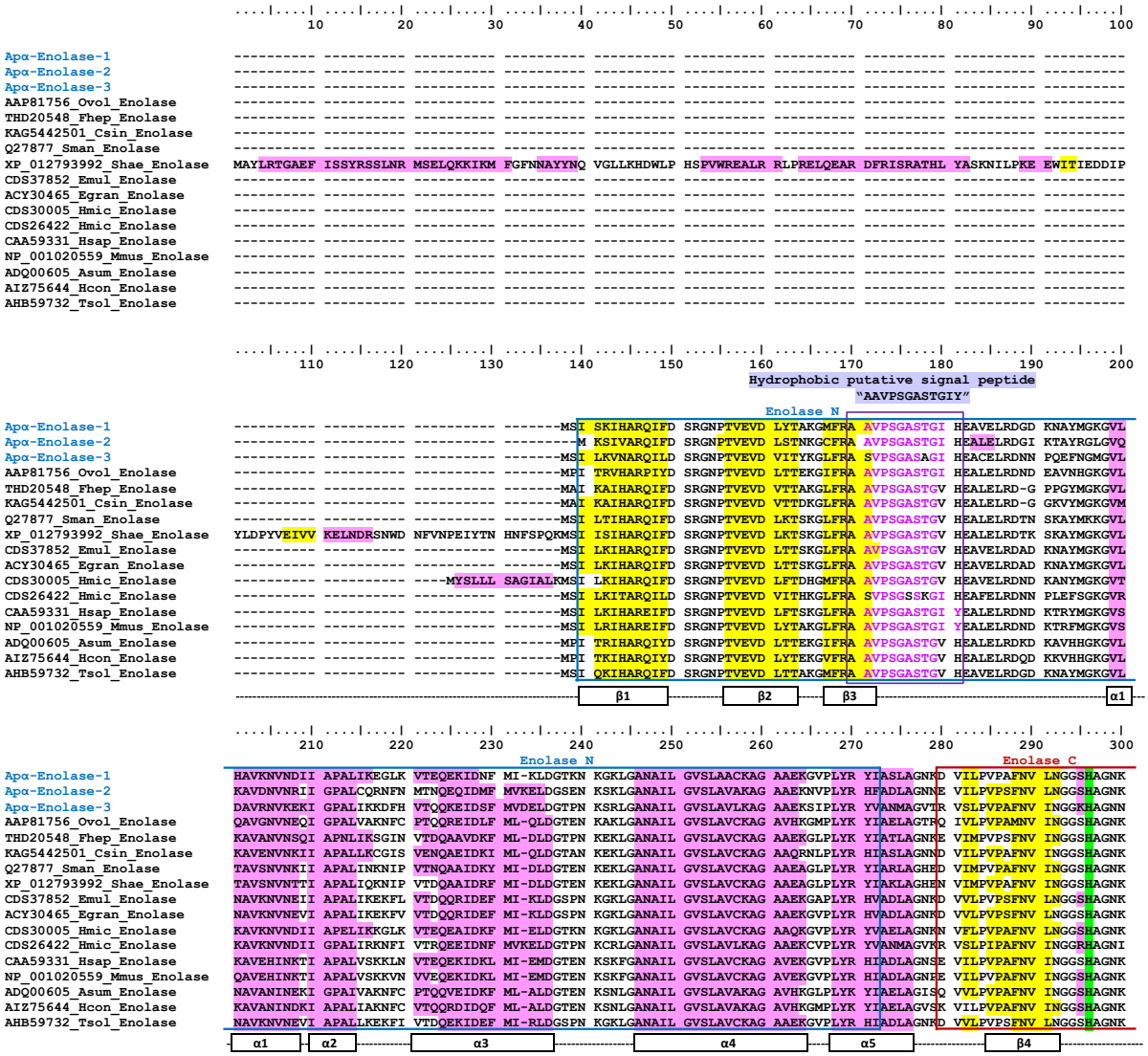

Figure 2.11 Multiple sequence alignment of the 3 novel α–Enolase from *Anoplocephala perfoliata* (Apα–Enolase–1, 2 and 3). Secondary protein structure prediction using the PSIPRED is presented below the alignment and comprises of 10 β–strands and 15 α–helices, highlighted in yellow and pink, respectively. The 5 essential residues necessary for proper catalytic function are highlighted in green (Pancholi, 2001). The hydrophobic putative signal peptide are in purple text (Jolodar *et al.*, 2003). The enolase fingerprint motif are in blue text and putative plasminogen–binding motif (Bergmann *et al.*, 2003; Bernal *et al.*, 2004) are marked by arrows (↑). The predicted N–and C–terminal Enolase domain profiles are indicated by blue–and red–boxes, respectively. **Abbreviations:** Ovol: *Onchocerca volvulus,* Asum: *Ascaris suum,* Hcon: *Haemonchus contortus*, Hsap: *Homo sapiens*, Mmus: *Mus musculus*, Fhep: *Fasciola hepatica*, Csin: *Clonorchis sinensis*, Sman: *Schistosoma mansoni,* Shae: *Schistosoma haematobium*, Hmic: *Hymenolepis microstoma*, Tsol: *Taenia solium*, Emul: *Echinococcus multilocularis*, Egra: *Echinococcus granulosus*.

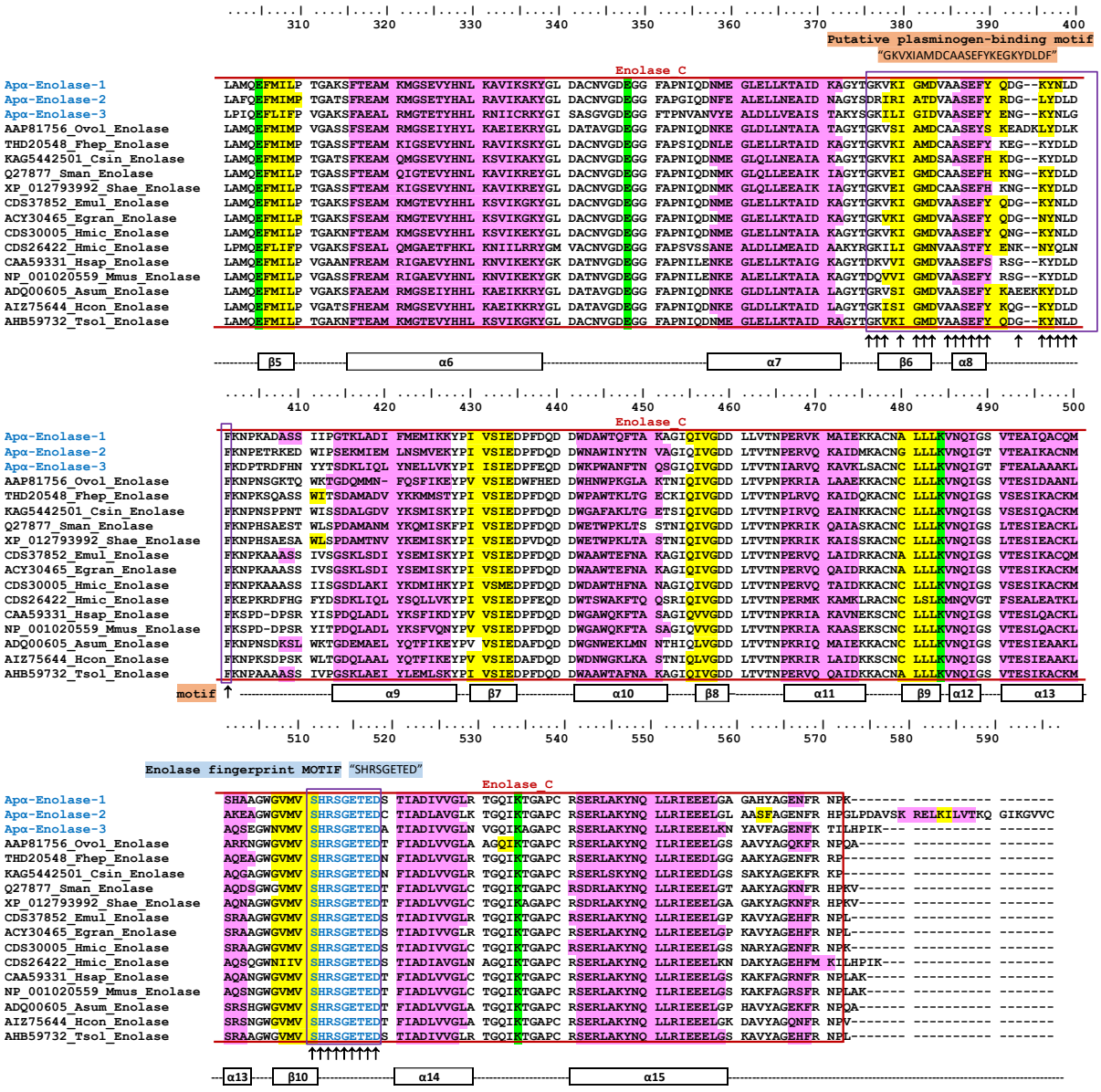

Figure 2.11–Continued 2. Multiple sequence alignment of the 3 novel α–Enolase from *Anoplocephala perfoliata* (Apα–Enolase–1, 2 and 3). Secondary protein structure prediction using the PSIPRED is presented below the alignment and comprises of 10 β–strands and 15 α–helices, highlighted in yellow and pink, respectively. The 5 essential residues necessary for proper catalytic function are highlighted in green (Pancholi, 2001). The hydrophobic putative signal peptide are in purple text (Jolodar *et al.*, 2003). The enolase fingerprint motif are in blue text and putative plasminogen–binding motif (Bergmann *et al.*, 2003; Bernal *et al.*, 2004) are marked by arrows (↑). The predicted N–and C–terminal Enolase domain profiles are indicated by blue– and red–boxes, respectively. **Abbreviations:** Ovol: *Onchocerca volvulus,* Asum: *Ascaris suum,* Hcon: *Haemonchus contortus*, Hsap: *Homo sapiens*, Mmus: *Mus musculus*, Fhep: *Fasciola hepatica*, Csin: *Clonorchis sinensis*, Sman: *Schistosoma mansoni,* Shae: *Schistosoma haematobium*, Hmic: *Hymenolepis microstoma*, Tsol: *Taenia solium*, Emul: *Echinococcus multilocularis*, Egra: *Echinococcus granulosus*.

A phylogenetic tree demonstrated that all 3 *A. perfoliata* α–Enolase sequences (Apα–Enolase–1, 2 and 3) clustered in a cestode specific clade on assessment of evolutionary relationships with 14 recognised α–Enolase proteins. Apα–Enolase–1 was characterised to the cluster of *T. solium* (accession number AHB59732), *E. multilocularis* (accession number CDS37852) and *E. granulosus* (accession number ACY30465) with a moderate bootstrap support (67%). However, Apα–Enolase–1 was well–characterised to *H. microstoma* α–Enolase sequence (accession number CDS30005) with a high bootstrap value (96%) (Figure 2.12). Apα–Enolase–2 and 3 were characterised to *H. microstoma* (accession number CDS26422 and CDS30005) which was moderately bootstrap supported (69%) and strongly bootstrap supported (100%), respectively (Figure 2.12).

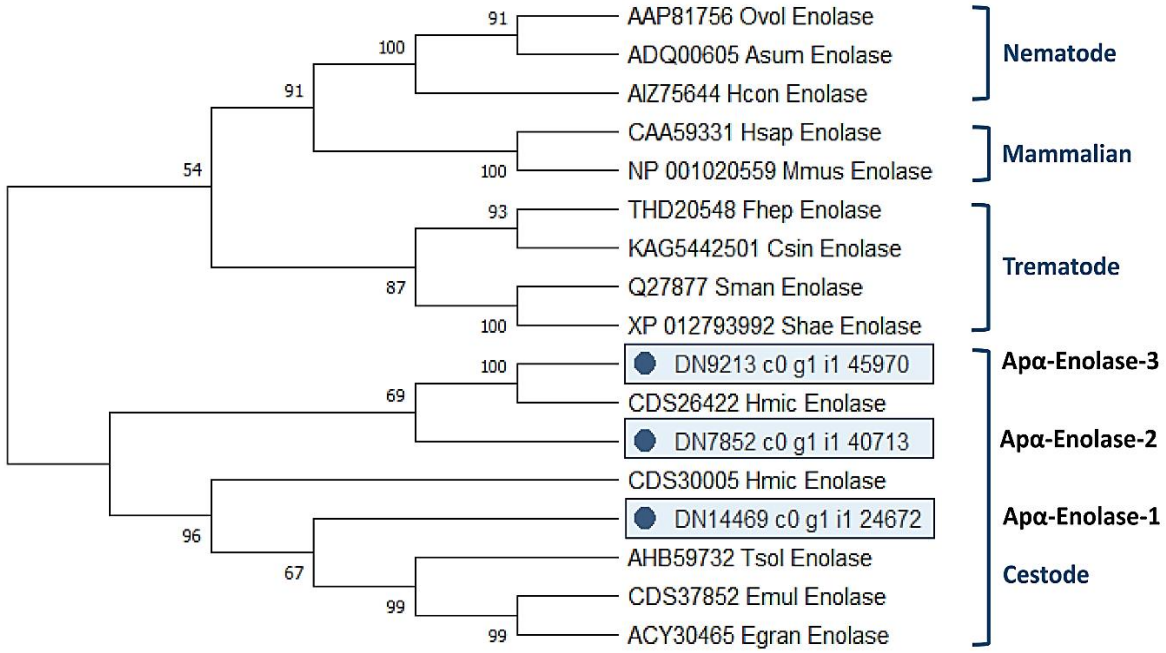

Figure 2.12 Maximum likelihood (ML) tree with JTT matrix–based model inferred from *Anoplocephala perfoliata* (AP) α–Enolase amino acid sequences. The bootstrap consensus tree inferred from 1000 replicates. Initial tree(s) for the heuristic search were obtained automatically by applying Neighbor–Joining and BioNJ algorithms to a matrix of pairwise distances estimated using a JTT model, and then selecting the topology with superior log likelihood value. A discrete Gamma distribution was used to model evolutionary rate differences among sites (5 categories (+G, parameter = 0.4176)). This analysis involved 17 amino acid sequences. There were a total of 597 positions in the final dataset. Evolutionary analyses were conducted in MEGA X. **Abbreviations:** Ovol: *Onchocerca volvulus,* Asum: *Ascaris suum,* Hcon: *Haemonchus contortus*, Hsap: *Homo sapiens*, Mmus: *Mus musculus*, Fhep: *Fasciola hepatica*, Csin: *Clonorchis sinensis*, Sman: *Schistosoma mansoni,* Shae: *Schistosoma haematobium*, Hmic: *Hymenolepis microstoma*, Tsol: *Taenia solium*, Emul: *Echinococcus multilocularis*, Egra: *Echinococcus granulosus*.

2.4 Discussion

In this chapter, the transcriptome of an adult equine tapeworm (*A. perfoliata*) was generated using *de novo* transcriptome assembly and the validity of the transcript assembly was confirmed using bioinformatics approaches. I also identified known key RNA sequences which are expressed as immune modulatory proteins in other platyhelminth species. I then further characterised the immune modulators, GSTs, HSP90s and α–Enolase within the adult *A. perfoliata* transcriptome. These discoveries provide an essential molecular knowledge for further proteomic analysis of the *A. perfoliata* secretome.

2.4.1 Transcriptomics of *Anoplocephala perfoliata*

The equine tapeworm, *A. perfoliata*, remains a neglected parasite with molecular information being limited to the full mitochondrial (mt) genome (Guo, 2015). Hence, there is a lack of understanding of host–parasite interactions. Therefore, in the absence of an *A. perfoliata* reference genome, I generated a transcriptome of the adult worm to improve the fundamental biology of *A. perfoliata* itself and characterise key genes associated with the host–parasite interface, as have been demonstrated previously for other helminths (Robinson *et al.*, 2009; Cantacessi *et al.*, 2012; Pan *et al.*, 2014; Huson *et al.*, 2018). To my knowledge, this is the first *de novo* transcriptome assembly of an adult equine tapeworm, *A. perfoliata*. While this transcriptome was generated from *A. perfoliata* samples within the United Kingdom and not globally representative, it still serves as a valuable resource for initiating future functional studies in *A. perfoliata.* The top 50 most highly represented transcripts demonstrate the expression of common conserved genes similar to other closely related cestodes including *E. granulosus* (Parkinson *et al.*, 2012; Debarba *et al.*, 2020), *H. microstoma* (Olson *et al.*, 2018; Preza *et al.*, 2021), *T. pisiformis* (Yang *et al.*, 2012) *and T. crassiceps* (García-Montoya *et al.*, 2016) at several life stages. Such commonly conserved genes included dynein light chain, Tegumental protein, Deoxyhypusine hydroxylase, 8 kDa Glycoprotein and Expressed conserved protein. Moreover, the *A. perfoliata* transcriptome aligned well to 3 closely related tapeworm species, namely *H. diminuta, E. granulosus* and *H. microstoma*.

The functional GO term enrichment analysis of *A. perfoliata* transcriptome when compared to closely related tapeworms, revealed that enriched GO terms observed in *E. granulosus* (Pan *et al.*, 2014; Liu *et al.*, 2017; Mohammadi *et al.*, 2021) *E. multilocularis* (Liu *et al.*, 2017), *H. diminuta* (Sulima *et al.*, 2018) and *H. microstoma* (Olson *et al.*, 2018; Preza *et al.*, 2021) are shared with *A. perfoliata*. These shared GO terms encompass various Biological Processes, including organic substance metabolic process, cellular metabolic process and primary metabolic process. Additionally, they encompass functional attributes, such as binding and catalytic activities within the Molecular Function category and cellular components, including cell parts or membranes (Pan *et al.*, 2014; Liu *et al.*, 2017; Olson *et al.*, 2018; Sulima *et al.*, 2018; Mohammadi *et al.*, 2021; Preza *et al.*, 2021). It is conceivable that closely related tapeworm species, from a phylogenetic standpoint, could share common biological functions or molecular–level processes with *A. perfoliata*. The similarity in primary function among the overrepresented genes in *A. perfoliata* and closely related tapeworm may be attributed to their evolutionary development of analogous functions, such as nutrient acquisition, immune evasion, and reproduction. Although, similar GO term enrichments suggest shared functions of *A. perfoliata* with closely related tapeworm (Pan *et al.*, 2014; Liu *et al.*, 2017; Olson *et al.*, 2018; Sulima *et al.*, 2018; Mohammadi *et al.*, 2021; Preza *et al.*, 2021).

However, information about the specific genes in various life stage and hosts, particularly those related to the host–parasite interplay, may not be provided. This gap in knowledge is evident from GO enrichment analyses conducted on different life stages of model tapeworms, such as *H. microstoma* (including eggs, cysticercoids, and adults) (Olson *et al.*, 2018; Preza *et al.*, 2021), *H. diminuta* (covering larvae and various regions of segmented worms) (Sulima *et al.*, 2018), and *E. granulosus* (encompassing the early stages of adults and cystic development) (Bai *et al.*, 2020). These analyses have revealed significant changes in gene expression patterns. Furthermore, the evidence of differences in host environments for *E. granulosus* protoscoleces has also shown differential expression of immune–related genes between cysts found in cattle and sheep (Pereira *et al.*, 2022). Therefore, it is imperative to conduct further research to explore specific genes and their functions associated with GO terms. This will provide a deeper understanding of the *A. perfoliata* transcriptome as well as its interactions with the host, *A. perfoliata*.

2.4.2 Novel key RNA sequences

At the host–parasite interface, immune modulation is imperative for parasite survival (Hewitson *et al.*, 2009; Gazzinelli-Guimaraes and Nutman, 2018), as such, many immune modulatory proteins have been identified in the secretome of platyhelminth species (Davis *et al.*, 2019; Wang *et al.*, 2020; Allen *et al.*, 2021). I have demonstrated that the *A. perfoliata* transcriptome contains evidence of immune modulators which have been characterised previously in two significant flatworms; namely *S. mansoni* and *F. hepatica*, with significant hits for 46 out of 76 bait immune modulators. Further investigation and characterisation of sequences within the *A. perfoliata* transcriptome was carried out for three novel immune modulatory proteins found in other helminths, GSTs, HSP90α and α–Enolase where it was demonstrated that members of all three protein superfamilies were identified in a consistent manner with related helminths (Alexandra *et al.*, 2003; Jolodar *et al.*, 2003; Marcilla *et al.*, 2007; Ramajo-Hernández *et al.*, 2007; Dowling *et al.*, 2010; LaCourse *et al.*, 2012; Maizels *et al.*, 2018; Wang *et al.*, 2022) Therefore, this provides further evidence to support exploration of the secretome, where many of these immune modulators may be found using proteomic studies. Demonstration of these proteins in the secretome, will provide initial evidence that these transcripts may produce functional proteins that are able to interact with the host to modulate the immune response.

2.4.2.1 Glutathione Transferase

In helminths, the GSTs are recognised as crucial multifunctional enzymes in Phase II detoxification of xenobiotics (Brophy *et al.*, 1989; Brophy and Barrett, 1990; Sheehan *et al.*, 2001), as a consequence of the limited activity documented for cytochrome P450s (CYP450) as Phase I detoxification enzymes (Precious and Barrett, 1989; Barrett, 1998, 2009; Torres-Rivera and Landa, 2008; Nelson, 2009; Pakharukova *et al.*, 2012). However, immunomodulatory roles in Sigma class (Alexandra *et al.*, 2003; Dowling *et al.*, 2010; LaCourse *et al.*, 2012) and Omega class GST (Wang *et al.*, 2022) have been increasingly revealed. Therefore, in the present work I identified the cytosolic GSTs family of *A. perfoliata*. Phylogenetic tree analysis of the *A. perfoliata* GST sequences demonstrated that three cytosolic GST classes including Sigma, Omega and Mu were present within the *A. perfoliata* transcriptome and were homologous with, and closely related to, other GST class members

from platyhelminths. As expected, the Theta, Delta, Epsilon and Kappa GST classes were not identified in the *A. perfoliata* transcriptome given that Theta are primarily mammalian (Meyer *et al.*, 1991; Rossjohn *et al.*, 1998) and Delta and Epsilon are insect specific (Friedman, 2011; ShouMin, 2012). Interestingly, Kappa are also primarily mammalian and named mitochondrial GST. However, Kappa were identified in the pine wood nematode, *Bursaphelenchus xylophilus*, suggesting (Espada *et al.*, 2016). Besides, Zeta class GSTs are not usually identified in helminths, however, Zeta were identified in trematodes: *F. gigantica* and *F. hepatica* (Morphew *et al.*, 2012) and in nematodes: *Caenorhabditis elegans* and *B. xylophilus* (Espada et al., 2016), suggesting that they may be involve in energy and lipid metabolism via Tyrosine pathway (Board *et al.*, 1997). Taken together, it was interesting to find out that Zeta class GSTs are not identified in the *A. perfoliata* transcriptome, which may indicate different roles for their metabolism.

All three of the identified GST classes found within the *A. perfoliata* transcriptome have been frequently identified as the major cytosolic GST classes of flatworms (Mu, Sigma and Omega class GSTs) (Fernández *et al.*, 2000; Chemale *et al.*, 2006; Nguyen *et al.*, 2010; LaCourse *et al.*, 2012; Morphew *et al.*, 2012; Iriarte *et al.*, 2012; Bae *et al.*, 2013; Bae *et al.*, 2016; Kim *et al.*, 2016; Arbildi *et al.*, 2017, 2021; Lopez-Gonzalez *et al.*, 2018; Huson *et al.*, 2018; Aguayo *et al.*, 2019; Stuart *et al.*, 2021). For example, in closely related cestodes; *E. granulosus* presents Mu class GST (EgGST1), Sigma class GST (EgGST2) and a representative matching both Omega and Sigma classes (EgGST3) (Fernández *et al.*, 2000; Iriarte *et al.*, 2012; Arbildi *et al.*, 2017, 2021; Lopez-Gonzalez *et al.*, 2018) and in *T. solium* a Sigma–like GST (TsGST2) has been identified (Nguyen *et al.*, 2010). In trematodes, four classes of GST (Mu, Sigma/Sigma like, Omega and Zeta classes GST) are primarily observed, for example in *F. hepatica* (Chemale *et al.*, 2006; LaCourse *et al.*, 2012; Aguayo *et al.*, 2019; Stuart *et al.*, 2021), *F. gigantica* (Morphew *et al.*, 2012), *C. sinensis* (Bae *et al.*, 2013; Bae *et al.*, 2016; Kim *et al.*, 2016) and *C. daubneyi* (Huson *et al.*, 2018). Due to the common expression of these Sigma, Omega and Mu class GSTs in platyhelminths, and their known functional roles (e.g. immunomodulatory (LaCourse *et al.*, 2012; Wang *et al.*, 2022) and detoxification (LaCourse *et al.*, 2012; Arbildi *et al.*, 2017; Kim *et al.*, 2017; Stuart *et al.*, 2021), it is possible that these enzymes are expressed and associated with an adaptation of *A. perfoliata* to survive in the host environment (LaCourse *et al.*, 2012; Wang *et al.*, 2022).

In the current study, I further investigated the Sigma and Omega class GSTs as potential immune modulators. Sigma class GST has been demonstrated to increase the prostaglandin synthase activity producing prostaglandin (PGE_2 and PGD_2) and is involved in the survival within the host during infections (Sommer *et al.*, 2003; LaCourse *et al.*, 2012). Furthermore, it is suggested that the role within prostaglandin synthase activity is a conserved role of sigma class GST (Thomson *et al.*, 1998; Flanagan and Smythe, 2011; LaCourse *et al.*, 2012). In *F. hepatica,* Sigma class GST possess immune–modulatory activity by inactivating Th2 immune responses and suppressing Th17 immune responses in host dendritic cells, allowing the parasite to survive for long–term parasitism and as such, causing chronic infection (Dowling *et al.*, 2010; LaCourse *et al.*, 2012). Omega class GSTs have a role in oxidative stress responses (Liebau *et al.*, 2000; Burmeister *et al.*, 2008; Kim *et al.*, 2016, 2017). Due to omega class GSTs primarily being expressed in the parasite reproductive system, it is suggested that the protection from stress damage is particularly relevant during maturation (Kim *et al.*, 2016; Wang *et al.*, 2022). Furthermore, a novel recombinant *F. hepatica* omega class GST (GSTO2) has been demonstrated to modulate the physiological functions of murine macrophages by inhibiting the viability of macrophages, promoting apoptosis and modulating cytokines the expression, thereby avoiding the host immune response for long–term parasitism (Wang *et al.*, 2022).

I identified 2 novel *A. perfoliata* Sigma class GSTs (ApGST–S1, GST–S2.1 and GST–S2.2) within the transcriptome, confirmed by secondary structure assessment, domain analysis and phylogenetic analysis. All *A. perfoliata* Sigma class GSTs were clustered well in the Sigma class GST clade, specifically as part of a cestode group. Moreover, the secondary characteristic structure prediction demonstrated the consistency and similarity with other cestodes and trematodes of the β–strand, α–helix, and random coils structures within the recognised Sigma class GST sequences, which are conserved regions of these proteins. Remarkably, the catalytic tyrosine residues (Y) positioned at the end of the first β–strand, which has been suggested as the key feature of the GSH binding site of the sigma class GST (Yamamoto *et al.*, 2007; Nguyen *et al.*, 2010; Iriarte *et al.*, 2012; Xie *et al.*, 2015; Bae *et al.*, 2016; Zhang *et al.*, 2020), was present in ApGST–S2.1 and S2.2. In ApGST–S1, the catalytic tyrosine residue (Y) positioning appeared shifted in the alignment one residue to the left. However, ApGST–S1 demonstrated similarity to *H. microstoma* Sigma–like GST (HmicGSTS2; accession number CDS25704) at the

'Y' residue position and as such was clustered alongside the *H. microstoma* Sigma–like GST in the phylogenetic tree (moderately bootstrap supported of 52%). Thus, ApGST–S1 is likely to still have a functional catalytic tyrosine residue important for Sigma class GSTs as *H. microstoma* Sigma–like GST (HmicGSTS2; accession number CDS25704). However, functionality of ApGST–S1, and other ApGSTs, requires further experimentation. Interestingly, the likely functional expressed protein ApGST–S1 was initially designated, through an Omicsbox annotation, as a Chain A, Glutathione S–transferase 28 Kda (GST class–Mu 28 kDa isozyme). Nevertheless, the domain and phylogenetic analysis demonstrated that ApGST–S1 is likely to be a Sigma class GST according to the similar amino acid conservation patterns to other Sigma class GST, demonstrating the importance of characterising proteins rather than relying on automated annotations.

I also identified 7 novel *A. perfoliata* Omega class GSTs (ApGST–O1 [1.1 and 1.2] to ApGST–O7), based on secondary characteristic structure prediction, phylogenetic tree analysis and key features. One potential further isoform was represented by a truncated sequence and so was excluded from analysis. The secondary characteristic structure prediction established the consistency and similarity of the β–strand, α–helix, and random coils structures with other cestodes and trematodes within the recognised Omega class GST and SspA sequences, which are conserved regions of these proteins. Likewise, all 7 novel *A. perfoliata* Omega class GSTs were homologous to recognised Omega class GSTs and the SspA sequence from the cestode clade GSTs in the phylogenetic tree, with a high bootstrap value (79%). Although, the phylogenetic tree revealed the *A. perfoliata* sequences were closer related to cestode SspA, for which GST activity is absent and does not bind glutathione (Hansen *et al.*, 2005), rather than other recognised Omega class GST sequences. Moreover, *A. perfoliata* were lacking of the proline–rich residues in the Omega class characteristic N–terminal extension (PXXP motif) (Morphew *et al.*, 2012). Importantly, all 7 novel *A. perfoliata* Omega class GST sequences had a high homology to other GSH–binding sites (Burmeister *et al.*, 2008; Kim *et al.*, 2016), containing the catalytic cysteine residue characteristic of Omega class GSTs at positions 32 (Cys^{32}) (Morphew *et al.*, 2012; Meng *et al.*, 2014; Kim *et al.*, 2016), as well as amino acid residues related to the Omega class GST key signature motifs (Chemale *et al.* 2006). Therefore, these preliminary discoveries support that *A. perfoliata* Omega class GST proteins likely belong to the Omega class of GST proteins according to their structural

enzymatic properties. It is implied that all 7 novel *A. perfoliata* Omega class GSTs are likely to possess similar functional characteristics to Omega class GST. Notably, because SspAs in cestodes have all of the characteristics of Omega class GSTs, including the key active site residue, which leads to the assumption that they are more likely to be Omega class GSTs. This could be an automated annotation issue based on the sequence similarity searching against protein databases that assigned them to SspAs.

Mu class GST have major roles in parasite general detoxification of xenobiotics and endogenously derived toxins as demonstrated in *E. granulosus* (EgGST1) (Arbildi *et al.*, 2017) and *F. hepatica* (Stuart *et al.*, 2021). Despite no documented role in immune modulation of the Mu class GSTs, in this chapter I examined the Mu class GSTs for completeness of the protein superfamily. *A. perfoliata* Mu class GST were identified in the largest proportion among other GST classes with 83 putative Mu class GSTs (87.37%) from a total of 95 GST sequences and demonstrated clustering in the cestode group. Likewise in the liver fluke, *F. gigantica* and *F. hepatica*, Mu class GSTs have been identified as the most abundant GST class (Morphew *et al.*, 2012; Stuart *et al.*, 2021). However, this is in contrast to transcriptome analysis of the rumen fluke, *C. daubneyi*, where the sigma–like GST class was the most abundant (Huson *et al.*, 2018), suggesting an essential role for the parasite's migration through the host. It has been reported that Mu class GST isoforms were majorly identified within the excretory secretory products (ESPs) of native forms of *F. hepatica* GSTs (Chemale *et al.*, 2006; Aguayo *et al.*, 2019). Hence, it would be of interest to explore *A. perfoliata* Sigma, Omega and Mu classes GSTs within the *A. perfoliata* secretome for further information. However, the resulting *A. perfoliata* Mu class GSTs identified in the current study need further characterisation and a better understanding as to their function and whether this is associated with parasite–host interactions.

2.4.2.2 Heat Shock Protein 90

Heat Shock Protein 90 (HSP90) is a molecular chaperone and a highly conserved protein involved in signal transduction, cell cycle control, stress management and folding, degradation and transport of proteins (Johnson, 2012; Roy *et al.*, 2012; Gillan and Devaney, 2014; Hoter *et al.*, 2018; Zininga *et al.*, 2018; Biebl and Buchner, 2019; Backe *et al.*, 2020). HSP90 has also been thought to be involved in host immune system modulation via platyhelminth secretomes (Liu *et al.*, 2009; Xu *et al.*, 2020), although information on the role

of HSP90 as an immune modulator in helminth infections is less extensive than other proteins, such as GSTs and α–Enolase. Within the *A. perfoliata* transcriptome, 5 novel HSP90s were identified (ApHSP90–1 [1.1 and 1.2], 2 [2.1, 2.2], 3, 4 and 5 [5.1 and 5.2]). All putative ApHSP90s were confirmed via secondary structure assessment and phylogenetic analysis with all 5 predicted as the HSP90α isoform via phylogenetics. It has been reported that only HSP90α isoforms are secreted from cells and are induced upon stress conditions, whereas HSP90β isoforms primarily operate intracellularly and are constitutively expressed (Langer *et al.*, 2003; Jayaprakash *et al.*, 2015; Hoter *et al.*, 2018). HSP90α proteins may be secreted by *A. perfoliata* which would support the importance of expression of HSP90α for production of proteins and suggest key roles in parasite–host invasion and interaction. On further assessment of the secondary structure and the molecular characteristics of HSP90s, only ApHSP90–4 contained the cytoplasmic HSP90 sequence motif 'MEEVD' whereas ApHSP90–5 (both 5.1 and 5.2) contained 'KEEL' which is 75% conserved to the 'KDEL' peptide sequences of the HSP90 endoplasmic reticulum (GRP94; 94–kDa glucose–regulated protein). As expected, there were no ApHSP90 sequences that contained the 'LKID' peptide sequences, which are specific to HSP90β (Skantar and Carta, 2004; Chen *et al.*, 2006; Hoter *et al.*, 2018). The 'LIP' and 'EDD' peptide sequences have been suggested as a signature sequences of HSP90α isoforms (Chen *et al.*, 2006), yet they were missing in all ApHSP90s. Interestingly, the 'IIP' and 'EDE' peptide sequences were found in ApHSP90–4 instead, which are similar to that observed in *E. granulosus* HSP90α (accession number XP_024345770 and CDI70178).

Three ApHSP90 sequences (ApHSP90–1.1, 1.2, 2.1, 2.2 and 3) were also shown to be closely related to other recognised cytosolic HSP90 sequences within the phylogenetic tree (*H. microstoma* accession number CDS28179, *E. granulosus* accession number CDS25067 and *E. multilocularis* accession number CDS39694). Therefore, ApHSP90–1, 2 and 3 may be the cytosolic HSP90 which are not specific to alpha (inducible isoform) or beta isoforms (constitutively expressed). Whereas ApHSP90–4 was clustered in a HSP90α cestode specific clade containing *E. granulosus* (accession number XP_024345770.1 and CDI70178.1). However, ApHSP90–5.1 and 5.2 were clustered into both cestode and trematode specific clades as well as HSP90s and HSP90α.

To this end, ApHSP90–1, 2, 3 and 4 are most likely to be cytosolic HSP90, of which ApHSP90–4 is most likely to be HSP90α–like, according to the molecular characteristics on signature sequences of HSP90α isoforms observed in *E. granulosus* HSP90α. Whereas ApHSP90–5 is most likely to be an endoplasmic reticulum HSP90. Based on the molecular characteristics of HSP90α, ApHSP90–4 may be expressed in response to stress in the environment in the host, as in pathological conditions, thus suggesting the modulation of the host immune response, facilitating the parasite survival within its host.

2.4.2.3 Alpha–Enolase

α–Enolase, also known as phosphopyruvate hydratase, is a glycolytic enzyme responsible for converting 2–phosphoglycerate (2–PG) into phosphoenolpyruvate (PEP) in the penultimate step of glycolysis (Fukano and Kimura, 2014). Additionally, α–Enolase is also considered a multi–functional protein due to acting as a plasminogen receptor and concentrating proteolytic plasmin activity on the cell surface (Díaz-Ramos *et al.*, 2012). Functional characterisations of the *Onchocerca volvulus* α–Enolase (Jolodar *et al.*, 2003) and *Echinostoma caproni* (Marcilla *et al.*, 2007) have suggested that this enzyme possesses immunomodulatory properties due to its ability to bind to plasminogen and promote plasmin–mediated proteolysis, which subsequently leads to the degradation of the host's extracellular matrix (Jolodar *et al.*, 2003; Ramajo-Hernández *et al.*, 2007; Maizels *et al.*, 2018). In total, 3 full length novel α–Enolases were identified (Apα–Enolase–1, 2, and 3) when exploring the *A. perfoliata* transcriptome, with the potential of two further isoforms that were represented by small fragments. Following phylogenetic analysis, all three novel Apα–Enolases were clustered well in the α–Enolase clade, specifically as part of a group.

Assessment of the primary amino acid sequence of the translated contig hits showed Apα–Enolase–1, 2 and 3 to conserve all five active site amino acid residues (His^{158}, Glu^{167}, $Glu2^{10}$, Lys^{343}, Lys^{394}, respective positions in human α–Enolase). Apα–Enolase–1, 2 and 3 also possessed similar secondary structure positioning when compared to α–Enolase of human, nematodes, trematodes and cestodes (10 β–strands and 15 α–helices) (Pancholi, 2001; Bergmann *et al.*, 2003; Jolodar *et al.*, 2003; Bernal *et al.*, 2004). Moreover, all three α–Enolase *A. perfoliata* sequences contained an enolase fingerprint motif, which is highly conserved in all known enolases (Babbitt *et al.*, 1996) as well as a domain for a hydrophobic putative signal peptide (91.7% complete for Ap–Enolase 1 and 2 and 75% complete for 3) (Jolodar *et al.*, 2003),

and putative plasminogen–binding motif (90.9%, 68.2% and 63.6% complete for Ap–Enolase 1, 2 and 3, respectively) (Bergmann *et al.*, 2003; Bernal *et al.*, 2004). This evidence suggests that these α–Enolase *A. perfoliata* proteins would exhibit similar enzymatic activity properties commonly associated with previously characterised α–Enolase proteins (Pancholi, 2001; Bergmann *et al.*, 2003; Jolodar *et al.*, 2003; Bernal *et al.*, 2004). To this end, Apα–Enolase–1, 2 and 3 are confirmed to be likely functional Apα–Enolase. However, the two Apα–Enolase fragments lacked the five catalytic active–site residues and comparable secondary structure patterning, which suggests enzymatic activity is not conserved in these two Apα–Enolase proteins and thus further investigation is required to confirm their enzymatic activity and full transcripts.

2.4.2.4 Sequence selection and genetic diversity assessment in immune modulators

After conducting the initial bioinformatics analysis, we obtained sequences for the three immune modulators. Notably, before constructing the phylogenetic tree, we performed a selection process where we excluded non–selected isoforms, very short sequences, alternative splice variants, and missing exons or fragmented split sequences. It **i**s important to highlight that this selection method was a manual process based on the most completed sequence regarding the multiple sequence alignments through Bioedit and insights from InterProScan results. Specific parameters or programmes were not employed for this selection. Consequently, the sequences that were excluded during this process may have represented gene duplications or distinct alleles, contributing to genetic variability within a population. Such genetic diversity can have significant implications for traits, adaptation, and evolution (Ranson *et al.*, 1998; García-Pérez *et al.*, 2023). These sequences might have represented genes with expression patterns differing from their isoforms within the family of related genes (Ranson *et al.*, 1998; García-Pérez *et al.*, 2023). In *Anopheles gambiae* class I GSTs, the gene *aggst1α* contains five coding exons that are alternatively spliced to produce four mature GST transcripts, generating multiple functional GST transcripts (Ranson *et al.*, 1998). This phenomenon is notably relevant within the GSTs family, demonstrate a multitude of isoforms in my study.

Therefore, future study should determine alternative spliced isoforms of a gene in total RNA using quantitative real–time or semi–quantitative PCR methods (Harvey and Cheng, 2016). Current methods can be employed in the detection of splice variants on RNA-level

information include prediction by clustering of expressed sequence tags, exon microarray, and mRNA sequencing (Florea, 2006). Moreover, programmes such as SplAdder identify alternative splicing events present in the augmented annotation graph; SingleSplice for Robust detection of alternative splicing in a population of single cells (Welch *et al.*, 2016); Bisbee predicts the protein–level effect of splice alterations (Halperin *et al.*, 2021) .

Hence, for future investigations, it is imperative to identify alternative spliced isoforms of a gene within total RNA samples. This can be accomplished through quantitative real-time or semi-quantitative PCR techniques (Harvey and Cheng, 2016). Contemporary methods for detecting splice variants at the RNA level encompass approaches such as prediction based on clustering of expressed sequence tags (EST), exon microarray analysis, and mRNA sequencing (Florea, 2006). Furthermore, specialized software programs, including *SplAdde*r for the identification of alternative splicing events within augmented annotation graphs, SingleSplice for robust detection of alternative splicing in single-cell populations (Welch *et al.*, 2016), and Bisbee for predicting the protein-level consequences of splice alterations (Halperin *et al.*, 2021), can be effectively employed to enhance our understanding of alternative splicing.

2.4.2.5 Resilient evolutionary relationships among novel immune modulatory proteins

After conducting phylogenetic analysis in the current study, most of the three immune modulators, including GSTs (Sigma and Omega classes GSTs), HSP90s, and α–Enolase, were clustered with their representatives in the cestode clade, showing strong bootstrap support (a high bootstrap value between 70–90% to 90–100%). Notably, some of them, as shown in a separate phylogenetic tree, exhibited weak bootstrap support (between 50 and 70%) for the branching patterns within the phylogenetic tree, including ApGST–S1, Apα–Enolase–1, and Apα–Enolase–2. Those weakly bootstrap supported branches should be subjected to further analysis to determine whether they accurately reflect true evolutionary relationships. Particularly further concerning the bootstrap value of the Mu class GSTs in some nodes of the GSTs phylogenetic tree, which have not been investigated.

The study of evolutionary relationships is dynamic, with new techniques and tools continually emerging, which, using multiple analytical methods or with traditional phylogenetic analysis, enhance the accuracy, reliability, and robustness of relationships in a phylogenetic tree (Kück *et al.*, 2010; Ribeiro *et al.*, 2012; Chang *et al.*, 2014; Z. Zhang *et al.*, 2017). It has been demonstrated in the research conducted by Zhang and colleagues in 2017,

when using the combine techniques to constructed the phylogenetic tree for two distinct sets of DNA sequences: one comprised bacterial 16S ribosomal RNA gene sequences, and the other featured genetic data from five homologous species. The Maximum likelihood (ML) and Bayesian inference (BI) methods were utilised to enhance the precision of the phylogenetic trees within the context of homologous data. Additionally, a multi-chain Markov chain Monte Carlo (MCMC) sampling technique was employed to identify the most optimal phylogenetic tree. This combined approach demonstrated improved accuracy of the phylogenetic trees, particularly enabling the detection of compositional heterogeneity within the experimental data (Zhang *et al.*, 2017). Prior to phylogenetic reconstruction, it is recommended to employ alignment masking tools, such as gBLOCKs (Castresana, 2000; Talavera and Castresana, 2007), trimAl (Capella-Gutiérrez *et al.*, 2009), ALISCORE (Kück *et al.*, 2010), and ClipKIT (Steenwyk *et al.*, 2020), to optimize the signal–to–noise ratio. These tools help eliminate unreliable positions in multiple sequence alignments (MSAs), thereby enhancing the topologies of the inferred trees, particularly in likelihood-based analyses. However, as suggested by Tan *et al.* (2015), while there was an increase in the proportion of well–supported branches in single-gene phylogeny reconstruction, phylogenetic trees obtained from filtered alignments often exhibited deteriorated performance (Tan *et al.*, 2015).

2.5 CONCLUSIONS

In the current study, I have presented the first *de novo* transcriptome inferred for adult *A. perfoliata* using Illumina RNA–sequencing and assembly, which is a rapid, effective technique, less expensive than full genome sequencing and allows better relation to the protein secretion from these individuals. Additionally, I have identified key RNA sequences likely expressed as proteins potentially involved in host–parasite interactions in the *A. perfoliata* transcriptome for three protein families; namely GSTs, HSP90s, andHSP90α–Enolase.

The discovery of *A. perfoliata* key RNA sequences including Sigma class GSTs, Omega class GST, Mu class GST, HSP90α and α–Enolase in the current study are still in the initial steps, based on the integrated *A. perfoliata* transcriptome and bioinformatics analysis. More work is needed, such as a deep characterisation in the crystal structural determination, biochemical or physiological functions. Importantly, the functionality as putative immune modulators will need to be completed to elucidate if they are involved in host immune modulation in *A. perfoliata* infected horses. Furthermore, the discovery of *A. perfoliata* key RNA sequences in this chapter will provide insight into whether these immune modulators proteins are specifically discovered in the EVs and ESP as well as secreted into the environment of the host and, consequently, capable of interacting with the host. Therefore, these novel protein families (GSTs, HSP90s and α–Enolase) will be further investigated in the *A. perfoliata* secretome via proteomic analysis in Chapter 3.

CHAPTER 3:

CHARACTERISATION OF THE ADULT *ANOPLOCEPHALA PERFOLIATA* SECRETOME TO REVEAL POTENTIAL IMMUNE MODULATORY PROTEINS

3.1 INTRODUCTION

Molecules secreted by helminth parasites into the host environment during the course of infection are termed excretory/secretory products (ESP) or secretome and contain a variety of soluble proteins, glycoproteins, carbohydrates, lipids and metabolites many of which are known to have an important role in helminth–mediated immunomodulation (Robinson *et al.*, 2009; Morphew *et al.*, 2011; Marcilla *et al.*, 2012; Victor *et al.*, 2012; Bień *et al.*, 2016; Vendelova *et al.*, 2016; Pan *et al.*, 2017; Wang *et al.*, 2017; Han *et al.*, 2019; Wangchuk *et al.*, 2019; Lawson *et al.*, 2019). Investigation of the ESP from tapeworms, such as the protoscoleces of *E. granulosus*, have demonstrated regulation of immune cell differentiation, such as B10, B17 and Th17 cells in infected mice, accompanied by a down regulation of the inflammatory response (Pan *et al.*, 2017)**.** Furthermore, *A. perfoliata* has been suggested to down–regulate T–cell responses in the horse in live infections, which was partly attributed to ESP*,* which inhibited growth and induced apoptosis of Jurkat cells (human T-cell line) *in vitro* (Lawson *et al.*, 2019). However, at present the active key component(s) in *A. perfoliata* ESP driving these potential host immunomodulatory mechanisms are yet unknown and need to be determined (Lawson *et al.*, 2019).

Extracellular vesicles (EVs) are lipid membrane–bound structures released from helminths as part of the ESP. Parasite EVs are released into the host extracellular environment and are likely candidates for intercellular communication and immunomodulation (Eichenberger *et al.*, 2018; Maizels *et al.*, 2018; Zakeri *et al.*, 2018). To date, EVs released from tapeworms have been identified in adult *H. diminuta* (Mazanec *et al.*, 2021) and *Taenia asiatica* (Liang *et al.*, 2019), and from various stages of *Taenia pisiformis* (Wang *et al.*, 2020), *E. granulosus* (Siles-Lucas *et al.*, 2017; Nicolao *et al.*, 2019; Zhou *et al.*, 2019; Wu *et al.*, 2021)*, Taenia crassiceps*, *M. corti* and *E. multilocularis* (Ancarola *et al.*, 2017). However, EVs from adult equine tapeworms, including *A. perfoliata*, have not yet been identified.

Key secretory proteins involved in immune modulation, host interaction and parasite survival have been identified as part of the ESP as free proteins or as components of EVs for a number of helminths. Such proteins identified include Annexins, Actins, Cathepsin proteases, Heat shock proteins (HSPs), Helminth defense molecules (HDMs), Glutathione transferases (GSTs) and Fatty–acid binding proteins (FABP), which have been identified from

platyhelminth species, *F. hepatica* (Robinson *et al.*, 2009; Marcilla *et al.*, 2012; Cwiklinski *et al.*, 2015; Davis *et al.*, 2019; de la Torre-Escudero *et al.*, 2019; Bennett *et al.*, 2020; Murphy *et al.*, 2020; Cwiklinski *et al.*, 2021), *C. daubneyi* (Rumen Fluke) (Huson *et al.*, 2018; Allen *et al.*, 2021), *S. japonicum* (Liu *et al.*, 2009) and *S. mansoni* (Kifle *et al.*, 2020). Furthermore, proteins exposed on the surface of EVs are likely essential in establishing direct connections between cells and their environment, thus implying key roles in parasite–host communication and interactions (Cwiklinski *et al.*, 2015; Buzás *et al.*, 2018; de la Torre-Escudero *et al.*, 2019; Murphy *et al.*, 2020; Allen *et al.*, 2021).

Proteomics is now recognised as a powerful tool for assessing protein profiles as part of a helminth secretome. A significant number of helminth secretome proteins have been identified and functionally characterised using a proteomic approach including potential immune modulation proteins in nematodes (Grzelak *et al.*, 2020; Kobpornchai *et al.*, 2020; Gillis-Germitsch *et al.*, 2021; Maruszewska-Cheruiyot *et al.*, 2021), trematodes (Ma *et al.*, 2021; Kenney *et al.*, 2022) and cestodes (Bień *et al.*, 2016; Mazanec *et al.*, 2021; Wu *et al.*, 2021). Furthermore, the hydrolytic surface–shaving techniques, releasing surface proteins of EVs for MS/MS identification gives insight into potential internalisation of EVs into host cells (Cwiklinski *et al.*, 2015; Buzás *et al.*, 2018; de la Torre-Escudero *et al.*, 2019; Murphy *et al.*, 2020; Allen *et al.*, 2021). Thus, in depth characterisation of helminth secretomes has the potential to uncover a greater understanding of pathological conditions as well as parasite–host interaction mechanisms during parasite infection.

3.1.1 AIMS AND OBJECTIVES

To facilitate an in–depth understanding of *A. perfoliata* molecular mechanisms of host–parasite interaction, I investigated the proteomics of the adult *A. perfoliata* secretome including whole EVs, EV surface expressed proteins, and EV depleted ESP. To achieve this aim, whole adult *A. perfoliata* from natural infections within the equine caecum were cultured *in vitro*. Adult *A. perfoliata* secretome was subsequently fractioned via size exclusion chromatography to obtain *A. perfoliata* whole EVs and EV depleted ESP. To confirm that adult *A. perfoliata* produce a secretome during *in vitro* maintenance, as in other platyhelminth species, morphology of EVs was characterised by Transmission Electron Microscopy (TEM) and Nanoparticle Tracking Analysis (NTA). Proteomic characterisation of adult *A. perfoliata* secretome were performed via GeLC (for whole EVs and ESP) and Gel free (for EV surface shaves) proteomic approaches. The *A. perfoliata* transcriptome (Chapter 2) was then exploited acting as an in–house searchable database for proteomic analysis to reveal key secretory proteins which have potential immunomodulatory properties expressed in the adult *A. perfoliata*, both in the EVs and EV depleted ESP.

3.2 MATERIALS AND METHODS

3.2.1 *A. perfoliata* collection and *in vitro* culture

Live adult *A. perfoliata* were collected according to the procedure outlined in Chapter 2, section 2.2.1. Subsequently, from each of the three horse replicates, 50 live adult *A. perfoliata* were cultured *in vitro,* following the method as previously described in Morphew et al. (2014). Briefly, following the PBS wash (for each replicate), 50 live adult *A. perfoliata* were transferred into 500 mL of pre–warmed (39°C) Dulbecco's modified Eagle's medium (DMEM, Gibco, Thermo Scientific), supplemented with 2.2 mM Calcium acetate, 2.7 mM Magnesium sulphate, 61 mM glucose, 15 mM HEPES (pH 7.0–7.6), gentamycin (5 µg/mL) and 1 µM serotonin. *A. perfoliata* were then cultured for 5 hours at 39^{o}C, whilst being transported back to the laboratory. All adult *A. perfoliata* remained alive (defined by worms still moving and responding to tapping on the media bottle) during the culture period. Following the culture period, adult *A. perfoliata* and large precipitated debris were removed, the culture supernatant was collected as *A. perfoliata* ESP and immediately stored at -80°C until further analysis.

3.2.2 Extracellular vesicle purification by size exclusion chromatography

EVs were purified from *A. perfoliata* culture media following the protocol described in Davis et al. (2019). Briefly, prior to EV purification, *A. perfoliata* ESP supernatant (Section 3.2.1) was thawed at 4°C and centrifuged (Heraeus Multifuge 3 S–R, Kendro Laboratory Products, Newtown, USA) at 4°C, firstly at 300 *x g* for 10 minutes, followed by 700 *x g* for 30 minutes to remove any cells and large debris. Subsequently, residual cells and debris were removed by filtering ESP supernatant through a 0.45 µm PES syringe membrane filter (diameter 33 mm, STARLAB, Milton Keynes, UK). *A. perfoliata* supernatant was concentrated using 10 KDa MWCO Amicon® Ultra–15 Centrifugal Filter Units (MerckMillipore, Merck Life Sciences, Dorset, UK), following the manufacturer's guidelines. Briefly, 500 mL of ESP supernatant was ultra–centrifuged (Heraeus Multifuge 3 S–R) at 3,000 x *g* for 20 minutes at 4°C until approximately 500 µL of ESP supernatant was retained in the filter unit and ready for further purification.

Following ultracentrifugation, *A. perfoliata* EVs were purified using a qEVoriginal size exclusion chromatography (SEC) column (70 nm; iZON Science, Oxford, UK), according to the manufacturer's protocol. Briefly, 10 mL of filtered PBS (pH 7.4; 0.22 µm, PES syringe membrane filter, diameter 33 mm; STARLAB) was firstly loaded through the qEVoriginal SEC column, followed by approximately 500 µL of ultra–centrifuged ESP supernatant. The first 3 mL of the filtration flow–through (Fractions 1 to 6) was discarded and SEC purified EVs collected from the next 1.5 mL of the filtration flow–through (EV enriched fractions 7 to 9; Böing et al. (2014); Hansen et al. (2019) into 1.5 mL microcentrifuge tube. Subsequently, 10 mL of filtered PBS was added to the qEVoriginal SEC column and the next 7.5 mL of the filtration flow–through collected as EV depleted SEC ESP >10 kDa. Both SEC purified EVs and SEC EV depleted ESP >10 kDa were stored at -80˚C until further proteomics analysis.

3.2.3 Characterization of extracellular vesicles released by *A. perfoliata*

3.2.3.1 Transmission Electron Microscopy (TEM) analysis

A. perfoliata SEC purified EV samples (n=3; Section 3.2.2; 1 replicate per TEM grid) for TEM analysis were prepared following the protocol according to Théry et al. (2006). Briefly, thawed SEC purified EVs (5 µL) were mixed gently with 4% (w/v) Paraformaldehyde (5 µL; PFA; Thermo Scientific). Subsequently Formvar/Carbon coated Copper TEM grids (400 Mesh; Agar Scientific, Stansted, UK) were transferred onto SEC purified EVs in 2% PFA, fixed for 20 minutes at room temperature and in darkness. Following fixing of EVs, each grid was then washed in filtered (0.22 µm) PBS (pH 7.4, Thermo Scientific) for 1 minute and fixed with 1% (v/v) glutaraldehyde solution (Sigma–Aldrich, Merck Life Sciences) for 5 minutes. At this point, each TEM grid was washed to remove any free EVs with distilled water for 2 minutes, a total of 8 times. Grids were then contrast–stained in Uranyl–Oxalate solution (pH 7.0, Thermo Scientific) for 5 minutes, followed by embedding in Methyl Cellulose–Uranyl Oxalate (Thermo Scientific) for 10 minutes on ice. Finally, TEM grids were air dried and stored at room temperature for further EV characterisation.

To analyse the characteristic morphology of *A. perfoliata* SEC purified EVs, TEM grids were assessed under Transmission Electron Microscope (JEM1010 Transmission Electron Microscope, Jeol , Tokyo, Japan) at 80 kV, as previously described in Davis et al. (2019). The size

(dimension) of 200 EVs per purification sample (n=3) imaged by TEM were measured (nm) using ImageJ (version 1.52a; https://imagej.nih.gov/ij/; Schneider *et al.*, 2012). The proportion of the size distribution of *A. perfoliata* SEC purified EVs were identified by the range of EV size at < 30 nm, 30–100 nm and > 100 nm (Raposo and Stoorvogel, 2013; Davis *et al.*, 2019).

3.2.3.2 Nanoparticle Tracking Analysis (NTA)

A. perfoliata SEC purified EVs (n=3; Section 3.2.2) underwent Nanoparticle Tracking Analysis at the Department of Veterinary Medicine, University of Cambridge. The size distribution and the number of particles (concentration) in each replicate were determined using a Nanosight NS500 system (Malvern Instruments, Malvern, UK) equipped with a green 532 nm laser and a high sensitivity electron multiplying charge-coupled device (EMCCD) camera (Andor Technology, Belfast, UK), following the manufacturer's instruction. Each *A. perfoliata* SEC purified EVs replicate was diluted in PBS (pH 7.4) at a 1:600 dilution to a final volume of 1 mL to obtain a concentration ranging between 1 x 10^6 and 1 x 10^9 particles/mL. Diluted SEC purified EVs were introduced into the measurement chamber through a 1 mL syringe. For each sample, 5 consecutive videos of the particles moving under Brownian motion were captured, with a camera level of 15. Each video lasted 60 seconds, with a delay of 12 seconds between videos taken. Subsequently, the captured video data were analysed using the NanoSight software (NTA version 3.2 Dev Build 3.2.16) to assess the particle size and concentration of SEC purified EVs, with the analysis setting set at a detection threshold of 5 (see the capture and analysis settings in Appendix 3.1).

3.2.3.3 Extracellular vesicle surface protein hydrolysis

Surface proteins of SEC purified EVs of *A. perfoliata* (n=3) were removed through hydrolysis with trypsin, as previously described by Allen *et al.* (2021). Briefly, each replicate of SEC purified EV sample (Section 3.2.2) was diluted with PBS to a final concentration of 200 µg in 250 µL total volume. Sequencing grade modified trypsin (25 µg/vial; Roche, U.K) was diluted with 50 mM Ammonium bicarbonate (AMBIC; pH 8.0; Thermo Scientific) to 100 µg/mL and added to the SEC purified EVs to obtain a final trypsin concentration of 50 µg/mL. Samples were incubated on dry bath/block heaters (Fisherbrand™, Thermo Scientific) at 37°C for 5 minutes. The treated SEC purified EVs were then ultra–centrifuged (S55–S rotor, Sorval

MX120 centrifuge, Thermo Scientific) at 100,000 × *g* for 1 hour at 4°C. The resulting supernatant was stored at -20°C for further gel free mass spectrometry analysis.

3.2.4 Secretome proteomics analysis

3.2.4.1 EV depleted ESP sample preparation for one dimensional sodium dodecyl sulfate polyacrylamide gel electrophoresis (1D SDS–PAGE)

Prior to protein quantification*, A. perfoliata* SEC EV depleted ESP >10 kDa (n=3; Section 3.2.2) were concentrated by Trichloroacetic acid (TCA)/ acetone precipitation as previously described in Morphew *et al.* (2014). Briefly, *A. perfoliata* SEC EV depleted ESP >10 kDa was concentrated with ice–cold 20% (w/v) TCA in 100% acetone (Thermo Scientific) at a ratio 1:1 in a conical centrifuge tube and incubated at -20 °C for 1 hour, during which time the tube was inverted 4 times, every 15 minutes. The mixed solution was aliquoted into to 2 mL centrifuge tubes and subsequently centrifuged (Heraeus Multifuge 3 S–R) at 21,000 x *g* for 20 minutes at 4°C. Following centrifugation, the supernatant was discarded and the pellet washed in 100% acetone (cooled on ice) and sonicated in an ultra–sonicating water bath (Fisherbrand FB11013, Thermo Scientific) for 30 seconds. All aliquots were pooled together and centrifuged (IEC Micromax Centrifuge, Thermo Scientific) at 21,000 x *g* for 20 minutes at 4°C, repeating the washing, sonicating and centrifugation steps once for the single combined aliquot. After the supernatant was discarded, the retained pellet was placed at -20°C with the lid open for 15 minutes to let the acetone evaporate, and subsequently stored at -20°C (with the lid closed) until further 1D SDS–PAGE.

3.2.4.2 Quantification of protein concentration in SEC purified EVs and SEC EV depleted ESP>10 kDa samples

The Qubit® Protein Assay Kit along with the Qubit® 2.0 Fluorometer (Invitrogen, Thermo Scientific) was employed to quantify the concentration of *A. perfoliata* SEC purified EVs (n=3; Section 3.2.2), according to the manufacturer's protocol. Due to the concentration of protein in SEC purified EV samples being low, samples were evaporated under a vacuum centrifugation (Heto Holton Maxi–Dry Plus, West Technology Systems, Bristol, UK) for 1 hour,

repeated until a final volume was approximately 500 µL and quantified using the Qubit® Protein Assay Kits, as described above.

The resultant pellets of *A. perfoliata* SEC EV depleted ESP >10 kDa (n=3; Section 3.2.4.1) were re–suspended in Isoelectric Focusing (IEF) Buffer Z (8 M urea, 2% w/v CHAPS ($C_{32}H_{58}N_2O_7S$), 33 mM Dithiothreitol). Suspended SEC EV depleted ESP >10 kDa samples were dissolved by sonicating in an ultra–sonicating water bath for 30 seconds and then placed on ice for 1 minute. Following that, samples were quantified using Bradford assay (Sigma–Aldrich, Merck Life Sciences; Bradford, 1976) according to the manufacturer's protocol, through an UV–visible spectrophotometer (Cary 50, Agilent Technologies, Cheshire, UK) at an absorbance measurement of A595 nm. All SEC purified EVs and SEC EV depleted ESP >10 kDa samples were stored at -20°C until further 1D SDS–PAGE electrophoresis.

3.2.4.3 One dimensional sodium dodecyl sulfate polyacrylamide gel electrophoresis

A. perfoliata SEC purified EVs (n=3) and SEC EV depleted ESP >10 kDa (n=3) samples (Section 3.2.4.2) were run on a mini 1D SDS–PAGE gel, 7 cm, 0.75 mm gel thickness, 12.5% resolving acrylamide gels, according to the protocol of Brunelle & Green (2014). Briefly, 12.5% resolving acrylamide gels (containing 30% w/v Acrylamide/Bisacrylamide stock solution 29:1, 10% Ammonium persulfate; TEMED, running gel buffer and ddH_2O) and stacking gels (containing 30% w/v Acrylamide/Bisacrylamide stock solution 29:1, 10% w/v Ammonium persulfate, TEMED, stacking gel buffer and ddH_2O) were prepared. Then a fresh 1x Tris/glycine/SDS electrophoresis buffer (25 mM Tris, 192 mM glycine, 0.1% SDS, pH 8.3; Bio–Rad Laboratories, Hertfordshire, UK) was prepared to fill the electrophoresis chamber (Bio–Rad Laboratories). All samples were mixed with 5 µL of 4x SDS buffer (containing 0.2 M Tris–HCl pH 6.8, 8.0% (w/v) Sodium dodecyl sulfate, 40% (v/v) Glycerol, 0.02% (v/v) Bromophenol blue and 5% β–mercaptoethanol). SEC purified EV samples were denatured by heating to 95°C for 10 minutes on the dry bath/block heaters (Fisherbrand™, Thermo Scientific), and centrifuged (IEC Micromax Centrifuge), at 21,000 x *g* for 10 minutes at room temperature. Samples were loaded onto the gel with 10 µg of protein. The gel was run at a constant voltage of 70 V (PowerPac 1000 Electrophoresis Power Supply, Bio–Rad Laboratories) for approximately 20 minutes until the bromophenol blue moved through the stacking gel, and the voltage then increased to 150 V until completion.

Completed 1D SDS–PAGE gels were then washed in distilled water, followed by fixing in 40% (v/v) ethanol (Thermo Scientific) and 10% (v/v) acetic acid (Thermo Scientific) on a rocker (SSL4, Cole–Parmer™ Stuart™ See–Saw Rocker, Thermo Scientific) for approximately 1 hour. After fixing, gels were washed twice in distilled water for 5 minutes and stained overnight with colloidal Coomassie™ Brilliant Blue (80% (v/v) dye stock solution and 20% (v/v) methanol, Thermo Scientific). Stained gels were washed twice in distilled water for 5 minutes followed by thoroughly de–staining in 1% (v/v) acetic acid (Thermo Scientific) until the gel background was clear. Gel images were acquired with a GS–800™ Calibrated Densitometer (Bio–Rad Laboratories), set for Coomassie stained gels at 400 dpi. One dimensional SDS–PAGE gels with separated protein bands of SEC purified EVs and SEC EV depleted ESP >10 kDa samples were stored in 1% (v/v) acetic acid (Thermo Scientific) until ready for further trypsin in–gel digestion.

3.2.4.4 Trypsin in–gel digestion

SDS PAGE lanes containing either *A. perfoliata* SEC purified EVs (n=3) and SEC EV depleted ESP >10 kDa (n=3; Section 3.2.4.3) were divided into 9 and 12 sections, respectively. Each of these sections were excised for in–gel digestion with trypsin, as previously described by Morphew *et al.* (2011). Briefly, excised gel bands were transferred into a 500 µL microcentrifuge tube (Thermo Scientific) and de–stained with mixed 50% (v/v) acetonitrile (ACN; Thermo Scientific) and 50% (v/v) 50 mM ammonium bicarbonate (AMBIC; pH 8.0; Thermo Scientific) at 37°C for 15 minutes. The supernatant was discarded and the process repeated until gel pieces were de–stained. Gel bands were then dehydrated in 100% ACN at 37°C for 15 minutes, and the gel dried at 50°C. Following drying, 10 mM dithiothreitol (DTT; Melford Laboratories, Suffolk, UK) in 50 mM AMBIC (15.4 mg DDT in 10 mL 50 mM AMBIC) was added to gel pieces and incubated at 80°C for 30 minutes before then incubating with 55 mM iodoacetamide (IAA; Sigma–Aldrich) in 50 mM AMBIC (102 mg IAA in 10 mL 50 mM AMBIC) at room temperature for 20 minutes. Gel pieces were washed with mixed 50% (v/v) ACN and 50% (v/v) 50 mM AMBIC at room temperature for 15 minutes, dehydrated with 100% ACN at room temperature for 15 minutes and then dried at 50°C. Gel pieces were rehydrated and digested with 50 mM AMBIC containing trypsin (Roche) at 10 ng/µL at 37˚C for approximately 16 hours. Gel pieces were then centrifuged at 10,000 *x g* for 10 minutes and then MilliQ water was added before placing on a shaker at room temperature for 10 minutes,

and the supernatant retained. A mixed solution of 50% (v/v) ACN and 5% (v/v) formic acid (Sigma–Aldrich) were again added to the gel pieces at room temperature for 60 minutes. Gel pieces were centrifuged briefly (IEC Micromax Centrifuge), the supernatant retained was added to the previously retained extraction. All retained supernatants containing peptides were dried (Heto Holton Maxi–Dry Plus) until pelleted ready for mass spectrometry analysis.

3.2.4.5 Liquid Chromatography–Tandem Mass Spectrometry (LC–MS/MS)

Liquid Chromatography Tandem Mass Spectrometry was performed at the Advanced Mass Spectrometry Facility, School of Biosciences, University of Birmingham as a commercial service. Briefly, dried peptide pellets of *A. perfoliata* SEC EVs (n=3; Section 3.2.4.4) and SEC EV depleted ESP >10 kDa (n=3; Section 3.2.4.4) were re–suspended in 20 µL of 0.1% v/v formic acid and then loaded to a 250 µL vial insert with an autosampler vial (Agilent Technologies, Cheshire, UK) to be analysed by Liquid Chromatography tandem mass spectrometry (Q Exactive™ HF Hybrid Quadrupole–Orbitrap™ Mass Spectrometer, Thermo Scientific) equipped with a TriVersa Nanomate (Advion, Harlow, UK) and nanoflow liquid chromatography system (Dionex, Thermo Scientific). EV surface peptides (n=3; section 3.2.3.3) were analysed directly on the same mass spectrometry set up.

3.2.4.6 Protein identification and Gene Ontology terms enrichment analysis (GOEA)

Protein identification of *A. perfoliata* proteomic profiles were performed through MASCOT hosted by IBERS, Aberystwyth University, according to the method described by Morphew et al. (2014). Briefly, the acquired MS/MS spectra (Mascot Generic Files; Section 3.2.4.5) were submitted to a MASCOT MS/MS ions search (Matrix Science, v2.6; www.matrixscience.com; Perkins et al., 1999) against the *A. perfoliata* transcriptome (Chapter 2, Section 2.3.2) and *Equus caballus* predicted coding sequences (CDS) from the genome (version 3.0; https://www.ensembl.org). Search parameters used the following: trypsin enzymatic cleavage with up to 1 missed cleavage allowed, fixed modifications to carbamidomethylation of cysteines with variable modifications set for Oxidation of methionine, fixing fragment monoisotopic mass error with peptide tolerances of ±1.2 Da and MS/MS of ±0.6 Da, peptide charge 1+, 2+ and 3+, monoisotopic, data format with MASCOT generic, Electrospray ionization (ESI) TRAP. The resulting identified proteins that indicate the identity or extensive homology, at $p<0.05$, were selected according to the individual MASCOT ions score with

scores set at greater than 48 for SEC EVs and SEC EV depleted ESP >10 kDa samples and 47 for EVs surface samples. Subsequently, unique peptides presented in at least 2 replicates were then used for searching against the *A. perfoliata* annotation database (obtained from the Omicsbox; Chapter 2, Section 2.3.3, Appendix 2.4) to assign the protein description and Gene Ontology (GO) terms.

The resulting number of proteins identified from MS/MS analysis within *A. perfoliata* proteomics datasets were then visualised in Venn–diagrams using InteractiVenn (http://www.interactivenn.net/; Heberle *et al.*, 2015). Gene Ontology terms enrichment analysis (GOEA) on gene sets of all proteomics datasets was performed using GOATOOLS python package (v0.5.9, https://github.com/tanghaibao/goatools; Klopfenstein et al., 2018) whether the GO terms were propagated up the hierarchy (prop) or were not propagated up the hierarchy (nop). A p value of $p<0.05$ identified significance.

3.2.5 Characterisation of potential immune modulators in *A. perfoliata* secretome

Putative immune modulatory sequences, particularly for three potential immune modulator protein families identified within *A. perfoliata* transcriptome (namely the Glutathione transferase (GSTs) Superfamily (Mu, Sigma and Omega class GST; Chapter 2, section 2.3.5.1–2.3.5.3), cytoplasmic Heat Shock Protein 90s (; Chapter 2, section 2.3.5.4) and Alpha–Enolases (α–Enolase; Chapter 2, section 2.3.5.5) were assessed for protein expression across all three secretome proteomic datasets (SEC whole EV, EV surface and EV depleted ESP).

3.3 RESULT

3.3.1. Morphological characterisation and size distribution of *A. perfoliata* SEC purified EVs by TEM

The characterisation of SEC purified *A. perfoliata* EVs by TEM confirmed that *A. perfoliata* secreted EVs during *in vitro* maintenance. TEM analysis demonstrated morphological characteristics of SEC purified *A. perfoliata* EVs to be a spherical shaped (cup–shaped) membrane surrounded by a phospholipid bilayer structure (Figure 3.1). The mean estimated particle size (mean ± SD) of SEC purified *A. perfoliata* EVs (3 replicates) measured by TEM was approximately 64.16 ± 28.50 nm in diameter (n = 200). TEM showed the greatest EV size was 214.57 nm whereas and the smallest EVs size was 30.17 nm. The proportion of the size distribution of SEC purified *A. perfoliata* exosome (30–100 nm) and microvesicles (100–1000 nm) determined by TEM was 86% and 14%, respectively (Figure 3.2).

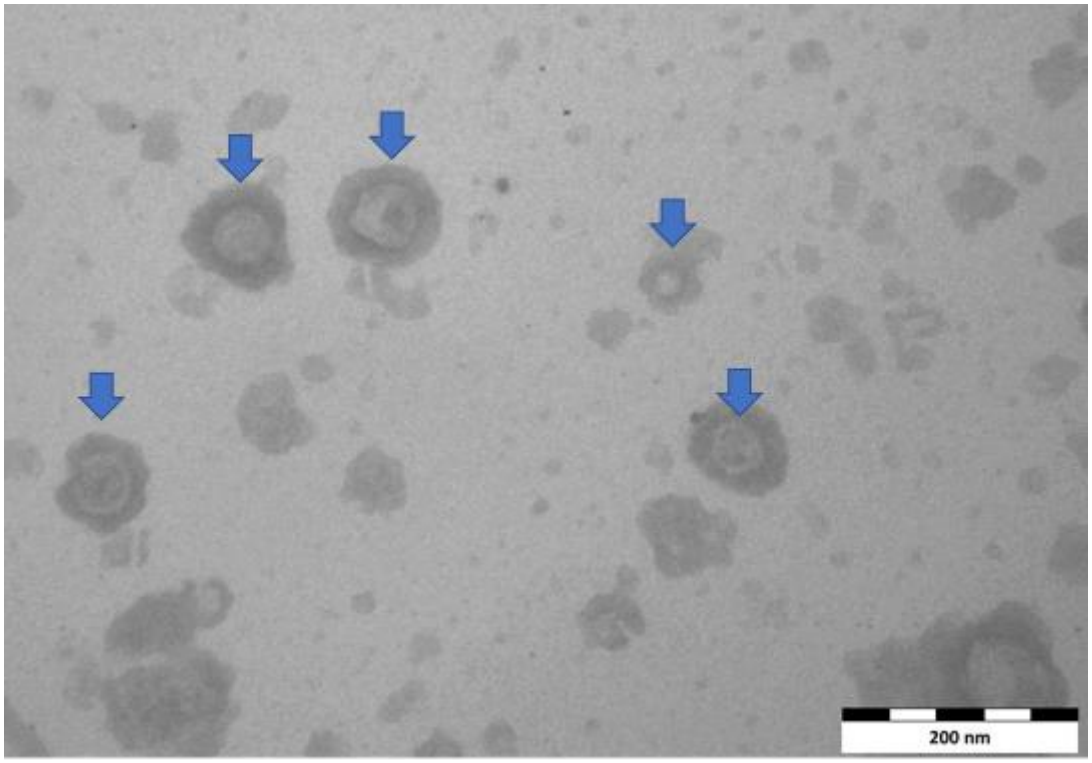

Figure 3.1 TEM image from SEC purified *A. perfoliata* derived EVs at 80 kV blue arrows demonstrate *A. perfoliata* secreted extracellular vesicles (scale bar = 200 nm). *A. perfoliata* EV morphology is demonstrated to be a spherical shaped membrane surrounded by a phospholipid bilayer structure.

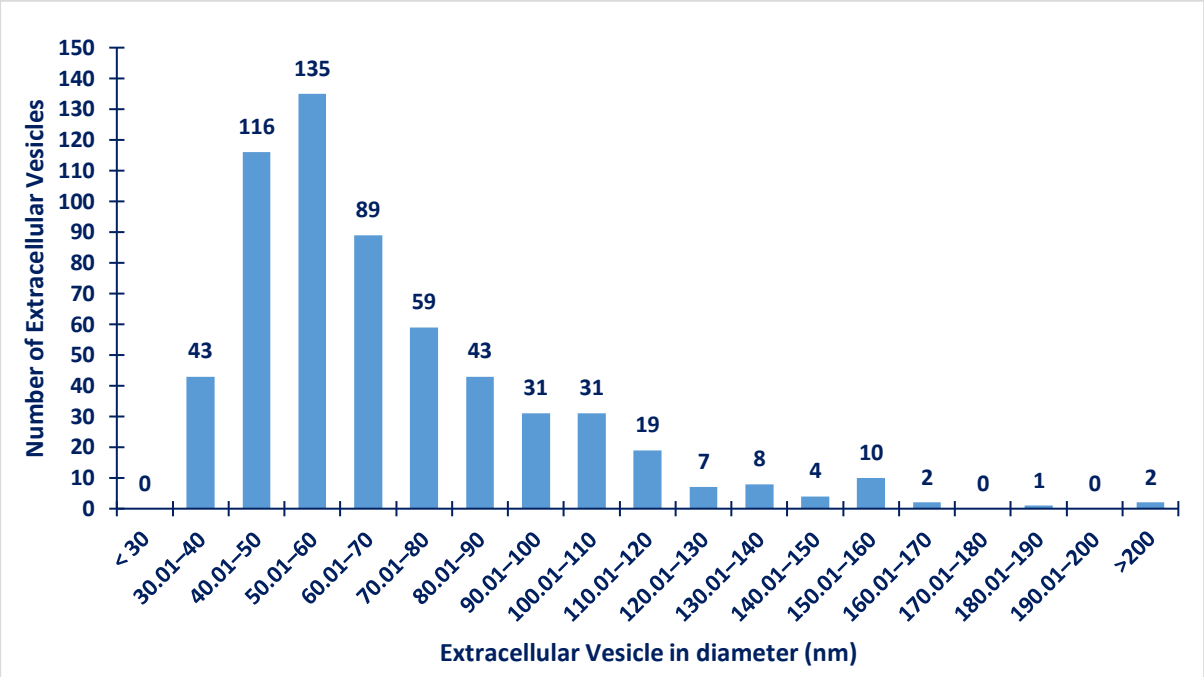

Figure 3.2 Size distribution of the isolated size exclusion chromatography (SEC) purified *A. perfoliata* EVs (cumulative data from 200 EVs per replicate, n = 3). The number of exosomes is shown in the size range of 30 to 100 nm (86%) and microvesicles in the size range of 100–1000 nm (14%).

3.3.2. Nanoparticle Tracking Analysis of *A. perfoliata* EVs

The characterisation of SEC purified *A. perfoliata* EVs by NTA also confirmed that *A. perfoliata* secreted EVs during *in vitro* maintenance (Figure 3.3–A). The mean estimated particle size (mean ± SD) of SEC purified *A. perfoliata* EVs (3 replicates) measured by NTA was approximately 199.1 ± 108.7 nm in diameter which the majority of the EV population were found to be 67–213 nm (Figure 3.3–B), with a mean concentration of 1.57 x 10^9 EV particles/mL (Table 3.1).

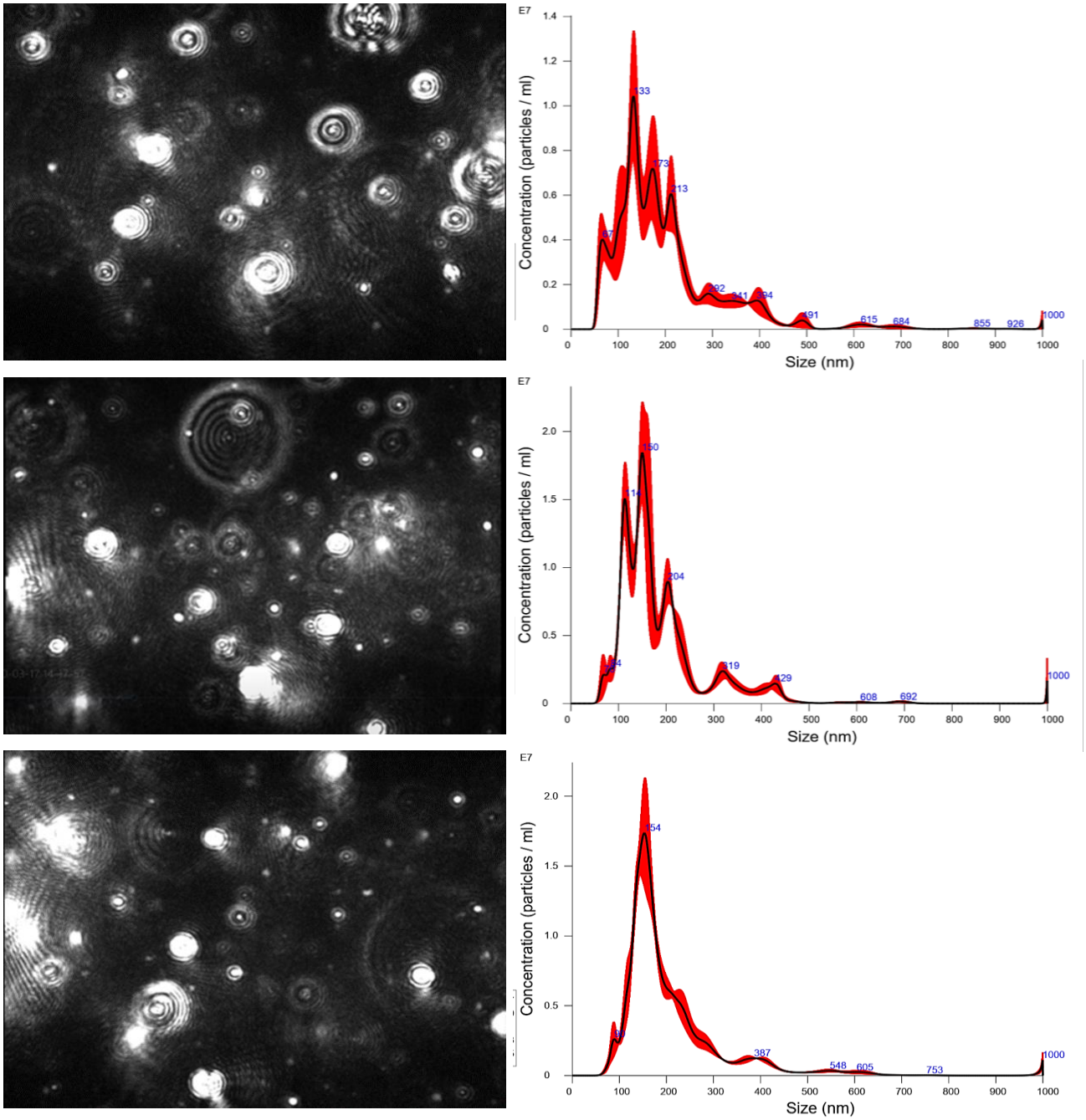

(A) **(B)**

Figure 3.3 A. Screenshots from video recorded nanoparticle tracking analysis through a Nanosight NS500 system demonstrating SEC purified *A. perfoliata* EV particles at a 1:600 dilution (n=3); B. EV particle size distribution and average finite track length adjustment (FTLA) concentration (EVs x 10^7/mL vs size in nm) of SEC purified *A. perfoliata* EVs at 1:600 dilution (n=3). Averaged FTLA concentration, as red areas, specify the standard deviation (SD) between measurements and blue numbers indicate the maxima of individual peaks.

Table 3.1 Summary statistics of nano–particle tracking analysis (NTA) of Size Exclusion Chromatography (SEC) purified *A. perfoliata* EVs. D10, D50 and D90 refer to the point at which the particle size distribution, up to and including 10, 50 and 90% of the total volume of material in the sample is 'contained'.

Parameters	Mean EVs ± SE
Mean (nm)	199.1 ± 5.3
Mode (nm)	144.7 ± 7.5
SD (nm)	108.7 ± 8.5
D10 (nm)	105.9 ± 2.6
D50 (nm)	168.3 ± 4.6
D90 (nm)	337.9 ± 14.7
Concentration (particles/mL)	$9.42 \times 10^{11} \pm 7.20 \times 10^{11}$
Concentration (particles/frame) 1:600 dilution	81.2 ± 6.1
Concentration (centres/frame) 1:600 dilution	116.1 ± 7.1

3.3.3. Protein profiling of *A. perfoliata* proteomics datasets

3.3.3.1 1D SDS–PAGE gels

The mean ± SD protein concentration of *A. perfoliata* SEC purified EVs (n=3) and SEC EV depleted ESP >10 kDa (n=3) quantified using Qubit™ Protein Assay was 1.70 ± 0.42 µg/µL and 3.59 ± 2.60 µg/µL, respectively. Three biological replicates of both *A. perfoliata* whole SEC purified EVs and SEC EV depleted ESP >10 kDa produced similar patterns of protein bands for each separate sample demonstrating the similarity amongst biological replicates. Protein bands in SEC EV depleted ESP >10 kDa demonstrated more frequent and dense proteins on 1D SDS–PAGE gels compared to the whole EVs (Figure 3.4). Each replicate lane was cut into equal sections and analysed using tandem mass spectrometry.

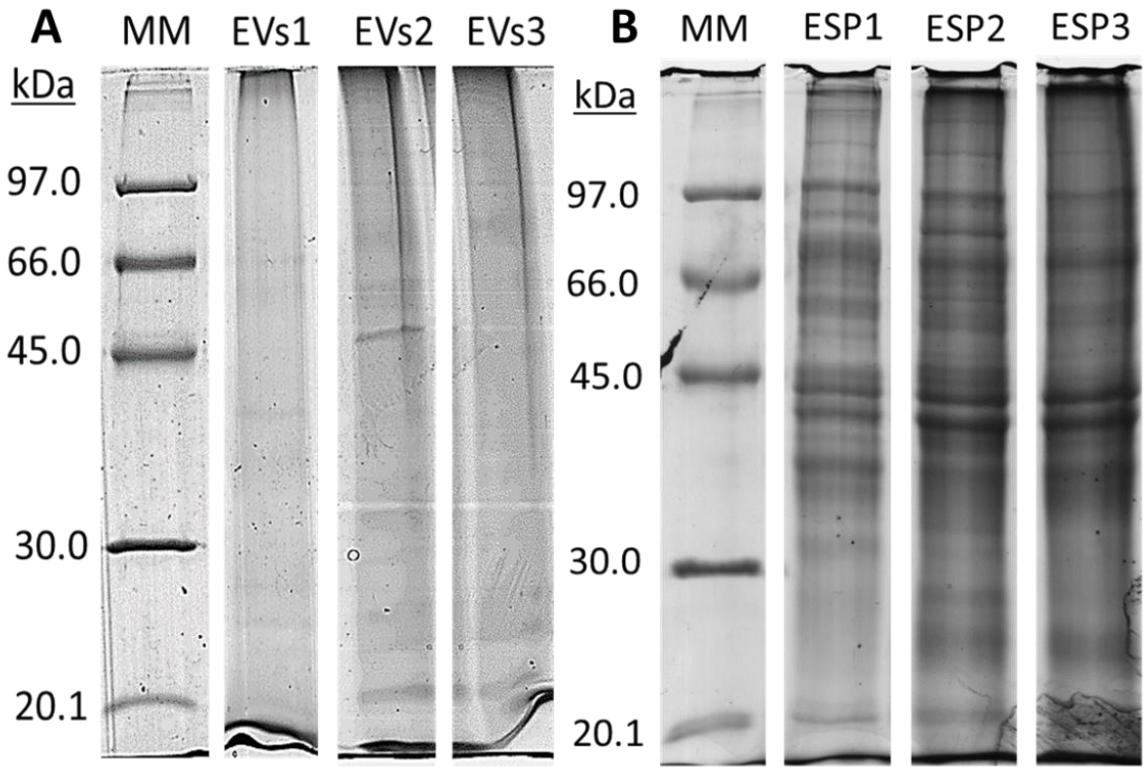

Figure 3.4 A. Protein profiles of *A. perfoliata* SEC purified EVs; B. SEC EV depleted ESP >10 kDa replicate 1, 2 and 3 displayed on a 12.5% 1D SDS–PAGE stained with Coomassie blue, loaded 10 µg protein/each lane. MM: Molecular weight markers.

3.3.3.2 Mass spectrometry datasets

The resulting three *A. perfoliata* mass spectrometry datasets including SEC whole EVs (GeLC approach), EV surface (Gel free approach) and EV depleted ESP >10 kDa (GeLC approach) were analysed through MASCOT via MS/MS Ion Search against the *A. perfoliata* transcriptome for protein identification. The full list of proteins identified in each *A. perfoliata* proteomics datasets is available in Appendix 3.2. A total of 315 proteins were identified from SEC *A. perfoliata* whole EVs, 301 proteins from the EV surface and 596 proteins from EV depleted ESP >10 kDa (Figure 3.5). All three proteomics datasets shared 107 proteins (Figure 3.5), with the most abundant proteins in all datasets being WD repeat and FYVE domain–containing protein 3 (Table 3.2–3.5, Appendix 3.2). Of a total 474 proteins identified in or on EVs, 142 identified proteins were common between whole EVs and the EV surface.

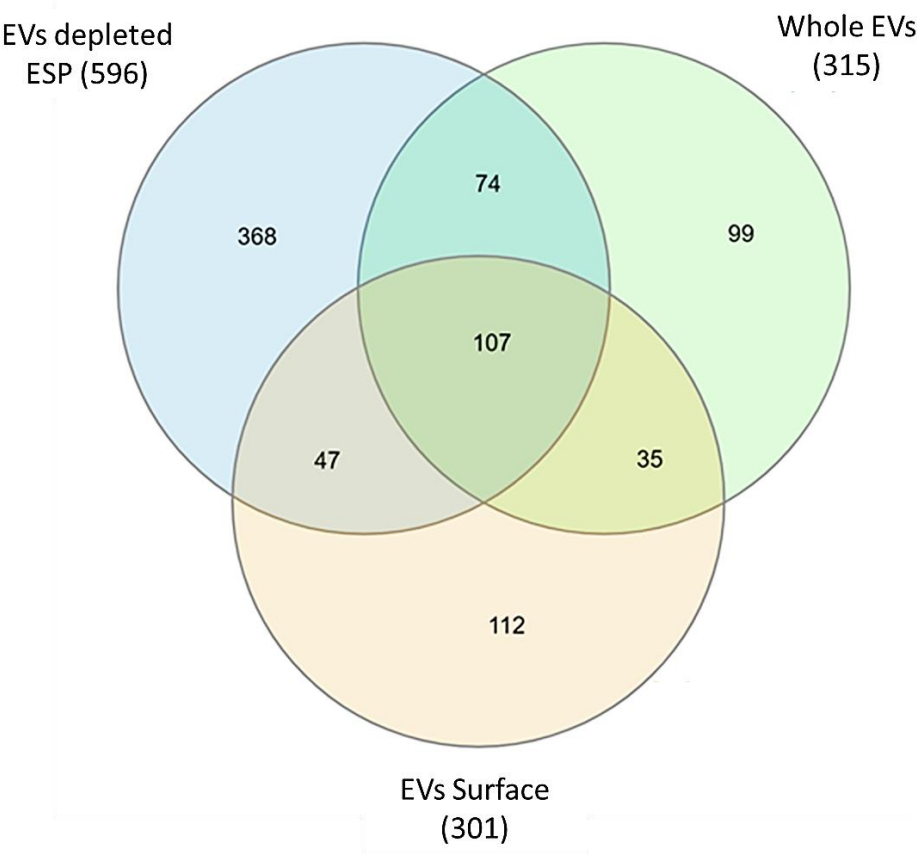

Figure 3.5 Venn–diagrams comparing the proteins identified in SEC *A. perfoliata* whole EVs, EV surface and EV depleted ESP >10 kDa retrieved from mass spectrometry analysis and MASCOT via MS/MS Ion Search against the *A. perfoliata* transcriptome.

Well–known identified EV markers of interest as defined by the Exocarta (http://www.exocarta.org/; Mathivanan *et al.*, 2012; Keerthikumar *et al.*, 2016) and Vesiclepedia databases (http://microvesicles.org/extracellular_vesicle_markers; Kalra *et al.*, 2012) in SEC *A. perfoliata* whole EV and EV surface proteomics datasets were noted amongst the top 50 most abundant proteins, such as annexin, actin, myosin, enolase, phosphoglycerate kinase, heat shock 70 kDa protein, molecular chaperone HtpG and programmed cell death 6–interacting protein (Table 3.2 and 3.3). On the surface of SEC *A. perfoliata* EVs, protein pumps and transporters were identified, such as ATP binding cassette subfamily B (MDR:TAP), multidrug resistance protein, V type proton ATPase 116 kDa subunit A, plasma membrane calcium–transporting ATPase 3 and solute carrier family 5 (Table 3.3).

Table 3.2 The top 50 most abundant proteins putatively identified in SEC *A. perfoliata* EV proteomic dataset by 1D SDS–PAGE, LC MS/MS (GeLC) and a MASCOT search, with significance threshold score above 48. Protein descriptions were given from Omicsbox. Protein hits shaded in grey and in bold represent known helminth immune modulators, as also identified in the *A. perfoliata* transcriptome (Appendix 3.2).

No.	Protein Description	Sequence ID	Number of sequenced peptides	MASCOT score
1	WD repeat and FYVE domain–containing protein 3	DN11838_c0_g1_i2_56054	78	1933
2	Actin, cytoplasmic type 5	DN10334_c0_g1_i3_17117	41	958
3	Myosin XV	DN10026_c0_g1_i2_27828	36	346
4	Myosin heavy chain 10 or non–muscle myosin IIB	DN10438_c0_g2_i2_34624	34	1235
5	Leucine–rich repeat–containing protein	DN11834_c0_g1_i11_56034	30	611
6	Otoferlin	DN10250_c0_g1_i1_26991	29	245
7	Fascin 2	DN10161_c0_g1_i1_59685	29	599
8	**Calpain A**	**DN9786_c0_g1_i1_72692**	**27**	**1113**
9	Annexin A7	DN8700_c0_g1_i1_600	26	747
10	Phosphoenolpyruvate carboxykinase	DN11364_c0_g2_i1_39228	25	691
11	Actin, cytoplasmic type 5	DN10334_c0_g1_i1_17115	24	865
12	Heat shock 70 kDa protein 4	DN12581_c0_g1_i2_73130	23	440
13	Expressed conserved protein	DN11921_c1_g2_i1_46303	22	400
14	Von Willebrand factor A domain containing protein	DN11931_c2_g1_i10_58523	22	396
15	Expressed conserved protein	DN7822_c0_g2_i1_27391	22	131
16	Annexin A7	DN7793_c0_g1_i1_23754	21	321
17	Aldo keto reductase family 1–member B4	DN11165_c0_g1_i1_24177	21	416
18	Expressed conserved protein	DN10367_c0_g1_i3_29401	21	473
19	Solute carrier family 5	DN12278_c0_g6_i1_68615	20	642
20	Tegumental antigen	DN5781_c0_g1_i1_2927	20	674
21	Programmed cell death 6– interacting protein	DN10491_c0_g3_i2_21343	19	303
22	Peroxidasin	DN10163_c0_g1_i1_35077	18	419
23	**Enolase**	**DN14469_c0_g1_i1_24672 (Apα–Enolase–1)**	**18**	**447**
24	Ubiquitin–60S ribosomal protein L40	DN12547_c0_g1_i1_46361	18	335
25	Annexin A13 (Annexin XIII)	DN9930_c0_g1_i1_67885	17	1023
26	Tegumental protein	DN15763_c0_g1_i1_57495	17	260
27	**Molecular chaperone HtpG/ Heat shock protein 90 alpha**	**DN11960_c0_g1_i1_46290 (Ap –4)**	**16**	**239**
28	Expressed conserved protein	DN8957_c0_g1_i1_66134	16	299
29	**Glycoprotein Antigen 5**	**DN9013_c0_g1_i2_47406**	**16**	**476**
30	Annexin A13 (Annexin XIII)	DN12676_c0_g1_i9_72045	15	480
31	Alpha 2 macroglobulin	DN12789_c0_g1_i5_70580	15	293
32	Phosphoglycerate kinase	DN11218_c0_g1_i1_75075	14	338
33	Annexin B9–like isoform X1	DN11220_c0_g1_i12_22997	14	650
34	Non–lysosomal glucosylceramidase	DN9975_c0_g1_i9_4448	14	274
35	Solute carrier family 5	DN10836_c0_g1_i4_11677	14	600
36	Basement membrane–specific heparan sulfate proteoglycan core protein	DN9818_c0_g2_i1_37822	14	237
37	Tegumental protein	DN118_c0_g1_i1_52814	14	417
38	H17g protein tegumental antigen	DN11977_c0_g1_i2_72857	14	357
39	Hypothetical transcript	DN9865_c0_g1_i1_63028	14	594
40	Cytosolic malate dehydrogenase	DN10181_c0_g1_i1_47181	13	139
41	Putative anoctamin	DN11493_c0_g1_i2_56859	13	145
42	Plasma membrane calcium–transporting ATPase 3	DN11817_c3_g5_i1_69816	13	234
43	Uncharacterised	DN6547_c0_g1_i3_66219	13	250
44	Annexin A13 (Annexin XIII)	DN12676_c0_g1_i5_72043	13	547
45	Von Willebrand factor A domain containing protein	DN10879_c1_g1_i8_12057	13	381
46	Annexin A4–like	DN12342_c0_g1_i2_39792	13	824
47	Carbonic anhydrase	DN11803_c0_g3_i1_69783	13	255
48	Annexin A7	DN11263_c0_g1_i4_60744	12	320
49	**Calpain**	**DN4288_c0_g1_i1_31793**	**12**	**321**
50	Unnamed protein product, partial	DN11248_c0_g2_i1_22893	12	267

Table 3.3 The top 50 most abundant proteins putatively identified on the SEC *A. perfoliata* EV surface proteomic dataset by Gel–free LC MS/MS and a MASCOT search, with significance threshold score above 47. Protein descriptions were given from Omicsbox. Protein hits shaded in grey and in bold represent known helminth immune modulators, as also identified in the *A. perfoliata* transcriptome (Appendix 3.2).

No.	Protein Description	Sequence ID	Number of sequenced peptides	MASCOT score
1	WD repeat and FYVE domain–containing protein 3	DN11838_c0_g1_i2_56054	72	1302
2	Expressed conserved protein	DN10367_c0_g1_i3_29401	50	1039
3	Myosin heavy chain 10 or non–muscle myosin IIB	DN10438_c0_g2_i2_34624	50	1372
4	P29	DN11822_c0_g2_i2_55872	44	1617
5	Basement membrane–specific heparan sulfate proteoglycan core protein	DN9818_c0_g2_i1_37822	44	470
6	Spectrin alpha chain	DN11694_c0_g1_i1_54338	37	686
7	Expressed conserved protein	DN11921_c1_g2_i1_46303	37	701
8	Myosin XV	DN10026_c0_g1_i2_27828	34	296
9	Collagen alpha–2(I) chain	DN6173_c0_g1_i4_63619	33	759
10	Expressed conserved protein	DN7822_c0_g2_i1_27391	32	114
11	Expressed conserved protein	DN10746_c0_g1_i6_22331	31	841
12	Annexin A7	DN8700_c0_g1_i1_600	30	1130
13	Leucine–rich repeat–containing protein	DN11834_c0_g1_i3_56030	29	596
14	Annexin A13 (Annexin XIII)	DN9930_c0_g1_i1_67885	29	1313
15	Microtubule actin cross linking factor 1	DN10747_c0_g1_i5_35870	28	231
16	Peroxidasin	DN10163_c0_g1_i1_35077	28	393
17	Spectrin alpha actinin	DN11195_c0_g3_i1_24267	28	231
18	Myosin heavy chain	DN11757_c0_g1_i1_61366	28	613
19	Heat shock 70 kDa protein 4	DN12581_c0_g1_i2_73130	27	634
20	**Calpain A**	**DN9786_c0_g1_i1_72692**	**26**	**931**
21	Expressed conserved protein	DN11614_c0_g2_i3_53973	24	338
22	Plasma membrane calcium–transporting ATPase 3	DN10463_c3_g1_i2_34420	23	329
23	Von Willebrand factor A domain containing protein	DN10879_c1_g1_i8_12057	23	310
24	**Enolase**	**DN14469_c0_g1_i1_24672 (Apα–Enolase–1)**	**23**	**474**
25	**Calpain**	**DN4288_c0_g1_i1_31793**	**23**	**333**
26	Galectin carbohydrate recognition domain	DN6894_c0_g1_i2_12735	21	631
27	Tegumental antigen	DN5781_c0_g1_i1_2927	21	1112
28	Uncharacterised	DN10801_c0_g1_i14_11633	20	594
29	Phosphoenolpyruvate carboxykinase	DN11364_c0_g2_i1_39228	20	253
30	**Molecular chaperone HtpG/ Heat shock protein 90 alpha**	**DN11960_c0_g1_i1_46290 (Ap –4)**	**20**	**372**
31	Annexin A7	DN7793_c0_g1_i1_23754	20	336
32	**Glycoprotein Antigen 5**	**DN9013_c0_g1_i2_47406**	**20**	**458**
33	Annexin A7	DN11263_c0_g1_i4_60744	20	355
34	H17g protein tegumental antigen	DN11977_c0_g1_i2_72857	19	470
35	Programmed cell death 6–interacting protein	DN10491_c0_g3_i2_21343	19	645
36	Expressed conserved protein	DN12262_c0_g1_i1_68587	18	203
37	Actin modulator protein	DN8972_c0_g1_i1_2323	17	395
38	Otoferlin	DN10250_c0_g1_i1_26991	17	527
39	Ornithine aminotransferase	DN9481_c0_g1_i1_55273	17	289
40	Unnamed protein product	DN12187_c0_g1_i1_66436	17	335
41	Fascin 2	DN10161_c0_g1_i1_59685	16	535
42	Actin, cytoplasmic type 5	DN10334_c0_g1_i3_17117	16	570
43	Calmodulin	DN5211_c0_g1_i2_35332	16	381
44	Expressed conserved protein	DN8957_c0_g1_i1_66134	16	681
45	Paramyosin	DN10354_c0_g1_i1_3720	15	299
46	Serine/threonine kinase	DN8156_c0_g1_i2_52113	15	212
47	Protein kinase C and casein kinase substrate in neurons protein 1	DN7152_c0_g1_i2_8970	15	456
48	Tegumental protein	DN118_c0_g1_i1_52814	14	205
49	Lysyl oxidase	DN7852_c0_g1_i1_1626	14	189
50	Phosphoglycerate kinase	DN11218_c0_g1_i1_75075	14	123

Table 3.4 The top 50 most abundant proteins putatively identified in SEC *A. perfoliata* EV depleted ESP >10 kDa proteomic datasets by 1D SDS–PAGE, LC MS/MS and a MASCOT search, with significance threshold score above 48. Protein descriptions were given from Omicsbox. Protein hits shaded in grey and in bold represent known helminth immune modulators, as also identified in the *A. perfoliata* transcriptome (Appendix 3.2).

No.	Protein Description	Sequence ID	Number of sequenced peptides	MASCOT score
1	WD repeat and FYVE domain–containing protein 3	DN11838_c0_g1_i2_56054	292	6943
2	Basement membrane–specific heparan sulfate proteoglycan core protein	DN9818_c0_g2_i1_37822	169	2575
3	**Enolase**	**DN14469_c0_g1_i1_24672 (Apα–Enolase–1)**	**146**	**5177**
4	Alpha 2 macroglobulin	DN12789_c0_g1_i5_70580	118	2655
5	Ornithine aminotransferase	DN9481_c0_g1_i1_55273	106	2044
6	Aldo keto reductase family 1–member B4	DN10754_c1_g2_i7_35857	96	3057
7	Deoxyhypusine hydroxylase	DN10922_c1_g1_i5_14239	95	1993
8	Protein disulfide–isomerase	DN9431_c0_g1_i1_5402	91	3042
9	Peroxidasin	DN10163_c0_g1_i1_35077	89	2110
10	Cytosolic malate dehydrogenase	DN10181_c0_g1_i1_47181	75	1053
11	Heat shock 70 kDa protein 4	DN12581_c0_g1_i2_73130	74	1512
12	Actin, cytoplasmic type 5	DN10334_c0_g1_i3_17117	68	1765
13	Glycogen phosphorylase	DN9054_c0_g2_i1_35634	63	865
14	Fascin 2	DN10161_c0_g1_i1_59685	62	952
15	Lysosomal alpha–glucosidase	DN10704_c0_g1_i4_9857	60	932
16	Gynecophoral canal protein	DN2510_c0_g1_i1_41860	59	991
17	Phosphoenolpyruvate carboxykinase	DN11364_c0_g2_i1_39228	57	1088
18	Protein disulfide–isomerase A3	DN6375_c0_g1_i1_15550	55	1134
19	Von Willebrand factor A domain containing protein	DN10879_c1_g1_i8_12057	53	1406
20	**Calpain A**	**DN9786_c0_g1_i1_72692**	**52**	**1568**
21	Spectrin alpha chain	DN11694_c0_g1_i1_54338	50	513
22	Putative zinc binding dehydrogenase	DN10593_c0_g1_i11_28936	50	1031
23	Phosphoglycerate kinase	DN11218_c0_g1_i1_75075	50	958
24	Fructose–bisphosphate aldolase	DN10221_c0_g1_i1_65390	46	909
25	NADP–dependent malic enzyme	DN8932_c0_g1_i2_2337	45	1210
26	Actin modulator protein	DN8953_c0_g1_i6_52210	45	977
27	EF hand family protein	DN9944_c0_g2_i4_42845	42	1195
28	Expressed conserved protein	DN11614_c0_g2_i3_53973	41	201
29	**Molecular chaperone HtpG/ Heat shock protein 90 alpha**	**DN11960_c0_g1_i1_46290 (Ap –4)**	**41**	**801**
30	Spectrin alpha actinin	DN11195_c0_g3_i1_24267	40	467
31	Basement membrane–specific heparan sulfate proteoglycan core protein	DN9714_c0_g1_i3_20481	40	770
32	Beta galactosidase	DN10618_c0_g1_i1_32785	39	752
33	Transketolase	DN9107_c0_g1_i1_32351	39	985
34	Glucose–6–phosphate isomerase	DN10660_c0_g1_i2_45795	38	709
35	Puromycin sensitive aminopeptidase	DN10270_c0_g1_i2_26817	37	706
36	Calsyntenin 1	DN10458_c0_g1_i1_34309	37	638
37	Gynecophoral canal protein	DN7995_c0_g1_i1_6847	37	653
38	Glycerol kinase	DN8664_c0_g1_i1_13160	37	1104
39	Peptidyl–glycine alpha–amidating monooxygenase A	DN8251_c0_g1_i1_16141	36	725
40	Hypothetical transcript	DN9865_c0_g1_i1_63028	36	642
41	Adenylosuccinate synthetase	DN10697_c0_g3_i1_6876	36	810
42	Glucose–6–phosphate 1–dehydrogenase	DN11811_c2_g4_i1_55908	35	1378
43	Myosin heavy chain 10 or non–muscle myosin IIB	DN12309_c0_g1_i3_64783	35	70
44	Expressed conserved protein	DN11119_c0_g1_i2_24053	34	662
45	Putative actin–interacting protein 1	DN1602_c0_g1_i1_69974	34	218
46	Expressed conserved protein	DN7822_c0_g2_i1_27391	34	595
47	Puromycin sensitive aminopeptidase	DN10270_c0_g1_i1_26816	33	488
48	Phosphoglucomutase	DN12341_c1_g3_i1_64791	33	449
49	Ubiquitin modifier activating enzyme 1	DN11247_c1_g1_i4_75101	33	784
50	Peptidyl prolyl cis trans isomerase B	DN4872_c0_g1_i1_43079	32	202

3.3.3.3. Gene ontology enrichment analysis

A total of 173 GO terms were not propagated up the hierarchy ($p<0.05$ identified significance), of which 45, 42 and 86 GO terms were enriched in SEC whole EVs, the EV surface and EV depleted ESP >10 kDa, respectively. The comparison of GO term enrichment from all 3 proteomics datasets is presented in Figure 3.6, with 20 GO terms were enriched across all secretome proteomic datasets. Most GO terms being in the Biological Process group, of which calcium ion binding was found to be the most enriched, followed by Arp2/3 complex–mediated actin nucleation, microtubule–based process and gluconeogenesis.

Seven GO terms enriched in EV samples only were all categorised in biological process, with carbohydrate transmembrane transport being the most enriched followed by transmembrane transport, inorganic anion transport, peptidyl–lysine modification to peptidyl–hypusine, calcium–mediated signalling, protein phosphorylation and protein processing. In the SEC EV surface protein samples, the 3 most enriched GO terms were categorised in Biological Process including bile acid and bile salt transport, seryl–tRNA aminoacylation and urea cycle whereas the 3 enriched GO terms categorised in Cellular Component included membrane, virion and nascent polypeptide–associated complex. The top 5 most enriched GO terms in SEC EV depleted ESP >10 kDa were categorised in Biological Process included carbohydrate metabolic process, formaldehyde catabolic process, negative regulation of endopeptidase activity, proteolysis involved in cellular protein catabolic process and proteolysis.

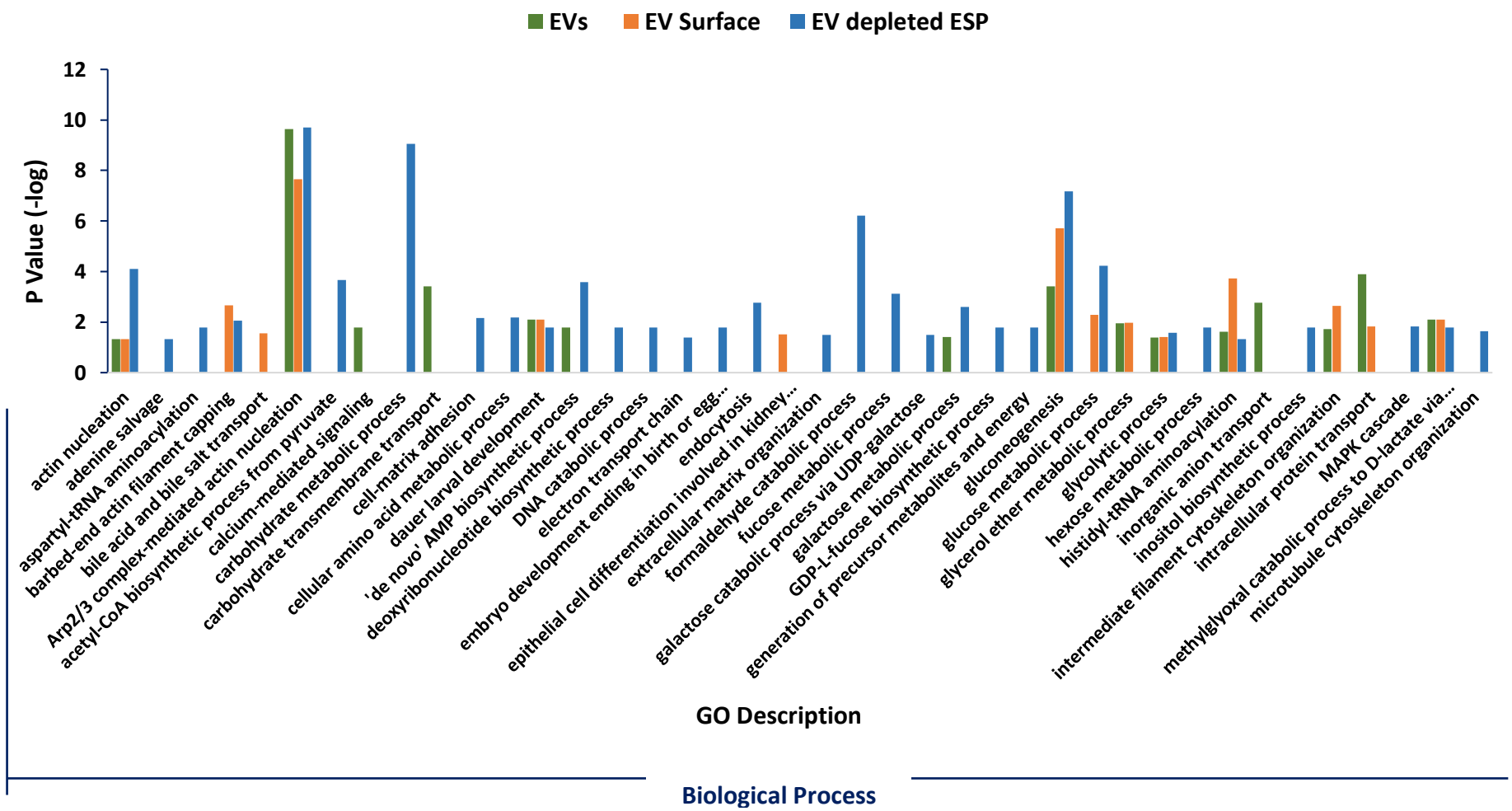

Figure 3.6 Gene ontology enrichment analysis using GOATOOLS in python comparing all 3 proteomic datasets from the *A. perfoliata* secretome compared to *A. perfoliata* transcriptome for the Biological Process, Molecular function and Cellular Component functional categories. GO terms were not propagated up the hierarchy (nop) (p<0.05 identified significance) and where enriched in all or any of the 3 proteomic datasets were presented using –log transformation of p_uncorrected value and GO description.

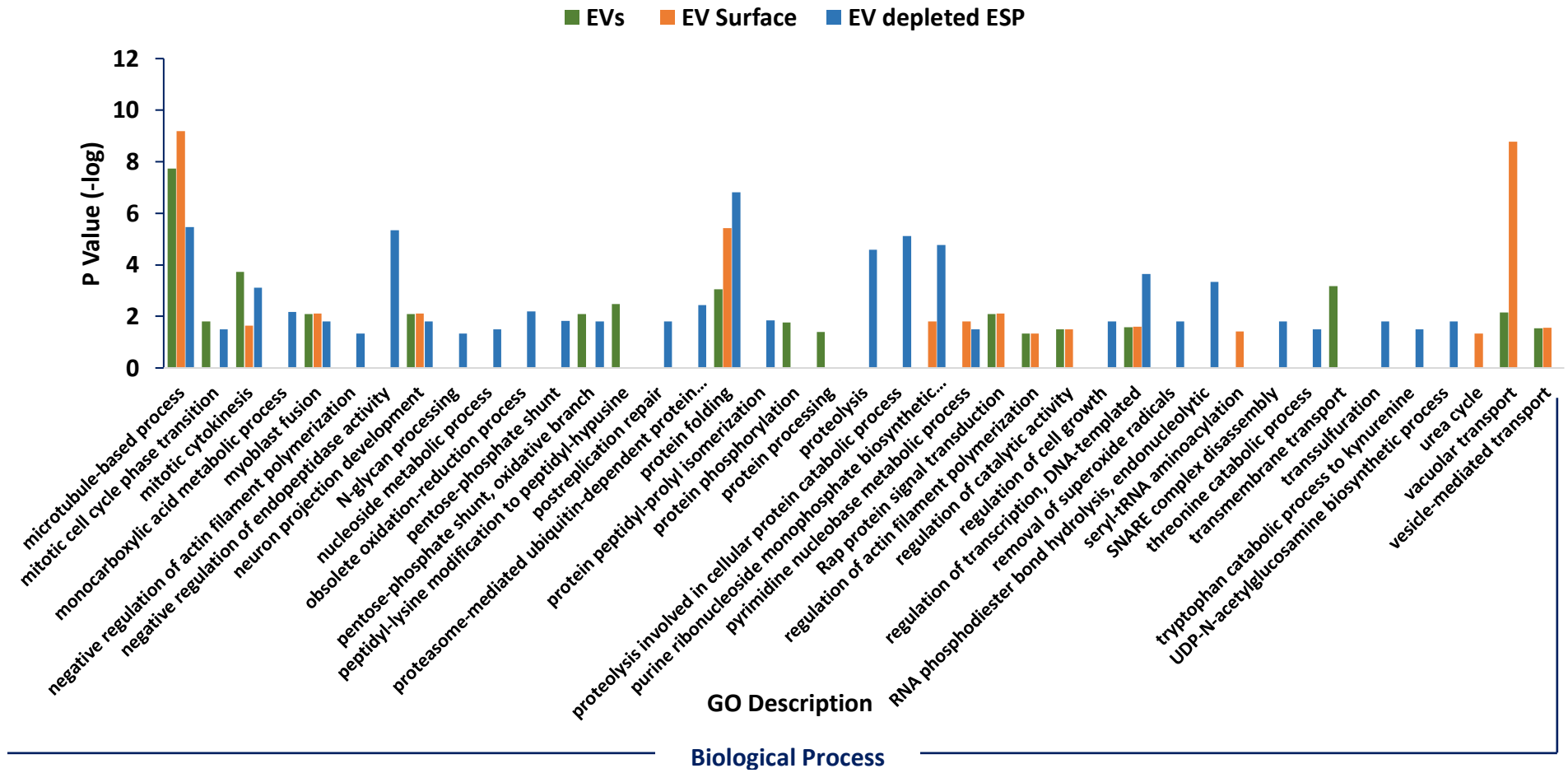

Figure 3.6–continued 2. Gene ontology enrichment analysis using GOATOOLS in python comparing all 3 proteomic datasets from the *A. perfoliata* secretome compared to *A. perfoliata* transcriptome for the Biological Process, Molecular function and Cellular Component functional categories. GO terms were not propagated up the hierarchy (nop) (p<0.05 identified significance) and where enriched in all or any of the 3 proteomic datasets were presented using –log transformation of p_uncorrected value and GO description.

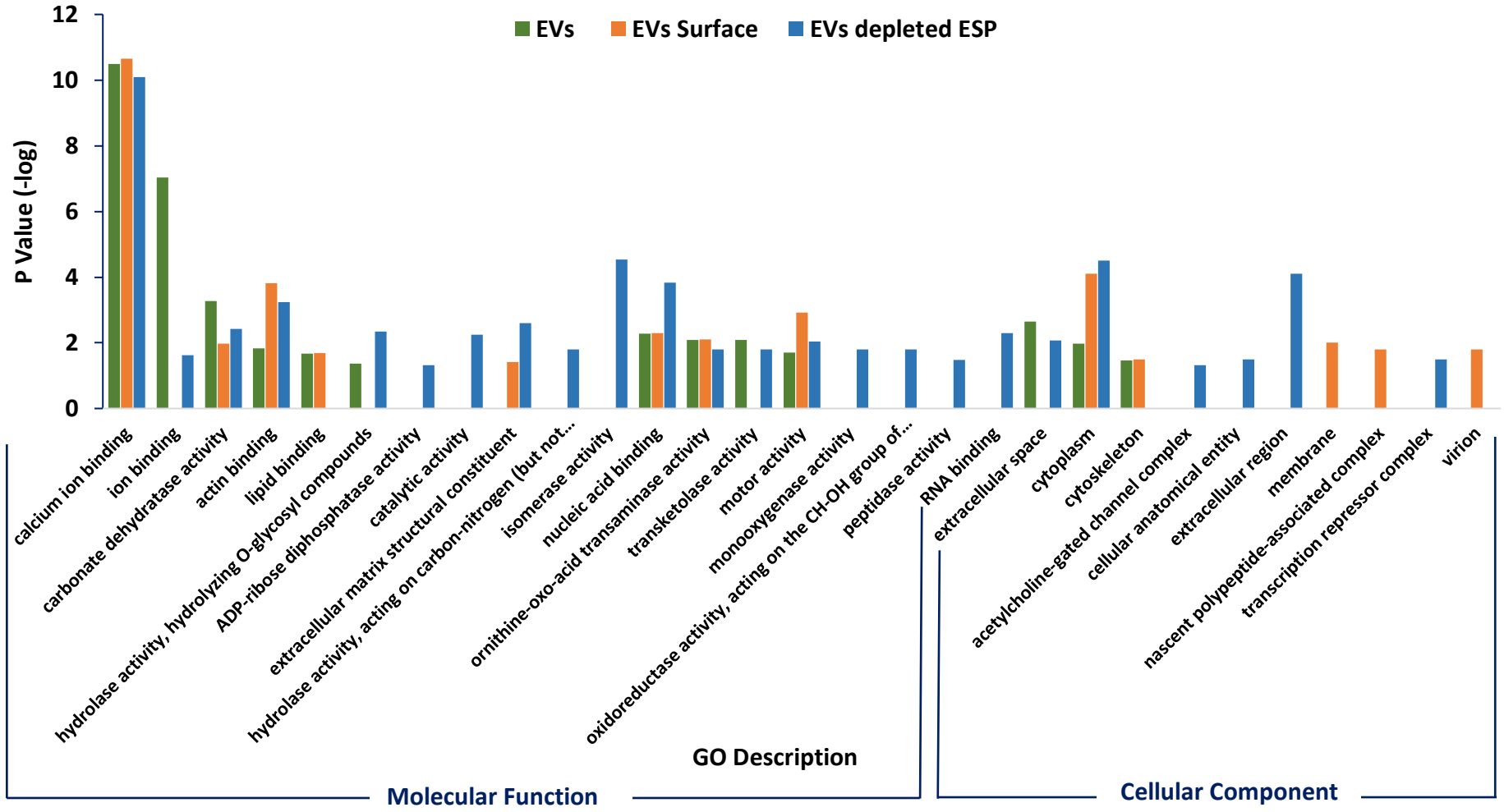

Figure 3.6–continued 3. Gene ontology enrichment analysis using GOATOOLS in python comparing all 3 proteomic datasets from the *A. perfoliata* secretome compared to *A. perfoliata* transcriptome for the Biological Process, Molecular function and Cellular Component functional categories. GO terms were not propagated up the hierarchy (nop) (p<0.05 identified significance) and where enriched in all or any of the 3 proteomic datasets were presented using –log transformation of p_uncorrected value and GO description.

3.3.4. Potential immune modulators are expressed in the *A. perfoliata* secretome

The 462 putative immune modulatory sequences identified within the *A. perfoliata* transcriptome (Chapter 2, Section 2.3.5) were also assessed in the *A. perfoliata* proteomic data. A total of 50 putative immune modulator sequences were identified as expressed proteins across all three datasets, including 22 expressed in SEC whole EVs, 16 on the EV surface and 41 in the EV depleted ESP >10 kDa (Table 3.2–3.4; Appendix 3.2).

Key secretory proteins linked to the host–parasite interface such as enolase and calpain were identified in the top 50 most abundant of *A. perfoliata* EV depleted ESP >10 kDa (Table 3.4; Appendix 3.2). Of note, only a single Sigma class GST (ApGST–S1) and a single Omega class GST (ApGST–O4) were identified across all three proteomic datasets, but at a relatively low abundance (352nd and 145th, respectively within the EV depleted ESP >10 kDa; Appendix 3.3). When assessing the proteomics datasets for and α–Enolase, one (Ap –4) and two α–Enolases (Apα–Enolase–1 and 2) were observed across all three proteomic datasets analysed (Table 3.2–3.4; Appendix 3.2). Ap –4 and Apα–Enolase–1 were highly abundant in the analysis, both featuring in the top 30 of all three datasets (27th and 23rd in whole EVs, 30th and 24th on the EV surface and 29th and 3rd in the ESP >10 kDa, respectively; Table 3.2–3.4; Appendix 3.2). However, Apα–Enolase–2 was identified within the EV depleted ESP >10 kDa proteomic dataset at very low abundance (top 425th; Appendix 3.2).

3.4. DISCUSSION

The parasite secretome during infection is known to have an essential role in host–parasite interactions (Robinson *et al.*, 2009; Morphew *et al.*, 2011; Marcilla *et al.*, 2012; Nono *et al.*, 2012; Bień *et al.*, 2016; Vendelova *et al.*, 2016; Wang *et al.*, 2017; Pan *et al.*, 2017; Han *et al.*, 2019; Wangchuk *et al.*, 2019; Lawson *et al.*, 2019; Nicolao *et al.*, 2019). Therefore, in this chapter, I focused on secretome proteomics of the equine tapeworm, *A. perfoliata* and identified that *A. perfoliata* secrete EVs during *in vitro* maintenance. With the use of the *A. perfoliata* transcriptome (Chapter 2, Section 2.3.2), I established the first proteomic analysis of the *A. perfoliata* secretome including purified EVs, the EV surface and EV depleted ESP >10 kDa proteomes. Furthermore, we explored key proteins of importance linked to immune regulation, demonstrating putative proteins involved in host–pathogen interactions, thus paving the way for further functional studies.

3.4.1 *A. perfoliata* secrete EVs during *in vitro* maintenance

The choice of a SEC column was used for isolation and purification of *A. perfoliata* EVs as it has previously been demonstrated to reduce non–EV contamination in *F. hepatica* ESP and is therefore suggested for further downstream helminth EV studies (Davis *et al.*, 2019). Secretion of *A. perfoliata* EVs was initially confirmed by the morphological characterisation using TEM and NTA analysis. TEM revealed that SEC purified *A. perfoliata* EVs have the typical morphology characteristic of EVs, with a spherical or cup–shaped membrane surrounded by a phospholipid bilayer structure. Furthermore, EVs with a diameter ranging from 32–215 nm, categorised as exosomes (30–100 nm; 86%) and microvesicles (100–1000 nm; 14%), were consistent with EVs released from other tapeworms (Table 3.5). In comparison, the NTA analysis also defined the majority of the SEC purified *A. perfoliata* EV population (67–213 nm in diameter) in ranges similar to other tapeworms (Table 3.5). Although *A. perfoliata* were seen to secrete larger vesicles than other tapeworms, yet were closest to those released from *T. pisiformis* cysticercus (50–150 nm), *E. multilocularis* metacestode (112–170 nm) and *E. granulosus* protoscoleces, metacestodes (30–390 nm) (Table 3.5). Importantly, the combined results of both TEM and NTA reveal that EVs are secreted during *in vitro* maintenance and that *A. perfoliata* EVs are amenable to isolation and purification by SEC.

Table 3.5 The characterisation of EVs secreted from cestode species during *in vitro* maintenance using Transmission Electron Microscopy (TEM) and Nanoparticle Tracking Analysis (NTA). NF: information is not shown.

	TEM/Cryo–EM		NTA	
Species	**Morphology**	**Size (nm in diameter)**	**Major particle size (nm in diameter)**	**References**
A. perfoliata adult	spherical/cup–shaped vesicles with lipid bilayer–bound membrane structures	32–215	67–213	Current work
H. diminuta adult	cup–shaped vesicles	NF	80 –90	Mazanec *et al.* (2021)
T. asiatica adult	spherical vesicles	30–150	50– 80	Liang *et al.* (2019)
T.pisiformis cysticercus	spherical/cup–shaped vesicles with lipid bilayer–bound membrane structures	30–150	50–150	Wang *et al.* (2020)
E. granulosus protoscoleces, metacestodes	cup–shaped structures	25–150 nm	30–90	Nicolao *et al.* (2019)
E. granulosus metacestodes	vesicles	NF	80– 100	Siles-Lucas *et al.* (2017)
E. granulosus protoscoleces	vesicles with round or oval membranes	<200 nm	30–200	Zhou *et al.* (2019)
E. granulosus protoscoleces	oval or spherical, with negatively–stained membrane	NF	2K; 450– 950 10K; 220–390 110 K; 60–150	Wu *et al.* (2021)
E. multilocularis metacestode	NF	NF	112–170	Ancarola *et al.* (2020)
T. crassiceps metacestode	round–shaped membrane–bound structures	<100 nm & >100 nm	NF	Ancarola *et al.* (2017)
M. corti metacestode	round–shaped membrane–bound structures	<100 nm & >100 nm	NF	Ancarola *et al.* (2017)

3.4.2 General characteristics and profiles of *A. perfoliata* proteome

For further characterization of the SEC *A. perfoliata* secretome protein profile, I performed 1D SDS–PAGE and/or LC MS/MS (GeLC approach for whole EVs and EV depleted ESP >10 kDa; Gel free approach for EV surface) and reported the identification of a total of 315 proteins from SEC *A. perfoliata* whole EVs, 301 proteins from the EV surface and a further 596 proteins from EV deleted ESP >10 kDa. Interestingly, WD repeat and FYVE domain–containing protein 3 (WDFY3) were found as the most abundant protein across all 3 secretome datasets. In humans, WDFY3 is known as Autophagy–Linked FYVE (Alfy/WDFY3) which has been implicated in neurodevelopmental disorder (Dragich *et al.*, 2016; Napoli *et al.*, 2018; Le Duc *et al.*, 2019). However, it is yet unexplored how WDFY3 may be involved in parasite functioning and the host–parasite interaction.

Key secretory proteins, such as GSTs, HSP90s and enolase were secreted by *A. perfoliata* as free proteins in SEC EV depleted ESP >10 kDa during *in vitro* maintenance in the current study, which shows similarity to other cestodes (Victor *et al.*, 2012; Virginio *et al.*, 2012; Wang *et al.*, 2015; Bień *et al.*, 2016). In addition, proteins identified in *H. diminuta* ESP (Bień *et al.*, 2016), like Peroxidasin, Expressed conserved protein, NADP–dependent malic enzyme, Deoxyhypusine hydroxylase, and particularly, Basement membrane–specific heparan sulfate proteoglycan core protein, were also presented in the fifty most abundant proteins in *A. perfoliata* EV depleted ESP. Consistently, those proteins presented in the ESP of other cestodes, were also identified in this SEC *A. perfoliata* EV depleted ESP.

The protein profile of *A. perfoliata* EVs also demonstrated a number of common EV markers in the top 50 abundant proteins, which have been reported in Exocarta database (Mathivanan *et al.*, 2012; Keerthikumar *et al.*, 2016), Vesiclepedia (Kalra *et al.*, 2012) (Table 3.6). Furthermore, many proteins identified in *A. perfoliata* EVs were correlated well with common EVs in previous cestode studies (Ancarola *et al.*, 2017; Liang *et al.*, 2019; Nicolao *et al.*, 2019; Zhou *et al.*, 2019; Wang *et al.*, 2020; Mazanec *et al.*, 2021; Wu *et al.*, 2021) (Table 3.6; Appendix 3.2) as such proteins corresponded to the cytoskeleton (Actin, Tubulin and Dynein); proteins involved in vesicle trafficking/vesicle biogenesis (Annexin and Otoferlin); pumps, transporters and carriers (14–3–3 family proteins, Solute carrier family 5 and Fatty acid–binding protein); metabolism (Calpain, Enolase, Gyceraldehyde–3–phosphate dehydrogenase and Phosphoenolpyruvate carboxykinase). Interestingly, proteins such as H17 tegumental antigen, Tegumental antigen and Tegumental protein, which were found in abundance in *A. perfoliata* whole EVs, have been suggested as typical components in EVs from parasitic flatworms such as *H. diminuta* (Mazanec *et al.*, 2021)*, E. granulosus* (Siles-Lucas *et al.*, 2017; Nicolao *et al.*, 2019; Wu *et al.*, 2021) *T. asiatica* (Liang *et al.*, 2019), *T. crassiceps* and *M. corti* (Ancarola *et al.*, 2017), *F. hepatica* (Cwiklinski *et al.*, 2015) and *C. daubneyi* (Allen *et al.*, 2021).

Table 3.6 The top 50 most abundant proteins putatively identified in the SEC *A. perfoliata* EVs compared to common EV markers from Vesiclepedia, Exocarta databases and others cestodes EVs. Protein in bold indicates the homologue in *A. perfoliata* EVs (Ancarola *et al.*, 2017; Liang *et al.*, 2019).

No.	*A.perfoliata*	Vesiclepedia database	Exocarta database	*T. asiatica*	*T. crassiceps*	*M. corti*
1	WD repeat and FYVE domain–containing protein 3	**Programmed cell death 6 interacting protein**	CD9 molecule/antigen	**Calpain A**	**Annexin**	**Annexin**
2	**actin, cytoplasmic type 5**	Glyceraldehyde–3–phosphate dehydrogenase	Heat shock protein 8	Serpin B6	Myoferlin	Myoferlin
3	**myosin XV**	Heat shock protein 8	**Programmed cell death 6 interacting protein**	Serine protease inhibitor	**Otoferlin**	**Otoferlin**
4	**putative myosin–10 (Myosin heavy chain, nonmuscle IIb)**	**Actin, beta**	Glyceraldehyde–3–phosphate dehydrogenase	GPCR, family 3, C terminal	Vacuolar protein sorting associated protein 4A	Vacuolar protein sorting associated protein 4A
5	Leucine–rich repeat–containing protein	**Annexin A2**	**Actin, beta**	Arginyl tRNA synthetase, cytoplasmic	Rab	Rab
6	**otoferlin**	CD9 molecule/antigen	**Annexin A2**	**Otoferlin**	ADP–ribosylation factor	ADP–ribosylation factor
7	fascin 2	Pyruvate kinase, muscle	CD63 molecule	Plasma membrane calcium transporting ATPase	Transforming protein RhoA	Transforming protein RhoA
8	**calpain A**	**Heat shock protein 90kDa alpha (cytosolic), class A member 1**	**Syndecan binding protein (syntenin)**	Heat shock protein 83	BRO1 domain containing protein BROX	BRO1 domain containing protein BROX
9	**Annexin A7**	**Enolase 1, (alpha)**	**Enolase 1, (alpha)**	**Endophilin B1**	Clathrin	**Actin**
10	**phosphoenolpyruvate carboxykinase**	**Annexin A5**	**Heat shock protein 90kDa alpha (cytosolic), class A member 1**	**Annexin**	**Actin**	Tubulin
11	**Heat shock 70 kDa protein 4**	**Heat shock protein 90kDa alpha (cytosolic), class B member 1**	Tumor susceptibility gene 101	Rab3	Tubulin	Dynein
12	**von Willebrand factor A domain containing protein**	CD63 molecule	Pyruvate kinase, muscle	Lipid transport protein, N terminal	Dynein	**Heat shock 70 kDa**
13	aldo keto reductase family 1 member B4	Tyrosine 3–monooxygenase/tryptophan 5–monooxygenase activation protein, zeta polypeptide	Lactate dehydrogenase A	Phospholipid transporting ATPase IIB	**Heat shock 70 kDa**	Ferritin
14	**solute carrier family 5**	Tyrosine 3–monooxygenase/tryptophan 5–monooxygenase activation protein, epsilon polypeptide	Eukaryotic translation elongation factor 1 alpha 1	Major vault protein	Ferritin	Fatty acid binding protein
15	**tegumental antigen**	Eukaryotic translation elongation factor 1 alpha 1	Tyrosine 3–monooxygenase/tryptophan 5–monooxygenase activation protein, zeta polypeptide	Arginyl tRNA protein transferase 1	Fatty acid binding protein	Gyceraldehyde–3–phosphate dehydrogenase
16	**Programmed cell death 6–interacting protein**	**Phosphoglycerate kinase 1**	**Phosphoglycerate kinase 1**	**Solute carrier family 5**	Gyceraldehyde–3–phosphate dehydrogenase	**Phosphoenolpyruvate carboxykinase**

Table 3.6–Continued 2. The top 50 most abundant proteins putatively identified in the SEC *A. perfoliata* EVs compared to common EV markers from Vesiclepedia, Exocarta databases and others cestodes EVs. Protein in bold indicates the homologue in *A. perfoliata* EVs (Ancarola *et al.*, 2017; Liang *et al.*, 2019).

No.	*A.perfoliata*	Vesiclepedia database	Exocarta database	*T. asiatica*	*T. crassiceps*	*M. corti*
17	peroxidasin	Clathrin, heavy chain (Hc)	Eukaryotic translation elongation factor 2	Filamin	**Phosphoenolpyruvate carboxykinase**	**Cytosolic malate dehydrogenase**
18	**enolase**	Peptidylprolyl isomerase A (cyclophilin A)	Aldolase A, fructose–bisphosphate	Alpha actinin, sarcomeric	**Cytosolic malate dehydrogenase**	6–phosphogluconate dehydrogenase
19	ubiquitin–60S ribosomal protein L40	**Syndecan binding protein (syntenin)**	**Heat shock protein 90kDa alpha (cytosolic), class B member 1**	**Actin interacting protein 1**	6–phosphogluconate dehydrogenase	**Phosphoglycerate kinase**
20	**tegumental protein**	Aldolase A, fructose–bisphosphate	**Annexin A5**	Synaptotagmin protein 4 like	**Phosphoglycerate kinase**	**Enolase**
21	**molecular chaperone HtpG/ alpha**	Eukaryotic translation elongation factor 2	Fatty acid synthase	Mastin	**Enolase**	Elongation factor
22	glycoprotein Antigen 5	Albumin	Tyrosine 3–monooxygenase/ tryptophan 5–monooxygenase activation protein, epsilon polypeptide	14–3–3 protein	Elongation factor	Eukaryotic translation initiation factor
23	**alpha 2 macroglobulin**	Triosephosphate isomerase 1	Clathrin, heavy chain (Hc)	Synaptotagmin	Eukaryotic translation initiation factor	**Calpain**
24	**Phosphoglycerate kinase**	Valosin containing protein	CD81 molecule	Synaptotagmin 2	**Calpain**	Synaptobrevin YKT6
25	**annexin B9–like isoform X1**	Cofilin 1 (non–muscle)	Albumin	14–3–3 protein beta:alpha	BAR–domain containing proteina	Ras protein Rap
26	non lysosomal glucosylceramidase	Moesin	Valosin containing protein	Gelsolin	Synaptic vesicle membrane protein VAT 1a	Calcium binding protein
27	**H17g protein tegumental antigen**	ATPase, Na+/K+ transporting, alpha 1 polypeptide	Triosephosphate isomerase 1	**Cytoplasmic actin**	Syntaxina	**H17g protein, tegumental antigen (FERM ezrin/ radixin/ moesin)**
28	Basement membrane–specific heparan sulfate proteoglycan core protein	Peroxiredoxin 1	Peptidylprolyl isomerase A (cyclophilin A)	Syntenin 1	Syntaxin–binding proteina	Receptor Mediated Endocytosis family member
29	**cytosolic malate dehydrogenase**	**Myosin, heavy chain 9, non–muscle**	Moesin	Thioredoxin peroxidase	Synaptotagmina	Alpha actinin sarcomeric
30	putative anoctamin	Ezrin	Cofilin 1 (non–muscle)	**Phosphoenolpyruvate carboxykinase**	N–ethylmaleimide sensitive factor attachmenta	**Actin modulator protein**
31	Plasma membrane calcium–transporting ATPase 3	CD81 molecule	Peroxiredoxin 1	Transitional endoplasmic reticulum ATPase	Ras protein Rap	Ras gtpase
32	**Annexin A13 (Annexin XIII)**	**Annexin A6**	Profilin 1	**Enolase**	Calcium binding protein	Ras protein
33	carbonic anhydrase	Flotillin 1	RAP1B, member of RAS oncogene family	Fructose 1,6 bisphosphate aldolase	**H17g protein, tegumental antigen (FERM ezrin/ radixin/ moesin)**	Ras–related protein O–RAL
34	**annexin A4–like**	Tyrosine 3–monooxygenase/tryptophan 5–monooxygenase activation protein, beta polypeptide	Integrin, beta 1 (fibronectin receptor, beta polypeptide, antigen CD29 includes MDF2, MSK12)	6 phosphofructokinase	**p29 (endophilin B1/BAR–domain containing protein)**	Guanine nucleotide binding protein G(q) subunit

Table 3.6–Continued 3. The top 50 most abundant proteins putatively identified in the SEC *A. perfoliata* EVs compared to common EV markers from Vesiclepedia, Exocarta databases and others cestodes EVs, Protein in bold indicates the homologue in *A. perfoliata* EVs (Ancarola *et al.*, 2017; Liang *et al.*, 2019).

No.	*A.perfoliata*	Vesiclepedia database	Exocarta database	*T. asiatica*	*T. crassiceps*	*M. corti*
35	**calpain**	Lactate dehydrogenase B	HSPA5 heat shock protein family A (Hsp70) member 5	phosphoglucomutase 2	Ts8B1	UPF0047 domain containing protein
36	**P29**	Solute carrier family 3 (activators of dibasic and neutral amino acid transport), member 2	Solute carrier family 3 (activators of dibasic and neutral amino acid transport), member 2	Glucose 6 phosphate isomerase	14–3–3	cGMP dependent protein kinase
37	microtubule actin cross linking factor 1	Guanine nucleotide binding protein (G protein), beta polypeptide 1	Histone cluster 1, H4a	Phosphoglycerate kinase 1	Receptor Mediated Endocytosis family member	Thioredoxin fold
38	**actin modulator protein**	Profilin 1	G Protein Subunit Beta 2	Cytosolic malate dehydrogenase	Alpha actinin sarcomeric	Immunoglobulins
39	**syndecan binding protein syntenin**	Tumor susceptibility gene 101	ATPase, Na+/K+ transporting, alpha 1 polypeptide	Glyceraldehyde 3 phosphate dehydrogenase (GAPDH)	**Actin modulator protein**	Complement factors
40	NADP–dependent malic enzyme	Tyrosine 3–monooxygenase/tryptophan 5–monooxygenase activation protein, theta polypeptide	Tyrosine 3–monooxygenase/tryptophan 5–monooxygenase activation protein, theta polypeptide	Triosephosphate isomerase	Ras gtpase	
41	Deoxyhypusine hydroxylase	Guanine nucleotide binding protein (G protein), alpha inhibiting activity polypeptide 2	Flotillin 1	Alkaline phosphatase	Ras protein	
42	**Annexin A5**	Chloride intracellular channel 1	Filamin A	Telomerase protein component 1	Ras–related protein O–RAL	
43	lysyl oxidase	**Annexin A1**	Chloride intracellular channel 1	**Calpain**	Guanine nucleotide binding protein G(q) subunit	
44	glycerol kinase	Integrin, beta 1 (fibronectin receptor, beta polypeptide, antigen CD29 includes MDF2, MSK12)	Cell division cycle 42 (GTP binding protein, 25kDa)	Protein of unknown function DUF590	UPF0047 domain containing protein	
45	**Putative actin–interacting protein 1**	Lactate dehydrogenase A	Chaperonin containing TCP1, subunit 2 (beta)	Ras protein Rab 2A	cGMP dependent protein kinase	
46	protein kinase C and casein kinase substrate	Fatty acid synthase	**Alpha–2–Macroglobulin**	Prostaglandin H2 D isomerase	Thioredoxin fold	
47	endophilin B2	Cell division cycle 42 (GTP binding protein, 25kDa)	Tyrosine 3–monooxygenase/tryptophan 5–monooxygenase activation protein, gamma polypeptide	Peptidylprolyl isomerase A	Immunoglobulins	
48	Band 3 anion transport protein	RAP1B, member of RAS oncogene family	Tubulin Alpha 1b	**H17 g protein, tegumental antigen**	Complement factors	
49	glutathione S–transferase	Chaperonin containing TCP1, subunit 2 (beta)	Rac Family Small GTPase 1	**Von Willebrand factor A domain containing protein**		
50	paramyosin	Tyrosine 3–monooxygenase/ tryptophan 5–monooxygenase activation protein, gamma polypeptide	Galectin 3 Binding Protein	**Tegumental protein**		

Since parasite derived EVs likely interact with receptors on the host cell plasma membrane, the outer surface proteins of parasite–derived EVs play crucial roles in establishing cell to cell communication, mediating cellular uptake, affecting immune recognition and representing effector molecules (Buzás *et al.*, 2018). The surface proteins of EVs from trematodes have been characterised in *F. hepatica* (Cwiklinski *et al.*, 2015; de la Torre-Escudero *et al.*, 2019; Murphy *et al.*, 2020) and *C. daubneyi* (Allen *et al.*, 2021), but have not yet been characterised in a cestode species. Thus, this is the first study to provide a proteome profile for the EV surface of a cestode species. Surface hydrolysis and gel free proteomics led to the identification of 301 surface proteins of *A. perfoliata* EVs, including many well–known EV markers, which have been also identified in *F. hepatica* (de la Torre-Escudero *et al.*, 2019) and *C. daubneyi* (Allen *et al.*, 2021), such as CD63 antigen, Annexin, Glyceraldehyde 3–phosphate dehydrogenase and programmed cell death 6 interacting protein.

CD63, a known cell surface antigen as part of the tetraspanin family and primarily a structural protein associated with membranes of intracellular vesicles (Andreu and Yáñez-Mó, 2014), was identified on the *A. perfoliata* EV surface, although not in the top 50 most abundant proteins. Cathepsins, have crucial roles as digestive enzymes in parasitic helminths involved in the host tissue invasion and migration, protein degradation and immune suppression (Robinson *et al.*, 2008; Caffrey *et al.*, 2018). Interestingly, Cathepsins (B, D and L) which are commonly found on the surface of trematode EVs (de la Torre-Escudero *et al.*, 2019; Allen *et al.*, 2021) were not observed on the *A. perfoliata* EV surface, perhaps reflecting the relative importance of larger EVs secreted from the parasite digestive tract, that are absent from cestodes (Margulis and Chapman, 2009).

A total of 142 proteins were shared between the whole EVs and EV surface, which was expected as the surface proteins were not removed prior to analysing the whole EVs. Of those exclusively expressed by the surface were proteins likely involved in important functions of EV uptake and interaction. Notable was the identification of a Leucine–rich repeat–containing protein, proteins often involved in protein–protein interactions (Gay *et al.*, 1991; Kobe and Kajava, 2001). Leucine–rich repeat 1 (LRR1) plays a role in the regulation of the cell cycle through the modulation of protein phosphatase type 1 (PP1) activity in *Toxoplasma gondii* (Daher *et al.*, 2007), *S. mansoni* (Daher *et al.*, 2006), *Plasmodium falciparum* (Daher *et al.*,

2006; Pierrot *et al.*, 2018) and *Plasmodium berghei* (Fréville *et al.*, 2022) and inhibit *P. falciparum* growth *in vitro* (Pierrot *et al.*, 2018). In addition, Spectrins were identified which are a major component of the membrane skeleton that lines the plasma membrane and suggested to participate in cell–cell contact, cell adhesion (Machnicka *et al.*, 2019, 2020) and endocytosis (Li, 2022). αII–Spectrins deficiency affects cell adhesion on fibronectin and laminin and cell motility *in vitro* (Metral *et al.*, 2009; Machnicka *et al.*, 2020). Therefore, the identification of these proteins suggests key roles of the EV surface to bind to cells.

When examining the role of the identified proteins, the majority of GO terms associated with *A. perfoliata* whole EVs were enriched in the biological processes group. However, calcium ion binding in the molecular category was found to be the most enriched across all secretome samples, a process involved in EV biogenesis (Savina *et al.*, 2003; Abels and Breakefield, 2016; Taylor *et al.*, 2020). Glycolytic process and phosphorylation enzymes such as phosphoenolpyruvate carboxykinase, phosphoglycerate kinase, glyceraldehyde–3–phosphate dehydrogenase and glucose 6 phosphate were also identified on the surface of *A. perfoliata* which are crucial enzyme activities providing a source of energy for helminths (Mansour and Mansour, 2002; Barrett, 2009) and likely reflect the EV site of origin from the cestode tegument given the lack of a digestive tract in *A. perfoliata* (Margulis and Chapman, 2009). Glycogen or glucose, although sporadically available in the caecum, are likely an easy source of energy in the host's gut which are absorbed directly through their tegument (Chappell, 1980; Barrett, 2009). Additionally, membrane transport proteins on the surface of *A. perfoliata* EVs such as solute carrier family 5, plasma membrane calcium–transporting ATPase 3, band 3 anion transport protein particularly the pumps protein; ATP binding cassette subfamily B (MDR:TAP) and multidrug resistance protein were observed on the *A. perfoliata* EV surface similar to *F. hepatica* EVs (de la Torre-Escudero *et al.*, 2019). These transport enzyme activities are likely to enhance the carbohydrate metabolism mechanisms in or between cells providing more nutrient and energy uptake to *A. perfoliata*.

Hence, these protein profiles support and highlight the validity of the *A. perfoliata* secretome, particularly indicating consistent markers in tapeworm EVs that were verified as common EV markers in other parasitic flatworms (Ancarola *et al.*, 2017; Liang *et al.*, 2019; Nicolao *et al.*, 2019; Allen *et al.*, 2021; Mazanec *et al.*, 2021; Wu *et al.*, 2021).

3.4.3. Potential immune modulators identified in *A. perfoliata* secretome

The development of the first transcriptome for *A. perfoliata* (Chapter 2, Section 2.3.2), provides support to explore key proteins of importance linked to the host–parasite interface as has been demonstrated previously for other helminths (Robinson *et al.*, 2009; Cantacessi *et al.*, 2012; Pan *et al.*, 2014; Huson *et al.*, 2018). At the host–parasite interface, immune modulation is imperative for parasite survival (Hewitson *et al.*, 2009; Gazzinelli-Guimaraes and Nutman, 2018) and consequently many putative immune modulatory proteins have been identified in platyhelminth species (Ancarola *et al.*, 2017; Davis *et al.*, 2019; Liang *et al.*, 2019; Nicolao *et al.*, 2019; Wang *et al.*, 2020; Allen *et al.*, 2021; Mazanec *et al.*, 2021; Wu *et al.*, 2021). The current transcriptome and proteomic analysis of *A. perfoliata* has identified 462 unique transcripts as homologues of recognised immune modulators in other helminth species (Chapter 2, Section 2.3.5). Of the 50 transcripts identified as expressed proteins across all three datasets, 22 were expressed in SEC whole EVs, 16 on the EV surface and 41 in the EV depleted ESP >10 kDa (Table 3.2–3.4, Appendix 3.2). In addition, GSTs, HSP90α, Enolase, Calpain/Calpain A, Cysteine protease, CD63 antigen, Cathepsin (L, D) and thioredoxin glutathione reductase are functionally expressed given their presence as part of the secretome (whole EVs, EV surface and EV depleted ESP >10 kDa). Whereas CD63 antigen and Cathepsin (L, D) are unique to the *A. perfoliata* EV surface and EV depleted ESP >10 kDa, respectively (Appendix 3.2). Three notable immune modulators were identified in the top 30 most abundant proteins across the *A. perfoliata* secretome, including Enolase (whole EVs, EV surface and EV depleted ESP >10 kDa), HSP90α (whole EVs, EV surface and EV depleted ESP >10 kDa) and, Calpain/ Calpain A (whole EVs, EV surface and EV depleted ESP >10 kDa) (Table 3.2–3.4, Appendix 3.2). Other notable immune modulators, included Sigma and Omega class GST which were only identified in EV depleted ESP >10 kDa and with relative low abundances (Table 3.4; Appendix 3.2).

Enolase, is a multifunctional protein necessary for host immune system evasion by binding with plasminogen or fibrinogen and activating plasmin–mediated proteolysis (Díaz-Ramos *et al.*, 2012; Fukano and Kimura, 2014; Ayón-Núñez *et al.*, 2018a; Ayón-Núñez*et al.*, 2018b). Binding to plasminogen or fibrinogen results in the degradation of the host's extracellular matrix and the prevention of clot formation around the parasites (Jolodar *et al.*, 2003; Marcilla *et al.*, 2007; Ramajo-Hernández *et al.*, 2007; Wang *et al.*, 2011; Figueiredo *et al.*,

2015; Maizels *et al.*, 2018; Jiang *et al.*, 2019). My findings demonstrate that Apα–Enolase–1 was observed as the third most abundant protein in SEC *A. perfoliata* EV depleted ESP >10 kDa, 23rd in whole EVs, 24th in EV surface (Table 3.2–3.4; Appendix 3.2). Enolase was also found to be the most abundant in other cestode ESP, *E. granulosus* (Wang *et al.*, 2015) and *T. solium* (Victor *et al.*, 2012). It is implied that the high expression of Apα–Enolase in SEC *A. perfoliata* secretome, particularly in whole EVs, may play an essential role in the host immunity evasion and establishment of *A. perfoliata* in the host. However, *A. perfoliata* are not blood sucking worms, the pathological changes during *A. perfoliata* infection primarily causes a localised inflammation at the site of attachment, particularly the caecal mucosa (Lawson *et al.*, 2019). Thus, Apα–Enolase is likely to play another role in *A. perfoliata* infections, rather than being involved in blood clot formation.

Annexins are a family of proteins usually present in the plasma membrane, involved in a wide range important biological processes such as membrane traffic and organisation activities and regulation of Ca^{2+} ion channel activity (Gerke and Moss, 2002; Hofmann *et al.*, 2010; Song *et al.*, 2021). Annexin B1, derived from *T. solium* metacestodes have an ability to down–regulate the host immune response by inducing apoptosis of human eosinophils (Yan *et al.*, 2008). Immunisation with recombinant Annexin B30 derived from *C. sinensis* (rCsANXB30) strongly induced IgG1 and cytokines IL–10 levels in spleen cells, indicating that immune responses both humoral and cellular in rats are triggered by Annexin (He *et al.*, 2014). Therefore, the discovery of 8 (A4, A7, A13 and B9) Annexins in SEC *A. perfoliata* EVs and 4 Annexins (A7 and A13) on the EV surface in the top 50 most abundant proteins, suggests that Annexins secreted by *A. perfoliata* may trigger the host immune responses for furthering survival within the host. However, different Annexin groups have been identified in the SEC *A. perfoliata* secretome. Therefore, each annexin group will need to be elucidated for their distinct immune modulatory functions to further resolve their function (Cantacessi *et al.*, 2013).

Calpain is a calcium–dependent, non–lysosomal cysteine protease that exists in the cytosol as an inactive proteolytic enzyme. Moreover, Calpain is involved in numerous inflammation–associated diseases in human (Ji *et al.*, 2016). Calpain identified in *S. mansoni and S. japonicum* has been mainly investigated as a vaccine candidate. However information on Calpains as immune modulators is currently brief (Molehin, 2020). Notably, Calpain expressed in the tegument external surface and excretory organs of schistosomes (Siddiqui

et al., 1993; Kumagai *et al.*, 2005; Wang *et al.*, 2017&2018; Chaimon *et al.*, 2019) has the ability to cleave plasma fibronectin (Wang *et al.*, 2017; Chaimon *et al.*, 2019) and blood coagulation protein high molecular weight kininogen (HK) (Wang *et al.*, 2018). Taken together, these functions aid in host immune evasion and parasite survival by regulating blood coagulation and inflammation where the parasite resides. Therefore, highly expressed calpain across the three components of the *A. perfoliata* secretome (8th in whole EVs, 20th in Surface EVs and 20th in EV depleted ESP; Table 3.2–3.4; Appendix 3.2), highlights a role in host immune invasion as suggested for Schistosomes, although, as for Enolase, the role of blood coagulation in *A. perfoliata* is unlikely. Thus, the specific role of calpain in *A. perfoliata* needs to be further investigated.

Thus, through a proteomic led approach, I have demonstrated the potential for an immune modulatory role of the *A. perfoliata* secretome, and some specific targets to examine, that may have wide ranging effects on the host immune response to the parasite or acting as virulence factors during infection. However, the functionality of these putative immune modulators secreted by *A. perfoliata* such as Sigma and Omega class GSTs, α and α–Enolase, now requires further investigation as demonstrated for *F. hepatica* (LaCourse *et al.*, 2012; Wang *et al.*, 2022)

3.5 CONCLUSIONS

In this chapter, I have successfully isolated and purified the *A. perfoliata* secretome using SEC and profiled each protein component, demonstrating the potential functions of the SEC fractioned *A. perfoliata* secretome involved in the parasite–host immune response. I have confirmed that adult *A. perfoliata* secrete EVs during *in vitro* maintenance by characterising the morphology with TEM and NTA analysis. Comprehensive proteomics coverage of the *A. perfoliata* secretome (SEC whole EVs, EV surface expressed proteins, and EV depleted ESP >10 kDa) supported by transcriptomics has revealed several key secretory molecules as putative immune modulators secreted by *A. perfoliata*. However, their immunomodulatory activities need to be further elucidated whether they play a role in the modulation of the horse host immunity by completing functional studies.

CHAPTER 4:

IN VITRO IMMUNOMODULATORY EFFECTS OF *ANOPLOCEPHALA PERFOLIATA* EXTRACELLULAR VESICLES ON THP–1 CELLS

4.1 INTRODUCTION

A. perfoliata is one of the most prevalent tapeworm species that infect horses around the world (Gasser *et al.*, 2005; Nielsen, 2016). A light infection (< 20 *A. perfoliata*) are often asymptomatic, whereas a severe infection from large clusters of *A. perfoliata* (> 100 *A. perfoliata*) at the ileocecal junction (Pearson *et al.*, 1993; Fogarty *et al.*, 1994; Williamson *et al.*, 1997) leads to a localised caecal mucosal tissue damage and inflammatory response (Lawson *et al.*, 2019). However, it is still unclear how *A. perfoliata* interacts with the horse host or modulates the horse immune response to aid prolonged survival within the host environment.

During helminth infections, the T helper type 2 (Th2) immune response is predominant for protective immunity against infection, thus limiting tissue damage and allowing chronic infection to occur (Else *et al.*, 1994; Liew *et al.*, 1997; Turner *et al.*, 2003; Min *et al.*, 2004; Chen *et al.*, 2012). For instance, mice infected with the nematode *N. brasiliensis* indicate a strong Th2–type immune response, demonstrated by high levels of Immunoglobulin E (IgE), Interleukin–4 (IL–4), and IL–13 production (Finkelman *et al.*, 1997). Likewise, RAW264.7 macrophages stimulated *in vitro* by exosome–like vesicles from the larval stage of the cestode, *T. pisiformis,* produced mainly Th2 related bioactive molecules including Arginase–1 (Arg–1), IL–4, IL–6, IL–10 and IL–13 (Wang *et al.*, 2020). However, in *T. crassiceps*, Th1 response may plays a critical role in protection against infection, whereas Th2 response through IL–10 is associated with heavy parasite intensities (Terrazas *et al.*, 1999). It was demonstrated that *T. crassiceps* infected mice treated with recombinant murine Th1–cytokines (IFN–γ and IL–2) had lower parasite numbers than control mice, whereas treated with Th2 (IL–10) increased in number of parasite loads (Terrazas *et al.*, 1999). In the same time, mice treated with anti–Interferon gamma (IFN–γ) monoclonal antibody demonstrated a dramatic increase in susceptibility, whereas mice treated with anti–IL–10 monoclonal antibody had a lower parasite intensity than control mice (Terrazas *et al.*, 1999). Moreover, in *T. crassiceps* a mix of Th1/Th2 response with high levels of both Interferon gamma (IFN–γ) and IL–4 produced by in splenocytes host cells has been demonstrated in chronic infections (Peón *et al.*, 2013). A mixed Th1/ Th2 adaptive immune response with *F. hepatica* EV–specific total Immunoglobulin G (IgG) antibodies in BALB/c mice has also been induced by *F. hepatica*

extracellular vesicles (EVs) (Murphy *et al.*, 2020). As such, it is clear that many factors are involved in the immune response of the host during helminth infections, which have been demonstrated both *in vivo* and *in vitro.*

EVs secreted as part of the ESPs by live parasitic helminths contains various important bioactive molecules such as lipids, proteins, metabolites, genomic DNA, RNAs, and non–coding RNAs (Zamanian *et al.*, 2015; de la Torre-Escudero *et al.*, 2019; Liu *et al.*, 2019; Meningher *et al.*, 2020; Hautala *et al.*, 2022). To date, growing research in EVs has revealed a wide range of roles in the host–parasite interaction (Wang *et al.*, 2015, 2020; Zheng *et al.*, 2017; Eichenberger *et al.*, 2018; Liu *et al.*, 2019; Zhou *et al.*, 2019; Murphy *et al.*, 2020; Yang *et al.*, 2021). Particularly, various key immune modulatory proteins identified in EVs derived from helminths have been shown to modulate the host immune response (Drurey and Maizels, 2021; Sánchez-López *et al.*, 2021). EV cargo molecules are likely delivered to the recipient cells through uptake of the EVs by the host cell, as demonstrated *in vitro* for several platyhelminths such as, *Echinococcus* spp. (Nicolao *et al.*, 2019; Wu *et al.*, 2021; Yang *et al.*, 2021), *T. asiatica* (Liang *et al.*, 2019), *Schistosoma* spp. (Zhu *et al.*, 2016; Liu *et al.*, 2019; Kifle, Chaiyadet, *et al.*, 2020; Meningher *et al.*, 2020), *F. hepatica* (de la Torre-Escudero *et al.*, 2019), *O. viverrini* (Chaiyadet *et al.*, 2015)*, and E. caproni* (Marcilla *et al.*, 2012). As a consequence of EV uptake, there are alterations to the recipient cells such as cell viability, cell proliferation and cytokine production as part of the immune response of the recipient cells (Chaiyadet *et al.*, 2015; Meningher *et al.*, 2020). For example, EVs from *O. viverrini* drove human cholangiocytes proliferation *in vitro,* as well as increased IL–6 secretion and changes in protein expression associated with endocytosis, wound repair, and cancer (Chaiyadet *et al.*, 2015). In *S. mansoni,* EV miRNA were taken up *in vitro* by primary Th cells, resulting in downregulation of T helper cell differentiation (Meningher *et al.*, 2020). Furthermore, stimulation of sheep peripheral blood mononuclear cells (PBMCs) with *E. granulosus* EVs upregulated mRNA expression of IL–10, IRF5 and TNF–α, but downregulated IL–1β, IL–17, and CD14 in (Yang *et al.*, 2021).

However, there is limited research that investigates an interaction between *A. perfoliata* and the immune response of the horse host. Lawson *et al.* (2019) investigated the role of *A perfoliata* ESP in modulating *in vitro* immune responses, demonstrating that *A. perfoliata* ESP had the ability to inhibit the proliferation of human T–cell line Jurkat and down–

regulate cytokine transcription by Concanavalin–A stimulated equine lymphocyte. The present thesis has identified potential immune modulators expressed in the *A. perfoliata* transcriptome (Chapter 2). Furthermore, we have confirmed that *A. perfoliata* release EVs which express potential immune modulators at the protein level as part of the EVs (Chapter 3). Thus, there is evidence to suggest that EVs secreted by *A. perfoliata* may be able to modulate the host immune system, however, functional studies are needed to confirm putative immunomodulatory actions to increase my understanding of these complex parasite–host interactions.

4.1.1 AIMS AND OBJECTIVES

This chapter aimed to investigate whether *A. perfoliata* EVs have immunomodulatory functions and the ability to modulate the mammalian immune response, as demonstrated in other platyhelminth species such as *Echinococcus* spp., *Schistosoma* spp. and *F. hepatica*. In the absence of an established equine host cell model, an *in vitro* model using THP–1 cells as a host cell co–cultured with *A. perfoliata* EVs was employed to achieve this aim. Firstly, uptake of *A. perfoliata* EVs, dyed with a lipid dye, by THP1–cells was evaluated using laser confocal microscopy and flow cytometry. Cell viability post exposure to *A. perfoliata* EVs was determined using Trypan blue, MTT assay and flow cytometry. Finally, multiplex *in vitro* cytokine secretion from THP–1 cells following exposure to *A. perfoliata* EVs was performed.

It was hypothesised that THP–1 cells would uptake *A. perfoliata* EVs *in vitro*. As a consequence of uptake, it was hypothesised that EVs would impact cell viability and expression of key cytokines secreted by THP–1 cells including Th1–type/pro–inflammatory cytokines: Tumor necrosis factor (TNF–α), Interleukin 1–alpha (IL1–α), Interleukin–1 beta (IL–1β) and Interferon gamma (IFN–γ) and Th2–type/anti–inflammatory cytokines: Interleukin–4 (IL–4) and Interleukin–5 (IL–5).

4.2 MATERIALS AND METHODS

4.2.1 THP–1 cell culture and maintenance

THP–1 cells (kind donation from Royal Veterinary College, London) were cultured following ATCC product information (https://www.atcc.org/products/tib-202). Briefly, cells were cultured in complete RPMI 1640 cell culture medium containing GlutaMAX™ and 25 mM HEPES (Gibco™, Thermo Fisher Scientific, Loughborough, UK), supplemented with 10% heat–inactivated foetal bovine serum (FBS), 1% penicillin–streptomycin (10,000 IU/mL), 1% Minimum Essential Medium (MEM), non–essential amino acids solution (MEM–NEAA, 100X) and 0.1% Beta–2–mercaptoethanol (Gibco™, Thermo Fisher Scientific, Loughborough, UK), in T25 cell culture flasks (Thermo Fisher Scientific, Loughborough, UK). Cells were cultured in a humidified incubator at 37°C, with 5% CO_2. Once THP–1 cells reached approximately 80% confluency (cell density of 8×10^5 to 1.0×10^6 viable cells/mL), cell viability was determined. Briefly, THP–1 cells were stained with trypan blue at a 1:1 ratio (0.4%, filtered 0.22 µm; Gibco™, Thermo Fisher Scientific, Loughborough, UK) and viable and dead cells counted using a Fast–Read 102® cell counting slide (Biosigma, Venice, Italy), under the light microscope. A viable cell percentage between 80–90% was deemed acceptable to be used for further experiments.

4.2.2 THP–1 Cells differentiation

THP–1 monocyte cells were differentiated into macrophages as previously described in Daigneault *et al.* (2010). In each experiment, THP–1 cells were seeded into experimental plates at defined cell densities (described in subsequent sections). Prior to cell stimulation, a stock solution of Vitamin D_3 at 100 mM (1α,25–Dihydroxyvitamin D_3, Enzo Life Sciences, New York, USA) was prepared by dissolving 50 µg Vitamin D_3 (Enzo Life Sciences, New York, USA) in 100 µL dimethyl sulfoxide (DMSO; MP Biomedicals, California, USA) and 1.1 mL RPMI 1640 medium (Gibco™, Thermo Fisher Scientific, Loughborough, UK). Cells were then stimulated by adding 100 nM of Vitamin D_3 (1:1000 dilution of the stock solution into culture medium) and incubated in a humidified incubator, at 37°C with 5% CO_2 for 72 hours. After differentiation and a total of 24 hours prior to adding any experimental treatments, the FBS in the culture medium was changed to 10% Exosome–Depleted FBS (Gibco™, Thermo Fisher Scientific, Loughborough, UK).

4.2.3 Confocal microscopy to determine cell uptake of *A. perfoliata* EVs

4.2.3.1 Fluorescent labelling of *A. perfoliata* EVs

A total of 200 µg of *A. perfoliata* SEC purified EVs (n=3; derived from Chapter 3, Section 3.2.2) and a PBS control (n=3; equal volume to equate to PBS used in purified EVs samples) were pipetted into a 3 kDa MWCO, Amicon® Ultra 0.5 mL Centrifugal Filters (Merck Millipore, Merck Life Sciences, Darmstadt, Germany). Subsequently, samples were ultra–centrifuged (IEC Micromax Centrifuge), at 14,000 x *g* for 10 minutes at 4°C, until the final volume of samples were reduced to approximately 20 µL. Samples were recovered by reverse spinning (IEC Micromax Centrifuge), at 1,000 x *g* for 2 minutes at 4°C.

Both EVs and PBS control were labelled with PKH26 Red Fluorescent Cell Linker Kits for General Cell Membrane Labelling (Sigma–Aldrich, Merck Life Sciences, Darmstadt, Germany), following the manufacturer's procedure with modification, according to van der Vlist *et al.*, (2012) and Zhang *et al.* (2020). Briefly, the 20 µL of sample from ultracentrifugation was diluted with 80 µL of diluent C, rapidly mixed with 100 µL PKH26 dye solution (3 µL of PKH26 to 100 µL diluent C) and incubated for 5 minutes at room temperature with periodic mixing. Unincorporated dye was removed immediately after incubation using an exosome spin column kit (MW 3000; Invitrogen, Thermo Fisher Scientific, Loughborough, UK), following the manufacturer's protocol and Zhang *et al.* (2020). In brief, to remove via Exosome spin columns Kits, 100 µL of each labelled sample was transferred into the rehydrated exosome spin column and the column placed into the elution tube and then centrifuged (IEC Micromax Centrifuge), at 750 *×g* for 2 minutes at 4°C. At this point, unincorporated dye was removed, whilst PKH26–labelled samples were eluted into the elution tube. PKH26–labelled *A. perfoliata* SEC purified EV (n=3) and control samples (n=3) were then stored in the dark at 4°C overnight, prior to being added to uptake experiments.

4.2.3.2 Confocal microscopy

Prior to differentiation, THP–1 cells were seeded onto glass sterile cover slips in 24 well flat bottom cell culture plates (Costar™, Corning Incorporated, New York, USA), at a density of 1 x 10^5 viable cells/mL. Glass coverslips had previously been coated overnight at 4 °C with collagen (Collagen type I, rat tail, 1:50 with PBS and 20 % FBS; Gibco™, Thermo Fisher Scientific, Loughborough, UK), which was removed and cover slips washed three times with

PBS prior to seeding of cells. Following differentiation of THP–1 cells and change of FBS to exosome–depleted FBS (section 4.2.2), cells were co–cultured with 40 µg/mL (equal to 20 µg per well) of PKH26–labelled *A. perfoliata* SEC purified EVs (n=3) and PKH26–labelled PBS control samples for 6, 12 and 24 hours, in triplicate. At the end of each timepoint, medium was removed and cells gently washed with PBS thrice. THP–1 macrophages were subsequently fixed with 4% Paraformaldehyde in PBS (Santa Cruz Biotechnology, Texas, USA) for 15 minutes at room temperature, and then washed with PBS thrice. All cover slips were transferred onto a glass slide for counterstaining with VECTASHIELD® antifade mounting medium (Vector Laboratories, Inc, California, USA) with 5 µL of DAPI (1 µg/mL; 4',6–diamidino–2–phenylindole, dihydrochloride; Thermo Fisher Scientific, Loughborough, UK) to detect the nucleus of the macrophages. Coverslips were sealed with nail polish, and the slides stored in the dark at 4 °C until imaging.

All slides were imaged with a Leica SP8 super resolution laser confocal microscope (Leica Microsystems, Wetzlar, Germany), using a 20X/0.75 dry lens (HC PL APO CS2), with a 2.4 zoom factor. Cells were imaged using LAS X CORE software (v3.3.0) at 200 × magnification, with the same parameters setting of standard excitation (EX)/ emission (EM) wavelength filters for DAPI (358 nm/461 nm) and PKH–26 (551 nm/567 nm) throughout image processing. The fluorescent intensity of the uptake THP–1 macrophages were quantified using ImageJ software (version 1.52a, https://imagej.nih.gov/ij/) according to Kifle *et al.* (2020) with modification. Briefly, a total of 30 cells were randomly selected per biological replicate (six cells per field of view for five fields of view equating to 30 cells in total). The fluorescent intensity of the uptake of PKH26–labelled *A. perfoliata* SEC purified EVs and PBS control by THP–macrophages was measured by drawing around selected cells to obtain the integrated density and area of the selected cells. Following that, a circle (dimension 0.75 x 0.75 cm) was drawn per technical fields next to selected cells that had no fluorescence as a fluorescence of background readings. The corrected total cell fluorescence (CTCF) was calculated using the formula: CTCF = Integrated Density – (Area of selected cell × Mean fluorescence of background readings). Subsequently, CTCF of the PBS controls were deducted from CTCF of PKH26–labelled *A. perfoliata* SEC purified EV samples to normalise the natural luminescence. Percentage uptake of EVs by THP–1 cells was obtained by dividing CTCF (after deduction with the integrated density) by the total integrated density then multiplying by 100.

4.2.4 Flow cytometry to determine cell uptake of *A. perfoliata* SEC purified EVs and cell viability

4.2.4.1 Fluorescent labelling of *A. perfoliata* EVs

EVs were labelled as in section 4.2.3.1 with a modification to the unincorporated dye removal stage. Briefly, excess dye from both PKH26–labelled *A. perfoliata* SEC purified EV and controls was removed for flow cytometry experiments using Amicon Ultra–0.5 Centrifugal Filter Unit (MerckMillipore, Merck Life Sciences, Dorset, UK), following the manufacturer's guidelines. Briefly, Amicon® Ultra filter units were washed with 200 µL of PBS then ultra–centrifuged (Heraeus Multifuge 3 S–R) at 14,000 x *g* for 20 minutes at 4°C. Subsequently, 200 µL of labelled sample was added and ultra–centrifuged as previously described. Retained labelled sample were then recovered by placing the Amicon® Ultra filter unit upside down and centrifuging at 1,000 *× g* for 2 minutes. The ultrafiltrate were then stored in the dark at 4°C overnight, prior to being added to uptake experiments.

4.2.4.2 Flow cytometry

Cells were seeded into 24 well flat bottom cell culture plates (Costar™, Corning Incorporated, New York, USA) at a density of 2 x 10^5 viable cells/mL and subsequently exposed to PKH26–labelled *A. perfoliata* SEC purified EVs (n=3; 40 µg/mL equal to 20 µg/ well) and the PBS control for 6, 12, and 24 hours. Following exposure, medium was removed and THP–1 macrophages were gently washed with PBS thrice, with each wash retained. THP–1 macrophages were removed from the wells by adding cell dissociation buffer (enzyme–free, PBS; Gibco™, Thermo Fisher Scientific, Loughborough, UK) into each well and incubated at room temperature for 15 minutes. Lifted cells were pooled together with previous PBS washes, centrifuged (Eppendorf™ Refrigerated Centrifuge 5424 R, Thermo Fisher Scientific, Loughborough, UK) at 600 *x g* for 10 minute and the cell pellet resuspended in 1 mL of PBS.

To determine the effect of *A. perfoliata* SEC purified EVs on cell viability, resuspended cells were stained with 1 µL of Near–IR fluorescence dye (Invitrogen™ LIVE/DEAD™ Fixable Near–IR Dead Cell Stain Kit, for 633 or 635 nm excitation; Thermo Fisher Scientific, Loughborough, UK), following the manufacturer's protocol. After staining, the cell pellet was suspended and fixed with 200 µL of 4% paraformaldehyde in PBS (Santa Cruz Biotechnology, Texas, USA) for 20 minutes at room temperature. Cells were centrifuged (Eppendorf™

Refrigerated Centrifuge 5424 R, Thermo Fisher Scientific, Loughborough, UK) at 600 *x g* for 10 minutes, the supernatant was discarded, and the cell pellet resuspended in 200 µL of nuclease–free Molecular Biology–Grade Water (HyClone™, 0.1 µm sterile filtered, Cytiva; Massachusetts, USA). Finally, resuspended cells were transferred into 96–well U–bottom plates to analyse via flow cytometry. A total of 10,000 cells per sample were analysed using the CytoFLEX LX Flow Cytometer via CytExpert software (version 2.4.0.28; Beckman Coulter, California, USA) at different time points. Flow cytometry data were exported in FCS3.0 files and were analysed using FlowJo software (version 10; FlowJo LLC, USA) whereby THP1 macrophages were first gated for major THP–1 macrophage population, then doublet discrimination was performed through singlet gating. Subsequently, viable THP–1 macrophages were assessed for uptake of *A. perfoliata* EVs using fluorescence marker gating (gating strategy described in Figure 4.3). Population data from each gate were exported from FlowJo via .csv files for subsequent analysis and fluorescence–activated cell sorting (FACS) plots were exported from FlowJo as Tag Image File Format (TIFF files) for presentation in figures. Total percentage uptake was calculated based on the proportion of viable cells that demonstrated uptake of *A. perfoliata* EVs.

4.2.5 Assessment of cell viability following exposure to *A. perfoliata* EVs

To further determine whether the *A. perfoliata* SEC purified EVs affect THP–1 macrophage cell viability, the cells were further assessed by Trypan Blue to assess the live to dead ratio and MTT (metabolic activity as a reflection of viable cells) assay.

THP–1 cells were seeded at 2 x 10^5 viable cells/mL into 12–well flat–bottom plates (Trypan Blue assay) or 2 x 10^4 viable cells/mL into 96–well flat–bottom plates (MTT assay), prior to differentiation and changing FBS to exosome depleted FBS, as previously described in Section 4.2.2. Differentiated THP–1 macrophages were exposed to 3 treatments for 24 hours; 40 µg/mL of *A. perfoliata* SEC purified EVs (3 biological replicates and 3 technical replicates; Chapter 3, Section 3.2.2), PBS control (n=3; added to wells in equal volume as each biological replicate of EVs) and 2% Triton X–100 as a positive control (n=3; Sigma–Aldrich, Merck Life Sciences, Darmstadt, Germany).

4.2.5.1 Trypan Blue Assay

Following exposure for 24 hours, the culture media was removed and cells lifted using cell dissociation buffer (Gibco™, Thermo Fisher Scientific, Loughborough, UK) as described in Section 4.2.4.2; note, the cell pellet was not resuspended in 1 mL of PBS. Lifted cells were then stained with Trypan blue at a 1:1 ratio (0.4%, 0.22 µm filtered; Gibco™, Thermo Fisher Scientific, Loughborough, UK), and live and/or dead cells counted using TC10™ Automated Cell Counter (Bio–Rad Laboratories, California, USA). The percentage of live cells per sample were calculated by dividing the live cell count by the total cell count and multiplying with 100.

4.2.5.2 MTT assay

Following exposure to the 3 treatments for 24 hours, cell culture supernatants were removed and stored at −80 °C until further analysis for cytokine secretion (Section 4.2.6). Cells and 9 empty wells as background controls were then incubated with 50 µL of RPMI 1640 culture medium (without any supplements) and 50 µL of MTT solution (3–(4,5–dimethylthiazol–2–yl)–2,5–diphenyl–2H–tetrazolium bromide, 5 mg/mL MTT in PBS; Invitrogen, Thermo Fisher Scientific, Loughborough, UK) per well at 37°C, with 5% CO_2 for 3 hours. After incubation, 150 µL of MTT solvent (4 mM HCl, Thermo Fisher Scientific, Loughborough, UK) with 0.1% NP40 (Sigma–Aldrich, Merck Life Sciences, Darmstadt, Germany) in isopropanol (Thermo Fisher Scientific, Loughborough, UK)) were added to each well, incubated in the dark with orbital shaking, at room temperature for 15 minutes, with manual pipetting every 5 minutes. Absorbance was then measured by Infinite® 200 PRO micro plate reader with Tecan i–control software (version 2.0.10.0; Männedorf, Switzerland) at 590 nm. To calculate cell viability, background readings were subtracted from all sample readings to correct the absorbance and mean PBS control reading were used as a control (healthy cells = 100% viability). Percentage cell viability (%) was calculated by dividing the mean treatment readings from all replicates by mean PBS control readings, then multiplying with 100.

4.2.6. Determination of cytokine secretion following exposure to *A. perfoliata* EVs

Following exposure to 40 µg/mL of *A. perfoliata* SEC purified EVs for 24 hours, cytokine secretion in the supernatants was quantified via an immunology multiplex bead–based assay for measurement of the following 6 cytokines: TNF, IL1–α, IL1–β, IFN–γ, IL–4 and IL–5 (HCYTA–60K, MILLIPLEX® Human Cytokine/ Chemokine/ Growth Factor Panel A; Millipore, Merck Life Sciences, Massachusetts, USA). Prior to quantification, the cell culture supernatants (Section 4.2.5.2) were defrosted and centrifuged at 10,000 *x g*, for 10 minutes to collect the cell–free supernatant and all samples quantified without diluting. The Multiplex assay was performed in duplicate, following the manufacturer's instructions. A standard curve was constructed for each cytokine, with the following ranges of concentration in pg/mL: TNF–α (6.4–100,000); IL1–α (4.8–75,000); IL1–β (1.6–25,000); IFN–γ (1.3–20,000); IL–4 (0.64–10,000) and IL–5 (0.64–10,000). The Multiplex plate was read on a Luminex®200™ with xPONENT® software (version 4.3.229.0; xMAP® Technologies, Luminex Corporation, Texas, USA). For all cytokine analysis, cytokine concentration was quantified via the median fluorescence intensity (MFI) data, using Five Parameter Logistic (5PL) to fit the standard curve.

4.2.7 Statistical analysis

Prior to analysis, data were assessed for normal distribution by assessment for skewness within Genstat (21st Edition; VSN International, Hemel Hempstead, UK). All data in this chapter were confirmed to be normally distributed and so were not transformed prior to analysis. All statistical analyses were completed in GenStat (21st Edition; VSN International, Hemel Hempstead, UK). Statistical significance was considered if $P < 0.05$ and statistical trend considered if $P < 0.1$.

The percentage uptake by THP–1 macrophages via confocal microscopy and flow cytometry at 6, 12 and 24 hours and percentage cell viability after exposure to *A. perfoliata* SEC purified EVs for 24 hours via Trypan blue and MTT assays were analysed using one–way analysis of variance (ANOVA). Post–hoc Tukey's honestly significant difference (HSD) test was used to compare treatment groups (PBS control, EVs and Triton–X 100 EV exposed) in a pairwise method. A paired Student's t test was used to assess percentage cell viability by flow cytometry at 6, 12 and 24 hours and the cytokine secretion between control samples and EV exposed.

4.3 RESULTS

4.3.1 THP–1 macrophages uptake *A. perfoliata* EVs

Both confocal microscopy and flow cytometry demonstrated that THP–1 macrophages uptake *A. perfoliata* SEC purified EVs *in vitro* following 6, 12 and 24 hours of exposure to EVs (Figure 4.1 and 4.2A–B).

Based on confocal microscopy, PKH26 labelled *A. perfoliata* EVs were clearly demonstrated inside the cytoplasm of THP–1 macrophages, demonstrated by the red fluorescence signal (Figure 4.1; 4.2A–B). Only a low fluorescence signal was observed when cells were exposed to PKH26–labelled PBS control, demonstrating specific uptake of EVs, rather than the PKH26 dye alone (Figure 4.1; 4.2A–B). The percentage uptake demonstrated no significant difference in the corrected total cell fluorescence (CTCF) (P = 0.435; Figure 4.2A). and percentage uptake (P = 0.799; Figure 4.2B) between the 6, 12 and 24 hour time points. Numerically, the greatest uptake of *A. perfoliata* EVs was at 24 hours (72.61 ± 2.16% (Mean ± SEM; Figure 4.2B), therefore, the timepoint at 24 hours was used for further cell viability assessment via Trypan blue and MTT assays.

Quantification of EV uptake via flow cytometry also demonstrated clear uptake of *A. perfoliata* EVs by singlet, viable THP–1 cells (the overall mean uptake = 96.16 ± 1.33% % (Mean ± SEM); Figure 4.2C), with no significant difference between uptake at 6, 12 and 24 hours (P = 0.593; Figure 4.2C).

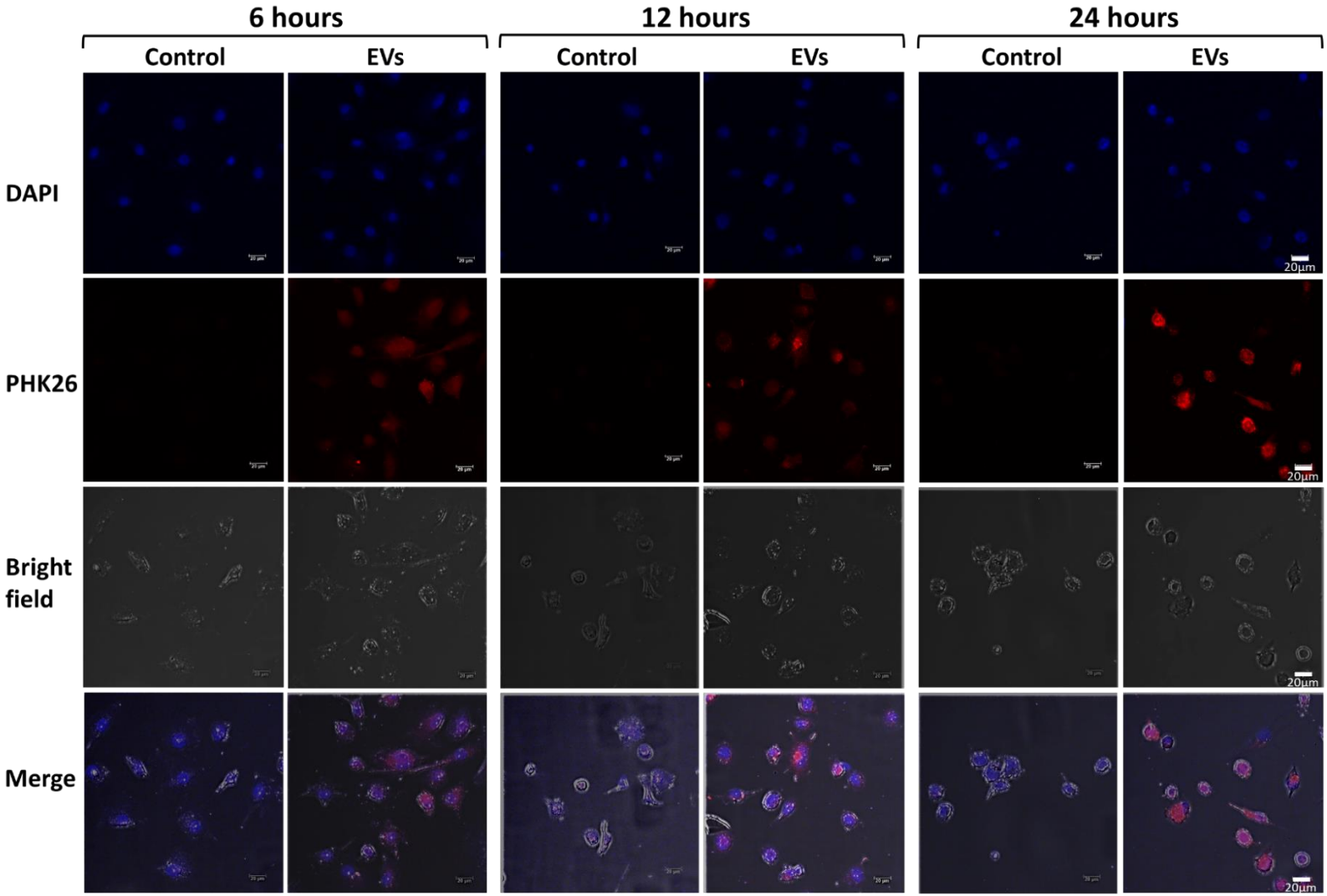

Figure 4.1 Uptake of *A. perfoliata* SEC purified EVs by THP–1 macrophages via confocal analysis at 6, 12 and 24 hours. THP–1 cells were exposed to 40 µg/mL PKH26–labelled *A. perfoliata* SEC purified EVs (n=3) and PKH26–labelled PBS control (n=3). The fluorescence microscopy images from top to bottom show: DAPI to demonstrate the cell nuclei, PKH26 to demonstrate labelled EVs, Bright field to demonstrate cell and the Merged fields. Images were taken at 200 × magnification. Scale bars: 20 µm.

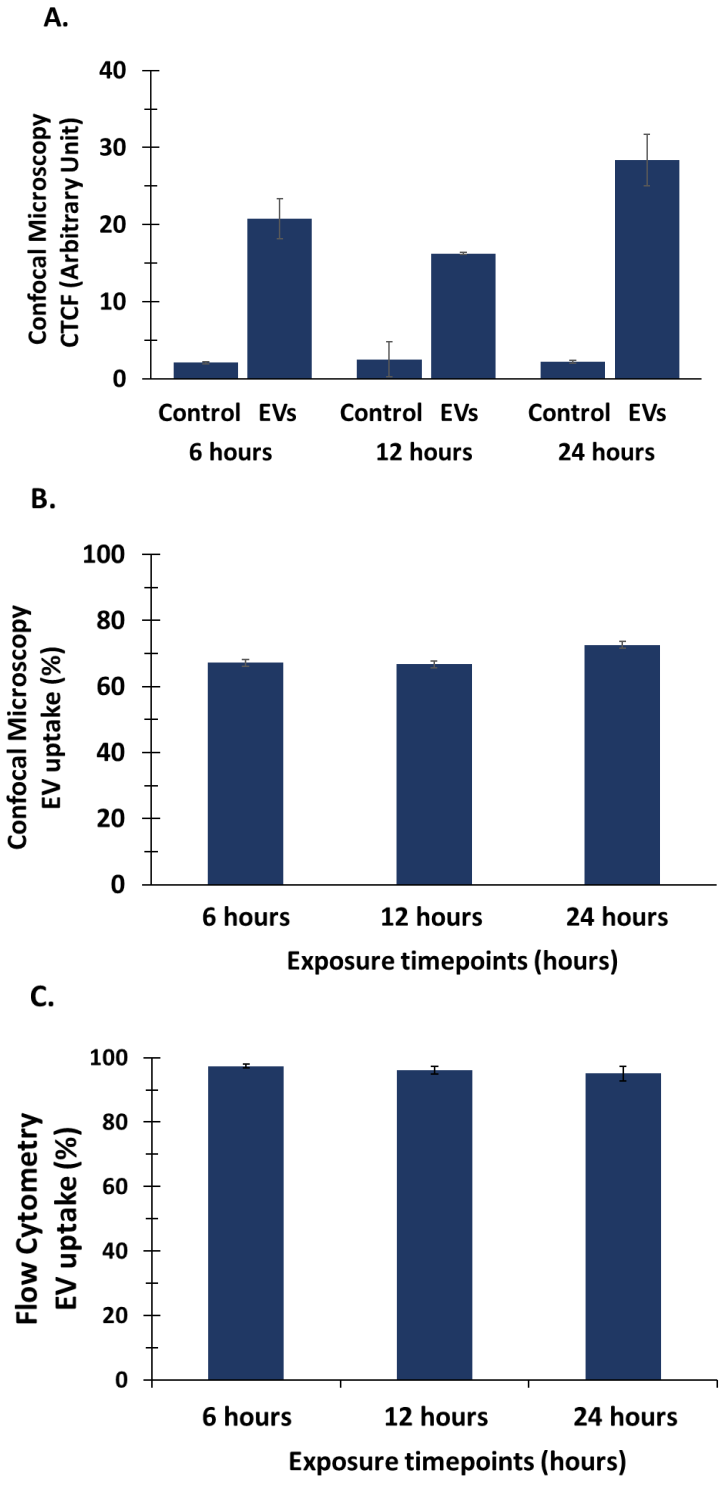

Figure 4.2 Confocal and flow cytometry analyses of 40 µg/mL of PKH26–labelled *A. perfoliata* SEC purified EVs (n=3) and PKH26–labelled PBS control (n=3), demonstrating uptake of EVs by THP–1 macrophages after co–culture for 6, 12 and 24 hours. No significant differences in EV uptake were demonstrated between exposure time points for (A) mean corrected total cell fluorescence (CTCF) via confocal microscope (P=0.799), (B) percentage EV uptake via confocal microscope (P=0.435) and (C) percentage EV uptake via flow cytometry (P = 0.593).

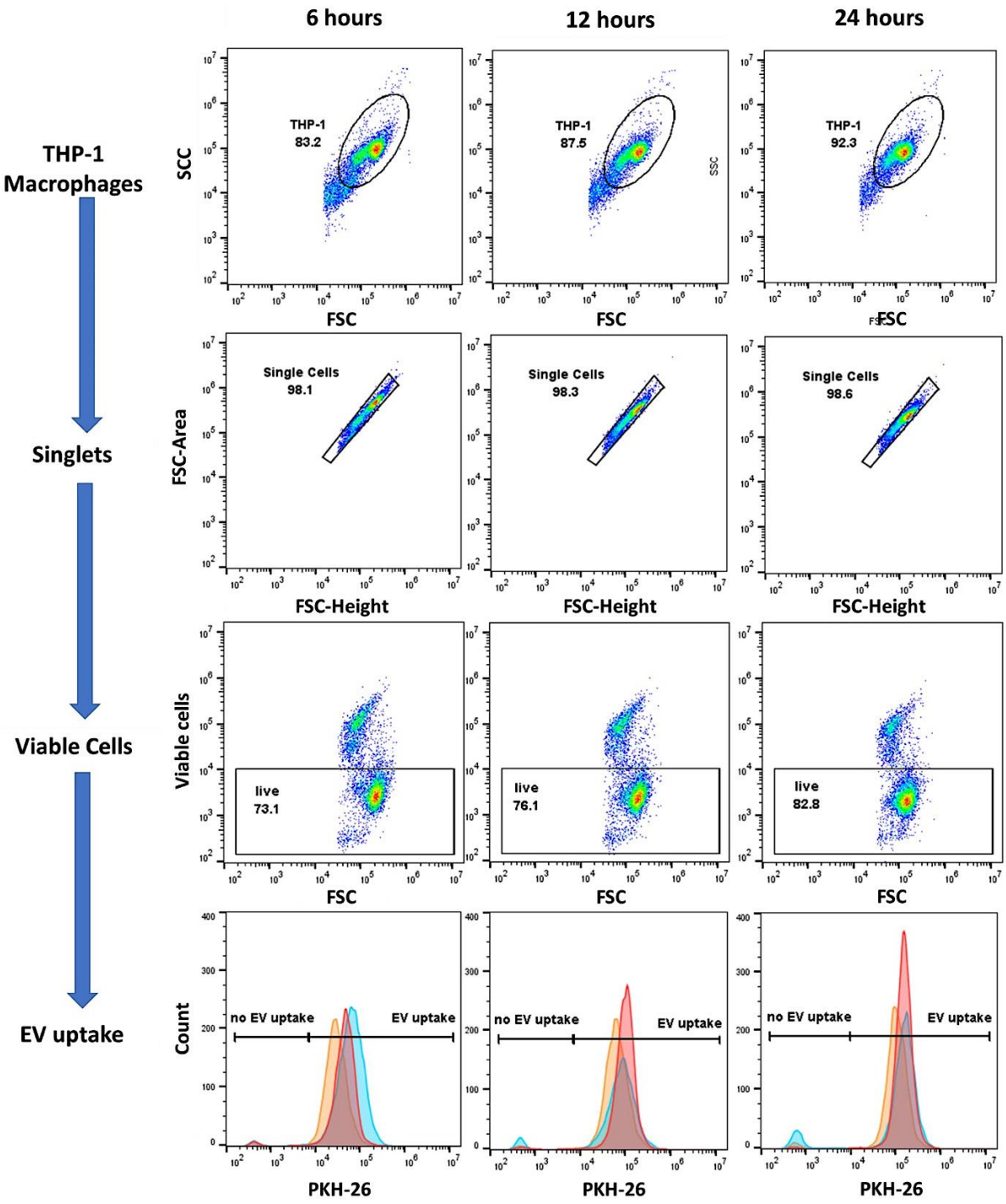

Figure 4.3 Representative flow cytometry gating strategy for THP–1 macrophages population sorting for EV uptake post exposure to 40 µg/mL of PKH26–labelled *A. perfoliata* SEC purified EVs (n=3) and PKH26–labelled PBS control (n=3), demonstrating uptake of EVs by THP–1 macrophages after co–culture for 6, 12 and 24 hours. The gating strategy from top to bottom, reveals the following: the major THP–1 macrophage population, singlet THP–1 macrophages, viable THP–1 macrophages, and THP–1 macrophages that have taken up *A. perfoliata* EVs. Replicates 1, 2 and 3 of samples were presented in red, blue and orange, respectively. **Abbreviations:** forward scatter (FSC), side scatter (SSC).

4.3.2 *A. perfoliata* EVs affect cell viability of THP–1 macrophages

The assessment of cell viability of THP–1 macrophages post exposure to *A. perfoliata* SEC purified EVs *in vitro* at 24 hours by trypan blue and MTT assays demonstrated a significantly decreased cell viability by 30% ($P < 0.001$; Figure 4.4A) and 36.2% ($P < 0.001$, Figure 4.4B), respectively, compared to the PBS controls. In all assays, the Triton X positive control significantly reduced cell viability to negligible levels, compared to the PBS control and EV exposed ($P < 0.001$; Figure 4.4A–B).

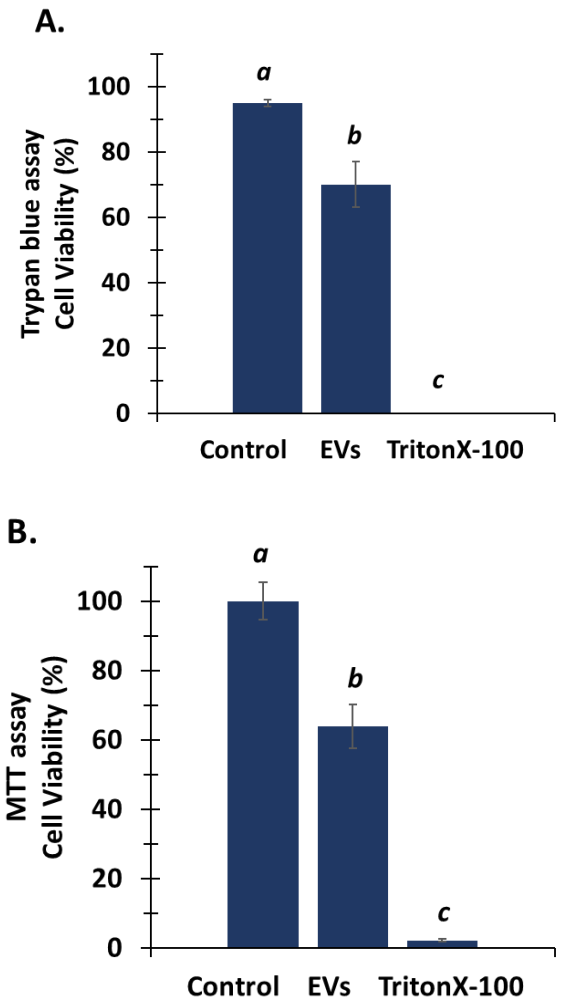

Figure 4.4 Cell viability of THP–1 macrophages after co–culture with SEC *A. perfoliata* EVs *in vitro* at 24 hours via (A) Trypan blue assay and (B) MTT assay, expressed as percentage. Different letters (a–c) indicate significant difference $P < 0.001$ in cell viability between cells exposed to PBS controls, 40 µg/mL of SEC *A. perfoliata* EV, and 2% Triton X–100 (positive control). Error bars represent the SEM.

Flow cytometry analysis of cell viability of singlets THP–1 macrophages *in vitro* post exposure to PKH26–labelled *A. perfoliata* EVs at 6, 12 and 24 hours *in vitro* (Figure 4.3), demonstrated that there were no significant differences in cell viability between the 3 exposure timepoints (P = 0.154, Figure 4.5). However, cell viability decreased by 23.3%, 23.5 % and 17.4% post EV exposure *in vitro* at 6, 12 and 24 hours, respectively, compared to the control. Viability of THP–1 cells exposed to *A. perfoliata* EVs at 12 hours demonstrated a significant difference to the PBS control (P = 0.009, Figure 4.5). However, there were no differences in cell viability between *A. perfoliata* EV exposed and PBS control cells at 6 and 24 hours (P > 0.05).

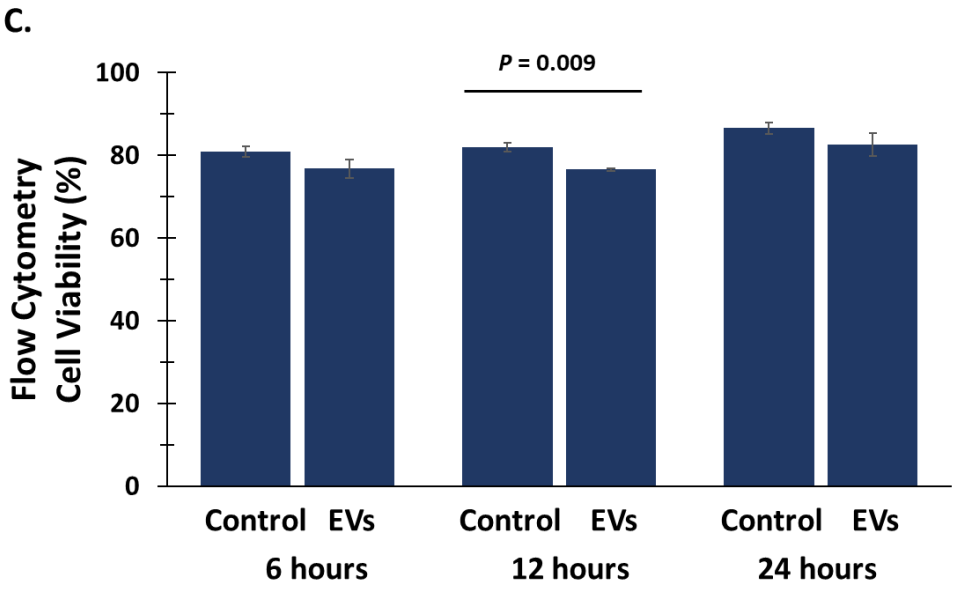

Figure 4.5 Flow cytometry analysis on cell viability of THP–1 macrophages post exposure to 40 µg/mL of PKH26–labelled *A. perfoliata* SEC purified EVs (n=3) and PKH26–labelled PBS control (n=3) after co–culture for 6,12 and 24 hours. THP–1 macrophages were stained with Near–IR fluorescence dye for 633 or 635 nm excitation to assess cell viability. No significant differences in cell viability between the 3 exposure timepoints (P = 0.154) and between *A. perfoliata* EV exposed and PBS control cells at 6 and 24 hours (P > 0.05). At 12 hours demonstrated a significant difference between *A. perfoliata* EV exposed and PBS control cells (P = 0.009), error bars represent SEM.

4.3.3 *A. perfoliata* EVs affect cytokine production of THP–1 macrophages

A. perfoliata EVs induced a significant increase in secretion of IL1–α ($P < 0.001$), IL1–β ($P = 0.016$) and TNF–α ($P = 0.03$) and a statistical trend for an increase in IFN–γ ($P = 0.095$; Figure 4.6). However, there was no effect on IL–4 ($P = 0.307$; Figure 4.6). The levels of IL–5 in the assay were too low (ranging from 95.1 fg/mL to 127.6 fg/mL) to determine significant differences between controls and EV exposed and so were removed from the analysis.

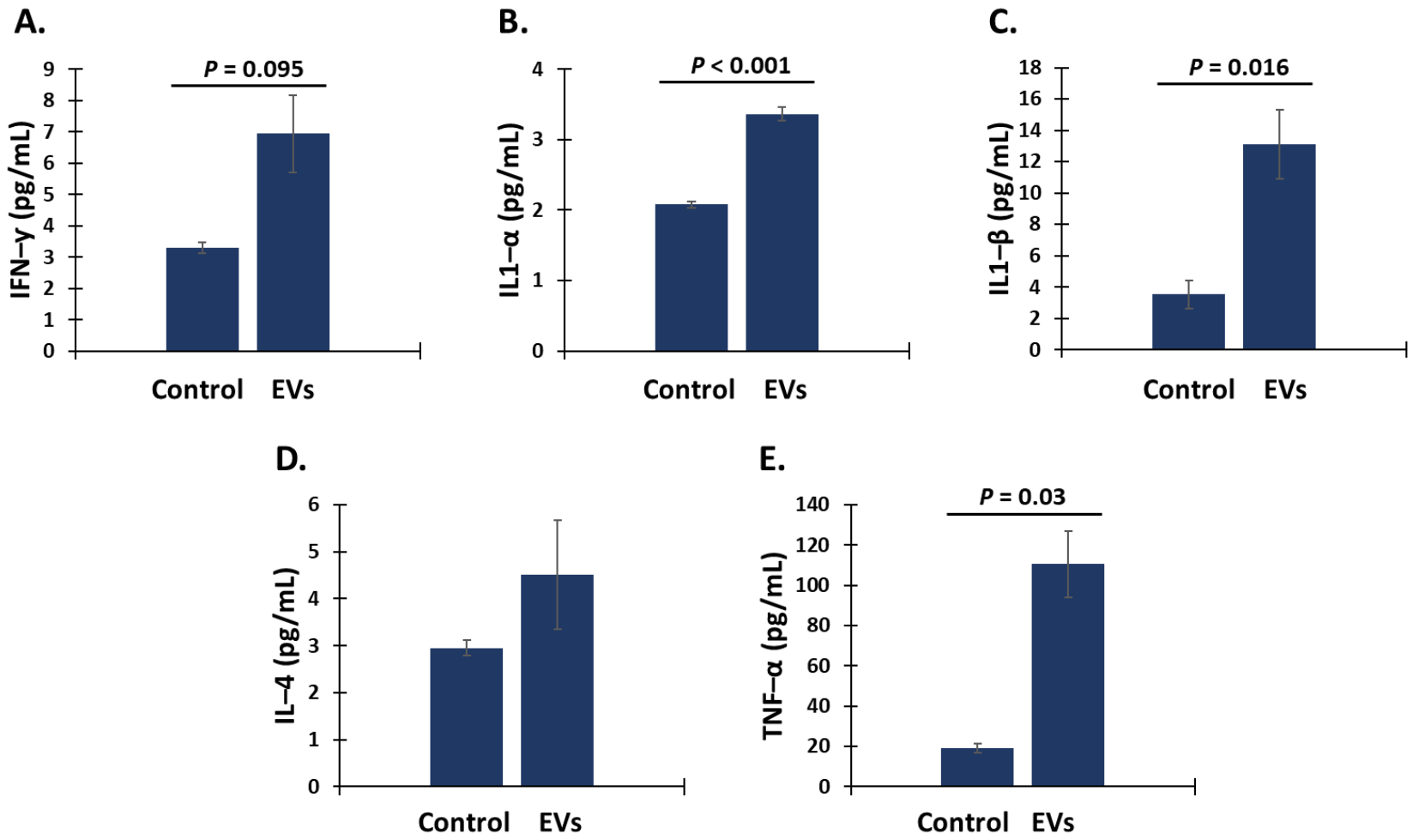

Figure 4.6 Cytokines released by THP–1 macrophages post exposure to PBS control and 40 µg/mL of SEC *A. perfoliata* EV for 24 hours are expressed as mean of calculated concentration pg/mL, error bars represent SEM. The cytokine level from A–E: (A) Interferon–gamma (IFN–γ), (B) Interleukin–1 alpha (IL1–α), (C) Interleukin–1 beta (IL–1β), (D) interleukin–4 (IL–4), (E) Tumour necrosis factor–α (TNF–α). Statistical significance was considered if $P < 0.05$ and statistical trend considered if $P < 0.1$.

4.4. DISCUSSION

I have previously demonstrated key secretory molecules as putative immune modulators in the *A. perfoliata* secretome, and identified 22 putative immune modulatory proteins within EVs which had been purified from the *A. perfoliata* secretome (Chapter 3). EVs from several helminth species have been confirmed to be involved in cell–to–cell communication or in the modulation of the host immunity (Wang *et al.*, 2015, 2020; Zheng *et al.*, 2017; Eichenberger *et al.*, 2018; Liu *et al.*, 2019; Zhou *et al.*, 2019; Murphy *et al.*, 2020; Yang *et al.*, 2021). However, as my work only suggests immune modulatory roles of *A. perfoliata* EVs, based on putative proteins, these functions of *A. perfoliata* EVs need to be investigated. Therefore, in this study, I assessed the immune modulatory functions of *A. perfoliata* SEC purified EVs on THP–1 macrophages *in vitro*, as a mammalian immune cell model. I confirmed that THP–1 macrophages can uptake *A. perfoliata* EVs and uptake reached as much as 97.33% in viable cells after 24 hours of exposure. Furthermore, uptake of the EVs decreased cell viability by 30%, whilst inducing a Th–1 cytokine response via increased secretion of IL1–α, IL1–β and TNF–α from THP–1 macrophages. As such, to my knowledge, I have demonstrated for the first time that *A. perfoliata* derived EVs can be taken up and interact with a mammalian immune cell *in vitro* in an immunomodulatory manner, thus confirming the suggested immunomodulatory function of EVs in Chapter 3.

4.4.1 *A. perfoliata* SEC purified EVs can enter THP–1 macrophages

The red fluorescence signal observed in the cytoplasm of THP–1 macrophages post exposure to PKH26–labelled *A. perfoliata* SEC purified EVs at 6, 12 and 24 hours *in vitro* via both confocal microscopy and flow cytometry analysis, indicates an uptake of *A. perfoliata* EVs by THP–1 macrophages. These data complement others who have demonstrated EV uptake in immune cells such as cestodes: *E. granulosus* and *T. asiatica*; trematodes: *S. mansoni*, *F. hepatica, O. viverrini* and *E. caproni* and nematodes: *H. polygyrus, T. muris, A. suum* and *Nippostrongylus brasiliensis* (Table 4.1). Importantly, EV uptake was relatively comparable across time points for both methods employed with no significant differences observed; albeit the greatest uptake for confocal analysis was at 24 hours post exposure (72.6%) and after 6 hours via flow cytometry analysis (97.3%). Notably, increased uptake for

THP–1 cells as analysed by flow cytometry is likely due to the removal of dead cells during the flow cytometry workflow (See Section 4.4.2). The percentage uptake of EVs within the present study is greater than that previously reported for uptake of *E. granulosus* EVs (a cestode related to *A. perfoliata*) by sheep peripheral blood mononuclear cells (PBMCs) and murine hepatic cells (NCTC1469) (20.3–60%) (Wu *et al.*, 2021; Yang *et al.*, 2021; Table 4.1). Whereas, after 6 hours of EV exposure, uptake of *A. perfoliata* EVs by THP–macrophages via confocal microscopy was lower (67.2%) than uptake of *O. viverrini* EVs by human cholangiocytes (90.6%) as assessed by 3D structured illumination microscopy (Chaiyadet *et al.*, 2015). However, in the current work, EV uptake was higher as assessed by flow cytometry (97.3%). This suggests that, even though uptake was detected during the same time frame, the level of uptake throughout the cell population can be different, possibly depending on the species derived EVs, types of EVs, recipient cells or, very likely, the technique used to assess the uptake depending on cell viability. Thus, further investigation on these factors are required. Similarly, murine hepatic cells exhibited varying uptake levels at 24 hours for three distinct sub populations of *E. granulosus* protoscoleces EVs, which were differentiated by size using centrifugal methods. These subpopulations, namely 2 K, 10 K, and 110 K EVs, demonstrated uptake levels of 20.3%, 36.8%, and 44.5%, respectively (Wu *et al.*, 2021). Although currently, only one type of EV has been characterised in *A. perfoliata* (Chapter 3), the size of EVs in each helminth varies (Table 3.5, Chapter3), implying that EV size influences the rate of uptake by host cells (Wu *et al.*, 2021).

Fluorescently labelled helminth EVs have been demonstrated to be taken up by different cell types such as human umbilical vein endothelial cells, human cholangiocytes, MODE–K cells, bone marrow dendritic cell, rat intestinal epithelial cancer cells and murine hepatic cells (Table 4.1). From the current study, THP–1 cells were used for the uptake of PKH26–labelled *A. perfoliata* EVs revealing an uptake level within the middle of the range for published studies (40–100%; Table 4.1) up to and including 6 hours (67.2%) that were exposed to EVs as assessed by confocal microscopy. This may reflect the choice of host cell, given that THP–1 cells are not derived from a natural host of *A. perfoliata*. Despite some *in vitro* EV uptake studies such as in *E. granulosus* (Wu *et al.*, 2021), *T. asiatica* (Liang *et al.*, 2019), *S. mansoni* (Kuipers *et al.*, 2020), *S. japonicum* (Zhu *et al.*, 2016)*, E. caproni* (Marcilla *et al.*, 2012), *N. brasiliensis* (Eichenberger *et al.*, 2018) and *B. malayi* (Ricciardi *et al.*, 2021) not quantifying

EV uptake within cells, the uptake was confirmed post exposure to EVs at 6 hours or less (Table 4.1). Interestingly, uptake of *S. mansoni* derived EVs (exosome–like vesicles and larger microvesicles) where the same recipient cell was used, THP–1 cells, demonstrated a higher uptake of up to 100% (assessed via confocal microscopy) within 2 hours post exposure to EVs (Kifle *et al.*, 2020). Therefore, earlier time points should also be investigated to elucidate whether *A. perfoilata* EVs can be taken up by THP–1 cells in less than 6 hours of exposure (Table 4.1).

It has been reported that EVs contain biological molecules as a cargo which are likely transferred to recipient cells via uptake (Zamanian *et al.*, 2015; Liu *et al.*, 2019; Meningher *et al.*, 2020). Of interest are key immune modulatory molecules which play an important role in mediation of parasite–host interactions and immune responses (Drurey and Maizels, 2021; Sánchez-López *et al.*, 2021). Accordingly, when *A. perfoliata* secretes EVs into the host environment during infection, EV cargo molecules are likely transported after being taken up by host cells, potentially leading to biological effects within those recipient cells. Following incorporation, EVs containing key immune modulatory proteins may regulate the process of *A. perfoliata* infection within the host. To confirm this hypothesis, the functional impact consequences of *A. perfoliata* EV uptake by mammalian cells, cell viability and cytokine production were further investigated.

Table 4.1 *In vitro* EV uptake studies in cestodes, trematodes and nematodes by recipient cells

Species	Recipient cells	EVs Dye	Technique	Uptake result	References
Echinococcus granulosus **(110 K HF EVs)**	PBMCs	PKH26	confocal microscopy	uptake was detected post 12 and 24 hours at 24 hours: uptake > 40%	Yang *et al.* (2021)
Echinococcus granulosus protoscoleces **(2 K, 10 K & 110 K EVs)**	Murine hepatic cells (NCTC1469)	PKH26	fluorescent microscopy, flow cytometry	uptake was detected post 4 hours, time–dependent manner at 24 hours: 2K (20.3%), 10K (36.8%) and 110K (44.5%)	Wu *et al.* (2021)
Echinococcus granulosus protoscoleces	BMDCs	PKH26	confocal microscopy, flow cytometry	at 30 minutes: uptake > 40%	Nicolao *et al.* (2019)
Taenia asiatica	Colorectal cancer cell lines (LoVo)	PKH67	confocal microscopy	confirmed uptake at 6 hours	Liang *et al.* (2019)
Schistosoma mansoni **(ELVs, MVs)**	HUVECs	PKH–67	confocal microscopy	ELVs at 30 minutes (68%), 1 hour (98%), 2 hours (99.7 %) MVs at 30 minutes (93%), 1 hour (99%), 2 hours (100%)	Kifle *et al.* (2020)
Schistosoma mansoni **(ELVs, MVs)**	THP–1 human monocytes	PKH–67	confocal microscopy	ELVs at 30 minutes (86%), 1 hour (86%), 2 hours (99%) MVs at 30 minutes (92%), 1 hour (95%), 2 hours (100%)	Kifle *et al.* (2020)
Schistosoma mansoni ***(*****6, 3 and 1.5 x10^9 EV/mL*)***	moDCs	PKH26	Confocal microscopy	confirmed uptake by the CD1a+ moDCs post 2 h, at 37°C, dose–dependent manner, no binding/uptake at 4°C uptake did not change with LPS stimulation or in the presence of IL–1β+TNF–α 20 µg/ mL αDC–SIGN/CD209 blocked uptake after 48 h	Kuipers *et al.* (2020)
Schistosoma japonicum	Murine hepatic cells (NCTC1469)	PKH67	fluorescence microscopy	confirmed uptake post 1 hour	Zhu *et al.* (2016)
Schistosoma japonicum **(EV miRNAs)**	Murine macrophage (RAW264.7)	Exo–Glow exosome labeling kit	fluorescent microscopy	confirmed uptake at 4 hours	Liu *et al.* (2019)
Fasciola hepatica **(15 k & 120 k EVs)**	Murine macrophage (RAW264.7)	PKH26	confocal microscopy	confirmed uptake at 6 hours	de la Torre-Escudero *et al.* (2019)
Echinostoma Caproni	Rat intestinal epithelial cancer cells: IEC–18	FM4–64	confocal microscopy	uptake was detected post 30 minutes, 37°C at the cell surface; at 4°C was observed outside cells	Marcilla *et al.* (2012)
Opisthorchis viverrini	Human cholangiocytes (H69)	AF488	3D–SIM	at 30 minutes: uptake 62.44%, at 6 hours: uptake 90.57% uptake was blocked by antibodies to an EV recombinant tetraspanin (TSP)	Chaiyadet *et al.* (2015)

Abbreviation: HF: Hydatid fluid, ELVs: Exosome–like vesicles, MVs: Larger microvesicles, PBMCs: Peripheral blood mononuclear cells, BMDCs: Bone marrow dendritic cells, HUVECs: Human umbilical vein endothelial cells, BMDMs: Bone marrow–derived macrophages, moDCs: Monocyte–derived dendritic cells, FACS: fluorescence–activated cell sorting, 3D–SIM: 3–dimensional structured illumination microscopy.

Table 4.1–Continued 2 *In vitro* EV uptake studies in cestodes, trematodes and nematodes by recipient cells.

Species	Recipient cells	EVs Dye	Technique	Uptake result	References
Heligmosomoides polygyrus	Murine epithelial cell line MODE–K cells	PKH67	confocal microscopy, flow cytometry, FACS	after 1 hour: uptake > 60%	Buck *et al.* (2014)
Heligmosomoides polygyrus **2.5–5 µg EVs per 200,000 cells**	BMDMs MODE–K small intestinal epithelial cell line RAW246.7 macrophage cell line,	PKH67 CellVue Claret dye	confocal microscopy, flow cytometry,	uptake steadily increased over 24 hr in all cells after 1 hour: RAW264.7 & BMDMs uptake 14–23%, epithelial cells 10% after 24 hours: RAW264.7 & BMDMs uptake 97–98%, MODE–K 55% Cytochalasin D blocked EV uptake at 1 and 24 hr post–incubation, with 1% & 8% of cells PKH67+ LPS pre–treatment repressed uptake: after 1 hour: BMDMs (4%), naive BMDMs (17%), IL–4/IL–13 BMDMs (21%) after 24 hours: BMDMs (60%), naive BMDMs (90%), IL–4/IL–13 BMDMs (82%)	Coakley *et al.* (2017)
Nippostrongylus brasiliensis	Murine Small Intestinal Organoids	PKH26	confocal microscopy	confirmed uptake post 3 hours	Eichenberger *et al.* (2018a)
Trichuris muris **(exosome–like EVs)**	Murine colonic organoids	PKH26	confocal microscopy	uptake was detected post 30 minutes, at 37°C: epithelial organoid cells (% CTF 4.04), central lumen (0.59)	Eichenberger *et al.* (2018b)
Ascaris suum **(exosome–like EVs)**	Canine enteroids	PKH67	confocal microscopy	uptake through the epithelial cells and into the enteroid lumen within 24 h	Chandra *et al.* (2019)
Brugia malayi	Murine macrophages	PKH67	Confocal microscopy	at 6 hours: uptake 40–50% to some degree uptake 10% at markedly higher levels	Zamanian *et al.* (2015)
Brugia malayi **microfilarial (mf) stage (exosome–like EVs)**	THP–1 cells PKH26 –labelled Human moDCs	Exo–Red dye PKH67	confocal microscopy, flow cytometry	THP–1 cells; uptake were detected within 10 minutes, signal increased at 1–24 hours moDCs: some mf–derived EV products diffused throughout the cytoplasm with some appearing in the nucleus of the dendritic cell	Ricciardi *et al.* (2021)

Abbreviation: HF: Hydatid fluid, ELVs: Exosome–like vesicles, MVs: Larger microvesicles, PBMCs: Peripheral blood mononuclear cells, BMDCs: Bone marrow dendritic cells, HUVECs: Human umbilical vein endothelial cells, BMDMs: Bone marrow–derived macrophages, moDCs: Monocyte–derived dendritic cells, FACS: fluorescence–activated cell sorting, 3D–SIM: 3–dimensional structured illumination microscopy.

4.4.2 Host cell viability is decreased following exposure to *A. perfoliata* EVs.

To date, little evidence has been reported as to the effect of EVs derived from parasites and protozoa on host cell viability using the trypan blue, MTT assay and flow cytometry (de Souza Gonçalves *et al.*, 2018; Ofir-Birin *et al.*, 2018; Retana Moreira *et al.*, 2019). A previous study in *A. perfoliata* studied the impact of *A. perfoliata* ESP on cell proliferation and viability of human T-cell line Jurkat J6 cells over 72 hours *in vitro* (Lawson et al., 2019). MTT assay demonstrated that *A. perfoliata* ESP inhibited the growth of the human T-cell line Jurkat. Moreover, annexin binding and 7–AAD assay, via flow cytometry, demonstrated that *A. perfoliata ESP* induced cell death as a result of cell membrane permeability loss. It is known that EVs derived from helminths are a component of ESP, therefore, I expected that *A. perfoliata* EVs would be able to exhibit a similar effect on THP–1 macrophages as that demonstrated by *A. perfoliata* ESP (Lawson et al., 2019).

From my findings, uptake of *A. perfoliata* EVs by THP–1 macrophages caused a significant reduction in viability of THP–1 macrophages, as assessed by trypan blue and MTT assays at 24 hours and flow cytometry at 12 hours. Notably, the lower percentage of EV uptake in confocal analysis is likely explained by the selectivity of flow cytometry for live cells. We observed 20–30% non–viable cells using flow cytometry, trypan blue, and MTT assays, which better explains the resulting uptake of EVs within the confocal analysis of 60–70%. Herein, I show that *A. perfoliata* EVs at 40 mg/mL can reduce THP–1 cell viability following EV uptake. These findings were similar to those in *A. perfoliata* ESP (Lawson *et al.*, 2019) and EVs of tissue–culture cell–derived trypomastigotes of the *Trypanosoma cruzi* (Pan4 strain). For the *T. cruzi* analysis, cell viability in Vero cells and HL–1 cardiomyocyte cells *in vitro* decreased likely through changes in cell permeability during or after the EV–cell interaction after 24 hours (Retana Moreira *et al.*, 2019). It is implied that interaction between *A. perfoliata* EVs and THP–1 macrophages was established, in which *A. perfoliata* EVs may participate in the permeabilization mechanism of host cells, allowing other molecules to enter the cells and cause further cell damage (Retana Moreira *et al.*, 2019). Interestingly, *Plasmodium falciparum* infected RBC–derived EVs did not effect cell growth of THP–1 cells after 72 hours post EV uptake (Ofir-Birin *et al.*, 2018).

Therefore, my findings warrant further research in a broader range of EV roles in modulating host cell viability, such as to confirm a level of lethality to EV uptake, or to determine if EV uptake is a passive process, evaluate EV–host cell co–culture at 4°C, or an active process, evaluate EV–host cell co–culture at 37°C. Furthermore, additional studies on other responses and cell health in culture are needed to determine whether *A. perfoliata* EVs have an impact on cell proliferation and cell permeability, as demonstrated in other platyhelminths. For example, EVs derived from *E. granulosus* protoscoleces have immunosuppressive effects by inhibiting the proliferation of murine T lymphocyte, CD4+ T cells, and CD8+ T cells in a dose–dependent manner after 72 hours of co–culture (Zhou *et al.*, 2019). Whereas, EVs derived from *O. viverrini* promoted human cholangiocytes cell proliferation at 72 hours (Chaiyadet *et al.*, 2015).

4.4.3 *A. perfoliata* EVs instigate a cytokine response from THP–1 macrophages

Following uptake of *A. perfoliata* SEC purified EVs by THP–1 macrophages, cytokine secretion from EV exposed cells was examined. Even though the EVs appeared to be killing THP–1 machrophages and so there were less cells available, those remaining THP–1 machrophages were still able to produce and increase the quantity of key cytokines when exposed to EVs compared to the control, demonstrating clear immunomodulatory effects of *A. perfoliata* EVs.

I quantified a total of 6 cytokines secreted by Th1 cells as pro–inflammatory cytokines including TNF–α, IL1–α, IL1–β, and IFN–γ; and Th2 cells as anti–inflammatory cytokines including IL–4 and IL–5. In total, secretion of 3 of the examined cytokines, IL1–α, IL1–β and TNF–α, were significantly increased ($P < 0.05$) compared to the control, whilst, IFN–γ tended to increase post exposure to *A. perfoliata* EVs 24 hours *in vitro* ($P < 0.1$). Conversely, secretion of IL–4 was not significantly altered post exposure to EVs, compared to the control ($P > 0.05$). IL–5 was secreted at a very low level in all samples and so was not analysed further. The increase in IL1–α, IL1–β and TNF–α after exposure to *A. perfoliata* EVs correlates well with the predominant expression of inflammatory cytokines secreted normally during macrophage stimulation; namely TNF–α, IL–1, IL–6, IL–8, and IL–12 (Duque and Descoteaux, 2014; Rolot and Dewals, 2018). As such, this study demonstrates that *A. perfoliata* EVs exert

immunomodulatory properties through modulating cytokine production by THP–macrophages.

It has been shown that the expression of key cytokines from my findings were similar, however also contrast to some cytokines expression from previous reports in cestodes, trematodes and nematodes (Table 4.2). For example, an increased production of IFN–γ by THP–1 macrophages post exposure to *A. perfoliata* EVs *in vitro* contrasts findings in an *in vitro* study whereby IFN–γ was inhibited in murine PBMCs exposed to a high dose (24 µg) of *E. granulosus* protoscoleces EVs (Zhou *et al.*, 2019), RAW264.7 macrophages exposed to *Taenia pisiformis* EVs (Wang *et al.*, 2020) and mice induced with *N. brasiliensis* EVs (Eichenberger *et al.*, 2018a). IFN–γ is a predominant pro–inflammatory cytokine in the Th1 response, playing a critical role in the control of intracellular pathogens, including protozoan parasitic infections, during acute infection (Kak *et al.*, 2018). Therefore, it is possible that EVs may function similarly to intracellular pathogens by stimulating the production of IFN–γ. It is suggested that the increase of IFN–γ within THP–macrophages likely represents an early response, inducing Th1–type immune activity against the interaction of *A. perfoliata* EVs with THP–macrophages. It is likely that *A. perfoliata* EV proteins, either within the EV or present on the surface, may bind to pattern recognition receptors, such as TLR2 or 4, as has been demonstrated for other parasites (Han *et al.*, 2019; Murphy *et al.*, 2020) leading to the eventual secretion of IFN–γ through cascade signalling. Alternative parasite systems that do not secrete IFN–γ may not activate host cells in the same manner, as the EV contents derived from these parasites are likely to be significantly different from those derived from *A. perfoliata*.

TNF–α, IL–1α and IL–1β are pro–inflammatory cytokines. *S. japonicum* EVs have been demonstrated to induce RAW264.7 cell proliferation and elevate TNF–α level to contribute to schistosome survival (Liu *et al.*, 2019). Moreover, TNF–α, IL–1α and IL–1β have been reported to play a critical role in the mucosal Th2 responses and a protective role in chronic infection during, *Trichuris muris* infections (Artis *et al.*, 1999; Helmby and Grencis, 2004). TNF–α secretion was significantly increased after *A. perfoliata* EV stimulation matching the findings for sheep PBMCs that were exposed to *E. granulosus*, 110 K hydatid fluid (HF) EVs *in vitro* (Yang *et al.*, 2021), RAW264.7 cells exposed to *S. japonicum* EVs at 5– 40 ng/µL (Wang *et al.*, 2015) and mice injected with 10 µg/mL *F. hepatica* EVs stimulated BMDCs (Murphy *et al.*, 2020), although this was in contrast to murine PBMCs exposed to a high dose of *E. granulosus*

protoscoleces EVs (Zhou *et al.*, 2019). From my findings, IL–1α and IL–1β were also significant increased post exposure to *A. perfoliata* EVs, which is in contrast to another *in vitro* study in *E. multilocularis*, where metacestodes EVs suppressed IL–1α and IL–1β secretion from murine RAW264.7 cells (Zheng *et al.*, 2017) and IL–1β following *E. granulosus* 110K HF EVs which suppressed IL–1 β secretion from Sheep PBMCs cells (Yang *et al.*, 2021). As TNF–α, IL–1α and IL–1β levels were increased in the current study, it is suggested that *A. perfoliata* EVs primarily drive Th1–type immune activity of THP–1 macrophages, contributing to the survival of the parasite within the host (Wang *et al.*, 2015; Liu *et al.*, 2019). Once the interaction establishes, they may be important components in the development and regulation of Th2–cytokine–mediated responses, particularly at mucosal sites during infection, which is important for worm expulsion, as demonstrated in nematodes (Artis *et al.*, 1999; Helmby and Grencis, 2004).

Despite both *A. perfoliata* and *Echinococcus* species being closely related cestodes, it is clear that the underlying immune responses directed by EVs are different from one another. However, the differences in cytokine expression may be influenced by using different recipient cells or varying dosages of EVs (Zhou *et al.*, 2019; Yang *et al.*, 2021). In an *A. perfoliata* investigation, Lawson et al. (2019) demonstrated that in the early stages of a natural infection, there were moderate changes to Th2 cytokines and high levels of TGF–β transcripts in the mucosa close to the attachment site, compared to both the attachment site and the non–infected controls. Whereas in the late stage of infection, transcripts encoding Th2 cytokines, IL–4 and IL–13, and the Th1 cytokine IFN–γ were all significantly reduced at the attachment site and close to the attachment site compared to the non–infected controls. However, in the late stage of infection, regulatory cytokines, IL–10 and TGF–β, and transcription factor, FOXP3, at the tissue adjacent to parasite attachment site were increased compared to the attachment site and the non–infected controls. Yet at the parasite attachment site, it was demonstrated that there was an active inflammatory response, through a decrease in anti–inflammatory IL–10 but an increase of pro–inflammatory IL–1 and IL–6. These results mostly contrast with my study on both natural infection and *A. perfoliata* ESP, which suppress Th1/Th2 cytokines and downregulate cytokine transcription, with the exception of the increase in IL-1, which directly relates to my study. In comparison to the current study, I observed the immunomodulatory properties of *A perfoliata* EVs alone at specific exposure timepoints *in vitro*. Due to the complex interaction from naturally *A.*

perfoliata infection in horses as well as an *in vitro* exposure to *A. perfoliata* ESP containing wide range of biomolecules interacting with the EVs, different responses may occur.

IL–4 has a key role in host defence from parasite invasion in nematodes (Urban *et al.*, 1991; Urban Jr. *et al.*, 1995; Finkelman *et al.*, 1997). However, IL–4 levels were not significantly increased post exposure to *A. perfoliata* EVs at 40 mg/mL for 24 hours in the present study. Future work should investigate longer exposure times to EVs, such as 36 to 72 hours, which may demonstrate alternative responses through IL–4 secretion.

The present study suggests that *A. perfoliata* EVs may interact with host cells in generating Th1 responses, given the range of cytokines expressed in the current work in comparison to alternative helminth studies (Table 4.2). Thereby, *A. perfoliata* EVs primarily elicits the Th1–mediated immunity response of THP–1 macrophages as a host cells to infection, characterised by a significant increase of type 1 cytokines; IL1–α, IL1–β, TNF–α and tendency to increase IFN–γ post EV exposure for 24 hours *in vitro*. Following IL1–α, IL1–β, TNF–α induction it is likely that Th–2 mediated immunity response generates at a later stage of infection. However, cytokines quantified in the current study were limited in number, thus may not certify the total effect of *A. perfoliata* EVs, which is likely to be much more complex. THP–1 macrophages may require a longer exposure time to be exposed to *A. perfoliata* EVs in order to elicit Th2–mediated immune responses, likewise *A. perfoliata* may also mediate THP–1 macrophages to prolong Th2–immune responses within THP–1 macrophages. Thus, more examination of the full repertoire of cytokines such as IL–2, IL–6, IL–10, IL–12, IL–13 and IL–17 as well as the wider transcriptome changes are required for further study. Moreover, the role of *A. perfoliata* EVs on both type 1 and 2 immune responses remains to be further elucidated yet this work has driven my understanding of EV immune interaction.

Table 4.2 *In vitro* effect of cestodes, trematodes and nematodes derived–EVs on the expression of cytokines of recipient cells**.**

Species	Cell type	Method	Effect	References
Echinococcus granulosus **(110K HF EVs)**	Sheep PBMCs	ELISA	Upregulated IL–10, IRF5 and TNF–α Downregulated IL–1β, IL–17, and CD14 Unchanged IL–6	Yang *et al.* (2021)
Echinococcus granulosus **protoscoleces**	Murine PBMCs	Cytometric Bead Array Mouse Th1/Th2/Th17 Cytokine Kit	After 3 days, inhibit the proliferation of murine lymphocyte, CD4+ T cells, and CD8+ T cells in a dose–dependent manner Low dose 6 μg: promote IL–2 and IL–4; inhibit IL–10 High dose 24 μg: promote IL–4; inhibit IL–6, IL–17A, TNF and IFN–γ	Zhou *et al.* (2019)
Echinococcus granulosus **protoscoleces**	CF–1 mice BMDCs	Flow cytometry	Approximately 70–90% of the cells were CD11c+ Increase in CD86 and with down–regulation of the expression of MHC–II molecules	Nicolao *et al.* (2019)
Echinococcus multilocularis **metacestodes**	Murine RAW264.7 macrophages	qPCR, sELISA	Suppression of NO production via downregulation of iNOS by 0.86–fold Suppression of IL–1α and IL–1β by 0.56– and 0.68–fold IL–6, IL–4 and IL–10 were still stably expressed	Zheng *et al.* (2017)
Taenia pisiformis **Cysticercus (50 μg/mL EVs)**	RAW264.7 macrophages	qPCR, ELISA	Induced the macrophages polarization toward the M2 phenotype & produced a Th2–type immune response. Significantly increased Arg–1, IL–4, IL–6, IL–10 and IL–13 in EVs treated cells Significantly decreased iNOS, IFN–γ and IL–12 in EVs treated cells	Wang *et al.* (2020)
Opisthorchis viverrini	human cholangiocytes (H69)	ELISA	Stimulated IL–6	Chaiyadet *et al.* (2015)
Schistosoma mansoni	moDCs	ELISA	Increased IL–6, IL–10 and IL–12	Kuipers *et al.* (2020)
Schistosoma japonicum	RAW264.7 cell line	ELISA	significantly increased iNOS expression, TNF–α secretion Arg–1 and IL–12 had no significant change IL–10, and IL–13 expression was not reliably detected	Wang *et al.* (2015)
Trichinella spiralis **(muscle larvae EVs 2.5, 1 & 0.25 μg/mL)** **ES L1 (50 μg/mL)**	PBMCs	LEGENDPlex Human Th Cytokine Panel	EVs concentration of 2.5 μg/mL increased IL–6, IL–10 Decreased IL17a incubated with ES L1 and EVs	Kosanović *et al.* (2019)

Abbreviation: HF: Hydatid Fluid, PBMCs: Peripheral blood mononuclear cells, BMDCs: Bone Marrow–derived Dendritic Cells, moDCs: Human monocyte–derived dendritic cells, sELISA: sandwich enzyme–linked immunosorbent assay, NO: nitric oxide, iNOS: inducible nitric oxide synthase, IRF–5: Interferon regulatory factor 5, CD: cluster of differentiation, MHC: major histocompatibility complex molecules.

4.4.4 Study limitations

In the current study, PBS was utilised as a negative control group across all experiments, as PBS solution was used in the isolation of EVs. PBS is considered as non–immunostimulatory because it does not contain any immunogenic components that could activate the immune system (Wang *et al.*, 2015). Importantly, the PBS solution used was a calcium and magnesium–free formulation. Previous research has shown that PBS containing calcium and magnesium can elicit short–term responses in chemokine IL–8 secretion, such as, by human PBMCs within 30 minutes to 24 hours post–incubation (Lichtenauer *et al.*, 2011). Furthermore, it is not advisable to use PBS for resuspending cell samples before assessing cell viability with automated cell counters, as it may lead to reduced cell viability and increased variability (Chen *et al.*, 2017). In my study, cell dissociation buffer was employed for both lifting and resuspending cells. Consequently, there was no adverse impact of PBS on my research. However, to ensure the highest quality of results, it is recommended to include a negative control comprising untreated THP-1 cells. The untreated THP–1 cells control serves to eliminate non–specific responses and ensure that any observed specific cytokine responses from THP–1 cells to *A. perfoliata* EVs stimulation are not influenced by contamination or experimental artifacts. Additionally, it is crucial to incorporate a positive control to assess the functionality of the immune response and validate the precision of cytokine measurement methods. Consequently, a well–recognised immunostimulant, lipopolysaccharide (LPS) is recommend to introduce as a positive control (Schildberger *et al.*, 2013).

4.5 CONCLUSIONS

In this chapter, I have for the first time confirmed that *A. perfoliata* EVs are able to be labelled with the lipid dye PKH26 and are subsequently taken up by THP–1 macrophages *in vitro*, demonstrating the potential role of EVs in the parasite–host interaction and communication. I have also first revealed that *A. perfoliata* EVs have the potential to modulate the host immune response by decreasing cell viability after exposure to *A. perfoliata* EVs by 30%. Furthermore, *A. perfoliata* EVs modulate the host immune response *in vitro* to increase secretion of key cytokines (IL1–α, IL1–β, TNF–α and IFN–γ) as primarily a Th1–driven immune response.

However, the complete function of *A. perfoliata* EVs remains to be fully defined. Therefore, the transcription level of key cytokine gene expression, greater cytokine investigation and RNA sequencing analysis post exposure to *A. perfoliata* EVs should be further performed. Moreover, to understand their functional role in the pathogenesis or host–parasite interactions, the unique immune modulatory proteins expressed in *A. perfoliata* EVs should be further investigated. This knowledge will provide an insight into immunomodulatory properties for *A. perfoliata* EVs which is useful to extend a development of diagnostic tools as well as parasite control.

CHAPTER 5:

THE IMPACT OF PRAZIQUANTEL ON THE EQUINE MICROBIOME USING AN *IN VITRO* HINDGUT MICROBIAL FERMENTATION MODEL

5.1 INTRODUCTION

5.1.1 Hindgut microbiome in equine nutrition and health

Horses are hindgut fermenters, with microbes within the hindgut playing an important role in driving the fermentation processes of fibrous digesta that is not fully digested and absorbed prior to the hindgut, thus providing nutrients and energy to the host and maintaining intestinal homeostasis (Costa and Weese, 2012). Volatile fatty acids (VFAs) are the core end products of metabolism by microbial fermentation in the hindgut, which are used by the horse as an energy source (Argenzio *et al.*, 1974; Bergman, 1990). These VFAs include the short–chain fatty acids (SCFAs) acetic, butyric and propionic acid and account for approximately 30% of the horse's maintenance energy (Glinsky *et al.*, 1976). Even though microbes support the maintenance of intestinal homeostasis, it is common for the microbial community in the hindgut of horses to experience dysregulation or changes (Dougal *et al.*, 2013; Ericsson *et al.*, 2016; Edwards *et al.*, 2020). This can be attributed to a limited number of species within the core microbial population (Dougal *et al.*, 2013; Ericsson *et al.*, 2016; Edwards *et al.*, 2020). Therefore, the equine hindgut microbiome can be influenced by a variety of factors whether it be horse–related or environment–related factors (Garber *et al.*, 2020; Theelen *et al.*, 2021; Chaucheyras-Durand *et al.*, 2022).

Alterations to the equine hindgut microbiome are likely to impact on equine hindgut nutritional health, as well as metabolic diseases or disorders, such as colic and laminitis (Milinovich *et al.*, 2008; Costa *et al.*, 2012; Steelman *et al.*, 2012; Moreau *et al.*, 2014; Stewart *et al.*, 2019; T. Park, Cheong, *et al.*, 2021; Tuniyazi *et al.*, 2021). An increasing awareness that medication, such as antibiotics (Costa *et al.*, 2015; Arnold *et al.*, 2020; Collinet *et al.*, 2021; Liepman *et al.*, 2022) and anthelmintics (Rowe, 2017; Crotch-Harvey *et al.*, 2018; Peachey *et al.*, 2018, 2019; Kunz *et al.*, 2019; Walshe *et al.*, 2019, 2021; Daniels *et al.*, 2020; Dini. Hu *et al.*, 2021; Boisseau *et al.*, 2022) may also alter the unstable microbiome of the horse. Anthelmintics that target gastrointestinal parasites of the hindgut may have further consequences, as their action is targeted in the region of this essential hindgut microbiome.

5.1.2 Praziquantel mechanism of action and impact on the equine hindgut microbiome

PZQ has been widely employed for the treatment and control of human schistosomiasis, trematodes and cestodes (Chai, 2013). The mechanism of action is primarily achieved by disrupting their outer integument layer through the regulation of calcium homeostasis, resulting in severe muscle spasms and paralysis (Pica-Mattoccia *et al.*, 2008; Thomas and Timson, 2020; Park *et al.*, 2021; Nogueira *et al.*, 2022). When worms are exposed to PZQ, the cell membrane permeability to calcium is immediately changed, leading to a rapid influx of calcium within the worms (Pica-Mattoccia *et al.*, 2008; Park *et al.*, 2021). This increase in calcium triggers spasmodic contractions of the worms' muscles and rapid vacuolisation of the worm surface (Pica-Mattoccia *et al.*, 2008; Park *et al.*, 2021). At present, the molecular mechanism of action of the PZQ remains poorly understood. Therefore, molecular mechanisms have been extensively researched (Nogueira *et al.*, 2022), including PZQ's induction of changes in the operation of voltage–gated calcium channels (VOCC) through the modulation of a distinct channel β subunit in Schistosoma (Kohn *et al.*, 2003; Chen *et al.*, 2004; Greenberg, 2005; Nogi *et al.*, 2009), its activation of a calcium–sensitive transient receptor potential (TRP) channel (Park *et al.*, 2019) and transient receptor potential melastatin ion channel ($TRPM_{PZQ}$) (Park *et al.*, 2021). However, there is no direct evidence regarding the molecular mechanism by which PZQ affects *A. perfoliata* infection. Since PZQ is effective against both trematodes and cestodes (Chai, 2013), it is likely that PZQ has a similar mechanism of action in *A. perfoliata*.

As the treatment and control of *A. perfoliata* is targeted within the caecal environment (Grubbs *et al.*, 2003; Barrett *et al.*, 2004; Slocombe, 2006; Lyons *et al.*, 2017) it is important to understand the effect of the drug on the microbial environment within the caecum. In relation to the impact of PZQ on the GIT microbiome, studies involving PZQ treatment for *S. mansoni* (Schneeberger *et al.*, 2018), *Schistosoma haematobium* (Kay *et al.*, 2015; Ajibola *et al.*, 2023), *Opisthorchis felineus* infection (Sokolova *et al.*, 2021) in children did not demonstrated a significant alteration in the overall taxonomic profiling and diversity of the GIT microbiome. Consequently, it is plausible that PZQ treatment for *A. perfoliata* in horses may not significantly affect the equine GIT microbiome. However, both *A. perfoliata* and PZQ represent a substantial threat to the fragile equine GIT microbiome. Limited understanding of *A. perfoliata* and the host–parasite interaction will likely compromise continued

sustainable control. There is evidence in horses that the presence of intestinal helminths (Clark *et al.*, 2018; Peachey *et al.*, 2018, 2019; Walshe *et al.*, 2019, 2021; Slater *et al.*, 2021) and anthelmintic treatments (Rowe, 2017; Peachey *et al.*, 2018; Kunz *et al.*, 2019; Walshe *et al.*, 2019) can alter the equine hindgut microbiome bacterial richness, diversity or functionality. When considering anthelmintic treatments for *A. perfoliata* in horses, the utilisation of a combined formulation of PZQ and moxidectin yielded no substantial alterations in the overall microbiota population or composition (Kunz *et al.*, 2019). Nevertheless, an observed modification in the alpha diversity of the faecal microbiota suggested a potential individual impact within the horse's hindgut. It is noteworthy that this effect could not be quantified in a live animal study (Kunz *et al.*, 2019). At present, the exposure of PZQ alone and the effect that this has on the equine hindgut microbiome has been neglected. *In vitro* fermentation models have been commonly utilised as a model of hindgut fermentation for horses (Murray *et al.*, 2012, 2014; Biddle *et al.*, 2013; Elghandour *et al.*, 2016; de la Fuente *et al.*, 2017; Leng *et al.*, 2019; Daniels *et al.*, 2020; Kujawa *et al.*, 2020; Gandarillas *et al.*, 2021; MacNicol *et al.*, 2022). The use of equine faeces as a microbial inoculum has been validated by Lowman *et al.* (1999) and avoids the need for collection of caecal matter. Therefore, in the current study, *in vitro* fermentation models are a useful and non–invasive tool to investigate the impact of PZQ on the equine GIT microbiome.

5.1.3 AIMS AND OBJECTIVES

This chapter aimed to investigate if PZQ causes changes in the functionality of the equine hindgut microbiome, based on microbial fermentation activities and products associated with microbial fermentation. To achieve this aim, an *in vitro* hindgut fermentation model was exposed to PZQ at three dosage levels, related to doses recommended *in vivo* (low dose 0.03 mmol/L, recommended dose 0.08 mmol/L, and high dose 0.13 mmol/L). Hindgut fermentation kinetics, as well as fermentation products and metabolites were monitored. The kinetics of a gas production profile over a 72–hour fermentation period were analysed using the exponential model of Ørskov and McDonald (1979). pH, VFA production, ammonia and lactate were all determined and supported by metabolome fingerprinting to give an indication if there were likely changes in the microbiome.

It was hypothesised that microbiome fermentation activities in the equine hindgut based on microbial activities and fermentation products would be altered after exposure to PZQ at dosage levels of a low dose 0.03 mmol/L, a recommended dose 0.08 mmol/L, and a high dose 0.13 mmol/L.

5.2. MATERIALS AND METHODS

5.2.1 *In vitro* hindgut microbial fermentation model

5.2.1.1 Animals

All research was approved by the Animal Welfare and Ethical Review Board at Aberystwyth University. Five healthy adult horses at the Lluest Equine Centre, Llanbadarn Campus, Aberystwyth University were used in this study to provide a faecal inoculum for the hindgut fermentation model. Horses were varied in breed, age (mean ± SD of 17 ± 2.4 years) and sex (3 geldings and 2 mares), with a mean body weight (BW; mean ± SD) of 679.6 ± 114.9 kg. All horses were individually stabled, and their exercise routines were consistent (exercised daily for a maximum of 1 hour ridden and horse walker in the morning). They were fed a meadow hay diet (as–fed basis of 2% dry matter intake based on ideal BW) twice daily (provided at 08:00 and 16:00 h) and had free access to water. They received a parasite control programme at least one month prior to the experiment, of Equest Pramox oral gel for nematodes, cestodes or arthropod infections and Fasinex™ oral drench for liver fluke infection (fascioliasis), according to a faecal egg count result.

5.2.1.2 Faecal Sampling and microbial inoculum preparation

Freshly voided faeces (from horses in section 5.2.1.1, n=5) were used as a faecal inoculum for *in vitro* hindgut fermentation studies. Faecal samples were collected in the morning, immediately following defecation. All samples were collected from the centre of the faecal mass and approximately 1.2 kg of faeces per horse were transferred into a pre–warmed vacuum insulated flask. All flasks containing fresh faecal contents were subsequently transported to the laboratory within 1 hour of collection and kept warm for preparation of the inoculum.

A modified Van Soest culture medium (fermentation buffer) was made by homogenising the equine faecal samples in the incubation buffer (containing 50% (v/v) distilled water, 0.2 g/L trypticase peptone, 0.1% (v/v) micromineral solution, 20% (v/v) buffer solution, 20% (v/v) micromineral solution, 1% (v/v) resazurin solution and 4% (v/v) reducing solution) at 1:2 w/v ratio, in a blender, for 1 minute. The homogenised suspension was strained through 4 layers of muslin and the liquid subsequently transferred to a pre–gassed conical flask

with CO_2 on a heat plate at 39 °C. Gassing was continued whilst setting up the experiment to maintain an anaerobic environment for the modified Van Soest culture medium.

5.2.1.3 Substrates

Meadow hay and barley (Castle Horse Feeds, Hereford, UK) were used as a fermentation substrate for *in vitro* hindgut microbial fermentation (de la Fuente *et al.*, 2017). To prepare these substrates, both feedstuffs were oven–dried separately at 60 °C for 24 hours followed by grinding through a 1 mm Wiley mill screen grinder (Hammer Mill, Christy Norris, Ipswich, UK), to mimic mechanical digestion. Dried, ground hay and barley were mixed by weight at a 70:30 ratio and were subsequently subjected to a pre–caecal digestion process by pepsin and pancreatin treatment to mimic digestion in the stomach and small intestine, following Calsamiglia and Stern (1995). Briefly, 10 g of mixed substrates were weighed into 50 μm^2 Dacron bags. All bags were submerged in a solution of 2 g/L pepsin (Thermo Scientific, Loughborough, UK) in 0.075 M HCl (Thermo Scientific, Loughborough, UK), at 38 °C for 30 minutes, followed by rinsing in clean flowing water for 10 minutes. Subsequently, bags were submerged in a solution of 0.1% pancreatin (Origin: porcine pancreas; Sigma–Aldrich, Merck Life Science, Germany) in distilled water (pH=8), at 38 °C for 60 minutes, and rinsed in clean flowing water for 10 minutes. Finally, pre–caecal digested substrate bags were dried overnight at 60 °C, reweighed and stored in an airtight container prior to the experiment.

5.2.1.4 Praziquantel preparation

The PZQ (Sigma–Aldrich, Merck Life Science, Germany) concentration was determined based on the average adult horse BW at 500 kg, relative to an average volume of a caecum of 30 L (de Boom, 1975). Three different PZQ dosages were chosen to be used, based on the recommended dose rate of 1.5 mg/kg BW for a 500 kg horse by Equimax Oral Gel (Active ingredient: ivermectin (200 µg/kg) and PZQ (1.5 mg/kg); Virbac Ltd., Bury St. Edmunds, UK) from the NOAH Compendium of Data Sheets for Animal Medicines (https://www.noahcompendium.co.uk/) and related to concentrations of wormer provided to the 30 L caecum. A lower and higher dose rate than the recommended dose were chosen, based on literature on the effective reduction of *A. perfoliata* eggs after a single oral administration dose at 0.5, 1.5 and 2.5 mg/kg BW, respectively (Grubbs *et al.*, 2003; Barrett *et al.*, 2004; Slocombe, 2006; Lyons *et al.*, 2017). Thus, when the average 30 L volume of a

caecum was related to the 30 mL volume of the fermentation vessels used in the experiment, the following PZQ treatment groups were used; control 0.00 mmol/L, low dose 0.03 mmol/L, recommended dose 0.08 mmol/L, and high dose 0.13 mmol/L.

A PZQ stock solution of 130 mmol/L was prepared by dissolving 1 g of PZQ in 24.622 mL of dimethyl sulfoxide (DMSO; MP Biomedicals, California, USA). The PZQ–DMSO stock solution (130 mmol/L) was further diluted within fermentation vessels to obtain the relevant volume according to PZQ concentrations at low dose (0.03 mmol/L), recommended dose (0.08 mmol/L) and high dose (0.13 mmol/l) maintaining DMSO at a final concentration of 0.1%. DMSO was used in the control vessels to match the final concentration of DMSO included in the PZQ vessels (0.1%).

5.2.1.5 *In vitro* hindgut microbial fermentation experimental design

An *in vitro* hindgut microbial fermentation experiment was employed following the *in vitro* gas production technique (Theodorou *et al.*, 1994), with modifications as described in Murray *et al.* (2012&2014) and Daniels *et al.* (2020). Briefly, 120 mL Wheaton bottles (Thermo Scientific, Loughborough, UK) were used as the fermentation vessels. Each PZQ treatment assigned in section 5.2.1.4 was run in 5 replicates, with and without substrate (blank), resulting in a total number of 40 fermentation vessels being used per horse (Figure 5.1).

In each substrate fermentation vessel, 0.3 g of pre–caecal digested substrate (section 5.2.1.3) was added, and no substrate in the blank fermentation vessel (Figure 5.1); relevant concentrations of PZQ at 0.03 mmol/L, 0.08 mmol/L, and 0.13 mmol/L or the control (0 mmol/L PZQ, DMSO at 0.1% v/v) were also included (Figure 5.1). A total of 30 mL modified Van Soest culture medium, including the faecal inoculum (Section 5.2.1.2) was then added to each fermentation vessel using an automatic peristaltic pump dispenser (Perimatic GP II, Jencons Scientific Ltd, UK), whilst gassing with CO_2 (both substrate and blank vessels). Fermentation vessels were sealed using a rubber stopper with an aluminium crimp seal followed by releasing gas using a 23–gauge needle, before incubation at 39 °C. The beginning of incubation was set as time point 0 hours and the vessels were incubated for a total of 72 hours. Headspace gas pressure was measured at 2, 4, 6, 8, 12, 24, 48, and 72 hours using a Tracker 220 Pressure transducer (Data Track Process Instruments, Christchurch, UK),

according to the transducer technique of Theodorou *et al.* (1994) to assess microbial fermentation parameters.

At 24 and 72 hours post–fermentation, one fermentation vessel per treatment was sacrificed (both substrate and blank) and stored at –20°C until further analysis of bacterial fermentation metabolite products including VFAs, ammonia and lactate concentrations, as well as the metabolome. Additionally, pH was measured using a pH meter (ACCUMET AR10, Thermo Fisher Scientific, Loughborough, UK).

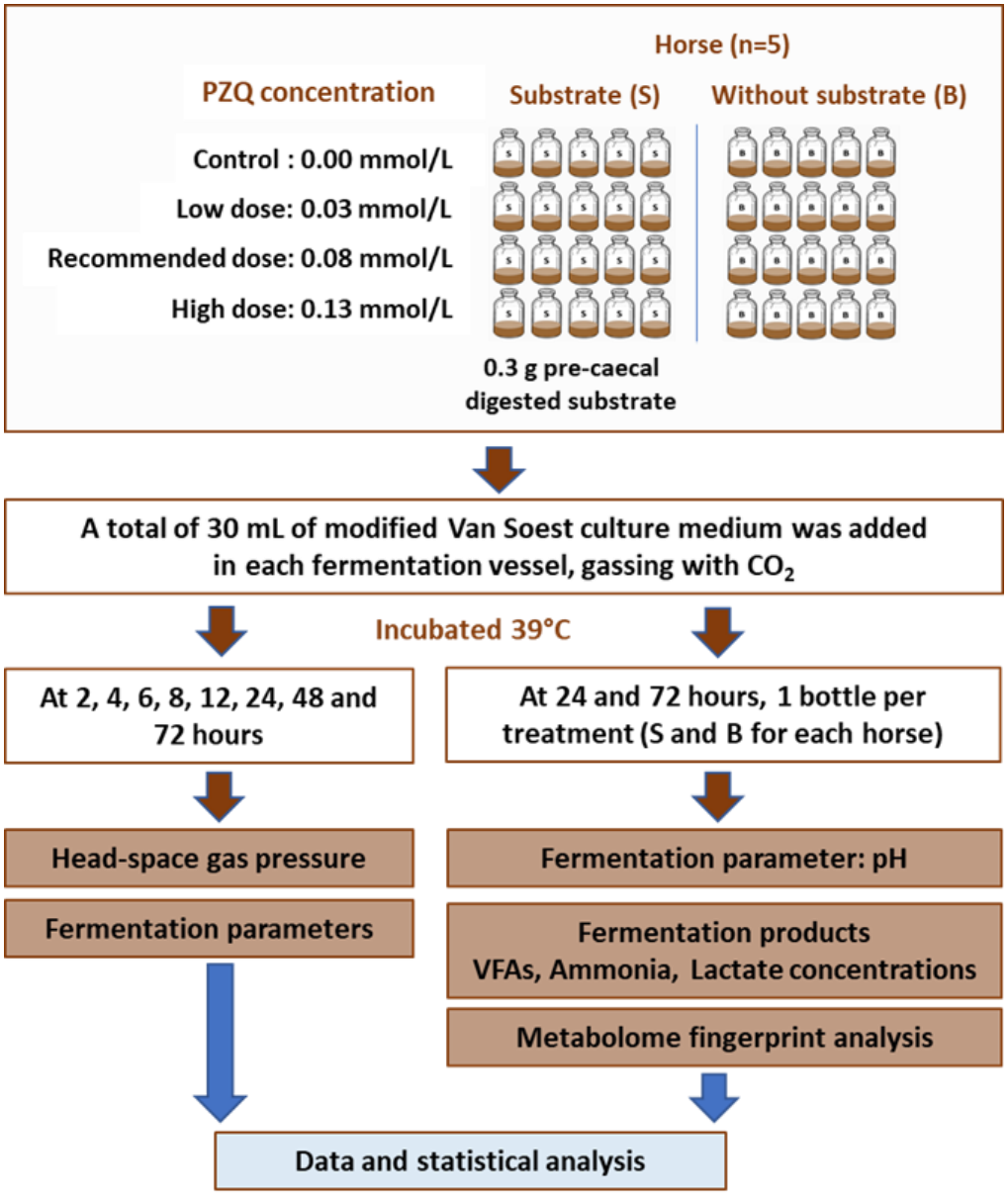

Figure 5.1 The workflow and experimental design used in the equine *in vitro* hindgut microbial fermentation experiment, investigating exposure to three different concentrations of PZQ.

5.2.2 Fermentation kinetics analysis

To describe the hindgut microbial fermentation profiles following exposure to PZQ at various dosage levels, the exponential model developed by Ørskov and McDonald (1979) was utilised to model the gas production profiles in GenStat (20th Edition; VSN International, Hemel Hempstead, UK). The model used the equation $Y = a+b\ (1-e^{-ct})$, where "Y" is the cumulative gas production (mL), "t" is time in hours, "a" is a gas produced at time point 0, "b" is the maximum gas produced, "a+b" describes the maximum potential of fermentation and "c" is a constant rate of gas production.

Prior to inputting the data set into the model, headspace gas pressure readings in the psi unit were corrected for the equivalent of the substrate at 1 g by multiplying with the value of 0.33. Additionally, the psi readings observed in the blank fermentation vessel were deducted from the substrate fermentation vessel as any background fermentation. The resulting headspace gas pressure (substrate and substrate–blank) was then used to model the fermentation profiles using the exponential Ørskov and McDonald model, as described above.

5.2.3. Microbial fermentation products analysis

5.2.3.1 Volatile Fatty Acids (VFAs)

VFA concentrations (acetic, propionic, butyric, valeric, caproic, heptanoic acids and total VFAs) after 24 and 72 hours fermentation periods following exposure to PZQ at various dosage levels were analysed by gas–liquid chromatography as described by Stewart and Duncan (1985). Briefly, 4 mL of fermented culture medium (section 5.2.1.5) was collected from the substrate vessel and mixed with 1 mL of 20% (w/v) orthophosphoric acid containing 20 mM 2–ethyl butyric acid (Sigma–Aldrich, Merck Life Science, Germany), as the internal standard. The mixed suspension was centrifuged (Heraeus Biofuge® Primo, Kendro Laboratory Products, Bishop's Stortford, UK), at 5000 x *g* for 5 minutes and the resulting supernatant filtered through a 0.45 µm PES membrane syringe filter (Captiva Econofilter, Agilent Technologies, California, USA). The filtered supernatant sample was transferred into a 2 mL gas chromatography vial (Chromacol 2–CV, Thermo Scientific, Loughborough, UK), capped with an aluminium crimp cap (Thermo Scientific, Loughborough, UK) and stored at –20 °C for subsequent VFAs analysis.

Samples underwent gas chromatography using a Varian CP3380 and autosampler Varian CP8400, equipped with a HP–FFAP column; 15 m length × 0.53 mm I.D. × 1 µm film thickness (J & W Scientific, California, U.S.A.) following Stewart and Duncan (1985). The Varian Galaxie Chromatography Workstation (software version 1.9.3.2.) was then used to obtain the concentration of each VFA in mmol/L. The proportion of the total VFAs that each VFA contributed (the % data) were calculated to standardise absolute values between samples prior to the statistical analysis.

5.2.3.2 Ammonia and lactate

For ammonia and lactate analyses, 12 mL of fermented culture medium (section 5.2.1.5) was collected from vessels with substrate after 24 and 72 hours of microbial fermentation and centrifuged (Heraeus Biofuge® Primo, Kendro Laboratory Products, Bishop's Stortford, UK), at 8,000 *x g* for 5 minutes. The resulting supernatant was considered a strongly coloured sample according to a manufacturer's protocol. Consequently, a proportion of 0.2 g polyvinylpolypyrrolidone (PVPP; Sigma–Aldrich, Merck Life Science, Germany) per 10 mL sample was added. Tubes were subsequently vortexed vigorously for 5 min (Whirlimixer™, Thermo Scientific, Loughborough, UK), followed by centrifuging (Heraeus Biofuge® Primo, Kendro Laboratory Products, Bishop's Stortford, UK) at 8,000 x *g* for 5 minutes and filtering through a 0.45 µm PES syringe membrane filter (STARLAB, Milton Keynes, UK) (Thermo Scientific, Loughborough, UK). The filtered supernatant was stored at –20 °C for subsequent determination of ammonia and lactate concentrations.

Ammonia and lactate (L–, D– and Total) concentrations were determined using the commercially available Ammonia Assay Kit (Rapid; K–AMIAR; Megazyme, Wicklow, Ireland) and Enzytec™ Generic D–/L–Lactic acid (R–Biopharm Rhône, Ltd, Glasgow), respectively, following the manufacturer's protocols. Assays were performed in a 96 well flat–bottomed micro–titre plate (Thermo Scientific, Loughborough, UK) and absorption read using Hidex Sense Microplate Reader (Hidex, Turku, Finland) at 340 nm absorbance and 25 °C. The concentration of ammonia and lactate (L–, D– and Total) was determined from the OD values and internal standards, using the equations according to the manufacturer's protocol.

5.2.3.3 Fourier Transform Infrared Spectroscopy for metabolome

The metabolome was assessed after 24 and 72 hours fermentation by Fourier Transform Infrared Spectroscopy (FTIR), as described by Dougal *et al.* (2012) and Blackmore *et al.* (2013). Briefly, 4 mL of fermented culture medium (section 5.2.1.5) was collected from vessels with substrate (Thermo Fisher Scientific, Loughborough, UK) and stored at –20 °C until further analysis. Prior to analysis, the samples were thawed, vortexed (Whirlimixer™, Thermo Fisher Scientific, Loughborough, UK) for 5 minutes and re–frozen at –20 °C, this process was repeated a further two times to break up cells within the samples. Following the final vortex, 15 µL of each sample was pipetted onto a FTIR plate in triplicate and oven–dried at 40 °C for 1 hour, or until fully dried. The samples were then put through a VERTEX 70v spectrophotometer with HTS–XT (Bruker Optik GmbH, Germany) to assess metabolome fingerprint. Triplicate infrared spectra were collected and read at a range of 4000–600 cm^{-1} and a resolution of 4 cm^{-1}. To minimise loading variation, spectra were normalised by conversion to relative values across samples. OPUS (version 6.5; Bruker Optik GmbH, Germany) was used to collect data and a mean of the normalised triplicate infrared spectra was calculated for further statistical analysis.

5.2.4 Statistical analyses

5.2.4.1 Microbial fermentation parameters and products

Prior to analysis, data were assessed for normal distribution by assessment of skewness within Genstat (21st Edition; VSN International, Hemel Hempstead, UK). Where skewed data of VFAs were identified they were corrected by transformation using either $\log_{10}$ or square root transformation prior to the data analysis. All data analysis was completed in GenStat (21st Edition; VSN International, Hemel Hempstead, UK). A statistical significance was considered if $P < 0.05$ and statistical trend considered if $P < 0.1$.

Fermentation parameters for substrate and substrate–blank were obtained from the exponential Ørskov and McDonald model ($Y = a+b\ (1-e^{-ct})$). Both the maximum potential of fermentation (a+b) and gas production rate (c) over the 72 hours fermentation period were analysed for differences in PZQ treatments using one–way Analysis of Variance (ANOVA).

Mean pH, VFAs (absolute quantifications, % contributions and the acetate: propionate ratio), ammonia and lactate concentrations after 24 and 72 hours microbial fermentation were analysed using one–way ANOVA for differences between PZQ treatments. Post–hoc Tukey's honestly significant difference (HSD) test was used to compare PZQ treatment groups in a pairwise method.

5.2.4.2 Metabolome fingerprint

Metabolome fingerprint spectra data were analysed by Principal Component Analysis (PCA) between PZQ dosage levels for each time point (24 and 72 hours) using PAST (Paleontological statistics software package for education and data analysis; version 4.03; Hammer *et al.*, 2001). To determine overall significant differences of the mean metabolome fingerprint profiles between PZQ treatment groups, one–way permutation multivariate analysis of variance (PERMANOVA; Anderson, 2017) in PAST software (version 4.03; Hammer *et al.*, 2001) was performed with unrestricted permutations of 9999 and similarity index of Bray–Curtis to calculate *P*–value. A statistical significance was considered if $P < 0.05$ and statistical trend considered if $P < 0.1$.

5.3 RESULTS

5.3.1 Fermentation kinetics profiles following PZQ treatment of an *in vitro* hindgut model of equine microbial fermentation

The mean cumulated gas produced consistently increased over 72 hours fermentation in the control and all PZQ treatments (0.03 mmol/L, 0.08 mmol/L and 0.13 mmol/L) (Figure 5.2). There was no indirect influence of PZQ concentrations on the model, based on the blank vessel fermentation parameters (Appendix 5.1).

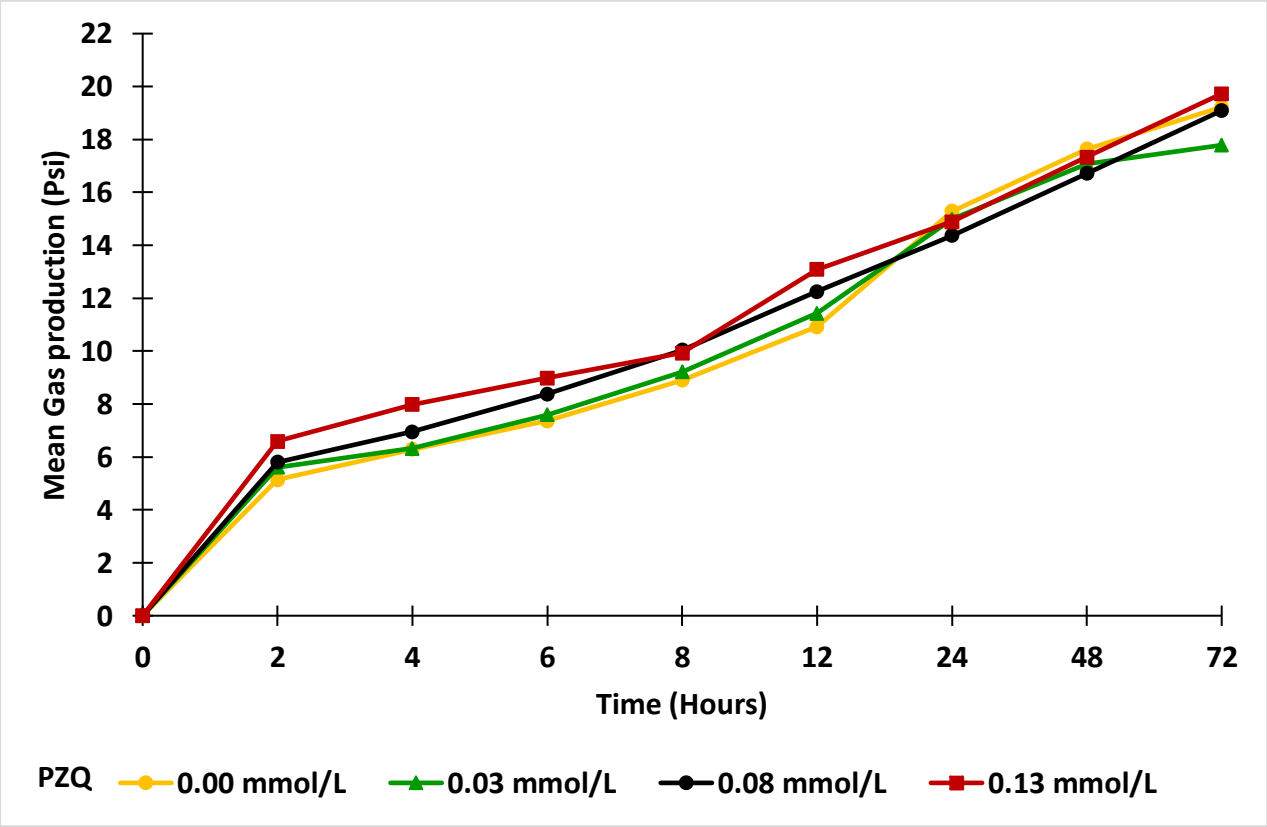

Figure 5.2 Cumulative gas production over a 72 hours fermentation period with a mixed diet of meadow hay: barley at 70:30 ratio in a hindgut model of equine microbial fermentation, incubated with PZQ at concentrations of 0.00 mmol/L (control), 0.03 mmol/L, 0.08 mmol/L and 0.13 mmol/L in DMSO at a final concentration of (v/v) 0.1%. Coloured in yellow, green, black and red, respectively.

There was no effect of PZQ on the gas production kinetics, compared to the control or between treatments, including the maximum potential of fermentation (a+b) (P = 0.615) and gas production rate (c) (P = 0.358) over the 72 hours fermentation period (Table 5.1). The mean pH data from the substrate fermentation vessels revealed no effect of any PZQ treatments on pH, compared to the control or between treatments after 24 (P = 0.389) and 72 hours (P = 0.384) microbial fermentation period (Table 5.1).

Table 5.1 The kinetics of gas production profile and pH over a 72 hours microbial fermentation period in an *in vitro* hindgut model of equine microbial fermentation. Data are presented as both the substrate incubated with PZQ at various dosage levels (0.00 mmol/L (control), 0.03 mmol/L, 0.08 mmol/L and 0.13 mmol/L) in 0.1% DMSO and the substrate minus the corresponding gas measured in blank vessels. Parameters modelled from cumulative gas production data using the exponential Ørskov and McDonald model; $Y=a+b\ (1-e(^{-ct}))$. Data are expressed as means and the standard error of the difference (SED). Data analysed by one–way Analysis of Variance (ANOVA), with statistical significance considered if $P < 0.05$ and statistical trend considered if $P < 0.1$.

Fermentation parameters	Praziquantel (mmol/L)				SED	*P* value
	0.00	**0.03**	**0.08**	**0.13**		
Substrate						
a+b	19.34	18.30	18.72	19.48	2.426	0.958
c	0.054	0.084	0.057	0.052	0.020	0.381
pH 24 hours	7.10	7.02	7.04	7.04	0.049	0.389
pH 72 hours	6.7	6.81	6.83	6.86	0.091	0.384
Substrate–Blank						
a+b	13.874	12.242	14.185	15.957	2.735	0.615
c	0.052	0.054	0.043	0.035	0.011	0.358

"a+b" describes the maximum potential of fermentation and "c" is a constant rate of gas production.

5.3.2 Fermentation products and metabolites

At 24 hours, there was no effect of PZQ treatment on propionate, acetate: propionate ratio, total other VFAs, ammonia and lactate concentrations (D–/L– and Total), compared to the control or between PZQ doses (Table 5.2; $P > 0.05$). A low dose of PZQ (0.03 mmol/L) demonstrated a significant increase in total butyrate level compared to control (0.00 mmol/L) and a high dose of PZQ treatment (0.13 mmol/L) at 24 hours (P = 0.023). A high dose of PZQ treatment (0.13 mmol/L) at 24 hours results in a trend for lower concentration (mM) of

acetate compared to the low dose of PZQ (P<0.1), although there was no difference from the control. However, when these data were standardised to total VFAs by converting to a percentage, it was demonstrated that there was a significantly lower proportion (%) of acetate, compared to both the control and low concentration of PZQ (P<0.05) low dose of PZQ treatment (0.03 mmol/L). Furthermore, this reduction in acetate between the high and low concentrations of PZQ, likely explained the statistical trend for lower production of total VFAs in the high dose PZQ treatment, compared to the low (*P* <0.1), but no difference from the control.

Table 5.2 Fermentation products and metabolites at 24 hours of fermentation of a mixed diet (meadow hay: barley at 70:30 ratio) in a hindgut model of equine fermentation incubated with PZQ treatment at various dosage levels (0.03 mmol/L, 0.08 mmol/L and 0.13 mmol/L) compared to control (0.00 mmol/L) in DMSO at 0.1%. Data are expressed as means and the standard error of the difference (SED). Data analysed by one–way Analysis of Variance (ANOVA), with statistical significance considered if *P* < 0.05. Different superscripts (a–c) following means in the same row indicate differences at *P* < 0.05 and statistical trend considered if *P* < 0.1.

Fermentation products	Praziquantel (mmol/L)				SED	P value
	0.00	0.03	0.08	0.13		
Absolute VFA concentrations						
Total VFA (mM)	31.00^{ab}	41.50^{b}	36.31^{ab}	29.19^{a}	4.340	0.058
Acetate (mM)	19.89^{ab}	27.61^{b}	23.58^{ab}	17.88^{a}	3.510	0.073
Propionate (mM)	5.18	6.26	5.59	4.86	0.904	0.471
Total Butyrate (mM)	5.44^{a}	6.95^{b}	6.35^{ab}	5.34^{a}	0.508	0.023
Total Others (mM)	0.48	0.67	0.80	1.11	0.343	0.354
VFA proportions						
Acetate (%)	65.34^{a}	65.42^{a}	64.63^{ab}	60.51^{b}	1.681	0.038
Propionate (%)	16.01	16.25	15.62	16.66	1.351	0.889
Total–Butyrate (%)	16.99	16.70	17.52	18.79	1.657	0.614
Total–Others (%)	1.66^{a}	1.64^{a}	2.23^{ab}	4.05^{b}	1.163	0.182
VFA ratios						
Acetate: Propionate: Butyrate ratio (mmol/100 mmol)	66:16:17	66:17:14	66:16:18	62:17:20	–	–
Acetate: Propionate Ratio	7.42	7.08	6.61	4.80	0.048	0.255
Acetate + Butyrate/ Propionate ratio	9.17	8.59	8.13	6.08	0.053	0.509
Ammonia (mM)	1.86	2.36	1.51	2.63	0.813	0.535
D–Lactate (mM)	0.059	0.054	0.053	0.096	0.017	0.157
L–Lactate (mM)	0.157	0.073	0.102	0.212	0.010	0.539
Total–Lactate (mM)	0.234	0.144	0.172	0.313	0.118	0.510

At 72 hours, there was no effect of PZQ treatments on mean VFAs and Lactate concentrations (D–/L– and Total) (Table 5.3; $P > 0.05$). Whereas there were significantly greater concentrations of ammonia following the high dose of PZQ treatment (0.013 mmol/L) compared to control (0.00 mmol/L), low dose (0.03 mmol/L) and recommended dose (0.08 mmol/L) of PZQ treatments ($P = 0.011$).

Table 5.3 Fermentation products and metabolites at 72 hours of fermentation of a mixed diet (meadow hay: barley at 70:30 ratio) in a hindgut model of equine fermentation incubated with PZQ treatment at various dosage levels (0.03 mmol/L, 0.08 mmol/L and 0.13 mmol/L) compared to control (0.00 mmol/L) in DMSO at 0.1%. Data are expressed as means and the standard error of the difference (SED). Data analysed by one–way Analysis of Variance (ANOVA), with statistical significance considered if $P < 0.05$. Different superscripts (a–c) following means in the same row indicate differences at $P < 0.05$ and statistical trend considered if $P < 0.1$.

Fermentation products	Praziquantel (mmol/L)				SED	P value
	0.00	0.03	0.08	0.13		
Absolute VFA concentrations						
Total VFA (mM)	51.04	47.18	46.38	42.93	5.970	0.614
Acetate (mM)	33.50	30.19	28.86	27.40	4.460	0.579
Propionate (mM)	8.26	8.76	9.16	7.93	1.059	0.676
Total Butyrate (mM)	8.01	7.07	7.13	6.43	1.041	0.530
Total Others (mM)	1.26	1.156	1.226	1.168	0.214	0.955
VFA proportions						
Acetate (%)	63.89	63.42	62.53	64.30	1.838	0.795
Propionate (%)	17.86	19.25	19.63	18.34	1.360	0.559
Total–Butyrate (%)	15.61	14.84	15.21	14.67	0.825	0.680
Total–Others (%)	2.65	2.49	2.63	2.69	0.379	0.956
VFA ratios						
Acetate: Propionate: Butyrate ratio (mmol/100 mmol)	66:18:16	65:20:15	64:20:16	66:19:15	–	–
Acetate: Propionate Ratio	6.61	4.80	4.02	4.67	0.014	0.492
Acetate + Butyrate/ Propionate ratio	8.01	5.77	4.91	5.60	0.013	0.436
Ammonia (mM)	2.03^{a}	2.04^{a}	1.72^{a}	5.35^{b}	17.26	0.011
D–Lactate (mM)	0.077	0.078	0.066	0.074	0.011	0.726
L–Lactate (mM)	0.077	0.035	0.055	0.055	0.026	0.457
Total–Lactate (mM)	0.177	0.137	0.131	0.152	0.026	0.349

5.3.3 The metabolome fingerprint

PCA analysis (PC1 and PC2, accounting for 99.33% and 99.31% of the variance at 24 and 72 hours, respectively) of the metabolome fingerprint (FTIR spectra data) at 24 (Figure 5.3) and 72 hours (Figure 5.4) demonstrated that there was no clear clustering of any PZQ treatment groups, suggesting that PZQ treatment did not affect the metabolome in the *in vitro* hindgut microbial fermentation model. Furthermore, a pairwise PERMANOVA demonstrated that there was no significant effect on the metabolome fingerprint profiles at 24 hours ($P = 0.1318$) or 72 hours ($P = 0.5347$) following treatment with any of the PZQ dosage levels (low dose 0.03 mmol/L, recommended dose 0.08 mmol/L and high dose 0.13 mmol/L), compared to the control.

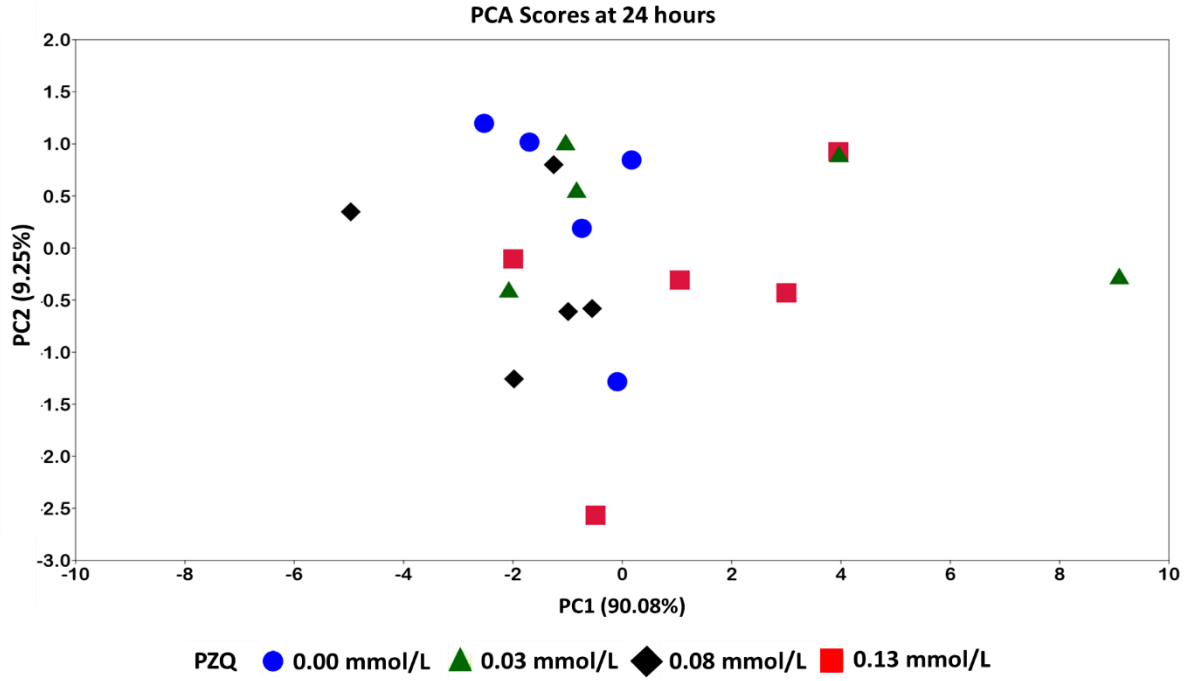

Figure 5.3 Principal component analysis (PCA) at 24 hours of fermentation of a mixed diet (meadow hay: barley at 70:30 ratio) in a hindgut model of equine fermentation incubated with praziquantel at concentration of 0.00 mmol/L (control), 0.03 mmol/L, 0.08 mmol/L and 0.13 mmol/L, coloured symbols in circle–blue, triangle–green, diamond–black and square–red, respectively. PC 1 and 2 demonstrated as a total of 99.33% of the variance.

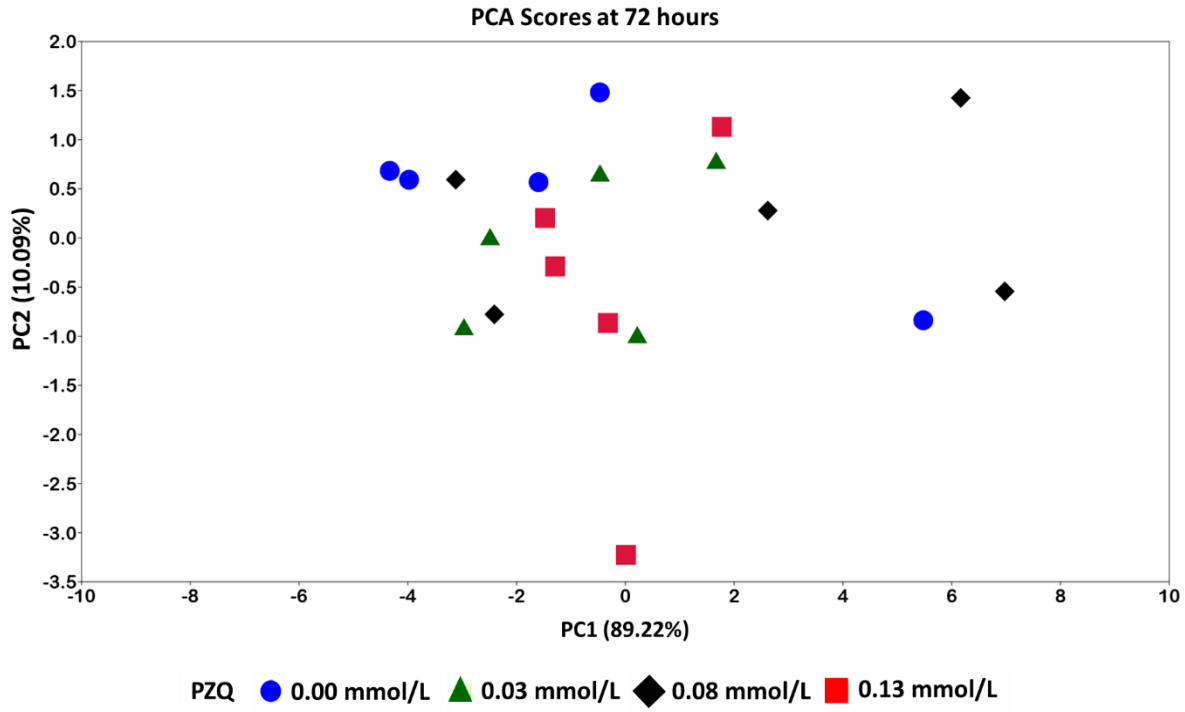

Figure 5.4 Principal component analysis (PCA) at 72 hours of fermentation of a mixed diet (meadow hay: barley at 70:30 ratio) in a hindgut model of equine fermentation incubated with praziquantel at concentration of 0.00 mmol/L (control), 0.03 mmol/L, 0.08 mmol/L and 0.13 mmol/L, coloured symbols in circle–blue, triangle–green, diamond–black and square–red, respectively. PC 1 and 2 demonstrated as a total of 99.31% of the variance.

5.4 DISCUSSION

In this chapter, I revealed the *in vitro* impact of PZQ treatment on the equine microbial fermentation activities and metabolome products at 3 different dosage levels, which related to a low, recommended and high concentration of PZQ, compared to no PZQ treatment. These fermentation parameters can provide a guide to the functionality of the equine hindgut. Therefore, the present study improves my understanding of the effect of the anthelmintic PZQ on the equine hindgut microbiome, using a widely used *in vitro* hindgut microbial fermentation model (Theodorou *et al.*, 1994). The overall result of the fermentation activities and products of the equine hindgut after exposure to PZQ treatments at the tested dosage levels suggests that there were minor alterations on the equine hindgut fermentation pathway which could impact on the nutritional functioning of the caecum.

5.4.1 Fermentation kinetics profiles over 72 hours following PZQ treatment

Changes in the intestinal microbiome following introduction of external factors to the equine hindgut microbiome can affect the microbial activity of the hindgut, including gas production and pH (Dougal *et al.*, 2012). There is limited work that has investigated the effect of both parasite infections and anthelmintic treatments on gastrointestinal microbial fermentation kinetics. This is the first study to investigate the impact of PZQ on microbial fermentation kinetics. Previous work has focussed on moxidectin, which is also a commonly used anthelmintic in horses, using a similar model to that in the present study. Daniels *et al.* (2020) revealed that the functional fermentation kinetics profile were temporally decreased, particularly the cumulative gas production and pH at 16 h after moxidectin administration compared to non–treated control group. Given this information perhaps a similar result might reflect to PZQ. However, in the present study, fermentation parameters obtained from the exponential model developed by Ørskov and McDonald (1979) demonstrated that the gas production accumulated over 72 hours (Ørskov and McDonald parameter Y – accumulated gas) did not differ between PZQ treated and the control. Thus, the present study indicates that the microbial fermentation activity within the *in vitro* hindgut model was still sustained in the presence of PZQ. Furthermore, my findings demonstrated no significant change on the fermentation parameters of maximum potential fermentation and gas production rate,

following PZQ at any dosage over 72 hours compared to the control *in vitro,* and in contrast to Daniels *et al.* (2020). It is implied that there were no alteration on the faecal bacteria related to substrate degradation functionality.

The pH indicates the abundance of fermentation products according to the microbial fermentation activity such as VFA, lactate and ammonia concentrations (Bergman, 1990; de Fombelle *et al.*, 2001; Coles *et al.*, 2005). The present study demonstrated that pH following any PZQ treatments including the control were constant in the optimal pH range within the large intestine of healthy horses *in vivo* (pH 6.2–7.2) (de Fombelle *et al.*, 2001, 2003) or in the *in vitro* fermentation of haylage from inoculum of the large intestine (pH 6.71–6.89) However, other anthelmintics, such as moxidectin and ivermectin, have been demonstrated to cause a decrease in pH in the *in vitro* hindgut fermentation model at 16 hours after moxidectin administration compared to those found at 0 hour (Daniels *et al.*, 2020) or pH of the caecal content at 24–48 hours after moxidectin (pH 6.6–6.7) and Ivermectin (pH 6.7–6.9) administration (Goachet *et al.*, 2004). These findings suggest a change in the cellulolytic bacterial population, including *Lactobacilli* and *Streptococci*, leading to reduced fermentation after administration of moxidectin and ivermectin. Particularly in Daniels *et al.* (2020), the decreased pH 16 hours following moxidectin treatment was associated to greater relative abundance of the acid metabolite formate. In addition on other anthelmintics, Goachet *et al.* (2004) demonstrated that fenbendazole did not impact on pH (pH 6.8) following administration at 24–48 hours. However, it must be noted that the overall pH readings following anthelmintics in Daniels *et al.* (2020) and Goachet *et al.* (2004) were greater than 6.2 which are consistent with those reported in the normal range (de Fombelle *et al.*, 2001, 2003; Kujawa *et al.*, 2020), suggesting there is unlikely to be a major change in overall bacterial functionality and a shift in bacterial community following these anthelmintics administration. It must be noted that an *in vitro* hindgut fermentation model is not reflective of the exact hindgut ecosystem, therefore this warrants further findings on the wider experiment such as an impact on the hindgut microbial structure, composition and community following PZQ administration.

5.4.2 Changes in fermentation products at 24 hours indicate a minor alteration in the microbiota functionality, following PZQ treatment in an *in vitro* model of equine hindgut microbial fermentation

After 24 hours of microbial fermentation within the present study, there was an alteration of specific VFA concentrations following PZQ treatment. However, no significant changes in ammonia and lactate concentration were detected.

I demonstrated that total butyrate levels significantly increased after exposure to a low dose of PZQ at 0.03 mmol/L compared to control and a high dose of PZQ, at 24 hours. Butyrate, is a SCFA produced by intestinal microbial fermentation of dietary fibres, provides the energy source for colonic epithelial cells, modulates oxidative stress in the colonic mucosa and maintains colonic homeostasis in humans (Roediger, 1980, 1989; Hague *et al.*, 1996; Hamer *et al.*, 2008, 2009; Furusawa *et al.*, 2013). Furthermore, butyrate aids the gut immune system and plays a protective role against problems related to colon in humans (Pryde *et al.*, 2002; Plöger *et al.*, 2012; Wang *et al.*, 2020; Yang *et al.*, 2020), although there is currently no evidence of these roles in horses. Increased levels of butyrate in the present study may be a response of the butyrate–producing bacteria to enhance the protection of gut epithelial cells while also maintaining intestinal homeostasis from PZQ impact in the horse. It is possible therefore that PZQ may increase populations of butyrate–producing bacteria, such as *Lachnospiraceae* (*Butyrivibrio* and *Eubacterium* spp.*), Clostridiales* family XIII *(Ruminococcus* and *Coprococcus)* (Collinet *et al.*, 2021; Mach *et al.*, 2021) or alter the metabolism of these bacterial species to be able to increase production of butyrate. To confirm whether the presence of PZQ has influenced the levels of butyrate, as well as the composition or relative abundance of butyrate–producing bacterial species, further investigations should be conducted, including quantitative PCR and sequencing analysis of the 16S ribosomal RNA (16S rRNA) gene (Vital *et al.*, 2013).

Acetate is a major SCFA produced by equine intestinal microbes from dietary fibres and is normally absorbed by the intestinal wall to then be further metabolised to generate ATP (Shepherd *et al.*, 2014). The presence of known acetate–producing bacteria, such as the *Fusobacteria* and *Spirochaetes* phyla, were found to be significantly positively correlated with acetate concentrations in equine *in vitro* culture studies (Leng *et al.*, 2019), suggesting that

changes in acetate concentrations also indicate a change in the relevant acetate producing bacteria within the model. In the present study, acetate levels as a proportion of the total VFAs were significantly lower after exposure to a high dose of PZQ at 0.013 mmol/L, compared to the 0.03 mmol/L, while total VFA levels showed a trend to be lower. This finding was similar to the findings of Kunz *et al.* (2019) who demonstrated higher abundances in a *Treponema* spp. of the *Spirochaetes* phylum following treatment at 48 hours using the combination of moxidectin and PZQ (2.5 mg/kg BW), where the dosage of PZQ was equal to the high dose in our study (0.013 mmol/L). Interestingly, Daniels *et al.* (2020) found no reductions in the relative abundance of *Spirochaetes* phylum after 16 hours of moxidectin treatment. In conjunction with Leng *et al.* (2019) and Daniels *et al.* (2020), the *Spirochaetes* phyla was found to be significantly positively correlated with acetate concentrations. Thus, it is assumed that PZQ at a high dose of 0.013 mmol/L may influence microbial fermentation dynamics, particularly bacterial communities producing acetate. Therefore, using inappropriate deworming practices through overdosing horses may cause a compromised or dysfunctional microbial ecosystem and trend toward a reduction in essential VFAs produced, such as acetate. If underproduction of acetate persists, it could lead to a lack of energy required for maintenance of the horse. Furthermore, Leng *et al.* (2019) reported that lower levels of acetate result from less carbohydrate availability, as some carbohydrate–fermenting bacteria cannot be supported. As all inoculum samples for the *in vitro* model were from horses fed only hay, and I used a mixed substrate of meadow hay and barley at a 70:30 ratio in my *in vitro* hindgut fermentation system for all samples, it can be deemed that my results are related to an exposure of PZQ rather than the type of feeds. As such, the findings in my study related to alterations in acetate production following the high dose of PZQ could demonstrate an effect of PZQ on carbohydrate or fibrolytic bacteria availability in the *in vitro* model of the equine hindgut microbiome.

Acetate, propionate and butyrate are important metabolites in maintaining hindgut homeostasis, and their proportions may predict the dynamic of microbial communities through their feed fermentation activity (Bergman, 1990; Lowman *et al.*, 1999). A typical molar ratio (mmol/100 mmol) of acetate, propionate and butyrate is approximately 67:24:9–72:20:7 in the caecum, 66:21:12–80:13:7 in the large intestine and 72:20:8 in faeces of hay–based–fed diet horses (de Fombelle *et al.*, 2003; Dougal *et al.*, 2012; Grimm *et al.*, 2017;

Muhonen *et al.*, 2021). My findings demonstrated that the overall molar ratio of acetate, propionate, and butyrate in the hindgut fermentation model in all PZQ treatments including the control at 24 hours ranged from 66:16:17 to 63:17:20 (Table 5.2) which were in the range to those found in horses. Furthermore, a molar ratio of acetate to propionate represents the acidotic environment associated with increased lactate concentration (Swyers *et al.*, 2008; Li *et al.*, 2012; Huson *et al.*, 2018), and acetate plus butyrate to propionate ratio infers fibrolytic activity (Sauvant *et al.*, 1994; de Fombelle *et al.*, 2001, 2003; Grimm *et al.*, 2017). However, I did not find a significant effect of PZQ on these VFA ratios. These findings together with the minor alteration in faecal microbial fermentation functionality via acetate and butyrate levels following PZQ exposure at a high dose and low dose for 24 hours, respectively, suggest the dynamic of the faecal microbial community is unlikely to establish. This hypothesis was also supported by the pH level over 24 hours fermentation that pH remained constant in the optimal ranges through PZQ at any dosage level as previously discussed in the fermentation kinetics profile (Section 5.4.1).

5.4.3 Fermentation products, ammonia at 72 hours suggest a faecal microbiota adaptation following PZQ treatment in an *in vitro* model of equine hindgut microbial fermentation

After a 72 hour microbial fermentation period, I found that changes to the VFAs demonstrated at 24 hours did not persist. However, production of ammonia was significantly greater following a high dose of PZQ at 0.013 mmol/L compared to control, a low dose and a recommended dose of PZQ.

Ammonia within the hindgut is normally produced from breaking down urea, amino acids and proteins by urease–producing bacteria, including many *Enterobacteriaceae*, specifically *Proteus mirabilis*, *Pseudomonas spp.*, *Klebsiella spp.*, *Staphylococcus spp.*, *Corynebacterium spp.*, *Ureaplasma ureolyticum* and *Proteus penneri* (Burne and Chen, 2000) and *Clostridium sordelli and Clostridium perfringens* (Desrochers *et al.*, 2003; Stickle *et al.*, 2006) which are implicated in host nitrogen balance (Vince *et al.*, 1973, 1976; Vince and Burridge, 1980). From my *in vitro* model, it is likely that the long–term exposure to a high dose of PZQ altered the equine hindgut microbiome. Particularly, an overgrowth of urease–producing bacteria could have occurred following a high dose of PZQ at 0.013 mmol/L, leading to more ammonia production. This hypothesis requires further investigation to determine

whether a proliferation of urease–producing bacteria was associated with the changes to ammonia levels. Thus, the analysis of urease–producing bacterial composition by 16S ribosomal RNA (16S rRNA) gene sequencing could be conducted to analyse the overall microbial composition both the diversity and relative abundance of various bacterial species, particularly urease–producing bacteria. Particularly, microbial DNA extraction kits and urease gene quantification using quantitative PCR (qPCR) to quantify the abundance of urease genes in the microbial DNA (Jesús *et al.*, 2020; Wu *et al.*, 2023).

Furthermore, when compared to the ammonia concentrations investigated from the caecum (7.3 mM), right dorsal colon (13.1 mM), and faeces (9.8 mM) of horses and ponies from Dougal *et al.* (2012), my ammonia concentration of the inoculum of faeces following a high dose of PZQ at 0.013 mmol/L (5.35 mM) was lower, suggesting at a high dose of PZQ is still likely safe to horses. However, from equine health perspectives, it is important to be concerned if an overdose or inappropriate dose is administered to horses over time. As high ammonia levels lead to altered permeability of the intestinal barrier, which may then develop secondary to intestinal dysfunction or diseases (Dunkel, 2010) inducing changes to microbial community causes alteration of the hindgut functionality and health (Costa *et al.*, 2012; T. Park, Cheong, *et al.*, 2021; Ayoub, 2022).

As the longer exposure with PZQ at any dosage level did not result in a persistence on changes in VFA concentrations described at 24 hours, it is suggested that there were temporary microbial functional changes at 24 hours. The active microbial community could then be able to balance the microbial ecosystem within the hindgut after PZQ exposure, avoiding further PZQ induced the shift of microbial community along with compromised hindgut homeostasis afterwards. Furthermore, it is possible that the media used in my *in vitro* hindgut fermentation model via the gas production technique contains buffers that could also support in pH buffering over time. A further consideration is that PZQ may have been metabolised by this point. As a result, there may not have been any PZQ left in the model to interact with the microbes present after 24 hours of fermentation period. Thus, as it was reported in the formation of monepantel metabolites with amide via the nitrile hydrolysis *in vivo* in sheep (Stuchlíková *et al.*, 2014). It is possible that PZQ may formed with its metabolites by microbes within the hindgut. This PZQ–metabolites formation could be further determined using the combination of ultra–high–performance liquid chromatography (UHPLC) and

quadrupole–time–of–flight analyser (QqTOF) mass spectrometry to prove the hypothesis (Stuchlíková *et al.*, 2014).

5.4.4 Metabolome fingerprint at 24 and 72 hours suggest no impact of PZQ treatment on the overall microbiome in an *in vitro* model of equine hindgut microbial fermentation

Metabolites produced by microbes in the gut after the fermentation of dietary compounds play a key role in regulating the host metabolism and immunity as well as maintaining host gut physiology and homeostasis (Argenzio *et al.*, 1974; Glinsky *et al.*, 1976; Bergman, 1990; Costa and Weese, 2012). Significant changes in gut microbiota–derived metabolites are associated with changes in microbe composition and function and as such, reflect gut function (Lavelle and Sokol, 2020; Agus *et al.*, 2021). For example, moxidectin administration in horses *in vivo* demonstrated a higher formate in faecal sample collected at 16 hours after moxidectin treatment *in vivo*, suggesting an alteration on the fermentation of carbohydrates metabolism (Daniels *et al.*, 2020).

The experiment in this chapter investigated changes over the whole metabolome of samples from the hindgut microbial fermentation model after exposure to PZQ at a low dose of 0.03 mmol/L, a recommended dose of 0.08 mmol/L and a high dose of 0.013 mmol at 24 hours and 72 hours. This investigation was very much a 'birds eye view' of the metabolome to provide a metabolic fingerprint, that has not been mined down to individual spectra. On assessment of the overall metabolome within the *in vitro* model following PZQ treatment for 24 and 72 hours, it was demonstrated that there were no large changes in the metabolome which could be detected through clustering of treatment samples. As such, if there were large shifts in the bacterial microbiome of the faecal inoculum or its functionality following PZQ at any dose, an effect on metabolome fingerprint would be expected. Based on these findings and of specific metabolites (as previously discussed, VFAs, ammonia and lactate), it is implied that PZQ does not have any wide–ranging effects on the health of the hindgut at the level of the microbiome through the functionality of equine faecal microbiome *in vitro,* as there was no change in the overall metabolites profile.

As there were only small changes detected in the microbial fermentation products described previously, a further in–depth evaluation of the metabolic profile is warranted, whereby further specific spectra are assessed to investigate other key metabolites. These analyses will provide a more definite view of certain aspects of the metabolome, which may further an understanding of the underlying mechanisms of the changes noted in the VFA and ammonia profiles following PZQ treatment. Furthermore, these investigations could identify potential biomarkers for the gut functionality and health.

5.4.5 Anthelmintic treatment effects on the hindgut microbiome

The common anthelmintics used in horses include fenbendazole, pyrantel, ivermectin, moxidectin and particularly my anthelmintic of interest, praziquantel. These anthelmintics have extensively been considered in relation to alterations to the gut microbiome and further consequence on the gut functionality and health following parasite treatment and control (Rowe, 2017; Crotch-Harvey *et al.*, 2018; Peachey *et al.*, 2018, 2019; Kunz *et al.*, 2019; Walshe *et al.*, 2019, 2021; Daniels *et al.*, 2020; Dini. Hu *et al.*, 2021; Boisseau *et al.*, 2022) (Chapter 1, Table 1.6). In the current study, I have not investigated the faecal microbiome directly. However, the results suggest that although there may be some changes to some specific species, it is unlikely that there is a large–scale change in diversity or shifts in populations following treatment with PZQ *in vitro*. Overall, the present *in vitro* study demonstrated some changes, but limited and short–lived effects on the functionality of the equine hindgut microbiome through a closed fermentation model. This study does however need further investigation into the microbial community, composition or structure through sequencing of the samples.

Previous research that has investigated the effect of anthelmintics on the equine hindgut microbiome has demonstrated mixed results *in vivo*, although overall results demonstrated some impacts (Chapter 1, Table 1.6). The present study is the first to assess the effects of PZQ alone on the equine hindgut, demonstrating limited effects of PZQ on hindgut microbial functionality over 72 hours *in vitro*. Previous work in horses has utilised *in vivo* methodologies to investigate PZQ in combination with moxidectin, where it was reported that in uninfected horses, free from *A. perfoliata* and cyathostomins *or* ascarids, there was a significant decrease in alpha diversity, but no effect on beta diversity of equine faecal

microbial communities 5 days after pre–treatment with PZQ in combination with moxidectin (Kunz *et al.*, 2019). Based on my findings, it may be that changes identified by Kunz *et al*. (2019) were from the effect of the moxidectin, rather than PZQ. Information on the effect of PZQ alone on the gastrointestinal microbiome *in vivo* can be derived from work in humans, due to the lack of information in horses. In children, PZQ treatment in *vivo* in *S. mansoni* (Schneeberger *et al.*, 2018) and *Opisthorchis felineus* infections (Sokolova *et al.*, 2021) demonstrated changes in the abundances of some bacteria such as an increase of butyrate–producing bacteria namely *Faecalibacterium* and decrease of *Megasphaera*, *Roseburia* (butyrate–producing bacteria) (Sokolova *et al.*, 2021), but was not related to a major shift in the gut taxonomic profiles or change in the microbial diversity, suggesting PZQ is safe for use with the gut microbiome (Schneeberger *et al.*, 2018; Sokolova *et al.*, 2021). Notably, there are obviously big differences in gastrointestinal anatomy between horses and humans and so although this gives some indication to what may happen in the horse, it cannot be conclusive.

Importantly, the current PZQ study in horses only takes into account a closed fermentation model, that utilises microbial inoculum but does not consider the wider environment of the animal, such as the host tissue or the presence of the parasites themselves that the PZQ is being used to treat. As such, the actual processes involved are likely to much more complex between the host, *A. perfoliata*, caecal microbiome and PZQ, necessitating further investigation to fully assess the effect of PZQ.

Interestingly, it is suggested that changes in intestinal microbiota may be associated with parasite death rather than following anthelmintic treatment (Peachey *et al.*, 2019; Walshe *et al.*, 2019; Daniels *et al.*, 2020; Hu *et al.*, 2021) (Chapter 1, Table 1.6). Walshe *et al.* (2019) suggests that effects of moxidectin on microbial diversity identified in their study may be associated with an inflammatory response after adult cyathostomins removal, rather than the effect of moxidectin treatment itself. Likewise, Boisseau *et al.*, (2022) demonstrated that the removal of cyathostomin following the pyrantel administration has a drastic and acute effect on the gut environment and microbiota composition. Therefore, the effect of PZQ on gut microbiome needs to be investigated further and compared between the presence and absence of *A. perfoliata* in conjunction with PZQ treatment, particularly in the *in vitro* hindgut fermentation system, to rule out the possibility that an alteration in gut microbiome is due to *A. perfoliata* infection rather than anthelmintic treatment.

5.4.6 Study limitations

There are limitations with the *in vitro* gas production model used to assess the equine hindgut fermentation activity in this study. The use of a closed microbial fermentation model of the equine large intestine may not support the growth and function of certain bacterial communities within the complexed ecosystem of the caecum. Furthermore, the substrates used may be not left within the system to be degraded by microbes within the system (Coles *et al.*, 2005). Leng *et al.* (2019) has reported in a continuous culture system, three–stage fermentation model, that without adding any fresh substrates, bacterial communities are often less diverse. The lack of diversity is represented by the identification of fewer unique operational taxonomic units (OTUs; 39 to 43% of the unique OTUs identified) (Leng *et al.*, 2019). Furthermore, Leng *et al.* (2019) suggest that other features of the host environment, such as epithelial cells and gut wall secretions may need to be added to the model to establish a more complete *in vitro* representation of the hind gut. Therefore, an alternative fermentation system that models more akin to *in vivo* horse feeding by adding refreshed daily substrates or additives is warranted. Specifically be an *in vitro* continuous rumen simulation systems or semi–continuous culture/fermentation systems such as rumen simulation technique (RUSITEC) or a modified RUSITEC for horses (EQUITEC) (Engelmann *et al.*, 2007; Kuhn, 2009; Vosmer *et al.*, 2012) or specifically to caecal content, namely caecum simulation technique (CAESITEC) (Meyer and Klingeberg-Kraus, 2002; Zeyner *et al.*, 2006) are recommeded for future experiments to support maintaining microbial communites under desired conditions (Deitmers *et al.*, 2022). Furthermore, the lack of PZQ being included in the *in vitro* pre–digestion process prior to microbial fermentation in the present study may not mimic the potential PZQ metabolic profile present within the foregut of the horse *in vivo*.

It has been noted that bacterial communities found in faeces are not exactly the representative of bacterial communities within caecum (Dougal *et al.*, 2012), where the majority of bacterial fermentation occurs. This discrepancy is further compounded given that bacterial communities, and their associated fermentation activity, in each part of the large intestine is also different (Dougal *et al.*, 2012, 2013; Fliegerova *et al.*, 2016). However, the use of faecal samples as a microbial inoculum for the model has been validated by Lowman *et al.* (1999) and provides a non–invasive sampling technique rather than using caecal fluid for

equine hindgut microbiome studies (Hastie *et al.*, 2008; Murray *et al.*, 2012, 2014; Leng *et al.*, 2019). Yet, as *A. perfoliata* is located in the caecum and so where PZQ would be exerting most effects, it would be useful to assess in the future work if there are any differences in PZQ effects in caecal inoculum models compared to faecal inoculum models.

5.5 CONCLUSIONS

The present study demonstrates the first investigation into the impact of PZQ on the equine hindgut microbiome fermentation. I demonstrated that there is no significant change in the fermentation kinetics profile over 72 hours and the metabolome profile at 24 and 72 hours after exposure to PZQ at doses related to a low recommended or high dose or PZQ, compared to the control. However, after exposure to PZQ at 24 hours, a low dose PZQ increased butyrate concentration and a high dose of PZQ (0.13 mmol/L) decreased acetate and tended to increase total VFAs. After exposure to PZQ at 72 hours, a high dose of PZQ (0.13 mmol/L) increased ammonia levels. As such, from these results, I suggest that PZQ treatment, especially at a higher than recommended doses, may alter the fermentation pathways in the equine hindgut based on microbial activities and fermentation products, which could impact on the nutritional functioning of the caecum. However, widespread changes in the microbiome are unlikely. Therefore, appropriate PZQ dosage administration is likely safe for equine hindgut microbiota, whereas inappropriate over–dosing of horses with PZQ may alter microbial activities in the equine hindgut and as such, lead to an issue with nutritional heath of the caecum.

The overall findings on bacterial functional information in this chapter warrant extensive investigation of PZQ impacts such as the correlation of the fermentation kinetics profile, products and key metabolites with the presence of known faecal microbial communities. To further characterise PZQ impact, samples from the present study should undergo both meta–taxonomy and meta–proteomics (potentially in conjunction with metagenomics) analysis for a complete assessment of PZQ induced alterations to the microbiome. An analysis of faecal/caecal/colonic microbiota composition, diversity and richness of the microbial communities via bacterial 16S ribosomal RNA (16S rRNA) amplicon sequencing together with operational taxonomic unit (OTU) assignments is required. Moreover, caecal or colonic fluid could be used as a source of inoculum to the *in vitro* hindgut model system with and without the presence of *A. perfoliata*, as well as performing an *in vivo* trial to further investigate PZQ impact.

CHAPTER 6:

GENERAL DISCUSSION

6.1 INTRODUCTION

The key motivation to complete this thesis was to drive an increased understanding of *A. perfoliata*, a neglected parasite for which symptoms are present in heavily infected horses and likely lead to colic. This body of work thus builds upon the recognised concern within the equine health sector in order to understand the interaction between *A. perfoliata* and the host.

Due to currently limited knowledge around the fundamental biology of *A. perfoliata*, research was undertaken to generate the first *A. perfoliata* transcriptome to improve my ability to perform in–depth molecular biology and functional genomics of *A. perfoliata*. Functional genomics, namely transcriptomics and proteomics, based approaches have further supported an investigation of putative *A. perfoliata* immune modulators which are likely involved in host–parasite interactions (Chapter 2 and 3; Appendix 6.1 Wititkornkul *et al.* (2021)). In doing so, the thesis has helped to facilitate an in–depth understanding of the potential molecular mechanisms of the *A. perfoliata* secretome that are employed to interact with the host, utilising a proteomic led analysis (Chapter 3). Furthermore, this approach has also supported the investigation into whether *A. perfoliata* EVs demonstrate immunomodulatory functions and thus influence the mammalian immune response (Chapter 4). Finally, the thesis has supported a praziquantel–equine hindgut microbiome interaction study which may be useful for future parasite management and control options (Chapter 5).

6.2 ADDRESSING THE THESIS AIMS

6.2.1 Transcriptomic and bioinformatic approaches for identifying key *A. perfoliata* immune modulators

A. perfoliata infection and interaction with the horse–host remains poorly understood due to a lack of fundamental knowledge, particularly in–depth molecular biology and functional genomics, which is required for a deeper understanding of the mechanism relevant to how *A. perfoliata* interacts with the host (Lawson *et al.*, 2019; Slater *et al.*, 2021). Complementary "omic" technologies, in conjunction with bioinformatic approaches have been employed to improve transcriptomic and proteomic profiling, such as in *E. granulosus* (Pan *et al.*, 2014; S. Liu *et al.*, 2017; Bai *et al.*, 2020; Debarba *et al.*, 2020; Fan *et al.*, 2020; Mohammadi *et al.*, 2021) *and F. hepatica* (Cwiklinski *et al.*, 2015; Cwiklinski *et al.*, 2021). However, perhaps unsurprisingly, a reference genome for *A. perfoliata* has not been completed despite recognition for its requirement (Guo, 2015, 2016). The development of a reference transcriptome is a highly acceptable alternative choice to support ongoing functional genomics in the continued absence of a reference genome (Chang *et al.*, 2015; Hölzer and Marz, 2019). In generating a reference or discovery transcriptome, further insights into RNA expression, particularly genes underlying the mechanisms associated with *A. perfoliata* infection, can be gained with high reproducibility and relatively low cost (Wang *et al.*, 2009; Nagalakshmi *et al.*, 2010; Li *et al.*, 2014; Kukurba and Montgomery, 2015).

Chapter 2 successfully addressed the thesis aim of resolving the lack of a molecular biology nucleotide–based reference database for *A. perfoliata* by generating the first *de novo* transcriptome of adult *A. perfoliata*. As such, this work provides an important resource for the functional implications of gene expression that can be linked to further proteomic analyses. The resolution of the *A. perfoliata* transcriptome, supported with bioinformatic approaches, provided a comprehensive analysis of key transcripts likely actively involved in *A. perfoliata* infection and host–parasite interaction, which will contribute to survival within the host (Hewitson *et al.*, 2009; Gazzinelli-Guimaraes and Nutman, 2018). Furthermore, the supporting bioinformatics approach confirmed the quality and biological validity of the transcript assembly given similarities to three closely related tapeworm species, namely *H. diminuta, E. granulosus* and *H. microstoma*.

When exploring the *A. perfoliata* transcriptome, using various bioinformatic approaches, for sequences of known immune modulatory proteins that have previously been characterised in two significant flatworms, namely *S. mansoni* and *F. hepatica*, this thesis discovered the expression of 462 key sequences, potentially demonstrating comparable immune modulatory functions, as demonstrated in flatworms. Of particular interest was the identification of three novel immune modulatory protein families within the *A. perfoliata* transcriptome, specifically GST (both Sigma and Omega classes), Heat shock protein 90 alpha and alpha–Enolase, in a consistent manner with related helminths (Alexandra *et al.*, 2003; Jolodar *et al.*, 2003; Marcilla *et al.*, 2007; Ramajo-Hernández *et al.*, 2007; Dowling *et al.*, 2010; LaCourse *et al.*, 2012; Maizels *et al.*, 2018; Wang *et al.*, 2022). The discovery of *A. perfoliata* key RNA sequences in this chapter provides further evidence to support future proteomic studies to examine if these immune modulatory transcripts may lead to functional proteins and are specifically identified within the *A. perfoliata* secretome. These proteins may be secreted into the host environment and as such capable of interacting directly or indirectly with the host, which is further investigated within Chapter 3.

It is noted that the three identified novel *A. perfoliata* key immune modulatory sequences have been characterised based on the integrated *A. perfoliata* transcriptome and bioinformatic analysis. However, each sequence has not been functionally confirmed as an immune modulator. Therefore, a future area of research could be performed on a deep functional characterisation, starting with production of recombinant or synthetic versions of identified target proteins, allowing experimentation such as the crystal structural determination and biochemical activity. More importantly, production of each target protein will allow the confirmation of their proposed immune modulatory activities. For example, *F. hepatica* omega–class GST (GSTO2) was synthetically produced and incubated with murine macrophages *in vitro*, whereby it was demonstrated to decrease cell viability, induce apoptosis and decrease mRNA expression of anti–inflammatory cytokines IL–10 and TGF–β (Wang *et al.*, 2022). Furthermore, *F. hepatica* sigma–class GST (FhGST–S1) when incubated with dendritic cells *in vitro* induced prostaglandin synthesis (LaCourse *et al.*, 2012). Once actions are identified *in vitro*, target proteins can also be assessed *in vivo*, such as in LaCourse *et al.* (2012) where the synthesised FhGST–S1 was used to vaccinate goats and demonstrated

an increase in immunoglobulin G (IgG) levels with a reduction of liver hepatic lesions associated with infection.

6.2.2 Future directions on *A. perfoliata* transcriptome

Further research on the transcriptome of *A. perfoliata* can uncover numerous dimensions to enhance our comprehension of its biology and its interactions with the host. An uncharted research domain involves conducting comparative transcriptomic analyses of *A. perfoliata* sourced from diverse geographical locations or host populations. This exploration can illuminate genetic variations, potential adaptation mechanisms, and variations in virulence or host preference (Hahn *et al.*, 2020; Sistermans *et al.*, 2023). Furthermore, the investigation and comparison of the temporal expression dynamics of *A. perfoliata* transcripts engaged in critical biological processes throughout the life cycle, including various developmental stages and during host infection, is imperative. Specifically, it is essential to identify key transcripts that undergo upregulation or downregulation during *A. perfolita* infection (Pereira *et al.*, 2022). Notably, to investigate the broader context of their roles in host–parasite interactions, computational approaches can be harnessed to predict gene regulatory networks (GRNs), signalling pathways involving the key transcripts, or host–parasite protein–protein interaction (PPI) networks (Dyer *et al.*, 2007; Ahn *et al.*, 2017; Soyemi *et al.*, 2018; Paludo *et al.*, 2020; Cui *et al.*, 2021). Additionally, further validation and functional studies are indispensable to deepen our comprehension, focusing on the expression patterns and functional significance of the prioritised key transcripts. Experimental techniques such as qRT–PCR, *in situ* hybridization, or immunohistochemistry can be employed for this purpose (Britos *et al.*, 2007; Camicia *et al.*, 2008; Förster *et al.*, 2018). Perturbing the expression of these transcripts through techniques like RNA interference (RNAi) or gene editing is required to assess their influence on infection dynamics or host immune responses (Lalawmpuii and Lalrinkima, 2023).

Given the focus of this thesis on the transcriptome (Chapter 2), and considering that PZQ is the drug commonly used for *A. perfoliata* treatment, it would be intriguing to investigate the transcriptomic changes in *A. perfoliata* following PZQ treatment. This analysis aims to identify genes or pathways that exhibit differential expression in response to PZQ and explore their potential role in PZQ response and resistance mechanisms.

6.2.3 Isolation and proteomic characterisation of the *A. perfoliata* secretome

It is well established that helminth parasites secrete bioactive molecules during infection. More recently, this knowledge has expanded to include EVs, which make a significant contribution to the secretome. EVs are also recognised to contain key secretory proteins that are likely involved in intercellular communication and immunomodulation of the host (Eichenberger *et al.*, 2018; Maizels *et al.*, 2018; Zakeri *et al.*, 2018). Using a proteomic lead approach, in conjunction with transcriptome reference databases and bioinformatics support, I undertook the first proteomic profiling of the *A. perfoliata* secretome, providing an in–depth understanding of the likely molecular mechanisms involved in the host–parasite interaction and in host immune modulation (Wititkornkul *et al.*, 2021), as also demonstrated for nematodes (Grzelak *et al.*, 2020; Kobpornchai *et al.*, 2020; Gillis-Germitsch *et al.*, 2021; Maruszewska-Cheruiyot *et al.*, 2021), trematodes (Ma *et al.*, 2021; Kenney *et al.*, 2022) and cestodes (Bień *et al.*, 2016; Mazanec *et al.*, 2021; Wu *et al.*, 2021). At this point, the proteome of the *A. perfoliata* secretome had not yet been investigated, yet since completion of this study (Wititkornkul *et al.*, 2021), an additional investigation has since been published complementing this work (Hautala *et al.*, 2022). Hautala *et al.* (2022) additionally incorporated an aspect of immunoproteomic, therefore supporting the identification and immune recognition of proteins within the *A. perfoliata* secretome. However, more functional studies are required, such as those completed within this thesis (Chapter 4) to identify potential immune modulatory properties of the secretome components, either with the use of whole EVs or individual immune modulatory proteins which were previously identified in Chapter 2.

Thus, Chapter 3 successfully addressed the thesis aim of resolving the lack of the proteomic profile of adult *A. perfoliata* secretome including whole EVs, EV surface expressed proteins, and EV depleted ESP >10 kDa. This thesis is the first to successfully perform an *in vitro* maintenance of *A. perfoliata* from natural infections within the equine caecum and obtain the *in vitro* secretome. The secretome was then fractioned using size exclusion chromatography to obtain *A. perfoliata* whole EVs and EV depleted ESP >10 kDa. In doing so, this thesis is the first to confirm that *A. perfoliata* actively secrete EVs as a part of their complete secretome. Identified EVs demonstrated similar morphology to EVs from other closely related cestodes such as *H. diminuta* (Mazanec *et al.*, 2021) and *E. granulosus* (Siles-

Lucas *et al.*, 2017; Nicolao *et al.*, 2019; Zhou *et al.*, 2019; Wu *et al.*, 2021) as characterised via TEM and NTA. However, the secretion of EVs in helminths has thus far been limited to *in vitro* maintenance investigations. Therefore, it is of importance to examine the predicted *in vivo* secretion of EVs to confirm EV release within the host. Potential meta–proteomics studies (Marzano *et al.*, 2017; Starr *et al.*, 2018; Issa Isaac *et al.*, 2019; Armengaud, 2023) may provide the solution if EVs could be successfully purified from infected host caecal contents. This highlights the potential that EV protein profiles may vary between *in vitro* maintenance conditions, such as incubation times, incubation media and the stage of worm, compared to EVs naturally released *in vivo*.

The characterisation of *A. perfoliata* EVs revealed many common EV markers which have been reported in Exocarta (Mathivanan *et al.*, 2012; Keerthikumar *et al.*, 2016) and Vesiclepedia (Kalra *et al.*, 2012) and are consistent to common EVs in previous cestode studies (Ancarola *et al.*, 2017; Liang *et al.*, 2019; Nicolao *et al.*, 2019; Zhou *et al.*, 2019; Wang *et al.*, 2020; Mazanec *et al.*, 2021; Wu *et al.*, 2021). In addition, this thesis is the first study to provide a proteome profile for the EV surface of a cestode species via surface hydrolysis and gel free proteomics revealing many well–known EV markers, comparable to those identified in *F. hepatica* (de la Torre-Escudero *et al.*, 2019) and *C. daubneyi* (Allen *et al.*, 2021). These identified proteins indicate the validity of the *A. perfoliata* secretome in this thesis.

When looking at the 462 putative immune modulatory sequences previously identified within the *A. perfoliata* transcriptome, this thesis confirmed a total of 50 putative immune modulators. Sigma and Omega class GSTs, HSP90–α isoform, α–Enolase, and Calpain, were expressed at the protein level and contributed to part of the *A. perfoliata* secretome. Given the recognised roles of EVs in cell–cell communication and the documented evidence of helminth EVs modulating host immune cells (Drurey and Maizels, 2021; Sánchez-López *et al.*, 2021), confirmation of *A. perfoliata* EV immunomodulatory activity was therefore a priority and was elucidated within Chapter 4.

Interestingly, momentum has been gathering on the presence of a conserved class of small non–coding RNAs (microRNAs, miRNAs) within EVs derived from alternative platyhelminths such as in *S. japonicum* (Zhu *et al.*, 2016), *E. multilocularis* (Zheng *et al.*, 2017; Ding *et al.*, 2019), *M. corti, T. crassiceps* (Ancarola *et al.*, 2017) and *Taenia pisiformis* (Wang *et al.*, 2020). miRNAs have since had immune modulatory roles assigned to them and have thus been associated

with host–parasite interactions and parasite survival (Rojas-Pirela *et al.*, 2022). Therefore, future characterisation of miRNAs secreted in *A. perfoliata* EVs could be performed to provide the deeper insight into further mechanisms likely involved in the host–parasite interaction.

The most research in helminths EV biogenesis have been studied in trematodes such as *F. hepatica*, whereby *in vitro* maintenance demonstrated that larger EVs are primarily derived from gastrodermal cells, secreted via excretory pores, whilst smaller EVs are derived from multivesicular bodies within the tegumental syncytium (Cwiklinski *et al.*, 2015; Davis *et al.*, 2019; Bennett *et al.*, 2020). In comparison to cestodes, where a digestive tract is absent (Margulis and Chapman, 2009), EVs derived from *H. diminuta* (Mazanec *et al.*, 2021), *E. multilocularis*, *T. crassiceps* and *M. corti* (Ancarola *et al.*, 2017) were observed budding from the tegument, around the surface and among the scolex, neck and proglottids. Accordingly, different EV sub–populations were shown to be secreted by trematodes (Cwiklinski *et al.*, 2015; Davis *et al.*, 2019; Bennett *et al.*, 2020) and cestodes (Wu *et al.*, 2021; Yang *et al.*, 2021), whereby each sub–population of EVs have distinct size, cargo molecules and site of origin, suggesting a distinct role in host–parasite interaction. As a result, future research is needed to determine whether *A. perfoliata* EVs are released from excretory pores or directly from the tegument as well as whether different EV sub–populations are secreted. Additionally, performing gene expression analysis using techniques like quantitative PCR (qPCR) or RNA sequencing to examine changes in gene expression patterns induced by *Anoplocephala perfoliata* EVs could be performed.

6.2.4 Immunomodulatory activity of *A. perfoliata* EVs on the host immune response

The success of an integrated *A. perfoliata* transcriptomic (Chapter 2) and proteomic approach to support the protein composition of the secretome (Chapter 3) (Wititkornkul *et al.*, 2021), allow for further in depth–discovery of EV markers and potential immune modulators within the *A. perfoliata* secretome. As demonstrated in other platyhelminths, EVs are taken up by host immune cells *in vitro* resulting in an alteration on the host immune cell response (Sánchez-López *et al.*, 2021). Therefore, an immunomodulatory activity and function of *A. perfoliata* EVs were confirmed and elucidated in Chapter 4.

Chapter 4 successfully addressed the thesis aim of resolving the investigation of *A. perfoliata* EVs on immunomodulatory activities and elucidating the ability to modulate the

mammalian immune response *in vitro*. It is firstly important to asses whether the mammalian host immune cell is able to uptake the *A. perfoliata* EVs, as such the initial investigations assessed uptake of *A. perfoliata* EVs by THP–1 macrophages using confocal microscopy and flow cytometry. This thesis confirmed that *A. perfoliata* EVs were taken up by THP–1 macrophages, as demonstrated for other helminth EVs (Chapter 4, Table 4.1). However, at present this work does not demonstrate a mode of action of the uptake process. Given the importance of the surface molecules of EVs, which are likely play a key role in cell–cell communication as well as mediate EV uptake (de la Torre-Escudero *et al.*, 2019), future work should verify this EV uptake by using EV surface proteins such as tetraspanin in *O. viverrini* (Chaiyadet *et al.*, 2015, 2019, 2022) and *S. mansoni* (Kifle *et al.*, 2020), glycosidase in *F. hepatica* (de la Torre-Escudero *et al.*, 2019) and Cytochalasin D in *H. polygyrus* (Coakley *et al.*, 2017) to block EV uptake. If these EV surface molecules block EV uptake, further interactions on the THP–1 macrophages such as cell viability and cytokine production will likely be inhibited (Chaiyadet *et al.*, 2015, 2019, 2022; Coakley *et al.*, 2017; de la Torre-Escudero *et al.*, 2019; Kifle *et al.*, 2020; Kuipers *et al.*, 2020). Since the percentage of uptake varies between helminth species, host cell types and exposure time (Chapter 4, Table 4.1), additional research into the uptake of *A. perfoliata* EVs with other host cells are required, particularly using dendritic cells, Th lymphocytes, organoids tissue (large intestine and caecum) or caecal epithelial cells of the horse in the *in vitro* co–culture system (Britton *et al.*, 2023). Furthermore, I previously discussed the role of miRNAs present in *A. perfoliata* EVs in Section 6.2.2, which may provide an in–depth mechanisms likely involved in the host–parasite interaction. Thus, an uptake of miRNAs by the mammalian immune cells could be further performed.

When looking at consequence of EV uptake by THP–macrophages, to elucidate whether *A. perfoliata* EV uptake influences the host immune response, cell viability and cytokine production within THP–macrophages were investigated. This thesis is the first in platyhelminths to utilise three methods including trypan blue, MTT assays and flow cytometry to quantify cell viability post EV uptake. Cell viability of THP–1 macrophages decreased following exposure to EVs from 6 to 24 hours *in vitro*. Moreover, Th1 cytokines (TNF–α, IL1–α and IL1–β with IFN–γ tended to increase) were predominantly released from EV exposed THP–1 macrophages after 24 hours *in vitro*. Taken together these findings confirm that an

interaction between *A. perfoliata* EVs and THP–1 macrophages was established post EV uptake. Given the focus of this thesis on the immunomodulatory activity and function of *A. perfoliata* EVs, future study at the molecular level, such as the analysis of differential gene expression (Chen *et al.*, 2012; Buck *et al.*, 2014; Zhu *et al.*, 2016; Zawistowska-Deniziak *et al.*, 2017; Kifle *et al.*, 2020) and cytokine gene expression (Zheng *et al.*, 2017; Lawson *et al.*, 2019) in *A. perfoliata* EV exposed THP–1 macrophages is essential to facilitate in–depth analyses of immune regulation involved in host–parasite interaction.

Apart from the effect of *A. perfoliata* EVs on cell proliferation, cell apoptosis and cell permeability, as well as complete cytokine profiles in the investigation as previously discussed in Chapter 4. However, the interaction between the host and parasite is complex and the response might differ within the *in vitro* conditions used in the present study, compared to the whole animal *in vivo*. Therefore, an *in vivo* experiment by administration of *A. perfoliata* EVs in laboratory animals (Sánchez-López *et al.*, 2021) or in naturally *A. perfoliata* infected horses could be useful in comparison to the potential *in vivo* and *in vitro* immunomodulatory functions and effects of *A. perfoliata* EVs. Furthermore, individual putative immune modulatory proteins identified in Chapter 3 may be also applied to elucidate their immune modulatory activity and function. Interestingly, an *ex vivo* tissue explant culture with an equine caecal tissue such as caecal lamina propria (Pittaway *et al.*, 2014; Lawson *et al.*, 2019), where *A. perfoliata* attach during infection may provide greater specificity of *A. perfoliata* EVs interactions within the host environment. Thus, an investigation on the internalisation and localisation of *A. perfoliata* EVs within the explants or cells using fluorescence microscopy or other imaging techniques should be further performed.

6.2.5 Praziquantel–equine hindgut microbiome interactions

PZQ is a choice anthelmintic for the control of *A. perfoliata* which, in the majority, reside attached to the caecal wall at the ileocaecal valve (Gasser *et al.*, 2005; Nielsen, 2016). Thus, *A. perfoliata in vivo* is in intimate contact with the host and the caecal contents. The equine hindgut, inclusive of the caecum, is a habitat for microbes to enhance fermentation of fibre, providing nutrients and energy to the host horse and supporting hindgut homeostasis (Argenzio *et al.*, 1974; Bergman, 1990; Costa and Weese, 2012). However, treatment of *A. perfoliata* with PZQ may have further consequences on the fragile equine hindgut

microbiome, which is prone to fluctuations in microbial composition as a result of various factors (Garber *et al.*, 2020; Theelen *et al.*, 2021; Chaucheyras-Durand *et al.*, 2022). The majority of equine hindgut microbiome studies utilise either a faecal microbiome sampling technique or *in vitro* models of the equine hindgut. This work employed an *in vitro* hindgut microbial fermentation model using a batch system for *in vitro* gas production, which allows a variety of doses of PZQ to be tested in a more controlled manner (Theodorou *et al.*, 1994).

Chapter 5 successfully addressed the thesis aim of resolving the investigation of PZQ on the functionality of the equine hindgut microbiome based on microbial fermentation activities and products associated with microbial fermentation using an *in vitro* hindgut microbial fermentation model (Theodorou *et al.*, 1994). The study utilised faeces of horses as an initial inoculum with meadow hay and barley at 70:30 ratio as a substrate and investigated three different PZQ dosages representing a low dose (0.03 mmol/L), a recommended treatment dose (0.08 mmol/L) and a high dose (0.13 mmol/L) of PZQ compared to a control (0.00 mmol/L) on the *in vitro* fermentation over 72 hours.

The work in this thesis chapter provides the first evidence on the investigation of the impact of PZQ on the equine hindgut microbial fermentation activity. The overall result of the fermentation activities and products of the equine hindgut after exposure to PZQ treatments at the tested dosage levels suggests that there were minor alterations on the equine hindgut fermentation pathway which could impact on the nutritional functioning of the caecum. It is highlighted that there was no major change to the functioning of the equine microbiome, yet, PZQ at a higher (0.13 mmol/L) than recommended dose likely alters the fermentation pathways in the equine hindgut demonstrated by increased butyrate and decreased acetate level at 24 hours and increased ammonia at 72 hours. Furthermore, the thesis findings demonstrate that appropriate PZQ dosage administration is safe for equine hindgut microbiota, whereas inappropriate over–dosing of horses with PZQ may alter microbial activities in the equine hindgut and as such, lead to an issue with nutritional heath of the caecum. These findings need further investigation, especially *in vivo*.

The *in vitro* gas production model used in this study is a batch culture–based system (Coles *et al.*, 2005). Thus, all the provided substrate is likely to have been degraded over the fermentation period, resulting in alterations to the equine hindgut fermentation activity and growth and function of certain bacterial communities such as fibrolytic bacteria (Wunderlich

et al., 2023) potentially being unsupported. Therefore, a semi–continuous, dynamic *in vitro* fermentation system such as EQUITEC (Deitmers *et al.*, 2022) and CAESITEC (Zeyner *et al.*, 2006; Dill *et al.*, 2007), are recommended whereby substrates are refreshed daily, more akin to the regular feeding of a horse.

There are various future experiments that could be performed for the extensive investigation and complete assessment of PZQ induced alterations to the microbiome such as investigation on the correlation of the fermentation kinetics profile, fermentation products and specific known key metabolites and with the presence of known faecal/caecal/colonic microbial communities by meta–taxonomy in conjunction with metagenomics and/or meta–proteomic analysis. Moreover, an *in vitro* hindgut model system or an *ex vivo* explant culture of caecal tissue with and without the presence of *A. perfoliata*, as well as performing an *in vivo* trial to further investigate PZQ impact would be very useful for further investigation to provide an insight into the interaction between parasite, host and hindgut microbiome.

Given the focus of this thesis on the secretome components, it would also be prudent to investigate the impact of such secretome components on the *in vitro* microbiome. Initially, experiments would likely start with *A. perfoliata* derived EVs but may also examine key secretome proteins or potential secreted antimicrobial peptides (AMPs) (Rooney et al., 2022). Finally, with the revelation that EVs are likely players in anthelmintic exposure (Davis *et al.*, 2020), it would be interesting to examine the role *A. perfoliata* EVs on PZQ uptake. Furthermore, additional *in vitro* hindgut model studies examining PZQ exposure, with the inclusion of *A. perfoliata*, will allow investigation into PZQ uptake by EVs. These EVs may not solely derive from *A. perfoliata* but also encompass those from microbial origins.

6.3 CONCLUSIONS

The research conducted throughout this thesis has addressed all of the aims. I contributed to the study of *A. perfoliata* by generating its transcriptome and providing support. This led to the characterisation of the secretome and the remarkable discovery of EVs in *A. perfoliata*. I confirmed that *A. perfoliata* EVs have immunomodulatory functions and the ability to modulate the mammalian immune response. In addition, I demonstrated the impact of PZQ on equine hindgut microbiota activity *in vitro*. Therefore, future work should now consider how *A. perfoliata* EVs or key components within EVs could be further expanded from the laboratory to clinical application as potential biomarkers, diagnostics and therapeutic tools, as well as vaccine candidates for *A. perfoliata* infected horses. Furthermore, utilising immune–proteomics could be essential for the discovery of immune interactions and recognition, which may lead to a better understanding of further diagnostics or vaccine candidates.

Novel datasets generated by the transcriptomic, proteomic and bioinformatic approaches in this thesis can be applied to future studies allowing further comprehensive studies on *A. perfoliata.* This first equine flatworm transcriptome (with exception of *Fasciola* spp.) would allow a comparative study with the other cestodes. Ultimately, these novel datasets provide numerous opportunities for the broader helminth community. For instance, the transcriptome dataset enables researchers interested in genetic comparative studies to conduct comparative work, as demonstrated in a recent publication by Hautala *et al.* (2022) on *A. perfoliata*. Furthermore, the proteomics datasets of *A. perfoliata* secretome offer valuable resources for those investigating the biology of EVs in helminths. These datasets can be utilised for comparative analyses of EVs biogenesis and for the development of common biomarkers among helminths. Moreover, my work is beneficial to individuals interested in discovering potential biomarkers or developing diagnostic tools, such as the Equisal tapeworm saliva test kit. It also caters to those in need of identifying potential drug targets and vaccine candidates. Lastly, the practical implications of PZQ administration, especially at high doses, on hindgut microbiota in my study are of practical concern for the treatment and control of *A. perfoliata.*

To this end, this thesis significantly advances my understanding of *A. perfoliata*, the *A. perfoliata* secretome, the interaction of *A. perfoliata* EVs with the host and the effect of PZQ on equine hindgut microbiota. The generated datasets will enable broader research, which is not only for *A. perfoliata* but also a wide spectrum of disciplines and backgrounds in other helminth species.

7.0 REFERENCES

Abbott, J.B., Mellor, D.J., Barrett, E.J., Proudman, C.J. and Love, S. (2008) 'Serological changes observed in horses infected with *Anoplocephala perfoliata* after treatment with praziquantel and natural reinfection', *Veterinary Record*, 162(2), pp. 50–53. Available at: https://doi.org/10.1136/vr.162.2.50.

Abels, E.R. and Breakefield, X.O. (2016) 'Introduction to Extracellular Vesicles: Biogenesis, RNA Cargo Selection, Content, Release, and Uptake', *Cellular and molecular neurobiology*. 2016/04/06, 36(3), pp. 301–312. Available at: https://doi.org/10.1007/s10571-016-0366-z.

Afgan, E. *et al.* (2018) 'The Galaxy platform for accessible, reproducible and collaborative biomedical analyses: 2018 update', *Nucleic Acids Research*, 46(W1), pp. W537–W544. Available at: https://doi.org/10.1093/nar/gky379.

Aguayo, V., Valdés Fernandez, B.N., Rodríguez-Valentín, M., Ruiz-Jiménez, C., Ramos-Benítez, M.J., Méndez, L.B. and Espino, A.M. (2019) '*Fasciola hepatica* GST downregulates NF-κB pathway effectors and inflammatory cytokines while promoting survival in a mouse septic shock model', *Scientific Reports 2019 9:1*, 9(1), pp. 1–16. Available at: https://doi.org/10.1038/s41598-018-37652-x.

Agus, A., Clément, K. and Sokol, H. (2021) 'Gut microbiota-derived metabolites as central regulators in metabolic disorders', *Gut*, 70(6), pp. 1174 LP – 1182. Available at: https://doi.org/10.1136/gutjnl-2020-323071.

Ahn, C.S., Kim, J.G., Han, X., Kang, I. and Kong, Y. (2017) 'Comparison of *Echinococcus multilocularis* and *Echinococcus granulosus* hydatid fluid proteome provides molecular strategies for specialized host-parasite interactions', *Oncotarget*, 8(57), pp. 97009–97024. Available at: https://doi.org/10.18632/oncotarget.20761.

Ajibola, O., Penumutchu, S., Gulumbe, B., Aminu, U. and Belenky, P. (2023) 'Longitudinal Analysis of the Impacts of Urogenital Schistosomiasis on the Gut microbiota of Adolescents in Nigeria', pp. 1–19.

Alberro, A., Iparraguirre, L., Fernandes, A. and Otaegui, D. (2021) 'Extracellular Vesicles in Blood: Sources, Effects, and Applications', *International journal of molecular sciences*, 22(15), p. 8163. Available at: https://doi.org/10.3390/ijms22158163.

Alexandra, S., Rainer, R., Peter, F., Hans, S., D., W.R. and Eva, L. (2003) 'A Dominant Role for Extracellular Glutathione S-Transferase from *Onchocerca volvulus* Is the Production of Prostaglandin D2', *Infection and Immunity*, 71(6), pp. 3603–3606. Available at: https://doi.org/10.1128/IAI.71.6.3603-3606.2003.

Allen, N.R., Taylor-Mew, A.R., Wilkinson, T.J., Huws, S., Phillips, H., Morphew, R.M. and Brophy, P.M. (2021) 'Modulation of Rumen Microbes Through Extracellular Vesicle Released by the Rumen Fluke *Calicophoron daubneyi*', *Frontiers in Cellular and Infection Microbiology*, 11, p. 263. Available at: https://doi.org/10.3389/fcimb.2021.661830.

Almiñana, C., Rudolf Vegas, A., Tekin, M., Hassan, M., Uzbekov, R., Fröhlich, T., Bollwein, H. and Bauersachs, S. (2021) 'Isolation and Characterization of Equine Uterine Extracellular Vesicles: A Comparative Methodological Study', *International journal of molecular sciences*, 22(2), p. 979. Available at: https://doi.org/10.3390/ijms22020979.

Alsaqabi, S.M. (2014) 'Praziquantel: A Review', *Journal of Veterinary Science & Technology*, 05(05). Available at: https://doi.org/10.4172/2157-7579.1000200.

Altschul, S.F., Madden, T.L., Schäffer, A.A., Zhang, J., Zhang, Z., Miller, W. and Lipman, D.J. (1997) 'Gapped BLAST and PSI-BLAST: a new generation of protein database search programs', *Nucleic acids*

research, 25(17), pp. 3389–3402. Available at: https://doi.org/10.1093/nar/25.17.3389.

Ancarola, M.E., Lichtenstein, G., Herbig, J., Holroyd, N., Mariconti, M., Brunetti, E., Berriman, M., Albrecht, K., Marcilla, A., Rosenzvit, M.C., Kamenetzky, L., Brehm, K. and Cucher, M. (2020) 'Extracellular non-coding RNA signatures of the metacestode stage of *Echinococcus multilocularis*', *PLOS Neglected Tropical Diseases*, 14(11), p. e0008890. Available at: https://doi.org/10.1371/journal.pntd.0008890.

Ancarola, M.E., Marcilla, A., Herz, M., Macchiaroli, N., Pérez, M., Asurmendi, S., Brehm, K., Poncini, C., Rosenzvit, M. and Cucher, M. (2017) 'Cestode parasites release extracellular vesicles with microRNAs and immunodiagnostic protein cargo', *International Journal for Parasitology*, 47(10–11), pp. 675–686. Available at: https://doi.org/10.1016/j.ijpara.2017.05.003.

Anderson, M.J. (2017) 'Permutational Multivariate Analysis of Variance (PERMANOVA)', in *Wiley StatsRef: Statistics Reference Online*, pp. 1–15. Available at: https://doi.org/https://doi.org/10.1002/9781118445112.stat07841.

Andreu, Z. and Yáñez-Mó, M. (2014) 'Tetraspanins in extracellular vesicle formation and function', *Frontiers in Immunology*, 5(SEP), p. 442. Available at: https://doi.org/10.3389/fimmu.2014.00442.

Andrews, P. (1985) 'Praziquantel: mechanisms of anti-schistosomal activity', *Pharmacology & Therapeutics*, 29(1), pp. 129–156. Available at: https://doi.org/https://doi.org/10.1016/0163-7258(85)90020-8.

Andrews, P., Thomas, H., Pohlke, R. and Seubert, Jür. (1983) 'Praziquantel', *Medicinal Research Reviews*, 3(2), pp. 147–200. Available at: https://doi.org/https://doi.org/10.1002/med.2610030204.

Andrews, S. (2010) 'FastQC: a quality control tool for high throughput sequence data'. Available at: http://www.bioinformatics.babraham.ac.uk/projects/fastqc.

Andrews, S., Krueger, F., Seconds-Pichon, A., Biggins, F. and Wingett, S. (2015) 'FastQC. A quality control tool for high throughput sequence data. Babraham Bioinformatics', 1(1), p. undefined-undefined. Available at: https://www.bioinformatics.babraham.ac.uk/projects/fastqc/%0Ahttp://www.bioinformatics.bbsrc.ac.uk/projects/fastqc/ (Accessed: 25 June 2021).

Arbildi, P., La-Rocca, S., Kun, A., Lorenzatto, K.R., Monteiro, K.M., Zaha, A., Mourglia-Ettlin, G., Ferreira, H.B. and Fernández, V. (2021) 'Expression and distribution of glutathione transferases in protoscoleces of *Echinococcus granulosus* sensu lato', *Acta Tropica*, 221, p. 105991. Available at: https://doi.org/10.1016/J.ACTATROPICA.2021.105991.

Arbildi, P., Turell, L., López, V., Alvarez, B. and Fernández, V. (2017) 'Mechanistic insights into EgGST1, a Mu class glutathione S-transferase from the cestode parasite *Echinococcus granulosus*', *Archives of biochemistry and biophysics*, 633, pp. 15–22. Available at: https://doi.org/10.1016/J.ABB.2017.08.014.

Argenzio, R., Southworth, M. and Stevens, C. (1974) 'Sites of organic acid production and absorption in the equine gastrointestinal tract', *American Journal of Physiology-Legacy Content*, 226(5), pp. 1043–1050. Available at: https://doi.org/10.1152/ajplegacy.1974.226.5.1043.

Armengaud, J. (2023) 'Metaproteomics to understand how microbiota function: The crystal ball predicts a promising future', *Environmental Microbiology*, 25(1), pp. 115–125. Available at: https://doi.org/https://doi.org/10.1111/1462-2920.16238.

Arnold, C.E., Isaiah, A., Pilla, R., Lidbury, J., Coverdale, J.S., Callaway, T.R., Lawhon, S.D., Steiner, J. and Suchodolski, J.S. (2020) 'The cecal and fecal microbiomes and metabolomes of horses before and after metronidazole administration', *PLOS ONE*. Edited by C. Ratnasekhar, 15(5), p. e0232905. Available at:

https://doi.org/10.1371/journal.pone.0232905.

Artis, D., Humphreys, N.E., Bancroft, A.J., Rothwell, N.J., Potten, C.S. and Grencis, R.K. (1999) 'Tumor Necrosis Factor α Is a Critical Component of Interleukin 13–Mediated Protective T Helper Cell Type 2 Responses during Helminth Infection', *Journal of Experimental Medicine*, 190(7), pp. 953–962. Available at: https://doi.org/10.1084/jem.190.7.953.

Ayón-Núñez, D.A., Fragoso, G., Bobes, R.J. and Laclette, J.P. (2018) 'Plasminogen-binding proteins as an evasion mechanism of the host's innate immunity in infectious diseases', *Bioscience Reports*, 38(5), p. BSR20180705. Available at: https://doi.org/10.1042/BSR20180705.

Ayón-Núñez, D.A., Fragoso, G., Espitia, C., García-Varela, M., Soberón, X., Rosas, G., Laclette, J.P. and Bobes, R.J. (2018) 'Identification and characterization of *Taenia solium* enolase as a plasminogen-binding protein', *Acta Tropica*, 182, pp. 69–79. Available at: https://doi.org/https://doi.org/10.1016/j.actatropica.2018.02.020.

Ayoub, C. (2022) 'Fecal Microbiota of Healthy horses and horses with Colitis and its association with Laminitis and Survival'. University of Guelph.

Babbitt, P.C., Hasson, M.S., Wedekind, J.E., Palmer, D.R.J., Barrett, W.C., Reed, G.H., Rayment, I., Ringe, D., Kenyon, G.L. and Gerlt, J.A. (1996) 'The Enolase Superfamily: A General Strategy for Enzyme-Catalyzed Abstraction of the α-Protons of Carboxylic Acids', *Biochemistry*, 35(51), pp. 16489–16501. Available at: https://doi.org/10.1021/bi9616413.

Back, H., Nyman, A. and Osterman Lind, E. (2013) 'The association between *Anoplocephala perfoliata* and colic in Swedish horses—A case control study', *Veterinary Parasitology*, 197(3), pp. 580–585. Available at: https://doi.org/10.1016/j.vetpar.2013.07.020.

Backe, S.J., Sager, R.A., Woodford, M.R., Makedon, A.M. and Mollapour, M. (2020) 'Post-translational modifications of Hsp90 and translating the chaperone code', *The Journal of biological chemistry*. 2020/06/11, 295(32), pp. 11099–11117. Available at: https://doi.org/10.1074/jbc.REV120.011833.

Bae, Y.-A., Ahn, D.-W., Lee, E.-G., Kim, S.-H., Cai, G.-B., Kang, I., Sohn, W.-M. and Kong, Y. (2013) 'Differential Activation of Diverse Glutathione Transferases of *Clonorchis sinensis* in Response to the Host Bile and Oxidative Stressors', *PLOS Neglected Tropical Diseases*, 7(5), p. e2211. Available at: https://doi.org/10.1371/journal.pntd.0002211.

Bae, Y.-A., Kim, J.-G. and Kong, Y. (2016) 'Phylogenetic characterization of *Clonorchis sinensis* proteins homologous to the sigma-class glutathione transferase and their differential expression profiles', *Molecular and Biochemical Parasitology*, 206(1), pp. 46–55. Available at: https://doi.org/https://doi.org/10.1016/j.molbiopara.2016.01.002.

Bai, Y., Zhang, Z., Jin, L., Zhu, Y., Zhao, L., Shi, B., Li, J., Guo, G., Guo, B., McManus, D.P., Wang, S. and Zhang, W. (2020) 'Dynamic Changes in the Global Transcriptome and MicroRNAome Reveal Complex miRNA-mRNA Regulation in Early Stages of the Bi-Directional Development of *Echinococcus granulosus* Protoscoleces', *Frontiers in Microbiology*, 11, p. 654. Available at: https://doi.org/10.3389/FMICB.2020.00654/BIBTEX.

Baietti, M.F., Zhang, Z., Mortier, E., Melchior, A., Degeest, G., Geeraerts, A., Ivarsson, Y., Depoortere, F., Coomans, C., Vermeiren, E., Zimmermann, P. and David, G. (2012) 'Syndecan–syntenin–ALIX regulates the biogenesis of exosomes', *Nature Cell Biology*, 14(7), pp. 677–685. Available at: https://doi.org/10.1038/ncb2502.

Bain, S.A. and Kelly, J.D. (1977) 'Prevalence and pathogenicity of *Anoplocephala perfoliata* in a horse population in South Auckland', *New Zealand Veterinary Journal*, 25(1–2), pp. 27–28. Available at: https://doi.org/10.1080/00480169.1977.34343.

Baltrušis, P., Halvarsson, P. and Höglund, J. (2019) 'Molecular detection of two major gastrointestinal parasite genera in cattle using a novel droplet digital PCR approach', *Parasitology Research*, 118(10), pp. 2901–2907. Available at: https://doi.org/10.1007/s00436-019-06414-7.

Baltrušis, P. and Höglund, J. (2023) 'Digital PCR: modern solution to parasite diagnostics and population trait genetics', *Parasites and Vectors*, 16(1), pp. 1–9. Available at: https://doi.org/10.1186/s13071-023-05756-7.

Barclay, W.P., Phillips, T.N. and Foerner, J.J. (1982) 'Intussusception associated with *Anoplocephala perfoliata* infection in five horses.', *Journal of the American Veterinary Medical Association*, 180(7), pp. 752–753.

Barrett, E.J., Farlam, J. and Proudman, C.J. (2004) 'Field trial of the efficacy of a combination of ivermectin and praziquantel in horses infected with roundworms and tapeworms', *Veterinary Record*, 154(11), pp. 323–325. Available at: https://doi.org/10.1136/vr.154.11.323.

Barrett, J. (1997) 'Helminth detoxification mechanisms', in *Journal of Helminthology*. Cambridge University Press, pp. 85–89. Available at: https://doi.org/10.1017/s0022149x0001573x.

Barrett, J. (1998) 'Cytochrome P450 in parasitic protozoa and helminths', *Comparative biochemistry and physiology. Part C, Pharmacology, toxicology & endocrinology*, 121(1–3), pp. 181–183. Available at: https://doi.org/10.1016/S0742-8413(98)10039-7.

Barrett, J. (2009) 'Forty years of helminth biochemistry', *Parasitology*. 2009/03/06, 136(12), pp. 1633–1642. Available at: https://doi.org/10.1017/S003118200900568X.

Belkaid, Y. and Hand, T.W. (2014) 'Role of the Microbiota in Immunity and Inflammation', *Cell*, 157(1), pp. 121–141. Available at: https://doi.org/10.1016/J.CELL.2014.03.011.

Bennett, A.P.S., de la Torre-Escudero, E., Oliver, N.A.M., Huson, K.M. and Robinson, M.W. (2020) 'The cellular and molecular origins of extracellular vesicles released by the helminth pathogen, *Fasciola hepatica*', *International Journal for Parasitology*, 50(9), pp. 671–683. Available at: https://doi.org/10.1016/j.ijpara.2020.03.015.

Berg, G. *et al.* (2020) 'Correction to: Microbiome definition re-visited: old concepts and new challenges', *Microbiome*, 8(1), p. 119. Available at: https://doi.org/10.1186/s40168-020-00905-x.

Bergman, E.N. (1990) 'Energy contributions of volatile fatty acids from the gastrointestinal tract in various species', *Physiological Reviews*, 70(2), pp. 567–590. Available at: https://doi.org/10.1152/physrev.1990.70.2.567.

Bergmann, S., Wild, D., Diekmann, O., Frank, R., Bracht, D., Chhatwal, G.S. and Hammerschmidt, S. (2003) 'Identification of a novel plasmin(ogen)-binding motif in surface displayed α-enolase of *Streptococcus pneumoniae*', *Molecular Microbiology*, 49(2), pp. 411–423. Available at: https://doi.org/https://doi.org/10.1046/j.1365-2958.2003.03557.x.

Bernal, D., de la Rubia, J.E., Carrasco-Abad, A.M., Toledo, R., Mas-Coma, S. and Marcilla, A. (2004) 'Identification of enolase as a plasminogen-binding protein in excretory–secretory products of *Fasciola hepatica*', *FEBS Letters*, 563(1), pp. 203–206. Available at: https://doi.org/https://doi.org/10.1016/S0014-5793(04)00306-0.

Beroza, G.A. (1983) 'Cecal perforation and peritonitis associated with *Anoplocephala perfoliata* infection in three horses', *J. Am. Vet. Med. Assoc.*, 183, pp. 804–806.

Beroza, G.A., Marcus, L.C., Williams, R. and Bauer, S.M. (1986) 'Laboratory diagnosis of *Anoplocephala perfoliata* infection in horses', *Proceedings of the American Association of Equine Practicioners*, 32, pp. 435–439.

Biddle, A.S., Black, S.J. and Blanchard, J.L. (2013) 'An In Vitro Model of the Horse Gut Microbiome Enables Identification of Lactate-Utilizing Bacteria That Differentially Respond to Starch Induction', *PLOS ONE*, 8(10), p. e77599. Available at: https://doi.org/10.1371/journal.pone.0077599.

Biebl, M.M. and Buchner, J. (2019) 'Structure, function, and regulation of the hsp90 machinery', *Cold Spring Harbor Perspectives in Biology*, 11(9), p. a034017. Available at: https://doi.org/10.1101/cshperspect.a034017.

Bień, J., Sałamatin, R., Sulima, A., Savijoki, K., Bruce Conn, D., Näreaho, A. and Młocicki, D. (2016) 'Mass spectrometry analysis of the excretory-secretory (E-S) products of the model cestode *Hymenolepis diminuta* a reveals their immunogenic properties and the presence of new E-S proteins in cestodes', *Acta Parasitologica*, 61(2), pp. 429–442. Available at: https://doi.org/10.1515/ap-2016-0058.

Blackmore, T.M., Dugdale, A., Argo, C.M., Curtis, G., Pinloche, E., Harris, P.A., Worgan, H.J., Girdwood, S.E., Dougal, K., Newbold, C.J. and McEwan, N.R. (2013) 'Strong Stability and Host Specific Bacterial Community in Faeces of Ponies', *PLoS ONE*. Edited by M.-J. Virolle, 8(9), p. e75079. Available at: https://doi.org/10.1371/journal.pone.0075079.

Blandin, A., Dugail, I., Cariou, B., Lhomme, M., Lay, S. Le, Ponnaiah, M. and Ghesquie, V. (2023) 'Report Lipidomic analysis of adipose-derived extracellular vesicles reveals specific EV lipid sorting informative of the obesity metabolic state ll ll Lipidomic analysis of adipose-derived extracellular vesicles reveals specific EV lipid sorting informati'. Available at: https://doi.org/10.1016/j.celrep.2023.112169.

Blum, M. *et al.* (2021) 'The InterPro protein families and domains database: 20 years on', *Nucleic Acids Research*, 49(D1), pp. D344–D354. Available at: https://doi.org/10.1093/nar/gkaa977.

Board, G.P., Baker, T.R., Chelvanayagam, G. and Jermin, S.L. (1997) 'Zeta, a novel class of glutathione transferases in a range of species from plants to humans', *Biochemical Journal*, 328(3), pp. 929–935. Available at: https://doi.org/10.1042/bj3280929.

Boelow, H., Krücken, J., Thomas, E., Mirams, G. and von Samson-Himmelstjerna, G. (2022) 'Comparison of FECPAKG2, a modified Mini-FLOTAC technique and combined sedimentation and flotation for the coproscopic examination of helminth eggs in horses', *Parasites and Vectors*, 15(1), pp. 1–18. Available at: https://doi.org/10.1186/s13071-022-05266-y.

Bohórquez, A., Meana, A. and Luzón, M. (2012) 'Differential diagnosis of equine cestodosis based on E/S and somatic *Anoplocephala perfoliata* and *Anoplocephala magna* antigens', *Veterinary Parasitology*, 190(1), pp. 87–94. Available at: https://doi.org/https://doi.org/10.1016/j.vetpar.2012.06.001.

Bohórquez, A., Meana, A., Pato, N.F. and Luzón, M. (2014) 'Coprologically diagnosing *Anoplocephala perfoliata* in the presence of *A. magna*', *Veterinary Parasitology*, 204(3–4), pp. 396–401. Available at: https://doi.org/10.1016/J.VETPAR.2014.04.023.

Bohórquez, G.A., Luzón, M., Martín-Hernández, R. and Meana, A. (2015) 'New multiplex PCR method for the simultaneous diagnosis of the three known species of equine tapeworm', *Veterinary Parasitology*, 207(1–2), pp. 56–63. Available at: https://doi.org/10.1016/J.VETPAR.2014.11.002.

Böing, A.N., van der Pol, E., Grootemaat, A.E., Coumans, F.A.W., Sturk, A. and Nieuwland, R. (2014) 'Single-step isolation of extracellular vesicles by size-exclusion chromatography', *Journal of Extracellular Vesicles*, 3(1). Available at: https://doi.org/10.3402/jev.v3.23430.

Boisseau, M., Dhorne-Pollet, S., Bars-Cortina, D., Courtot, E., Serreau, D., Annonay, G., Lluch, J., Gesbert, A., Reigner, F., Sallé, G. and Mach, N. (2022) 'Species interactions, stability, and resilience of the gut microbiota - helminth assemblage in horses'. Available at: https://doi.org/10.21203/RS.3.RS-1955749/V1.

Bolger, A.M., Lohse, M. and Usadel, B. (2014) 'Trimmomatic: A flexible trimmer for Illumina sequence data', *Bioinformatics*, 30(15), pp. 2114–2120. Available at: https://doi.org/10.1093/bioinformatics/btu170.

de Boom, H.P.A. (1975) 'Functional anatomy and nervous control, of the equine alimentary tract', *Journal of the South African Veterinary Association*, 46(1), pp. 5–11. Available at: https://doi.org/10.10520/EJC-204bc15e0c.

Borup, A., Boysen, A.T., Ridolfi, A., Brucale, M., Valle, F., Paolini, L., Bergese, P. and Nejsum, P. (2022) 'Comparison of separation methods for immunomodulatory extracellular vesicles from helminths', *Journal of Extracellular Biology*, 1(5), p. e41. Available at: https://doi.org/https://doi.org/10.1002/jex2.41.

Boswinkel, M. and Sloet van Oldruitenborgh-Oosterbaan, M.M. (2007) 'Correlation between colic and antibody levels against *Anoplocephala perfoliata* in horses in the Netherlands', *Tijdschrift voor Diergeneeskunde*, 132, pp. 508–512.

Bracken, M.K., Wøhlk, C.B.M., Petersen, S.L. and Nielsen, M.K. (2012) 'Evaluation of conventional PCR for detection of Strongylus vulgaris on horse farms', *Veterinary Parasitology*, 184(2–4), pp. 387–391. Available at: https://doi.org/10.1016/j.vetpar.2011.08.015.

Bradford, M.M. (1976) 'A rapid and sensitive method for the quantitation of microgram quantities of protein utilizing the principle of protein-dye binding', *Analytical Biochemistry*, 72(1–2), pp. 248–254. Available at: https://doi.org/10.1016/0003-2697(76)90527-3.

Britos, L., Lalanne, A.I., Castillo, E., Cota, G., Señorale, M. and Marín, M. (2007) '*Mesocestoides corti* (syn. vogae, cestoda): Characterization of genes encoding cysteine-rich secreted proteins (CRISP)', *Experimental Parasitology*, 116(2), pp. 95–102. Available at: https://doi.org/https://doi.org/10.1016/j.exppara.2006.11.008.

Britton, C., Laing, R., McNeilly, T.N., Perez, M.G., Otto, T.D., Hildersley, K.A., Maizels, R.M., Devaney, E. and Gillan, V. (2023) 'New technologies to study helminth development and host-parasite interactions', *International Journal for Parasitology*, 53(8), pp. 393–403. Available at: https://doi.org/https://doi.org/10.1016/j.ijpara.2022.11.012.

Brophy, P.M. and Barrett, J. (1990) 'Glutathione transferase in helminths', *Parasitology*, 100 Pt 2(2), pp. 345–349. Available at: https://doi.org/10.1017/S0031182000061369.

Brophy, P.M., Southan, C. and Barrett, J. (1989) 'Glutathione transferases in the tapeworm *Moniezia expansa*', *Biochemical Journal*, 262(3), pp. 939–946. Available at: https://doi.org/10.1042/BJ2620939.

Brunelle, J.L. and Green, R. (2014) 'One-dimensional SDS-polyacrylamide gel electrophoresis (1D SDS-PAGE)', in *Methods in Enzymology*. Academic Press Inc., pp. 151–159. Available at: https://doi.org/10.1016/B978-0-12-420119-4.00012-4.

Buchan, D.W.A. and Jones, D.T. (2019) 'The PSIPRED Protein Analysis Workbench: 20 years on', *Nucleic Acids Research*, 47(W1), pp. W402–W407. Available at: https://doi.org/10.1093/nar/gkz297.

Buck, A.H., Coakley, G., Simbari, F., McSorley, H.J., Quintana, J.F., Le Bihan, T., Kumar, S., Abreu-Goodger, C., Lear, M., Harcus, Y., Ceroni, A., Babayan, S.A., Blaxter, M., Ivens, A. and Maizels, R.M. (2014) 'Exosomes secreted by nematode parasites transfer small RNAs to mammalian cells and modulate innate immunity', *Nature Communications*, 5(1), pp. 1–12. Available at: https://doi.org/10.1038/ncomms6488.

Bucknell, D.G., Gasser, R.B. and Beveridge, I. (1995) 'The prevalence and epidemiology of gastrointestinal parasites of horses in Victoria, Australia', *International Journal for Parasitology*, 25(6), pp. 711–724. Available at: https://doi.org/10.1016/0020-7519(94)00214-9.

Burmeister, C., LÜersen, K., Heinick, A., Hussein, A., Domagalski, M., Walter, R.D. and Liebau, E. (2008) 'Oxidative stress in Caenorhabditis elegans: protective effects of the Omega class glutathione transferase (GSTO-1)', *The FASEB Journal*, 22(2), pp. 343–354. Available at: https://doi.org/10.1096/FJ.06-7426COM.

Burne, R.A. and Chen, Y.-Y.M. (2000) 'Bacterial ureases in infectious diseases', *Microbes and Infection*, 2(5), pp. 533–542. Available at: https://doi.org/https://doi.org/10.1016/S1286-4579(00)00312-9.

Buschmann, D., Mussack, V. and Byrd, J.B. (2021) 'Separation, characterization, and standardization of extracellular vesicles for drug delivery applications', *Advanced Drug Delivery Reviews*, 174, pp. 348–368. Available at: https://doi.org/https://doi.org/10.1016/j.addr.2021.04.027.

Buzás, E.I., Tóth, E.Á., Sódar, B.W. and Szabó-Taylor, K.É. (2018) 'Molecular interactions at the surface of extracellular vesicles', *Seminars in immunopathology*. 2018/04/16, 40(5), pp. 453–464. Available at: https://doi.org/10.1007/s00281-018-0682-0.

Caffrey, C.R., Goupil, L., Rebello, K.M., Dalton, J.P. and Smith, D. (2018) 'Cysteine proteases as digestive enzymes in parasitic helminths', *PLOS Neglected Tropical Diseases*, 12(8), p. e0005840. Available at: https://doi.org/10.1371/JOURNAL.PNTD.0005840.

Calsamiglia, S. and Stern, M.D. (1995) 'A three-step in vitro procedure for estimating intestinal digestion of protein in ruminants2', *Journal of Animal Science*, 73(5), pp. 1459–1465. Available at: https://doi.org/10.2527/1995.7351459x.

Camicia, F., Paredes, R., Chalar, C., Galanti, N., Kamenetzky, L., Gutierrez, A. and Rosenzvit, M.C. (2008) 'Sequencing, bioinformatic characterization and expression pattern of a putative amino acid transporter from the parasitic cestode *Echinococcus granulosus*', *Gene*, 411(1), pp. 1–9. Available at: https://doi.org/https://doi.org/10.1016/j.gene.2007.11.023.

Cantacessi, C., Mulvenna, J., Young, N.D., Kasny, M., Horak, P., Aziz, A., Hofmann, A., Loukas, A. and Gasser, R.B. (2012) 'A deep exploration of the transcriptome and "excretory/secretory" proteome of adult Fascioloides magna', *Molecular & cellular proteomics : MCP*, 11(11), pp. 1340–53. Available at: https://doi.org/10.1074/mcp.M112.019844.

Cantacessi, C., Seddon, J.M., Miller, T.L., Leow, C.Y., Thomas, L., Mason, L., Willis, C., Walker, G., Loukas, A., Gasser, R.B., Jones, M.K. and Hofmann, A. (2013) 'A genome-wide analysis of annexins from parasitic organisms and their vectors', *Scientific Reports*, 3(1), p. 2893. Available at: https://doi.org/10.1038/srep02893.

Capella-Gutiérrez, S., Silla-Martínez, J.M. and Gabaldón, T. (2009) 'trimAl: A tool for automated alignment trimming in large-scale phylogenetic analyses', *Bioinformatics*, 25(15), pp. 1972–1973. Available at: https://doi.org/10.1093/bioinformatics/btp348.

Cappellano, G., Raineri, D., Rolla, R., Giordano, M., Puricelli, C., Vilardo, B., Manfredi, M., Cantaluppi, V., Sainaghi, P.P. and Castello, L. (2021) 'Circulating platelet-derived extracellular vesicles are a hallmark of Sars-Cov-2 infection', *Cells*, 10(1), p. 85.

Carmel, D.K. (1988) 'Tapeworm infection in horses', *Journal of equine veterinary science (USA)* [Preprint].

Castresana, J. (2000) 'Selection of Conserved Blocks from Multiple Alignments for Their Use in Phylogenetic Analysis', *Molecular Biology and Evolution*, 17(4), pp. 540–552. Available at: https://doi.org/10.1093/oxfordjournals.molbev.a026334.

Cattadori, I.M., Sebastian, A., Hao, H., Katani, R., Albert, I., Eilertson, K.E., Kapur, V., Pathak, A. and Mitchell, S. (2016) 'Impact of Helminth Infections and Nutritional Constraints on the Small Intestine Microbiota', *PLOS ONE*. Edited by E. Serrano Ferron, 11(7), p. e0159770. Available at:

https://doi.org/10.1371/journal.pone.0159770.

Chai, J.Y. (2013) 'Praziquantel treatment in trematode and cestode infections: An update', *Infection and Chemotherapy*, 45(1), pp. 32–43. Available at: https://doi.org/10.3947/ic.2013.45.1.32.

Chaimon, S., Limpanont, Y., Reamtong, O., Ampawong, S., Phuphisut, O., Chusongsang, P., Ruangsittichai, J., Boonyuen, U., Watthanakulpanich, D., O'Donoghue, A.J., Caffrey, C.R. and Adisakwattana, P. (2019) 'Molecular characterization and functional analysis of the *Schistosoma mekongi* Ca2+-dependent cysteine protease (calpain)', *Parasites & Vectors*, 12(1), p. 383. Available at: https://doi.org/10.1186/s13071-019-3639-9.

Chaiyadet, S., Sotillo, J., Krueajampa, W., Thongsen, S., Brindley, P.J., Sripa, B., Loukas, A. and Laha, T. (2019) 'Vaccination of hamsters with *opisthorchis viverrini* extracellular vesicles and vesicle-derived recombinant tetraspanins induces antibodies that block vesicle uptake by cholangiocytes and reduce parasite burden after challenge infection', *PLoS Neglected Tropical Diseases*, 13(5), pp. 1–15. Available at: https://doi.org/10.1371/journal.pntd.0007450.

Chaiyadet, S., Sotillo, J., Krueajampa, W., Thongsen, S., Smout, M., Brindley, P.J., Laha, T. and Loukas, A. (2022) 'Silencing of *Opisthorchis viverrini* Tetraspanin Gene Expression Results in Reduced Secretion of Extracellular Vesicles', *Frontiers in Cellular and Infection Microbiology*, 12(February), pp. 1–12. Available at: https://doi.org/10.3389/fcimb.2022.827521.

Chaiyadet, S., Sotillo, J., Smout, M., Cantacessi, C., Jones, M.K., Johnson, M.S., Turnbull, L., Whitchurch, C.B., Potriquet, J., Laohaviroj, M., Mulvenna, J., Brindley, P.J., Bethony, J.M., Laha, T., Sripa, B. and Loukas, A. (2015) 'Carcinogenic Liver Fluke Secretes Extracellular Vesicles That Promote Cholangiocytes to Adopt a Tumorigenic Phenotype', *The Journal of Infectious Diseases*, 212(10), pp. 1636–1645. Available at: https://doi.org/10.1093/infdis/jiv291.

Chandra, L. *et al.* (2019) 'Derivation of adult canine intestinal organoids for translational research in gastroenterology', *BMC Biology*, 17(1), p. 33. Available at: https://doi.org/10.1186/s12915-019-0652-6.

Chang, J.-M., Di Tommaso, P. and Notredame, C. (2014) 'TCS: A New Multiple Sequence Alignment Reliability Measure to Estimate Alignment Accuracy and Improve Phylogenetic Tree Reconstruction', *Molecular Biology and Evolution*, 31(6), pp. 1625–1637. Available at: https://doi.org/10.1093/molbev/msu117.

Chang, Z., Li, G., Liu, J., Zhang, Y., Ashby, C., Liu, D., Cramer, C.L. and Huang, X. (2015) 'Bridger: A new framework for de novo transcriptome assembly using RNA-seq data', *Genome Biology*, 16(1), pp. 1–10. Available at: https://doi.org/10.1186/S13059-015-0596-2/FIGURES/7.

Chappell, L.H. (1980) 'The biology of the external surfaces of helminth parasites', *Proceedings of the Royal Society of Edinburgh. Section B. Biological Sciences*, 79(1–3), pp. 145–172. Available at: https://doi.org/10.1017/s026972700001040x.

Chargaff, E. and West, R. (1946) 'The biological significance of the thromboplastic protein of blood', *Journal of Biological Chemistry*, 166(1), pp. 189–197. Available at: https://doi.org/https://doi.org/10.1016/S0021-9258(17)34997-9.

Chaucheyras-Durand, F., Sacy, A., Karges, K. and Apper, E. (2022) 'Gastro-Intestinal Microbiota in Equines and Its Role in Health and Disease: The Black Box Opens', *Microorganisms*. Available at: https://doi.org/10.3390/microorganisms10122517.

Chemale, G., Morphew, R., Moxon, J. V., Morassuti, A.L., LaCourse, E.J., Barrett, J., Johnston, D.A. and Brophy, P.M. (2006) 'Proteomic analysis of glutathione transferases from the liver fluke parasite, *Fasciola hepatica*', *PROTEOMICS*, 6(23), pp. 6263–6273. Available at: https://doi.org/10.1002/PMIC.200600499.

Chen, A., Leith, M., Tu, R., Tahim, G., Sudra, A. and Bhargava, S. (2017) 'Effects of diluents on cell culture viability measured by automated cell counter', 1, pp. 1–13. Available at: https://doi.org/10.1371/journal.pone.0173375.

Chen, B., Zhong, D. and Monteiro, A. (2006) 'Comparative genomics and evolution of the HSP90 family of genes across all kingdoms of organisms', *BMC Genomics*, 7(1), pp. 1–19. Available at: https://doi.org/10.1186/1471-2164-7-156.

Chen, F., Liu, Z., Wu, W., Rozo, C., Bowdridge, S., Millman, A., Van Rooijen, N., Urban, J.F., Wynn, T.A. and Gause, W.C. (2012) 'An essential role for TH2-type responses in limiting acute tissue damage during experimental helminth infection', *Nature Medicine*, 18(2), pp. 260–266. Available at: https://doi.org/10.1038/nm.2628.

Chen, K.-Y., Chen, Y.-J., Cheng, C.-J., Jhan, K.-Y. and Wang, L.-C. (2022) 'Benzaldehyde Attenuates the Fifth Stage Larval Excretory–Secretory Product of *Angiostrongylus cantonensis*-Induced Injury in Mouse Astrocytes via Regulation of Endoplasmic Reticulum Stress and Oxidative Stress', *Biomolecules* . Available at: https://doi.org/10.3390/biom12020177.

Chen, K.-Y., Lu, P.-J., Cheng, C.-J., Jhan, K.-Y., Yeh, S.-C. and Wang, L.-C. (2019) 'Proteomic analysis of excretory-secretory products from young adults of *Angiostrongylus cantonensis*', *Memorias do Instituto Oswaldo Cruz*. 2019/06/19, 114, pp. e180556–e180556. Available at: https://doi.org/10.1590/0074-02760180556.

Chen, L., Yu, J., Xu, J., Wang, W., Ji, L., Yang, C. and Yu, H. (2018) 'Comparative Transcriptomes Analysis of Taenia pisiformis at Different Development Stages', *bioRxiv*, p. 490276. Available at: https://doi.org/10.1101/490276.

Chen, Y., Li, M., Zhang, Y., He, L., Yamada, Y., Fitzmaurice, A., Shen, Y., Zhang, H., Tong, L. and Yang, J. (2004) 'Structural basis of the α1–β subunit interaction of voltage-gated Ca2+ channels', *Nature*, 429, pp. 675–680. Available at: https://doi.org/10.1038/nature02641.

Cheng, I.S., Sealy, B.C., Tiberti, N. and Combes, V. (2020) 'Extracellular vesicles, from pathogenesis to biomarkers: the case for cerebral malaria', *Extracellular vesicles, from pathogenesis to biomarkers: the case for cerebral malaria*, 4, p. 17. Available at: https://doi.org/10.20517/2574-1209.2020.08.

Cheng, S., Zhu, B., Luo, F., Lin, X., Sun, C., You, Y., Yi, C., Xu, B., Wang, J., Lu, Y. and Hu, W. (2022) 'Comparative transcriptome profiles of *Schistosoma japonicum* larval stages: Implications for parasite biology and host invasion', *PLOS Neglected Tropical Diseases*, 16(1), p. e0009889. Available at: https://doi.org/10.1371/journal.pntd.0009889.

Choudhary, V., Garg, S., Chourasia, R., Hasnani, J.J., Patel, P.V., Shah, T.M., Bhatt, V.D., Mohapatra, A., Blake, D.P. and Joshi, C.G. (2015) 'Transcriptome analysis of the adult rumen fluke *Paramphistomum cervi* following next generation sequencing', *Gene*, 570(1), pp. 64–70. Available at: https://doi.org/10.1016/j.gene.2015.06.002.

Clark, A., Sallé, G., Ballan, V., Reigner, F., Meynadier, A., Cortet, J., Koch, C., Riou, M., Blanchard, A. and Mach, N. (2018) 'Strongyle Infection and Gut Microbiota: Profiling of Resistant and Susceptible Horses Over a Grazing Season', *Frontiers in Physiology*, 9, p. 272. Available at: https://doi.org/10.3389/fphys.2018.00272.

Coakley, G., McCaskill, J.L., Borger, J.G., Simbari, F., Robertson, E., Millar, M., Harcus, Y., McSorley, H.J., Maizels, R.M. and Buck, A.H. (2017) 'Extracellular Vesicles from a Helminth Parasite Suppress Macrophage Activation and Constitute an Effective Vaccine for Protective Immunity', *Cell Reports*, 19(8), pp. 1545–1557. Available at: https://doi.org/10.1016/j.celrep.2017.05.001.

Coles, L.T., Moughan, P.J. and Darragh, A.J. (2005) 'In vitro digestion and fermentation methods, including gas production techniques, as applied to nutritive evaluation of foods in the hindgut of humans and other simple-stomached animals', *Animal Feed Science and Technology*, 123–124, pp. 421–444. Available at: https://doi.org/https://doi.org/10.1016/j.anifeedsci.2005.04.021.

Collinet, A., Grimm, P., Julliand, S. and Julliand, V. (2021) 'Multidimensional Approach for Investigating the Effects of an Antibiotic-Probiotic Combination on the Equine Hindgut Ecosystem and Microbial Fibrolysis', *Frontiers in microbiology*, 12, p. 646294. Available at: https://doi.org/10.3389/fmicb.2021.646294.

Cortés, A., Sotillo, J., Muñoz-Antolí, C., Trelis, M., Esteban, J.G. and Toledo, R. (2016) 'Definitive host influences the proteomic profile of excretory/secretory products of the trematode *Echinostoma caproni*', *Parasites & Vectors*, 9(1), p. 185. Available at: https://doi.org/10.1186/s13071-016-1465-x.

Cosgrove, J.S., Sheeran, J.J. and Sainty, T.J. (1986) 'INTUSSUSCEPTION ASSOCIATED WITH INFECTION WITH *ANOPLOCEPHALA-PERFOLIATA* IN A 2-YEAR OLD THOROUGHBRED', *Irish Veterinary Journal*, 40(2), pp. 35–36.

Costa, M.., Silva, G., Ramos, R.., Staempfli, H.., Arroyo, L.., Kim, P. and Weese, J.. (2015) 'Characterization and comparison of the bacterial microbiota in different gastrointestinal tract compartments in horses', *The Veterinary Journal*, 205(1), pp. 74–80. Available at: https://doi.org/10.1016/J.TVJL.2015.03.018.

Costa, M.C., Arroyo, L.G., Allen-Vercoe, E., Stämpfli, H.R., Kim, P.T., Sturgeon, A. and Weese, J.S. (2012) 'Comparison of the Fecal Microbiota of Healthy Horses and Horses with Colitis by High Throughput Sequencing of the V3-V5 Region of the 16S rRNA Gene', *PLoS ONE*. Edited by G.L. Hold, 7(7), p. e41484. Available at: https://doi.org/10.1371/journal.pone.0041484.

Costa, M.C., Stämpfli, H.R., Arroyo, L.G., Allen-Vercoe, E., Gomes, R.G. and Weese, J.S. (2015) 'Changes in the equine fecal microbiota associated with the use of systemic antimicrobial drugs', *BMC Veterinary Research*, 11(1), p. 19. Available at: https://doi.org/10.1186/s12917-015-0335-7.

Costa, M.C. and Weese, J.S. (2012) 'The equine intestinal microbiome.', *Animal health research reviews / Conference of Research Workers in Animal Diseases*. Cambridge University Press, pp. 121–128. Available at: https://doi.org/10.1017/S1466252312000035.

Craig, T.M., Scrutchfield, W.L., Thompson, J.A. and Bass, E.E. (2003) 'Comparison of Anthelmintic Activity of Pyrantel, Praziquantel, and Nitazoxanide against *Anoplocephala perfoliata* in Horses', pp. 68–70.

Crewe, C., Funcke, J.-B., Li, S., Joffin, N., Gliniak, C.M., Ghaben, A.L., An, Y.A., Sadek, H.A., Gordillo, R., Akgul, Y., Chen, S., Samovski, D., Fischer-Posovszky, P., Kusminski, C.M., Klein, S. and Scherer, P.E. (2021) 'Extracellular vesicle-based interorgan transport of mitochondria from energetically stressed adipocytes', *Cell Metabolism*, 33(9), pp. 1853-1868.e11. Available at: https://doi.org/https://doi.org/10.1016/j.cmet.2021.08.002.

Crotch-Harvey, L., Thomas, L.-A., Worgan, H.J., Douglas, J.-L., Gilby, D.E. and Mcewan, N.R. (2018) 'The effect of administration of fenbendazole on the microbial hindgut population of the horse', *Journal of Equine Science*, 29(2), pp. 47–51. Available at: https://doi.org/10.1294/jes.29.47.

Cui, Y., Wang, Xinrui, Xu, J., Liu, X., Wang, Xuelin, Pang, J., Song, Y., Yu, M., Song, W., Luo, X., Liu, M. and Sun, S. (2021) 'PROTEOMIC ANALYSIS OF *TAENIA SOLIUM* CYST FLUID BY SHOTGUN LC-MS/MS', *Journal of Parasitology*, 107(5), pp. 799–809. Available at: https://doi.org/10.1645/20-65.

Curwen, R.S., Ashton, P.D., Sundaralingam, S. and Wilson, R.A. (2006) 'Identification of Novel Proteases and Immunomodulators in the Secretions of Schistosome Cercariae That Facilitate Host Entry * ', *Molecular & Cellular Proteomics*, 5(5), pp. 835–844. Available at: https://doi.org/10.1074/mcp.M500313-MCP200.

Cwiklinski, Krystyna., Dalton, J.P., Dufresne, P.J., La Course, J., Williams, D.J.L., Hodgkinson, J. and Paterson, S. (2015) 'The *Fasciola hepatica* genome: gene duplication and polymorphism reveals adaptation to the host environment and the capacity for rapid evolution', *Genome Biology*, 16(1), p. 71. Available at: https://doi.org/10.1186/s13059-015-0632-2.

Cwiklinski, Krystyna, De La Torre-Escudero, E., Trelis, M., Bernal, D., Dufresne, P.J., Brennan, G.P., O'Neill, S., Tort, J., Paterson, S., Marcilla, A., Dalton, J.P. and Robinson, M.W. (2015) 'The Extracellular Vesicles of the Helminth Pathogen, *Fasciola hepatica*: Biogenesis Pathways and Cargo Molecules Involved in Parasite Pathogenesis', *Molecular & Cellular Proteomics*, 14(12), pp. 3258–3273. Available at: https://doi.org/https://doi.org/10.1074/mcp.M115.053934.

Cwiklinski, K., Robinson, M.W., Donnelly, S. and Dalton, J.P. (2021) 'Complementary transcriptomic and proteomic analyses reveal the cellular and molecular processes that drive growth and development of *Fasciola hepatica* in the host liver', *BMC Genomics*, 22(1), pp. 1–16. Available at: https://doi.org/10.1186/S12864-020-07326-Y/FIGURES/6.

Daher, W., Browaeys, E., Pierrot, C., Jouin, H., Dive, D., Meurice, E., Dissous, C., Capron, M., Tomavo, S., Doerig, C., Cailliau, K. and Khalife, J. (2006) 'Regulation of protein phosphatase type 1 and cell cycle progression by PfLRR1, a novel leucine-rich repeat protein of the human malaria parasite *Plasmodium falciparum*', *Molecular Microbiology*, 60(3), pp. 578–590. Available at: https://doi.org/https://doi.org/10.1111/j.1365-2958.2006.05119.x.

Daher, W., Cailliau, K., Takeda, K., Pierrot, C., Khayath, N., Dissous, C., Capron, M., Yanagida, M., Browaeys, E. and Khalife, J. (2006) 'Characterization of *Schistosoma mansoni* Sds homologue, a leucine-rich repeat protein that interacts with protein phosphatase type 1 and interrupts a G2/M cell-cycle checkpoint', *Biochemical Journal*, 395(2), pp. 433–441. Available at: https://doi.org/10.1042/BJ20051597.

Daher, W., Oria, G., Fauquenoy, S., Cailliau, K., Browaeys, E., Tomavo, S. and Khalife, J. (2007) 'A *Toxoplasma gondii* leucine-rich repeat protein binds phosphatase type 1 protein and negatively regulates its activity', *Eukaryotic Cell*, 6(9), pp. 1606–1617. Available at: https://doi.org/10.1128/EC.00260-07/ASSET/9A99AE93-09F4-4AF6-9906-F4B22EA2484B/ASSETS/GRAPHIC/ZEK0090729620009.JPEG.

Daigneault, M., Preston, J.A., Marriott, H.M., Whyte, M.K.B.B. and Dockrell, D.H. (2010) 'The Identification of Markers of Macrophage Differentiation in PMA-Stimulated THP-1 Cells and Monocyte-Derived Macrophages', *PLOS ONE*, 5(1), p. e8668. Available at: https://doi.org/10.1371/JOURNAL.PONE.0008668.

Daniels, S.P., Leng, J., Swann, J.R. and Proudman, C.J. (2020) 'Bugs and drugs: a systems biology approach to characterising the effect of moxidectin on the horse's faecal microbiome', *Animal Microbiome*, 2(1), pp. 1–14. Available at: https://doi.org/10.1186/s42523-020-00056-2.

Datta Chaudhuri, A., Dasgheyb, R.M., DeVine, L.R., Bi, H., Cole, R.N. and Haughey, N.J. (2020) 'Stimulus-dependent modifications in astrocyte-derived extracellular vesicle cargo regulate neuronal excitability', *Glia*, 68(1), pp. 128–144. Available at: https://doi.org/https://doi.org/10.1002/glia.23708.

Davis, C.N., Phillips, H., Tomes, J.J., Swain, M.T., Wilkinson, T.J., Brophy, P.M. and Morphew, R.M. (2019) 'The importance of extracellular vesicle purification for downstream analysis: A comparison of differential centrifugation and size exclusion chromatography for helminth pathogens', *PLOS Neglected Tropical Diseases*. Edited by G. Rinaldi, 13(2), p. e0007191. Available at: https://doi.org/10.1371/journal.pntd.0007191.

Davis, C.N., Winters, A., Milic, I., Devitt, A., Cookson, A., Brophy, P.M. and Morphew, R.M. (2020) 'Evidence of sequestration of triclabendazole and associated metabolites by extracellular vesicles of Fasciola hepatica', *Scientific Reports*, 10(1), p. 13445. Available at: https://doi.org/10.1038/s41598-020-69970-4.

Debarba, J.A., Sehabiague, M.P.C., Monteiro, K.M., Gerber, A.L., Vasconcelos, A.T.R., Ferreira, H.B. and Zaha, A. (2020) 'Transcriptomic analysis of the early strobilar development of *Echinococcus granulosus*', *Pathogens*, 9(6), pp. 1–12. Available at: https://doi.org/10.3390/pathogens9060465.

Deitmers, J.-H., Gresner, N. and Südekum, K.-H. (2022) 'Opportunities and limitations of a standardisation of the rumen simulation technique (RUSITEC) for analyses of ruminal nutrient degradation and fermentation and on microbial community characteristics', *Animal Feed Science and Technology*, 289, p. 115325. Available at: https://doi.org/https://doi.org/10.1016/j.anifeedsci.2022.115325.

Denegri, G.M. (1993) 'Review of oribatid mites as intermediate hosts of tapeworms of the Anoplocephalidae', *Experimental and Applied Acarology*, 17(8), pp. 567–580. Available at: https://doi.org/10.1007/BF00053486.

Desrochers, A.M., Dallap, B.L. and Wilkins, P.A. (2003) 'Clostridium sordelli Infection as a Suspected Cause of Transient Hyperammonemia in an Adult Horse', *Journal of Veterinary Internal Medicine*, 17(2), pp. 238–241. Available at: https://doi.org/https://doi.org/10.1111/j.1939-1676.2003.tb02441.x.

Devulder, J., Baker, J.R., Donnelly, L.E. and Barnes, P.J. (2021) 'Extracellular vesicles produced by airway epithelial cells in response to oxidative stress contain microRNAs associated with cellular senescence', *European Respiratory Journal*, 58(suppl 65), p. OA2696. Available at: https://doi.org/10.1183/13993003.congress-2021.OA2696.

Díaz-Ramos, À., Roig-Borrellas, A., García-Melero, A., López-Alemany, R., Díaz-Ramos, A., Roig-Borrellas, A., García-Melero, A. and López-Alemany, R. (2012) 'α-Enolase, a multifunctional protein: its role on pathophysiological situations', *Journal of biomedicine & biotechnology*. 2012/10/14, 2012, p. 156795. Available at: https://doi.org/10.1155/2012/156795.

Dicks, L.M.T., Botha, M., Dicks, E. and Botes, M. (2014) 'The equine gastro-intestinal tract: An overview of the microbiota, disease and treatment', *Livestock Science*, 160, pp. 69–81. Available at: https://doi.org/10.1016/j.livsci.2013.11.025.

Dill, B., Engelmann, W., Markuske, K.D. and Zeyner, A. (2007) 'Comparison of equine caecum content and faeces as inocula in a modified Rumen Simulation Technique', in *Proceedings of the Society of Nutrition Physiology*, p. 73.

Ding, J., He, G., Wu, J., Yang, J., Guo, X., Yang, X., Wang, Y., Kandil, O.M., Kutyrev, I., Ayaz, M. and Zheng, Y. (2019) 'miRNA-seq of *Echinococcus multilocularis* Extracellular Vesicles and Immunomodulatory Effects of miR-4989 ', *Frontiers in Microbiology* . Available at: https://www.frontiersin.org/articles/10.3389/fmicb.2019.02707.

Donnelly, S., O'Neill, S.M., Sekiya, M., Mulcahy, G. and Dalton, J.P. (2005) 'Thioredoxin peroxidase secreted by *Fasciola hepatica* induces the alternative activation of macrophages', *Infection and immunity*, 73(1), pp. 166–173. Available at: https://doi.org/10.1128/IAI.73.1.166-173.2005.

Dougal, K., Harris, P.A., Edwards, A., Pachebat, J.A., Blackmore, T.M., Worgan, H.J. and Newbold, C.J. (2012) 'A comparison of the microbiome and the metabolome of different regions of the equine hindgut', *FEMS Microbiology Ecology*, 82(3), pp. 642–652. Available at: https://doi.org/10.1111/j.1574-6941.2012.01441.x.

Dougal, K., de la Fuente, G., Harris, P.A., Girdwood, S.E., Pinloche, E., Geor, R.J., Nielsen, B.D., Schott, H.C., Elzinga, S. and Newbold, C.J. (2014) 'Characterisation of the Faecal Bacterial Community in Adult and Elderly Horses Fed a High Fibre, High Oil or High Starch Diet Using 454 Pyrosequencing', *PLoS ONE*. Edited by A.M. Ibekwe, 9(2), p. e87424. Available at: https://doi.org/10.1371/journal.pone.0087424.

Dougal, K., de la Fuente, G., Harris, P.A., Girdwood, S.E., Pinloche, E. and Newbold, C.J. (2013) 'Identification of a Core Bacterial Community within the Large Intestine of the Horse', *PLoS ONE*. Edited by R. Schuch, 8(10), p. e77660. Available at: https://doi.org/10.1371/journal.pone.0077660.

Dowling, D.J., Hamilton, C.M., Donnelly, S., La Course, J., Brophy, P.M., Dalton, J. and O'Neill, S.M. (2010) 'Major secretory antigens of the Helminth *Fasciola hepatica* activate a suppressive dendritic cell phenotype that attenuates Th17 cells but fails to activate Th2 immune responses', *Infection and Immunity*, 78(2), pp. 793–801. Available at: https://doi.org/10.1128/IAI.00573-09.

Doyle, L. and Wang, M. (2019) 'Overview of Extracellular Vesicles, Their Origin, Composition, Purpose, and Methods for Exosome Isolation and Analysis', *Cells*, 8(7), p. 727. Available at: https://doi.org/10.3390/cells8070727.

Dragich, J.M., Kuwajima, T., Hirose-Ikeda, M., Yoon, M.S., Eenjes, E., Bosco, J.R., Fox, L.M., Lystad, A.H., Oo, T.F., Yarygina, O., Mita, T., Waguri, S., Ichimura, Y., Komatsu, M., Simonsen, A., Burke, R.E., Mason, C.A. and Yamamoto, A. (2016) 'Autophagy linked FYVE (Alfy/WDFY3) is required for establishing neuronal connectivity in the mammalian brain', *eLife*, 5(September). Available at: https://doi.org/10.7554/eLife.14810.

Drogemuller, M., Beelitz, P., Pfister, K., Schnieder, T. and Samson-Himmelstjerna, G. von (2004) 'Amplification of ribosomal DNA of Anoplocephalidae: *Anoplocephala perfoliata* diagnosis by PCR as a possible alternative to coprological methods', *Veterinary Parasitology*, 124(3–4), pp. 205–215. Available at: https://doi.org/10.1016/j.vetpar.2004.07.012.

Drurey, C. and Maizels, R.M. (2021) 'Helminth extracellular vesicles: Interactions with the host immune system', *Molecular immunology*. 2021/07/07, 137, pp. 124–133. Available at: https://doi.org/https://doi.org/10.1016/j.molimm.2021.06.017.

Duarte, A.M., Jenkins, T.P., Latrofa, M.S., Giannelli, A., Papadopoulos, E., de Carvalho, L.M., Nolan, M.J., Otranto, D. and Cantacessi, C. (2016) 'Helminth infections and gut microbiota – a feline perspective', *Parasites & Vectors*, 9(1), p. 625. Available at: https://doi.org/10.1186/s13071-016-1908-4.

Le Duc, D. *et al.* (2019) 'Pathogenic WDFY3 variants cause neurodevelopmental disorders and opposing effects on brain size', *Brain*, 142(9), pp. 2617–2630. Available at: https://doi.org/10.1093/brain/awz198.

Dunkel, B. (2010) 'Intestinal hyperammonaemia in horses', *Equine Veterinary Education*, 22(7), pp. 340–345. Available at: https://doi.org/https://doi.org/10.1111/j.2042-3292.2010.00047.x.

Duque, G.A. and Descoteaux, A. (2014) 'Macrophage cytokines: Involvement in immunity and infectious diseases', *Frontiers in Immunology*, 5(OCT), pp. 1–12. Available at: https://doi.org/10.3389/fimmu.2014.00491.

Dyer, M.D., Murali, T.M. and Sobral, B.W. (2007) 'Computational prediction of host-pathogen protein–protein interactions', *Bioinformatics*, 23(13), pp. i159–i166. Available at: https://doi.org/10.1093/bioinformatics/btm208.

Edwards, G.B. (1986) 'Surgical management of intussusception in the horse', *Equine veterinary journal*, 18(4), pp. 313–321.

Edwards, J.E., Schennink, A., Burden, F., Long, S., van Doorn, D.A., Pellikaan, W.F., Dijkstra, J., Saccenti, E. and Smidt, H. (2020) 'Domesticated equine species and their derived hybrids differ in their fecal microbiota', *Animal Microbiome*, 2(1), p. 8. Available at: https://doi.org/10.1186/s42523-020-00027-7.

Eichenberger, R.M., Ryan, S., Jones, L., Buitrago, G., Polster, R., de Oca, M.M., Zuvelek, J., Giacomin, P.R., Dent, L.A., Engwerda, C.R., Field, M.A., Sotillo, J. and Loukas, A. (2018) 'Hookworm secreted extracellular vesicles interact with host cells and prevent inducible colitis in mice', *Frontiers in Immunology*, 9(APR), p. 850. Available at: https://doi.org/10.3389/fimmu.2018.00850.

Eichenberger, R.M., Sotillo, J. and Loukas, A. (2018) 'Immunobiology of parasitic worm extracellular vesicles', *Immunology and Cell Biology*. John Wiley and Sons Inc., pp. 704–713. Available at: https://doi.org/10.1111/imcb.12171.

Eichenberger, R.M., Talukder, M.H., Field, M.A., Wangchuk, P., Giacomin, P., Loukas, A. and Sotillo, J. (2018) 'Characterization of *Trichuris muris* secreted proteins and extracellular vesicles provides new insights into host–parasite communication', *Journal of Extracellular Vesicles*, 7(1), p. 1428004. Available at: https://doi.org/10.1080/20013078.2018.1428004.

Elghandour, M.M.Y., Kholif, A.E., López, S., Mendoza, G.D., Odongo, N.E. and Salem, A.Z.M. (2016) 'In Vitro Gas, Methane, and Carbon Dioxide Productions of High Fibrous Diet Incubated With Fecal Inocula From Horses in Response to the Supplementation With Different Live Yeast Additives', *Journal of Equine Veterinary Science*, 38, pp. 64–71. Available at: https://doi.org/https://doi.org/10.1016/j.jevs.2015.12.010.

Else, K.J., Finkelman, F.D., Maliszewski, C.R. and Grencis, R.K. (1994) 'Cytokine-mediated regulation of chronic intestinal helminth infection', *Journal of Experimental Medicine*, 179(1), pp. 347–351. Available at: https://doi.org/10.1084/jem.179.1.347.

Elsener, J. and Villeneuve, A. (2011) 'Does examination of fecal samples 24 hours after cestocide treatment increase the sensitivity of *Anoplocephala spp.* detection in naturally infected horses?', *Canadian Veterinary Journal*, 52(2), pp. 165–168. Available at: /pmc/articles/PMC3022452/?report=abstract (Accessed: 26 December 2020).

Elsner, C., Ergün, S. and Wagner, N. (2023) 'Biogenesis and release of endothelial extracellular vesicles: Morphological aspects', *Annals of Anatomy - Anatomischer Anzeiger*, 245, p. 152006. Available at: https://doi.org/https://doi.org/10.1016/j.aanat.2022.152006.

Engelmann, W., Dill, B., Markuske, K.D., Aschenbach, J. and Zeyner, A. (2007) 'Investigations on chronic incubationof equine caecum content with fructan in a modified "Rumen Simulation Technique"', *Proceedings of the Society of Nutrition Physiology*, 16, p. 74. Available at: https://www.scopus.com/inward/record.uri?eid=2-s2.0-84865964591&partnerID=40&md5=30887fc21506eea7c054eca073dc4b7c.

Ericsson, A.C., Johnson, P.J., Lopes, M.A., Perry, S.C. and Lanter, H.R. (2016) 'A Microbiological Map of the Healthy Equine Gastrointestinal Tract', *PLOS ONE*. Edited by H. Smidt, 11(11), p. e0166523. Available at: https://doi.org/10.1371/journal.pone.0166523.

Espada, M., Jones, J.T. and Mota, M. (2016) 'Characterization of glutathione S transferases from the plant-parasitic nematode, *Bursaphelenchus xylophilus*', *Nematology*, 18(6), pp. 697–709. Available at: https://doi.org/10.1163/15685411-00002985.

Fan, J., Wu, H., Li, K., Liu, X., Tan, Q., Cao, W., Liang, B. and Ye, B. (2020) 'Transcriptomic Features of *Echinococcus granulosus* Protoscolex during the Encystation Process', *The Korean Journal of Parasitology*, 58(3), p. 287. Available at: https://doi.org/10.3347/KJP.2020.58.3.287.

Ferguson, G.D. and Bridge, W.J. (2019) 'The glutathione system and the related thiol network in *Caenorhabditis elegans*', *Redox biology*, 24, p. 101171. Available at: https://doi.org/10.1016/j.redox.2019.101171.

Fernandes, K.A., Kittelmann, S., Rogers, C.W., Gee, E.K. and Bolwell, C.F. (2014) 'Faecal Microbiota of Forage-Fed Horses in New Zealand and the Population Dynamics of Microbial Communities following Dietary Change', *PLoS ONE*, 9(11), p. 112846. Available at: https://doi.org/10.1371/journal.pone.0112846.

Fernández, V., Chalar, C., Martínez, C., Musto, H., Zaha, A. and Fernández, C. (2000) '*Echinococcus granulosus*: Molecular Cloning and Phylogenetic Analysis of an Inducible Glutathione S-Transferase', *Experimental Parasitology*, 96(3), pp. 190–194. Available at: https://doi.org/10.1006/EXPR.2000.4571.

Fesseha, H., Aliye, S., Mathewos, M. and Nigusie, K. (2022) 'Prevalence and risk factors associated with donkey gastrointestinal parasites in Shashemane and Suburbs, Oromia Region, Ethiopia', *Heliyon*, 8(12). Available at: https://doi.org/10.1016/j.heliyon.2022.e12244.

Figueiredo, B.C., Da'dara, A.A., Oliveira, S.C. and Skelly, P.J. (2015) 'Schistosomes Enhance Plasminogen Activation: The Role of Tegumental Enolase', *PLOS Pathogens*, 11(12), p. e1005335. Available at: https://doi.org/10.1371/JOURNAL.PPAT.1005335.

Finkelman, F.D., Shea-Donohue, T., Goldhill, J., Sullivan, C.A., Morris, S.C., Madden, K.B., Gause, W.C. and Urban, J.F. (1997) 'Cytokine Regulation Of Host Defense Against Parasitic Gastrointestinal Nematodes:Lessons from Studies with Rodent Models*', *Annual Review of Immunology*, 15(1), pp. 505–533. Available at: https://doi.org/10.1146/annurev.immunol.15.1.505.

Flanagan, J.U. and Smythe, M.L. (2011) 'Sigma-class glutathione transferases', *Drug Metabolism Reviews*, 43(2), pp. 194–214. Available at: https://doi.org/10.3109/03602532.2011.560157.

Fliegerova, K., Mura, E., Mrázek, J. and Moniello, G. (2016) 'A comparison of microbial profiles of different regions of the equine hindgut', *Livestock Science*, 190, pp. 16–19. Available at: https://doi.org/10.1016/J.LIVSCI.2016.05.015.

Florea, L. (2006) 'Bioinformatics of alternative splicing and its regulation', *Briefings in Bioinformatics*, 7(1), pp. 55–69. Available at: https://doi.org/10.1093/bib/bbk005.

Fogarty, U., Del Piero, F., Purnell, R.E. and Mosurski, K.R. (1994) 'Incidence of *Anoplocephala perfoliata* in horses examined at an Irish abattoir', *Veterinary Record*, 134(20), pp. 515–518. Available at: https://doi.org/10.1136/vr.134.20.515.

de Fombelle, A., Julliand, V., Drogoul, C. and Jacotot, E. (2001) 'Feeding and microbial disorders in horses: 1-effects of an abrupt incorporation of two levels of barley in a hay diet on microbial profile and activities', *Journal of Equine Veterinary Science*, 21(9), pp. 439–445. Available at: https://doi.org/https://doi.org/10.1016/S0737-0806(01)70018-4.

de Fombelle, A., Varloud, M., Goachet, A.-G., Jacotot, E., Philippeau, C., Drogoul, C. and Julliand, V. (2003) 'Characterization of the microbial and biochemical profile of the different segments of the digestive tract in horses given two distinct diets', *Animal Science*. 2016/08/18, 77(2), pp. 293–304. Available at: https://doi.org/DOI: 10.1017/S1357729800059038.

Förster, S., Koziol, U., Schäfer, T., Duvoisin, R., Cailliau, K., Vanderstraete, M., Dissous, C. and Brehm, K. (2018) 'The role of fibroblast growth factor signalling in *Echinococcus multilocularis* development and host-parasite interaction', *PLoS Neglected Tropical Diseases*, 13(3), pp. 1–27. Available at: https://doi.org/10.1371/journal.pntd.0006959.

Freitas, D., Balmaña, M., Poças, J., Campos, D., Osório, H., Konstantinidi, A., Vakhrushev, S.Y., Magalhães, A. and Reis, C.A. (2019) 'Different isolation approaches lead to diverse glycosylated extracellular vesicle populations', *Journal of Extracellular Vesicles*, 8(1), p. 1621131. Available at: https://doi.org/10.1080/20013078.2019.1621131.

Fréville, A., Gnangnon, B., Tremp, A.Z., De Witte, C., Cailliau, K., Martoriati, A., Aliouat, E.M., Fernandes, P., Chhuon, C., Silvie, O., Marion, S., Guerrera, I.C., Dessens, J.T., Pierrot, C. and Khalife, J. (2022) '*Plasmodium berghei* leucine-rich repeat protein 1 downregulates protein phosphatase 1 activity and is required for efficient oocyst development', *Open Biology*, 12(8), p. 220015. Available at: https://doi.org/10.1098/rsob.220015.

Fricke, W.F., Song, Y., Wang, A.-J., Smith, A., Grinchuk, V., Pei, C., Ma, B., Lu, N., Urban, J.F., Shea-Donohue, T. and Zhao, A. (2015) 'Type 2 immunity-dependent reduction of segmented filamentous bacteria in mice infected with the helminthic parasite *Nippostrongylus brasiliensis*', *Microbiome*, 3(1), p. 40. Available at: https://doi.org/10.1186/s40168-015-0103-8.

Friedman, R. (2011) 'Genomic organization of the glutathione S-transferase family in insects', *Molecular Phylogenetics and Evolution*, 61(3), pp. 924–932. Available at: https://doi.org/10.1016/J.YMPEV.2011.08.027.

Fu, L., Niu, B., Zhu, Z., Wu, S. and Li, W. (2012) 'CD-HIT: Accelerated for clustering the next-generation sequencing data', *Bioinformatics*, 28(23), pp. 3150–3152. Available at: https://doi.org/10.1093/bioinformatics/bts565.

Fukano, K. and Kimura, K. (2014) 'Measurement of enolase activity in cell lysates', in *Methods in Enzymology*. Academic Press Inc., pp. 115–124. Available at: https://doi.org/10.1016/B978-0-12-416618-9.00006-6.

Furusawa, Y. *et al.* (2013) 'Commensal microbe-derived butyrate induces the differentiation of colonic regulatory T cells', *Nature*, 504(7480), pp. 446–450. Available at: https://doi.org/10.1038/nature12721.

Gandarillas, M., Keim, J.P. and Gapp, E.M. (2021) 'Associative Effects between Forages and Concentrates on *In Vitro* Fermentation of Working Equine Diets', *Animals*. Available at: https://doi.org/10.3390/ani11082212.

Gao, J., Zhang, X., Jiang, L., Li, Y. and Zheng, Q. (2022) 'Tumor endothelial cell-derived extracellular vesicles contribute to tumor microenvironment remodeling', *Cell Communication and Signaling*, 20(1), p. 97. Available at: https://doi.org/10.1186/s12964-022-00904-5.

Garber, A., Hastie, P. and Murray, J.A. (2020) 'Factors Influencing Equine Gut Microbiota: Current Knowledge', *Journal of Equine Veterinary Science*, 88, p. 102943. Available at: https://doi.org/10.1016/J.JEVS.2020.102943.

García-Montoya, G.M., Mesa-Arango, J.A., Isaza-Agudelo, J.P., Agudelo-Lopez, S.P., Cabarcas, F., Barrera, L.F. and Alzate, J.F. (2016) 'Transcriptome profiling of the cysticercus stage of the laboratory model *Taenia crassiceps*, strain ORF', *Acta Tropica*, 154, pp. 50–62. Available at: https://doi.org/10.1016/j.actatropica.2015.11.001.

García-Pérez, R., Ramirez, J.M., Ripoll-Cladellas, A., Chazarra-Gil, R., Oliveros, W., Soldatkina, O., Bosio, M., Rognon, P.J., Capella-Gutierrez, S., Calvo, M., Reverter, F., Guigó, R., Aguet, F., Ferreira, P.G., Ardlie, K.G. and Melé, M. (2023) 'The landscape of expression and alternative splicing variation across human traits', *Cell Genomics*, 3(1). Available at: https://doi.org/10.1016/j.xgen.2022.100244.

Gasser, R.B., Williamson, R.M.C. and Beveridge, I. (2005) '*Anoplocephala perfoliata* of horses - Significant scope for further research, improved diagnosis and control', *Parasitology*, pp. 1–13. Available at: https://doi.org/10.1017/S0031182004007127.

Gasteiger, E., Gattiker, A., Hoogland, C., Ivanyi, I., Appel, R.D. and Bairoch, A. (2003) 'ExPASy: The proteomics server for in-depth protein knowledge and analysis', *Nucleic Acids Research*, 31(13), pp. 3784–3788. Available at: https://doi.org/10.1093/nar/gkg563.

Gay, N.J., Packman, L.C., Weldon, M.A. and Barna, J.C. (1991) 'A leucine-rich repeat peptide derived from the Drosophila Toll receptor forms extended filaments with a beta-sheet structure', *FEBS letters*, 291(1), pp. 87–91. Available at: https://doi.org/10.1016/0014-5793(91)81110-t.

Gazzinelli-Guimaraes, P.H. and Nutman, T.B. (2018) 'Helminth parasites and immune regulation', *F1000Research*, 7, p. F1000 Faculty Rev-1685. Available at: https://doi.org/10.12688/f1000research.15596.1.

Gebara, N., Scheel, J., Skovronova, R., Grange, C., Marozio, L., Gupta, S., Giorgione, V., Caicci, F., Benedetto, C., Khalil, A. and Bussolati, B. (2022) 'Single extracellular vesicle analysis in human amniotic fluid shows evidence of phenotype alterations in preeclampsia', *Journal of Extracellular Vesicles*, 11(5), p. e12217. Available at: https://doi.org/https://doi.org/10.1002/jev2.12217.

Gehlen, H., Wulke, N., Ertelt, A., Nielsen, M.K., Morelli, S., Traversa, D., Merle, R., Wilson, D. and von Samson-Himmelstjerna, G. (2020) 'Comparative analysis of intestinal helminth infections in colic and non-colic control equine patients', *Animals*, 10(10), pp. 1–13. Available at: https://doi.org/10.3390/ani10101916.

GergóCS, V., Garamvölgyi, Á., Homoródi, R. and Hufnagel, L. (2011) 'Seasonal change of oribatid mite communities (acari, oribatida) in three different types of microhabitats in an oak forest', *Applied Ecology and Environmental Research*, 9(2), pp. 181–195. Available at: https://doi.org/10.15666/aeer/0902_181195.

Gerke, V. and Moss, S.E. (2002) 'Annexins: From Structure to Function', *Physiological Reviews*, 82(2), pp. 331–371. Available at: https://doi.org/10.1152/physrev.00030.2001.

Getachew, A.M., Innocent, G., Proudman, C.J., Trawford, A., Feseha, G., Reid, S.W.J., Faith, B. and Love, S. (2012) 'Equine cestodosis: a sero-epidemiological study of *Anoplocephala perfoliata* infection in Ethiopia', *Veterinary Research Communications*, 36(2), pp. 93–98. Available at: https://doi.org/10.1007/s11259-012-9516-z.

Getachew, A.M., Innocent, G., Proudman, C.J., Trawford, A., Feseha, G., Reid, S.W.J., Faith, B. and Love, S. (2013) 'Field efficacy of praziquantel oral paste against naturally acquired equine cestodes in Ethiopia', *Parasitology Research*, 112(1), pp. 141–146. Available at: https://doi.org/10.1007/s00436-012-3117-1.

Getachew, M., Trawford, A., Feseha, G. and Reid, S.W.J. (2010) 'Gastrointestinal parasites of working donkeys of Ethiopia', *Tropical Animal Health and Production*, 42(1), pp. 27–33. Available at: https://doi.org/10.1007/s11250-009-9381-0.

Gillan, V. and Devaney, E. (2014) 'Nematode Hsp90: Highly conserved but functionally diverse', *Parasitology*, 141(9), pp. 1203–1215. Available at: https://doi.org/10.1017/S0031182014000304.

Gillis-Germitsch, N., Kockmann, T., Asmis, L.M., Tritten, L. and Schnyder, M. (2021) 'The Angiostrongylus vasorum Excretory/Secretory and Surface Proteome Contains Putative Modulators of the Host Coagulation', *Frontiers in Cellular and Infection Microbiology*, 11, p. 753320. Available at: https://doi.org/10.3389/fcimb.2021.753320.

Gilroy, R., Leng, J., Ravi, A., Adriaenssens, E.M. and Oren, A. (2021) 'Metagenomic investigation of the equine faecal microbiome reveals extensive taxonomic and functional diversity'.

Glendinning, L., Nausch, N., Free, A., Taylor, D.W. and Mutapi, F. (2014) 'The microbiota and helminths: sharing the same niche in the human host', *Parasitology*, 141(10), pp. 1255–1271. Available at: https://doi.org/10.1017/S0031182014000699.

Glinsky, M.J., Smith, R.M., Spires, H.R. and Davis, C.L. (1976) 'Measurement of Volatile Fatty Acid Production Rates in the Cecum of the Pony', *Journal of Animal Science*, 42(6), pp. 1465–1470. Available at: https://doi.org/10.2527/jas1976.4261465x.

Goachet, A.G., Ricard, J.M., Jacotot, E., Varloud, M. and Julliand, V. (2004) 'Effet de l'administration Orale de Trois Anthelminthiques Sur La Microflore Colique Du Cheval', *Proceedings of the Journées de l'Association Vétérinaire Équine Française, Pau, France*, pp. 21–23.

Goecks, J., Nekrutenko, A., Taylor, J., Afgan, E., Ananda, G., Baker, D., Blankenberg, D., Chakrabarty, R., Coraor, N., Goecks, J., Von Kuster, G., Lazarus, R., Li, K., Taylor, J. and Vincent, K. (2010) 'Galaxy: a comprehensive approach for supporting accessible, reproducible, and transparent computational research in the life sciences', *Genome Biology*, 11(8), pp. 1–13. Available at: https://doi.org/10.1186/gb-2010-11-8-r86.

Górniak, W., Cholewińska, P., Szeligowska, N., Wołoszyńska, M., Soroko, M. and Czyż, K. (2021) 'Effect of Intense Exercise on the Level of Bacteroidetes and Firmicutes Phyla in the Digestive System of Thoroughbred Racehorses', *Animals : an Open Access Journal from MDPI*, 11(2), pp. 1–9. Available at: https://doi.org/10.3390/ANI11020290.

Götz, S., García-Gómez, J.M., Terol, J., Williams, T.D., Nagaraj, S.H., Nueda, M.J., Robles, M., Talón, M., Dopazo, J. and Conesa, A. (2008) 'High-throughput functional annotation and data mining with the Blast2GO suite', *Nucleic Acids Research*, 36(10), pp. 3420–3435. Available at: https://doi.org/10.1093/nar/gkn176.

Gourbal, B.E.F., Guillou, F., Mitta, G., Sibille, P., Thèron, A., Pointier, J.-P. and Coustau, C. (2008) 'Excretory–secretory products of larval *Fasciola hepatica* investigated using a two-dimensional proteomic approach', *Molecular and Biochemical Parasitology*, 161(1), pp. 63–66. Available at: https://doi.org/https://doi.org/10.1016/j.molbiopara.2008.05.002.

Grabherr, M.G. *et al.* (2011) 'Full-length transcriptome assembly from RNA-Seq data without a reference genome', *Nature Biotechnology*, 29(7), pp. 644–652. Available at: https://doi.org/10.1038/nbt.1883.

Greenberg, R.M. (2005) 'Are Ca2+ channels targets of praziquantel action?', *International Journal for Parasitology*, 35(1), pp. 1–9. Available at: https://doi.org/https://doi.org/10.1016/j.ijpara.2004.09.004.

Grimm, P., Philippeau, C. and Julliand, V. (2017) 'Faecal parameters as biomarkers of the equine hindgut microbial ecosystem under dietary change', *Animal*, 11(7), pp. 1136–1145. Available at: https://doi.org/10.1017/S1751731116002779.

Grubbs, S., Amodie, D., Rulli, D., Wulster-Radcliffe, M., Reinemeyer, C., Yazwinski, T., Tucker, C., Hutchens, D., Smith, L., Patterson, D. and Basilio, P. (2003) 'Field evaluation of moxidectin/praziquantel oral gel in horses', *Veterinary Therapeutics*, 4(3), pp. 249–256. Available at: https://europepmc.org/article/med/15136986 (Accessed: 23 December 2020).

Grzelak, S., Stachyra, A., Stefaniak, J., Mrówka, K., Moskwa, B. and Bień-Kalinowska, J. (2020) 'Immunoproteomic analysis of *Trichinella spiralis* and *Trichinella britovi* excretory-secretory muscle larvae proteins recognized by sera from humans infected with Trichinella', *PloS one*, 15(11), pp. e0241918–e0241918. Available at: https://doi.org/10.1371/journal.pone.0241918.

Guan, S., Yu, H., Yan, G., Gao, M., Sun, W. and Zhang, X. (2020) 'Characterization of Urinary Exosomes Purified with Size Exclusion Chromatography and Ultracentrifugation', *Journal of Proteome Research*, 19(6), pp. 2217–2225. Available at: https://doi.org/10.1021/acs.jproteome.9b00693.

Guillou, F., Roger, E., Moné, Y., Rognon, A., Grunau, C., Théron, A., Mitta, G., Coustau, C. and Gourbal, B.E.F. (2007) 'Excretory–secretory proteome of larval *Schistosoma mansoni* and *Echinostoma caproni*, two parasites of Biomphalaria glabrata', *Molecular and Biochemical Parasitology*, 155(1), pp. 45–56. Available at: https://doi.org/https://doi.org/10.1016/j.molbiopara.2007.05.009.

Guo, A. (2015) 'The complete mitochondrial genome of *Anoplocephala perfoliata*, the first representative for the family Anoplocephalidae', *Parasites & Vectors*, 8(1), p. 549. Available at: https://doi.org/10.1186/s13071-015-1172-z.

Guo, A. (2016) 'Complete Mitochondrial Genome of *Anoplocephala magna* Solidifying the Species.', *The Korean journal of parasitology*, 54(3), pp. 369–73. Available at: https://doi.org/10.3347/kjp.2016.54.3.369.

Haas, B.J. *et al.* (2013) 'De novo transcript sequence reconstruction from RNA-seq using the Trinity platform for reference generation and analysis', *Nature Protocols*, 8(8), pp. 1494–1512. Available at: https://doi.org/10.1038/nprot.2013.084.

Hague, A., Butt, A.J. and Paraskeva, C. (1996) 'The role of butyrate in human colonic epithelial cells: an energy source or inducer of differentiation and apoptosis?', *Proceedings of the Nutrition Society*. 2007/02/28, 55(3), pp. 937–943. Available at: https://doi.org/DOI: 10.1079/PNS19960090.

Hahn, M.A., Rosario, K., Lucas, P. and Dheilly, N.M. (2020) 'Characterization of viruses in a tapeworm: phylogenetic position, vertical transmission, and transmission to the parasitized host', *The ISME Journal*, 14(7), pp. 1755–1767. Available at: https://doi.org/10.1038/s41396-020-0642-2.

Hall, B.G. (2013) 'Building phylogenetic trees from molecular data with MEGA', *Molecular Biology and Evolution*, 30(5), pp. 1229–1235. Available at: https://doi.org/10.1093/molbev/mst012.

Hall, T.A. (1999) 'BioEdit: a user-friendly biological sequence alignment editor and analysis program for Windows 95/98/NT', in *Nucleic acids symposium series*. [London]: Information Retrieval Ltd., c1979-c2000., pp. 95–98.

Halperin, R.F. *et al.* (2021) 'Improved methods for RNAseq-based alternative splicing analysis', *Scientific Reports*, 11(1), p. 10740. Available at: https://doi.org/10.1038/s41598-021-89938-2.

Hamer, H.., Jonkers, D., Venema, K., Vanhoutvin, S., Troost, F.J. and Brummer, R.-J. (2008) 'Review article: the role of butyrate on colonic function', *Alimentary Pharmacology & Therapeutics*, 27(2), pp. 104–119. Available at: https://doi.org/https://doi.org/10.1111/j.1365-2036.2007.03562.x.

Hamer, H.M., Jonkers, D.M.A.E., Bast, A., Vanhoutvin, S.A.L.W., Fischer, M.A.J.G., Kodde, A., Troost, F.J., Venema, K. and Brummer, R.-J.M. (2009) 'Butyrate modulates oxidative stress in the colonic mucosa of healthy humans', *Clinical Nutrition*, 28(1), pp. 88–93. Available at: https://doi.org/https://doi.org/10.1016/j.clnu.2008.11.002.

Hammer, D.A.T., Ryan, P.D., Hammer, Ø. and Harper, D.A.T. (2001) 'Past: Paleontological Statistics Software Package for Education and Data Analysis', *Palaeontologia Electronica*, 4(1), p. 178. Available at: http://palaeo-electronica.orghttp//palaeo-electronica.org/2001_1/past/issue1_01.htm. (Accessed: 7 November 2022).

Han, C., Yu, J., Zhang, Z., Zhai, P., Zhang, Y., Meng, S., Yu, Y., Li, X. and Song, M. (2019) 'Immunomodulatory effects of *Trichinella spiralis* excretory-secretory antigens on macrophages', *Experimental Parasitology*, 196, pp. 68–72. Available at: https://doi.org/10.1016/j.exppara.2018.10.001.

Han, X., Aslanian, A. and Yates III, J.R. (2008) 'Mass spectrometry for proteomics', *Current opinion in chemical biology*, 12(5), pp. 483–490. Available at: https://doi.org/10.1016/j.cbpa.2008.07.024.

Hansen, A.M., Gu, Y., Li, M., Andrykovitch, M., Waugh, D.S., Jin, D.J. and Ji, X. (2005) 'Structural Basis for the Function of Stringent Starvation Protein A as a Transcription Factor *', *Journal of Biological Chemistry*, 280(17), pp. 17380–17391. Available at: https://doi.org/10.1074/JBC.M501444200.

Hansen, Eline P., Fromm, B., Andersen, S.D., Marcilla, A., Andersen, K.L., Borup, A., Williams, A.R., Jex, A.R., Gasser, R.B., Young, N.D., Hall, R.S., Stensballe, A., Ovchinnikov, V., Yan, Y., Fredholm, M., Thamsborg, S.M. and Nejsum, P. (2019) 'Exploration of extracellular vesicles from *Ascaris suum* provides evidence of parasite–host cross talk', *Journal of Extracellular Vesicles*, 8(1), p. 1578116. Available at: https://doi.org/10.1080/20013078.2019.1578116.

Hansen, M.S., Gregersen, S.B. and Rasmussen, J.T. (2022) 'Bovine milk processing impacts characteristics of extracellular vesicle isolates obtained by size-exclusion chromatography', *International Dairy Journal*, 127, p. 105212. Available at: https://doi.org/https://doi.org/10.1016/j.idairyj.2021.105212.

Hao, W.-L. and Lee, Y.-K. (2004) 'Microflora of the Gastrointestinal Tract BT - Public Health Microbiology: Methods and Protocols', in J.F.T. Spencer and A.L. Ragout de Spencer (eds). Totowa, NJ: Humana Press, pp. 491–502. Available at: https://doi.org/10.1385/1-59259-766-1:491.

Harnett, W. (2014) 'Secretory products of helminth parasites as immunomodulators', *Molecular and Biochemical Parasitology*. Elsevier, pp. 130–136. Available at: https://doi.org/10.1016/j.molbiopara.2014.03.007.

Harvey, S.E. and Cheng, C. (2016) 'Methods for Characterization of Alternative RNA Splicing BT - Long Non-Coding RNAs: Methods and Protocols', in Y. Feng and L. Zhang (eds). New York, NY: Springer New York, pp. 229–241. Available at: https://doi.org/10.1007/978-1-4939-3378-5_18.

Hastie, P.M., Mitchell, K. and Murray, J.-A.M.D. (2008a) 'Semi-quantitative analysis of *Ruminococcus flavefaciens*, *Fibrobacter succinogenes* and *Streptococcus bovis* in the equine large intestine using real-time polymerase chain reaction', *British Journal of Nutrition*. 2008/04/01, 100(3), pp. 561–568. Available at: https://doi.org/DOI: 10.1017/S0007114508968227.

Hautala, K., Pursiainen, J., Näreaho, A., Nyman, T., Varmanen, P., Sukura, A., Nielsen, M.K. and Savijoki, K. (2022) 'Label-free quantitative proteomics and immunoblotting identifies immunoreactive and other excretory-secretory (E/S) proteins of *Anoplocephala perfoliata* ', *Frontiers in Immunology* . Available at: https://www.frontiersin.org/articles/10.3389/fimmu.2022.1045468.

He, L., Ren, M., Chen, X., Wang, X., Li, S., Lin, J., Liang, C., Liang, P., Hu, Y., Lei, H., Bian, M., Huang, Y., Wu, Z., Li, X. and Yu, X. (2014) 'Biochemical and immunological characterization of annexin B30 from Clonorchis sinensis excretory/secretory products', *Parasitology Research*, 113(7), pp. 2743–2755. Available at: https://doi.org/10.1007/s00436-014-3935-4.

Heberle, H., Meirelles, V.G., da Silva, F.R., Telles, G.P. and Minghim, R. (2015) 'InteractiVenn: A web-based tool for the analysis of sets through Venn diagrams', *BMC Bioinformatics*, 16(1), p. 169. Available at: https://doi.org/10.1186/s12859-015-0611-3.

Helmby, H. and Grencis, R.K. (2004) 'Interleukin 1 plays a major role in the development of Th2-mediated immunity', *European Journal of Immunology*, 34(12), pp. 3674–3681. Available at: https://doi.org/10.1002/EJI.200425452.

Hewitson, J.P., Grainger, J.R. and Maizels, R.M. (2009) 'Helminth immunoregulation: the role of parasite secreted proteins in modulating host immunity', *Molecular and biochemical parasitology*. 2009/05/03, 167(1), pp. 1–11. Available at: https://doi.org/10.1016/j.molbiopara.2009.04.008.

Hinney, B., Wirtherle, N.C., Kyule, M., Miethe, N., Zessin, K.H. and Clausen, P.H. (2011) 'Prevalence of helminths in horses in the state of Brandenburg, Germany', *Parasitology Research*, 108(5), pp. 1083–1091. Available at: https://doi.org/10.1007/s00436-011-2362-z.

Hofmann, A., Osman, A., Leow, C.Y., Driguez, P., McManus, D.P. and Jones, M.K. (2010) 'Parasite annexins - New molecules with potential for drug and vaccine development', *BioEssays*, 32(11), pp. 967–976. Available at: https://doi.org/10.1002/bies.200900195.

Höglund, J., Ljungström, B.-L., Nilsson, O. and Uggla, A. (1995) 'Enzyme-linked immunosorbent assay (ELISA) for the detection of antibodies to *Anoplocephala perfoliata* in horse sera', *Veterinary Parasitology*, 59(2), pp. 97–106. Available at: https://doi.org/10.1016/0304-4017(94)00755-2.

Höglund, N., Koho, N., Rossi, H., Karttunen, J., Mustonen, A.-M., Nieminen, P., Rilla, K., Oikari, S. and Mykkänen, A. (2022) 'Isolation of Extracellular Vesicles From the Bronchoalveolar Lavage Fluid of Healthy and Asthmatic Horses ', *Frontiers in Veterinary Science* . Available at: https://www.frontiersin.org/article/10.3389/fvets.2022.894189.

Holm-Martin, M., Levot, G.W. and Dawson, K.L. (2005) 'Control of endoparasites in horses with a gel containing moxidectin and praziquantel', *Veterinary Record*, 156(26), pp. 835–838. Available at: https://doi.org/10.1136/vr.156.26.835.

Holm, J.B., Sorobetea, D., Kiilerich, P., Ramayo-Caldas, Y., Estellé, J., Ma, T., Madsen, L., Kristiansen, K. and Svensson-Frej, M. (2015) 'Chronic *Trichuris muris* Infection Decreases Diversity of the Intestinal Microbiota and Concomitantly Increases the Abundance of Lactobacilli', *PLOS ONE*. Edited by I.C. Allen, 10(5), p. e0125495. Available at: https://doi.org/10.1371/journal.pone.0125495.

Hölzer, M. and Marz, M. (2019) 'De novo transcriptome assembly: A comprehensive cross-species comparison of short-read RNA-Seq assemblers', *GigaScience*, 8(5). Available at: https://doi.org/10.1093/GIGASCIENCE/GIZ039.

Hooper, L. V., Littman, D.R. and Macpherson, A.J. (2012) 'Interactions Between the Microbiota and the Immune System', *Science*, 336(6086), pp. 1268–1273. Available at: https://doi.org/10.1126/science.1223490.

Hoshino, A., Kim, H.S., Bojmar, L., Gyan, K.E., Cioffi, M., Hernandez, J., Zambirinis, C.P., Rodrigues, G., Molina, H. and Heissel, S. (2020) 'Extracellular vesicle and particle biomarkers define multiple human cancers', *Cell*, 182(4), pp. 1044–1061.

Hoter, A., El-Sabban, M. and Naim, H. (2018) 'The HSP90 Family: Structure, Regulation, Function, and Implications in Health and Disease', *International Journal of Molecular Sciences*, 19(9), p. 2560. Available at: https://doi.org/10.3390/ijms19092560.

Houlden, A., Hayes, K.S., Bancroft, A.J., Worthington, J.J., Wang, P., Grencis, R.K. and Roberts, I.S. (2015) 'Chronic Trichuris muris Infection in C57BL/6 Mice Causes Significant Changes in Host Microbiota and Metabolome: Effects Reversed by Pathogen Clearance', *PLOS ONE*. Edited by C.H. Kim, 10(5), p. e0125945. Available at: https://doi.org/10.1371/journal.pone.0125945.

Hovhannisyan, L., Czechowska, E. and Gutowska-Owsiak, D. (2021) 'The Role of Non-Immune Cell-Derived Extracellular Vesicles in Allergy ', *Frontiers in Immunology* . Available at: https://www.frontiersin.org/articles/10.3389/fimmu.2021.702381.

Hreinsdóttir, I., Hreinsdóttir, A., Eydal, M., Tysnes, K.R. and Robertson, L.J. (2019) '*Anoplocephala perfoliata* Infection in Horses in Iceland: Investigation of Associations between Intensity of Infection and Lesions', *Journal of Parasitology*, 105(2), p. 379. Available at: https://doi.org/10.1645/18-159.

Hu, Dini, Chao, Y., Zhang, B., Wang, C., Qi, Y., Ente, M., Zhang, D., Li, K. and Mok, K.M. (2021) 'Effects of *Gasterophilus pecorum* infestation on the intestinal microbiota of the rewilded Przewalski's horses in China', *PLOS ONE*, 16(5), p. e0251512. Available at: https://doi.org/10.1371/journal.pone.0251512.

Hu, Dini., Yang, J., Qi, Y., Li, B., Li, K. and Mok, K.M. (2021) 'Metagenomic Analysis of Fecal Archaea, Bacteria, Eukaryota, and Virus in Przewalski's Horses Following Anthelmintic Treatment', *Frontiers in Veterinary Science*, 8, p. 868. Available at: https://doi.org/10.3389/fvets.2021.708512.

Huang, H.-I., Lin, J.-Y., Chiang, H.-C., Huang, P.-N., Lin, Q.-D. and Shih, S.-R. (2020) 'Exosomes Facilitate Transmission of Enterovirus A71 From Human Intestinal Epithelial Cells', *The Journal of Infectious Diseases*, 222(3), pp. 456–469. Available at: https://doi.org/10.1093/infdis/jiaa174.

Huang, S.-Y., Yue, D.-M., Hou, J.-L., Zhang, X.-X., Zhang, F., Wang, C.-R. and Zhu, X.-Q. (2019) 'Proteomic analysis of *Fasciola gigantic*a excretory and secretory products (FgESPs) interacting with buffalo serum of different infection periods by shotgun LC-MS/MS', *Parasitology Research*, 118(2), pp. 453–460. Available at: https://doi.org/10.1007/s00436-018-6169-z.

Huang, Y. *et al.* (2013) 'The carcinogenic liver fluke, *Clonorchis sinensis*: new assembly, reannotation and analysis of the genome and characterization of tissue transcriptomes', *PloS one*, 8(1). Available at: https://doi.org/10.1371/JOURNAL.PONE.0054732.

Huang, Y., Niu, B., Gao, Y., Fu, L. and Li, W. (2010) 'CD-HIT Suite: A web server for clustering and comparing biological sequences', *Bioinformatics*, 26(5), pp. 680–682. Available at: https://doi.org/10.1093/bioinformatics/btq003.

Hur, Y.H., Cerione, R.A. and Antonyak, M.A. (2020) 'Extracellular vesicles and their roles in stem cell biology', *Stem Cells*, 38(4), pp. 469–476. Available at: https://doi.org/10.1002/stem.3140.

Huson, K.M., Morphew, R.M., Allen, N.R., Hegarty, M.J., Worgan, H.J., Girdwood, S.E., Jones, E.L., Phillips, H.C., Vickers, M., Swain, M., Smith, D., Kingston-Smith, A.H. and Brophy, P.M. (2018) 'Polyomic tools for an emerging livestock parasite, the rumen fluke *Calicophoron daubneyi*; identifying shifts in rumen functionality', *Parasites and Vectors*, 11(1), p. 617. Available at: https://doi.org/10.1186/s13071-018-3225-6.

Iriarte, A., Arbildi, P., La-Rocca, S., Musto, H. and Fernández, V. (2012) 'Identification of novel glutathione transferases in *Echinococcus granulosus*. An evolutionary perspective', *Acta Tropica*, 123(3), pp. 208–216. Available at: https://doi.org/10.1016/j.actatropica.2012.05.010.

Issa Isaac, N., Philippe, D., Nicholas, A., Raoult, D. and Eric, C. (2019) 'Metaproteomics of the human gut microbiota: Challenges and contributions to other OMICS', *Clinical Mass Spectrometry*, 14, pp. 18–30. Available at: https://doi.org/https://doi.org/10.1016/j.clinms.2019.06.001.

Jalili, V., Afgan, E., Gu, Q., Clements, D., Blankenberg, D., Goecks, J., Taylor, J. and Nekrutenko, A. (2020) 'Erratum: The Galaxy platform for accessible, reproducible and collaborative biomedical analyses: 2020 update (Nucleic Acids Research (2020) DOI: 10.1093/nar/gkaa434)', *Nucleic Acids Research*. Oxford University Press, pp. 8205–8207. Available at: https://doi.org/10.1093/nar/gkaa554.

Janis, C. (1976) 'THE EVOLUTIONARY STRATEGY OF THE EQUIDAE AND THE ORIGINS OF RUMEN AND CECAL DIGESTION', *Evolution*, 30(4), pp. 757–774. Available at: https://doi.org/10.1111/j.1558-5646.1976.tb00957.x.

Jawad, A.Q. and Alfatlawi, M.A.A. (2023) 'Molecular study and DNA sequence analysis of *Theileria annulata* in cattle in Al-Hilla, Iraq', *Iraqi Journal of Veterinary Sciences*, 37(2), pp. 425–429. Available at: https://doi.org/10.33899/ijvs.2022.135154.2450.

Jayaprakash, P., Dong, H., Zou, M., Bhatia, A., O'Brien, K., Chen, M., Woodley, D.T. and Li, W. (2015) 'Hsp90α and Hsp90β together operate a hypoxia and nutrient paucity stress-response mechanism during wound healing', *Journal of Cell Science*, 128(8), pp. 1475–1480. Available at: https://doi.org/10.1242/jcs.166363.

Jefferies, J.R., Campbell, A.M., Rossum, A.J. van, Barrett, J. and Brophy, P.M. (2001) 'Proteomic analysis of *Fasciola hepatica* excretory-secretory products', *PROTEOMICS*, 1(8), pp. 1128–1132. Available at: https://doi.org/10.1002/1615-9861(200109)1:9<1128::AID-PROT1128>3.0.CO;2-0.

Jenkins, S.J., Hewitson, J.P., Jenkins, G.R. and Mountford, A.P. (2005) 'Modulation of the host's immune response by schistosome larvae', *Parasite Immunology*, 27(10–11), pp. 385–393. Available at: https://doi.org/https://doi.org/10.1111/j.1365-3024.2005.00789.x.

Jesús, S., Sofía, B., Miguel, S., Carlos, R.J., Javier, S.-V., Antonio, G., Montserrat, R.-G., Alicia, B., Elena, L.-G., Eva, G., Carlos, S. and Gloria, R. (2020) 'Real-Time PCR for Diagnosing *Helicobacter pylori* Infection in Patients with Upper Gastrointestinal Bleeding: Comparison with Other Classical Diagnostic Methods', *Journal of Clinical Microbiology*, 50(10), pp. 3233–3237. Available at: https://doi.org/10.1128/jcm.01205-12.

Ji, J., Su, L. and Liu, Z. (2016) 'Critical role of calpain in inflammation (Review)', *Biomed Rep*, 5(6), pp. 647–652. Available at: https://doi.org/10.3892/br.2016.785.

Jiang, P., Zao, Y.J., Yan, S.W., Song, Y.Y., Yang, D.M., Dai, L.Y., Liu, R.D., Zhang, X., Wang, Z.Q. and Cui, J. (2019) 'Molecular characterization of a *Trichinella spiralis* enolase and its interaction with the host's plasminogen', *Veterinary Research*, 50(1), pp. 1–12. Available at: https://doi.org/10.1186/S13567-019-0727-Y/FIGURES/10.

Jiang, Y., Cai, X., Yao, J., Guo, H., Yin, L., Leung, W. and Xu, C. (2020) 'Role of Extracellular Vesicles in Influenza Virus Infection ', *Frontiers in Cellular and Infection Microbiology* . Available at: https://www.frontiersin.org/articles/10.3389/fcimb.2020.00366.

Johnson, J.L. (2012) 'Evolution and function of diverse Hsp90 homologs and cochaperone proteins', *Biochimica et Biophysica Acta (BBA) - Molecular Cell Research*, 1823(3), pp. 607–613. Available at: https://doi.org/10.1016/j.bbamcr.2011.09.020.

Johnston, C.J.C. *et al.* (2017) 'A structurally distinct TGF-β mimic from an intestinal helminth parasite potently induces regulatory T cells', *Nature communications*, 8(1), p. 1741. Available at: https://doi.org/10.1038/s41467-017-01886-6.

Johnstone, R.M., Adam, M., Hammond, J.R., Orr, L. and Turbide, C. (1987) 'Vesicle formation during reticulocyte maturation. Association of plasma membrane activities with released vesicles (exosomes).', *Journal of Biological Chemistry*, 262(19), pp. 9412–9420. Available at: https://doi.org/https://doi.org/10.1016/S0021-9258(18)48095-7.

Jolodar, A., Fischer, P., Bergmann, S., Büttner, D.W., Hammerschmidt, S. and Brattig, N.W. (2003) 'Molecular cloning of an α-enolase from the human filarial parasite *Onchocerca volvulus* that binds human plasminogen', *Biochimica et Biophysica Acta - Gene Structure and Expression*, 1627(2–3), pp. 111–120. Available at: https://doi.org/10.1016/S0167-4781(03)00083-6.

Jones, D.T. (1999) 'Protein secondary structure prediction based on position-specific scoring matrices', *Journal of Molecular Biology*, 292(2), pp. 195–202. Available at: https://doi.org/10.1006/jmbi.1999.3091.

Jones, P., Binns, D., Chang, H.Y., Fraser, M., Li, W., McAnulla, C., McWilliam, H., Maslen, J., Mitchell, A., Nuka, G., Pesseat, S., Quinn, A.F., Sangrador-Vegas, A., Scheremetjew, M., Yong, S.Y., Lopez, R. and Hunter, S. (2014) 'InterProScan 5: Genome-scale protein function classification', *Bioinformatics*, 30(9), pp. 1236–1240. Available at: https://doi.org/10.1093/bioinformatics/btu031.

Julliand, V. and Grimm, P. (2016) 'HORSE SPECIES SYMPOSIUM: The microbiome of the horse hindgut: History and current knowledge1', *Journal of Animal Science*, 94(6), pp. 2262–2274. Available at: https://doi.org/10.2527/jas.2015-0198.

Jung, A.L., Schmeck, B., Wiegand, M., Bedenbender, K. and Benedikter, B.J. (2021) 'The clinical role of host and bacterial-derived extracellular vesicles in pneumonia', *Advanced Drug Delivery Reviews*, 176, p. 113811. Available at: https://doi.org/https://doi.org/10.1016/j.addr.2021.05.021.

Jürgenschellert, L., Krücken, J., Austin, C.J., Lightbody, K.L., Bousquet, E. and von Samson-Himmelstjerna, G. (2020) 'Investigations on the occurrence of tapeworm infections in German horse populations with comparison of different antibody detection methods based on saliva and serum samples', *Parasites & Vectors*, 13(1), p. 462. Available at: https://doi.org/10.1186/s13071-020-04318-5.

Kak, G., Raza, M. and Tiwari, B.K. (2018) 'Interferon-gamma (IFN-γ): Exploring its implications in infectious diseases', 9(1), pp. 64–79. Available at: https://doi.org/doi:10.1515/bmc-2018-0007.

Kalluri, R. and McAndrews, K.M. (2023) 'The role of extracellular vesicles in cancer', *Cell*, 186(8), pp. 1610–1626. Available at: https://doi.org/10.1016/j.cell.2023.03.010.

Kalra, H. *et al.* (2012) 'Vesiclepedia: A Compendium for Extracellular Vesicles with Continuous Community Annotation', *PLoS Biology*, 10(12), p. e1001450. Available at: https://doi.org/10.1371/journal.pbio.1001450.

Kania, S.A. and Reinemeyer, C.R. (2005) '*Anoplocephala perfoliata* coproantigen detection: a preliminary study', *Veterinary Parasitology*, 127(2), pp. 115–119. Available at: https://doi.org/10.1016/j.vetpar.2004.10.003.

Kay, G.L., Millard, A., Sergeant, M.J., Midzi, N., Gwisai, R., Mduluza, T., Ivens, A., Nausch, N., Mutapi, F. and Pallen, M. (2015) 'Differences in the Faecal Microbiome in *Schistosoma haematobium* Infected Children vs. Uninfected Children', *PLOS Neglected Tropical Diseases*. Edited by A.R. Jex, 9(6), p. e0003861. Available at: https://doi.org/10.1371/journal.pntd.0003861.

Keerthikumar, S., Chisanga, D., Ariyaratne, D., Al Saffar, H., Anand, S., Zhao, K., Samuel, M., Pathan, M., Jois, M., Chilamkurti, N., Gangoda, L. and Mathivanan, S. (2016) 'ExoCarta: A Web-Based Compendium of Exosomal Cargo', *Journal of Molecular Biology*, 428(4), pp. 688–692. Available at: https://doi.org/10.1016/J.JMB.2015.09.019.

Keller, S., Ridinger, J., Rupp, A.-K., Janssen, J.W.G. and Altevogt, P. (2011) 'Body fluid derived exosomes as a novel template for clinical diagnostics', *Journal of Translational Medicine*, 9(1), p. 86. Available at: https://doi.org/10.1186/1479-5876-9-86.

Kenney, E.T., Mann, V.H., Ittiprasert, W., Rosa, B.A., Mitreva, M., Bracken, B.K., Loukas, A., Brindley, P.J. and Sotillo, J. (2022) 'Differential excretory/secretory proteome of the adult female and male stages of the human blood fluke, *Schistosoma mansoni*, *bioRxiv*, p. 2022.05.22.492965. Available at: https://doi.org/10.1101/2022.05.22.492965.

Keshtkar, S., Azarpira, N. and Ghahremani, M.H. (2018) 'Mesenchymal stem cell-derived extracellular vesicles: novel frontiers in regenerative medicine', *Stem Cell Research & Therapy*, 9(1), p. 63. Available at: https://doi.org/10.1186/s13287-018-0791-7.

Kifle, D.W., Chaiyadet, S., Waardenberg, A.J., Wise, I., Cooper, M., Becker, L., Doolan, D.L., Laha, T., Sotillo, J., Pearson, M.S. and Loukas, A. (2020) 'Uptake of *Schistosoma mansoni* extracellular vesicles by human endothelial and monocytic cell lines and impact on vascular endothelial cell gene expression', *International Journal for Parasitology*, 50(9), pp. 685–696. Available at: https://doi.org/10.1016/J.IJPARA.2020.05.005.

Kifle, D.W., Pearson, M.S., Becker, L., Pickering, D., Loukas, A. and Sotillo, J. (2020) 'Proteomic analysis of two populations of *Schistosoma mansoni*-derived extracellular vesicles: 15k pellet and 120k pellet vesicles', *Molecular and Biochemical Parasitology*, 236, p. 111264. Available at: https://doi.org/10.1016/j.molbiopara.2020.111264.

Kifle, D.W., Sotillo, J., Pearson, M.S. and Loukas, A. (2017) 'Extracellular vesicles as a target for the development of anti-helminth vaccines', *Emerging Topics in Life Sciences*. Edited by R. Docampo, 1(6), pp. 659–665. Available at: https://doi.org/10.1042/ETLS20170095.

Kim, J.-G.G., Ahn, C.-S.S., Kim, S.-H.H., Bae, Y.-A.A., Kwon, N.-Y.Y., Kang, I., Yang, H.-J.J., Sohn, W.-M.M. and Kong, Y. (2016) '*Clonorchis sinensis* omega-class glutathione transferases play major roles in the protection of the reproductive system during maturation and the response to oxidative stress', *Parasites & vectors*, 9(1), p. 337. Available at: https://doi.org/10.1186/s13071-016-1622-2.

Kim, Y., Cha, S.J., Choi, H.J. and Kim, K. (2017) 'Omega Class Glutathione S-Transferase: Antioxidant Enzyme in Pathogenesis of Neurodegenerative Diseases', *Oxidative Medicine and Cellular Longevity*, 2017. Available at: https://doi.org/10.1155/2017/5049532.

Kjaer, L.N., Lungholt, M.M., Nielsen, M.K., Olsen, S.N. and Maddox-Hyttel, C. (2007) 'Interpretation of serum antibody response to *Anoplocephala perfoliata* in relation to parasite burden and faecal egg count', *Equine Veterinary Journal*, 39(6), pp. 529–533. Available at: https://doi.org/10.2746/042516407X217876.

Klopfenstein, D. V., Zhang, L., Pedersen, B.S., Ramírez, F., Vesztrocy, A.W., Naldi, A., Mungall, C.J., Yunes, J.M., Botvinnik, O., Weigel, M., Dampier, W., Dessimoz, C., Flick, P. and Tang, H. (2018) 'GOATOOLS: A Python library for Gene Ontology analyses', *Scientific Reports*, 8(1). Available at: https://doi.org/10.1038/s41598-018-28948-z.

Kobe, B. and Kajava, A. V (2001) 'The leucine-rich repeat as a protein recognition motif', *Current Opinion in Structural Biology*, 11(6), pp. 725–732. Available at: https://doi.org/https://doi.org/10.1016/S0959-440X(01)00266-4.

Kobpornchai, P., Flynn, R.J., Reamtong, O., Rittisoonthorn, N., Kosoltanapiwat, N., Boonnak, K., Boonyuen, U., Ampawong, S., Jiratanh, M., Tattiyapong, M. and Adisakwattana, P. (2020) 'A novel cystatin derived from *Trichinella spiralis* suppresses macrophage-mediated inflammatory responses', *PLoS neglected tropical diseases*, 14(4), pp. e0008192–e0008192. Available at: https://doi.org/10.1371/journal.pntd.0008192.

Kohn, A.B., Roberts-Misterly, J.M., Anderson, P.A.V., Khan, N. and Greenberg, R.M. (2003) 'Specific sites in the Beta Interaction Domain of a schistosome Ca^{2+} channel β subunit are key to its role in sensitivity to the anti-schistosomal drug praziquantel', *Parasitology*, 127(4), pp. 349–356. Available at: https://doi.org/10.1017/S003118200300386X.

Konoshenko, M.Y., Lekchnov, E.A., Vlassov, A. V and Laktionov, P.P. (2018) 'Isolation of Extracellular Vesicles: General Methodologies and Latest Trends'. Available at: https://doi.org/10.1155/2018/8545347.

Kosanović, M., Cvetković, J., Gruden-Movsesijan, A., Vasilev, S., Svetlana, M., Ilić, N. and Sofronić-Milosavljević, L. (2019) '*Trichinella spiralis* muscle larvae release extracellular vesicles with immunomodulatory properties', *Parasite Immunology*, 41(10), pp. 1–5. Available at: https://doi.org/10.1111/pim.12665.

Kou, M., Huang, L., Yang, J., Chiang, Z., Chen, S., Liu, J., Guo, L., Zhang, X., Zhou, X., Xu, X., Yan, X., Wang, Y., Zhang, J., Xu, A., Tse, H. and Lian, Q. (2022) 'Mesenchymal stem cell-derived extracellular vesicles for immunomodulation and regeneration: a next generation therapeutic tool?', *Cell Death & Disease*, 13(7), p. 580. Available at: https://doi.org/10.1038/s41419-022-05034-x.

Kück, P., Meusemann, K., Dambach, J., Thormann, B., von Reumont, B.M., Wägele, J.W. and Misof, B. (2010) 'Parametric and non-parametric masking of randomness in sequence alignments can be improved and leads to better resolved trees', *Frontiers in Zoology*, 7(1), p. 10. Available at: https://doi.org/10.1186/1742-9994-7-10.

Kuhn, M. (2009) '*In-vitro*-Untersuchungen zum Einfluss von Erythromycin und Nahrungsreduktion auf mikrobielle Stoffwechselleistungen im Caecum des Pferdes'.

Kuipers, M.E., Nolte-'t Hoen, E.N.M., van der Ham, A.J., Ozir-Fazalalikhan, A., Nguyen, D.L., de Korne, C.M., Koning, R.I., Tomes, J.J., Hoffmann, K.F., Smits, H.H. and Hokke, C.H. (2020) 'DC-SIGN mediated internalisation of glycosylated extracellular vesicles from *Schistosoma mansoni* increases activation of monocyte-derived dendritic cells', *Journal of Extracellular Vesicles*, 9(1). Available at: https://doi.org/10.1080/20013078.2020.1753420.

Kujawa, T.J., van Doorn, D.A., Wambacq, W.A., Hesta, M. and Pellikaan, W.F. (2020) 'Evaluation of equine rectal inoculum as representative of the microbial activities within the horse hindgut using a fully automated in vitro gas production technique system', *Journal of animal science*, 98(3), p. skaa050. Available at: https://doi.org/10.1093/jas/skaa050.

Kukurba, K.R. and Montgomery, S.B. (2015) 'RNA Sequencing and Analysis', *Cold Spring Harbor Protocols*, 2015(11), p. pdb.top084970. Available at: https://doi.org/10.1101/PDB.TOP084970.

Kumagai, T., Maruyama, H., Hato, M., Ohmae, H., Osada, Y., Kanazawa, T. and Ohta, N. (2005) '*Schistosoma japonicum*: localization of calpain in the penetration glands and secretions of cercariae', *Experimental Parasitology*, 109(1), pp. 53–57. Available at: https://doi.org/https://doi.org/10.1016/j.exppara.2004.11.001.

Kumar, S., Stecher, G., Li, M., Knyaz, C. and Tamura, K. (2018) 'MEGA X: Molecular evolutionary genetics analysis across computing platforms', *Molecular Biology and Evolution*, 35(6), pp. 1547–1549. Available at: https://doi.org/10.1093/molbev/msy096.

Kunz, I.G.Z., Reed, K.J., Metcalf, J.L., Hassel, D.M., Coleman, R.J., Hess, T.M. and Coleman, S.J. (2019) 'Equine Fecal Microbiota Changes Associated With Anthelmintic Administration', *Journal of Equine Veterinary Science*, 77, pp. 98–106. Available at: https://doi.org/10.1016/j.jevs.2019.01.018.

de la Fuente, G., Jones, E., Jones, S. and Newbold, C.J. (2017) 'Functional Resilience and Response to a Dietary Additive (Kefir) in Models of Foregut and Hindgut Microbial Fermentation In Vitro', *Frontiers in Microbiology*, 8(JUN), p. 1194. Available at: https://doi.org/10.3389/fmicb.2017.01194.

de la Torre-Escudero, E., Gerlach, J.Q., Bennett, A.P.S.S., Cwiklinski, K., Jewhurst, H.L., Huson, K.M., Joshi, L., Kilcoyne, M., O'Neill, S., Dalton, J.P. and Robinson, M.W. (2019) 'Surface molecules of extracellular vesicles secreted by the helminth pathogen Fasciola hepatica direct their internalisation by host cells', *PLoS Neglected Tropical Diseases*. Edited by R.B. Gasser, 13(1), p. e0007087. Available at: https://doi.org/10.1371/journal.pntd.0007087.

LaCourse, E.J., Perally, S., Morphew, R.M., Moxon, J. V., Prescott, M., Dowling, D.J., O'Neill, S.M., Kipar, A., Hetzel, U., Hoey, E., Zafra, R., Buffoni, L., Pérez Arévalo, J., Brophy, P.M., Arévalo, J., Brophy, P.M., Pérez Arévalo, J. and Brophy, P.M. (2012) 'The Sigma class glutathione transferase from the liver fluke *Fasciola hepatica*', *PLoS neglected tropical diseases*. 2012/05/29. Edited by M.K. Jones, 6(5), pp. e1666–e1666. Available at: https://doi.org/10.1371/journal.pntd.0001666.

Lalawmpuii, K. and Lalrinkima, H. (2023) 'Genetic manipulations in helminth parasites', *Journal of Parasitic Diseases*, 47(2), pp. 203–214. Available at: https://doi.org/10.1007/s12639-023-01567-w.

Lane, R.E., Korbie, D., Hill, M.M. and Trau, M. (2018) 'Extracellular vesicles as circulating cancer biomarkers: opportunities and challenges', *Clinical and Translational Medicine*, 7(1), p. e14. Available at: https://doi.org/https://doi.org/10.1186/s40169-018-0192-7.

Langer, T., Rosmus, S. and Fasold, H. (2003) 'Intracellular localization of the 90 kDA heat shock protein (HSP90α) determined by expression of a EGFP—HSP90α-fusion protein in unstressed and heat stressed 3T3 cells', *Cell Biology International*, 27(1), pp. 47–52. Available at: https://doi.org/https://doi.org/10.1016/S1065-6995(02)00256-1.

Lavelle, A. and Sokol, H. (2020) 'Gut microbiota-derived metabolites as key actors in inflammatory bowel disease', *Nature reviews. Gastroenterology & hepatology*, 17(4), pp. 223–237. Available at: https://doi.org/10.1038/s41575-019-0258-z.

Lawson, A.L., Pittaway, C.E., Sparrow, R.M., Balkwill, E.C., Coles, G.C., Tilley, A. and Wilson, A.D. (2019) 'Analysis of caecal mucosal inflammation and immune modulation during *Anoplocephala perfoliata* infection of horses', *Parasite Immunology*, 41(11), p. e12667. Available at: https://doi.org/10.1111/pim.12667.

Le, L.H.M., Steele, J.R., Ying, L., Schittenhelm, R.B. and Ferrero, R.L. (2023) 'A new isolation method for bacterial extracellular vesicles providing greater purity and improved proteomic detection of vesicle proteins', *Journal of Extracellular Biology*, 2(5), p. e84. Available at: https://doi.org/https://doi.org/10.1002/jex2.84.

Lee, D.L. and Tatchell, R.J. (1964) 'Studies on the tapeworm *Anoplocephala perfoliata* (Goeze, 1782)', *Parasitology*, 54(03), p. 467. Available at: https://doi.org/10.1017/S0031182000082512.

Leng, J., Walton, G., Swann, J., Darby, A., La Ragione, R. and Proudman, C. (2019) '"Bowel on the Bench": Proof of Concept of a Three-Stage, In Vitro Fermentation Model of the Equine Large Intestine', *Applied and environmental microbiology*, 86(1), pp. e02093-19. Available at: https://doi.org/10.1128/AEM.02093-19.

Letunic, I. and Bork, P. (2018) '20 years of the SMART protein domain annotation resource', *Nucleic Acids Research*, 46(D1), pp. D493–D496. Available at: https://doi.org/10.1093/nar/gkx922.

Letunic, I., Khedkar, S. and Bork, P. (2021) 'SMART: Recent updates, new developments and status in 2020', *Nucleic Acids Research*, 49(D1), pp. D458–D460. Available at: https://doi.org/10.1093/nar/gkaa937.

Li, D. (2022) 'Role of Spectrin in Endocytosis', *Cells 2022, Vol. 11, Page 2459*, 11(15), p. 2459. Available at: https://doi.org/10.3390/CELLS11152459.

Li, R.W., Li, W., Sun, J., Yu, P., Baldwin, R.L. and Urban, J.F. (2016) 'The effect of helminth infection on the microbial composition and structure of the caprine abomasal microbiome.', *Scientific reports*, 6, p. 20606. Available at: https://doi.org/10.1038/srep20606.

Li, R.W., Wu, S., Li, W., Huang, Y. and Gasbarre, L.C. (2011) 'Metagenome Plasticity of the Bovine Abomasal Microbiota in Immune Animals in Response to *Ostertagia Ostertagi* Infection', *PLoS ONE*. Edited by R.K. Aziz, 6(9), p. e24417. Available at: https://doi.org/10.1371/journal.pone.0024417.

Li, S. *et al.* (2014) 'Multi-platform assessment of transcriptome profiling using RNA-seq in the ABRF next-generation sequencing study', *Nature biotechnology*, 32(9), pp. 915–925. Available at: https://doi.org/10.1038/NBT.2972.

Li, S., Chen, X., Zhou, J., Xie, Z., Shang, M., He, L., Liang, P., Chen, T., Mao, Q., Liang, C., Li, X., Huang, Y. and Yu, X. (2020) 'Amino acids serve as an important energy source for adult flukes of *Clonorchis sinensis*', *PLOS Neglected Tropical Diseases*, 14(4), p. e0008287. Available at: https://doi.org/10.1371/journal.pntd.0008287.

Li, S., Khafipour, E., Krause, D.O., Kroeker, A., Rodriguez-Lecompte, J.C., Gozho, G.N. and Plaizier, J.C. (2012) 'Effects of subacute ruminal acidosis challenges on fermentation and endotoxins in the rumen and hindgut of dairy cows', *Journal of Dairy Science*, 95(1), pp. 294–303. Available at: https://doi.org/https://doi.org/10.3168/jds.2011-4447.

Li, W. and Godzik, A. (2006) 'Cd-hit: A fast program for clustering and comparing large sets of protein or nucleotide sequences', *Bioinformatics*, 22(13), pp. 1658–1659. Available at: https://doi.org/10.1093/bioinformatics/btl158.

Li, W., Jaroszewski, L. and Godzik, A. (2001) 'Clustering of highly homologous sequences to reduce the size of large protein databases', *Bioinformatics*, 17(3), pp. 282–283. Available at: https://doi.org/10.1093/bioinformatics/17.3.282.

Li, W., Jaroszewski, L. and Godzik, A. (2002) 'Tolerating some redundancy significantly speeds up clustering of large protein databases', *Bioinformatics*, 18(1), pp. 77–82. Available at: https://doi.org/10.1093/bioinformatics/18.1.77.

Li, W.H., Yang, Y., Zhang, N.Z., Wang, J.K., Liu, Y.J., Li, L., Yan, H. Bin, Jia, W.Z. and Fu, B. (2021) 'Comparative Transcriptome Analyses of the Developmental Stages of *Taenia multiceps*', *Frontiers in Veterinary Science*, 8, p. 707. Available at: https://doi.org/10.3389/FVETS.2021.677045/BIBTEX.

Liang, P., Mao, L., Zhang, S., Guo, X., Liu, G., Wang, L., Hou, J., Zheng, Y. and Luo, X. (2019) 'Identification and molecular characterization of exosome-like vesicles derived from the *Taenia asiatica* adult worm', *Acta Tropica*, 198, p. 105036. Available at: https://doi.org/10.1016/j.actatropica.2019.05.027.

Lichtenauer, M., Nick, S., Hoetzenecker, K., Mangold, A., Mitterbauer, A., Hacker, S., Zimmermann, M. and Ankersmit, H.J. (2011) 'Effect of PBS solutions on chemokine secretion of human peripheral blood mononuclear cells', *American Laboratory*, 43(1), pp. 30–33.

Liebau, E., Eschbach, M.L., Tawe, W., Sommer, A., Fischer, P., Walter, R.D. and Henkle-Dührsen, K. (2000) 'Identification of a stress-responsive *Onchocerca volvulus* glutathione S-transferase (Ov-GST-3) by RT-PCR differential display', *Molecular and Biochemical Parasitology*, 109(2), pp. 101–110. Available at: https://doi.org/10.1016/S0166-6851(00)00232-2.

Liepman, R.S., Swink, J.M., Habing, G.G., Boyaka, P.N., Caddey, B., Costa, M., Gomez, D.E. and Toribio, R.E. (2022) 'Effects of Intravenous Antimicrobial Drugs on the Equine Fecal Microbiome', *Animals* . Available at: https://doi.org/10.3390/ani12081013.

Liew, F.Y., Vickerman, K. and Grencis, R.K. (1997) 'Th2–mediated host protective immunity to intestinal nematode infections', *Philosophical Transactions of the Royal Society of London. Series B: Biological Sciences*, 352(1359), pp. 1377–1384. Available at: https://doi.org/10.1098/rstb.1997.0123.

Lightbody, K.L., Davis, P.J. and Austin, C.J. (2016) 'Validation of a novel saliva-based ELISA test for diagnosing tapeworm burden in horses', *Veterinary Clinical Pathology*, 45(2), pp. 335–346. Available at: https://doi.org/10.1111/vcp.12364.

Lightbody, K.L., Matthews, J.B., Kemp-Symonds, J.G., Lambert, P.A. and Austin, C.J. (2018) 'Use of a saliva-based diagnostic test to identify tapeworm infection in horses in the UK', *Equine Veterinary Journal*, 50(2), pp. 213–219. Available at: https://doi.org/10.1111/evj.12742.

Lightowlers, M.W. and Rickard, M.D. (1988) 'Excretory–secretory products of helminth parasites: effects on host immune responses', *Parasitology*. 2011/08/23, 96(S1), pp. S123–S166. Available at: https://doi.org/DOI: 10.1017/S0031182000086017.

Lindenberg, F., Krych, L., Kot, W., Fielden, J., Frøkiær, H., van Galen, G., Nielsen, D.S. and Hansen, A.K. (2019) 'Development of the equine gut microbiota', *Scientific Reports*, 9(1), p. 14427. Available at: https://doi.org/10.1038/s41598-019-50563-9.

Line, K., Isupov, M.N., LaCourse, E.J., Cutress, D.J., Morphew, R.M., Brophy, P.M. and Littlechild, J.A. (2019) 'X-ray structure of *Fasciola hepatica* Sigma class glutathione transferase 1 reveals a disulfide bond to support stability in gastro-intestinal environment', *Scientific Reports*, 9(1), pp. 1–9. Available at: https://doi.org/10.1038/s41598-018-37531-5.

Liu, F., Cui, S.J., Hu, W., Feng, Z., Wang, Z.Q. and Han, Z.G. (2009) 'Excretory/secretory proteome of the adult developmental stage of human blood fluke, *Schistosoma japonicum*', *Molecular and Cellular Proteomics*, 8(6), pp. 1236–1251. Available at: https://doi.org/10.1074/mcp.M800538-MCP200.

Liu, G.-H., Xu, M.-J., Song, H.-Q., Wang, C.-R. and Zhu, X.-Q. (2016) 'De novo assembly and characterization of the transcriptome of the pancreatic fluke *Eurytrema pancreaticum* (trematoda: Dicrocoeliidae) using Illumina paired-end sequencing', *Gene*, 576(1), pp. 333–338. Available at: https://doi.org/10.1016/J.GENE.2015.10.045.

Liu, J., Zhu, L., Wang, J., Qiu, L., Chen, Y., Davis, R.E. and Cheng, G. (2019) '*Schistosoma japonicum* extracellular vesicle mirna cargo regulates host macrophage functions facilitating parasitism', *PLoS Pathogens*, 15(6). Available at: https://doi.org/10.1371/journal.ppat.1007817.

Liu, P., Yu, S., Cui, Y., He, J., Yu, C., Wen, Z., Pan, Y., Yang, K., Song, L. and Yang, X. (2017) 'Cloning of HSP90, expression and localization of HSP70/90 in different tissues including lactating/non-lactating yak (Bos grunniens) breast tissue', *PLOS ONE*. Edited by G. Multhoff, 12(7), p. e0179321. Available at: https://doi.org/10.1371/journal.pone.0179321.

Liu, R., Cheng, W.J., Ye, F., Zhang, Y.D., Zhong, Q.P., Dong, H.F., Tang, H. Bin and Jiang, H. (2020) 'Comparative Transcriptome Analyses of *Schistosoma japonicum* Derived From SCID Mice and BALB/c Mice: Clues to the Abnormality in Parasite Growth and Development', *Frontiers in Microbiology*, 11, p. 274. Available at: https://doi.org/10.3389/FMICB.2020.00274/BIBTEX.

Liu, S., Zhou, X., Hao, L., Piao, X., Hou, N. and Chen, Q. (2017) 'Genome-Wide transcriptome analysis reveals extensive alternative splicing events in the protoscoleces of *Echinococcus granulosus* and *Echinococcus multilocularis*', *Frontiers in Microbiology*, 8(MAY), p. 929. Available at: https://doi.org/10.3389/FMICB.2017.00929/BIBTEX.

Liu, X., Fan, H., Ding, X., Hong, Z., Nei, Y., Liu, Z., Li, G. and Guo, H. (2014) 'Analysis of the gut microbiota by high-throughput sequencing of the v5-v6 regions of the 16s rRNA gene in donkey', *Current Microbiology*, 68(5), pp. 657–662. Available at: https://doi.org/10.1007/s00284-014-0528-5.

Lopez-Gonzalez, V., La-Rocca, S., Arbildi, P. and Fernandez, V. (2018) 'Characterization of catalytic and non-catalytic activities of EgGST2-3, a heterodimeric glutathione transferase from *Echinococcus granulosus*', *Acta Tropica*, 180, pp. 69–75. Available at: https://doi.org/10.1016/J.ACTATROPICA.2018.01.007.

Lopez, E., Srivastava, A.K., Burchfield, J., Wang, Y.-W., Cardenas, J.C., Togarrati, P.P., Miyazawa, B., Gonzalez, E., Holcomb, J.B., Pati, S. and Wade, C.E. (2019) 'Platelet-derived- Extracellular Vesicles Promote Hemostasis and Prevent the Development of Hemorrhagic Shock', *Scientific Reports*, 9(1), p. 17676. Available at: https://doi.org/10.1038/s41598-019-53724-y.

Lowman, R.S., Theodorou, M.K., Hyslop, J.J., Dhanoa, M.S. and Cuddeford, D. (1999) 'Evulation of an in vitro batch culture technique for estimating the in vivo digestibility and digestible energy content of equine feeds using equine faeces as the source of microbial inoculum', *Animal Feed Science and Technology*, 80(1), pp. 11–27. Available at: https://doi.org/10.1016/S0377-8401(99)00039-5.

Lyons, E.T., Bellaw, J.L., Dorton, A.R. and Tolliver, S.C. (2017) 'Efficacy of moxidectin and an ivermectin-praziquantel combination against ascarids, strongyles, and tapeworms in Thoroughbred yearlings in field tests on a farm in Central Kentucky in 2016', *Veterinary Parasitology: Regional Studies and Reports*, 8, pp. 123–126. Available at: https://doi.org/10.1016/j.vprsr.2017.03.006.

Lyons, E.T., Bolin, D.C., Bryant, U.K., Cassone, L.M., Jackson, C.B., Janes, J.G., Kennedy, L.A., Loynachan, A.T., Boll, K.R., Burkhardt, A.S., Langlois, E.L., Minnis, S.M., Welsh, S.C. and Scare, J.A. (2018) 'Postmortem examination (2016–2017) of weanling and older horses for the presence of select species of endoparasites: *Gasterophilus spp., Anoplocephala spp.* and *Strongylus spp.* in specific anatomical sites', *Veterinary Parasitology: Regional Studies and Reports*, 13, pp. 98–104. Available at: https://doi.org/10.1016/j.vprsr.2018.01.004.

Lyons, E.T., Tolliver, S.C., Drudge, J.H., Swerczek, T.W. and Crowe, M.W. (1987) 'Common internal parasites found in the stomach, large intestine, and cranial mesenteric artery of thoroughbreds in Kentucky at necropsy (1985 to 1986)', *American journal of veterinary research*, 48(2), pp. 268–273. Available at: http://europepmc.org/abstract/MED/2950814.

Lyons, E.T., Tolliver, S.C., Stamper, S., Drudge, J.H. and Granstrom, D.E. (1995) '*Anoplocephala perfoliata* (Cestoda) in equids', 56(June 1993), pp. 255–257.

Ma, X.-X., Qiu, Y.-Y., Chang, Z.-G., Gao, J.-F., Jiang, R.-R., Li, C.-L., Wang, C.-R. and Chang, Q.-C. (2021) 'Identification of Myoferlin, a Potential Serodiagnostic Antigen of Clonorchiasis, via Immunoproteomic Analysis of Sera From Different Infection Periods and Excretory-Secretory Products of *Clonorchis sinensis* ', *Frontiers in Cellular and Infection Microbiology* . Available at: https://www.frontiersin.org/article/10.3389/fcimb.2021.779259.

Mach, N., Foury, A., Kittelmann, S., Reigner, F., Moroldo, M., Ballester, M., Esquerré, D., Rivière, J., Sallé, G., Gérard, P., Moisan, M.-P. and Lansade, L. (2017) 'The Effects of Weaning Methods on Gut Microbiota Composition and Horse Physiology', *Frontiers in Physiology*, 8, p. 535. Available at: https://doi.org/10.3389/fphys.2017.00535.

Mach, N., Lansade, L., Bars-Cortina, D., Dhorne-Pollet, S., Foury, A., Moisan, M.-P. and Ruet, A. (2021) 'Gut microbiota resilience in horse athletes following holidays out to pasture', *Scientific Reports*, 11(1), p. 5007. Available at: https://doi.org/10.1038/s41598-021-84497-y.

Machnicka, B., Grochowalska, R., Bogusławska, D.M. and Sikorski, A.F. (2019) 'The role of spectrin in cell adhesion and cell–cell contact', *Experimental Biology and Medicine*, 244(15), pp. 1303–1312. Available at: https://doi.org/10.1177/1535370219859003.

Machnicka, B., Ponceau, A., Picot, J., Colin, Y. and Lecomte, M.-C. (2020) 'Deficiency of αII-spectrin affects endothelial cell–matrix contact and migration leading to impairment of angiogenesis in vitro', *Cellular & Molecular Biology Letters*, 25(1), p. 3. Available at: https://doi.org/10.1186/s11658-020-0200-y.

Mackie, R.I. and Wilkins, C.A. (1988) 'Enumeration of anaerobic bacterial microflora of the equine gastrointestinal tract.', *Applied and Environmental Microbiology*, 54(9).

MacNicol, J.L., Renwick, S., Ganobis, C.M., Allen-Vercoe, E., Weese, J.S. and Pearson, W. (2022) 'A Comparison of Methods to Maintain the Equine Cecal Microbial Environment In Vitro Utilizing Cecal and Fecal Material', *Animals*. Available at: https://doi.org/10.3390/ani12152009.

Maizels, R.M. (2013) '*Toxocara canis*: molecular basis of immune recognition and evasion', *Veterinary parasitology*. 2012/12/20, 193(4), pp. 365–374. Available at: https://doi.org/10.1016/j.vetpar.2012.12.032.

Maizels, R.M. and Page, A.P. (1990) 'Surface associated glycoproteins from Toxocara canis larval parasites', *Acta Tropica*, 47(5), pp. 355–364. Available at: https://doi.org/https://doi.org/10.1016/0001-706X(90)90036-Y.

Maizels, R.M., Philipp, M. and Ogilvie, B.M. (1982) 'Molecules on the Surface of Parasitic Nematodes as Probes of the Immune Response in Infection', *Immunological Reviews*, 61(1), pp. 109–136. Available at: https://doi.org/https://doi.org/10.1111/j.1600-065X.1982.tb00375.x.

Maizels, R.M., Smits, H.H. and McSorley, H.J. (2018) 'Modulation of Host Immunity by Helminths: The Expanding Repertoire of Parasite Effector Molecules', *Immunity*, 49(5), pp. 801–818. Available at: https://doi.org/10.1016/j.immuni.2018.10.016.

Malmuthuge, N. and Guan, L.L. (2016) 'Gut microbiome and omics: a new definition to ruminant production and health', *Animal Frontiers*, 6(2), pp. 8–12. Available at: https://doi.org/10.2527/af.2016-0017.

Mansour, T.E. and Mansour, J.M. (2002) 'Energy Metabolism in Parasitic Helminths: Targets for Antiparasitic Agents', in T.E. Mansour (ed.) *Chemotherapeutic Targets in Parasites: Contemporary Strategies*. Cambridge: Cambridge University Press, pp. 33–57. Available at: https://doi.org/DOI: 10.1017/CBO9780511546440.004.

Marchiondo, A.A., White, G.W., Smith, L.L., Reinemeyer, C.R., Dascanio, J.J., Johnson, E.G. and Shugart, J.I. (2006) 'Clinical field efficacy and safety of pyrantel pamoate paste (19.13% w/w pyrantel base) against Anoplocephala spp. in naturally infected horses', *Veterinary Parasitology*, 137(1–2), pp. 94–102. Available at: https://doi.org/10.1016/j.vetpar.2005.12.019.

Marcilla, A., Pérez-García, A., Espert, A., Bernal, D., Muñoz-Antolí, C., Esteban, J.G. and Toledo, R. (2007) '*Echinostoma caproni*: Identification of enolase in excretory/secretory products, molecular cloning, and functional expression', *Experimental Parasitology*, 117(1), pp. 57–64. Available at: https://doi.org/10.1016/J.EXPPARA.2007.03.011.

Marcilla, A., Trelis, M., Cortés, A., Sotillo, J., Cantalapiedra, F., Minguez, M.T., Valero, M.L., Sánchez del Pino, M.M., Muñoz-Antoli, C., Toledo, R. and Bernal, D. (2012) 'Extracellular Vesicles from Parasitic Helminths Contain Specific Excretory/Secretory Proteins and Are Internalized in Intestinal Host Cells', *PLoS ONE*, 7(9), p. e45974. Available at: https://doi.org/10.1371/journal.pone.0045974.

Margulis, L. and Chapman, M.J. (2009) *Kingdoms and domains: an illustrated guide to the phyla of life on Earth*. Academic Press.

Marley, S., Hutchens, D., Reinemeyer, C., Holste, J., Paul, A., Rehbein, S., Harris, J. and Dhupa, S. (2004) 'Antiparasitic activity of an ivermectin and praziquantel combination paste in horses', *Veterinary Therapeutics*, 5(2).

Maruszewska-Cheruiyot, M., Szewczak, L., Krawczak-Wójcik, K., Głaczyńska, M. and Donskow-Łysoniewska, K. (2021) 'The production of excretory-secretory molecules from *Heligmosomoides polygyrus bakeri* fourth stage larvae varies between mixed and single sex cultures', *Parasites & Vectors*, 14(1), p. 106. Available at: https://doi.org/10.1186/s13071-021-04613-9.

Marzano, V., Mancinelli, L., Bracaglia, G., Del Chierico, F., Vernocchi, P., Di Girolamo, F., Garrone, S., Tchidjou Kuekou, H., D'Argenio, P., Dallapiccola, B., Urbani, A. and Putignani, L. (2017) '"Omic" investigations of protozoa and worms for a deeper understanding of the human gut "parasitome"', *PLOS Neglected Tropical Diseases*, 11(11), p. e0005916. Available at: https://doi.org/10.1371/journal.pntd.0005916.

Maslowski, K.M. and MacKay, C.R. (2011) 'Diet, gut microbiota and immune responses', *Nature Immunology*, pp. 5–9. Available at: https://doi.org/10.1038/ni0111-5.

Mathewos, M., Girma, D., Fesseha, H., Yirgalem, M. and Eshetu, E. (2021) 'Prevalence of Gastrointestinal Helminthiasis in Horses and Donkeys of Hawassa District, Southern Ethiopia', *Veterinary Medicine International*. Edited by B.O. Bebe, 2021, p. 6686688. Available at: https://doi.org/10.1155/2021/6686688.

Mathivanan, S., Fahner, C.J., Reid, G.E. and Simpson, R.J. (2012) 'ExoCarta 2012: database of exosomal proteins, RNA and lipids', *Nucleic Acids Research*, 40(D1), pp. D1241–D1244. Available at: https://doi.org/10.1093/NAR/GKR828.

Mathivanan, S., Ji, H. and Simpson, R.J. (2010) 'Exosomes: Extracellular organelles important in intercellular communication', *Journal of Proteomics*, 73(10), pp. 1907–1920. Available at: https://doi.org/https://doi.org/10.1016/j.jprot.2010.06.006.

Matthews, J.B. and Burden, F.A. (2013) 'Common helminth infections of donkeys and their control in temperate regions', *Equine Veterinary Education*, 25(9), pp. 461–467. Available at: https://doi.org/https://doi.org/10.1111/eve.12018.

Mazanec, H., Koník, P., Gardian, Z. and Kuchta, R. (2021) 'Extracellular vesicles secreted by model tapeworm Hymenolepis diminuta: biogenesis, ultrastructure and protein composition', *International Journal for Parasitology*, 51(5), pp. 327–332. Available at: https://doi.org/10.1016/j.ijpara.2020.09.010.

McKenney, E.A., Williamson, L., Yoder, A.D., Rawls, J.F., Bilbo, S.D. and Parker, W. (2015) 'Alteration of the rat cecal microbiome during colonization with the helminth Hymenolepis diminuta.', *Gut microbes*, 6(3), pp. 182–93. Available at: https://doi.org/10.1080/19490976.2015.1047128.

Meana, A., Luzon, M., Corchero, J. and Gómez-Bautista, M. (1998) *Reliability of coprological diagnosis of Anoplocephala perfoliata infection*, *Veterinary Parasitology*. Available at: https://doi.org/10.1016/S0304-4017(97)00145-3.

Meana, A., Pato, N.F., Martín, R., Mateos, A., Pérez-García, J. and Luzón, M. (2005) 'Epidemiological studies on equine cestodes in central Spain: Infection pattern and population dynamics', *Veterinary Parasitology*, 130(3–4), pp. 233–240. Available at: https://doi.org/10.1016/j.vetpar.2005.03.040.

Mekonnen, G.G., Tedla, B.A., Pickering, D., Becker, L., Wang, L., Zhan, B., Bottazzi, M.E., Loukas, A., Sotillo, J. and Pearson, M.S. (2020) '*Schistosoma haematobium* Extracellular Vesicle Proteins Confer Protection in a Heterologous Model of Schistosomiasis', *Vaccines* . Available at: https://doi.org/10.3390/vaccines8030416.

Meng, F., Zhang, Y., Liu, F., Guo, X. and Xu, B. (2014) 'Characterization and Mutational Analysis of Omega-Class GST (GSTO1) from *Apis cerana cerana*, a Gene Involved in Response to Oxidative Stress', *PLOS ONE*, 9(3), p. e93100. Available at: https://doi.org/10.1371/JOURNAL.PONE.0093100.

Meningher, T., Barsheshet, Y., Ofir-Birin, Y., Gold, D., Brant, B., Dekel, E., Sidi, Y., Schwartz, E., Regev-Rudzki, N., Avni, O. and Avni, D. (2020) 'Schistosomal extracellular vesicle-enclosed miRNAs modulate host T helper cell differentiation', *EMBO reports*, 21(1). Available at: https://doi.org/10.15252/embr.201947882.

Metral, S., Machnicka, B., Bigot, S., Colin, Y., Dhermy, D. and Lecomte, M.-C. (2009) 'αII-Spectrin Is Critical for Cell Adhesion and Cell Cycle*', *Journal of Biological Chemistry*, 284(4), pp. 2409–2418. Available at: https://doi.org/https://doi.org/10.1074/jbc.M801324200.

Meyer, D.J., Coles, B., Pemble, S.E., Gilmore, K.S., Fraser, G.M. and Ketterer, B. (1991) 'Theta, a new class of glutathione transferases purified from rat and man', *The Biochemical journal*, 274 (Pt 2, pp. 409–414. Available at: https://doi.org/10.1042/bj2740409.

Meyer, H. and Klingeberg-Kraus, S. (2002) 'Entwicklung der fisteltechnik am verdauungskanal von equiden', *Pferdeheilkunde*, 18, pp. 633–639.

Mezerova, J., Koudela, B. and Vojtkova, M. (2007) 'Equine colic caused by tape worms-5 clinical case reports', *Praktische Tierarzt*, 88(1), pp. 26-+.

Michael McAloon, F. (2004) 'Oribatid mites as intermediate hosts of *Anoplocephala manubriata*, cestode of the Asian elephant in India', *Experimental & Applied Acarology*, 32(3), pp. 181–185. Available at: https://doi.org/10.1023/B:APPA.0000021795.02103.d0.

Midha, A., Janek, K., Niewienda, A., Henklein, P., Guenther, S., Serra, D.O., Schlosser, J., Hengge, R. and Hartmann, S. (2018) 'The intestinal roundworm *Ascaris suum* releases antimicrobial factors which interfere with bacterial growth and biofilm formation', *Frontiers in cellular and infection microbiology*, 8, p. 271.

Miles, S., Mourglia-Ettlin, G. and Fernández, V. (2022) 'Expanding the family of Mu-class glutathione transferases in the cestode parasite *Echinococcus granulosus* sensu lato', *Gene*, 835, p. 146659. Available at: https://doi.org/10.1016/J.GENE.2022.146659.

Milinovich, G.J., Burrell, P.C., Pollitt, C.C., Klieve, A. V, Blackall, L.L., Ouwerkerk, D., Woodland, E. and Trott, D.J. (2008) 'Microbial ecology of the equine hindgut during oligofructose-induced laminitis', *The ISME Journal*, 2(11), pp. 1089–1100. Available at: https://doi.org/10.1038/ismej.2008.67.

Mills, J.T., Schwenzer, A., Marsh, E.K., Edwards, M.R., Sabroe, I., Midwood, K.S. and Parker, L.C. (2019) 'Airway Epithelial Cells Generate Pro-inflammatory Tenascin-C and Small Extracellular Vesicles in Response to TLR3 Stimuli and Rhinovirus Infection ', *Frontiers in Immunology* . Available at: https://www.frontiersin.org/articles/10.3389/fimmu.2019.01987.

Min, B., Prout, M., Hu-Li, J., Zhu, J., Jankovic, D., Morgan, E.S., Urban, J.F., Dvorak, A.M., Finkelman, F.D., LeGros, G. and Paul, W.E. (2004) 'Basophils Produce IL-4 and Accumulate in Tissues after Infection with a Th2-inducing Parasite', *Journal of Experimental Medicine*, 200(4), pp. 507–517. Available at: https://doi.org/10.1084/JEM.20040590.

Miranda-Miranda, E., Cossio-Bayugar, R., Aguilar-Díaz, H., Narváez-Padilla, V., Sachman-Ruíz, B. and Reynaud, E. (2021) 'Transcriptome assembly dataset of anthelmintic response in *Fasciola hepatica*', *Data in Brief*, 35, p. 106808. Available at: https://doi.org/10.1016/J.DIB.2021.106808.

Mistry, J., Chuguransky, S., Williams, L., Qureshi, M., Salazar, G.A., Sonnhammer, E.L.L., Tosatto, S.C.E., Paladin, L., Raj, S., Richardson, L.J., Finn, R.D. and Bateman, A. (2021) 'Pfam: The protein families database in 2021', *Nucleic Acids Research*, 49(D1), pp. D412–D419. Available at: https://doi.org/10.1093/nar/gkaa913.

Mohammadi, M.A., Harandi, M.F., McManus, D.P. and Mansouri, M. (2021) 'Genome-wide transcriptome analysis of the early developmental stages of *Echinococcus granulosus* protoscoleces reveals extensive alternative splicing events in the spliceosome pathway', *Parasites and Vectors*, 14(1), pp. 1–14. Available at: https://doi.org/10.1186/S13071-021-05067-9/TABLES/5.

Molehin, A.J. (2020) 'Schistosomiasis vaccine development: update on human clinical trials', *Journal of Biomedical Science*, 27(1), pp. 1–7. Available at: https://doi.org/10.1186/s12929-020-0621-y.

Monguió-Tortajada, M., Gálvez-Montón, C., Bayes-Genis, A., Roura, S. and Borràs, F.E. (2019) 'Extracellular vesicle isolation methods: rising impact of size-exclusion chromatography', *Cellular and Molecular Life Sciences*, 76(12), pp. 2369–2382. Available at: https://doi.org/10.1007/s00018-019-03071-y.

Moreau, M.M., Eades, S.C., Reinemeyer, C.R., Fugaro, M.N. and Onishi, J.C. (2014) 'Illumina sequencing of the V4 hypervariable region 16S rRNA gene reveals extensive changes in bacterial communities in the cecum following carbohydrate oral infusion and development of early-stage acute laminitis in the horse', *Veterinary Microbiology*, 168(2–4), pp. 436–441. Available at: https://doi.org/10.1016/J.VETMIC.2013.11.017.

Morphew, R.M., Eccleston, N., Wilkinson, T.J., McGarry, J., Perally, S., Prescott, M., Ward, D., Williams, D., Paterson, S., Raman, M., Ravikumar, G., Khalid Saifullah, M., Abbas Abidi, S.M., McVeigh, P., Maule, A.G., Brophy, P.M. and LaCourse, E.J. (2012) 'Proteomics and *in Silico* Approaches To Extend Understanding of the Glutathione Transferase Superfamily of the Tropical Liver Fluke *Fasciola gigantica*', *Journal of Proteome Research*, 11(12), pp. 5876–5889. Available at: https://doi.org/10.1021/pr300654w.

Morphew, R.M., MacKintosh, N., Hart, E.H., Prescott, M., LaCourse, E.J. and Brophy, P.M. (2014) 'In vitro biomarker discovery in the parasitic flatworm *Fasciola hepatica* for monitoring chemotherapeutic treatment', *EuPA Open Proteomics*, 3, pp. 85–99. Available at: https://doi.org/10.1016/j.euprot.2014.02.013.

Morphew, R.M., Wright, H.A., LaCourse, E.J., Porter, J., Barrett, J., Woods, D.J. and Brophy, P.M. (2011) 'Towards Delineating Functions within the Fasciola Secreted Cathepsin L Protease Family by Integrating In Vivo Based Sub-Proteomics and Phylogenetics', *PLoS Neglected Tropical Diseases*. Edited by J.P. Dalton, 5(1), p. e937. Available at: https://doi.org/10.1371/journal.pntd.0000937.

Morrison, P.K., Newbold, C.J., Jones, E., Worgan, H.J., Grove-White, D.H., Dugdale, A.H., Barfoot, C., Harris, P.A. and Argo, C.M. (2018) 'The Equine Gastrointestinal Microbiome: Impacts of Age and Obesity', *Frontiers in Microbiology*, 9. Available at: https://doi.org/10.3389/FMICB.2018.03017.

Mossallam, S.F., Abou-El-Naga, I.F., Abdel Bary, A., Elmorsy, E.A. and Diab, R.G. (2021) '*Schistosoma mansoni* egg-derived extracellular vesicles: A promising vaccine candidate against murine schistosomiasis', *PLOS Neglected Tropical Diseases*, 15(10), p. e0009866. Available at: https://doi.org/10.1371/journal.pntd.0009866.

Mshelia, E.S., Adamu, L., Wakil, Y., Turaki, U.A., Gulani, I.A. and Musa, J. (2018) 'The association between gut microbiome, sex, age and body condition scores of horses in Maiduguri and its environs', *Microbial Pathogenesis*, 118, pp. 81–86. Available at: https://doi.org/https://doi.org/10.1016/j.micpath.2018.03.018.

Muhonen, S., Sadet-Bourgeteau, S. and Julliand, V. (2021) 'Effects of Differences in Fibre Composition and Maturity of Forage-Based Diets on the Microbial Ecosystem and Its Activity in Equine Caecum and Colon Digesta and Faeces', *Animals*. Available at: https://doi.org/10.3390/ani11082337.

Mulcahy, L.A., Pink, R.C. and Carter, D.R.F. (2014) 'Routes and mechanisms of extracellular vesicle uptake', *Journal of Extracellular Vesicles*, 3(1), p. 24641. Available at: https://doi.org/10.3402/jev.v3.24641.

Murphy, A., Cwiklinski, K., Lalor, R., O'connell, B., Robinson, M.W., Gerlach, J., Joshi, L., Kilcoyne, M., Dalton, J.P. and O'Neill, S.M. (2020) '*Fasciola hepatica* Extracellular Vesicles isolated from excretory-secretory products using a gravity flow method modulate dendritic cell phenotype and activity', *PLOS Neglected Tropical Diseases*, 14(9), p. e0008626. Available at: https://doi.org/10.1371/journal.pntd.0008626.

Murray, J.A.M.D., McMullin, P., Handel, I. and Hastie, P.M. (2012) 'The effect of freezing on the fermentative activity of equine faecal inocula for use in an *in vitro* gas production technique', *Animal Feed Science and Technology*, 178(3–4), pp. 175–182. Available at: https://doi.org/10.1016/j.anifeedsci.2012.09.013.

Murray, J.M.D., McMullin, P., Handel, I. and Hastie, P.M. (2014) 'Comparison of intestinal contents from different regions of the equine gastrointestinal tract as inocula for use in an *in vitro* gas production technique', *Animal Feed Science and Technology*, 187, pp. 98–103. Available at: https://doi.org/10.1016/j.anifeedsci.2013.10.005.

Nagalakshmi, U., Waern, K. and Snyder, M. (2010) 'RNA-Seq: a method for comprehensive transcriptome analysis', *Current protocols in molecular biology*, Chapter 4(SUPPL. 89). Available at: https://doi.org/10.1002/0471142727.MB0411S89.

Napoli, E., Song, G., Panoutsopoulos, A., Riyadh, M.A., Kaushik, G., Halmai, J., Levenson, R., Zarbalis, K.S. and Giulivi, C. (2018) 'Beyond autophagy: a novel role for autism-linked Wdfy3 in brain mitophagy', *Scientific Reports*, 8(1), pp. 1–19. Available at: https://doi.org/10.1038/s41598-018-29421-7.

Nawaz, M., Malik, M.I., Zhang, H., Hassan, I.A., Cao, J., Zhou, Y., Hameed, M., Hussain Kuthu, Z. and Zhou, J. (2020) 'Proteomic Analysis of Exosome-Like Vesicles Isolated From Saliva of the Tick *Haemaphysalis longicornis*', *Frontiers in Cellular and Infection Microbiology*. Available at: https://www.frontiersin.org/articles/10.3389/fcimb.2020.542319.

Nelson, D.R. (2009) 'The Cytochrome P450 Homepage', *Human Genomics 2009 4:1*, 4(1), pp. 1–7. Available at: https://doi.org/10.1186/1479-7364-4-1-59.

Nguyen, D.B., Thuy Ly, T.B., Wesseling, M.C., Hittinger, M., Torge, A., Devitt, A., Perrie, Y. and Bernhardt, I. (2016) 'Characterization of Microvesicles Released from Human Red Blood Cells', *Cellular Physiology and Biochemistry*, 38(3), pp. 1085–1099. Available at: https://doi.org/10.1159/000443059.

Nguyen, D.B., Tran, H.T., Kaestner, L. and Bernhardt, I. (2022) 'The Relation Between Extracellular Vesicles Released From Red Blood Cells, Their Cargo, and the Clearance by Macrophages ', *Frontiers in Physiology* . Available at: https://www.frontiersin.org/articles/10.3389/fphys.2022.783260.

Nguyen, H.A., Bae, Y.A., Lee, E.G., Kim, S.H., Diaz-Camacho, S.P., Nawa, Y., Kang, I. and Kong, Y. (2010) 'A novel sigma-like glutathione transferase of *Taenia solium* metacestode', *International Journal for Parasitology*, 40(9), pp. 1097–1106. Available at: https://doi.org/10.1016/j.ijpara.2010.03.007.

Nicolao, M.C., Rodriguez Rodrigues, C. and Cumino, A.C. (2019) 'Extracellular vesicles from *Echinococcus granulosus* larval stage: Isolation, characterization and uptake by dendritic cells', *PLoS Neglected Tropical Diseases*, 13(1), p. e0007032. Available at: https://doi.org/10.1371/journal.pntd.0007032.

Nielsen, M.K. (2016) 'Equine tapeworm infections: Disease, diagnosis and control', *Equine Veterinary Education*, 28(7), pp. 388–395. Available at: https://doi.org/10.1111/eve.12394.

Nielsen, M.K. (2023) 'Apparent treatment failure of praziquantel and pyrantel pamoate against anoplocephalid tapeworms', *International Journal for Parasitology: Drugs and Drug Resistance*, 22(May), pp. 96–101. Available at: https://doi.org/10.1016/j.ijpddr.2023.06.002.

Nilsson, O., Ljungström, B.-L., Höglund, J., Lundquist, H. and Uggla, A. (1995) '*Anoplocephala perfoliata* in horses in Sweden: prevalence, infection levels and intestinal lesions', *Acta Veterinaria Scandinavica*, 36, pp. 319–328.

Nogi, T., Zhang, D., Chan, J.D. and Marchant, J.S. (2009) 'A Novel Biological Activity of Praziquantel Requiring Voltage-Operated Ca2+ Channel β Subunits: Subversion of Flatworm Regenerative Polarity', *PLOS Neglected Tropical Diseases*, 3(6), p. e464. Available at: https://doi.org/10.1371/journal.pntd.0000464.

Nogueira, R.A., Lira, M.G.S., Licá, I.C.L., Frazão, G.C.C.G., dos Santos, V.A.F., Filho, A.C.C.M., Rodrigues, J.G.M., Miranda, G.S., Carvalho, R.C. and Nascimento, F.R.F. (2022) 'Praziquantel: An update on the mechanism of its action against schistosomiasis and new therapeutic perspectives', *Molecular and Biochemical Parasitology*, 252, p. 111531. Available at: https://doi.org/10.1016/j.molbiopara.2022.111531.

Nono, J.K., Lutz, M.B. and Brehm, K. (2020) 'Expansion of Host Regulatory T Cells by Secreted Products of the Tapeworm *Echinococcus multilocularis*', *Frontiers in Immunology*. Available at: https://www.frontiersin.org/article/10.3389/fimmu.2020.00798.

Nono, J.K., Pletinckx, K., Lutz, M.B. and Brehm, K. (2012) 'Excretory/secretory-products of *Echinococcus multilocularis* larvae induce apoptosis and tolerogenic properties in dendritic cells in vitro', *PLoS Neglected Tropical Diseases*, 6(2), p. e1516. Available at: https://doi.org/10.1371/journal.pntd.0001516.

Norris, J.K., Steuer, A.E., Gravatte, H.S., Slusarewicz, P., Bellaw, J.L., Scare, J.A. and Nielsen, M.K. (2018) 'Determination of the specific gravity of eggs of equine strongylids, *Parascaris spp*., and *Anoplocephala perfoliata*', *Veterinary parasitology*, 260, pp. 45–48. Available at: https://doi.org/10.1016/j.vetpar.2018.08.004.

Ofir-Birin, Y., Abou karam, P., Rudik, A., Giladi, T., Porat, Z. and Regev-Rudzki, N. (2018) 'Monitoring Extracellular Vesicle Cargo Active Uptake by Imaging Flow Cytometry', *Frontiers in Immunology* . Available at: https://www.frontiersin.org/articles/10.3389/fimmu.2018.01011.

Olson, P.D., Zarowiecki, M., James, K., Baillie, A., Bartl, G., Burchell, P., Chellappoo, A., Jarero, F., Tan, L.Y., Holroyd, N. and Berriman, M. (2018) 'Genome-wide transcriptome profiling and spatial expression analyses identify signals and switches of development in tapeworms', *EvoDevo*, 9(1), pp. 1–29. Available at: https://doi.org/10.1186/s13227-018-0110-5.

Opadokun, T. and Rohrbach, P. (2021) 'Extracellular vesicles in malaria: an agglomeration of two decades of research', *Malaria Journal*, 20(1), p. 442. Available at: https://doi.org/10.1186/s12936-021-03969-8.

Ørskov, E.R. and McDonald, I. (1979a) 'The estimation of protein degradability in the rumen from incubation measurements weighted according to rate of passage', *The Journal of Agricultural Science*. 2009/03/27, 92(2), pp. 499–503. Available at: https://doi.org/DOI: 10.1017/S0021859600063048.

Ørskov, E.R. and McDonald, I. (1979b) 'The estimation of protein degradability in the rumen from incubation measurements weighted according to rate of passage', *The Journal of Agricultural Science*. 2009/03/27, 92(2), pp. 499–503. Available at: https://doi.org/DOI: 10.1017/S0021859600063048.

Owen, R.A., Jagger, D.W. and Quan-Taylor, R. (1989) 'Caecal intussusceptions in horses and the significance of *Anoplocephala perfoliata*.', *The Veterinary record*, pp. 34–37. Available at: https://doi.org/10.1136/vr.124.2.34.

Pakharukova, M.Y., Ershov, N.I., Vorontsova, E. V., Katokhin, A. V., Merkulova, T.I. and Mordvinov, V.A. (2012) 'Cytochrome P450 in fluke *Opisthorchis felineus*: Identification and characterization', *Molecular and Biochemical Parasitology*, 181(2), pp. 190–194. Available at: https://doi.org/10.1016/J.MOLBIOPARA.2011.11.005.

Paludo, G.P., Thompson, C.E., Miyamoto, K.N., Guedes, R.L.M., Zaha, A., De Vasconcelos, A.T.R., Cancela, M. and Ferreira, H.B. (2020) 'Cestode strobilation: Prediction of developmental genes and pathways', *BMC Genomics*, 21(1), pp. 1–16. Available at: https://doi.org/10.1186/s12864-020-06878-3.

Palviainen, M., Saraswat, M., Varga, Z., Kitka, D., Neuvonen, M., Puhka, M., Joenväärä, S., Renkonen, R., Nieuwland, R., Takatalo, M. and Siljander, P.R.M. (2020) 'Extracellular vesicles from human plasma and serum are carriers of extravesicular cargo—Implications for biomarker discovery', *PLOS ONE*, 15(8), p. e0236439. Available at: https://doi.org/10.1371/journal.pone.0236439.

Pan, W., Hao, W.T., Shen, Y.J., Li, X.Y., Wang, Y.J., Sun, F.F., Yin, J.H., Zhang, J., Tang, R.X., Cao, J.P. and Zheng, K.Y. (2017) 'The excretory-secretory products of *Echinococcus granulosus* protoscoleces directly regulate the differentiation of B10, B17 and Th17 cells', *Parasites and Vectors*, 10(1), pp. 1–11. Available at: https://doi.org/10.1186/s13071-017-2263-9.

Pan, W., Shen, Y., Han, X., Wang, Ying, Liu, H., Jiang, Y., Zhang, Y., Wang, Yanjuan, Xu, Y. and Cao, J. (2014) 'Transcriptome Profiles of the Protoscoleces of *Echinococcus granulosus* Reveal that Excretory-Secretory Products Are Essential to Metabolic Adaptation', *PLoS Neglected Tropical Diseases*, 8(12), p. e3392. Available at: https://doi.org/10.1371/journal.pntd.0003392.

Pancholi, V. (2001) 'Multifunctional α-enolase: Its role in diseases', *Cellular and Molecular Life Sciences*. Birkhauser Verlag Basel, pp. 902–920. Available at: https://doi.org/10.1007/PL00000910.

Papaiakovou, M., Littlewood, D.T.J., Doyle, S.R., Gasser, R.B. and Cantacessi, C. (2022) 'Worms and bugs of the gut: the search for diagnostic signatures using barcoding, and metagenomics–metabolomics', *Parasites & Vectors*, 15(1), p. 118. Available at: https://doi.org/10.1186/s13071-022-05225-7.

Park, S.-K., Friedrich, L., Yahya, N.A., Rohr, C.M., Chulkov, E.G., Maillard, D., Rippmann, F., Spangenberg, T. and Marchant, J.S. (2021) 'Mechanism of praziquantel action at a parasitic flatworm ion channel', *Science translational medicine*, 13(625), p. eabj5832. Available at: https://doi.org/10.1126/scitranslmed.abj5832.

Park, S.K., Gunaratne, G.S., Chulkov, E.G., Moehring, F., McCusker, P., Dosa, P.I., Chan, J.D., Stucky, C.L. and Marchant, J.S. (2019) 'The anthelmintic drug praziquantel activates a schistosome transient receptor potential channel', *Journal of Biological Chemistry*, 294(49), pp. 18873–18880. Available at: https://doi.org/10.1074/jbc.AC119.011093.

Park, T., Cheong, H., Yoon, J., Kim, A., Yun, Y. and Unno, T. (2021) 'Comparison of the Fecal Microbiota of Horses with Intestinal Disease and Their Healthy Counterparts', *Veterinary sciences*, 8(6), p. 113. Available at: https://doi.org/10.3390/vetsci8060113.

Park, T., Yoon, J., Kim, A., Unno, T. and Yun, Y. (2021) 'Comparison of the Gut Microbiota of Jeju and Thoroughbred Horses in Korea', *Veterinary Sciences*, 8(5), p. 81. Available at: https://doi.org/10.3390/vetsci8050081.

Parkinson, J., Wasmuth, J.D., Salinas, G., Bizarro, C. V., Sanford, C., Berriman, M., Ferreira, H.B., Zaha, A., Blaxter, M.L., Maizels, R.M. and Fernández, C. (2012) 'A Transcriptomic Analysis of *Echinococcus granulosus* Larval Stages: Implications for Parasite Biology and Host Adaptation', *PLoS Neglected Tropical Diseases*, 6(11), p. e1897. Available at: https://doi.org/10.1371/journal.pntd.0001897.

Pashkirova, E.Y. (1941) 'Contribution to the Study of the Biology [Oribatid hosts] of the Tapeworm *Anoplocephala perfoliata* (Goeze, 1782), parasitic in the Horse.', *G. R. Acad. Sci. USRR*, 30(6). Available at: https://www.cabdirect.org/cabdirect/abstract/19431000217 (Accessed: 24 May 2019).

Paßlack, N., Vahjen, W. and Zentek, J. (2020) 'Impact of Dietary Cellobiose on the Fecal Microbiota of Horses', *Journal of Equine Veterinary Science*, 91, p. 103106. Available at: https://doi.org/10.1016/j.jevs.2020.103106.

Patro, R., Duggal, G., Love, M.I., Irizarry, R.A. and Kingsford, C. (2017) 'Salmon provides fast and bias-aware quantification of transcript expression', *Nature Methods*, 14(4), pp. 417–419. Available at: https://doi.org/10.1038/nmeth.4197.

Paveley, R.A., Aynsley, S.A., Cook, P.C., Turner, J.D. and Mountford, A.P. (2009) 'Fluorescent Imaging of Antigen Released by a Skin-Invading Helminth Reveals Differential Uptake and Activation Profiles by Antigen Presenting Cells', *PLOS Neglected Tropical Diseases*, 3(10), p. e528. Available at: https://doi.org/10.1371/journal.pntd.0000528.

Pavone, S., Veronesi, F., Genchi, C., Fioretti, D.P., Brianti, E. and Mandara, M.T. (2011) 'Pathological changes caused by *Anoplocephala perfoliata* in the mucosa/submucosa and in the enteric nervous system of equine ileocecal junction', *Veterinary Parasitology*, 176(1), pp. 43–52. Available at: https://doi.org/10.1016/J.VETPAR.2010.10.041.

Paz, E.A., Chua, E.G., Hassan, S.U., Greeff, J.C., Palmer, D.G., Liu, S., Lamichhane, B., Sepúlveda, N., Liu, J., Tay, C.Y. and Martin, G.B. (2022) 'Bacterial communities in the gastrointestinal tract segments of helminth-resistant and helminth-susceptible sheep', *Animal Microbiome*, 4(1), p. 23. Available at: https://doi.org/10.1186/s42523-022-00172-1.

Peachey, L.E., Castro, C., Molena, R.A., Jenkins, T.P., Griffin, J.L. and Cantacessi, C. (2019) 'Dysbiosis associated with acute helminth infections in herbivorous youngstock - observations and implications', *Scientific reports*, 9(1), p. 11121. Available at: https://doi.org/10.1038/s41598-019-47204-6.

Peachey, L.E., Jenkins, T.P. and Cantacessi, C. (2017) 'This Gut Ain't Big Enough for Both of Us. Or Is It? Helminth–Microbiota Interactions in Veterinary Species', *Trends in Parasitology*, 33(8), pp. 619–632. Available at: https://doi.org/10.1016/J.PT.2017.04.004.

Peachey, L.E., Molena, R.A., Jenkins, T.P., Di Cesare, A., Traversa, D., Hodgkinson, J.E. and Cantacessi, C. (2018) 'The relationships between faecal egg counts and gut microbial composition in UK Thoroughbreds infected by cyathostomins', *International Journal for Parasitology*, 48(6), pp. 403–412. Available at: https://doi.org/10.1016/j.ijpara.2017.11.003.

Pearson, G.R., Davies, L.W., White, A.L. and O'Brien, J.K. (1993) 'Pathological lesions associated with *Anoplocephala perfoliata* at the ileo-caecal junction of horses.', *The Veterinary record*, 132(8), pp. 179–182. Available at: https://doi.org/10.1136/vr.132.8.179.

Peón, A.N., Espinoza-Jiménez, A. and Terrazas, L.I. (2013) 'Immunoregulation by *Taenia crassiceps* and Its Antigens', *BioMed Research International*. Edited by M. Rodríguez-Sosa, 2013, p. 498583. Available at: https://doi.org/10.1155/2013/498583.

Pereira, I., Hidalgo, C., Stoore, C., Baquedano, M.S., Cabezas, C., Bastías, M., Riveros, A., Meneses, C., Cancela, M., Ferreira, H.B., Sáenz, L. and Paredes, R. (2022) 'Transcriptome analysis of *Echinococcus granulosus* sensu stricto protoscoleces reveals differences in immune modulation gene expression between cysts found in cattle and sheep', *Veterinary Research*, pp. 1–12. Available at: https://doi.org/10.1186/s13567-022-01022-3.

Perkins, D.N., Pappin, D.J.C., Creasy, D.M. and Cottrell, J.S. (1999) 'Probability-based protein identification by searching sequence databases using mass spectrometry data', *ELECTROPHORESIS*, 20(18), pp. 3551–3567. Available at: https://doi.org/10.1002/(SICI)1522-2683(19991201)20:18<3551::AID-ELPS3551>3.0.CO;2-2.

Petri, R.M., Schwaiger, T., Penner, G.B., Beauchemin, K.A., Forster, R.J., McKinnon, J.J. and McAllister, T.A. (2013) 'Characterization of the Core Rumen Microbiome in Cattle during Transition from Forage to Concentrate as Well as during and after an Acidotic Challenge', *PLoS ONE*. Edited by X. Ren, 8(12), p. e83424. Available at: https://doi.org/10.1371/journal.pone.0083424.

Pica-Mattoccia, L., Orsini, T., Basso, A., Festucci, A., Liberti, P., Guidi, A., Marcatto-Maggi, A.L., Nobre-Santana, S., Troiani, A.R., Cioli, D. and Valle, C. (2008) '*Schistosoma mansoni*: Lack of correlation between praziquantel-induced intra-worm calcium influx and parasite death', *Experimental Parasitology*, 119(3), pp. 332–335. Available at: https://doi.org/10.1016/j.exppara.2008.03.012.

Pierrot, C., Zhang, X., Zhangi, G., Fréville, A., Rebollo, A. and Khalife, J. (2018) 'Peptides derived from *Plasmodium falciparum* leucine-rich repeat 1 bind to serine/threonine phosphatase type 1 and inhibit parasite growth in vitro', *Drug Design, Development and Therapy*, 12, p. 85. Available at: https://doi.org/10.2147/DDDT.S153095.

Pittaway, C.E., Lawson, A.L., Coles, G.C. and Douglas Wilson, A. (2014) 'Systemic and mucosal IgE antibody responses of horses to infection with *Anoplocephala perfoliata*', *Veterinary Parasitology*, 199(1), pp. 32–41. Available at: https://doi.org/10.1016/j.vetpar.2013.10.005.

Plöger, S., Stumpff, F., Penner, G.B., Schulzke, J.-D., Gäbel, G., Martens, H., Shen, Z., Günzel, D. and Aschenbach, J.R. (2012) 'Microbial butyrate and its role for barrier function in the gastrointestinal tract', *Annals of the New York Academy of Sciences*, 1258(1), pp. 52–59. Available at: https://doi.org/https://doi.org/10.1111/j.1749-6632.2012.06553.x.

Prada, I., Gabrielli, M., Turola, E., Iorio, A., D'Arrigo, G., Parolisi, R., De Luca, M., Pacifici, M., Bastoni, M., Lombardi, M., Legname, G., Cojoc, D., Buffo, A., Furlan, R., Peruzzi, F. and Verderio, C. (2018) 'Glia-to-neuron transfer of miRNAs via extracellular vesicles: a new mechanism underlying inflammation-induced synaptic alterations', *Acta Neuropathologica*, 135(4), pp. 529–550. Available at: https://doi.org/10.1007/s00401-017-1803-x.

Prasanphanich, N.S., Mickum, M.L., Heimburg-Molinaro, J. and Cummings, R.D. (2013) 'Glycoconjugates in host-helminth interactions', *Frontiers in immunology*, 4, p. 240. Available at: https://doi.org/10.3389/fimmu.2013.00240.

Precious, W.Y. and Barrett, J. (1989) 'The possible absence of cytochrome P-450 linked xenobiotic metabolism in helminths', *Biochimica et Biophysica Acta (BBA) - General Subjects*, 992(2), pp. 215–222. Available at: https://doi.org/10.1016/0304-4165(89)90013-5.

Preza, M., Calvelo, J., Langleib, M., Hoffmann, F., Castillo, E., Koziol, U. and Iriarte, A. (2021) 'Stage-specific transcriptomic analysis of the model cestode *Hymenolepis microstoma*', *Genomics*, 113(2), pp. 620–632. Available at: https://doi.org/10.1016/j.ygeno.2021.01.005.

Proudman, C.. and Trees, A.. (1999) 'Tapeworms as a Cause of Intestinal Disease in Horses', *Parasitology Today*, 15(4), pp. 156–159. Available at: https://doi.org/10.1016/S0169-4758(99)01416-7.

Proudman, C. and Edwards, G. (1992) 'Validation of a centrifugation/flotation technique for the diagnosis of equine cestodiasis', *Veterinary Record*, 131(4), pp. 71–72. Available at: https://doi.org/10.1136/vr.131.4.71.

Proudman, C.J. and Edwards, G.B. (1993) 'Are tapeworms associated with equine colic? A case control study', *Equine Veterinary Journal*, 25(3), pp. 224–226. Available at: https://doi.org/10.1111/j.2042-3306.1993.tb02948.x.

Proudman, C.J., French, N.P. and Trees, A.J. (1998) 'Tapeworm infection is a significant risk factor for spasmodic colic and ileal impaction colic in the horse', *Equine Veterinary Journal*, 30(3), pp. 194–199. Available at: https://doi.org/10.1111/j.2042-3306.1998.tb04487.x.

Proudman, C.J. and Holdstock, N.B. (2000) 'Investigation of an outbreak of tapeworm-associated colic in a training yard', *Equine Veterinary Journal*, 32(S32), pp. 37–41. Available at: https://doi.org/https://doi.org/10.1111/j.2042-3306.2000.tb05332.x.

Proudman, C.J. and Trees, A.J. (1996) 'Use of excretory/secretory antigens for the serodiagnosis of *Anoplocephala perfoliata* cestodosis', *Veterinary Parasitology*, 61(3), pp. 239–247. Available at: https://doi.org/10.1016/0304-4017(95)00837-3.

Pryde, S.E., Duncan, S.H., Hold, G.L., Stewart, C.S. and Flint, H.J. (2002) 'The microbiology of butyrate formation in the human colon', *FEMS Microbiology Letters*, 217(2), pp. 133–139. Available at: https://doi.org/10.1111/j.1574-6968.2002.tb11467.x.

Ramajo-Hernández, A., Pérez-Sánchez, R., Ramajo-Martín, V. and Oleaga, A. (2007) '*Schistosoma bovis*: Plasminogen binding in adults and the identification of plasminogen-binding proteins from the worm tegument', *Experimental Parasitology*, 115(1), pp. 83–91. Available at: https://doi.org/10.1016/J.EXPPARA.2006.07.003.

Ramírez, A.L., Herrera, G., Muñoz, M., Vega, L., Cruz-Saavedra, L., García-Corredor, D., Pulido-Medellín, M., Bulla-Castañeda, D.M., Giraldo, J.C. and Bernal, M.C. (2021) 'Describing the intestinal microbiota of Holstein Fasciola-positive and-negative cattle from a hyperendemic area of fascioliasis in central Colombia', *PLoS Neglected Tropical Diseases*, 15(8), p. e0009658.

Ranson, H., Collins, F. and Hemingway, J. (1998) 'The role of alternative mRNA splicing in generating heterogeneity within the *Anopheles gambiae* class I glutathione S-transferase family', *Proceedings of the National Academy of Sciences*, 95(24), pp. 14284–14289. Available at: https://doi.org/10.1073/pnas.95.24.14284.

Raposo, G. and Stoorvogel, W. (2013) 'Extracellular vesicles: Exosomes, microvesicles, and friends', *Journal of Cell Biology*. The Rockefeller University Press, pp. 373–383. Available at: https://doi.org/10.1083/jcb.201211138.

Rausch, S., Held, J., Fischer, A., Heimesaat, M.M., Kühl, A.A., Bereswill, S. and Hartmann, S. (2013) 'Small Intestinal Nematode Infection of Mice Is Associated with Increased Enterobacterial Loads alongside the Intestinal Tract', *PLoS ONE*. Edited by I.C. Allen, 8(9), p. e74026. Available at: https://doi.org/10.1371/journal.pone.0074026.

Ravera, F., Femmino', S., Penna, C., Franchin, L., Angelini, F., Tapparo, M., Lopatina, T., Espolin Fladmark, K., Alloatti, G., Camussi, G., D'Ascenzo, F., Pagliaro, P. and Brizzi, M.F. (2020) 'Endothelial cell-derived extracellular vesicles exert cardio-protective effect via their protein cargo', *European Heart Journal*, 41(Supplement_2), p. ehaa946.3767. Available at: https://doi.org/10.1093/ehjci/ehaa946.3767.

Redman, C.A., Robertson, A., Fallon, P.G., Modha, J., Kusel, J.R., Doenhoff, M.J. and Martin, R.J. (1996) 'Praziquantel: An urgent and exciting challenge', *Parasitology Today*, 12(1), pp. 14–20. Available at: https://doi.org/https://doi.org/10.1016/0169-4758(96)80640-5.

Rehbein, S., Lindner, T., Visser, M. and Winter, R. (2011) 'Evaluation of a double centrifugation technique for the detection of Anoplocephala eggs in horse faeces', *Journal of Helminthology*, 85(04), pp. 409–414. Available at: https://doi.org/10.1017/S0022149X10000751.

Rehbein, S., Visser, M. and Winter, R. (2013) 'Prevalence, intensity and seasonality of gastrointestinal parasites in abattoir horses in Germany', *Parasitology Research*, 112(1), pp. 407–413. Available at: https://doi.org/10.1007/s00436-012-3150-0.

Rehbein, S., Visser, M., Yoon, S. and Marley, S.E. (2007) 'Efficacy of a combination ivermectin/praziquantel paste against nematodes, cestodes and bots in naturally infected ponies', *Veterinary Record*, 161(21), pp. 722–724. Available at: https://doi.org/10.1136/vr.161.21.722.

Respondek, F., Goachet, A.G. and Julliand, V. (2008) 'Effects of dietary short-chain fructooligosaccharides on the intestinal microflora of horses subjected to a sudden change in diet', *Journal of Animal Science*, 86(2), pp. 316–323. Available at: https://doi.org/10.2527/jas.2006-782.

Retana Moreira, L., Rodríguez Serrano, F. and Osuna, A. (2019) 'Extracellular vesicles of *Trypanosoma cruzi* tissue-culture cell-derived trypomastigotes: Induction of physiological changes in non-parasitized culture cells', *PLOS Neglected Tropical Diseases*, 13(2), p. e0007163. Available at: https://doi.org/10.1371/journal.pntd.0007163.

Reynolds, L.A., Smith, K.A., Filbey, K.J., Harcus, Y., Hewitson, J.P., Redpath, S.A., Valdez, Y., Yebra, M.J., Finlay, B.B. and Maizels, R.M. (2014) 'Commensal-pathogen interactions in the intestinal tract: *lactobacilli* promote infection with, and are promoted by, helminth parasites', *Gut microbes*, 5(4), pp. 522–532.

Rhoads, M.L. (1981) 'Cholinesterase in the parasitic nematode, *Stephanurus dentatus*. Characterization and sex dependence of a secretory cholinesterase.', *Journal of Biological Chemistry*, 256(17), pp. 9316–9323. Available at: https://doi.org/https://doi.org/10.1016/S0021-9258(19)52549-2.

Ribeiro, P.L., Rapini, A., Silva, U.C.S. e and Berg, C. van den (2012) 'Using multiple analytical methods to improve phylogenetic hypotheses in Minaria (Apocynaceae)', *Molecular Phylogenetics and Evolution*, 65(3), pp. 915–925. Available at: https://doi.org/https://doi.org/10.1016/j.ympev.2012.08.019.

Ricciardi, A., Bennuru, S., Tariq, S., Kaur, S., Wu, W., Elkahloun, A.G., Arakelyan, A., Shaik, J., Dorward, D.W., Nutman, T.B. and Tolouei Semnani, R. (2021) 'Extracellular vesicles released from the filarial parasite *Brugia malayi* downregulate the host mTOR pathway', *PLOS Neglected Tropical Diseases*, 15(1), p. e0008884. Available at: https://doi.org/10.1371/journal.pntd.0008884.

Roba, H.M. and Hiko, A. (2022) 'Study on Prevalence of Gastrointestinal Tract of Helminthiasis in Equine in and Around Chole District East Arsi Zone, Oromia Regional State, Central Ethiopia', *Veterinary and Animal Sciences*, 4(2).

Robinson, M.W., Dalton, J.P. and Donnelly, S. (2008) 'Helminth pathogen cathepsin proteases: it's a family affair', *Trends in Biochemical Sciences*, 33(12), pp. 601–608. Available at: https://doi.org/10.1016/J.TIBS.2008.09.001.

Robinson, M.W., Menon, R., Donnelly, S.M., Dalton, J.P. and Ranganathan, S. (2009) 'An integrated transcriptomics and proteomics analysis of the secretome of the helminth pathogen *Fasciola hepatica*: Proteins associated with invasion and infection of the mammalian host', *Molecular and Cellular Proteomics*, 8(8), pp. 1891–1907. Available at: https://doi.org/10.1074/mcp.M900045-MCP200.

Roediger, W.E. (1980) 'Role of anaerobic bacteria in the metabolic welfare of the colonic mucosa in man.', *Gut*, 21(9), pp. 793 LP – 798. Available at: https://doi.org/10.1136/gut.21.9.793.

Roediger, W.E. (1989) 'Short chain fatty acids as metabolic regulators of ion absorption in the colon', *Acta veterinaria Scandinavica. Supplementum*, 86, pp. 116–125. Available at: http://europepmc.org/abstract/MED/2699772.

Roelfstra, L., Betschart, B. and Pfister, K. (2006) 'A study on the seasonal epidemiology of *Anoplocephala spp*.-infection in horses and the appropriate treatment using a praziquantel gel (Droncit® 9% oral gel)', *Berliner und Munchener Tierarztliche Wochenschrift*, 119(7–8), pp. 312–315. Available at: https://europepmc.org/article/med/17009715 (Accessed: 27 December 2020).

Rogawski, R. and Sharon, M. (2022) 'Characterizing Endogenous Protein Complexes with Biological Mass Spectrometry', *Chemical Reviews*, 122(8), pp. 7386–7414. Available at: https://doi.org/10.1021/acs.chemrev.1c00217.

Rojas-Pirela, M., Andrade-Alviárez, D., Quiñones, W., Rojas, M.V., Castillo, C., Liempi, A., Medina, L., Guerrero-Muñoz, J., Fernández-Moya, A. and Ortega, Y.A. (2022) 'microRNAs: Critical Players during Helminth Infections', *Microorganisms*, 11(1), p. 61.

Rolot, M. and Dewals, B.G. (2018) 'Macrophage activation and functions during helminth infection: Recent advances from the laboratory mouse', *Journal of Immunology Research*, 2018. Available at: https://doi.org/10.1155/2018/2790627.

Rooney, J., Northcote, H.M., Williams, T.L., Cortés, A., Cantacessi, C. and Morphew, R.M. (2022) 'Parasitic helminths and the host microbiome – a missing "extracellular vesicle-sized" link?', *Trends in Parasitology*, 38(9), pp. 737–747. Available at: https://doi.org/10.1016/J.PT.2022.06.003.

Rossjohn, J., McKinstry, W.J., Oakley, A.J., Verger, D., Flanagan, J., Chelvanayagam, G., Tan, K.-L., Board, P.G. and Parker, M.W. (1998) 'Human theta class glutathione transferase: the crystal structure reveals a sulfate-binding pocket within a buried active site', *Structure*, 6(3), pp. 309–322. Available at: https://doi.org/https://doi.org/10.1016/S0969-2126(98)00034-3.

Rossum, A.J. van, Brophy, P.M., Tait, A., Barrett, J. and Jefferies, J.R. (2001) 'Proteomic identification of glutathione S-transferases from the model nematode *Caenorhabditis elegans*', *PROTEOMICS*, 1(11), pp. 1463–1468. Available at: https://doi.org/https://doi.org/10.1002/1615-9861(200111)1:11<1463::AID-PROT1463>3.0.CO;2-H.

Rowe, J. (2017) *Two Pyrantel Anthelmintics Alter Equine Fecal Microbiota Honors Research Thesis Presented in Partial Fulfillment of the Requirements for Graduation with Honors Research Distinction*. The Ohio State University. Available at: https://kb.osu.edu/handle/1811/86981 (Accessed: 12 February 2021).

Roy, N., Nageshan, R.K., Ranade, S. and Tatu, U. (2012) 'Heat shock protein 90 from neglected protozoan parasites', *Biochimica et Biophysica Acta (BBA) - Molecular Cell Research*, 1823(3), pp. 707–711. Available at: https://doi.org/10.1016/j.bbamcr.2011.12.003.

Ryan, S., Shiels, J., Taggart, C.C., Dalton, J.P. and Weldon, S. (2020) '*Fasciola hepatica*-Derived Molecules as Regulators of the Host Immune Response', *Frontiers in immunology*, 11, p. 2182. Available at: https://doi.org/10.3389/fimmu.2020.02182.

Ryu, S.H., Bak, U.B., Kim, J.G., Yoon, H.J., Seo, H.S., Kim, J.T., Park, J.Y. and Lee, C.W. (2001) 'Cecal rupture by *Anoplocephala perfoliata* infection in a thoroughbred horse in Seoul Race Park, South Korea.', *Journal of veterinary science (Suwon-si, Korea)*, 2(3), pp. 189–193. Available at: https://doi.org/10.4142/jvs.2001.2.3.189.

Salem, S.E., Maddox, T.W., Berg, A., Antczak, P., Ketley, J.M., Williams, N.J. and Archer, D.C. (2018) 'Variation in faecal microbiota in a group of horses managed at pasture over a 12-month period', *Scientific Reports*, 8(1), p. 8510. Available at: https://doi.org/10.1038/s41598-018-26930-3.

Sallé, G., Guillot, J., Tapprest, J., Foucher, N., Sevin, C. and Laugier, C. (2020) 'Compilation of 29 years of postmortem examinations identifies major shifts in equine parasite prevalence from 2000 onwards', *International Journal for Parasitology*, 50(2), pp. 125–132. Available at: https://doi.org/10.1016/j.ijpara.2019.11.004.

Samoil, V., Dagenais, M., Ganapathy, V., Aldridge, J., Glebov, A., Jardim, A. and Ribeiro, P. (2018) 'Vesicle-based secretion in schistosomes: Analysis of protein and microRNA (miRNA) content of exosome-like vesicles derived from *Schistosoma mansoni*', *Scientific Reports*, 8(1), p. 3286. Available at: https://doi.org/10.1038/s41598-018-21587-4.

Sánchez-López, C.M., Trelis, M., Bernal, D. and Marcilla, A. (2021) 'Overview of the interaction of helminth extracellular vesicles with the host and their potential functions and biological applications', *Molecular Immunology*, 134, pp. 228–235. Available at: https://doi.org/https://doi.org/10.1016/j.molimm.2021.03.020.

Sánchez-López, C.M., Trelis, M., Jara, L., Cantalapiedra, F., Marcilla, A. and Bernal, D. (2020) 'Diversity of extracellular vesicles from different developmental stages of *Fasciola hepatica*', *International Journal for Parasitology*, 50(9), pp. 663–669. Available at: https://doi.org/10.1016/j.ijpara.2020.03.011.

Sartorio, M.G., Pardue, E.J., Scott, N.E. and Feldman, M.F. (2023) 'Human gut bacteria tailor extracellular vesicle cargo for the breakdown of diet- and host-derived glycans', *Proceedings of the National Academy of Sciences*, 120(27), p. e2306314120. Available at: https://doi.org/10.1073/pnas.2306314120.

Sauvant, D., Chapoutot, P. and Archimède, H. (1994) 'La digestion des amidons par les ruminants et ses conséquences', *Productions animales*, 7(2), pp. 115–124.

Savina, A., Furlán, M., Vidal, M. and Colombo, M.I. (2003) 'Exosome release is regulated by a calcium-dependent mechanism in K562 cells', *Journal of Biological Chemistry*, 278(22), pp. 20083–20090. Available at: https://doi.org/10.1074/jbc.M301642200.

Schildberger, A., Rossmanith, E., Eichhorn, T., Strassl, K. and Weber, V. (2013) 'Cells Exhibit Different Cytokine Expression Patterns following Stimulation with Lipopolysaccharide', 2013.

Schneeberger, P.H.H., Coulibaly, J.T., Panic, G., Daubenberger, C., Gueuning, M., Frey, J.E. and Keiser, J. (2018) 'Investigations on the interplays between *Schistosoma mansoni*, praziquantel and the gut microbiome', *Parasites & Vectors*, 11(1), p. 168. Available at: https://doi.org/10.1186/s13071-018-2739-2.

Schneider, C.A., Rasband, W.S. and Eliceiri, K.W. (2012) 'NIH Image to ImageJ: 25 years of image analysis', *Nature Methods*, 9(7), pp. 671–675. Available at: https://doi.org/10.1038/nmeth.2089.

Schoster, A., Arroyo, L.G., Staempfli, H.R. and Weese, J.S. (2013) 'Comparison of microbial populations in the small intestine, large intestine and feces of healthy horses using terminal restriction fragment length polymorphism', *BMC research notes*, 6, p. 91. Available at: https://doi.org/10.1186/1756-0500-6-91.

Schoster, A., Staempfli, H.R., Guardabassi, L.G., Jalali, M. and Weese, J.S. (2017) 'Comparison of the fecal bacterial microbiota of healthy and diarrheic foals at two and four weeks of life', *BMC Veterinary Research*, 13(1), p. 144. Available at: https://doi.org/10.1186/s12917-017-1064-x.

Shanawany, E.E. El, Hassan, S.E., Abdel-Rahman, A.A.-H. and Abdel-Rahman, E.H. (2019) '*Toxocara vitulorum* cuticle glycoproteins in the diagnosis of calves' toxocariasis', *Veterinary world*. 2019/02/20, 12(2), pp. 288–294. Available at: https://doi.org/10.14202/vetworld.2019.288-294.

Sheehan, D., Meade, G., Foley, V.M. and Dowd, C.A. (2001) 'Structure, function and evolution of glutathione transferases: Implications for classification of non-mammalian members of an ancient enzyme superfamily', *Biochemical Journal*. Portland Press Ltd, pp. 1–16. Available at: https://doi.org/10.1042/0264-6021:3600001.

Shepherd, M.L., Ponder, M.A., Burk, A.O., Milton, S.C. and Swecker Jr, W.S. (2014) 'Fibre digestibility, abundance of faecal bacteria and plasma acetate concentrations in overweight adult mares', *Journal of nutritional science*, 3, pp. e10–e10. Available at: https://doi.org/10.1017/jns.2014.8.

Shepherd, M.L., Swecker, W.S., Jensen, R. V. and Ponder, M.A. (2012) 'Characterization of the fecal bacteria communities of forage-fed horses by pyrosequencing of 16S rRNA V4 gene amplicons', *FEMS Microbiology Letters*, 326(1), pp. 62–68. Available at: https://doi.org/10.1111/j.1574-6968.2011.02434.x.

Shimano, S. (2004) 'Oribatid mites (Acari: Oribatida) as an intermediate host of Anoplocephalid cestodes in Japan', *Applied Entomology and Zoology*, 39(1), pp. 1–6. Available at: https://doi.org/10.1303/aez.2004.1.

ShouMin, F. (2012) 'Insect glutathione S-transferase: a review of comparative genomic studies and response to xenobiotics.', *Bulletin of Insectology*, 65(2), pp. 265–271. Available at: http://www.bulletinofinsectology.org/.

Siddiqui, A.A., Zhou, Y., Podesta, R.B., Karcz, S.R., Tognon, C.E., Strejan, G.H., Dekaban, G.A. and Clarke, M.W. (1993) 'Characterization of Ca^{2+}-dependent neutral protease (calpain) from human blood flukes, Schistosoma mansoni', *Biochimica et Biophysica Acta (BBA) - Molecular Basis of Disease*, 1181(1), pp. 37–44. Available at: https://doi.org/https://doi.org/10.1016/0925-4439(93)90087-H.

Siles-Lucas, M., Sánchez-Ovejero, C., González-Sánchez, M., González, E., Falcón-Pérez, J.M., Boufana, B., Fratini, F., Casulli, A. and Manzano-Román, R. (2017) 'Isolation and characterization of exosomes derived from fertile sheep hydatid cysts', *Veterinary Parasitology*, 236, pp. 22–33. Available at: https://doi.org/https://doi.org/10.1016/j.vetpar.2017.01.022.

Sirois, R.J. (2013) 'Comparison of the fecal microbiota of horses before and after treatment for parasitic helminths: massively parallel sequencing of the v4 region of the 16S ribosomal RNA gene'.

Sistermans, T., Hartke, J., Stoldt, M., Libbrecht, R. and Foitzik, S. (2023) 'The influence of parasite load on transcriptional activity and morphology of a cestode and its ant intermediate host', *Molecular Ecology*, 32(15), pp. 4412–4426. Available at: https://doi.org/https://doi.org/10.1111/mec.16995.

Sivanantham, A. and Jin, Y. (2022) 'Impact of Storage Conditions on EV Integrity/Surface Markers and Cargos', *Life* . Available at: https://doi.org/10.3390/life12050697.

Skantar, A.M. and Carta, L.K. (2004) 'Molecular characterization and phylogenetic evaluation of the hsp90 gene from selected nematodes', *Journal of nematology*, 36(4), pp. 466–480. Available at: http://www.barc.usda. (Accessed: 15 June 2021).

Skotarek, S.L., Colwell, D.D. and Goater, C.P. (2010) 'Evaluation of diagnostic techniques for *Anoplocephala perfoliata* in horses from Alberta, Canada', *Veterinary Parasitology*, 172(3–4), pp. 249–255. Available at: https://doi.org/10.1016/J.VETPAR.2010.05.005.

Šlapeta, J., Dowd, S.E., Alanazi, A.D., Westman, M.E. and Brown, G.K. (2015) 'Differences in the faecal microbiome of non-diarrhoeic clinically healthy dogs and cats associated with *Giardia duodenalis* infection: impact of hookworms and coccidia', *International Journal for Parasitology*, 45(9–10), pp. 585–594. Available at: https://doi.org/10.1016/J.IJPARA.2015.04.001.

Slater, R., Frau, A., Hodgkinson, J., Archer, D. and Probert, C. (2021) 'A comparison of the colonic microbiome and volatile organic compound metabolome of *Anoplocephala perfoliata* infected and non-infected horses: A pilot study', *Animals*, 11(3), pp. 1–22. Available at: https://doi.org/10.3390/ani11030755.

Slocombe, J.O. (1979) 'Prevalence and treatment of tapeworms in horses.', *The Canadian veterinary journal = La revue veterinaire canadienne*, 20(5), pp. 136–40. Available at: http://www.ncbi.nlm.nih.gov/pubmed/487360 (Accessed: 21 May 2019).

Slocombe, J.O.D. (2006) 'A modified critical test and its use in two dose titration trials to assess efficacy of praziquantel for *Anoplocephala perfoliata* in equids', in *Veterinary Parasitology*. Elsevier, pp. 127–135. Available at: https://doi.org/10.1016/j.vetpar.2005.10.025.

Slocombe, J.O.D., Heine, J., Barutzki, D. and Slacek, B. (2007) 'Clinical trials of efficacy of praziquantel horse paste 9% against tapeworms and its safety in horses', *Veterinary Parasitology*, 144(3–4), pp. 366–370. Available at: https://doi.org/10.1016/j.vetpar.2006.09.038.

Sokolova, T.S., Petrov, V.A., Saltykova, I. V, Dorofeeva, Y.B., Tyakht, A. V, Ogorodova, L.M. and Fedorova, O.S. (2021) 'The impact of *Opisthorchis felineus* infection and praziquantel treatment on the intestinal microbiota in children', *Acta Tropica*, 217, p. 105835. Available at: https://doi.org/https://doi.org/10.1016/j.actatropica.2021.105835.

Sommer, A., Rickert, R., Fischer, P., Steinhart, H., Walter, R.D. and Liebau, E. (2003) 'A dominant role for extracellular glutathione S-transferase from *Onchocerca volvulus* is the production of prostaglandin D2', *Infection and Immunity*, 71(6), pp. 3603–3606. Available at: https://doi.org/10.1128/IAI.71.6.3603-3606.2003/ASSET/F9D4CF8F-1CDC-4D5B-9B8F-5DE768F1259A/ASSETS/GRAPHIC/II0631537002.JPEG.

Sommer, F. and Bäckhed, F. (2013) 'The gut microbiota — masters of host development and physiology', *Nature Reviews Microbiology*, 11(4), pp. 227–238. Available at: https://doi.org/10.1038/nrmicro2974.

Song, H., He, X., Du, X., Hua, R., Xu, J., He, R., Xie, Y., Gu, X., Peng, X. and Yang, G. (2021) 'Molecular characterization and expression analysis of annexin B3 and B38 as secretory proteins in *Echinococcus granulosus*', *Parasites & Vectors*, 14(1), p. 103. Available at: https://doi.org/10.1186/s13071-021-04596-7.

Sotillo, J., Pearson, M.S., Becker, L., Mekonnen, G.G., Amoah, A.S., van Dam, G., Corstjens, P.L.A.M., Murray, J., Mduluza, T., Mutapi, F. and Loukas, A. (2019) 'In-depth proteomic characterization of *Schistosoma haematobium*: Towards the development of new tools for elimination', *PLOS Neglected Tropical Diseases*, 13(5), p. e0007362. Available at: https://doi.org/10.1371/journal.pntd.0007362.

Sotillo, J., Robinson, M.W., Kimber, M.J., Cucher, M., Ancarola, M.E., Nejsum, P., Marcilla, A., Eichenberger, R.M. and Tritten, L. (2020) 'The protein and microRNA cargo of extracellular vesicles from parasitic helminths – current status and research priorities', *International Journal for Parasitology*, 50(9), pp. 635–645. Available at: https://doi.org/https://doi.org/10.1016/j.ijpara.2020.04.010.

Sotillo, J., Valero, M.L., Sánchez Del Pino, M.M., Fried, B., Esteban, J.G., Marcilla, A. and Toledo, R. (2010) 'Excretory/secretory proteome of the adult stage of *Echinostoma caproni*', *Parasitology Research*, 107(3), pp. 691–697. Available at: https://doi.org/10.1007/s00436-010-1923-x.

de Souza Gonçalves, D., da Silva Ferreira, M., Liedke, S.C., Gomes, K.X., de Oliveira, G.A., Leão, P.E.L., Cesar, G.V., Seabra, S.H., Cortines, J.R., Casadevall, A., Nimrichter, L., Domont, G.B., Junqueira, M.R., Peralta, J.M. and Guimaraes, A.J. (2018) 'Extracellular vesicles and vesicle-free secretome of the protozoa *acanthamoeba castellanii* under homeostasis and nutritional stress and their damaging potential to host cells', *Virulence*, 9(1), pp. 818–836. Available at: https://doi.org/10.1080/21505594.2018.1451184.

Soyemi, J., Isewon, I., Oyelade, J. and Adebiyi, E. (2018) 'Inter-Species/Host-Parasite Protein Interaction Predictions Reviewed', *Current Bioinformatics*, 13(4), pp. 396–406. Available at: https://doi.org/10.2174/1574893613666180108155851.

Sperotto, R.L., Kremer, F.S., Aires Berne, M.E., Costa de Avila, L.F., da Silva Pinto, L., Monteiro, K.M., Caumo, K.S., Ferreira, H.B., Berne, N. and Borsuk, S. (2017) 'Proteomic analysis of *Toxocara canis* excretory and secretory (TES) proteins', *Molecular and Biochemical Parasitology*, 211, pp. 39–47. Available at: https://doi.org/https://doi.org/10.1016/j.molbiopara.2016.09.002.

Stam, J., Bartel, S., Bischoff, R. and Wolters, J.C. (2021) 'Isolation of extracellular vesicles with combined enrichment methods', *Journal of Chromatography B*, 1169, p. 122604. Available at: https://doi.org/https://doi.org/10.1016/j.jchromb.2021.122604.

Starr, A.E., Deeke, S.A., Li, L., Zhang, X., Daoud, R., Ryan, J., Ning, Z., Cheng, K., Nguyen, L.V.H., Abou-Samra, E., Lavallée-Adam, M. and Figeys, D. (2018) 'Proteomic and Metaproteomic Approaches to Understand Host–Microbe Interactions', *Analytical Chemistry*, 90(1), pp. 86–109. Available at: https://doi.org/10.1021/acs.analchem.7b04340.

Steelman, S.M., Chowdhary, B.P., Dowd, S., Suchodolski, J. and Janečka, J.E. (2012) 'Pyrosequencing of 16S rRNA genes in fecal samples reveals high diversity of hindgut microflora in horses and potential links to chronic laminitis', *BMC Veterinary Research*, 8(1), p. 231. Available at: https://doi.org/10.1186/1746-6148-8-231.

Steenwyk, J.L., Buida, T.J., Li, Y., Shen, X.X. and Rokas, A. (2020) 'ClipKIT: A multiple sequence alignment trimming software for accurate phylogenomic inference', *PLoS Biology*, 18(12), pp. 1–17. Available at: https://doi.org/10.1371/journal.pbio.3001007.

Steiner, K., Garbe, A., Diekmann, H.W. and Nowak, H. (1976) 'The fate of praziquantel in the organism I. Pharmacokinetics in animals', *European Journal of Drug Metabolism and Pharmacokinetics*, 1(2), pp. 85–95. Available at: https://doi.org/10.1007/BF03189262.

Stewart, C.S. and Duncan, S.H. (1985) 'The Effect of Avoparcin on Cellulolytic Bacteria of the Ovine Rumen', *Microbiology*, 131(3), pp. 427–435. Available at: https://doi.org/10.1099/00221287-131-3-427.

Stewart, H.L., Southwood, L.L., Indugu, N., Vecchiarelli, B., Engiles, J.B. and Pitta, D. (2019) 'Differences in the equine faecal microbiota between horses presenting to a tertiary referral hospital for colic compared with an elective surgical procedure', *Equine Veterinary Journal*, 51(3), pp. 336–342. Available at: https://doi.org/10.1111/EVJ.13010.

Stickle, J.E., McKnight, C.A., Williams, K.J. and Carr, E.A. (2006) 'Diarrhea and hyperammonemia in a horse with progressive neurologic signs', *Veterinary Clinical Pathology*, 35(2), pp. 250–253. Available at: https://doi.org/https://doi.org/10.1111/j.1939-165X.2006.tb00125.x.

Stirewalt, M.A. (1963) 'CHEMICAL BIOLOGY OF SECRETIONS OF LARVAL HELMINTHS*', *Annals of the New York Academy of Sciences*, 113(1), pp. 36–53. Available at: https://doi.org/10.1111/J.1749-6632.1963.TB40656.X.

Straat, M., Böing, A.N., Tuip-De Boer, A., Nieuwland, R. and Juffermans, N.P. (2015) 'Extracellular Vesicles from Red Blood Cell Products Induce a Strong Pro-Inflammatory Host Response, Dependent on Both Numbers and Storage Duration', *Transfusion Medicine and Hemotherapy*, 43(4), pp. 302–305. Available at: https://doi.org/10.1159/000442681.

Stuart, R.B., Zwaanswijk, S., MacKintosh, N.D., Witikornkul, B., Brophy, P.M., Morphew, R.M., RB, S., S, Z., ND, M., B, W., PM, B. and RM, M. (2021) 'The soluble glutathione transferase superfamily: role of Mu class in triclabendazole sulphoxide challenge in *Fasciola hepatica*.', *Parasitology research*, 120(3), pp. 979–991. Available at: https://doi.org/10.1007/s00436-021-07055-5.

Stuchlíková, L., Jirásko, R., Vokřál, I., Valát, M., Lamka, J., Szotáková, B., Holčapek, M. and Skálová, L. (2014) 'Metabolic pathways of anthelmintic drug monepantel in sheep and in its parasite (Haemonchus contortus)', *Drug Testing and Analysis*, 6(10), pp. 1055–1062. Available at: https://doi.org/https://doi.org/10.1002/dta.1630.

Suades, R., Padró, T., Vilahur, G. and Badimon, L. (2022) 'Platelet - released extracellular vesicles : the effects of thrombin activation', *Cellular and Molecular Life Sciences*, 79(3), pp. 1–16. Available at: https://doi.org/10.1007/s00018-022-04222-4.

Sulima, A., Savijoki, K., Bień, J., Näreaho, A., Sałamatin, R., Conn, D.B. and Młocicki, D. (2018) 'Comparative Proteomic Analysis of *Hymenolepis diminuta* Cysticercoid and Adult Stages ', *Frontiers in Microbiology* . Available at: https://www.frontiersin.org/article/10.3389/fmicb.2017.02672.

Swyers, K.L., Burk, A.O., Hartsock, T.G., Ungerfeld, E.M. and Shelton, J.L. (2008) 'Effects of direct-fed microbial supplementation on digestibility and fermentation end-products in horses fed low- and high-starch concentrates1', *Journal of Animal Science*, 86(10), pp. 2596–2608. Available at: https://doi.org/10.2527/jas.2007-0608.

Szemplinski, K.L., Thompson, A., Cherry, N., Guay, K., Smith, W.B., Brady, J. and Jones, T. (2020) 'Transporting and Exercising Unconditioned Horses: Effects on Microflora Populations', *Journal of Equine Veterinary Science*, 90, p. 102988. Available at: https://doi.org/https://doi.org/10.1016/j.jevs.2020.102988.

Talavera, G. and Castresana, J. (2007) 'Improvement of Phylogenies after Removing Divergent and Ambiguously Aligned Blocks from Protein Sequence Alignments', *Systematic Biology*, 56(4), pp. 564–577. Available at: https://doi.org/10.1080/10635150701472164.

Tan, G., Muffato, M., Ledergerber, C., Herrero, J., Goldman, N., Gil, M. and Dessimoz, C. (2015) 'Current methods for automated filtering of multiple sequence alignments frequently worsen single-gene phylogenetic inference', *Systematic Biology*, 64(5), pp. 778–791. Available at: https://doi.org/10.1093/sysbio/syv033.

Tavassoli, M., Dalir-Naghadeh, B. and Esmaeili-Sani, S. (2010) 'Prevalence of gastrointestinal parasites in working horses', *Polish journal of veterinary sciences*, 13(2), pp. 319–324. Available at: http://europepmc.org/abstract/MED/20731187.

Taylor, J., Azimi, I., Monteith, G. and Bebawy, M. (2020) 'Ca2+ mediates extracellular vesicle biogenesis through alternate pathways in malignancy', *Journal of Extracellular Vesicles*, 9(1). Available at: https://doi.org/10.1080/20013078.2020.1734326.

Terrazas, L.I., Cruz, M., Rodríguez-Sosa, M., Bojalil, R., García-Tamayo, F. and Larralde, C. (1999) 'Th1-type cytokines improve resistance to murine cysticercosis caused by *Taenia crassiceps*', *Parasitology Research*, 85(2), pp. 135–141. Available at: https://doi.org/10.1007/s004360050522.

The Monster Hunter's Guide to Veterinary Parasitology (2018) *Anoplocephala sp.* Available at: https://www.veterinaryparasitology.com/anoplocephala.html (Accessed: 31 March 2019).

Theelen, M.J.P., Luiken, R.E.C., Wagenaar, J.A., Sloet van Oldruitenborgh-Oosterbaan, M.M., Rossen, J.W.A. and Zomer, A.L. (2021) 'The Equine Faecal Microbiota of Healthy Horses and Ponies in The Netherlands: Impact of Host and Environmental Factors', *Animals*. Available at: https://doi.org/10.3390/ani11061762.

Theodorou, M.K., Williams, B.A., Dhanoa, M.S., McAllan, A.B. and France, J. (1994) 'A simple gas production method using a pressure transducer to determine the fermentation kinetics of ruminant feeds', *Animal Feed Science and Technology*, 48(3–4), pp. 185–197. Available at: https://doi.org/10.1016/0377-8401(94)90171-6.

Théry, C., Amigorena, S., Raposo, G. and Clayton, A. (2006) 'Isolation and Characterization of Exosomes from Cell Culture Supernatants and Biological Fluids', *Current Protocols in Cell Biology*, 30(1), pp. 3.22.1-3.22.29. Available at: https://doi.org/https://doi.org/10.1002/0471143030.cb0322s30.

Théry, C., Boussac, M., Véron, P., Ricciardi-Castagnoli, P., Raposo, G., Garin, J. and Amigorena, S. (2001) 'Proteomic Analysis of Dendritic Cell-Derived Exosomes: A Secreted Subcellular Compartment Distinct from Apoptotic Vesicles', *The Journal of Immunology*, 166(12), pp. 7309 LP – 7318. Available at: https://doi.org/10.4049/jimmunol.166.12.7309.

Thomas, M.C. and Timson, J.D. (2018) 'The Mechanism of Action of Praziquantel: Six Hypotheses', *Current Topics in Medicinal Chemistry*, pp. 1575–1584. Available at: https://doi.org/http://dx.doi.org/10.2174/1568026618666181029143214.

Thomas, M.C. and Timson, J.D. (2020) 'The Mechanism of Action of Praziquantel: Can New Drugs Exploit Similar Mechanisms?', *Current Medicinal Chemistry*, pp. 676–696. Available at: https://doi.org/http://dx.doi.org/10.2174/0929867325666180926145537.

Thomson, A.M., Meyer, D.J. and Hayes, J.D. (1998) 'Sequence, catalytic properties and expression of chicken glutathione-dependent prostaglandin D2 synthase, a novel class Sigma glutathione S-transferase', *Biochemical Journal*, 333(2), pp. 317–325. Available at: https://doi.org/10.1042/bj3330317.

Tomczuk, K., Grzybek, M., Szczepaniak, K., Studzińska, M., Demkowska-Kutrzepa, M., Roczeń-Karczmarz, M., Abbass, Z.A., Kostro, K. and Junkuszew, A. (2017) 'Factors affecting prevalence and abundance of *A.perfoliata* infections in horses from south-eastern Poland', *Veterinary Parasitology*, 246, pp. 19–24. Available at: https://doi.org/10.1016/J.VETPAR.2017.08.027.

Tomczuk, K., Kostro, K., Grzybek, M., Szczepaniak, K., Studzińska, M., Demkowska-Kutrzepa, M. and Roczeń-Karczmarz, M. (2015) 'Seasonal changes of diagnostic potential in the detection of *Anoplocephala perfoliata* equine infections in the climate of Central Europe', *Parasitology Research*, 114(2), pp. 767–772. Available at: https://doi.org/10.1007/s00436-014-4279-9.

Tomczuk, K., Kostro, K., Szczepaniak, K.O., Grzybek, M., Studzińska, M., Demkowska-Kutrzepa, M. and Roczeń-Karczmarz, M. (2014) 'Comparison of the sensitivity of coprological methods in detecting *Anoplocephala perfoliata* invasions.', *Parasitology research*, 113(6), pp. 2401–6. Available at: https://doi.org/10.1007/s00436-014-3919-4.

Torres-Rivera, A. and Landa, A. (2008) 'Glutathione transferases from parasites: A biochemical view', *Acta Tropica*, 105(2), pp. 99–112. Available at: https://doi.org/10.1016/J.ACTATROPICA.2007.08.005.

Traversa, D., Fichi, G., Campigli, M., Rondolotti, A., Iorio, R., Proudman, C.J., Pellegrini, D. and Perrucci, S. (2008) 'A comparison of coprological, serological and molecular methods for the diagnosis of horse infection with *Anoplocephala perfoliata* (Cestoda, Cyclophyllidea)', *Veterinary Parasitology*, 152(3–4), pp. 271–277. Available at: https://doi.org/10.1016/J.VETPAR.2007.12.032.

Tsai, I.J. *et al.* (2013) 'The genomes of four tapeworm species reveal adaptations to parasitism', *Nature*, 496(7443), pp. 57–63. Available at: https://doi.org/10.1038/nature12031.

Tuniyazi, M., He, J., Guo, J., Li, S., Zhang, N., Hu, X. and Fu, Y. (2021) 'Changes of microbial and metabolome of the equine hindgut during oligofructose-induced laminitis', *BMC Veterinary Research*, 17(1), p. 11. Available at: https://doi.org/10.1186/s12917-020-02686-9.

Turner, J.D., Faulkner, H., Kamgno, J., Cormont, F., Van Snick, J., Else, K.J., Grencis, R.K., Behnke, J.M., Boussinesq, M. and Bradley, J.E. (2003) 'Th2 Cytokines Are Associated with Reduced Worm Burdens in a Human Intestinal Helminth Infection', *The Journal of Infectious Diseases*, 188(11), pp. 1768–1775. Available at: https://doi.org/10.1086/379370.

Urban, J.F., Katona, I.M., Paul, W.E. and Finkelman, F.D. (1991) 'Interleukin 4 is important in protective immunity to a gastrointestinal nematode infection in mice.', *Proceedings of the National Academy of Sciences*, 88(13), pp. 5513–5517. Available at: https://doi.org/10.1073/pnas.88.13.5513.

Urban Jr., J.F., Maliszewski, C.R., Madden, K.B., Katona, I.M. and Finkelman, F.D. (1995) 'IL-4 treatment can cure established gastrointestinal nematode infections in immunocompetent and immunodeficient mice', *Journal of Immunology*, 154(9), pp. 4675–4684. Available at: https://www.scopus.com/inward/record.uri?eid=2-s2.0-0029004498&partnerID=40&md5=baa65999ec37b4b66048d00704e06eb2.

Valadi, H., Ekström, K., Bossios, A., Sjöstrand, M., Lee, J.J. and Lötvall, J.O. (2007) 'Exosome-mediated transfer of mRNAs and microRNAs is a novel mechanism of genetic exchange between cells', *Nature Cell Biology*, 9(6), pp. 654–659. Available at: https://doi.org/10.1038/ncb1596.

Venable, E.B., Bland, S.D., McPherson, J.L. and Francis, J. (2016) 'Role of the gut microbiota in equine health and disease', *Animal Frontiers*, 6(3), pp. 43–49. Available at: https://doi.org/10.2527/af.2016-0033.

Venable, E.B., Fenton, K.A., Braner, V.M., Reddington, C.E., Halpin, M.J., Heitz, S.A., Francis, J.M., Gulson, N.A., Goyer, C.L., Bland, S.D., Cross, T.-W.L., Holscher, H.D. and Swanson, K.S. (2017) 'Effects of Feeding Management on the Equine Cecal Microbiota', *Journal of Equine Veterinary Science*, 49, pp. 113–121. Available at: https://doi.org/10.1016/J.JEVS.2016.09.010.

Vendelova, E., Camargo de Lima, J., Lorenzatto, K.R., Monteiro, K.M., Mueller, T., Veepaschit, J., Grimm, C., Brehm, K., Hrčková, G., Lutz, M.B., Ferreira, H.B. and Nono, J.K. (2016) 'Proteomic Analysis of Excretory-Secretory Products of *Mesocestoides corti* Metacestodes Reveals Potential Suppressors of Dendritic Cell Functions', *PLoS Neglected Tropical Diseases*, 10(10), p. 5061. Available at: https://doi.org/10.1371/journal.pntd.0005061.

Victor, B., Kanobana, K., Gabriël, S., Polman, K., Deckers, N., Dorny, P., Deelder, A.M. and Palmblad, M. (2012) 'Proteomic analysis of *Taenia solium* metacestode excretion-secretion proteins', *Proteomics*, 12(11), pp. 1860–1869. Available at: https://doi.org/10.1002/pmic.201100496.

Vince, A., Dawson, A.M., Park, N. and O'Grady, F. (1973) 'Ammonia production by intestinal bacteria', *Gut*, 14(3), pp. 171 LP – 177. Available at: https://doi.org/10.1136/gut.14.3.171.

Vince, A., Down, P.F., Murison, J., Twigg, F.J. and Wrong, O.M. (1976) 'Generation of ammonia from non-urea sources in a faecal incubation system', *Clinical science and molecular medicine*, 51(3), pp. 313–322. Available at: https://doi.org/10.1042/cs0510313.

Vince, A.J. and Burridge, S.M. (1980) 'Ammonia production by intestinal bacteria: the effects of lactose, lactulose and glucose', *Journal of Medical Microbiology*, 13(2), pp. 177–191. Available at: https://doi.org/10.1099/00222615-13-2-177.

Virginio, V.G., Monteiro, K.M., Drumond, F., De Carvalho, M.O., Vargas, D.M., Zaha, A. and Ferreira, H.B. (2012) 'Excretory/secretory products from *in vitro*-cultured *Echinococcus granulosus* protoscoleces', *Molecular and Biochemical Parasitology*, 183(1), pp. 15–22. Available at: https://doi.org/10.1016/j.molbiopara.2012.01.001.

Vital, M., Penton, C.R., Wang, Q., Young, V.B., Antonopoulos, D.A., Sogin, M.L., Morrison, H.G., Raffals, L., Chang, E.B., Huffnagle, G.B., Schmidt, T.M., Cole, J.R. and Tiedje, J.M. (2013) 'A gene-targeted approach to investigate the intestinal butyrate-producing bacterialcommunity', *Microbiome*, 1(1), p. 8. Available at: https://doi.org/10.1186/2049-2618-1-8.

van der Vlist, E.J., Nolte-'t Hoen, E.N.M., Stoorvogel, W., Arkesteijn, G.J.A. and Wauben, M.H.M. (2012) 'Fluorescent labeling of nano-sized vesicles released by cells and subsequent quantitative and qualitative analysis by high-resolution flow cytometry', *Nature Protocols*, 7(7), pp. 1311–1326. Available at: https://doi.org/10.1038/nprot.2012.065.

Vosmer, J., Liesegang, A., Wanner, M., Zeyner, A., Suter, D., Hoelzle, L. and Wichert, B. (2012) 'Fermentation of six different forages in the semi-continuous fermentation technique Caesitec', *Journal of animal physiology and animal nutrition*, 96(5), pp. 860–869.

Walden, H.S., Jordan, M.E. and DiPietro, J.A. (2014) 'Chapter 58 - Cestodes', in D.C. Sellon and M.T.B.T.-E.I.D. (Second E. Long (eds). St. Louis: W.B. Saunders, pp. 490-494.e2. Available at: https://doi.org/https://doi.org/10.1016/B978-1-4557-0891-8.00058-0.

Walk, S.T., Blum, A.M., Ewing, S.A.-S., Weinstock, J. V and Young, V.B. (2010) 'Alteration of the murine gut microbiota during infection with the parasitic helminth *Heligmosomoides polygyrus.*', *Inflammatory bowel diseases*, 16(11), pp. 1841–9. Available at: https://doi.org/10.1002/ibd.21299.

Walker, S., Busatto, S., Pham, A., Tian, M., Suh, A., Carson, K., Quintero, A., Lafrence, M., Malik, H., Santana, M.X. and Wolfram, J. (2019) 'Theranostics Extracellular vesicle-based drug delivery systems for cancer treatment', 9(26). Available at: https://doi.org/10.7150/thno.37097.

Walshe, N., Duggan, V., Cabrera-Rubio, R., Crispie, F., Cotter, P., Feehan, O. and Mulcahy, G. (2019) 'Removal of adult cyathostomins alters faecal microbiota and promotes an inflammatory phenotype in horses', *International Journal for Parasitology* [Preprint]. Available at: https://doi.org/10.1016/J.IJPARA.2019.02.003.

Walshe, N., Mulcahy, G., Crispie, F., Cabrera-Rubio, R., Cotter, P., Jahns, H. and Duggan, V. (2021) 'Outbreak of acute larval cyathostominosis - A "perfect storm" of inflammation and dysbiosis', *Equine veterinary journal*. 2020/10/06, 53(4), pp. 727–739. Available at: https://doi.org/10.1111/evj.13350.

Wang, L., Cen, S., Wang, G., Lee, Y., Zhao, J., Zhang, H. and Chen, W. (2020) 'Acetic acid and butyric acid released in large intestine play different roles in the alleviation of constipation', *Journal of Functional Foods*, 69, p. 103953. Available at: https://doi.org/https://doi.org/10.1016/j.jff.2020.103953.

Wang, L., Li, Z., Shen, J., Liu, Z., Liang, J., Wu, X., Sun, X. and Wu, Z. (2015) 'Exosome-like vesicles derived by *Schistosoma japonicum* adult worms mediates M1 type immune- activity of macrophage', *Parasitology Research*, 114(5), pp. 1865–1873. Available at: https://doi.org/10.1007/s00436-015-4373-7.

Wang, L.Q., Liu, T.L., Liang, P.H., Zhang, S.H., Li, T.S., Li, Y.P., Liu, G.X., Mao, L. and Luo, X.N. (2020) 'Characterization of exosome-like vesicles derived from *Taenia pisiformis* cysticercus and their immunoregulatory role on macrophages', *Parasites and Vectors*, 13(1), pp. 1–16. Available at: https://doi.org/10.1186/s13071-020-04186-z.

Wang, Q., Da'dara, A.A. and Skelly, P.J. (2017) 'The human blood parasite *Schistosoma mansoni* expresses extracellular tegumental calpains that cleave the blood clotting protein fibronectin', *Scientific Reports*, 7(1), p. 12912. Available at: https://doi.org/10.1038/s41598-017-13141-5.

Wang, Q., Da'dara, A.A. and Skelly, P.J. (2018) 'The blood fluke *Schistosoma mansoni* cleaves the coagulation protein high molecular weight kininogen (HK) but does not generate the vasodilator bradykinin', *Parasites & Vectors*, 11(1), p. 182. Available at: https://doi.org/10.1186/s13071-018-2704-0.

Wang, T., Ma, G., Ang, C.-S., Korhonen, P.K., Koehler, A. V, Young, N.D., Nie, S., Williamson, N.A. and Gasser, R.B. (2019) 'High throughput LC-MS/MS-based proteomic analysis of excretory-secretory products from short-term *in vitro* culture of *Haemonchus contortus*', *Journal of Proteomics*, 204, p. 103375. Available at: https://doi.org/https://doi.org/10.1016/j.jprot.2019.05.003.

Wang, T., Van Steendam, K., Dhaenens, M., Vlaminck, J., Deforce, D., Jex, A.R., Gasser, R.B. and Geldhof, P. (2013) 'Proteomic Analysis of the Excretory-Secretory Products from Larval Stages of *Ascaris suum* Reveals High Abundance of Glycosyl Hydrolases', *PLOS Neglected Tropical Diseases*, 7(10), p. e2467. Available at: https://doi.org/10.1371/journal.pntd.0002467.

Wang, X. *et al.* (2011) 'Clonorchis sinensis enolase: Identification and biochemical characterization of a glycolytic enzyme from excretory/secretory products', *Molecular and Biochemical Parasitology*, 177(2), pp. 135–142. Available at: https://doi.org/10.1016/J.MOLBIOPARA.2011.02.011.

Wang, Xia, Tian, L., Lu, J. and Ng, I.O.-L. (2022) 'Exosomes and cancer - Diagnostic and prognostic biomarkers and therapeutic vehicle', *Oncogenesis*, 11(1), p. 54. Available at: https://doi.org/10.1038/s41389-022-00431-5.

Wang, Xifeng, Zhao, C., Zhang, G., Zhang, K., Li, Z., Shang, Y., Ning, C., Ji, C., Xia, X., Cai, X., Qiao, J. and Meng, Q. (2022) 'Molecular characterization of a novel GSTO2 of *Fasciola hepatica* and its roles in modulating murine macrophages', *Parasite (Paris, France)*. 2022/03/22, 29, p. 16. Available at: https://doi.org/10.1051/parasite/2022016.

Wang, Y., Bai, X., Zhu, H., Wang, X., Shi, H., Tang, B., Boireau, P., Cai, X., Luo, X., Liu, M. and Liu, X. (2017) 'Immunoproteomic analysis of the excretory-secretory products of *Trichinella pseudospiralis* adult worms and newborn larvae', *Parasites and Vectors*, 10(1), pp. 1–9. Available at: https://doi.org/10.1186/s13071-017-2522-9.

Wang, Y., Xiao, D., Shen, Y., Han, X., Zhao, F., Li, X., Wu, W., Zhou, H., Zhang, J. and Cao, J. (2015) 'Proteomic analysis of the excretory/secretory products and antigenic proteins of *Echinococcus granulosus* adult worms from infected dogs', *BMC Veterinary Research*, 11(1), p. 119. Available at: https://doi.org/10.1186/s12917-015-0423-8.

Wang, Y., Zhou, H., Shen, Y., Wang, Yanjuan, Wu, W., Liu, H., Yuan, Z. and Xu, Y. (2015) 'Impairment of dendritic cell function and excretory-secretory products : a potential mechanism of immune evasion adopted by *Echinococcus granulosus*', *BMC Immunology*, pp. 1–10. Available at: https://doi.org/10.1186/s12865-015-0110-3.

Wang, Z., Gerstein, M. and Snyder, M. (2009) 'RNA-Seq: a revolutionary tool for transcriptomics', *Nature reviews. Genetics*, 10(1), p. 57. Available at: https://doi.org/10.1038/NRG2484.

Wangchuk, P., Kouremenos, K., Eichenberger, R.M., Pearson, M., Susianto, A., Wishart, D.S., McConville, M.J. and Loukas, A. (2019) 'Metabolomic profiling of the excretory–secretory products of hookworm and whipworm', *Metabolomics*, 15(7), p. 101. Available at: https://doi.org/10.1007/s11306-019-1561-y.

Wangwiwatsin, A., Protasio, A. V., Wilson, S., Owusu, C., Holroyd, N.E., Sanders, M.J., Keane, J., Doenhoff, M.J., Rinaldi, G. and Berriman, M. (2020) 'Transcriptome of the parasitic flatworm *schistosoma mansoni* during intra-mammalian development', *PLoS Neglected Tropical Diseases*, 14(5), pp. 1–25. Available at: https://doi.org/10.1371/journal.pntd.0007743.

Weimer, P.J. (1998) 'Manipulating ruminal fermentation: a microbial ecological perspective.', *Journal of Animal Science*, 76(12), p. 3114. Available at: https://doi.org/10.2527/1998.76123114x.

Weimer, P.J. (2015) 'Redundancy, resilience, and host specificity of the ruminal microbiota: implications for engineering improved ruminal fermentations', *Frontiers in Microbiology*, 6, p. 296. Available at: https://doi.org/10.3389/FMICB.2015.00296.

Welch, J.D., Hu, Y. and Prins, J.F. (2016) 'Robust detection of alternative splicing in a population of single cells', *Nucleic Acids Research*, 44(8), pp. e73–e73. Available at: https://doi.org/10.1093/nar/gkv1525.

Van Weyenberg, S., Sales, J. and Janssens, G.P.J. (2006) 'Passage rate of digesta through the equine gastrointestinal tract: A review', *Livestock Science*. Elsevier, pp. 3–12. Available at: https://doi.org/10.1016/j.livprodsci.2005.04.008.

White, R.R. and Artavanis-Tsakonas, K. (2012) 'How helminths use excretory secretory fractions to modulate dendritic cells', *Virulence*. Taylor and Francis Inc., pp. 668–677. Available at: https://doi.org/10.4161/viru.22832.

Whitfield-Cargile, C.M., Chamoun-Emanuelli, A.M., Cohen, N.D., Richardson, L.M., Ajami, N.J. and Dockery, H.J. (2018) 'Differential effects of selective and non-selective cyclooxygenase inhibitors on fecal microbiota in adult horses', *PloS one*, 13(8), pp. e0202527–e0202527. Available at: https://doi.org/10.1371/journal.pone.0202527.

Whitfield-Cargile, C.M., Coleman, M.C., Cohen, N.D., Chamoun-Emanuelli, A.M., DeSolis, C.N., Tetrault, T., Sowinski, R., Bradbery, A. and Much, M. (2021) 'Effects of phenylbutazone alone or in combination with a nutritional therapeutic on gastric ulcers, intestinal permeability, and fecal microbiota in horses', *Journal of veterinary internal medicine*. 2021/03/03, 35(2), pp. 1121–1130. Available at: https://doi.org/10.1111/jvim.16093.

Williamson, R., Beveridge, I. and Gasser, R. (1998) 'Coprological methods for the diagnosis of *Anoplocephala perfoliata* infection of the horse', *Australian Veterinary Journal*, 76(9), pp. 618–621. Available at: https://doi.org/10.1111/j.1751-0813.1998.tb10242.x.

Williamson, R.M.C., Gasser, R.B., Middleton, D. and Beveridge, I. (1997) 'The distribution of *Anoplocephala perfoliata* in the intestine of the horse and associated pathological changes', *Veterinary Parasitology*, 73(3–4), pp. 225–241. Available at: https://doi.org/10.1016/S0304-4017(97)00123-4.

Willing, B., Vörös, A., Roos, S., Jones, C., Jansson, A. and Lindberg, J.E. (2009) 'Changes in faecal bacteria associated with concentrate and forage-only diets fed to horses in training', *Equine Veterinary Journal*, 41(9), pp. 908–914. Available at: https://doi.org/https://doi.org/10.2746/042516409X447806.

Wilson, R.A. (2012) 'Virulence factors of schistosomes', *Microbes and Infection*, 14(15), pp. 1442–1450. Available at: https://doi.org/https://doi.org/10.1016/j.micinf.2012.09.001.

Wititkornkul, B., Hulme, B.J., Tomes, J.J., Allen, N.R., Davis, C.N., Davey, S.D., Cookson, A.R., Phillips, H.C., Hegarty, M.J., Swain, M.T., Brophy, P.M., Wonfor, R.E. and Morphew, R.M. (2021) 'Evidence of Immune Modulators in the Secretome of the Equine Tapeworm *Anoplocephala perfoliata*', *Pathogens*, 10(7). Available at: https://doi.org/10.3390/pathogens10070912.

Wu, H., Xie, X., Tang, Q., Huang, T., Tang, X., Jiao, B., Wang, R., Zhu, X., Ye, X., Ma, H. and Li, X. (2023) 'Epiberberine inhibits *Helicobacter pylori* and reduces host apoptosis and inflammatory damage by down-regulating urease expression', *Journal of Ethnopharmacology*, 318, p. 117046. Available at: https://doi.org/https://doi.org/10.1016/j.jep.2023.117046.

Wu, J., Cai, M., Yang, J., Li, Y., Ding, J., Kandil, O.M., Kutyrev, I., Ayaz, M. and Zheng, Y. (2021) 'Comparative analysis of different extracellular vesicles secreted by *Echinococcus granulosus* protoscoleces', *Acta Tropica*, 213, p. 105756. Available at: https://doi.org/https://doi.org/10.1016/j.actatropica.2020.105756.

Wu, S., Li, R.W., Li, W., Beshah, E., Dawson, H.D. and Urban Jr, J.F. (2012) 'Worm burden-dependent disruption of the porcine colon microbiota by *Trichuris suis* infection', *PloS one*, 7(4), p. e35470.

Wu, X., Fu, Y., Yang, D., Zhang, R., Zheng, W., Nie, H., Xie, Y., Yan, N., Hao, G., Gu, X., Wang, S., Peng, X. and Yang, G. (2012) 'Detailed Transcriptome Description of the Neglected Cestode *Taenia multiceps*', *PLOS ONE*, 7(9), p. e45830. Available at: https://doi.org/10.1371/JOURNAL.PONE.0045830.

Wunderlich, G., Bull, M., Ross, T., Rose, M. and Chapman, B. (2023) 'Understanding the microbial fibre degrading communities & processes in the equine gut', *Animal Microbiome* [Preprint]. Available at: https://doi.org/10.1186/s42523-022-00224-6.

Xie, Y., Zhou, X., Chen, L., Zhang, Z., Wang, C., Gu, X., Wang, T., Peng, X. and Yang, G. (2015) 'Cloning and characterization of a novel sigma-like glutathione S-transferase from the giant panda parasitic nematode, Baylisascaris schroederi', *Parasites and Vectors*, 8(1), p. 44. Available at: https://doi.org/10.1186/s13071-014-0629-9.

Xu, R., Rai, A., Chen, M., Suwakulsiri, W., Greening, D.W. and Simpson, R.J. (2018) 'Extracellular vesicles in cancer — implications for future improvements in cancer care', *Nature Reviews Clinical Oncology*, 15(10), pp. 617–638. Available at: https://doi.org/10.1038/s41571-018-0036-9.

Xu, Z., Ji, M., Li, C., Du, X., Hu, W., McManus, D.P. and You, H. (2020) 'A Biological and Immunological Characterization of *Schistosoma Japonicum* Heat Shock Proteins 40 and 90α', *International journal of molecular sciences*, 21(11), p. 4034. Available at: https://doi.org/10.3390/ijms21114034.

Yamamoto, K., Fujii, H., Aso, Y., Banno, Y. and Koga, K. (2007) 'Expression and characterization of a sigma-class glutathione S-transferase of the fall webworm, *Hyphantria cunea*', *Bioscience, Biotechnology and Biochemistry*, 71(2), pp. 553–560. Available at: https://doi.org/10.1271/bbb.60592.

Yan, H., Xue, G., Mei, Q., Ding, F., Wang, Y. and Sun, S. (2008) 'Calcium-dependent proapoptotic effect of *Taenia solium* metacestodes annexin B1 on human eosinophils: A novel strategy to prevent host immune response', *The International Journal of Biochemistry & Cell Biology*, 40(10), pp. 2151–2163. Available at: https://doi.org/https://doi.org/10.1016/j.biocel.2008.02.018.

Yang, D., Fu, Y., Wu, X., Xie, Y., Nie, H., Chen, L., Nong, X., Gu, X., Wang, S., Peng, X., Yan, N., Zhang, R., Zheng, W. and Yang, G. (2012) 'Annotation of the Transcriptome from *Taenia pisiformis* and Its Comparative Analysis with Three Taeniidae Species', *PLOS ONE*, 7(4), p. e32283. Available at: https://doi.org/10.1371/journal.pone.0032283.

Yang, J., Wu, J., Fu, Y., Yan, L., Li, Y., Guo, X., Zhang, Y., Wang, X., Shen, Y., Cho, W.C. and Zheng, Y. (2021) 'Identification of Different Extracellular Vesicles in the Hydatid Fluid of *Echinococcus granulosus* and Immunomodulatory Effects of 110 K EVs on Sheep PBMCs', *Frontiers in Immunology*, 0, p. 315. Available at: https://doi.org/10.3389/FIMMU.2021.602717.

Yang, L., Huang, S., Zhang, Z., Liu, Z. and Zhang, L. (2022) 'Roles and Applications of Red Blood Cell-Derived Extracellular Vesicles in Health and Diseases'.

Yang, W., Yu, T., Huang, X., Bilotta, A.J., Xu, L., Lu, Y., Sun, J., Pan, F., Zhou, J., Zhang, W., Yao, S., Maynard, C.L., Singh, N., Dann, S.M., Liu, Z. and Cong, Y. (2020) 'Intestinal microbiota-derived short-chain fatty acids regulation of immune cell IL-22 production and gut immunity', *Nature Communications*, 11(1), p. 4457. Available at: https://doi.org/10.1038/s41467-020-18262-6.

Yoo, W.G., Kim, D.W., Ju, J.W., Cho, P.Y., Kim, T.I., Cho, S.H., Choi, S.H., Park, H.S., Kim, T.S. and Hong, S.J. (2011) 'Developmental Transcriptomic Features of the Carcinogenic Liver Fluke, *Clonorchis sinensis*', *PLOS Neglected Tropical Diseases*, 5(6), p. e1208. Available at: https://doi.org/10.1371/JOURNAL.PNTD.0001208.

Young, N.D., Campbell, B.E., Hall, R.S., Jex, A.R., Cantacessi, C., Laha, T., Sohn, W.M., Sripa, B., Loukas, A., Brindley, P.J. and Gasser, R.B. (2010) 'Unlocking the Transcriptomes of Two Carcinogenic Parasites, *Clonorchis sinensis* and *Opisthorchis viverrini*', *PLoS Neglected Tropical Diseases*, 4(6). Available at: https://doi.org/10.1371/JOURNAL.PNTD.0000719.

Young, N.D., Hall, R.S., Jex, A.R., Cantacessi, C. and Gasser, R.B. (2010) 'Elucidating the transcriptome of *Fasciola hepatica* — A key to fundamental and biotechnological discoveries for a neglected parasite', *Biotechnology Advances*, 28(2), pp. 222–231. Available at: https://doi.org/https://doi.org/10.1016/j.biotechadv.2009.12.003.

Young, N.D., Jex, A.R., Cantacessi, C., Hall, R.S., Campbell, B.E., Spithill, T.W., Tangkawattana, S., Tangkawattana, P., Laha, T. and Gasser, R.B. (2011) 'A portrait of the transcriptome of the neglected trematode, *Fasciola gigantica*-biological and biotechnological implications', *PLoS Neglected Tropical Diseases*, 5(2). Available at: https://doi.org/10.1371/journal.pntd.0001004.

Zakeri, A., Hansen, E.P., Andersen, S.D., Williams, A.R. and Nejsum, P. (2018) 'Immunomodulation by Helminths: Intracellular Pathways and Extracellular Vesicles', *Frontiers in immunology*, 9(OCT), p. 2349. Available at: https://doi.org/10.3389/fimmu.2018.02349.

Zamanian, M., Fraser, L.M., Agbedanu, P.N., Harischandra, H., Moorhead, A.R., Day, T.A., Bartholomay, L.C. and Kimber, M.J. (2015) 'Release of Small RNA-containing Exosome-like Vesicles from the Human Filarial Parasite Brugia malayi', *PLOS Neglected Tropical Diseases*, 9(9), p. e0004069. Available at: https://doi.org/10.1371/journal.pntd.0004069.

Zawistowska-Deniziak, A., Basalaj, K., Strojny, B. and Mlocicki, D. (2017) 'New data on human macrophages polarization by *Hymenolepis diminuta* tapeworm-An in vitro study', *Frontiers in Immunology*, 8(FEB), pp. 1–15. Available at: https://doi.org/10.3389/fimmu.2017.00148.

Zerihun, A., Bersissa, K., Bojia, E., Ayele, G., Tesfaye, M. and Etana, D. (2011) 'Endoparasites of donkeys in Sululta and Gefersa districts of central Oromia, Ethiopia.', *Journal of Animal and veterinary Advances*, 10(14), pp. 1850–1854.

Zeyner, A., Dill, B., Engelmann, W. and Markuske, K.D. (2006) 'Suitability of equine caecum content as inoculum in a modified "rumen simulation technique"', in *Proceedings of the 10 th Congress of European Society of Veterinary and Comparative Nutrition*, pp. 5–7.

Zhang (2019) 'Comparative Transcriptomic Analysis of the Larval and Adult Stages of *Taenia pisiformis*', *Genes*, 10(7), p. 507. Available at: https://doi.org/10.3390/genes10070507.

Zhang, D., Lee, H. and Jin, Y. (2020) 'Delivery of Functional Small RNAs via Extracellular Vesicles *In Vitro* and I*n Vivo* BT - RNA Interference and CRISPR Technologies: Technical Advances and New Therapeutic Opportunities', in M. Sioud (ed.). New York, NY: Springer US, pp. 107–117. Available at: https://doi.org/10.1007/978-1-0716-0290-4_6.

Zhang, H.C., Yang, Y.J., Ma, K.X., Shi, C.Y., Chen, G.W. and Liu, D.Z. (2020) 'A novel sigma class glutathione S-transferase gene in freshwater planarian *Dugesia japonica*: cloning, characterization and protective effects in herbicide glyphosate stress', *Ecotoxicology*, 29(3), pp. 295–304. Available at: https://doi.org/10.1007/s10646-020-02173-9.

Zhang, J., Kumar, S., Jayachandran, M., Herrera Hernandez, L.P., Wang, S., Wilson, E.M. and Lieske, J.C. (2021) 'Excretion of urine extracellular vesicles bearing markers of activated immune cells and calcium/phosphorus physiology differ between calcium kidney stone formers and non-stone formers', *BMC Nephrology*, 22(1), p. 204. Available at: https://doi.org/10.1186/s12882-021-02417-8.

Zhang, M., Jin, K., Gao, L., Zhang, Z., Li, F., Zhou, F. and Zhang, L. (2018) 'Methods and Technologies for Exosome Isolation and Characterization', *Small Methods*, 2(9), p. 1800021. Available at: https://doi.org/https://doi.org/10.1002/smtd.201800021.

Zhang, X.-X., Cong, W., Elsheikha, H.M., Liu, G.-H., Ma, J.-G., Huang, W.-Y., Zhao, Q. and Zhu, X.-Q. (2017) 'De novo transcriptome sequencing and analysis of the juvenile and adult stages of *Fasciola gigantica*', *Infection, Genetics and Evolution*, 51, pp. 33–40. Available at: https://doi.org/10.1016/J.MEEGID.2017.03.007.

Zhang, X., Liu, Dianfeng, Gao, Y., Lin, C., An, Q., Feng, Y., Liu, Y., Liu, Da, Luo, H. and Wang, D. (2021) 'The Biology and Function of Extracellular Vesicles in Cancer Development', *Frontiers in Cell and Developmental Biology*, 9(November), pp. 1–9. Available at: https://doi.org/10.3389/fcell.2021.777441.

Zhang, X., Takeuchi, T., Takeda, A., Mochizuki, H. and Nagai, Y. (2022) 'Comparison of serum and plasma as a source of blood extracellular vesicles: Increased levels of platelet-derived particles in serum extracellular vesicle fractions alter content profiles from plasma extracellular vesicle fractions', *PLOS ONE*, 17(6), p. e0270634. Available at: https://doi.org/10.1371/journal.pone.0270634.

Zhang, Z., Guo, K., Pan, G., Tang, J. and Guo, F. (2017) 'Improvement of phylogenetic method to analyze compositional heterogeneity', *BMC Systems Biology*, 11(4), p. 79. Available at: https://doi.org/10.1186/s12918-017-0453-x.

Zhao, Y., Li, B., Bai, D., Huang, J., Shiraigo, W., Yang, L., Zhao, Q., Ren, X., Wu, J., Bao, W. and Dugarjaviin, M. (2016) 'Comparison of Fecal Microbiota of Mongolian and Thoroughbred Horses by High-throughput Sequencing of the V4 Region of the 16S rRNA Gene.', *Asian-Australasian journal of animal sciences*, 29(9), pp. 1345–52. Available at: https://doi.org/10.5713/ajas.15.0587.

Zheng, Y., Guo, X., Su, M., Guo, A., Ding, J., Yang, J., Xiang, H., Cao, X., Zhang, S., Ayaz, M. and Luo, X. (2017) 'Regulatory effects of *Echinococcus multilocularis* extracellular vesicles on RAW264.7 macrophages', *Veterinary Parasitology*, 235, pp. 29–36. Available at: https://doi.org/10.1016/J.VETPAR.2017.01.012.

Zhou, X., Wang, W., Cui, F., Shi, C., Ma, Y., Yu, Y., Zhao, W. and Zhao, J. (2019) 'Extracellular vesicles derived from *Echinococcus granulosus* hydatid cyst fluid from patients: isolation, characterization and evaluation of immunomodulatory functions on T cells', *International Journal for Parasitology*, 49(13–14), pp. 1029–1037. Available at: https://doi.org/10.1016/J.IJPARA.2019.08.003.

Zhu, L., Liu, Juntao, Dao, J., Lu, K., Li, H., Gu, H., Liu, Jinming, Feng, X. and Cheng, G. (2016) 'Molecular characterization of *S. japonicum* exosome-like vesicles reveals their regulatory roles in parasite-host interactions', *Nature Publishing Group* [Preprint]. Available at: https://doi.org/10.1038/srep25885.

Zininga, T., Ramatsui, L. and Shonhai, A. (2018) 'Heat Shock Proteins as Immunomodulants', *Molecules (Basel, Switzerland)*, 23(11), p. 2846. Available at: https://doi.org/10.3390/molecules23112846.

8.0 APPENDIX

All Appendix listed below is supplied on the enclosed USB Flash Drive.

Appendix 2.1 Immunomodulator bait peptide sequences retrieved from Genbank and NCBI Reference Sequence (http://www.ncbi.nlm.nih.gov/).

Appendix 2.2 List of recognised Glutathione S transferase (GSTs), and α-Enolase proteins sequences retrieved from Genbank database and NCBI Reference Sequence (http://www.ncbi.nlm.nih.gov/).

Appendix 2.4 Omicsbox functional annotation of *A. perfoliata* transcriptome.

Appendix 3.2 The full list of proteins identified in *A. perfoliata* secretome proteomics dataset.

Appendix 6.1 Wititkornkul, B., Hulme, B.J., Tomes, J.J., Allen, N.R., Davis, C.N., Davey, S.D., Cookson, A.R., Phillips, H.C., Hegarty, M.J., Swain, M.T., Brophy, P.M., Wonfor, R.E. and Morphew, R.M. (2021) 'Evidence of Immune Modulators in the Secretome of the Equine Tapeworm *Anoplocephala perfoliata'*, Pathogens, 10(7). Available at: https://doi.org/10.3390/pathogens10070912.

Appendix 2.3 RNA integrity of 6 biological replicates of *A. perfoliata* on 1% w/v agarose gel illustrated by clear 28S and 18S rRNA bands

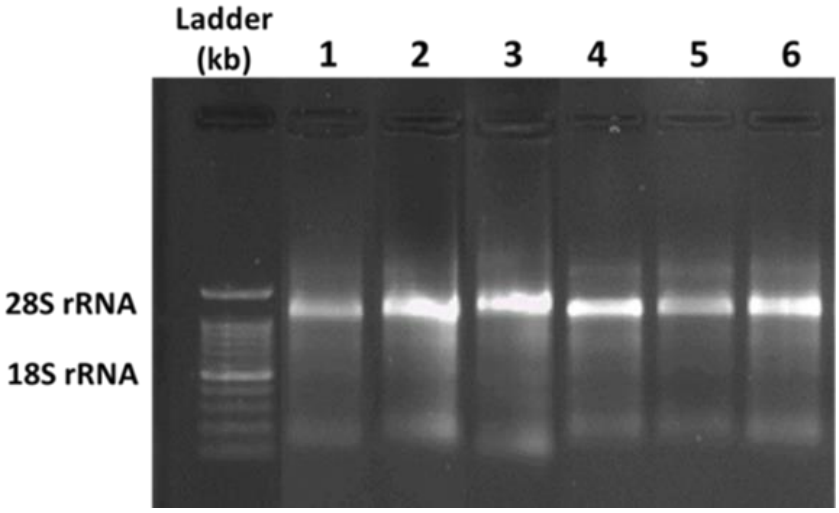

Appendix 3.1 The capture and analysis settings of NanoSight software to assess the particle size and concentration of SEC purified EVs.

Search parameters	**Setting**
Database	*Anoplocephala perfoliata* transcript
Taxonomy	All entries
Allow up to	1 missed cleavage
Enzyme	Trypsin
Fixed modifications	Carboxymethyl (C)
Variable modifications	Oxidation (M)
Peptide tolerance	±1.2 Da
MS/MS tolerance	±0.6 Da
Peptide Charge	1+, 2+ and 3+
Monoisotopic	Enable
Data format	Mascot generic
Instrument	ESI-TRAP
Decoy	Enable
Report top	Auto hit

Appendix 5.1 Cumulative gas production over a 72 hours fermentation period in the control (blank vessel in a hindgut model of equine microbial fermentation, incubated with PZQ at concentrations of 0.00 mmol/L (control), 0.03 mmol/L, 0.08 mmol/L and 0.13 mmol/L in DMSO at a final concentration of (v/v) 0.1%. Coloured in yellow, green, black and red, respectively).